Winter 12-15-2022

Development of Redox-Responsive Phenazine-Based Foldamers. Acylative Kinetic Resolution of Hydroxamic acids

Jingwei Yin
Washington University in St. Louis

WASHINGTON UNIVERSITY IN ST. LOUIS

Department of Chemistry

Dissertation Examination Committee:

Kevin Moeller, Chair

Vladimir Birman, Co-Chair

Jonathan Barnes

Alexei Demchenko

John-Stephen Taylor

Development of Redox-Responsive Phenazine-Based Foldamers. Acylative Kinetic Resolution of Hydroxamic Acids.

by

Jingwei Yin

A dissertation presented to

The Graduate School

of Washington University in

partial fulfillment of the

requirements for the degree

of Doctor of Philosophy

August 2022

St. Louis, Missouri

Table of Contents

List of Figures

List of Tables

List of Abbreviations

ABC: Amidine-based catalyst

Ac: Acetyl

Ar: Aryl

Boc: *tert*-Butoxycarbonyl

BTM: Benzotetramisole

CF3-PIP: 2-Phenyl-6-(trifluoromethyl)-2,3-dihydroimidazo[1,2-a]pyridine

Cl-PIQ: 7-Chloro-2-phenyl-1,2-dihydroimidazo[1,2-a]quinoline

DFT: density functional theory

DMF: N,N-Dimethylformamide

ent: enantiomer of

ee: enantiomeric excess

Et: ethyl

KR: Kinetic resolution

Me: methyl

p: para

Ph: phenyl

s: selectivity factor

THF: tetrahydrofuran

Acknowledgments

First, I would like to thank my advisor Professor Vladimir Birman. He has been an invaluable advisor. He has never hesitated to share his chemistry knowledge, experimental techniques and emotional support. I have learned a lot of chemistry from our group meeting discussions, our problem solving sessions, Chem 558, Chem 5522 and even our daily conversations. Still, there are so much more to learn. He has become the most important teacher in my life. Under his guidance, I was able to explore many interesting projects, some of which will be presented in this thesis.

Next, I would like to thank Professor Kevin Moeller, Professor Jonathan Barnes, and Professor John-Stephen Taylor for their valuable help and discussion on my projects. I would like to thank Professor Alexei Demchenko for serving on my dissertation committee.

My past and current lab mates Dr. Matthew Straub and Ruth Son have been giving me emotional support for many years, for which I am deeply grateful. I also want to thank Dr. Ali N. Khalilov, Dr. Pandi Muthupandi and our undergraduate student Ruby Ladd, for collaboration on our molecular switch project (Chapter 1). Dr. Xuesong Li and Dr. Ruihan Li and Yipei Zhang are experts in polymer and supramolecular chemistry, and their help on GPC and MALDI had been an essential part of the phenazine-based foldamer project (Chapter 2 & 3). I also want to thank Qiwei Jing, Dr. Tiandi Wu, Dr. Nai-Hua Yeh with their help in cyclic voltammetry and bulk electrolysis (Chapter 1-3). We also thank Dr. Nigam Rath (University of Missouri-Saint Louis) for providing crystallographic data.

I want to thank the chemistry department for all the seminars, classes and journal clubs, through which I gained a lot of knowledge. I am deeply grateful for the financial support from our

department. Especially on research funds, which allowed me to explore many projects over the years.

I shall not forget my parents. For years, they have always been inspiring me to do better. I would not have come to US to pursue for a Ph.D. degree without their support.

I want to express my profound gratitude towards my fiancé Su. I would not have come through graduate school without her constant support.

Lastly, I am grateful to my fatherland. The education system in China gave me access to the best education almost free of charge. Many of the knowledge and experience I had gained have been vital to my advancement. It has made me who I am.

Washington University in St. Louis

August, 2022

ABSTRACT OF THE DISSERTATION

Development of Redox-Responsive Phenazine-Based Foldamers. Acylative Kinetic Resolution of Hydroxamic Acids.

for Arts & Sciences Graduate Students

by

Jingwei Yin

Doctor of Philosophy in Chemistry

Washington University in St. Louis, 2022

Professor Vladimir Birman, Principal Investigator

Two different research directions have been presented in this thesis. The first project is about phenazine-based foldamers as molecular actuators. Researchers have been interested in the design and synthesis of foldamers and molecular actuators for years. We began our exploration by demonstrating that phenazine-1,6-dicarboxamides can function as redox-responsive molecular switches. We then designed and synthesized two generations of phenazine-based interleafed foldamers and studied their stability and redox behaviors under chemical and electrochemical conditions.

In the second project, we have developed the first acylative kinetic resolution on hydroxamic acids. Although chiral hydroxamic acids have extensive applications, synthetic methods towards them are not straightforward. On the other hand, with easy access to racemic hydroxamic acids, kinetic resolution provides an attractive approach to enantiomerically enriched hydroxamic acids. We examined three class of substrates with our method and obtained synthetically useful selectivity factors.

Part 1: Development of Redox-Responsive Phenazine-Based Foldamers.

Preface

For the vast majority of living organisms on our planet, muscles are the key to generate motions. The extension and contraction of actin and myosin fibers convert chemical energy into mechanical energy. By contrast, mankind adopted completely different ways of generating movement. For example, Aeolipile, the first engine invented by Heron in ancient Greece ca. 30-20 BCE, converted the power of heated steam into rotational motion. Some thirteen centuries later, Chinese developed the "flying crow", a propulsion device powered by gun powder. Ever since the industrial revolution, various engines have been invented, such as internal combustion engine, electric motor and jet propulsion. Today, with the help of such devices, we can surpass the capability of muscles to great extent. However, those existing motors have a common limitation. They generate rotational movements directly. Therefore, it is important to develop materials that mimic the extension and contraction motions of muscles, especially for applications in robotics and related areas.

There are several existing approaches to creating stimuli-responsive materials that mimic muscle movement. Among these, so-called molecular muscles discussed in more detail in the introduction to Chapter 2, have received considerable attention. However, one major problem with existing molecular muscle designs is that they are distributed randomly in a soft matrix. To fully mimic muscle movements, we need to design molecular muscles that can be aligned in one direction and thus generate unidirectional motion on macroscopic scale.

To design such molecular muscle, there are several important points we need to consider. First, a molecular muscle should be activated via a redox process. Electrochemical redox process is especially attractive as it can be reversed by switching the direction of current. Second, such

redox process should only require the transfer of electrons and protons, not large ions. A textbook example of such process is the oxidation of hydroquinone into p-benzoquinone.

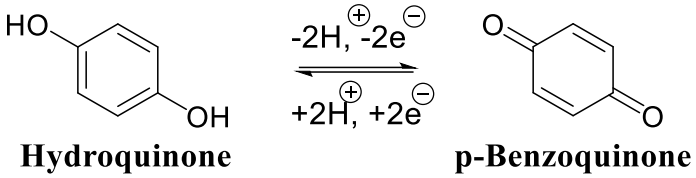

Figure 1. Redox process of hydroquinone and p-Benzoquinone.

Ultimately, molecular muscle should be assembled into an ordered state in the soft material. Side-by-side alignment of individual foldamers is expected to create a unidimensional extension and contraction upon actuation.

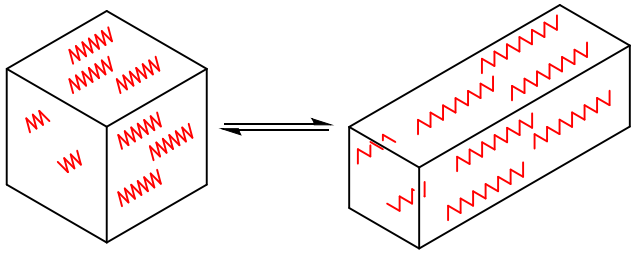

Figure 2. Desired molecular motor design.

Chapter 1: Phenazine-1,6-dicarbox-amides as redox responsive molecular switches

1.1 Introduction to molecular switches

A molecule that shifts between two or more stable states reversibly in response to an external stimulus can be viewed as molecular switch.[1] Over the years, numerous types of molecular switches have been developed, which can be categorized according to the stimuli required, such as irradiation,[2] protonation,[3] introduction of other ions,[4] or neutral organic molecules.[5] A few diverse examples of molecular switches are discussed below by way of illustration. Several more comprehensive reviews of the area may be found in the literature.[6]

Stiff stilbene based molecular switch was pioneered by Feringa et al.[7] At −55 ℃, light excited the double bonds into a single bond, enabling the rotation from (*P,P*)-*trans*-**1.1** to (*M,M*)-*cis*-**1.2**, with a 5:95 *trans*-**1.1** to *cis*-**1.2** ratio. Upon heating to 20 ℃, the unstable (*M,M*)-*cis*-**1.2** transformed to (*P,P*)-*cis*-**1.2** quickly and selectively. Subsequent photo irradiation at $\lambda \geq 280$ nm converted (*P,P*)-*cis*-**1.2** to (*M,M*)-*trans*-**1.1**, while heating to 60 ℃ reverted it back to (*P,P*)-*trans*-**1.1** (Figure 1-1).

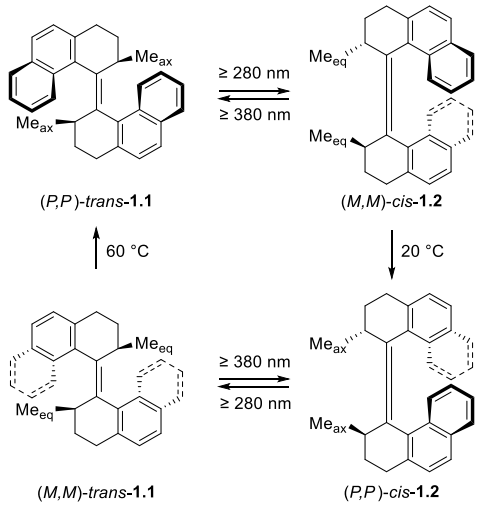

Figure 1-1. Stiff stilbene as a photoswitch.

Azobenzene is another example of photo switches, which can change between *Z*- and *E*-isomers upon photoirradiation or heating. Hecht *et al.*[8]synthesized *meta*-phenyleneethynylene) foldamers with an azobenzene core, which can transit between helix and random coil geometry by irradiation at different wavelengths (Figure 1-2). Hecht *et al.* [2(e)] later developed a library of acylhydrazone-based photoswitches. Herein, E- and Z-isomers have excellent separation of absorbance bands, good resistance and high quantum yields (Figure 1-3).

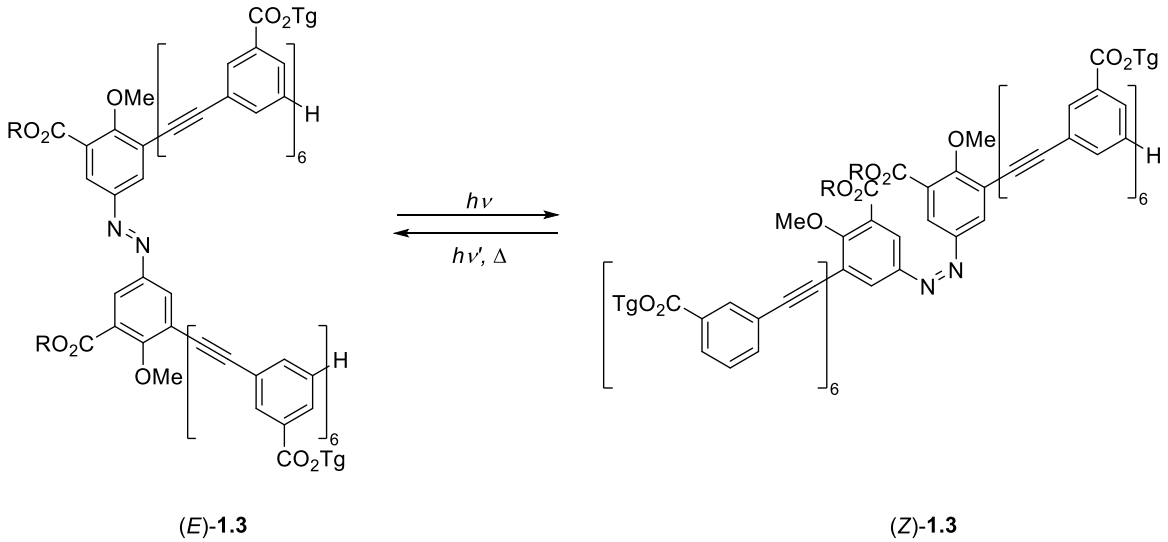

(*E*)-**1.3** (*Z*)-**1.3**

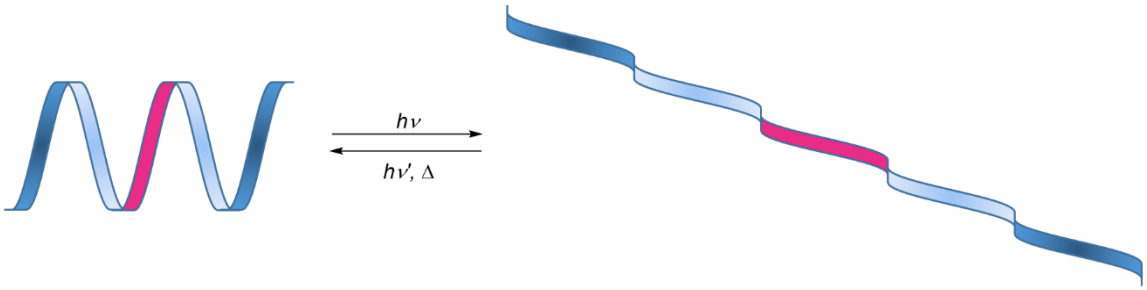

Figure 1-2. Photoswitchable foldamer with azobenzene core. Reprinted with permission from Ref. 8. Copyright 2006 John Wiley and Sons.

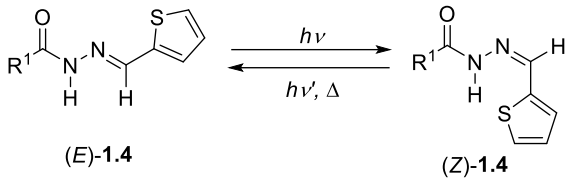

Figure 1-3. Acylhydrazone based photo switches.

A proton-activated molecular switch was reported by Huc *et al.*[9] Helical oligopyridine-dicarboxamide strand **1.5** adopted a folded geometry at neutral pH, which could unfold to a transitional linear conformation **1-(H$^+$)$_3$** by titration with 20 equivalents of TFA (pK_a = 0). Further protonation with an excess of TfOH (pK_a = −16) resulted in folding of **1-(H$^+$)$_3$** to **1-(H$^+$)$_7$** (Figure 1-4). Both **1-(H$^+$)$_3$** and **1-(H$^+$)$_7$** could reverse back to strand **1.5** once neutralized by Et_3N. The protonation/deprotonation process was fully reversible.

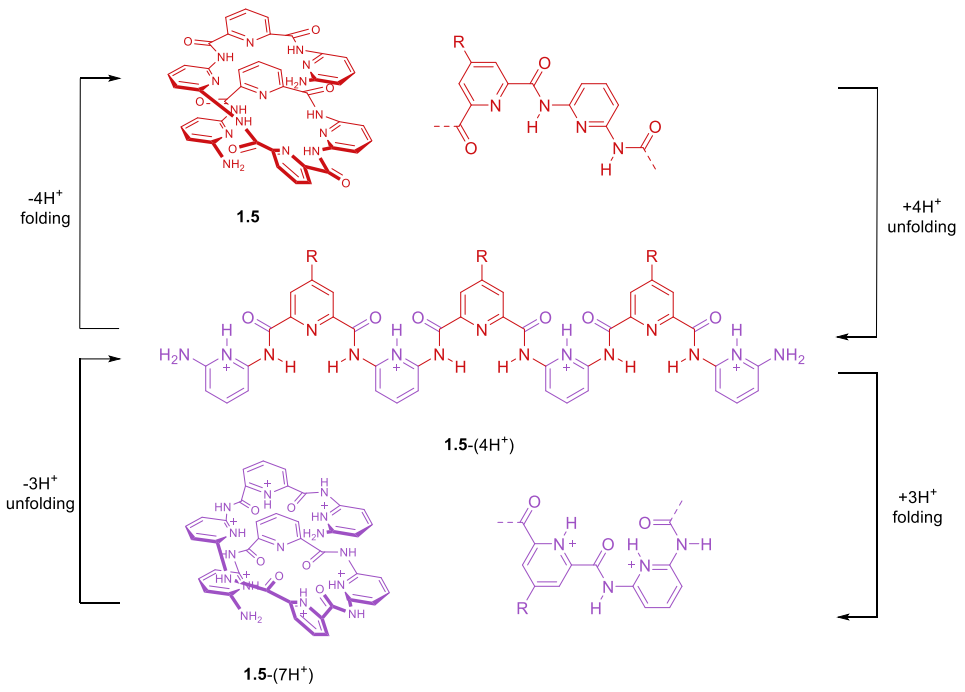

Figure 1-4. Proton activated molecular switch.

A copper (II) activated molecular hinge was reported by Haberhauer.[10] Steric repulsion of lone pairs 2, 2' plus proton 6 and 6' in (*S*)-**1.6** ensured the stable open conformation of the hinge, with dihedral angle of N—C—C—N ca. 180 °. After $Cu(OTf)_2$ was added, Cu^{2+} chelation turned the C—C bond ca. 180 °, making a closed hinge. Since 3 and 3' was connected via a chiral peptide strand, ***(R)*-1.6** is 42 kJ/mol (R = Ph) higher in energy than ***(S)*-1.6**. The reversibility was demonstrated by addition of cyclam to the mixture, which removed Cu^{2+} from the hinge, giving back the open conformation (Figure 1-5).

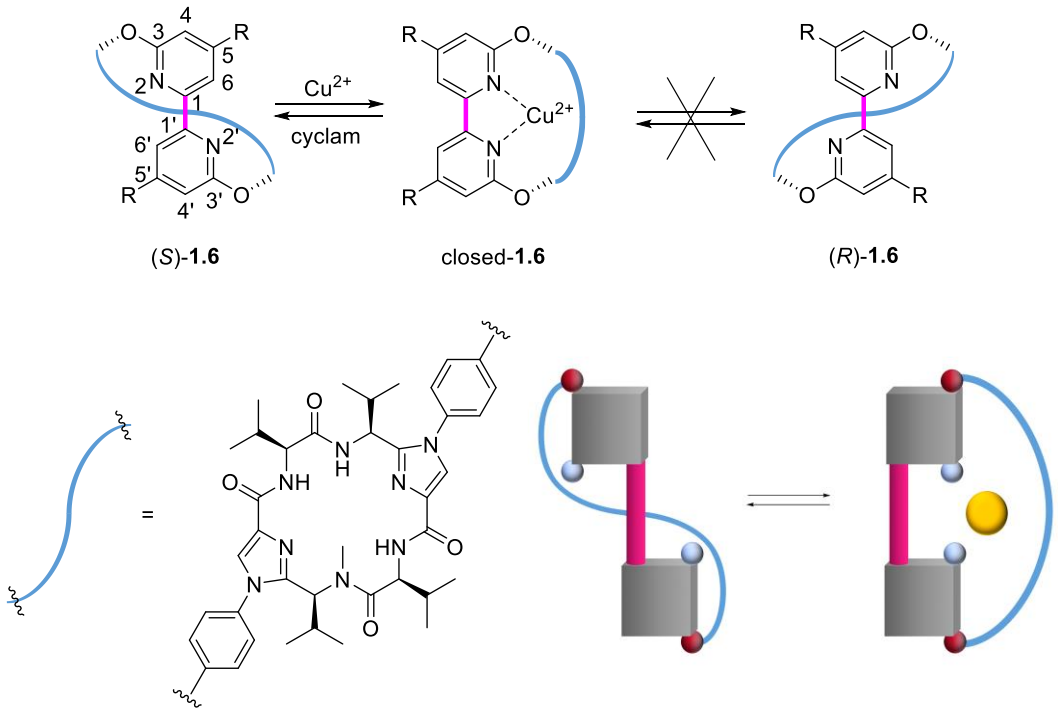

Figure 1-5. Copper (II) activated molecular hinge. Reprinted with permission from Ref. 10. Copyright 2008 John Wiley and Sons.

Powerful chelation properties of 2,2'-bipyridines were applied to the design of a molecular switch by Rebek *et al.*[11] Metal-free conformer *closed*-**1.7** has a cyclohexane inside its cavitand, conformationlly similar to *Ouroboros* - the ancient symbol of a serpent or dragon eating its own tail.[12] When *closed*-**1.7** was exposed to 1-adamantane-carbonitrile (AdCN), a potential guest for the cavity, no conformational change was observed. However, once $ZnBr_2$ was added to the mixture, chelation on 2,2'-bipyridine site caused the pyridine to take *syn*-conformation, opening up the host cavity. As a result, 45% of the AdCN was observed inside of the cavitand. As the addition of water washed out the $ZnBr_2$, *occupied*-**1.7** ejected AdCN it had absorbed, turning back to *closed*-**1.7** (Figure 1-6).

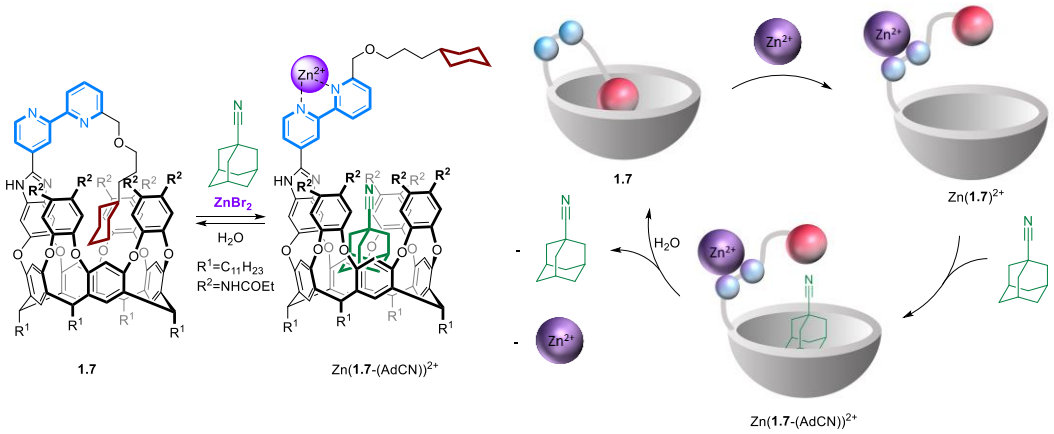

Figure 1-6. 2,2'-bipyridine-based molecular switch. Reprinted with permission from Ref. 11. Copyright 2010 John Wiley and Sons.

Besides cations as stimulus, Yu and Pan *et al.*[13] have reported an anion-meditated molecular switch on a macrocycle scaffold. Two units of di-Naphthoimidazole **1.8** and Pd^{2+} self-assembled to *bowl*-**1.8**, which could accommodate one nitrate anion via hydrogen bonds in a bowl conformation. Once non-coordinated anions such as $B(Ph)_4^-$ or PF_6^- was added to *bowl*-**1.8** in pure acetonitrile, a large conformational change was observed. In *bowl*-**1.8**, CH—O hydrogen bonding between the imidazolium hydrogens and the nitrate counter-ion providing the necessary enthalpic stabilization whereas in *chair*-**1.8**, CH-N hydrogen bonding conformation will reduce steric repulsion between arene unites. Upon addition of nitrate to *chair*-**1.8**, *bowl*-**1.8** was observed via ^{1}H NMR. Halogen anions Cl^-, Br^- and I^- were observed to destroy Pd-N bonds, which makes them inapplicable here (Figure 1-7).

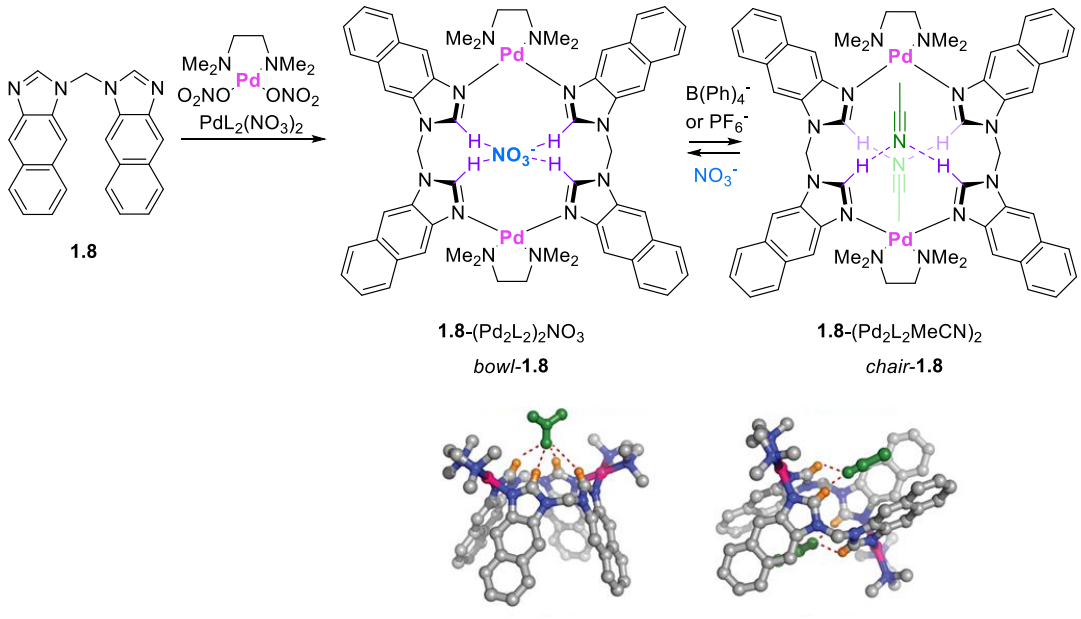

Figure 1-7. Anion-mediated molecular switch.

Neutral molecules have also been explored as stimuli for geometric changes. Ramakrishnan *et al.*[14] used **D2-NH_3^+** and **18-crown-6** to control the folding and unfolding of polyimide **1.9**. Multipoint interactions between -NH_3^+ and polyethylene chain, and the π-π stacking between electron rich ring **D2** and electron deficient ring on polyimide are two key factors for the folded geometry. To prove its reversibility, **18-crown-6** was titrated in order to capture **D2-NH_3^+** and a complete reversal was confirmed by ^{1}H NMR (Figure 1-8).

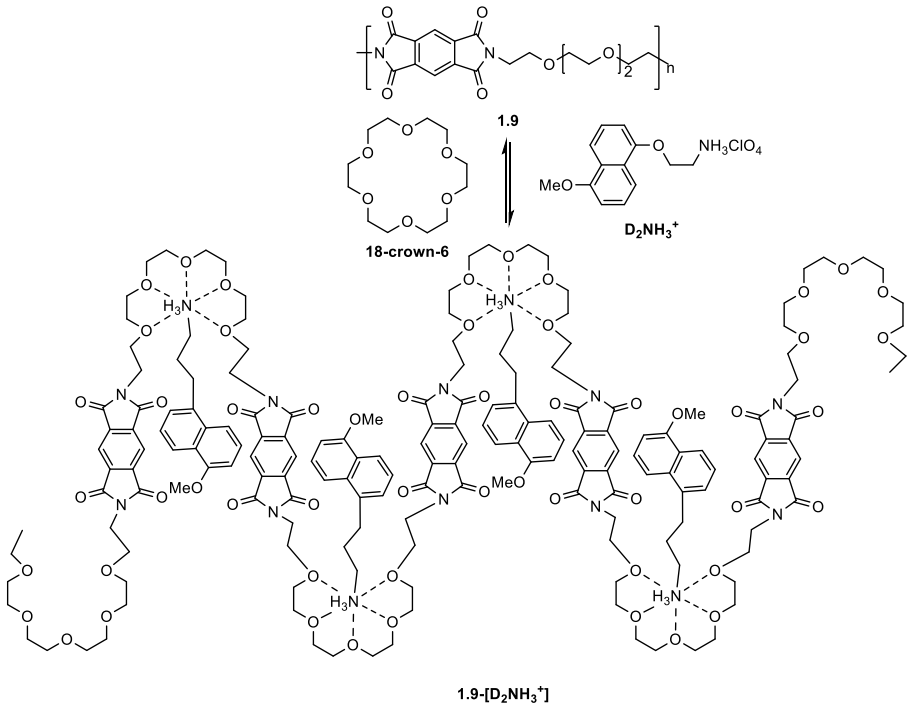

Figure 1-8. Folding induced by small molecules.

1.2 Phenazine-1,6-dicarboxamides as redox-responsive molecular switches.

As we have seen in the preceding section, a number of molecular switches have been designed that respond to irradiation, addition of ions or neutral molecules. Molecules that change their shape in response to changing their oxidation state are also known.[15] These, however, typically involve charged species and thus require migration of large ions. On the other hand, a shape-shifting redox-active molecule *that switches between two neutral states* would constitute an attractive molecular switch. Its electrochemical actuation would only rely on the flow of electrons and protons and could be reversed by switching the direction of the current. It could also be operated chemically via catalytic hydrogenation, i.e. using the cleanest available reductant. To our

knowledge, no molecular switch that satisfied these requirements had been described prior to our study described below.

The new type of molecular switch that we envisioned is based on phenazine-1,6-dicarboxyamides. Its mode of operation is illustrated in Figure 1-9. The orientation of carboxamide groups at C1 and C6 shown in structure **1.10** is dictated by hydrogen bonds to the phenazine nitrogens. Once reduced, phenazine ring turns from a hydrogen bond acceptor into a hydrogen bond donor. This newly forming hydrogen bonds will force two amide bonds to rotate almost 180 ° to the side.

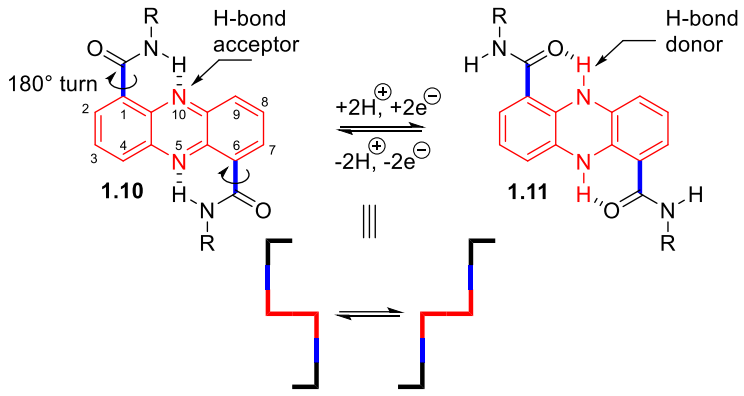

Figure 1-9. Proposed phenazine-1,6-dicarboxamide molecular switch.

To validate this idea, our group first required access to phenazine-1,6-dicarboxamides. Our synthetic route pioneered by Dr. Ali Khalilov in 2017 and later optimized when I joined this project is shown in (Figure 1-10). Hydrogenation of **1.12** leads quantitatively to **1.13**, with is then coupled with another equivalent of **1.12** to give **1.14** with 77% yield. Cyclization of **1.14** was achieved by refluxing it with 20 equivalents of sodium borohydride under basic conditions. Massive amount of gas was generated at the beginning; thus a 1-liter bump trap is recommended to replace the condenser throughout the reflux. The reaction mixture would first turn bright-yellow and then

slowly darken to brown. At the end of the reflux, the product was present in the dihydrophenazine form and still needed to be oxidized to **1.15**. Therefore, 30 wt% hydrogen peroxide was added during the work up. Multiple colors were observed during this process. I surmised that multiple charge transfer complexes were involved. The brown mixture first turned green and then red before finally settling on dark brown. To obtain reproducible results during later stages of the synthesis, I found it advantageous to rinse the crude diacid with acetone multiple times to wash away impurities. After this step, **1.15** was consistently obtained as a greenish brown solid.

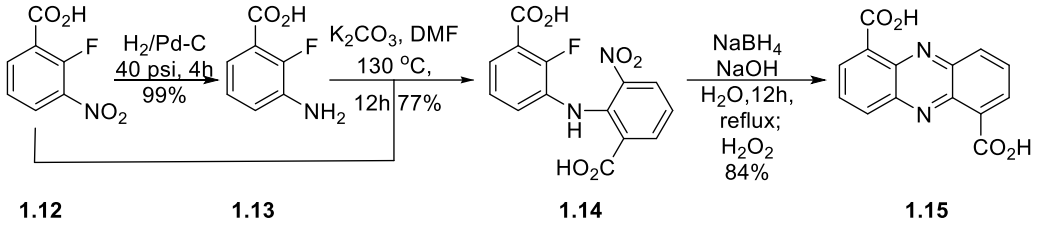

Figure 1-10. Synthesis of phenazine-1,6-dicarboxylic acid.

Amidation of phenazine-1,6-dicarboxylic acid **1.15** turned out to be non-trivial (Table 1). To begin with, **1.15** was insoluble in most organic solvents. It is soluble in K_2CO_3 or KOH solution (but not Na_2CO_3 or NaOH) and minimally soluble in DMF. Neat thionyl chloride was used in excess to try to make corresponding acyl chloride (entry 1). After 3 hours of reflux, the solution turned from brownish yellow to pink. Due to low solubility, the conversion could not be determined by ^{1}H NMR or TLC. Upon removal of excess thionyl chloride, excess butylamine was added directly to give **1.17** in 20% yield. While when added 5-tert-Butyl-2-methoxyaniline, **1.18** was not observed. Other activation methods did not seem promising (entry 2 and 3). Addition of propylphosphonic anhydride also resulted the solution to pink, but there was no conversion towards **1.17** or **1.18** (entry 4). Inspired by a literature example of using 1,1'-Carbonyldiimidazole for activation,[16] **1.15** in DMF was added 1,1'-Carbonyldiimidazole. The brownish yellow

suspension turned reddish within 30 minutes and slowly turned pale yellow in the next 24 hours. **1.18** is slightly soluble in methylene chloride and reacts with n-butylamine smoothly (entry 5).

Table 1-1. Amidation of phenazine-1,6-dicarboxylic acid.

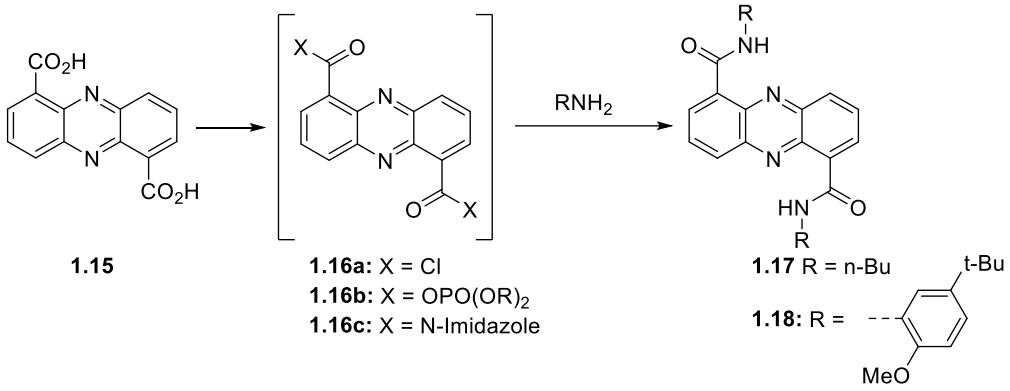

entry	Activation method	X	% yield	
			1.17	**1.18**
1	$SOCl_2$	**1.16a**	20%	NR
2	$(COCl)_2$, DMF	**1.16a**	20%	NR
3	$(NCCl)_3$, DMF	**1.16a**	15%	NR
4	T3P	**1.16b**	NR	NR
5	CDI	**1.16c**	90%	NR

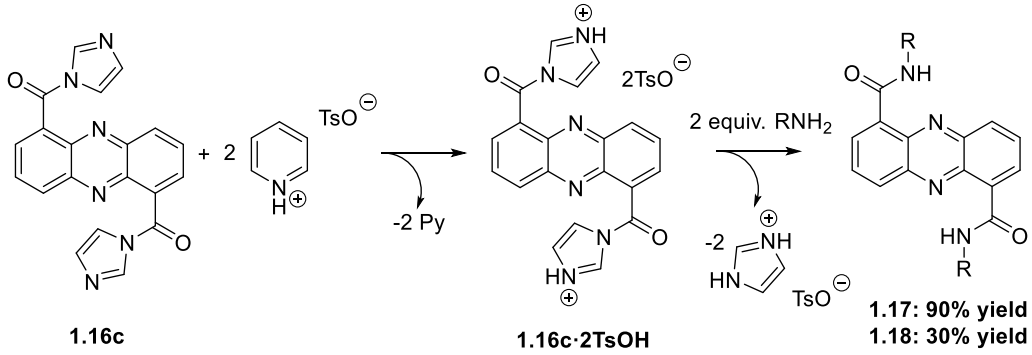

Figure 1-11. Activation of **1.16c** by PPTS.

N-acylimidazole can be activated via protonation.[17] **1.16c**·**2TsOH** would be a more reactive acyl donor than **1.16c** owning to better leaving group, imidazole trifluoromethanesulfonate salt (Figure 11). Indeed, when **1.16c** was heated to 135 ℃ in excess

molten pyridinium p-toluenesulfonate (PPTS), a moderate conversion to **1.18** was recorded. To further improve this acylation, we needed even better leaving groups.

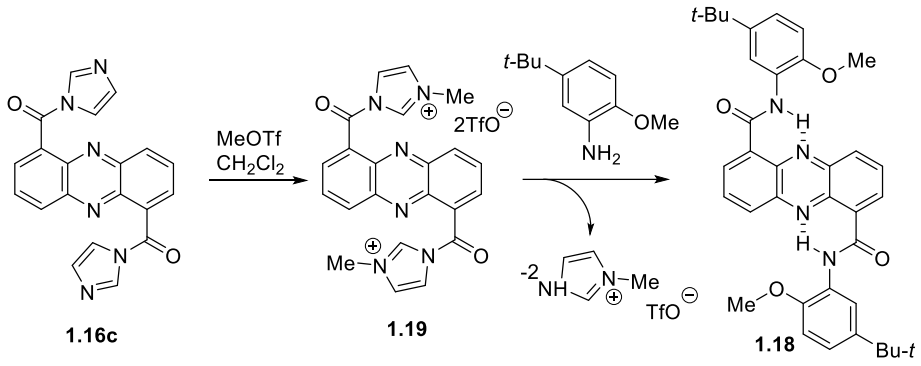

Figure 1-12. Synthesis of **1.18**.

Rapoport *et al*[18] reported that methylation on N-acylimidazoles greatly increases its reactivity by producing 3-methylimidazolium triflate as leaving group. Inspired by this finding, **1.16c** was treated with methyl triflate in CH_2Cl_2 to give **1.19**. Gratifyingly, **1.19** reacted smoothly to deliver **1.18** in 95% yield (Figure 12). As the continuation of this project, **1.19** became a vital compound to our synthesis. Therefore, several critical details are listed below to ensure its consistent quality.

The reaction of **1.16c** with methyl triflate was conveniently performed in a centrifuge test tube. The brownish product **1.19** forms a precipitate that tends to aggregate in the upper part of the tube above the liquid. Therefore, it is advisable to hand-shake the reaction mixture after about 30 min, so as to return the solid into the liquid suspension. The supernatant was usually dark brown.[a] Purification of **1.19c** was achieved by diluting the dark-brown reaction mixture with dry CH_2Cl_2,[b] centrifuging the test tube to collect the precipitate on the bottom, and removing the supernatant via syringe. The precipitate was re-suspended in fresh dry CH_2Cl_2, and the procedure repeated at least 5 times until the supernatant is clear.[c]

Notes:

a) Occasionally, the supernatant might turn green due to moisture. If so, the reaction should be considered compromised, and should be recycled with aqueous K_2CO_3 to recover the diacid.

b) Note that CH_2Cl_2 tends to evaporate quickly, causing the moisture in the air to freeze at the tip of the squeeze bottle. Therefore, it's recommended to use a cylinder to hold CH_2Cl_2 for this purpose.

c) The impurities of **1.19c** might not be fully visible by H NMR due to their poor solubility. In addition to H NMR, quality check should be performed by dissolving 10 mg of the product in 0.5 mL of dry acetonitrile. If the product dissolves at room temperature easily, then it should be considered excellent quality. If heat was needed to fully solvate the product, then this batch should be used with caution, knowing that the quality is substandard. If any solids still persisted after heating, this batch should be considered defective, even if the H NMR showed little impurities.

With **1.18** in hand, we began to evaluate its potential as a molecular switch (Figure 13). Its hydrogenation was performed at 20 psi in a Schlenk tube with an NMR tube attached to it so as to minimize the exposure of the dihydrophenazine form to air. After half an hour, the reaction mixture was transferred to the NMR tube by inverting the apparatus and flame sealing the NMR tube. A slight color change was observed during the hydrogenation (solution turned from orange to yellow), and ^{1}H NMR confirmed the quantitative conversion. According to NOESY spectra of **1.18** and **1.20**, protons **d** and **e** which had been in proximity with **a** in **1.18**, interacted with **c** in **1.20**. Proton **a** in **1.20** showed proximity to **x**. This change of nOe signals validated the expected unfolding of two amide bonds. Upon air exposure, compound **1.20** oxidized back to **1.18** within minutes.

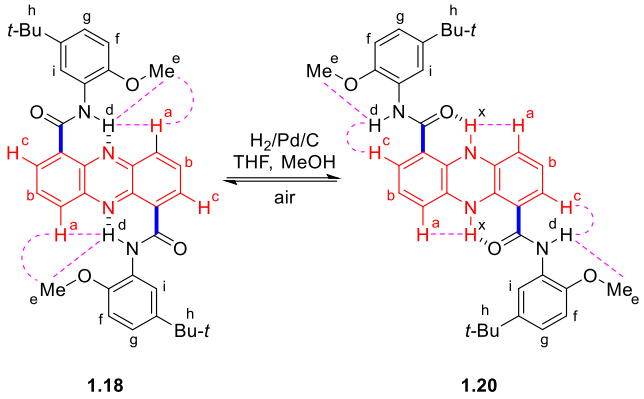

Figure 1-13. Redox studies of **1.18.**

Having demonstrated that our molecular switch can be actuated by hydrogenation, i.e., chemically, we wanted to evaluate its electrochemical reduction in protic and aprotic solvents (Figure 14). Since **1.18** was not soluble in methanol, **1.17** was tested instead via cyclic voltammetry (CV). Multiple scans were performed in THF and methanol to demonstrate complete redox reversibility of **1.17** in both solvents. While the CV in THF contains two distinct reduction waves, only one is observed in methanol.

THF, Scans 5-10 **Methanol, Scans 5-20**

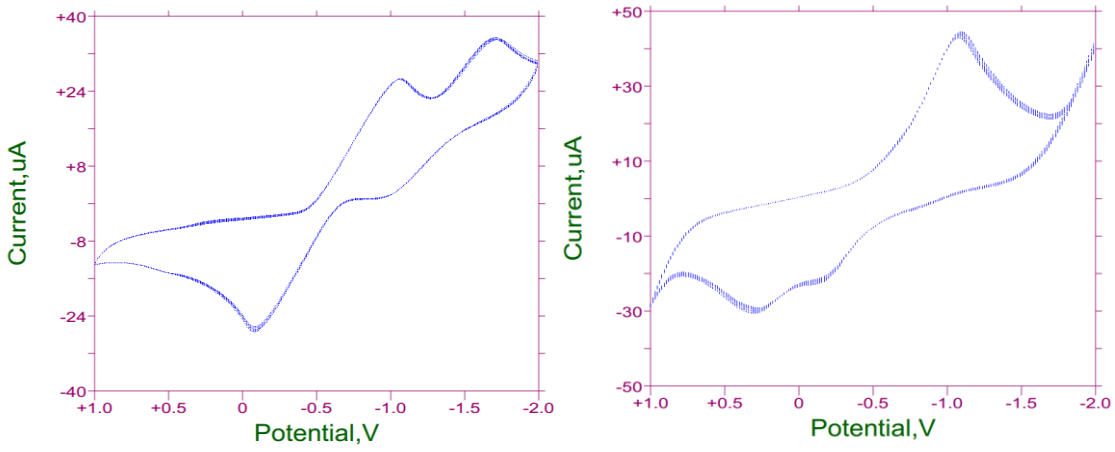

Figure 1-14. Synthesis and cyclic voltammetry of **1.17.**

In conclusion, we have synthesized phenazine-1,6-dicarboxyamides and demonstrated its ability as redox responsive molecular switch. In the next chapter, I will illustrate one of their applications: building a redox responsive molecular muscle.

1.3 Experimental

1.3.1. General

All reagents were obtained commercially and used as received unless specified otherwise. All reactions were carried out under argon, unless noted otherwise. Hydrogenations were carried out by first charging the reaction vessel with solid starting materials and palladium catalyst, then purging with argon, then adding the reaction solvents, and finally purging the vessel with hydrogen. ***Note:*** *mixtures of organic vapors or hydrogen with air have been observed to ignite spontaneously upon contact with an active palladium catalyst.* Solvents used for chromatography were ACS or HPLC grade. Reactions were monitored by thin layer chromatography (TLC) and by 1H NMR. Uniplate HLF (250 μm) silica gel plates were used for TLC analyses. Flash column chromatography was performed over Sorbent Technologies silica gel (40-63 mm). ^{1}H, ^{13}C and ^{19}F NMR spectra were recorded on a Mercury 300 MHz spectrometer and DD2 500 MHz and 600 MHz Agilent spectrometers. The chemical shifts are reported as δ values (ppm) relative to TMS using the residual $CHCl_3$ peak (7.26 ppm) as the reference. Melting points were measured on a Stuart SMP10 melting point apparatus. High-Resolution mass spectral analyses were performed at Washington University MS Center on a Bruker MaXis QTOF mass spectrometer using Electrospray Ionization (ESI) and Atmospheric Pressure Chemical Ionization (APCI) methods. Infrared spectra were recorded on a Bruker Alpha Platinum-ATR spectrophotometer.

1.3.2. Synthesis of 1,1'-(phenazine-1,6-dicarbonyl)bis(3-methyl-1H-imidazol-3-ium) ditriflate (1.19).

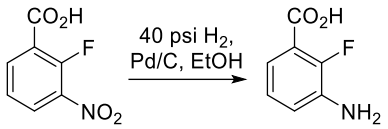

1.13

1.3.2a. 3-amino-2-fluorobenzoic acid (1.13).[19] A mixture of 2-fluoro-3-nitrobenzoic acid (5.0 g, 27 mmol), 10 wt% Pd/C (50 mg, 0.05 mmol) and 50 mL of EtOH was hydrogenated under 40 psi of pressure in a Parr shaker for 4 h. The mixture was filtered through Celite, dried with Na_2SO_4, and rotary evaporated to afford the product as a brown-pink solid, which was essentially pure by ^{1}H NMR. (4.1 g, 98% yield). **^{1}H NMR** (600 MHz, CD_3OD) δ 4.95(br, s, 3H), 6.93-6.96(t, J = 9 Hz, 1H), 7.00-7.02(t, J = 6 Hz, 1H), 7.13(t, J=9 Hz, 1H). **^{13}C NMR** (151 MHz, CD_3OD) δ 120.76, 122.08-122.12 (d, J=6 Hz), 124.99-125.02 (d, J=4.5 Hz), 138.34-138.43 (d, J=13.5 Hz), 151.40, 153.07, 168.38. **^{19}F NMR** (282 MHz, CD_3OD) δ 19F NMR (282 MHz, cdcl3) δ 1.71 - 1.63(m). **IR** (cm^{-1}):1683, 1485, 1417, 1296, 745; **HRMS** (ESI-TOF) m/z: calcd for $[C_7H_6FNO_2 + H]^+$, 156.0460 ; found, 156.0449. **mp:** 167-169 ℃.

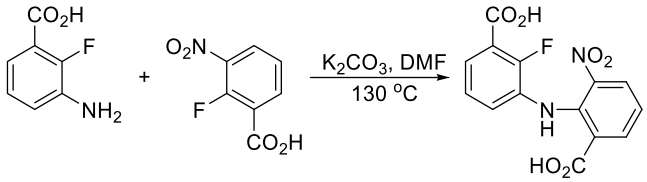

1.13 1.12 1.14

1.3.2b. 2-((3-carboxy-2-fluorophenyl)amino)-3-nitrobenzoic acid (1.14). A mixture of **S-1** (4.1 g, 26 mmol), 2-fluoro-3-nitrobenzoic acid (5.0 g, 27 mmol), K_2CO_3 (9.3 g, 56 mmol) and DMF (100 mL) was stirred at 130 ℃ for 12 h. After cooling, the reaction mixture was quenched with 50 mL of 6 M aqueous HCl and extracted with EtOAc (3×100 mL). The combined organic phase was dried over $MgSO_4$ and rotary evaporated. The residue was purified by flash chromatography (hexane/EtOAc/AcOH 66:33:1) to afford the product as a yellow solid (6.4 g, 77% yield). **^{1}H NMR** (500 MHz, CD_3OD) δ 4.92 (br, s, 3H), 7.06-7.11 (m, 3H), 7.55 (m, 3H）, 8.07-

8.09 (d, J = 10 Hz 1H), 8.30-8.32 (d, J = 10 Hz 1H). **^{13}C NMR** (126 MHz, CD_3OD) δ 120.38, 121.48, 124.10, 124.86-124.90 (d, J=5 Hz), 127.45, 132.14-132.18 (d, J=5 Hz), 132.28, 138.22, 140.83, 141.47, 154.50, 156.55, 167.27, 170.25. **^{19}F NMR** (282 MHz, $CDCl_3$) δ 19F NMR (282 MHz, CD_3OD) δ 25.88 (m). **IR** (cm^{-1}): 2908, 1682, 1260, 934, 774, 753, 739, 720; **HRMS** (ESI-TOF) m/z: calcd for $[C_{14}H_9FN_2O_6 + Na]^+$ 343.0342, found 343.0327. **mp:** 230-231 ℃.

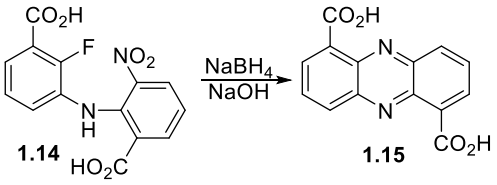

1.3.2c. Phenazine-1,6-dicarboxylic acid (1.15).[20] A solution of **S-2** (6.4 g, 20 mmol) in 400 mL of 3 M aqueous NaOH was treated with solid $NaBH_4$ (20.0 g, 535 mmol) added in small portions at room temperature, then refluxed overnight (10 h) and cooled to room temperature. The resulting yellow suspension was brought to pH 7 with 6 M aqueous HCl, at which point the precipitate turned green. The suspension was treated with 3% aqueous H_2O_2 (100 mL) and sparged with air overnight. The precipitate, which at this point was brown, was filtered off, rinsed on the filter with deionized water, and dried in a desiccator. The dry product was light-brown. (4.5 g, 84% yield). **^{1}H NMR** (300 MHz, as disodium salt, KOH, D_2O) δ 7.91 (s, 4H), 8.24 (s, 2H) . **^{13}C NMR** (126 MHz, D_2O) δ 126.72, 129.51, 129.56, 137.92, 138.23, 141.04, 174.50. **IR** (cm^{-1}):1740, 1394, 1230, 858, 754; **HRMS** (ESI-TOF) m/z: calcd for: $[C14H_8N_2O_4 + Na]^+$ 291.0376; found 291.1466. **mp:** >300 ℃.

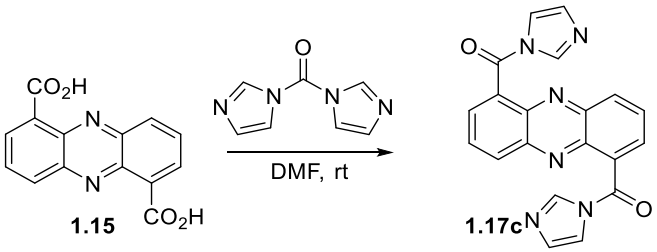

1.3.3d. 1,1'-(phenazine-1,6-dicarbonyl)bis-imidazole (1.17c).[14] A 10 mL centrifugation tube was charged with a stir bar, phenazine-1,6-dicarboxylic acid **3** (1.2 g, 4.47 mmol) and 5 mL of DMF. The resulting green suspension was stirred at room temperature and treated with solid CDI (2.5 g, 15.4 mmol) added in small portions. The reaction mixture quickly turned deep-red. After stirring overnight (ca. 12 h), the red color faded and a beige precipitate was observed. The mixture was diluted with 5 mL of Et_2O, stirred vigorously, and centrifuged. The supernatant was removed carefully via syringe. The procedure was repeated 4 more times leaving essentially pure product as a pale yellowish-beige powder, which was dried by rotary evaporation in the same tube (1.56 g, 94% yield).**^{1}H NMR** (600 MHz, $CDCl_3$) δ 7.16 (s, 2H), 7.52 (s, 2H), 7.86 (s, 2H), 7.97-7.99 (t, J = 6 Hz, 2H), 8.14-8.16 (d, J = 12 Hz, 2H), 8.36-8.38 (d, J = 12 Hz, 2H) **^{13}C NMR** (151 MHz, $CDCl_3$) δ 117.32, 130.22, 131.23, 132.10, 132.96, 133.93, 138.13, 164.41. **IR** (cm^{-1}):1721, 1537, 1410, 1383, 1288, 1237, 810, 748, 730, 677, 644; **HRMS** (ESI-TOF) m/z: calcd for $[C_{20}H_{12}N_6O_2 + H]^+$: 369.1095, found 369.1085. **mp:** 230 ℃ (dec).

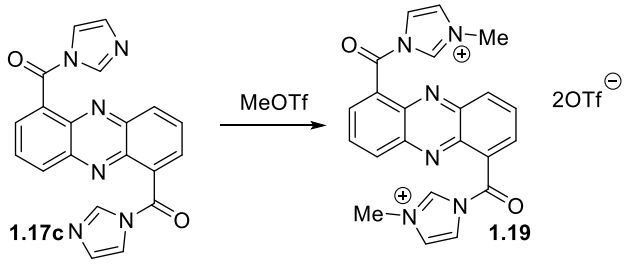

1.3.3e. 1,1'-(phenazine-1,6-dicarbonyl)bis(3-methyl-1H-imidazol-3-ium) triflate (1.19). A suspension of **1.17c** (1.56 g, 4.23 mmol) in 2 mL of CH_2Cl_2 stirring at room temperature in a centrifugation tube was treated with MeOTf (1.3 mL, 11.84 mmol) added slowly dropwise. After stirring for 2 h, the mixture was centrifuged and the supernatant removed via syringe. The precipitate was re-suspended in 5 mL of CH_2Cl_2 and the procedure repeated 3 more times. After drying by rotary evaporation in the same tube, the light-yellow microcrystalline product weighed

2.89 g (98% yield) and was sufficiently pure for the next step. **^{1}H NMR** (300 MHz, CD_3CN) δ 3.89 (s, 6H), 7.58-7.59 (m, 2H), 8.03-8.04 (m, 2H), 8.15-8.20 (dd, J_1 = 9 Hz, J_2 = 6 Hz, 2H), 8.40-8.44 (dd, J_1 = 3 Hz, J_2 = 9 Hz, 2H), 8.48-8.50 (dd, J_1 = 3 Hz, J_2 = 6 Hz, 2H), 9.08 (br, 2H). **^{13}C NMR** (151 MHz, CD_3CN) δ 120.77, 125.85, 130.05, 132.16, 136.16, 136.76, 140.17, 141.98, 143.42, 163.94. **IR** (cm^{-1}): 1745, 1256, 1167, 1028, 878, 749, 637, 618, 517; **mp:** 185 ℃ (dec).

1.3.3. SYNTHESIS AND REDUCTION OF MODEL COMPOUND 1.18.

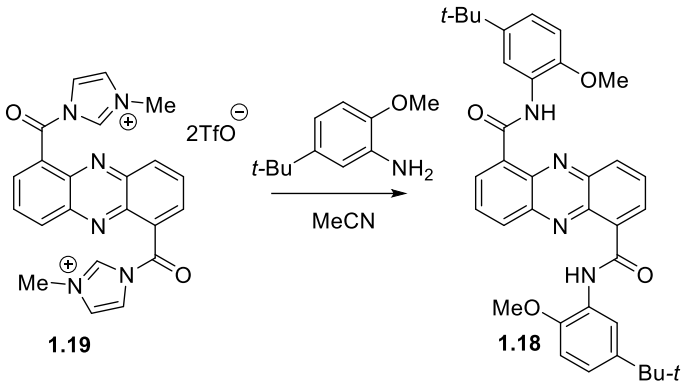

1.3.3a. N1,N6-bis(5-(tert-butyl)-2-methoxyphenyl)phenazine-1,6-dicarboxamide (1.18). To a suspension of **1.19** (270 mg, 0.39 mmol) in 1 mL MeCN stirring at room temperature was slowly added a solution of 5-(*t*-butyl)-2-methoxyaniline (170 mg, 0.93 mmol) in 1 mL MeCN. TLC indicated complete conversion after 30 min. The reaction mixture was rotary evaporated, the residue taken up in CH_2Cl_2, rinsed with water, and dried over $MgSO_4$. Flash chromatography (hexanes/EtOAc 2:1) afforded the product as a red-orange solid (226 mg, 98% yield). **^{1}H NMR** (600 MHz, CD_2Cl_2) δ 1.41 (s, 18H), 4.13 (s, 6H), 7.02 - 7.03 (d, 2H, J = 6 Hz), 7.19 - 7.20 (d, 2H, J = 6 Hz), 8.11 - 8.13 (t, 2H, J = 6 Hz), 8.52 - 8.53 (d, 2H, J = 6 Hz), 8.91 (s, 2H), 9.11 (s, 2H), 13.12 (s, 2H). **^{13}C NMR** (151 MHz, CD_2Cl_2) δ 31.92, 34.93, 56.77, 110.57, 119.00, 121.09, 128.81, 130.70, 131.97, 133.37, 136.56, 140.77, 141.99, 144.56, 147.73, 162.47. **IR** (cm^{-1}): 2950, 1662,

1591, 1528, 1255, 1220, 1178, 1139, 1030, 746. **HRMS** (ESI-TOF) m/z: calcd for: $[C_{36}H_{38}N_4O_4 + H]^+$: 591.2966, found 591.2940. **mp:** >300 ℃.

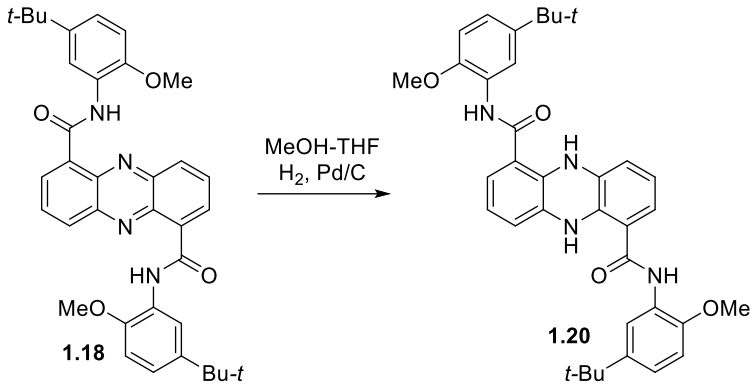

1.3.3b. N1,N6-bis(5-(tert-butyl)-2-methoxyphenyl)-5,10-dihydrophenazine-1,6-dicarboxamide (1.20). A pressure tube with a side arm was charged with **1.18** (34 mg, 0.058 mmol), 10 wt% Pd/C (5 mg, 0.005 mmol), THF (0.7 mL) and MeOH (0.7 mL) (**See Note in 1.3 general)** and connected to a hydrogen reservoir. The mixture was stirred magnetically under 20 psi of hydrogen pressure at room temperature for 2 h. The solvents were removed by evacuating the apparatus through the side arm and then purging it with argon. Degassed $CDCl_3$ (0.7 mL) was added via syringe under an argon blanket. The resulting suspension was withdrawn via syringe and filtered through a PTFE syringe filter (0.45 μm porosity) into an NMR tube filled with argon. A sample thus prepared contained ca. 95% pure dihydrophenazine **1.20** and was stable for 2 days in a capped NMR tube. Upon deliberate exposure to air, it converted back into **1.18** within 2 h. **^{1}H NMR** (600 MHz, CD_2Cl_2) δ 1.35 (s, 18H), 3.90 (s, 6H), 6.21 - 6.22 (d, 2H, J = 6 Hz), 6.38 - 6.41 (t, 2H, J = 6 Hz), 6.68 - 6.69 (d, 2H, J = 6 Hz), 6.87 - 6.89 (d, 2H, J = 6 Hz), 7.10 - 7.12 (dd, 2H, J_1 = 6 Hz, J_2 = 6 Hz), 8.39 (s, 2H), 8.42 - 8.43 (d, 2H, J = 6 Hz), 9.13 (s, 2H). ^{13}C NMR (151 MHz, CD_2Cl_2) δ 26.15, 30.65, 31.85, 34.88, 56.45, 68.32, 110.09, 113.65, 114.70, 117.98, 119.01, 120.48, 120.97, 127.54, 134.63, 137.71, 144.34, 146.97, 166.91.

1.3.4. Computational studies.

Energy profiles of simple models. The geometries of model phenazine-1,6-dicarboxamide **1.21** and its reduced form **1.22** were optimized at the B3LYP/6-31G* level of theory in gas phase. The dihedral angles of highlighted bonds in optimized **1.21** and **1.22** were found to be 173 ° and 17 °, respectively. The highlighted bonds were then constrained at dihedral angles ranging from 0 ° to 360 ° at 20 degree intervals and re-optimized. The resulting energy profiles are shown below.

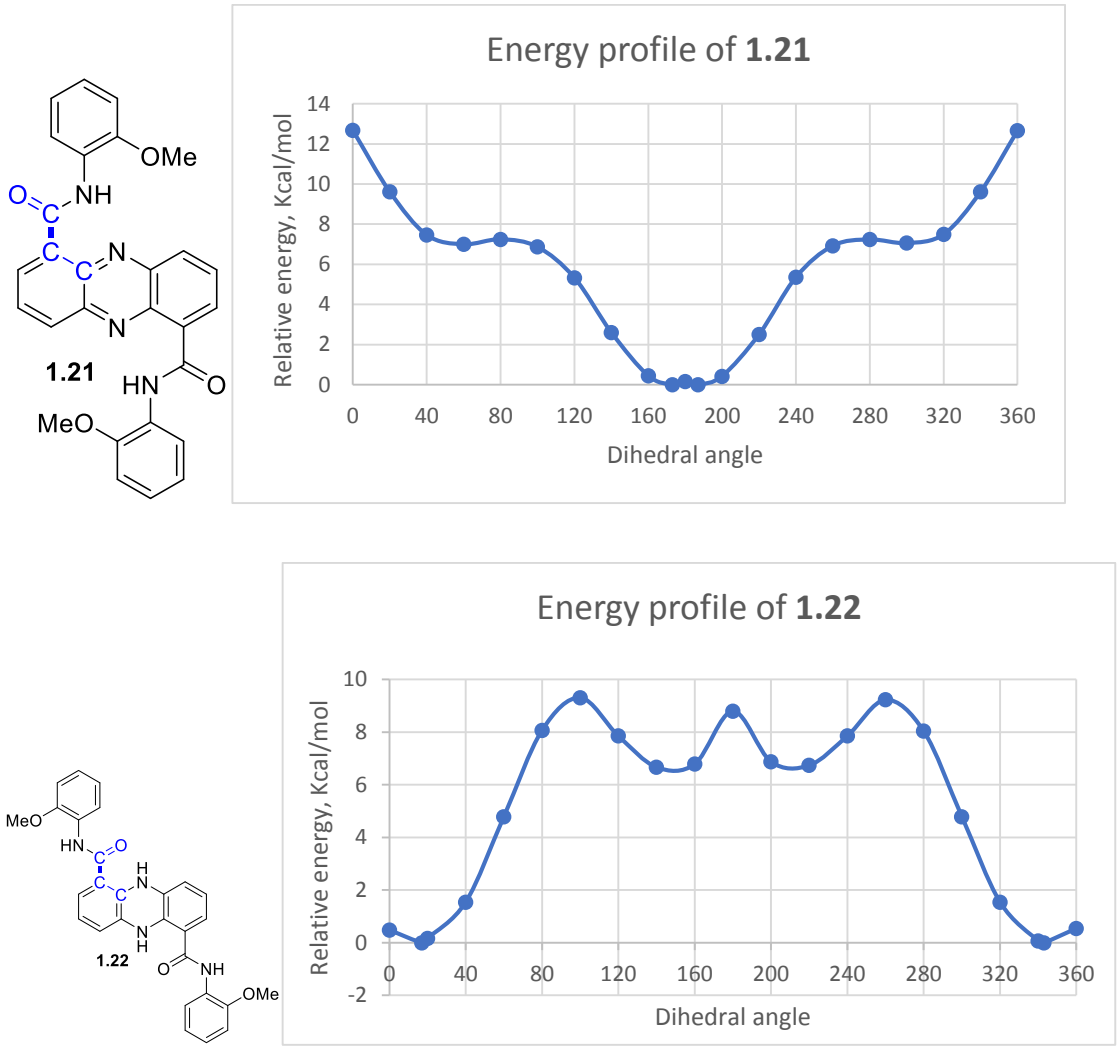

Figure 1-15. Energy profiles of simple models **1.21** and **1.22.**

1.3.5. 1D NMR spectra

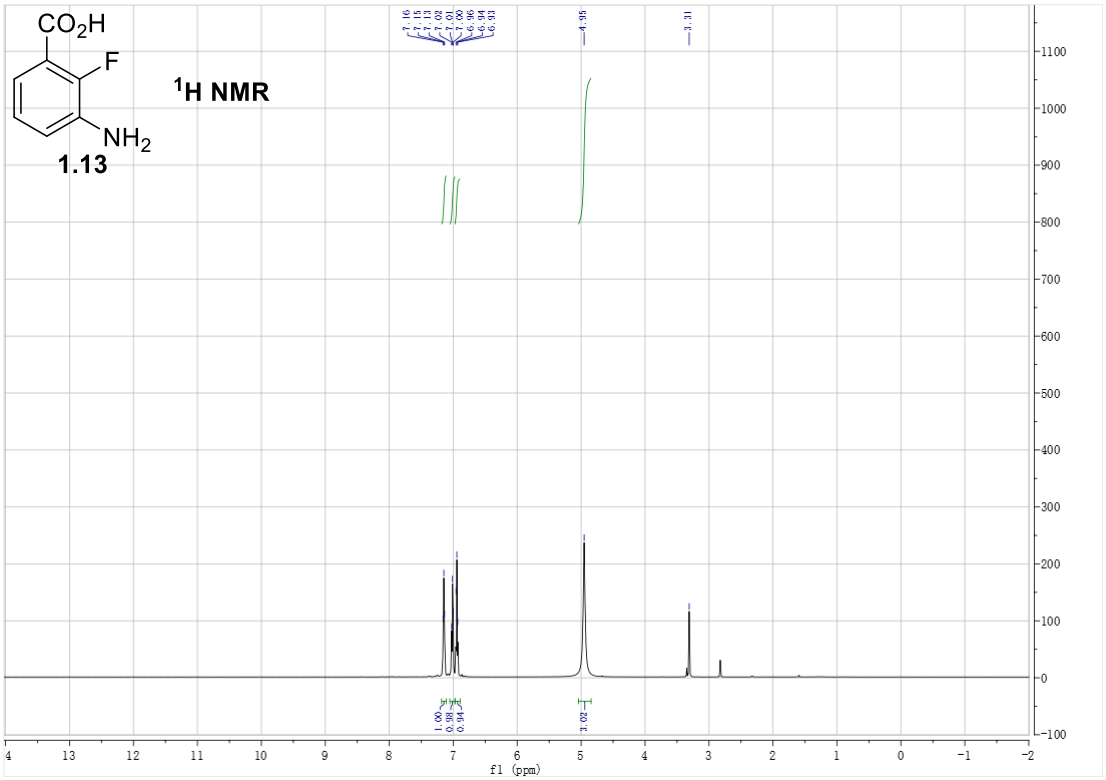

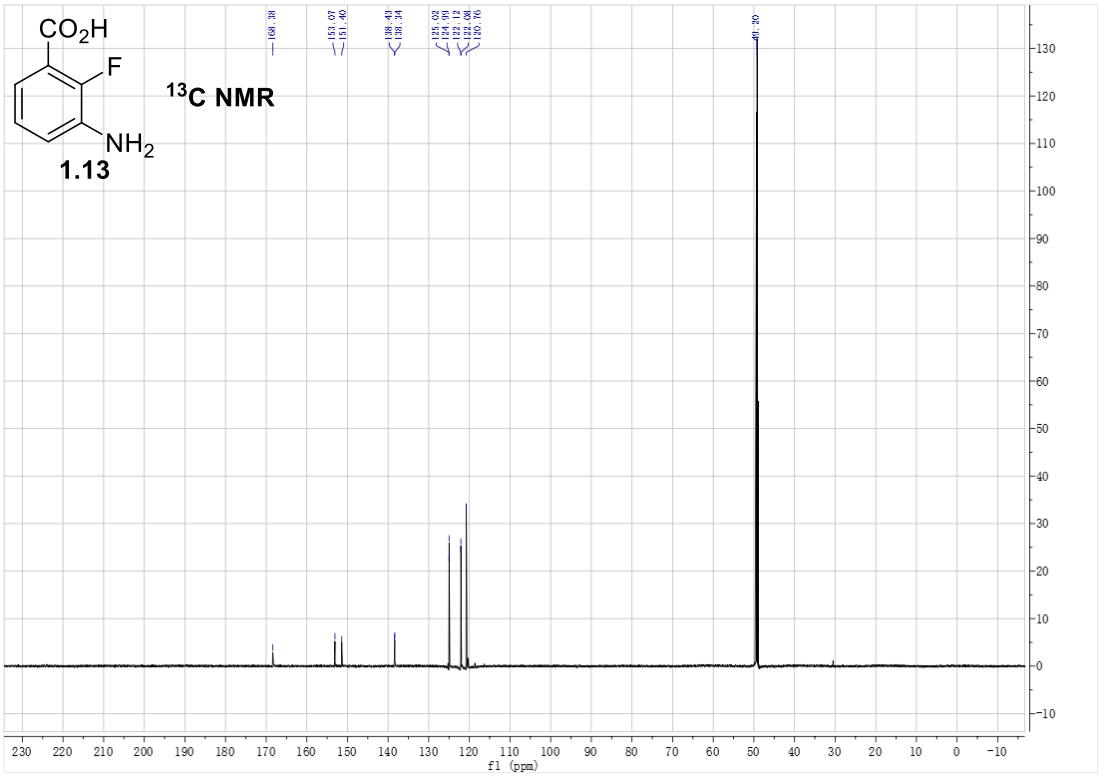

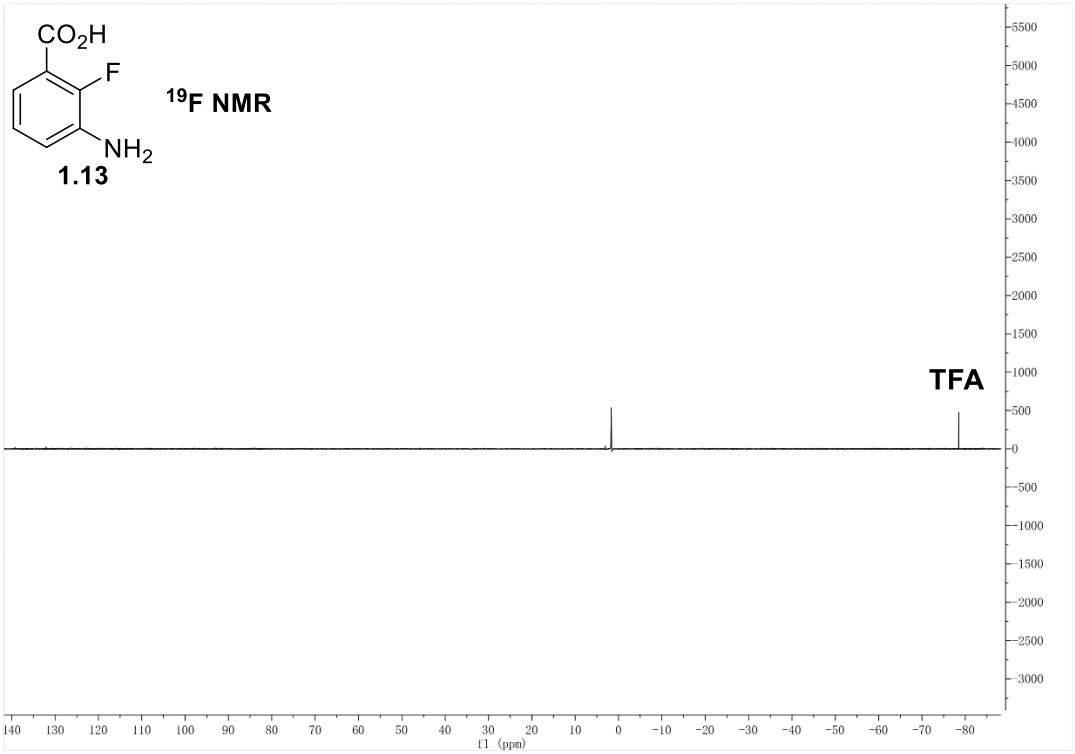
CO2H
F
NH2
1.13
19F NMR
TFA
f1 (ppm)

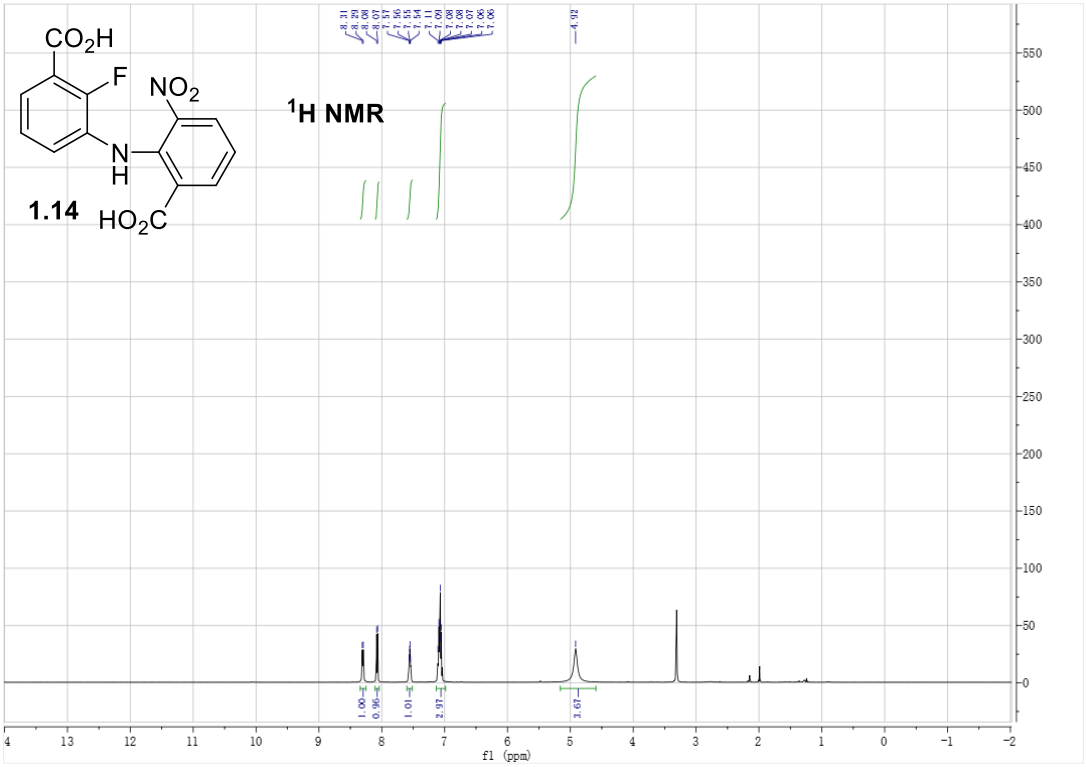
CO2H
F
NO2
N
H
HO2C
1.14
1H NMR
f1 (ppm)

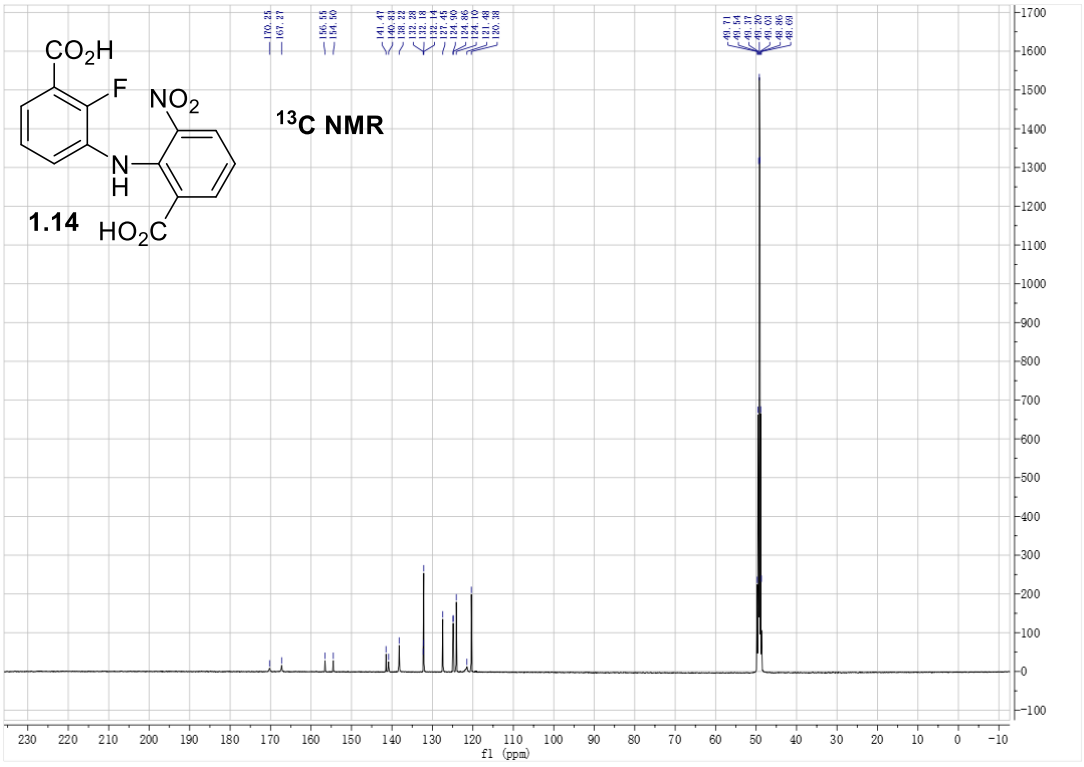
CO2H
F
NO2
N
H
HO2C
1.14
13C NMR
f1 (ppm)

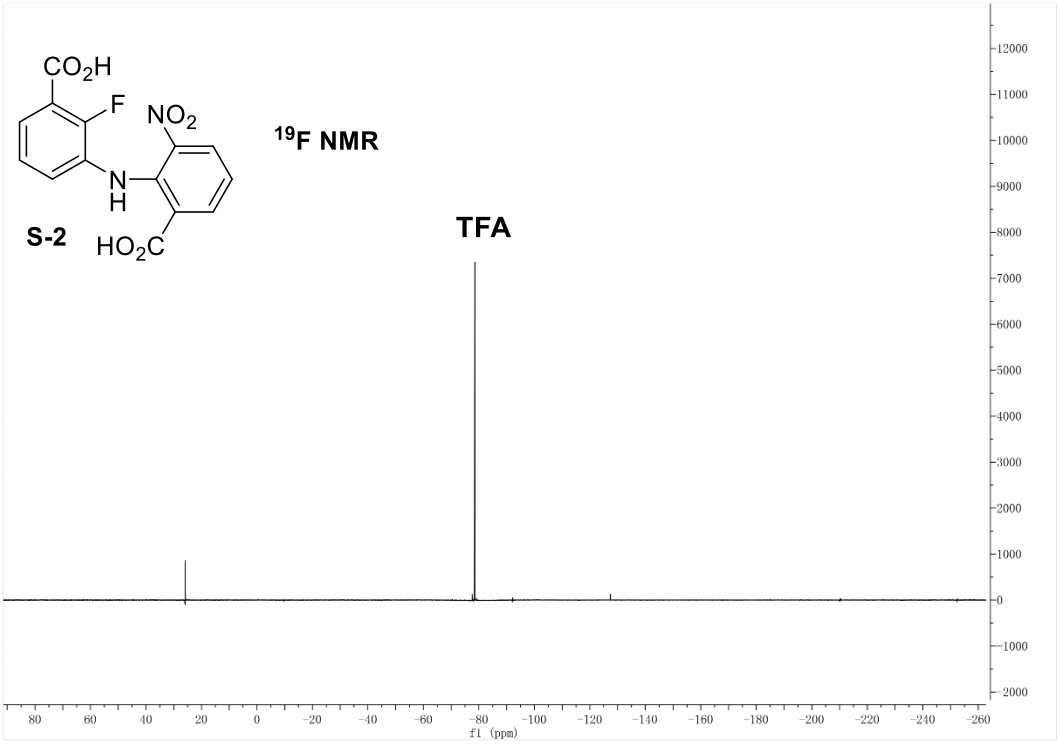
CO2H
F
NO2
N
H
HO2C
S-2
19F NMR
TFA
f1 (ppm)

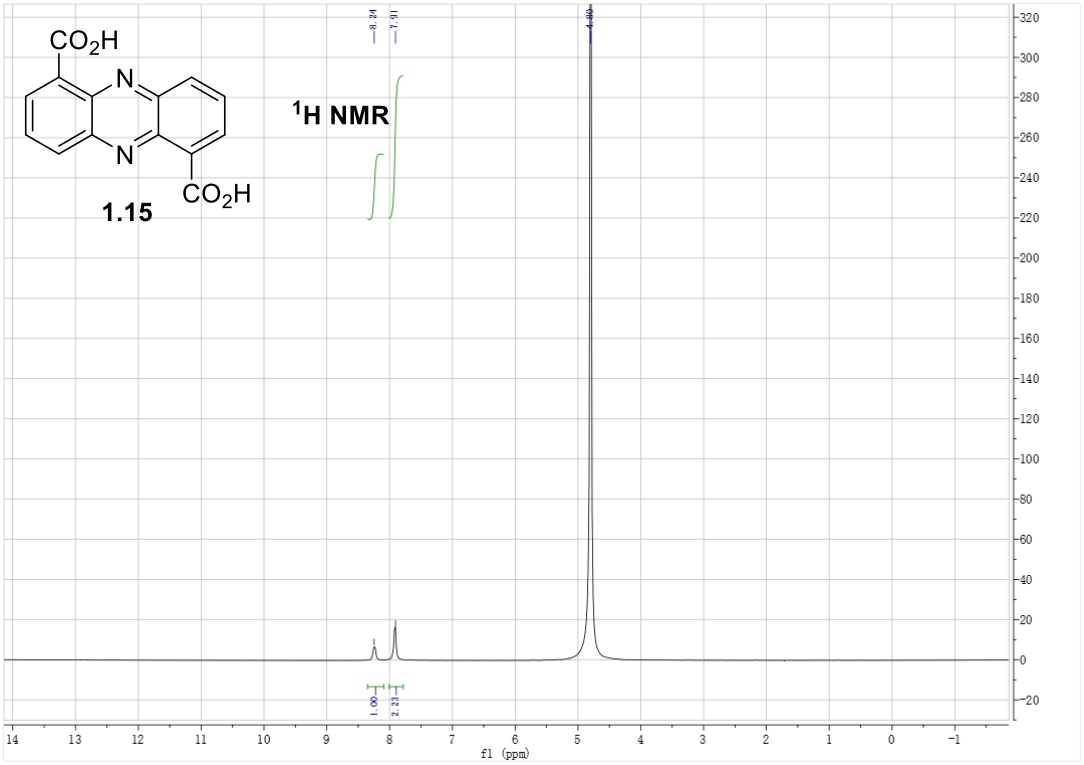
CO2H
N
N
CO2H
1.15
1H NMR
8.24
7.91
4.90
1.00
2.23
f1 (ppm)

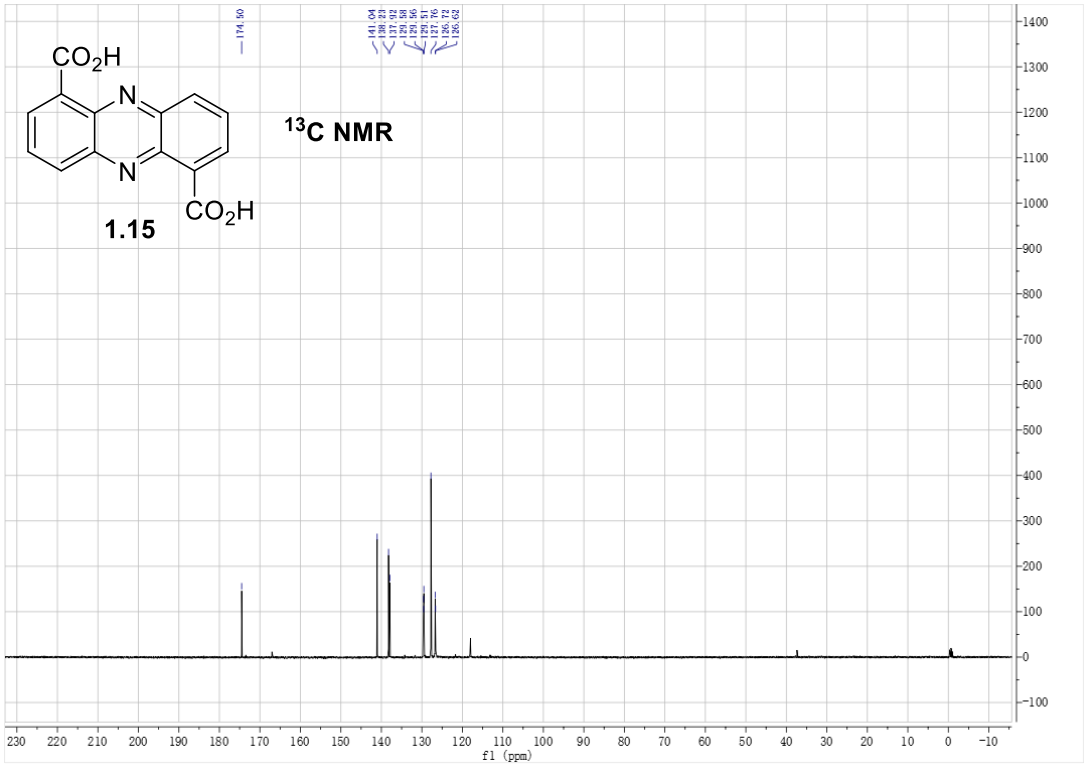
CO2H
N
N
CO2H
1.15
13C NMR
174.50
141.04
130.23
129.58
129.56
129.51
123.76
f1 (ppm)

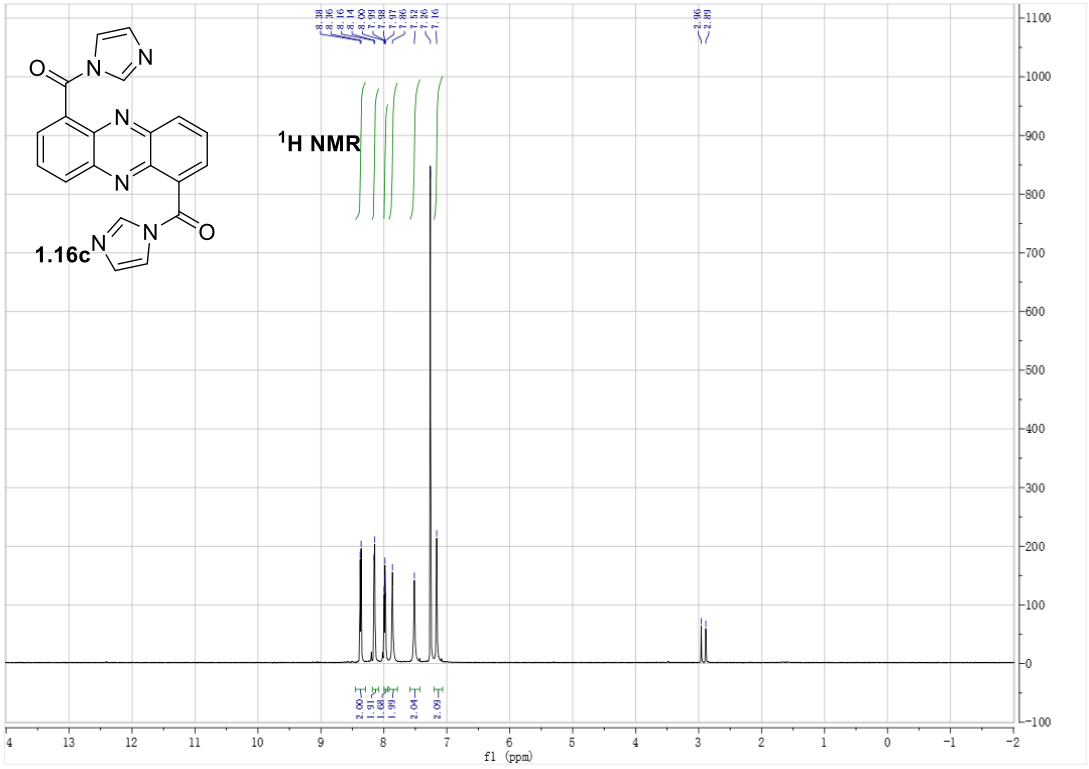
1.16c
^{1}H NMR
f1 (ppm)

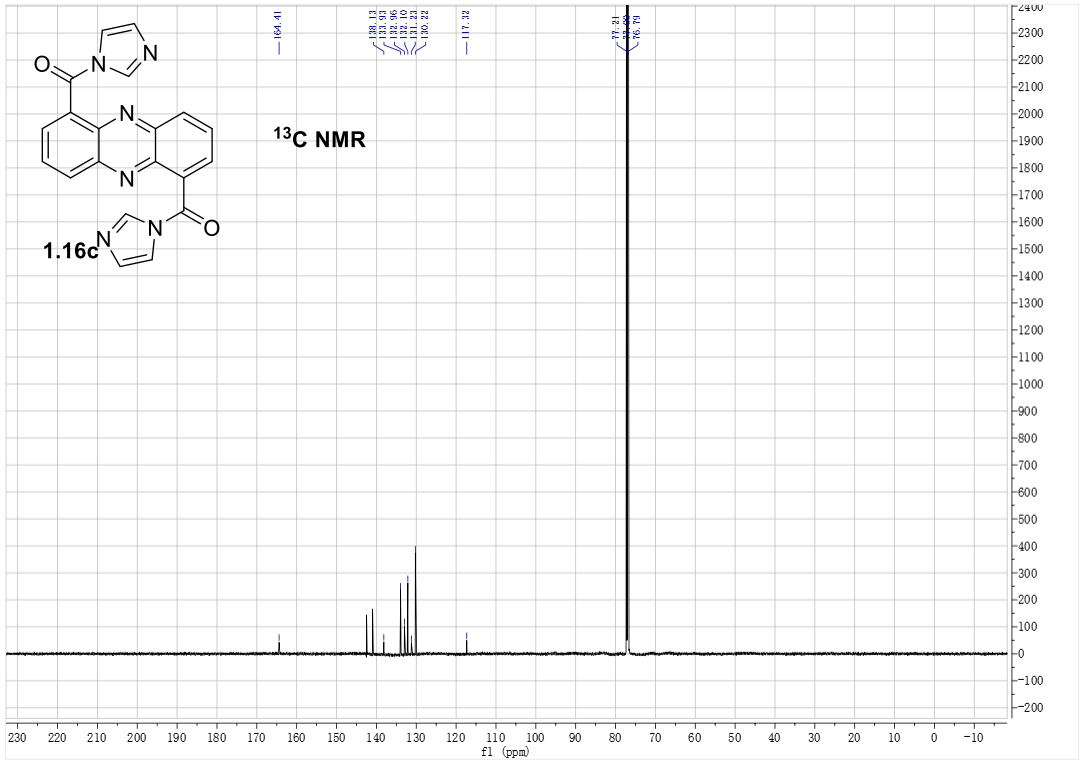
1.16c
^{13}C NMR
f1 (ppm)

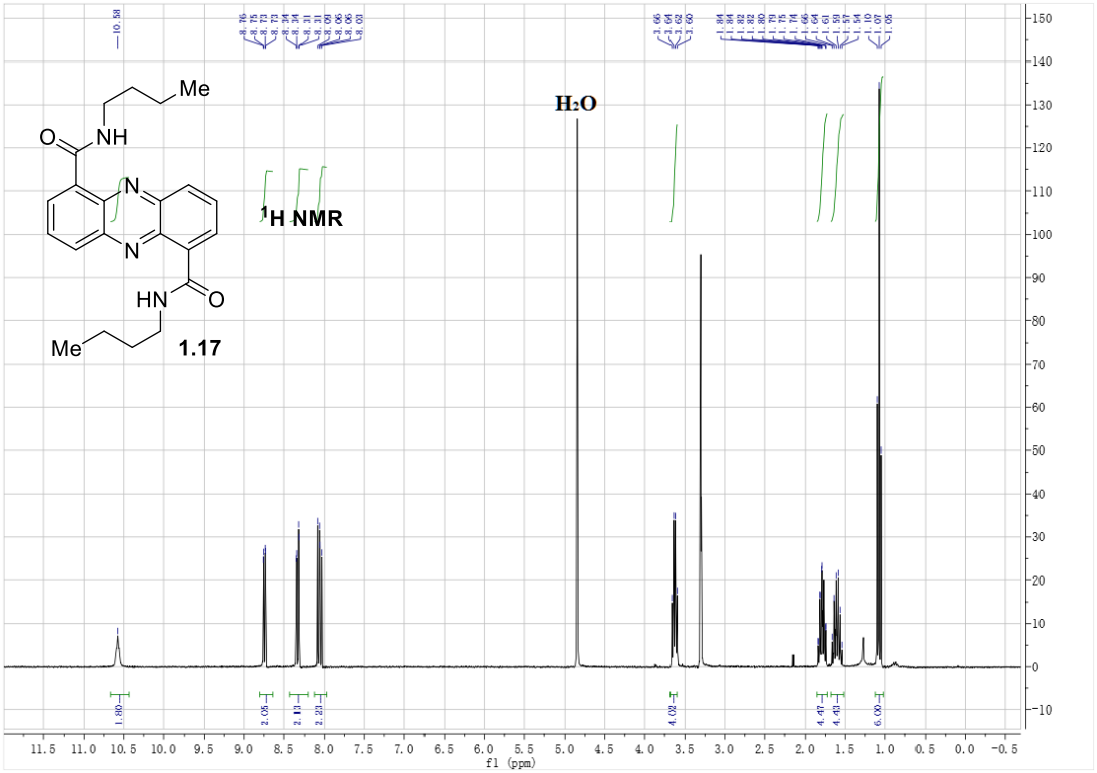
Me
O
NH
N
N
HN
O
Me
1.17
^{1}H NMR
H$_2$O
f1 (ppm)

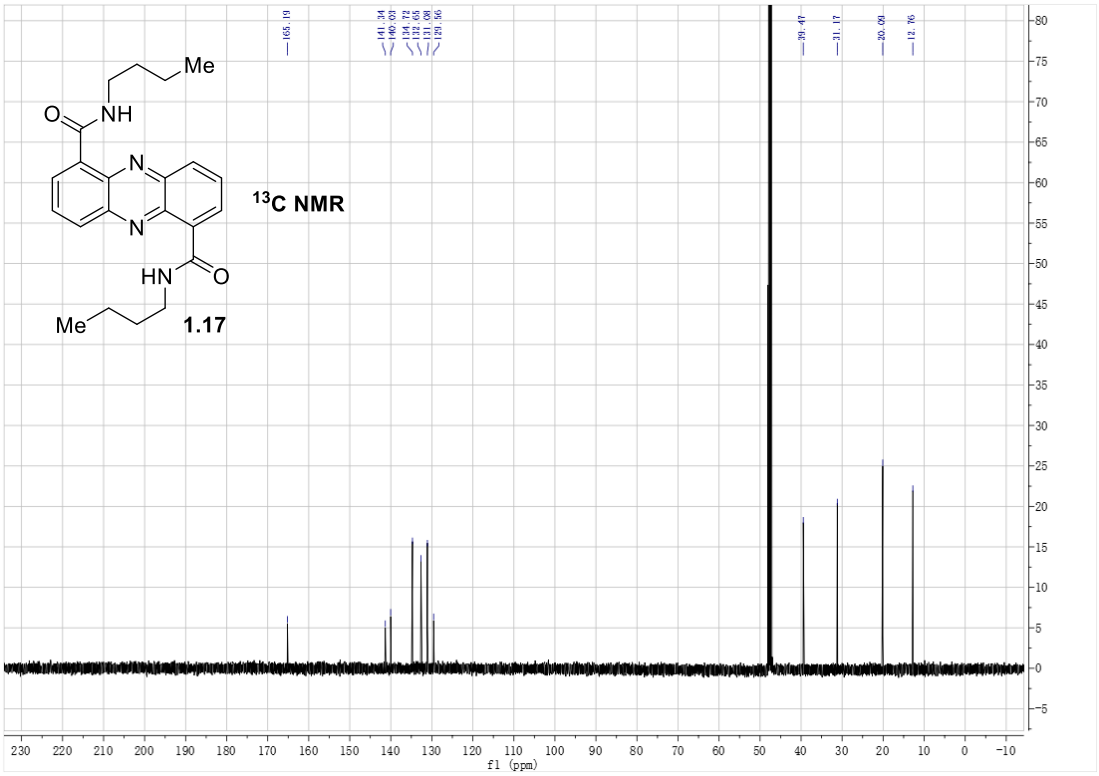
Me
O
NH
N
N
HN
O
Me
1.17
^{13}C NMR
f1 (ppm)

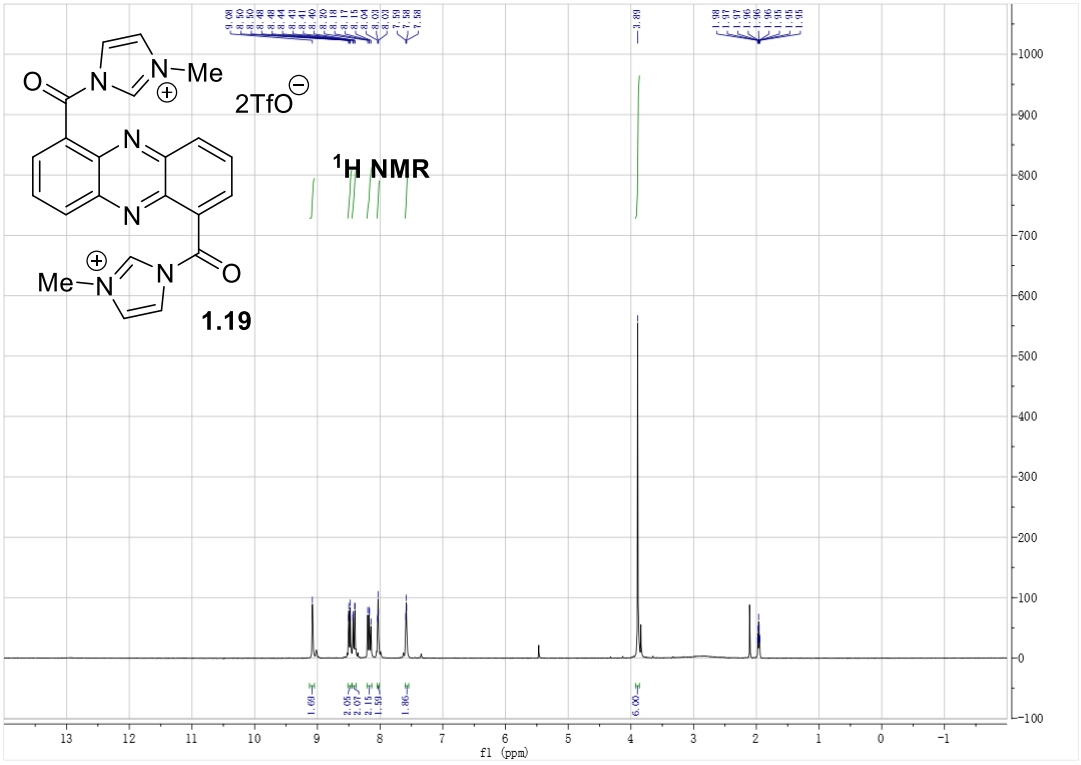
2TfO
1H NMR
1.19
f1 (ppm)

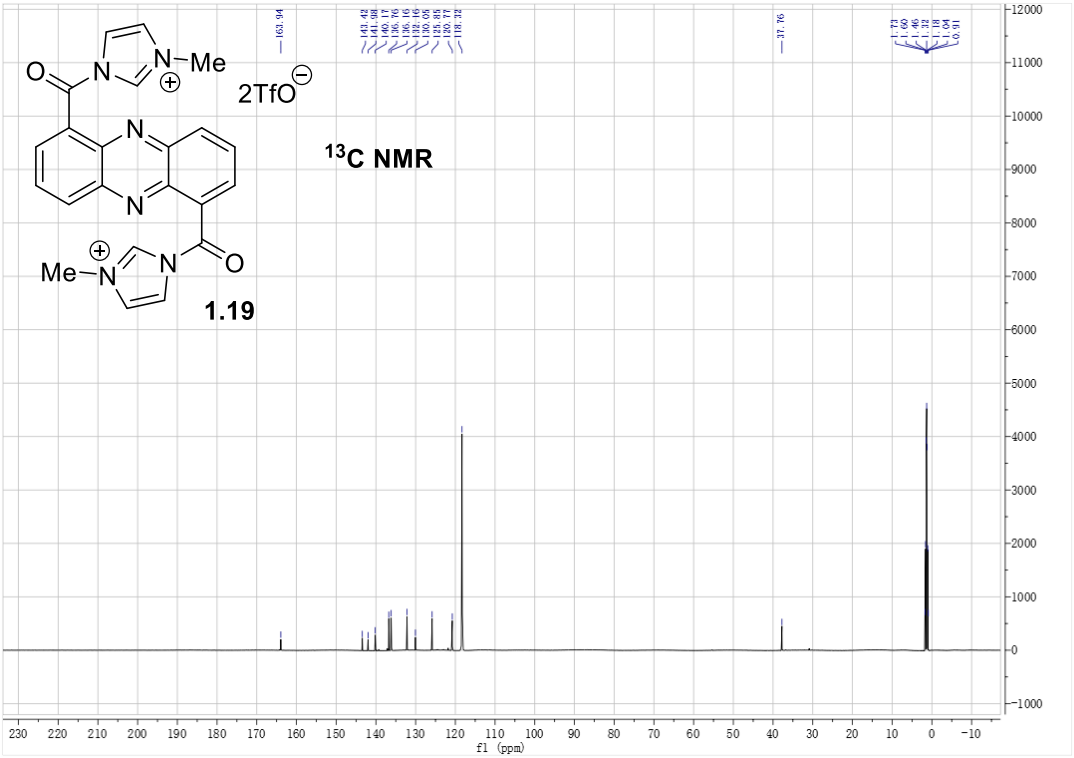
2TfO
13C NMR
1.19
f1 (ppm)

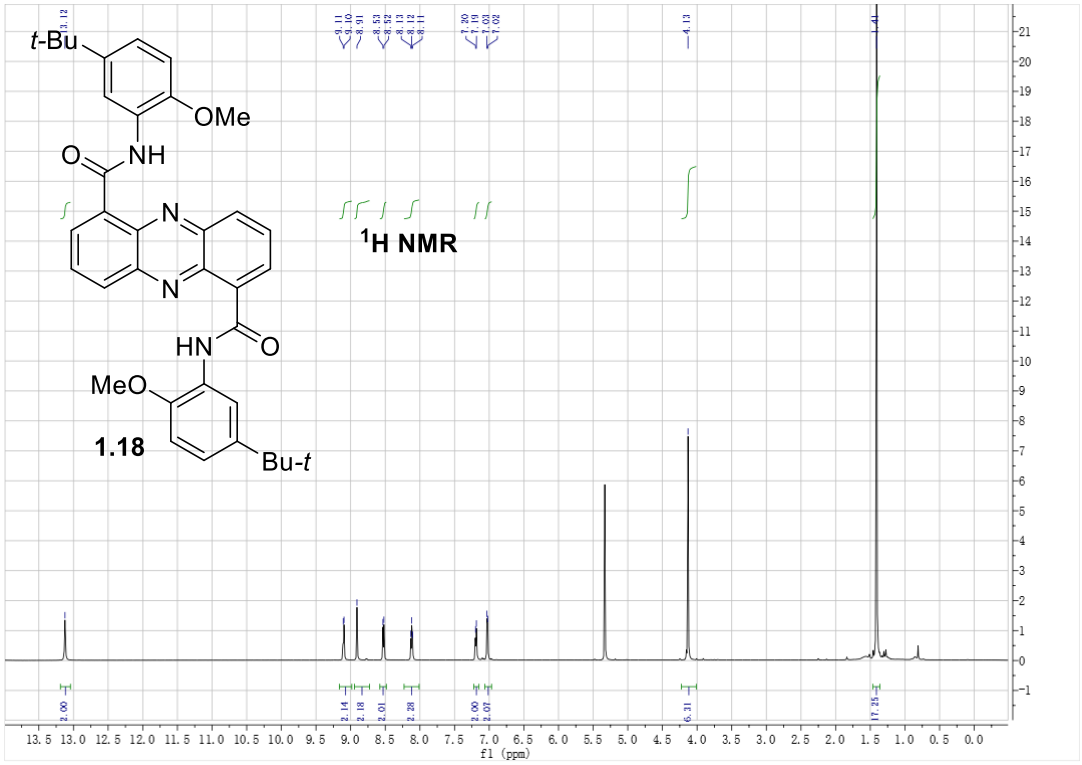
t-Bu
OMe
O
NH
N
N
HN
O
MeO
1.18
Bu-t
1H NMR
f1 (ppm)

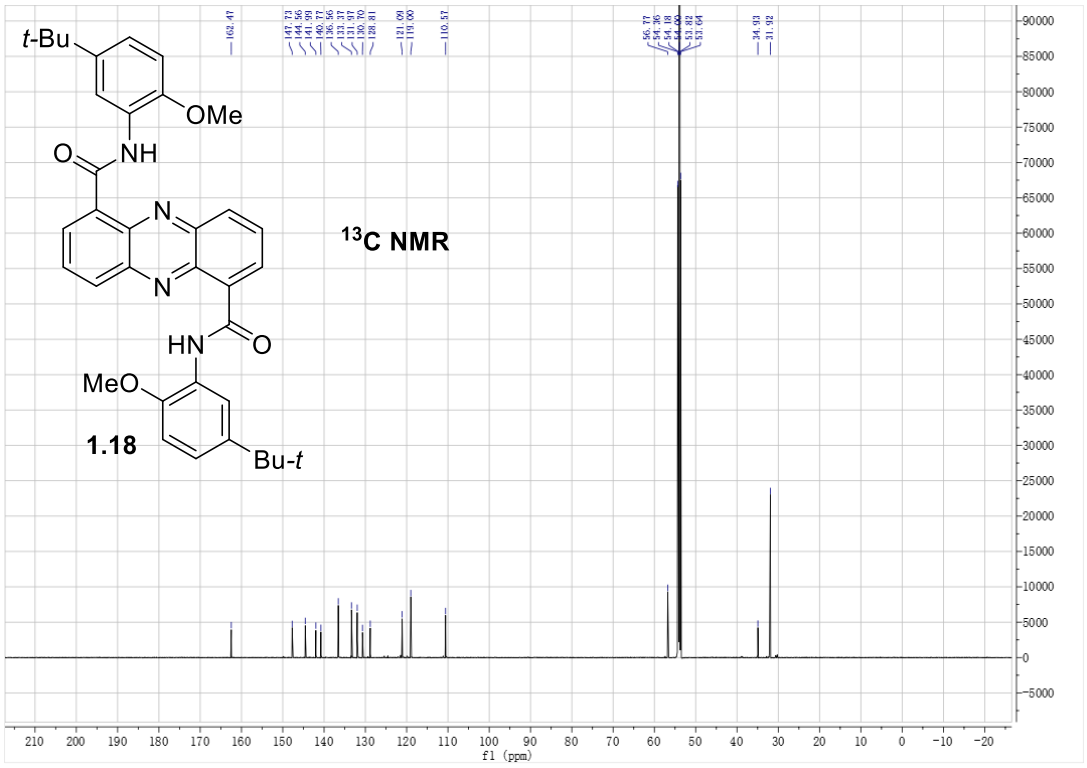
t-Bu
OMe
O
NH
N
N
HN
O
MeO
1.18
Bu-t
13C NMR
f1 (ppm)

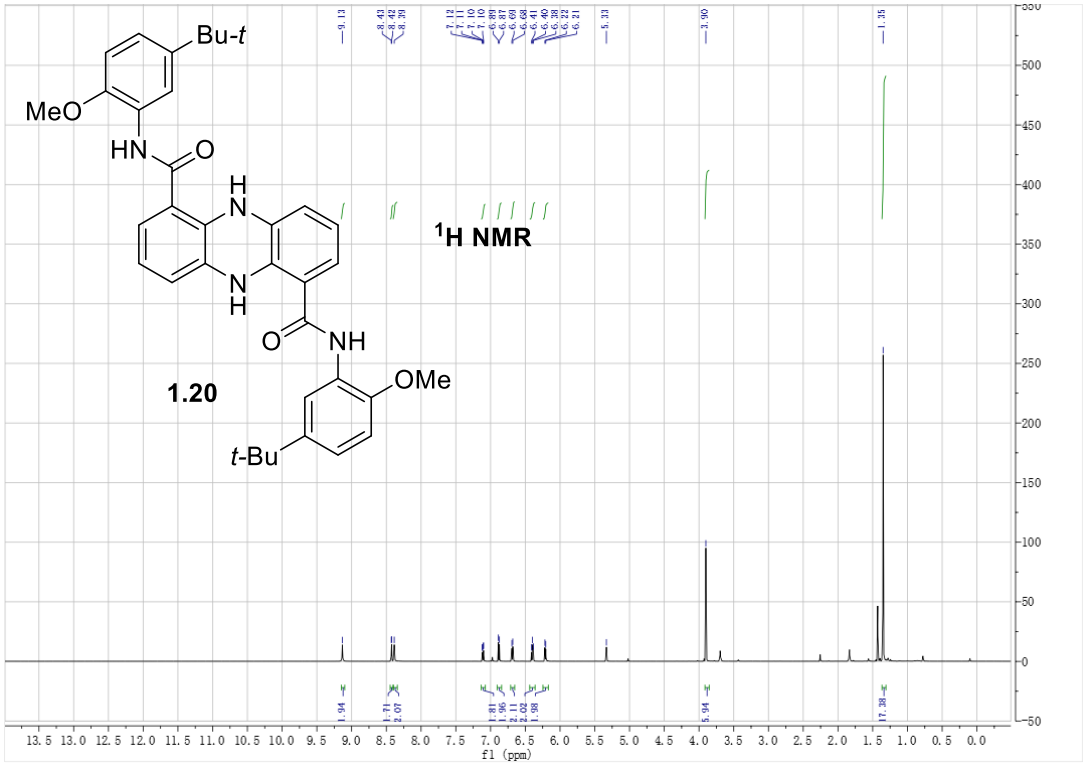
Bu-t
MeO
HN
O
H
N
N
H
O
NH
OMe
t-Bu
1.20
1H NMR
f1 (ppm)

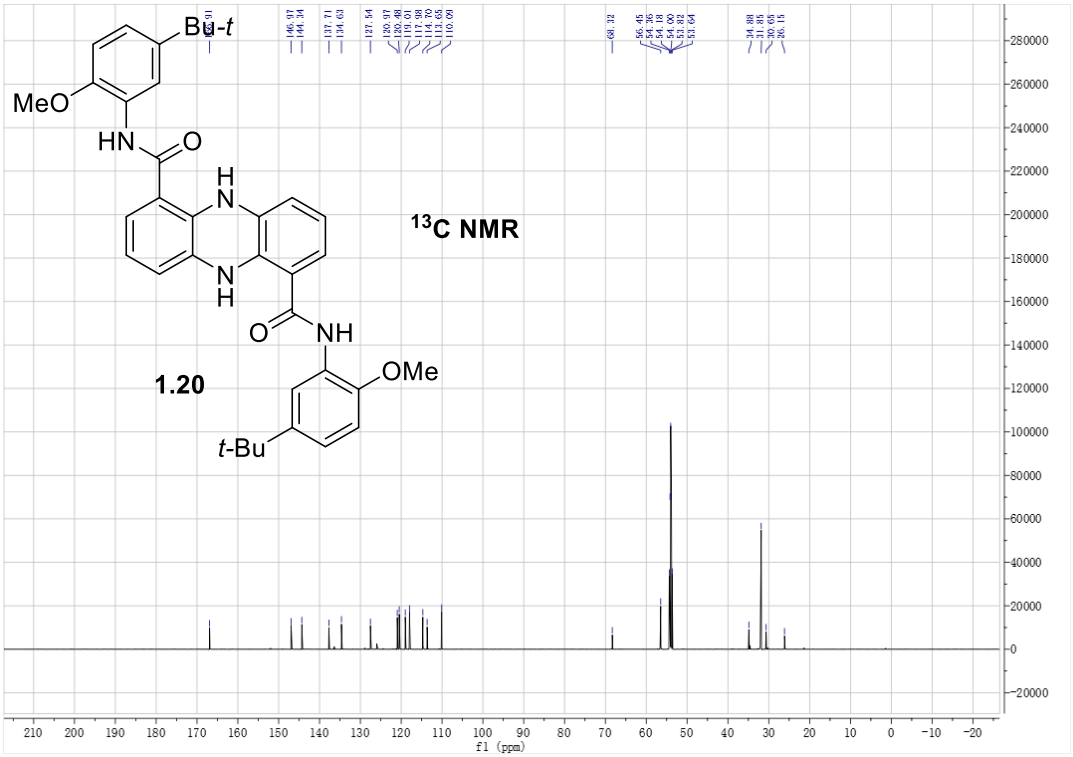
Bu-t
MeO
HN
O
H
N
N
H
O
NH
OMe
t-Bu
1.20
13C NMR
f1 (ppm)

1.3.6. 2D NMR Spectra.

NOESY Spectrum of **1.18**:

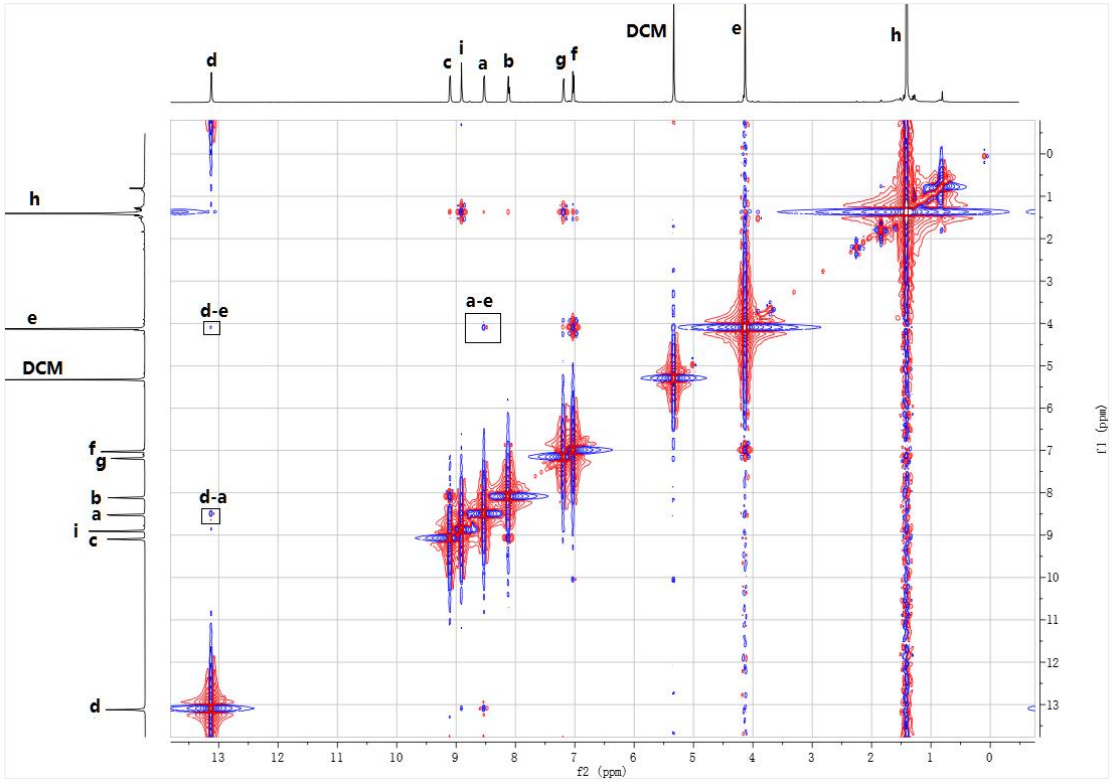

NOESY Spectrum of **1.20**

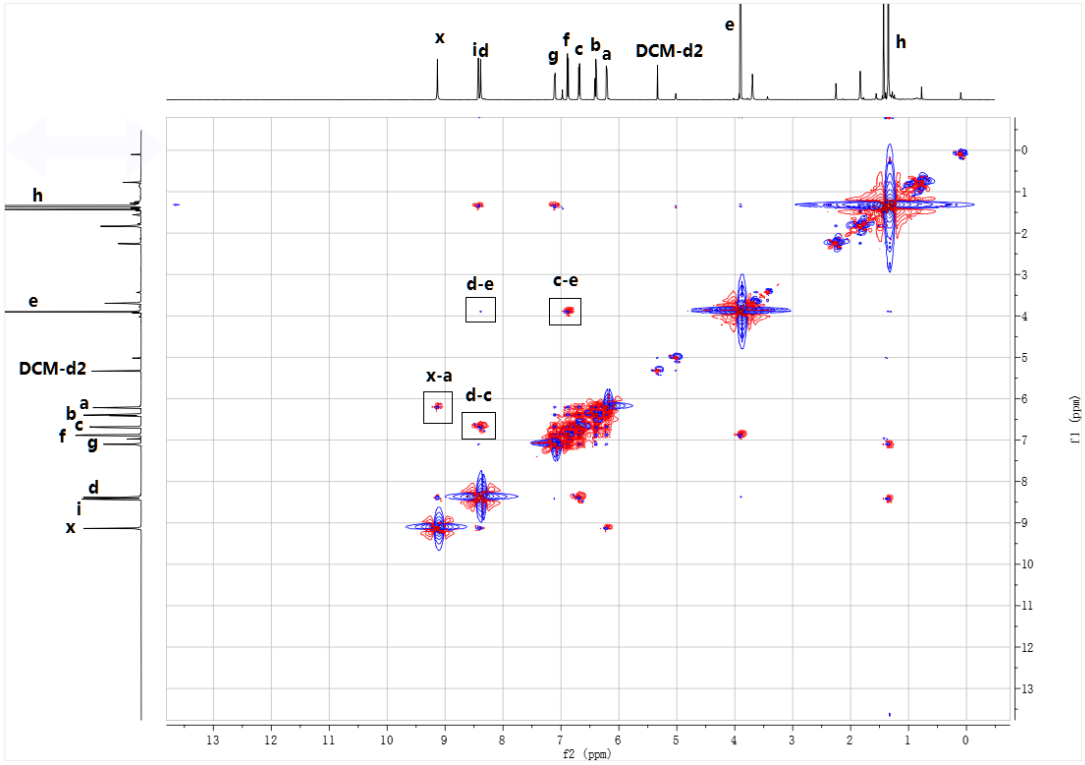

1.4. References

1. Molecular Machines & Motors (Structure and Bonding) J.-P. Sauvage Ed. ISBN 3-540-41382-0

2. (a) Khan, A.; Kaiser, C.; Hecht, S., Prototype of a Photoswitchable Foldamer. *Angew. Chem. Int. Ed.* **2006**, *45*, 1878-1881. (b) Bléger, D.; Hecht, S., Visible-Light-Activated Molecular Switches. *Angew. Chem., Int. Ed.* **2015**, *54*, 11338-11349. (c) Bandara, H. M. D.; Burdette, S. C. Photoisomerization in Different Classes of Azobenzene. *Chem. Soc. Rev.* **2012**, *41*, 1809-1825. (d) Irie, M., Diarylethenes for Memories and Switches. *Chem. Rev.* **2000**, *100*, 1685-1716. (e) van Dijken, D. J.; Kovaříček, P.; Ihrig, S. P.; Hecht, S., Acylhydrazones as Widely Tunable Photoswitches. *J. Am. Chem. Soc.* **2015**, *137*, 47, 14982-14991. (f) Tatum, L. A.; Su, X.; Aprahamian, I., Simple Hydrazone Building Blocks for Complicated Functional Materials. *Acc. Chem. Res.* **2014**, *47*, 2141-2149. (g) Su, X.; Aprahamian, I., Hydrazone-based switches, metallo-assemblies and sensors. *Chem. Soc. Rev.* **2014**, *43*, 1963-1981.

3. Dolain, C.; Maurizot, V.; Huc, I., Protonation-induced transition between two distinct helical conformations of a synthetic oligomer via a linear intermediate. *Angew. Chem., Int. Ed.* **2003**, *42*, 2738-2740.

4. Knipe, P. C.; Thompson, S.; Hamilton, A. D., Ion-mediated con-formational switches. *Chem. Sci*. **2015**, *6*, 1630-1639.

5. Ghosh, S.; Ramakrishnan, S., Small-molecule-induced folding of a synthetic polymer. *Angew. Chem., Int. Ed.* **2005**, *44*, 5441-5447. /For a review of approaches to controlling foldamer conformation, see: Barboiu, M.; Stadler, A.-M.; Lehn, J.-M., Controlled Folding, Motional, and

Constitutional Dynamic Processes of Polyheterocyclic Molecular Strands. *Angew. Chem., Int. Ed.* **2016**, *55*, 4130-4154.

6 (a) Zhang, J-L., Zhong, J-Q., Lin, J-D., Hu, W-P., Wu, K. Qin, Xu, G. Q., Weeb, A. T. S., Chen W. Towards single molecule switches. *Chem. Soc. Rev.*, **2015**, *44*, 2998-3022. (b) Dattler, D., Fuks, G., Heiser, J., Moulin, E., Perrot, A., Yao, X-Y., Giuseppone, N. Design of Collective Motions from Synthetic Molecular Switches, Rotors, and Motors. *Chem. Rev.* **2020**, *120*, 310-433.

7. N. Koumura, R. W. J. Zijlstra, R. A. van Delden, N. Harada and B. L. Feringa, Light-driven monodirectional molecular rotor. *Nature*, **1999**, *401*, 152-155.

8. Khan, A.; Kaiser, C.; Hecht, S., Prototype of a Photoswitchable Foldamer. *Angew. Chem. Int. Ed.* **2006**, *45*, 1878-1881.

9. Dolain, C.; Maurizot, V.; Huc, I., Protonation-induced transition between two distinct helical conformations of a synthetic oligomer via a linear intermediate. *Angew. Chem., Int. Ed.* **2003**, *42*, 2738-2740.

10. G. Haberhauer, Control of planar chirality: the construction of a copper‐ion‐controlled chiral molecular hinge. *Angew. Chem., Int. Ed.*, **2008**, *47*, 3635-3638.

11. F. Durola and J. Rebek, The Ouroborand: A Cavitand with a Coordination‐Driven Switching Device. *Angew. Chem., Int. Ed.*, **2010**, *49*, 3189-3191.

12. Plato, Timaeus, 360BC.

13. T.-Z. Xie, C. Guo, S.-Y. Yu and Y.-J. Pan, *Angew. Chem., Int. Ed.*, **2012**, *51*, 1177-1181.

14. Ghosh, S.; Ramakrishnan, S., Small-molecule-induced folding of a synthetic polymer. *Angew. Chem., Int. Ed.* **2005**, *44*, 5441-5447.

15. (a) Chen, Y., Huang, L., Chen, H., Chen, Z., Zhang, H., Xiao, Z. and Hong, W., Towards Responsive Single-Molecule Device. *Chin. J. Chem.*, **2021**, *39*, 421-439. (b) Ohtake, T.; Tanaka,

H.; Matsumoto, T.; Kimura, M.; Ohta, A., Redox-Driven Molecular Switches Consisting of Bis(benzodithiolyl)bithienyl Scaffold and Mesogenic Moieties: Synthesis and Complexes with Liquid Crystalline Polymer. *J. Org. Chem.* **2014,** *79*, 6590-6602. (c) Marsella, M. J.; Reid, R. J.; Estassi, S.; Wang, L.-S., Tetra[2,3-thienylene]: A Building Block for Single-Molecule Electromechanical Actuators. *J. Am. Chem. Soc.* **2002,** *124*, 12507-12510.

16. X, Zhu; M, Zhang; L, Yu; Z-H, Xu; D, Yang; X-Y, Du; Q, Wu; J, Li. *Natural Product Research.* **2019**, *33*, 17, 2453-2460.

17. Heller, S. T.; Sarpong, R. On the reactivity of imidazole carbamates and ureas and their use as esterification and amidation reagents. *Tetrahedron.* **2011**, *67*, 8851-8859.

18. Saha, A. K., Rapoport, H., Schultz, P. 1,1'-Carbonylbis(3-methylimidazolium) triflate: an efficient reagent for aminoacylations. *J. Am. Chem. Soc.*, **1989**, *111*, 13. 4856-4859.

19. Ferrins, L.; Rahmani, R.; Sykes, M. L.; Jones, A. J.; Avery, V. M.; Teston, E.; Almohaywi, B.; Yin, J. X.; Smith, J.; Hyland, C.; White, K. L.; Ryan, E.; Campbell, M.; Charman, S. A.; Kaiser, M.; Baell, J. B., 3-(Oxazolo[4,5-b]pyridin-2-yl)anilides as a novel class of potent inhibitors for the kinetoplastid Trypanosoma brucei, the causative agent for human African trypanosomiasis. *Eur. J. Med. Chem.* **2013**, *66*, 450-465.

20. (a) Rewcastle, G. W.; Denny, W. A., Unequivocal Synthesis of Phenazine-1-Carboxylic Acids: Selective Displacement of Fluorine During Alkaline Borohydride Reduction of N-(2-Fluorophenyl)-3-Nitroanthranilic Acids. *Synth. Commun.* **1987**, *17*, 1171-1179. (b) For an alternate synthetic route, see: Clark, T. W.; Sperry, J., Biomimetic synthesis of phenazine-1,6-dicarboxylic acid (PDC). *Synlett* **2012**, *23*, 2827-2829.

Chapter 2: Phenazine-based foldamers as redox responsive molecular muscles

2.1 Introduction to aromatic foldamers

Folded geometry has been observed in many biologically important molecules, such as DNA, RNA, and proteins.[1] Those folding patterns are pivotal for their functions. Moore used the term foldamer to describe any oligomer that folds into conformationally compact geometry in solution via noncovalent interactions between nonadjacent units.[2] For years, many examples of artificial foldmers have been described that mimic the structure and function of natural conformationally compact molecules.[3]

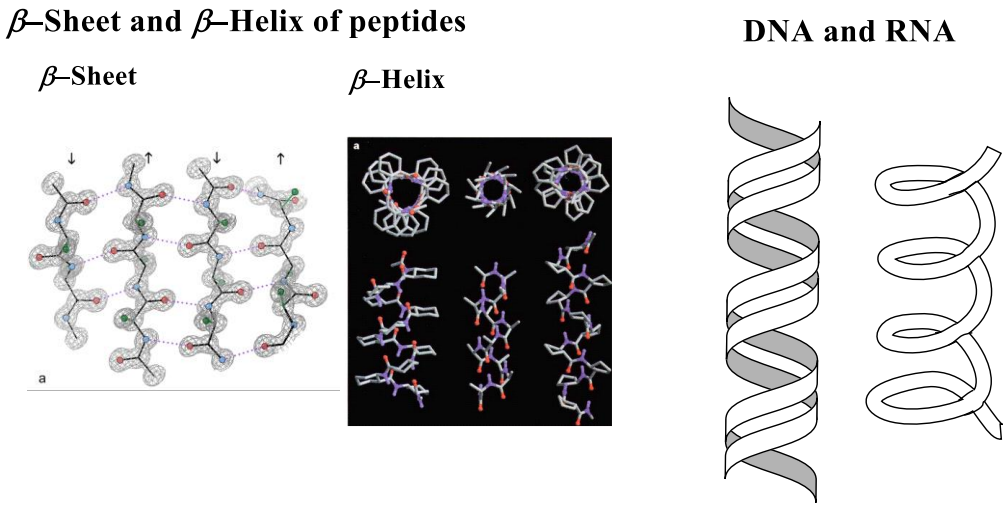

Figure 2-1. Examples of naturally occurring foldamers. Reprinted with permission from Ref. 1 (b). Copyright 1997 Springer Nature.

Aromatic foldamers is one of the most studied classes of foldamers, which are stabilized by π-π interactions and in most cases, intramolecular hydrogen bonding as well.[4] The first example

of an aromatic foldamer was reported in 1994, by Hamilton *et al.*[5] The folded geometry, validated by X-Ray structure, was held by N—H ···N(Py) hydrogen bonding (Figure 2-2). Since then, many aromatic foldamers have been synthesized. In 1999, Moore *et al.* reported a series of oligo(m-phenylene ethynylene)s based foldamers which are stabilized via π-π stacking.[6] The conformation of these foldamers may vary by solvents. In chloroform, oligomers tend to wrap around single-walled carbon nanotubes (SWCNTs), while in acetonitrile they form individual foldamers, releasing SWCNTs (Figure 2-3).[7]

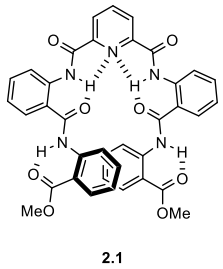

2.1

Figure 2-2. First aromatic foldamer by Hamilton group.

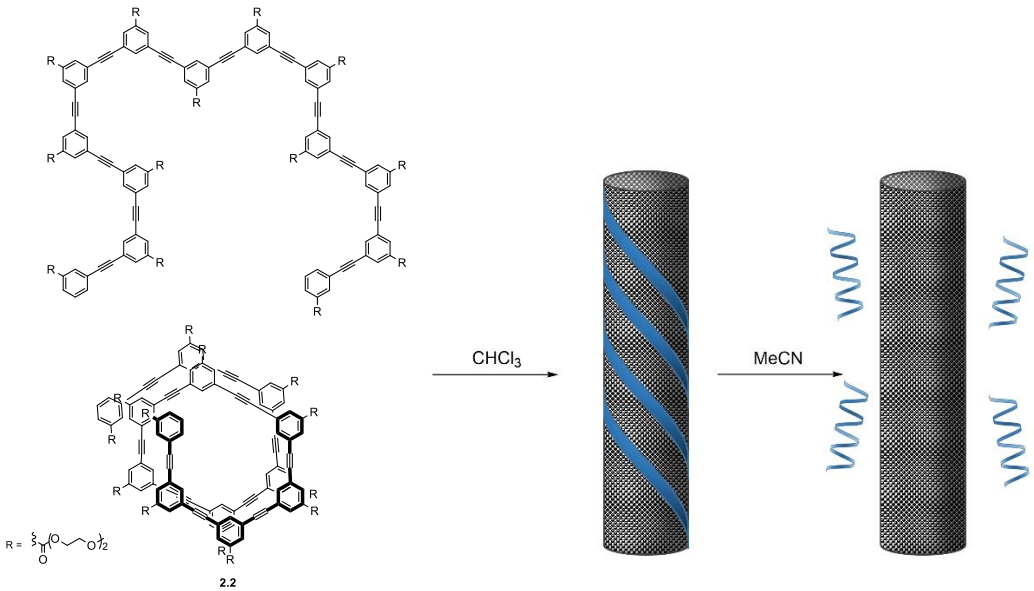

2.2

Figure 2-3. Oligo(m-phenylene ethynylene)s based foldamer. Remade with permission from Ref. 7. Copyright 2010 American Chemical Society.

Huc and Lehn *et al.*[8] constructed oligopyridine-dicarboxamides that folds into single helices in solution. The dimerization via hydrogen bonding between peripheral diamino-pyridine units of each strands opens the possibility for supramolecular double helices (Figure 2-4).

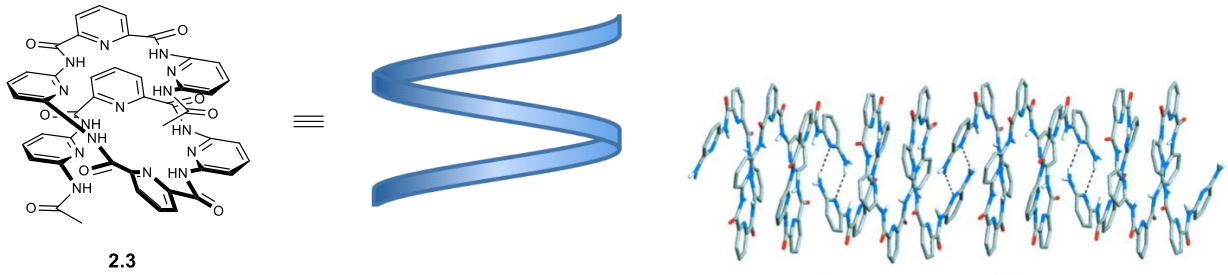

Figure 2-4. Oligopyridine-dicarboxamides based foldamers. Reprinted with permission from Ref. 8. Copyright 2001 John Wiley and Sons.

Huc *et al.*[9] also did extensive studies on quinoline based delta-peptide foldamers. Series of hydrogen bonding and π-π interactions provides great stability to **2.4**, as inversion of its chiral conformation is slow even in DMSO up to 120 ℃ (Figure 2-5). In 2016, 48-mer of this design was synthesized with a length ca. 7 nm.[10] There are extensive studies on this class of foldamers regarding their reactivity, [11] properties,[12] and applications.[13]

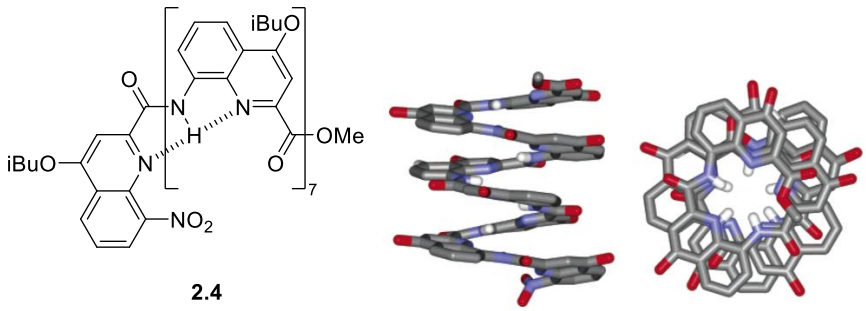

Figure 2-5. Quinoline based foldamers. Reprinted with permission from Ref. 9. Copyright 2003 American Chemical Society.

Li *et al.* [14] developed an aromatic hydrazide based foldamer. With a cavity of ca. 10.8 Å, **2.5** has the ability to host a saccharide molecule (Figure 2-6). Zeng *et al.* reported a pyridine based pentamer **2.6** that can self-assemble into a single helix with assistance of solvent.[15] It's very interesting that both helicities were observed when dichloromethane was trapped inside, while in the case of methanol, a single-handed helix forms via chiral crystallization without the use of chiral auxiliary or external stimuli (Figure 2-7).

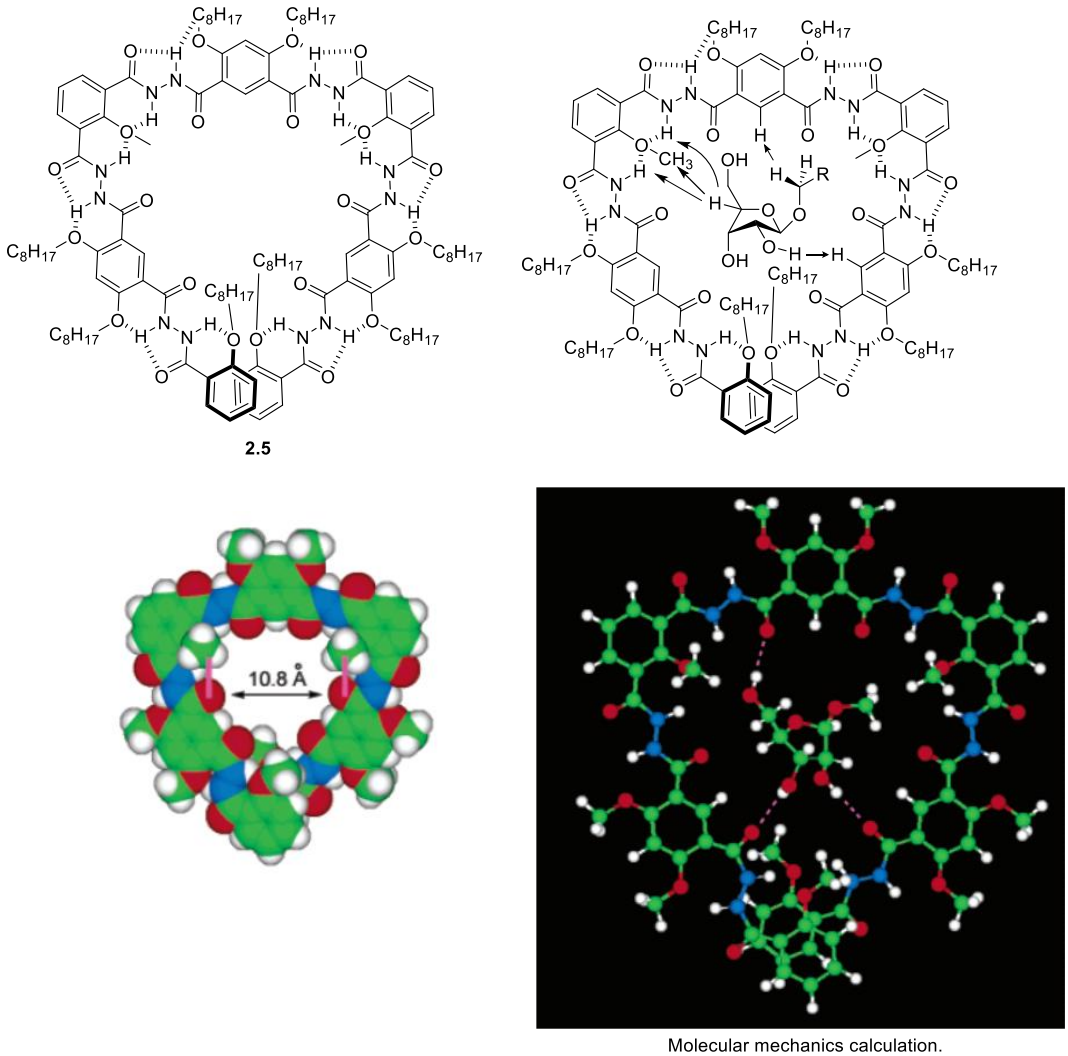

Figure 2-6. Aromatic hydrazide foldamer. Reprinted with permission from Ref. 14. Copyright 2004 American Chemical Society.

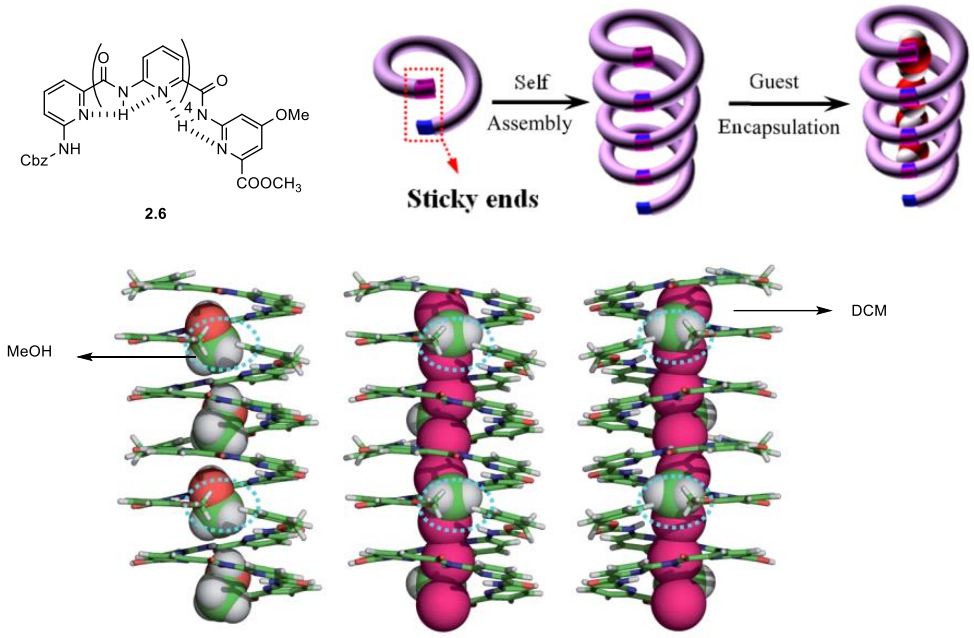

Figure 2-7. Chiral self-assembly of a pyridine-based foldamer by solvent. Reprinted with permission from Ref. 15. Copyright 2012 Royal Society of Chemistry.

2.2 Introduction to molecular muscles

Nature relies on muscle movements to transform chemical energy to mechanical energy. In modern society, this conversion is achieved via internal combustion engines that create rotational movements or, to a lesser extent, jet propulsion. These engines could be faster and stronger than muscles, but not as compact. That is why creation of artificial muscles able to mimic muscle movements under external stimuli is an important goal. Some examples of artificial muscle designs are listed here based off different types of stimulus.

Metal cations have been explored as stimulus for molecular muscles. Sauvage *et al.*[16] designed a rotaxane scaffold that can change length in response to different cations. The design relies on bidentate phenanthroline ligands and tridentate terpyridine ligands binding to metal

cations. Tetradentate cations, such as Cu^{2+}, can chelate to two phenanthroline ligands, giving an extended daisy chain **2.7-Cu^{2+}**. Pentadentate cations like Zn^{2+} tends to bind phenanthroline and terpyridine together, giving a contracted daisy chain **2.7-Zn^{2+}.** Both **2.7-Zn^{2+}** and **2.7-Cu^{2+}** can be demetallated by cyanides, making this process fully reversible (Figure 2-8).

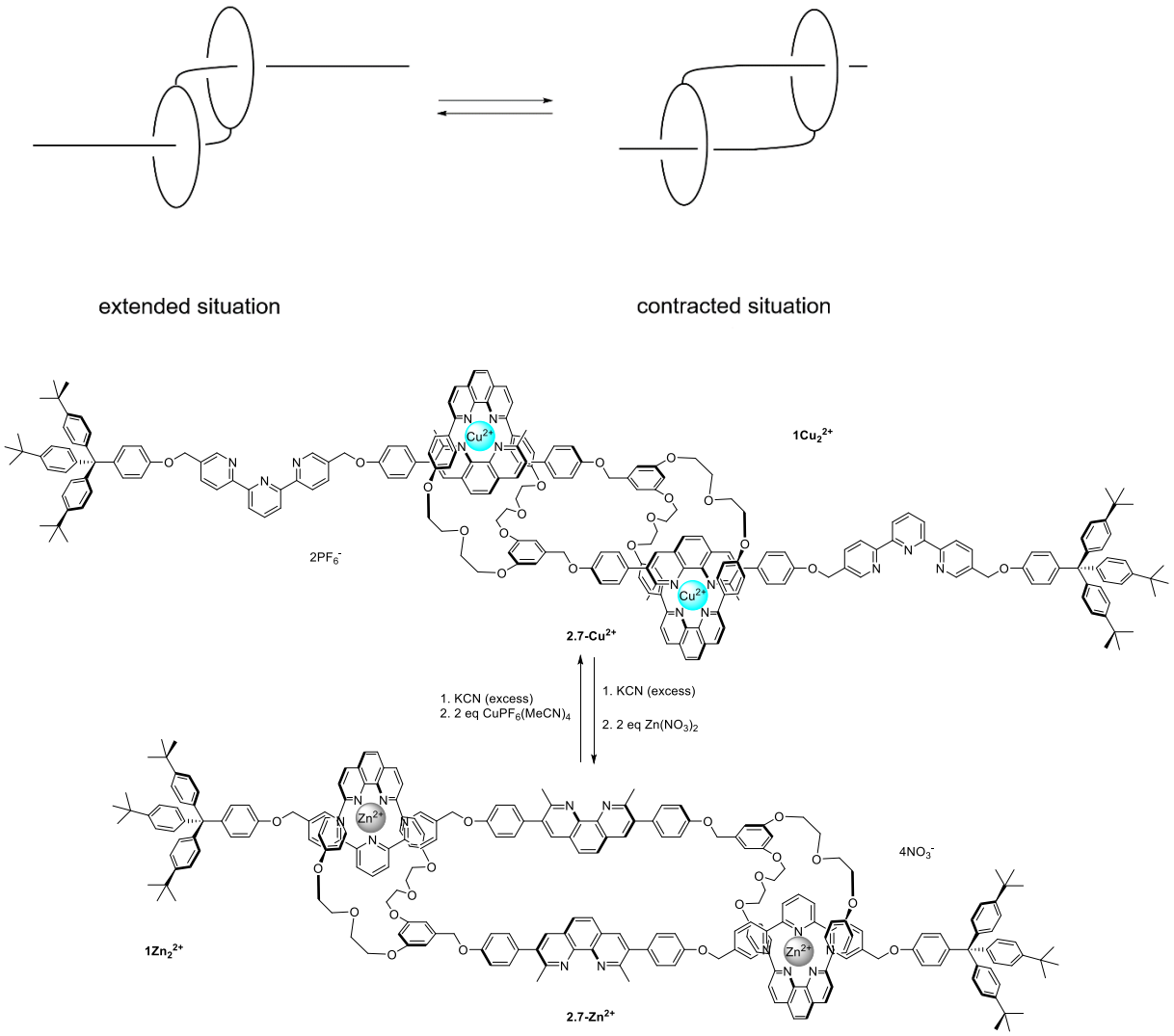

Figure 2-8. Sauvage's molecular muscle.

Lehn *et al.*[17] made a series of heterocyclic foldamers as a metal cation/pH mediated molecular muscles. Oligomers with pyridine and pyrimidine rings adopt folded structure due to

electronic repulsion from nitrogen atoms and π-π stackings. **2.8.3-H** and **2.8.5-H** give significant extension once chelated to Pb^{2+}, with almost 6-fold increase in length. With the assistance of cryptate complex **[Pb(II)-2.2.2]**, this folding and unfolding process become pH responsive. The addition of trifluoromethanesulfonic acid will release Pb^{2+} from cryptate, which will then be captured by the **2.8.3-H** or **2.8.5-H**. The demetallation of oligomers was triggered by deprotonation of [$2H^{+}$-2.2.2] with triethylamine. Completely folding was observed once Pb^{2+} was completely removed from **2.8.3-L** or **2.8.5-L**. To validate its reversibility, the system was titrated with acid/base three times. No sign of degradation was recorded (Figure 2-9).

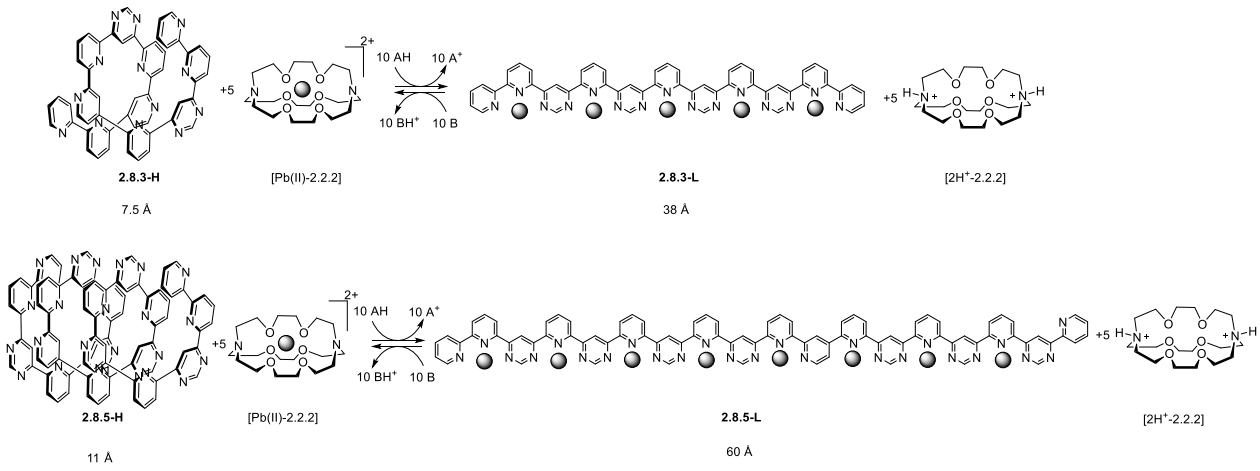

Figure 2-9. Foldamer based molecular muscle design.

Two more pH driven molecular devices were reported by Stoddard *et al.*[18] In single unit rotaxane **2.9,** Dibenzo[24]crown-8 can travel between its two docking sites. Under acidic conditions, dibenzo[24]crown-8 stays near the NH_2^{+} site, stabilized via hydrogen bonding. Upon treatment with base such as *t*-BuNP$(NMe_2)_3$, dibenzo[24]crown-8 moved to the bipyridinium site, connected by π-π interactions (Figure 2-10a). Later, they expanded this process to a tri-rotaxane **[2.12-H_3]$^{9+}$-Cap,** which worked as a molecular elevator. Pseudo-rotaxane **[2.12-H_3]$^{9+}$** was self-assembled by tris-crown ether **2.10** and the tris-ammoniumion **2.11**, with >99.9% binding

selectivity in $CHCl_3$-MeCN 2:1 solution. Capping group was introduced to limit the movements. With treatment of *t*-BuNP(NMe_2)$_3$, three crown ether rings in **[2.12-H$_3$]$^{9+}$-Cap** moved ca. 0.7 nm in stepwise other than concerted fashion with a force estimated to be 200 pN via from a thermodynamic analysis. Treatment of TFA fully restored this process (Figure 2-10b).

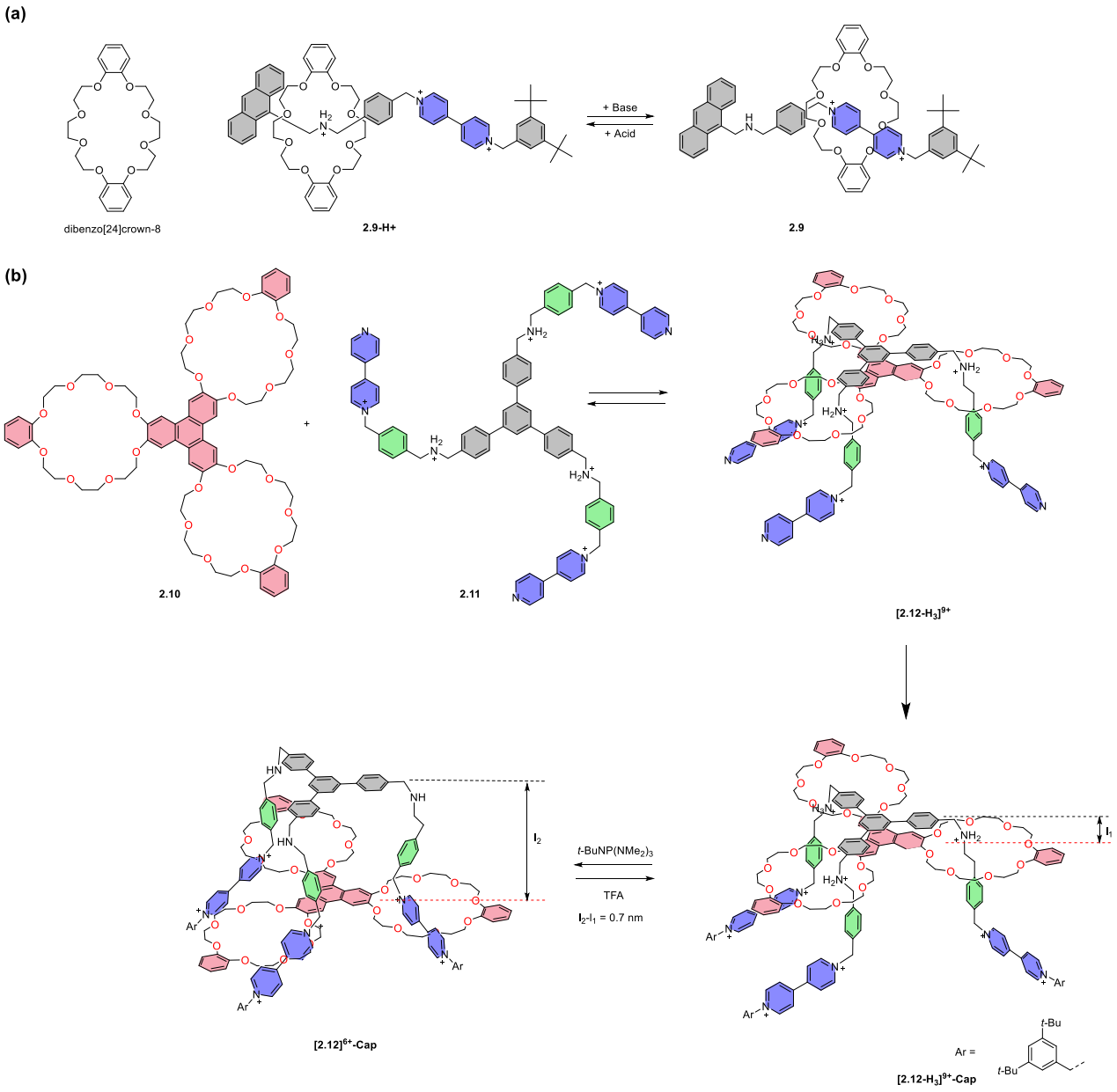

Figure 2-10. pH activated molecular elevator.

Azobenzene has been applied to many photoswitch designs as described in Chapter 1. Kaneda *et al.* [19] designed a daisy chain device with azobenzene and α-cyclodextrin. When both azobenzene groups are in *E* conformation, it resides inside α-cyclodextrin rings. Photo irridation at 366 nm in $CDCl_3$ gives 20% *ZE* and 5% *EE* isomer. Thermo relaxation can of *ZE* and *EE* can be achieved at 60 ℃. The estimated elongation is 0.7 nm (Figure 2-11).

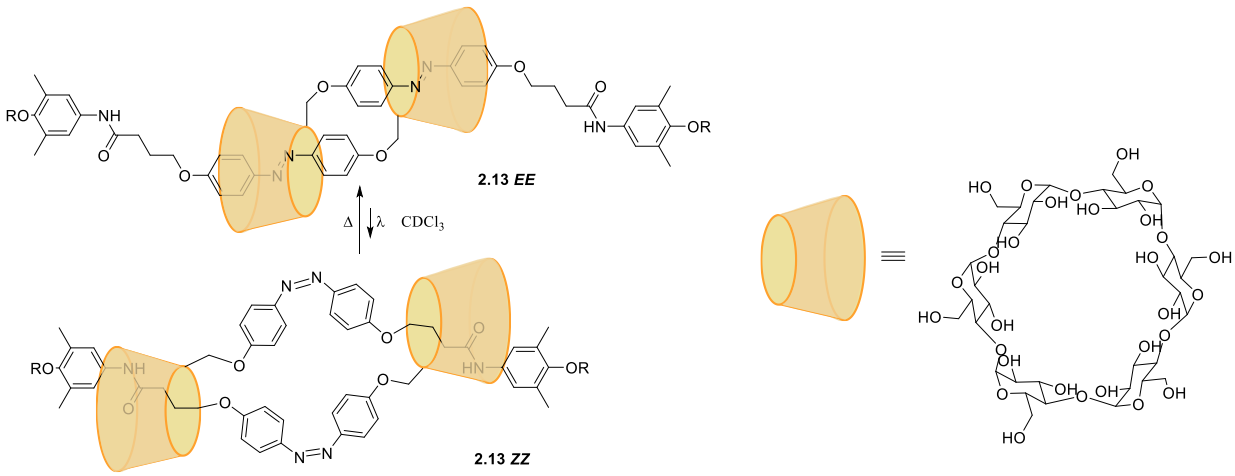

Figure 2-11. Rotaxane-based photo-responsive molecular muscle.

Inspired by Kaneda, Harada *et al.*[20] was able to improve the photo efficiency. With electronic tuning on azobenzene, conversion to 2.44 ZZ was about 80 % in methanol and 40% in water. However, long flexible ether chain reduced the effectiveness of the contraction length. 12*EE* has a hydrodynamic radius shortens from 4.4 nm to 3.6 nm (Figure 2-12).

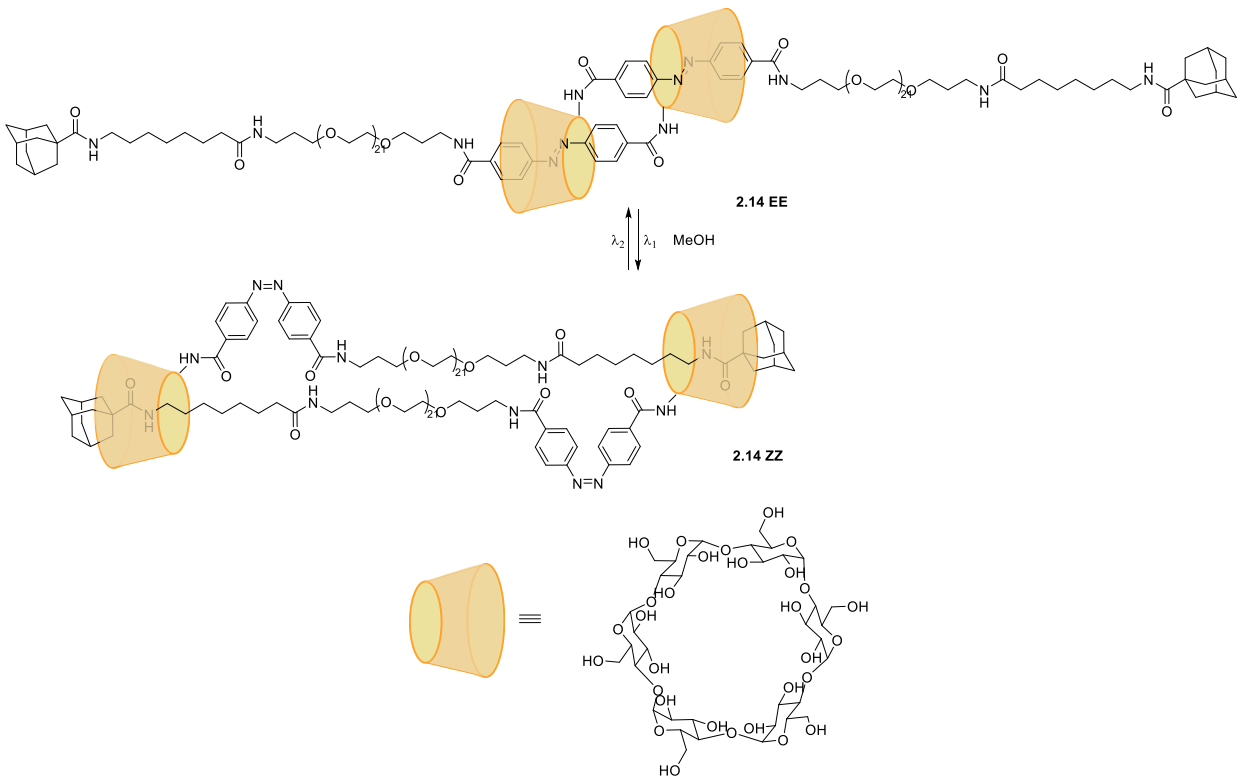

Figure 2-12. Improved design of photo-responsive molecular muscles.

Redox-driven molecular muscles have attracted a lot of attention. **2.15** is one of many redox-responsive daisy chains developed in Stoddard group[21] that function as molecular muscles. There are two stations for the electron rich 1,5-dioxynaphthalene and resorcinol rings: naphthalene diimide (NDI) and triazole ring, both of which are electron deficient. In the neutral state, electron rich ring almost exclusively stayed at NDI station in room temperature. The daisy chain contracted when NDI was electrochemically reduced to $NDI^{\bullet-}$ or $NDI^{2(\bullet-)}$. The increase of electron density on NDI moiety pushed the crown ether ring to the triazole station, thus the contraction (Figure 2-13).

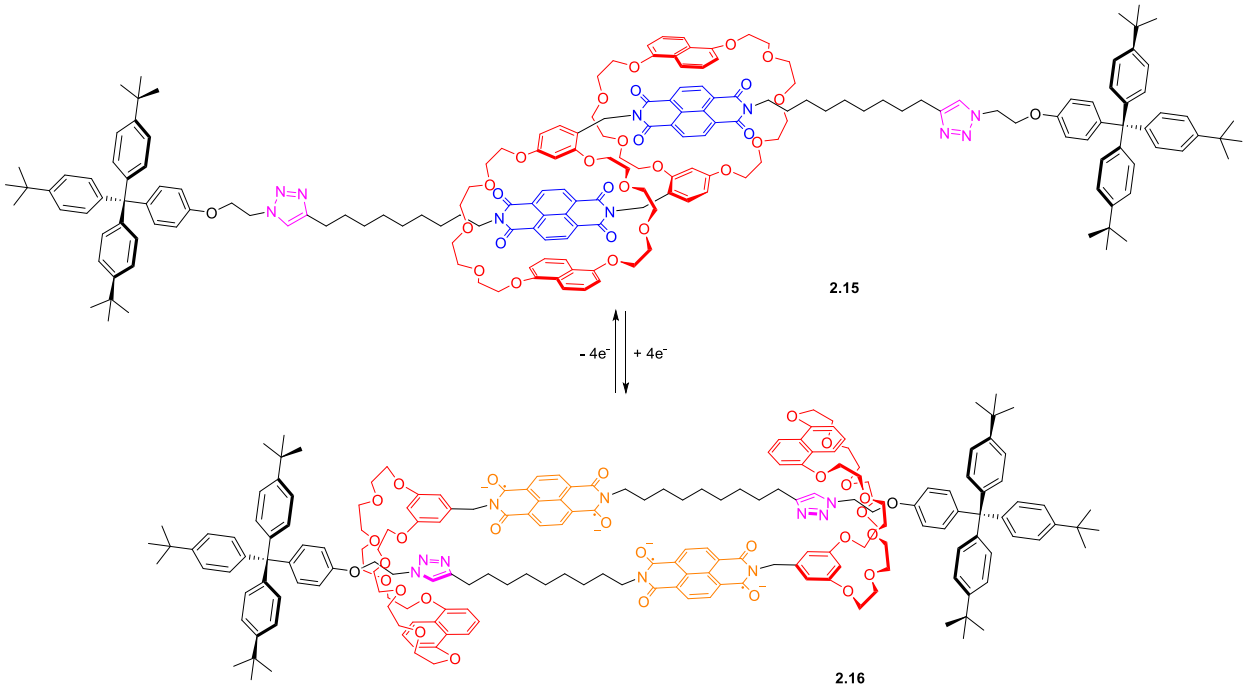

Figure 2-13. Electrochemically actuated daisy chain.

A redox responsive hydrogel was reported by Barnes *et al.*[22] Azide capped chain with 4,4'-bipyridine (BIPY) unites connected through hexaethylene glycol was cross linked with tetra-alkyne (TAXL) through click reaction. In the resulting hydrogel network, BIPY units are proposed to be linear. $Na_2S_2O_4$ was used to reduce BIPY to $BIPY^{\bullet -}$, which could form charge transfer complex and folded in to compact conformations, causing contraction on hydrogel. Air oxidation could restore this process and redox stimuli was cycled 4 times to demonstrate reversibility (Figure 2-14). Later, Barnes *et al.*[23] demonstrated this system also works effectively for a photoredox stimuli assisted via ruthenium catalyst.

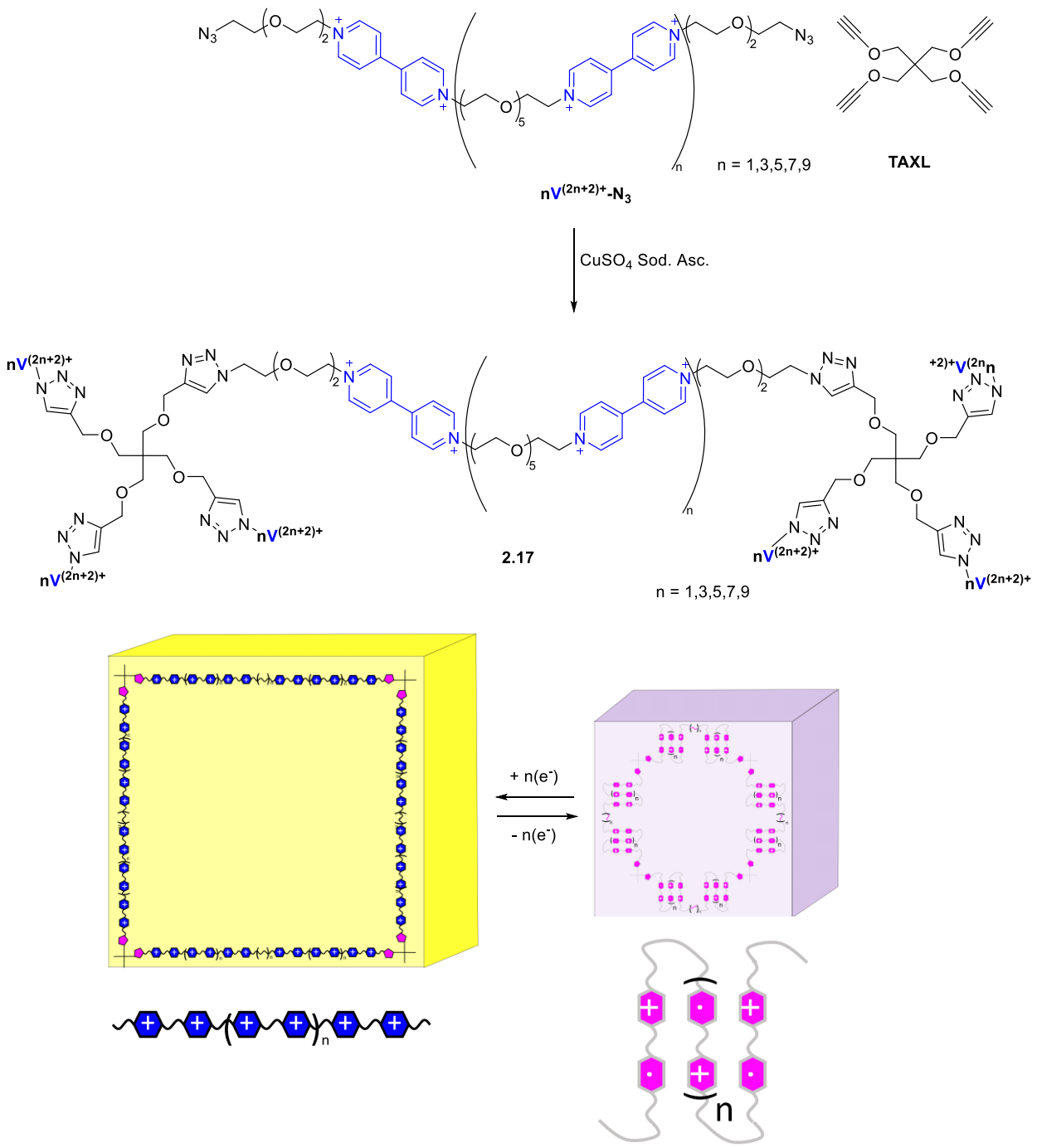

Figure 2-14. Redox responsive hydrogel. Remade with permission from Ref. 22. Copyright 2017 American Chemical Society.

Harada *et al.*[24] designed a redox responsive hydrogel **βCD-Fc-2.18** using guest-host interactions to control its sizes. The network was cross-linked with ferrocene (Fc) and β-cyclo-

dextrin (β-CD) units. The cross-link broke upon oxidation of ferrocene units, causing the gel to expand 11%. Subsequent reduction of ferrocene units would restore its binding with (β-CD), reverting the gel to original state. This hydrogel actuator could do mechanical work in the buffered solution, with output about 2.0 μJ (Figure 2-15).

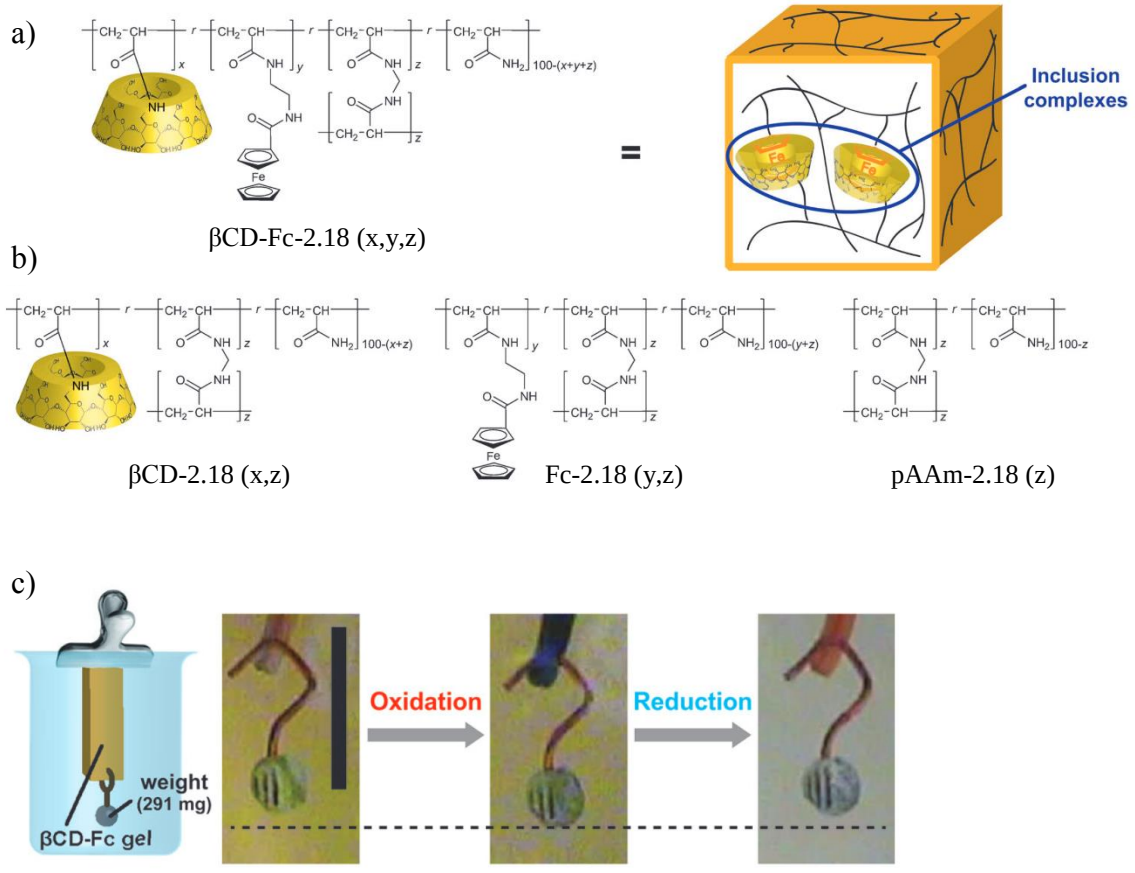

Figure 2-15. Redox-responsive molecular muscle design through guest-host interactions. Reprinted with permission from Ref. 24. Copyright 2013 John Wiley and Sons.

2.3 First generation phenazine-based interleafed foldamers as molecular muscles.

From a practical standing point, the most convenient way to actuate molecular muscles is via a redox process triggered by electricity. In Chapter 1, we have demonstrated that phenazine-1,6-dicarboxyamides are redox responsive molecular switches (Figure 2-16(a)). A chain composed of such molecular switches and cisoid spacers (shown in black) is predicted to fold into a butterfly-coil (Figure 2-16 (b)&(c)). This would encourage the phenazine moieties to stack in an offset, antiparallel orientation. With the help of computer-assisted modeling, we identified xanthene-4,5-diamines as promising candidates for this role. For example, tetramer **2.19** (depicted in Figure 2-16 (d) in extended form for ease of illustration) was predicted to fold as shown below.

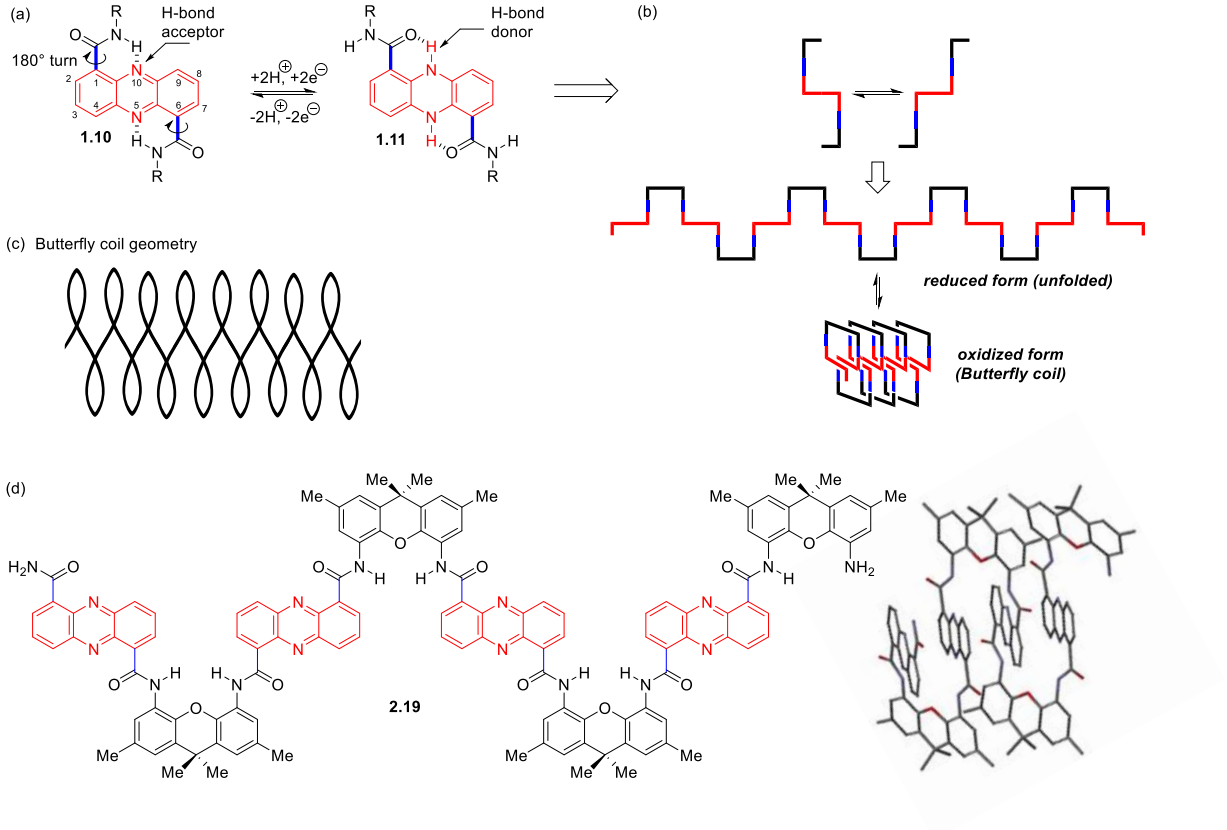

Figure 2-16. Proposed phenazine-based foldamer as molecular switches.

Synthesis of xanthene-4,5-diamine **2.24** started with **2.20** (Figure 2-17). There are a few vital details to secure 60% yield of **2.21** in this step. Nitrogen atmosphere was needed to prevent the oxidation of **2.20**. A mixture of **2.20** and methanesulfonic acid needed to be heated to 140 ℃ before the addition of acetone begins. Acetone was introduced over 12 hours using a syringe pump with a needle immersed below the surface of the reaction mixture. [25] Bromination smoothly delivered **2.21** in 75% yield. Flash chromatography or recrystallization in hexane is recommended to completely remove residual bromine, as needed for the next step. Conversion to diformamide **2.23** is also tricky.[26] The reaction needs to be at exactly 160 ℃ with an open flask for no more than 5 hours. The copper precipitate formed during the reaction was found to absorb **2.23**. Therefore, it is recommended to use THF during the filtration to boost the yield. During chromatography, **2.23** usually came out under the eluent of 40% acetone in hexane and would instantly crush out of the solution due to poor solubility. To ensure complete recovery from silica gel, dichloromethane was used in the last stage. Base hydrolysis of **2.23** produced **2.24** in 90% yield.

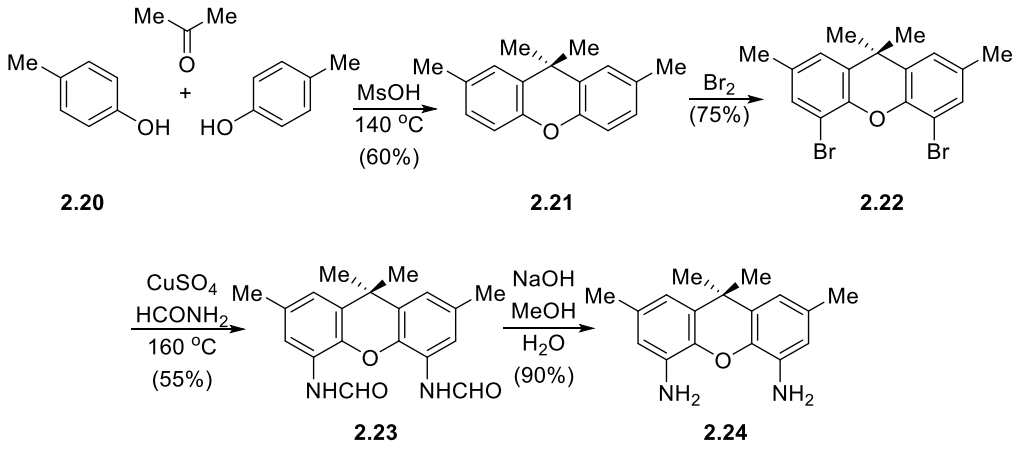

Figure 2-17. Synthesis of **2.24.**

With **2.24** in hand, we began to construct our foldamer. The single unit model **2.27** was pursued first (Figure 2-18). Acylation of **2.24** with **1.19** delivered **2.25** in 79% yield. **2.25** was not soluble in many organic solvents such as acetonitrile, acetone, and tetrahydrofuran (THF). It had good solubility in CH_2Cl_2, $CHCl_3$ and moderately soluble in dimethylformamide (DMF). Therefore, its purification was best achieved by washing away impurities after acylation with acetonitrile using the centrifuge technique mentioned in Chapter 1.

The geometry of **2.25** is also interesting. According to DFT calculations, two xanthene rings are twisted out of the plane of phenazine with dihedral angles of ca. 33 °. Two conformers are possible, one with C_2-symmetry that has two amino groups positioned in the same face of the phenazine while the other conformer has central symmetry with the amino groups on the opposite faces. Due to the reduced reactivity of the amino groups presumably due to hindrance, complete acylation of **2.25** required four equivalents of **2.26**.

DFT modeling suggested that two trimethoxyphenyl groups couldn't fit in the same face of the phenazine, forcing 2.27 to adopt centrosymmetrical conformation exclusively. While in solution, ^{1}H NMR and 2D NMR studies were able to confirm its folded geometry. Folded geometry of **2.27** in $CDCl_3$ resulted in strong shielding effects in the ^{1}H NMR spectrum. Chemical shifts of *ortho*-protons **m**/**m′** at δ 5.8 ppm were in much lower field compared to 7.3 ppm in simple 3,4,5-trimethoxybenzamides, indicating significant shielding effects from phenazine nucleus. Protic or polar solvents (80% CD_3OD-20% $CDCl_3$, DMSO-d_6) had little impact on this shielding effect. Moreover, this effect was largely the same upon heating to 75 ℃ in DMSO-d_6 or cooled down to –75 ℃ in CD_2Cl_2. While in NOESY spectrum, interactions between proton **d—l**, **d—a**, and **a—l** (see dashed lines) indicated a strong hydrogen bonding of proton **d** and **l** to phenazine nitrogens and the xanthene oxygens.

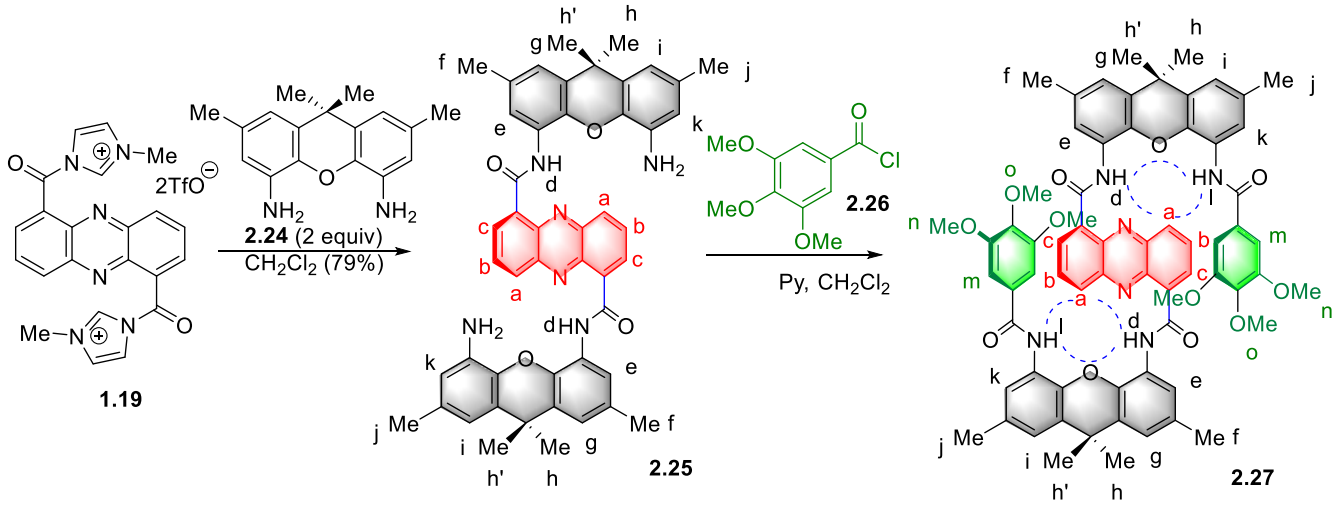

Figure 2-18. Synthesis of model compound **2.27**.

We were able to get a single crystal of **2.27** for X-ray diffraction study (Figure 2-19). Indeed, this folded geometry was stabilized by hydrogen bonding and π-stacking. The distances between proton **l**/proton **d** to phenazine nitrogen/xanthene oxygen are ca. 1.9 Å and 2.3 Å, which are within hydrogen bonding range. Two trimethoxyphenyl groups were found to be on the opposite faces of phenazine ring, with a distance of ca. 3.7 Å between the centers, suggesting their π-stacking to the phenazine ring.

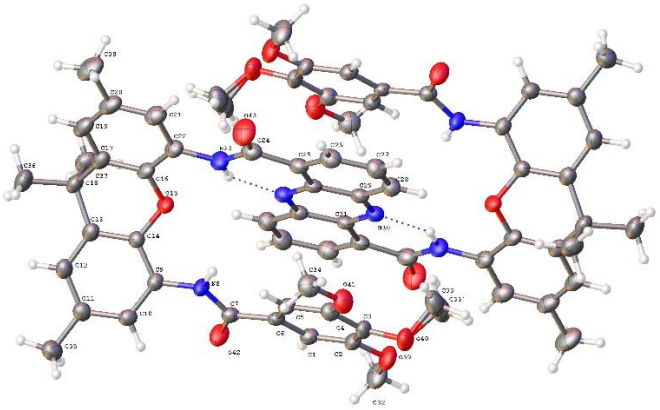

Figure 2-19. X-ray structure of **2.27**.

The stability of this folded conformation in solution was studied as well. **2.27** conceivably has two conformers due to its central symmetry (Figure 2-20). The energy barrier between those conformers can be determined via variable temperature NMR. The geminal methyl groups **h** and **h′** on the xanthene moieties were chosen to be examined in detail due to their diastereotopic nature. One sharp singlet peak was observed on ^{1}H NMR at ambient temperature (Figure 2-21). However, as the temperature went down to −42 ℃, separation began. According to Eyring-Polanyi equation.[27], we calculated an energy barrier of 10.9 Kcal/mol. As for aromatic protons **m/m′** and methyl groups **n/n′**, their broadening at −65 ℃ was the consequence of the slower rotation of the trimethoxyphenyl groups. Although our folded structure is thermodynamically favored, an energy barrier of 10.9 Kcal/mol adds certain degree of kinetic mobility to it.

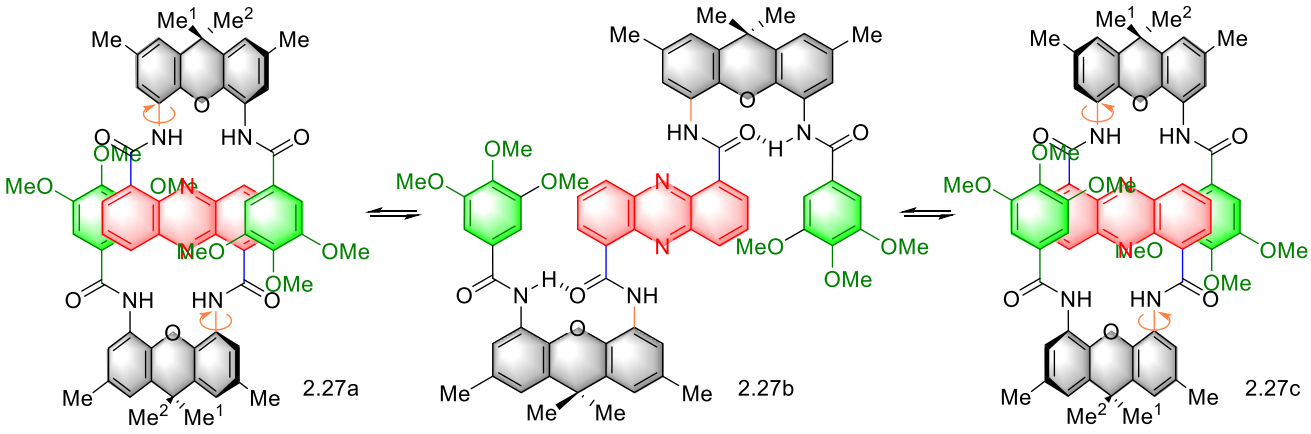

Figure 2-20. Double flip.

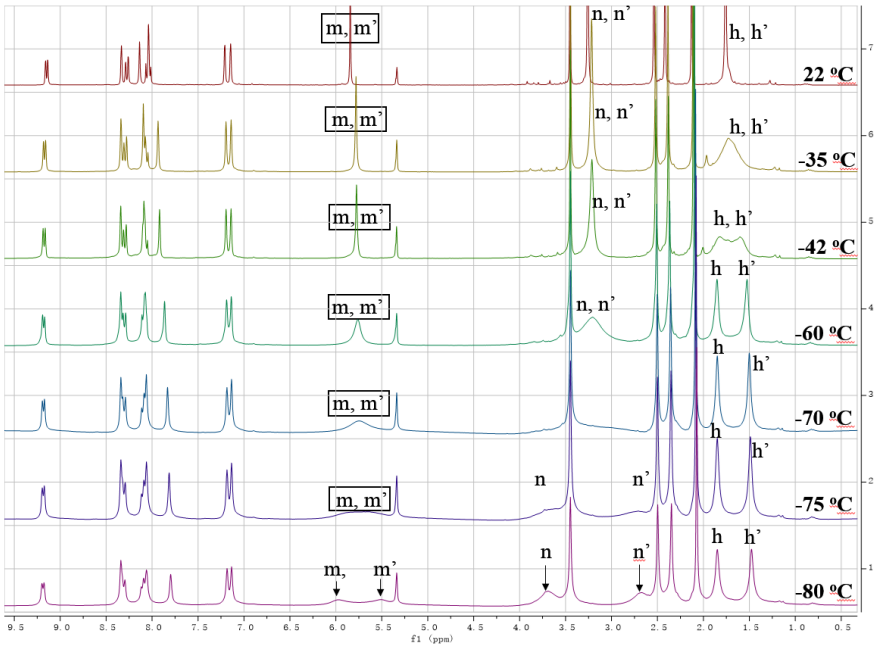

Figure 2-21. Variable-temperature experiment (300 MHz).

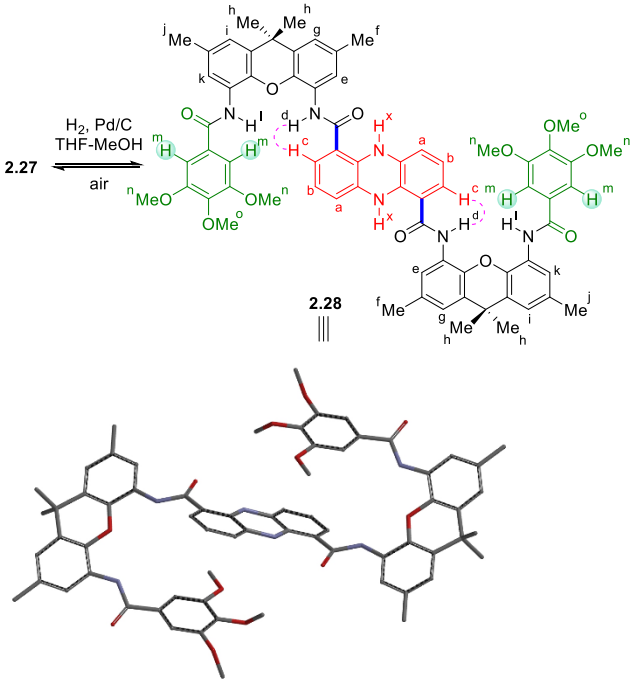

Figure 2-22. The unfolding of **2.27**.

Redox studies were carried out on this single unit model to evaluate its ability as a molecular switch. Catalytic hydrogenation of **2.24** was carried out similarly to that of **1.21**, only

to be much more challenging due to its poor solubility (Figure 2-22). Nevertheless, >95% conversion was confirmed by ^{1}H NMR. The first sign of its conformational change is aromatic protons **m**, which shifted from 5.8 to 7.0 ppm. This was consistent with the expected structure with diminished shielding. Furthermore, NOESY gave me more evidence of the unfolding. The two sets of amide protons **d** and **l** no longer displayed NOE with protons **a**. Instead, NOESY indicated the proximity of amide protons **d** to aromatic proton **c** on the dihydrophenazine nucleus. As with the **1.21**, dihydrophenazine **2.28** quickly oxidized back to **2.27** on exposure of its solution to air.

After the single unit model compound was confirmed to behave as intended, we set out to explore the synthesis of oligomers. Upon mixing equimolar amounts of **2.21** and **1.19** (Figure 2-23), the formation of bis-phenazine product **2.29** was detected. However, there were mono-phenazine derivative **2.25**[28] and cyclic dimer **2.30** present as well, in approximately 1:1:1 ratio. Isolation of these products turned out to be very difficult due to their low solubility. In fact, gel permeation chromatography was able to get **2.29** in pure form with 10% isolated yield. No evidence of formation of higher oligomers was seen in this case. The cyclic dimer byproduct **2.30** could also be prepared directly from **2.25** in high yield by treating it with **1.19**. Therefore, it is recommended to synthesize 2.25 via a protection/deprotection route from **2.21** to avoid formation of **2.29** and **2.30.** There are two possible forms of **2.30**, parallel (**2.30a**) and antiparallel (**2.30b**) orientation of the amide moieties, which are distinct and non-interchangeable. According to our DFT calculations, [29,30] **2.30b** is more stable. The ^{1}H NMR of **2.30** showed no line broadening at low temperatures, which indicated a C2-symmetric structure like **2.30b**.

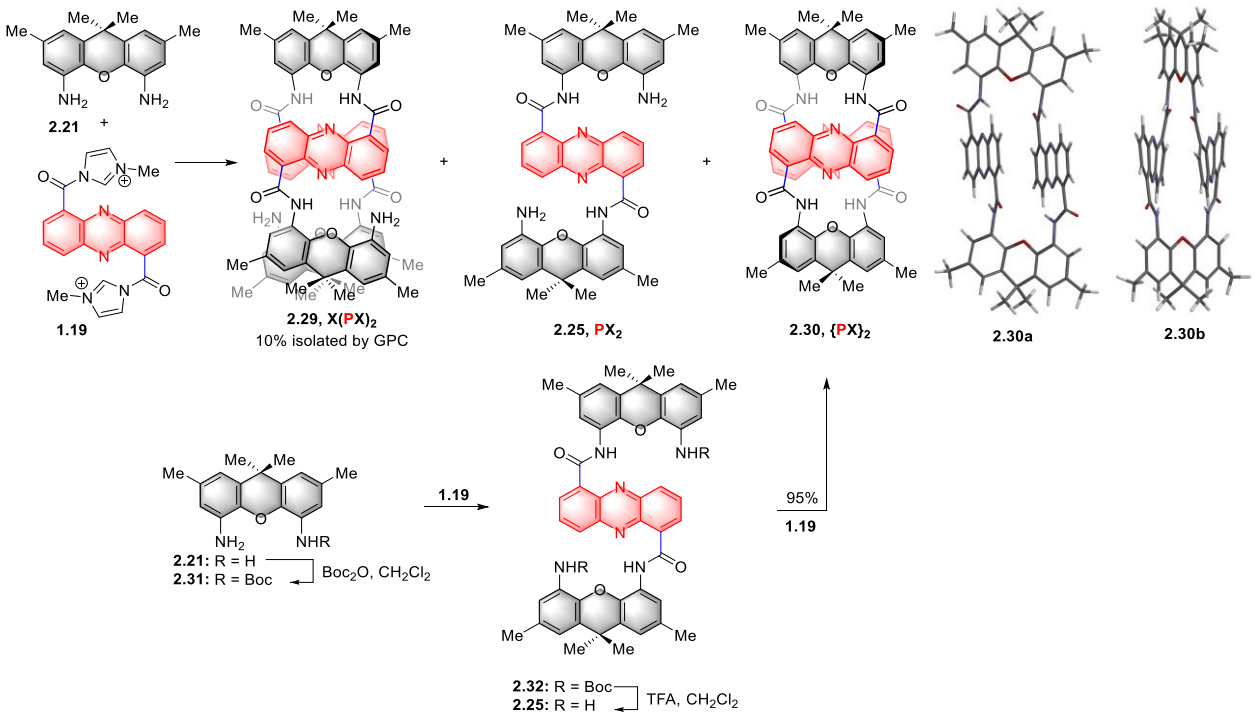

Figure 2-23. Attempted direct oligomerization.

We could use a suitable protection-deprotection strategy to avoid the undesired cyclization, however we were concerned by the poor solubility of **2.25**, which did not bode well for the future characterization and synthetic manipulation of higher oligomers. To improve their solubility, we decided to alternate phenazine units with 2,5-dialkoxy-*p*-phenylene groups, to which branched chains could be atached. The resulting "interleafed" oligomer **2.33** (Figure 2-24a) would be expected to fold into an achiral butterfly coil similar to the one we originally envisioned (Figure 2-16). This improvement came at the cost of a smaller relative extension upon reduction to **2.34** (50% vs. 110%, respectively) compared to the "all-phenazine" structure **2.19** [31], but it would still be sufficient to demonstrate the underlying design principle.

2,5-dialkoxy-*p*-phenylene spacer was synthesized from **2.35** in 4 steps as shown in Figure 2-24b. After some experimentation, it was found that the Williamson ether synthesis step (**2.36→2.37**) worked best using fine Cs_2CO_3 powder along with good stirring. The purity of acyl

chloride **2.39** turned out to be essential for its further use. Thus, after treatement of diacid **2.38** with thionyl chloride, all traces of the latter must be removed by co-evaporation with toluene leaving the final product **2.39** as an odorless, white or off-white solid. If a brownish sample of **2.39** is obtained, it may be recycled to **2.38** by refluxing with NaOH and repurified.

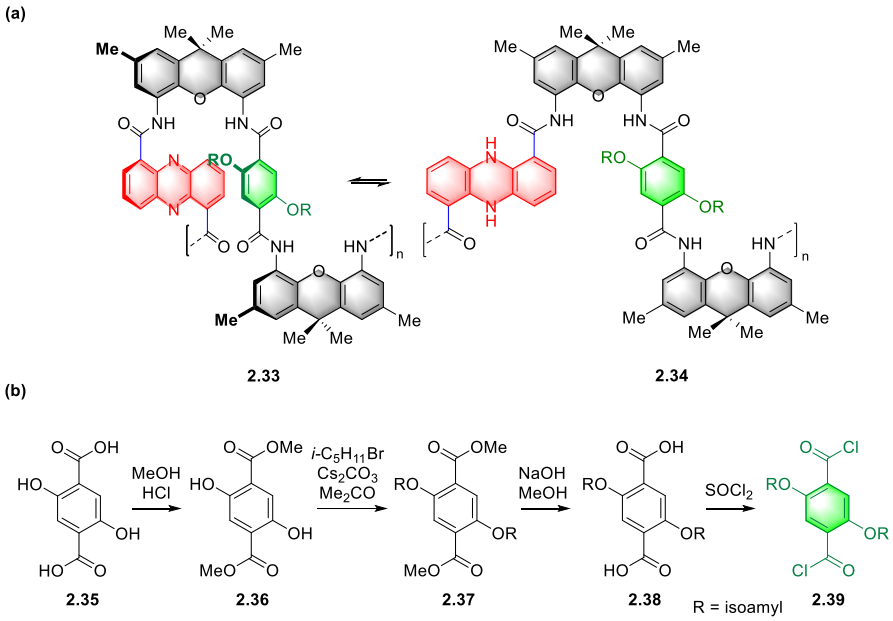

Figure 2-24. Design of interleafed butterfly coil **(a)** and preparation of bis-acyl chloride **2.39 (b)**.

In the first attempt to prepare oligomer **2.33** by adding diacyl chloride **2.39** slowly to excess **2.25**, none of the hoped-for product could be detected in the mixture. Instead, the reaction gave a high yield of macrocyclic product **2.38** (Figure 2-25). The same compound could also be prepared by reacting **2.40** with **1.19**. Once again, DFT calculations favored the diastereomer with the antiparallel orientation of the amide groups shown schematically in Figure 2-25. This prediction was also corroborated by the NOESY spectrum of **2.38**.

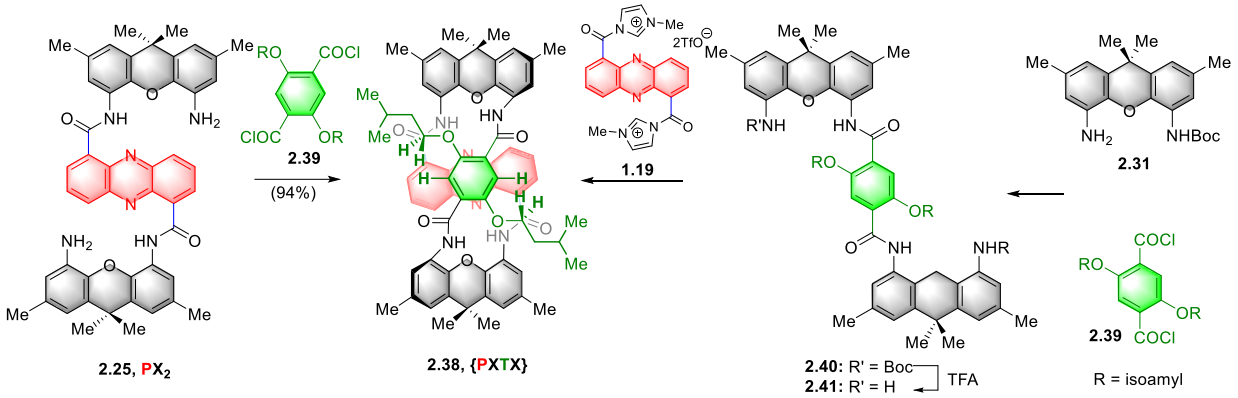

Figure 2-25. Synthesis of macrocycle **2.38**.

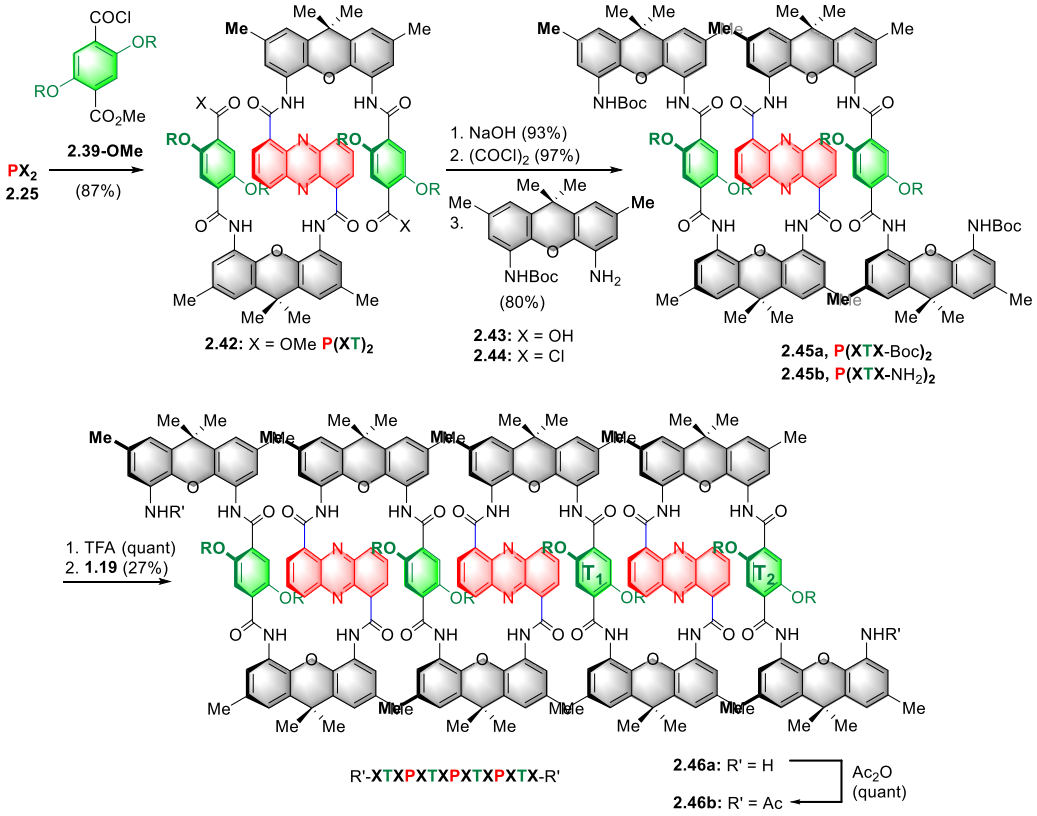

Figure 2-26. Synthesis of interleafed oligomer **2.46b**

While macrocycles **2.30** and **2.38** were interesting in their own right, multiphenazine oligomers needs to be studied for their redox behaviors, which would require a stepwise approach. Due to the ease to form such macrocycles from **2.25**, it is hypothesized that diamine intermediates

that's longer than **2.25** would be unlikely to adopt a conformation required for such cyclization. With this in mind, intermediate **2.42**was prepared via the route shown in Figure **2-26**. After capping with **2.39-OMe** (see experimental section for synthesis), **2.42** was subjected to base hydrolysis and converted to bis-acyl chloride **2.44. 2.44** is a very reactive acyl donor, and can be coupled with **2.31** easily. **2.45b** has lower reactivity towards **1.19** than **2.25**, probably due to its size. Thus, this acylation need freshly prepared **1.19** and heat to 80 ℃. It is recommended to add **1.19** in portions to reduce degradation at high temperature. Gratifyingly, no macrocycle was observed and the desired tris-phenazine oligomer **2.46a** was the major product obtained in pure form in 27% yield. Small quantities of longer oligomers were also detected in the course of its purification by gel permeation chromatography. From the practical standpoint, it's worth mentioning that 2,5-dialkoxy-*p*-phenylene groups indeed promoted the solubility on those oligomers. **2.42, 2.43, 2.44, 2.45a/b, and 2.46a/b** as well as **2.38**, possessed decent solubility in methylene chloride and chloroform, compared to bis-phenazine derivative **2.29** and cyclic homodimer **2.30**. Furthermore, **2.42, 2.43, 2.44, 2.45a/b, 2.46a** and **2.38** were well soluble in toluene and tetrahydrofuran and moderately soluble in acetone, but completely insoluble in polar solvents like acetonitrile and methanol. Indeed, this can be used to an advantage to remove all impurities. While our attempts to grow X-ray quality crystals of compounds **2.38**, **2.42** and **2.46a/b** were unsuccessful, extensive NMR characterization studies confirmed the thermodynamic and kinetic stability of their folded structures. Some of the most salient results are presented below.

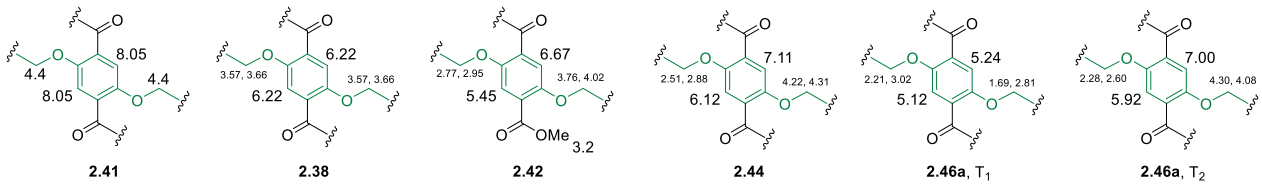

Figure 2-27. Chemical shifts of select protons (δ, ppm).

Shielding effects have been an interesting observation in many foldamers in this series. ^{1}H NMR study of model compound **2.27** allowed us to study its folding behavior in solution.[32] In particular, the upfield shift of the *ortho*-protons on the aroyl groups due to shielding by the phenazine nucleus provided the first evidence of its sandwiched structure illustrated in **2.27**. Therefore, we became interested to analyze the shielding effects in the additional phenazine derivatives that became available as our synthesis progress (Figure 2-27). As expected, the aromatic protons on the terephthaloyl moiety in macrocycle **2.38** were shifted upfield, compared to its "unshielded" precursor **2.41** (6.22 vs. 8.05 ppm).

Besides aromatic protons, the α-protons on the isoamyl side chains also showed appreciable upfield shifts (ca. 3.6 vs. 4.4 ppm), which was consistent with the expected face-to-face orientation of the benzene and phenazine nuclei. The corresponding protons in **2.27** and **2.28** displayed an interesting dichotomy: those pointing "inward", i.e. toward the phenazine nucleus, had considerably lower chemical shifts than those pointing outward. The shielding pattern of oligomer **2.46a** was also informative. While the aromatic protons on the "outer" terephthaloyl group T_2 appeared at 7.0 and 5.92 ppm, in line with the values seen in structures **2.42** and **2.44**, their counterparts on the "inner" group T_1 showed up at 5.24 and 5.12 ppm, reflecting the combined shielding effects of two phenazine moieties. Overall, these observations were in complete agreement with the expected thermodynamic preference for the folded conformations of oligomers **2.42**, **2.44**, and **2.46a**.

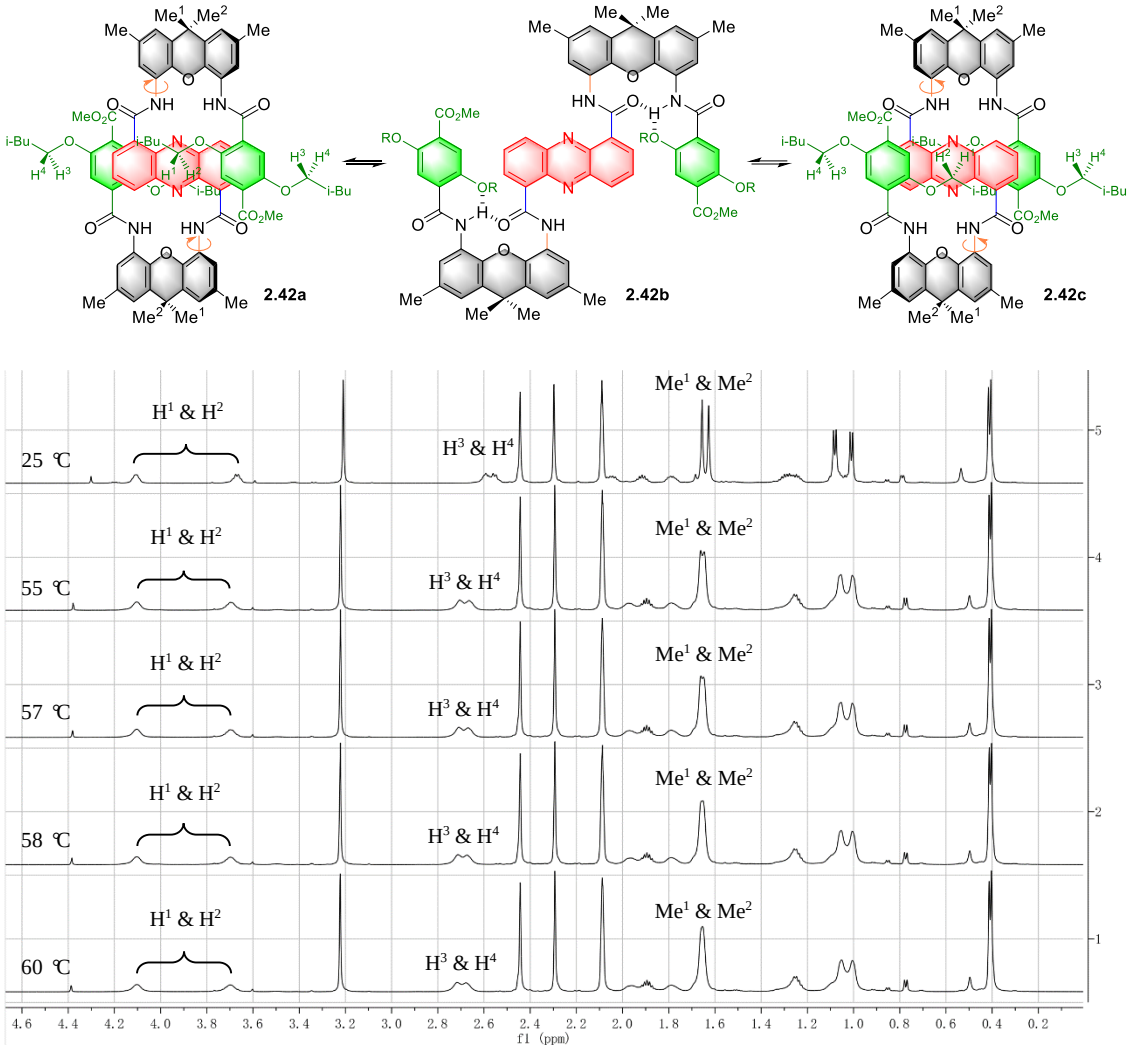

Figure 2-28. Line-broadening experiment with **2.42**.

Kinetic stability studies were done on the first single unit model **2.27,** and we estimated its inversion barrier to be at ca. 11 Kcal/mol. When we looked at the ^{1}H NMR of **2.42**, those geminal methyls are seen as *two singlets* at room temperature (Figure 2-28). Furthermore, the α-protons on the isoamyl side chains are also split into diastereotopic pairs. Heating and cooling experiments were performed with toluene as solvent. It's worth noting that heating to 60 ℃ made Me^1 and Me^2 coalesced, which put the inversion barrier at ca. 17 Kcal/mol.

On the basis of DFT calculations on simplified models of **2.27** and **2.42**,[33] we hypothesize that the *ortho*-alkoxy groups present in **2.42** and absent in **2.27** diminish the stabilizing hydrogen bonding interactions between the amide groups in the fully unfolded form (shown in **2.42b**) and thus raise the inversion barrier (estimated at ca. 7 Kcal/mol per sidearm for **2.27** and 9 Kcal/mol for **2.42**).

Likewise, extended oligomer **2.45a** is configurationally stable on NMR timescale at least up to 70 °C. It is also noteworthy that the "inner" dialkoxyphenylene groups display a remarkably wide separation of the diastereotopic pairs (up to 1.1 ppm, cf. **2.45a**, T_1 in Figure 2-27).

Then, chemical actuation of phenazine oligomers were studied. Although redox studies have been done on single phenazine unit **2.27**, greatly improved solubility and easily scalable synthesis gave us opportunity to investigate the redox process further. A modified redox protocol was established. This time, a valved NMR tube was used as the reaction vessel to carry out hydrogenation, which greatly simplified this procedure and secured a reliable process. It took almost 20 failures to get the initial results on **2.27** while this new procedure increased the success rate to almost 100%. Shaking a tetrahydrofuran solution of **2.42** in the presence of 8 mol% of palladium on carbon under 20 psi of hydrogen results in its clean conversion to dihydrophenazine **2.47** in 3 h. No further reduction or other side reactions occurred when stored under the same conditions for 24 h. After extensive NMR characterization on **2.47**, air was introduced back into the tube. **2.47** was oxidized back to the starting material within 5 minutes. Furthermore, this redox cycle was repeated 10 times without accumulation of any side products (besides water) or significant loss of catalytic activity (Figure 2-29). Analogously to our earlier study of model

compound **2.27**, the unfolding of **2.42** was evidenced by the disappearance of shielding experienced by the aromatic protons on the terephthaloyl side arms as well as changes in NOESY spectrum (see dashed lines).

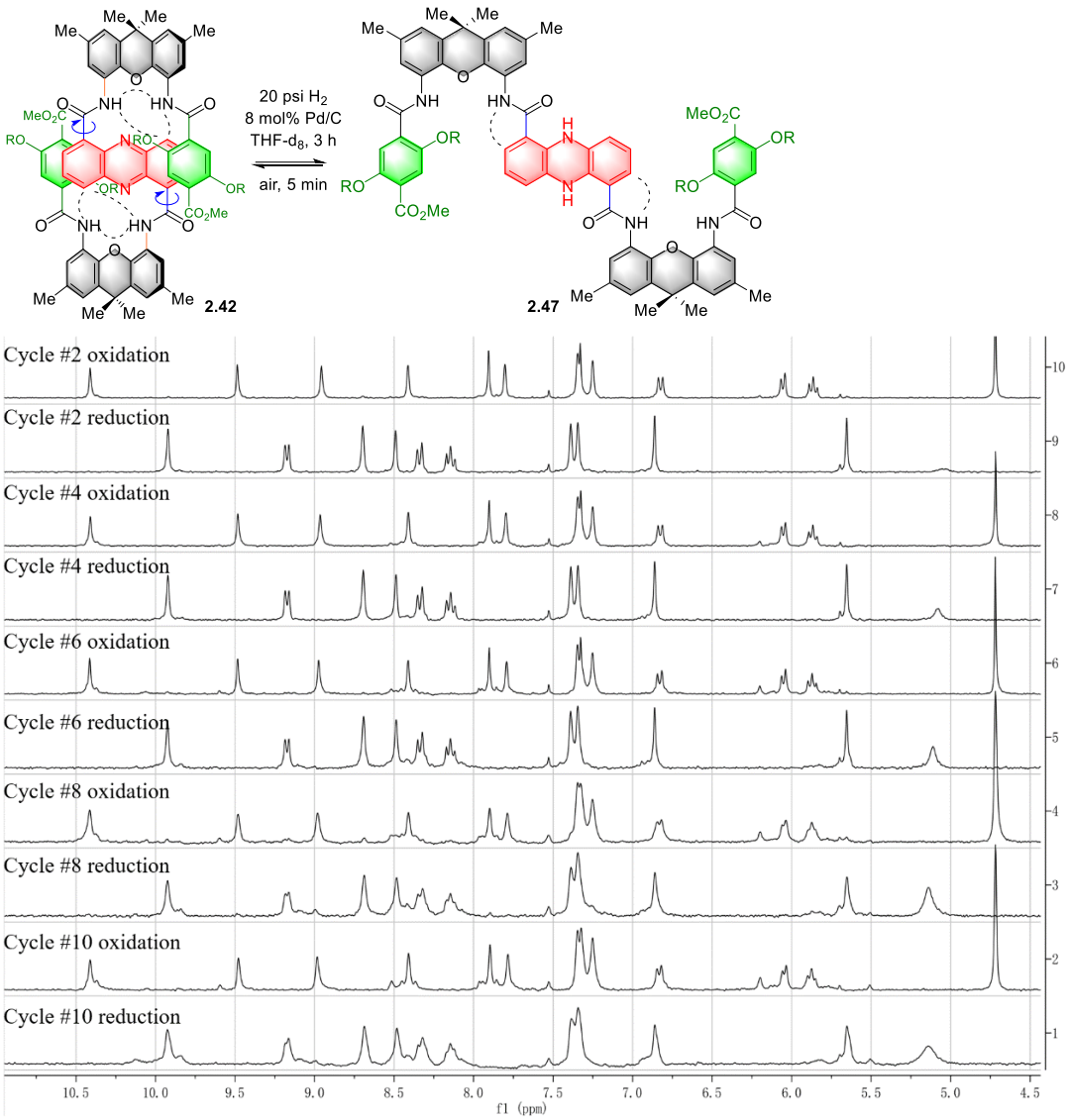

Figure 2-29. Redox cycling of **2.42** via catalytic hydrogenation.

This protocol was then applied to the redox cycling of the tris-phenazine oligomer **2.46a/b.** Chloroform was chosen instead of tetrahydrofuran as the solvent due to solubility issues. The unprotected **2.46a** was tested first. It underwent the reduction as expected, but

degraded significantly upon exposure of its reduced form to air. To improve its stability towards oxidation, **2.46a** was capped with acetic anhydride to **2.46b** (Figure 2-26). Fortunately, its N,N'-diacetylated derivative **2.46b** proved to be completely stable during 10 redox cycles (Figure 2-30). It is also noteworthy that a simple heterogeneous catalyst, palladium on carbon, proved to be as effective in this transformation as it was in the case of the smaller model compounds (**2.27** and **2.42**) and did not complicate the resulting NMR spectra.

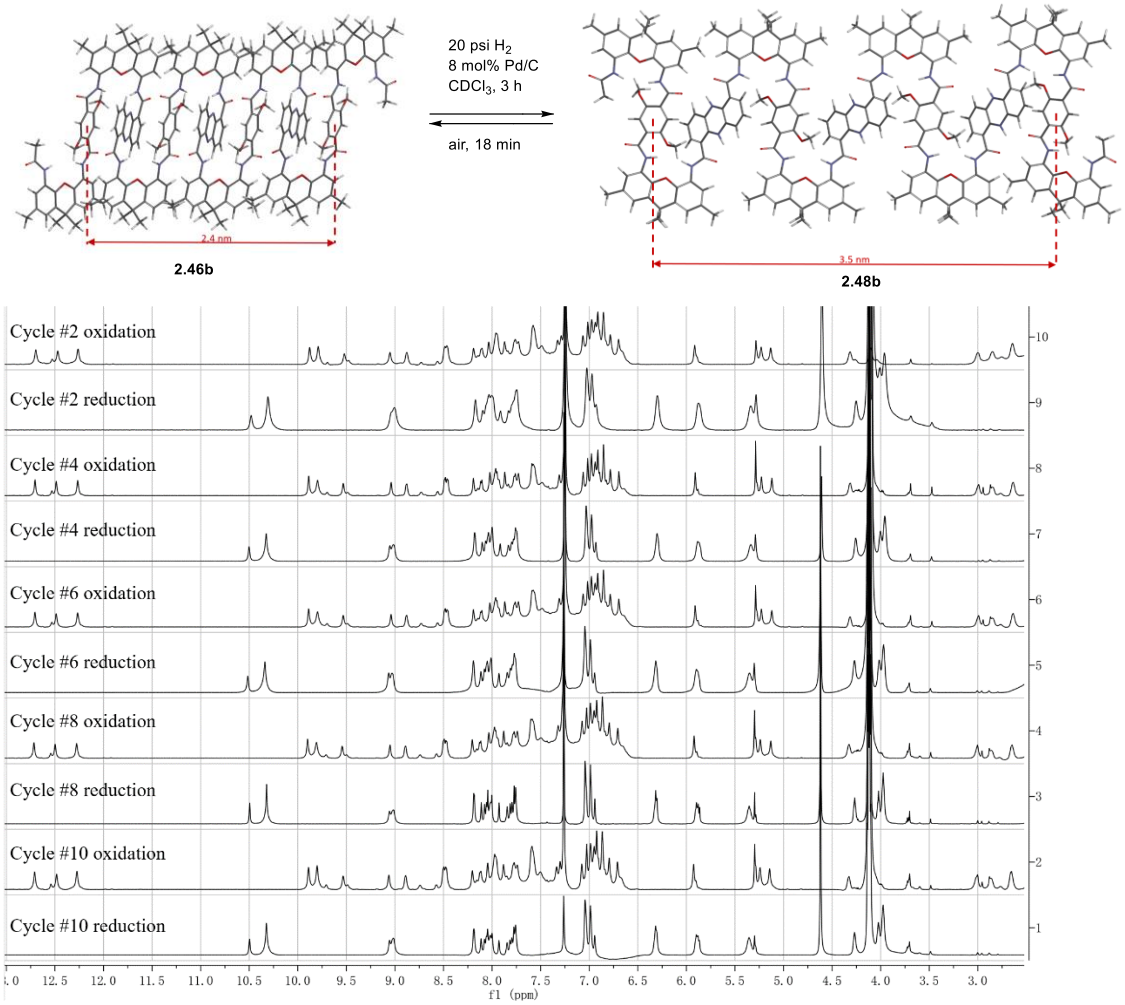

Figure 2-30. Redox cycling of **2.46b** via catalytic hydrogenation

By analogy with our original model system **2.17**, changes in the chemical shifts of the aromatic protons on the terephthalamide moieties proved to be highly diagnostic. As noted above (Figure 2-27), in the NMR spectra of the starting materials **2.42** and **2.46b** they occupied upfield positions (ca. 5-6 ppm) due to diamagnetic shielding by the phenazine groups. Upon reduction to the dihydrophenazine forms **2.47** and **2.48b**, however, they moved to ca. 7.2-8 ppm, which indicated that both molecules were now unfolded (Figure 2-31). In addition, the unfolded structure was supported by changes observed in the NOESY spectra of **2.46b** and **2.48b**. Overall, these results demonstrate that catalytic hydrogenation provides a simple and practical means of actuating a nanosized molecular muscle. [29]

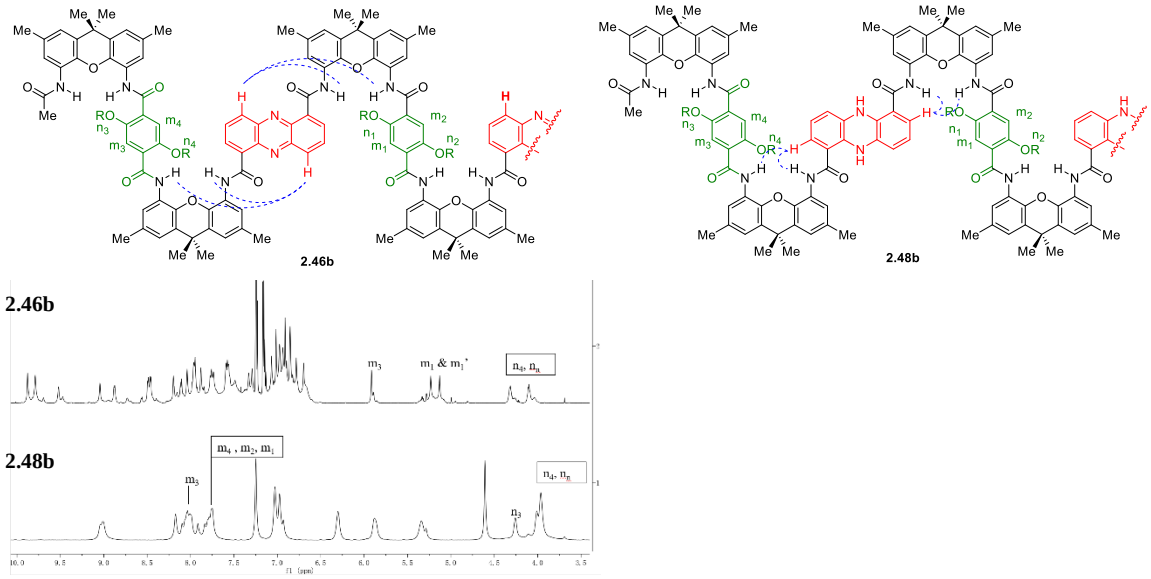

Figure 2-31. Diagnostic changes in chemical shifts and nOe.

Since we were aiming an electric activated molecular muscle design, we needed to explore electrochemical reduction-reoxidation of phenazine oligomers. A cyclic voltammetry experiment with **2.42** confirmed its stability for at least 40 redox cycles. After some experimentation, I developed a protocol for its bulk electrolysis using the apparatus

shown in Figure 2-32. Both cells were charged with a solution of **2.42** in $CDCl_3$-CD_3OD mixture with lithium perchlorate as a supporting electrolyte and hydrazine as a sacrificial reductant. After passing 5 F/mol of current through a divided cell, ^1H NMR indicated that half-cell A converted cleanly to dihydrophenazine **2.47**, while that in half-cell B remained intact. This is the first evidence that the electrochemical reduction is quantitative with no side product. To prove it's a reversible redox process, this experiment was repeated again. With **2.47** in half-cell A, and **2.42** remain unchanged in half-cell B, I *then reversed the current*. I confirmed that now the dihydrophenazine **2.47** in half-cell A oxidized back to **2.42**, while the starting phenazine in B got reduced.

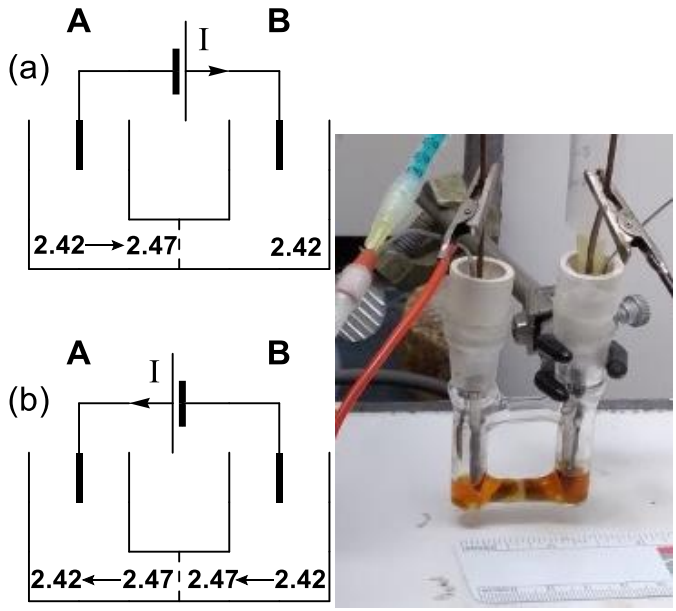

Figure 2-32. Electrochemical setup. Performed with **2.42** (7 mg, 0.005 mmol), N_2H_4-H_2O (25 μL, 0.5 mmol), and $LiClO_4$ (10 mg, 0.1 mmol) in 0.5 mL of 4:1 v/v $CDCl_3$-CD_3OD mixture.

In conclusion, we have, for the first time, constructed a tri-phenazine-based oligomer of nanometer size and shown that it undergoes a fully reversible extension-contraction in response to chemical and electrochemical reduction-oxidation. This

demonstration formed the basis for designing materials that would exhibit redox-responsive mechanical motion on macroscopic scale. It is also worth mentioning that, apart from its stimuli-responsive behavior, oligomer **2.46** provided the first example of a foldamer with the novel "butterfly coil" folding geometry distinct from both helical and regular achiral foldamers reported previously.[34] Development of other types of butterfly coil foldamers will be continued in the next chapter.

2.4 Experimental

2.4.1. Synthesis of 2,7,9,9-tetramethyl-9H-xanthene-4,5-diamine (2.24)

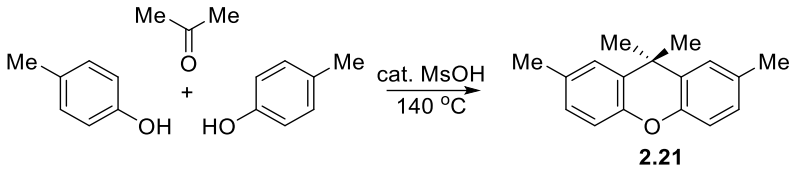

2.21

2.4.1a. 2,7,9,9-tetramethyl-9H-xanthene (2.21). Prepared via a modified patent procedure.[25] A mixture of *p*-cresol (20.0 g, 185 mmol) and methanesulfonic acid (0.45 mL, 6.9 mmol) was stirred at 140 ℃ under N_2 in a 100 mL, 3-necked flask equipped with a vertical reflux condenser and a thermometer. Using a syringe pump, acetone (4 mL, 54 mmol) was added over the course of 8 h via a steel needle passing through the condenser and immersed into the mixture. After the addition was complete, the mixture was heated at 140 ℃ for another 8 h. After cooling down to room temperature, the mixture was poured into 200 mL of 1 M NaOH and extracted with hexanes (300 mL×3) The combined extract was washed with 1 M NaOH, dried with $MgSO_4$ and rotary evaporated. The resulting brown oil was loaded onto a short silica gel column (6 cm H × 10 cm Ø) and eluted with ca. 1 L of hexanes. The pure chromatographic fractions were rotary evaporated to dryness

to afford the product as a white crystalline solid. If necessary, the product can be recrystallized from hexanes. (6.3 g, 48% yield based on acetone). **^{1}H NMR** (300 MHz, $CDCl_3$) δ 7.19 (s, 2H), 6.97 – 7.01 (m, 2H), 6.91 - 6.94 (m, 2H), 2.34 (s, 6H), 1.63 (s, 6H), 1.62 (s, 6H). **^{13}C NMR** (75 MHz, $CDCl_3$) δ 148.35, 131.94, 129.62, 127.91, 126.43, 115.98, 33.91, 32.39, 20.96. **IR** (cm^{-1}): 2966, 1489, 1362, 1292, 116, 1167, 1132, 1087, 1024, 1000, 941, 898, 809; **HRMS** (ESI-TOF) m/z: $[M + H]^+$ calcd for $C_{17}H_{19}O$, 239.1430 ; found 239.1456. **mp:** 138-140 ℃;

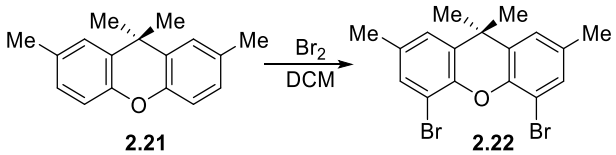

2.21 **2.22**

2.4.1b. 4,5-dibromo-2,7,9,9-tetramethyl-9H-xanthene (2.22).[26] A solution of **2.21** (8.167 g, 34 mmol) in 100 mL CH_2Cl_2 stirring at 0 ℃ was treated with bromine (5.5 mL, 106 mmol) added using a syringe pump over the course of 2 h and then allowed to warm up to room temperature. After complete conversion by TLC (another 2 h), the mixture was quenched with 100 mL of 10% Na_2SO_3 and extracted with CH_2Cl_2 (100 mL×3). The combined organic mixture was washed with brine, dried over $MgSO_4$, and rotary evaporated to dryness. The resulting yellow oil was eluted with hexanes through a short silica gel column (6 cm H ×10 cm Ø). Evaporation gave the product as a white solid (10.2 g, 76% yield). **^{1}H NMR** (300 MHz, $CDCl_3$) δ 7.29-7.30 (m, 2H), 7.11-7.12 (m, 2H), 2.32 (s, 6H), 1.59 (s, 6H). ^{13}C NMR (75 MHz, $CDCl_3$) δ 145.30, 133.72, 131.69, 131.67, 131.38, 125.34, 110.48, 35.29, 31.84, 20.74. **IR** (cm^{-1}): 2953, 1441, 1296, 1257, 1096, 901, 847, 789, 734, 556; **HRMS** (ESI-TOF) m/z: calcd for $[C_{17}H_{16}Br_2O + Na]^+$, 418.9617 ; found, 418.9433. **mp:** 158-160 ℃.

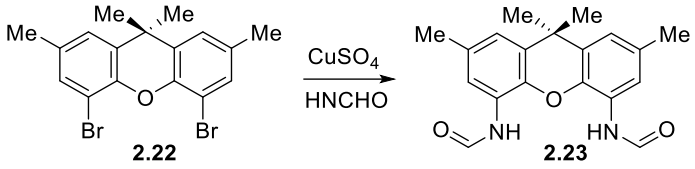

2.22 2.23

2.4.1c. N,N'-(2,7,9,9-tetramethyl-9H-xanthene-4,5-diyl)diformamide (2.23).[26]

A mixture of **S-5** (1.18 g, 3.2 mmol), anhydrous $CuSO_4$ (1.2 g, 7.5 mmol), $K_2CO_3 \cdot 1.5\ H_2O$ (12.5 mmol) and formamide (30 mL) was stirred at 160 ℃ for 8 h in a 100 mL round bottom flask equipped with a reflux condenser. After cooling to room temperature, the reaction mixture was poured into saturated aqueous NH_4Cl (100 mL) and CH_2Cl_2 (150 mL). The entire mixture (including the aqueous phase) was filtered through Celite. The Celite cake was rinsed with THF (200 mL). The combined filtrate was washed with saturated aqueous NH_4Cl and extracted with CH_2Cl_2 (200 mL ×3). The organic phase was dried with Na_2SO_4 and rotary evaporated. The residue was purified by flash chromatography (hexane/acetone 2:1) to afford the product as a white solid (768 mg, 74% yield). **^{1}H NMR** (300 MHz, $CDCl_3$) δ 10.85 - 10.89 (d, 1H, J = 9 Hz, -CHO), 10.58 - 10.61 (d, 1H, J = 9 Hz, -CHO), 9.78 (s, 1H, -NH), 8.83 - 8.97 (m, 2H, -NH), 8.54 - 8.55 (d, 1H, J = 3 Hz, aromatic), 8.17-8.18 (d, 1H, J = 3 Hz, aromatic), 6.94 - 7.07 (m, 5H, aromatic), 3.36 (s, 3H), 2.36 (s, 6H), 1.63 (s, 3H), 1.62 (s, 6H). **^{13}C NMR** (75 MHz, $CDCl_3$): δ 165.06, 164.01, 159.88, 138.21, 137.93, 136.95, 132.96, 132.94, 132.91, 131.08, 130.56, 129.12, 125.34, 125.32, 124.52, 123.40, 122.69, 121.44, 119.96, 116.83, 116.52, 34.16, 32.58, 32.42, 21.36, 21.17, 21.15. **IR** (cm^{-1}): 1675, 1614, 1536, 1416, 1289, 1226, 1173, 854 718, 622, 579, 509; **HRMS** (ESI-TOF) m/z: calcd for $[C_{19}H_{20}N_2O_3 + Na]^+$, 347.1366; found, 347.1362. **mp:** 235-237 ℃ (dec).

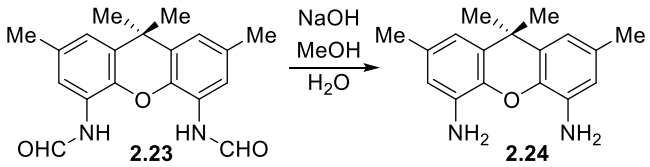

2.4.1d. 2,7,9,9-tetramethyl-9H-xanthene-4,5-diamine (2.26). A mixture of **2.23** (507 mg, 1.56 mmol) and EtOH (3 mL) was treated with aqueous NaOH (500 mg, 12.5 mmol in 1 mL H_2O) and refluxed for 1 h, at which time TLC analysis indicated full conversion. After cooling to room temperature, the mixture was diluted with EtOAc (20 mL), poured into brine, and extracted with EtOAc (20 mL ×3). The combined organic phase was washed with brine, dried with Na_2SO_4 and rotary evaporated to dryness. The residue was recrystallized from hexane to afford the product as a white powder (376.5 mg, 90% yield). **^{1}H NMR** (300 MHz, $CDCl_3$) δ 6.62 (s, 2H), 6.48 (s, 2H), 3.64 (br s, 4H), 2.26 (s, 6H), 1.58 (s, 6H). **^{13}C NMR** (151 MHz, $CDCl_3$) δ 136.48, 133.95, 131.93, 129.92, 116.00, 114.26, 34.05, 31.88, 21.11, 21.08. **IR** (cm-1):1625, 1476, 1273, 1212, 1165, 1031, 831, 554, **HRMS** (ESI-TOF) m/z: calcd for $[C_{17}H_{20}N_2O + H]^+$, 269.1648; found, 269.1643. **mp:** 50 ℃.

2.4.2. Synthesis and reduction of model compound 2.27.

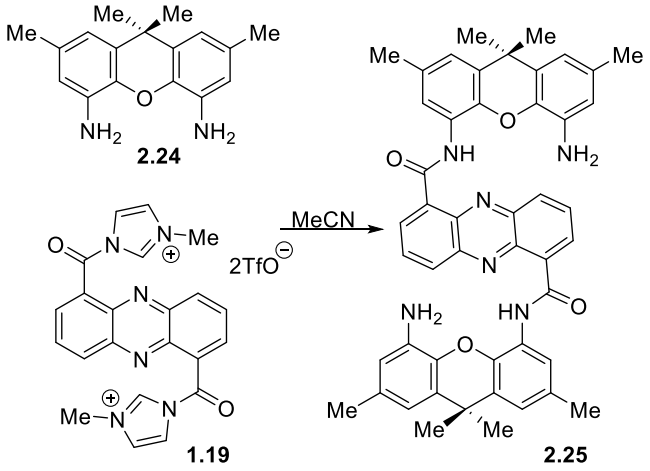

2.4.2a. N1,N6-bis(5-amino-2,7,9,9-tetramethyl-9H-xanthen-4-yl)phenazine-1,6-dicarboxamide (2.25). To a solution of **2.24** (1.94 g, 5.2 mmol) in 5 mL MeCN stirring at room temperature was slowly added a solution of **1.19** (1.81 g, 2.6 mmol) in 3 mL MeCN. Orange-red precipitate was observed almost immediately. After stirring for 12 h, the precipitate was separated by centrifugation, washed repeatedly with MeCN (7×5 mL), and dried under vacuum. The product thus obtained was essentially pure (1.62 g, 81% yield). **^{1}H NMR** (600 MHz, $CDCl_3$) δ 12.96 (s, 2H), 9.19 - 9.20 (d, 2H, J = 6 Hz), 8.67-8.69 (d, 2H, J = 6 Hz), 8.14 (s, 2H), 8.08 - 8.10 (t, 2H, J = 6 Hz), 7.09 (s, 2H), 6.68 (s, 2H), 6.40 (s, 2H), 2.44 (s, 6H), 2.28 (s, 6H), 1.70 (s, 12H). **^{13}C NMR** (151 MHz, $CDCl_3$) δ 162.14, 141.43, 140.56, 140.09, 137.01, 136.62, 134.18, 134.10, 132.88, 132.31, 131.43, 130.85, 130.63, 129.57, 125.64, 122.14, 121.55, 115.47, 114.08, 34.62, 31.52, 21.48, 21.20. **IR** (cm^{-1}): 1734, 1540, 1473, 1363, 748; **HRMS** (APCI-TOF) m/z: calcd for $[C_{48}H_{44}N_6O_4 + H]^+$: 769.3497, found: 769.3646. **mp:** >300 ℃.

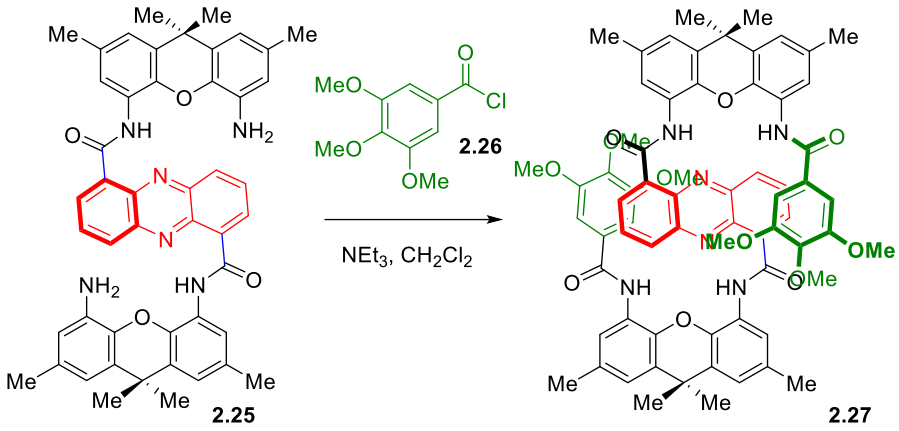

2.4.2b. N1,N6-bis(2,7,9,9-tetramethyl-5-(3,4,5-trimethoxybenzamido)-9H-xanthen-4-yl)phenazine-1,6-dicarboxamide (2.27). A suspension of **10** (116 mg, 0.15 mmol) in CH_2Cl_2 was treated successively with NEt_3 (45 µL, 0.33 mmol) and 3,4,5-trimethoxybenzoyl chloride **11** (77 mg, 0.33 mmol) added slowly at room temperature. TLC indicated complete conversion in 2 h. The mixture was quenched with saturated aqueous K_2CO_3 and extracted with CH_2Cl_2. The organic phase was rotary evaporated. A mixture of the crude product with 80 mL of saturated aqueous K_2CO_3 was refluxed for 2 h, allowed to cooling down to room temperature overnight, and then extracted with 100 mL of CH_2Cl_2. The organic extract was dried over $MgSO_4$ and rotary evaporated. The residue was recrystallized from acetone to afford essentially pure **2.27** (107 mg, 62% yield). **^{1}H NMR** (300 MHz, CD_2Cl_2) δ 13.21 (s, 2H), 9.13 - 9.16 (d, 2H, J=6 Hz), 8.33 (s, 2H), 8.26-8.28 (d, 2H, J=6 Hz), 8.13 (s, 2H), 8.01 - 8.06 (t, 2H, J=6 Hz), 7.20 (s, 2H), 7.14 (s, 2H), 5.84 (s, 4H), 3.45 (s, 6H), 3.25 (s, 12H), 2.53 (s, 6H), 2.41 (s, 6H), 1.75 (s, 12H). **^{13}C NMR** (126 MHz, CD_2Cl_2) δ 206.91, 164.54, 161.98, 152.32, 140.99, 140.16, 140.07, 139.97, 138.82, 137.12, 134.06, 133.87, 133.68, 132.10, 131.65, 131.24, 129.50, 128.98, 126.66, 126.52, 122.38, 121.69, 121.46, 119.74, 102.74, 60.14, 56.08, 35.33, 31.62, 31.14, 21.97,

21.83. **IR** (cm^{-1}): 3423, 1556, 1501, 1419, 1333, 1211, 1126, 855, 749, 569. **HRMS** (APCI-TOF) m/z: calcd for $[C_{68}H_{64}N_6O_{12}+H]^+$: 1157.4655, found 1158.4810. **mp:** >300 ℃.

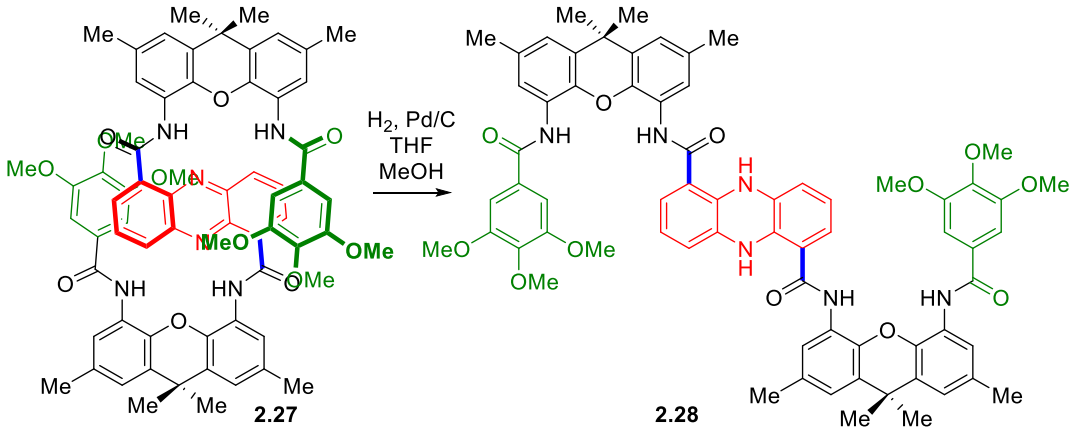

2.4.2c. N1,N6-bis(2,7,9,9-tetramethyl-5-(3,4,5-trimethoxybenzamido)-9H-xanthen-4-yl)-5,10-dihydro-phenazine-1,6-dicarboxamide (2.28). Compound 2.27 (30 mg, 0.026 mmol) was hydrogenated using 10 wt% Pd/C (5 mg, 0.005 mmol), 0.7 mL of THF and 0.7 mL of MeOH at 20 psi for 18 h as described above for 6. The solution of the product in $CDCl_3$ was stable when kept in an NMR tube sealed under argon. Upon deliberate exposure to air, however, it underwent over 90% oxidation within 20 min. ^{1}H NMR (600 MHz, $CDCl_3$) δ 8.88 (s, 2H), 8.03 (s, 2H), 7.93 (s, 2H), 7.67 - 7.69 (m, 4H), 7.06 (m, 4H), 7.02 (s, 4H), 6.26 - 6.27 (t, 2H, J = 6 Hz), 5.83 - 5.84 (d, 2H, J = 6 Hz), 5.47 - 5.48 (t, 2H, J = 6 Hz), 3.88 (s, 6H), 3.83 (s, 12H), 2.39 (s, 6H), 2.37 (s, 6H), 1.64 (s, 12H). ^{13}C NMR (151 MHz, $CDCl_3$) δ 166.39 - 166.50 (dd, J_1 = 4.5 Hz, J_2= 12 Hz), 165.71 - 165.79 (d, J = 12 Hz), 153.34, 141.26, 139.26 - 139.40 (d, J_1 = 9 Hz, J_2 = 4.5 Hz), 136.73 - 136.89 (d, J = 24 Hz), 133.53 - 133.62 (d, J= 13.5 Hz), 132.83 - 132.87 (d, J = 6 Hz), 130.87, 130.61, 130.47, 129.97, 128.79, 124.57 - 124.94 (dd, J_1 = 47 Hz, J_2 = 4 Hz), 122.53 - 122.73 (dd, J_1 = 24 Hz, J_2 = 6 Hz), 121.44 - 121.87 (dd, J = 20 Hz), 119.66, 117.51, 114.14 - 114.23 (d, J = 11 Hz), 111.63, 104.38, 60.81, 56.17, 34.50, 31.87, 21.40, 21.31.

2.4.3. Attempted direct synthesis of phenazine oligomers.

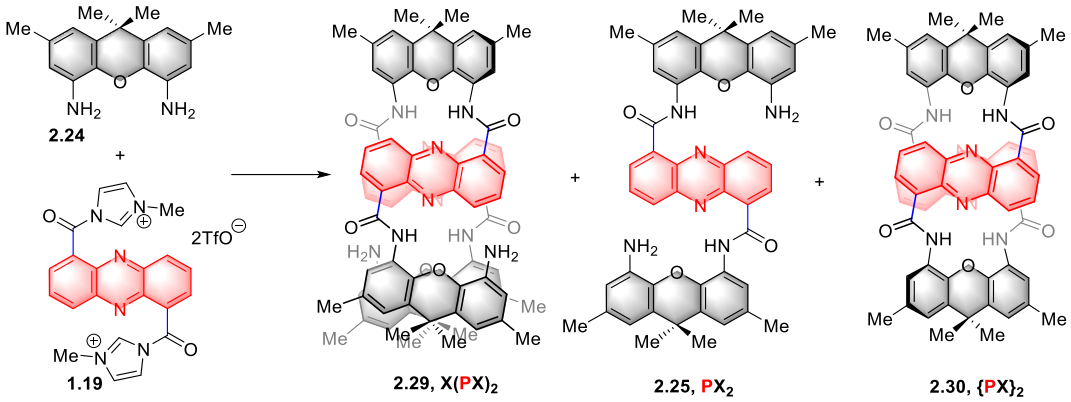

To a solution of **2.24** (20 mg, 0.075 mmol) in 10 mL CH_2Cl_2, a solution of freshly prepared **1.19** (52 mg, 0.075 mmol) in 10 mL acetonitrile was added dropwise at rt. After 30 min, TLC analysis indicated full conversion. The reaction was washed with 20 mL saturated K_2CO_3. The organic layer was dried with Na_2SO_4 and rotary evaporated to dryness. ^{1}H NMR analysis of the crude mixture indicated that the three products shown were present in approximately equal quantities. The crude mixture was diluted in $CDCl_3$, injected into preparative GPC, and eluted with $CHCl_3$. Fraction 5 yielded amber solid **2.29** (3 mg, 10% yield), fraction 2 yielded amber solid **2.25** (4 mg, 14% yield) and fraction 4 yielded amber solid **2.30** (1 mg, 1%).

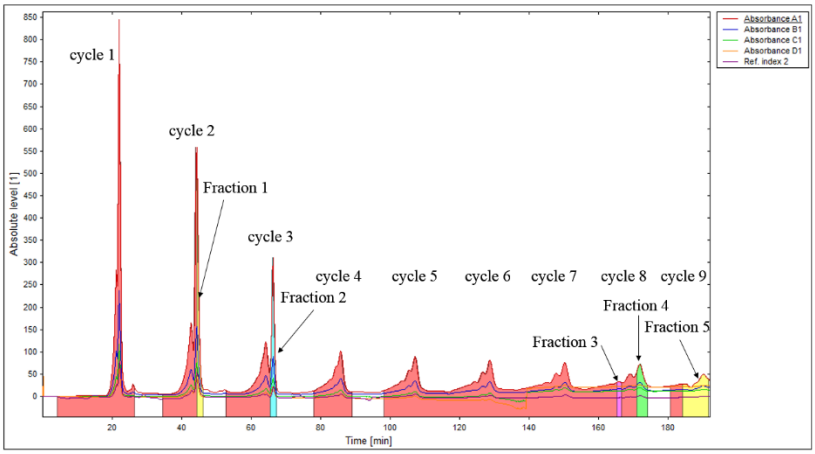

2.29: ^{1}H NMR (600 MHz, $CDCl_3$) δ 12.88 (s, 2H), 11.92 (s, 2H), 9.05 - 9.06 (d, J = 6 Hz, 2H), 8.34 (s, 2H),), 8.29 - 8.31 (d, J = 6 Hz, 2H), 8.18 - 8.21 (t, J = 6 Hz, 2H), 8.12 - 8.13 (d, J = 6 Hz, 2H), 8.02 - 8.04 (t, J = 6 Hz, 2H), 7.67 - 7.69 (t, J = 6 Hz, 2H), 7.21 (s, 2H), 7.09 (s, 2H), 6.57 (s, 2H), 5.85 (s, 2H), 1.50 (s, 12H), 2.50 (s, 6H), 2.46 (s, 6H), 2.16 (s, 6H), 1.86 (s, 6H). **^{13}C NMR** (151 MHz, $CDCl_3$) δ 161.92, 161.42, 140.21, 139.56, 139.31, 138.91, 138.83, 138.02, 136.87, 136.04, 135.84, 133.77, 133.65, 133.11, 132.68, 132.28, 132.07, 130.65, 130.47, 130.20, 129.99, 129.78, 127.30, 125.90, 125.29, 122.71, 122.57, 121.65, 121.26, 115.57, 114.04, 94.78, 34.50, 34.35, 32.21, 31.52, 29.70, 21.57, 21.51, 21.02. **IR (cm^{-1}):** 1697.2, 1551.6, 1448.4, 750.8. **MALDI-TOF** m/z: calcd for $[C_{79}H_{69}N_{10}O_7 + Na]^+$, 1292.524; found, 1291.806; calcd for $[C_{79}H_{69}N_{10}O_7 + K]^+$, 1308.498; found, 1308.325.

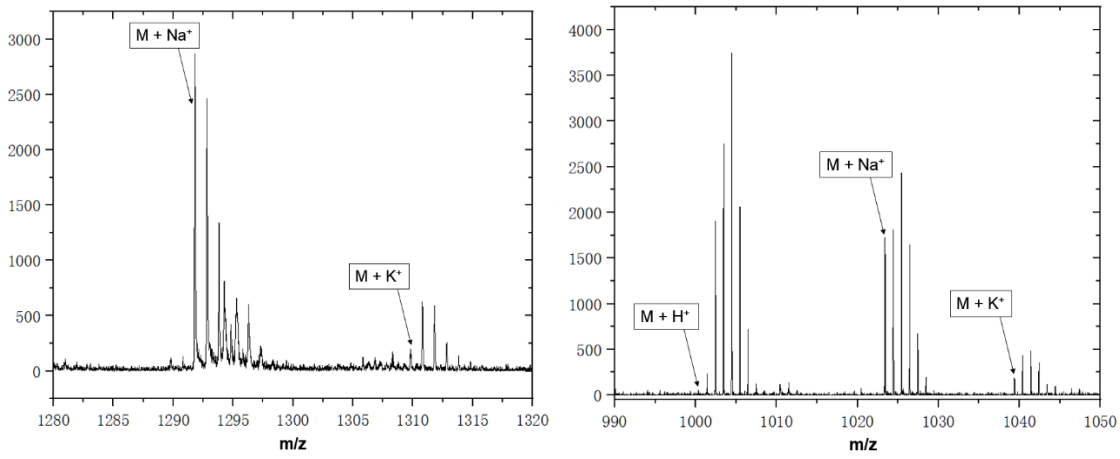

2.25: ^{1}H NMR (600 MHz, $CDCl_3$) δ 13.24 (s, 2H), 9.25 - 9.26 (d, J = 6 Hz, 2H), 8.48 - 8.49 (s, J = 6 Hz, 2H), 8.09 - 8.10 (d, J = 6 Hz, 2H), 8.09 (s, 2H), 7.88 (s, 2H), 7.12 (s, 4H), 6.95 (s, 4H), 2.46 (s, 6H), 2.37 (s, 6H), 1.72 (s, 12H). The data matched those previously described for this compound.

2.30: **^{1}H NMR** (600 MHz, $CDCl_3$) δ 12.21 (s, 4H), 8.29 - 8.30 (d, J = 6 Hz, 4H), 8.20 - 8.21 (d, J = 6 Hz, 4H), 7.73 (s, 4H), 7.65 - 7.68 (t, J = 6 Hz, 4H), 7.22 (s, 4H), 2.45 (s, 12H), 1.26 (s, 12H). **IR (cm^{-1}):** 1683.4, 1576.4, 1467.1, 754.2. MALDI-TOF m/z: calcd. for $[C_{62}H_{48}N_8O_6 + H]^+$, 1001.378, found 1001.441; calcd. for $[C_{62}H_{48}N_8O_6 + Na]^+$, 1023.359, found 1023.397; calcd. for $[C_{62}H_{48}N_8O_6 + K]^+$, 1039.333, found 1039.391.

2.4.4. Independent synthesis of cyclic dimer 2.30.

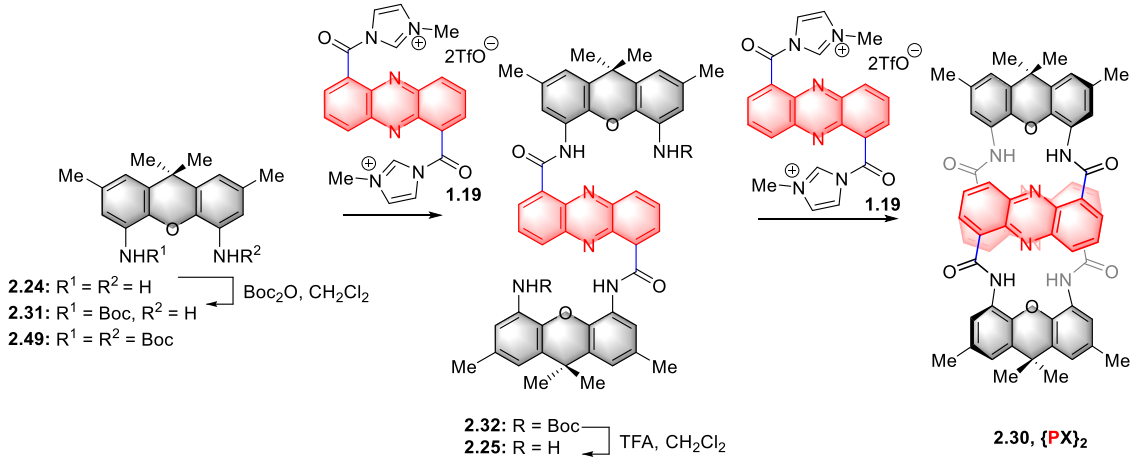

Note: *The synthesis of PX_2* ***15*** *described below, while less direct than the one originally reported,[1] provides the product with more consistent quality and therefore has been preferred in this study.*

3a. ***Preparation of XBoc 2.31.*** To a solution of **2.24** (500 mg, 1.87 mmol) in 10 mL CH_2Cl_2 stirring at rt was added Boc_2O (420 mg, 1.96 mmol) and 2 µL AcOH. After 4 hours, the reaction was quenched by 1 mL aqueous ammonia, then washed with 10 mL saturated NaCl. The combined organic layer was dried with Na_2SO_4 and rotary evaporated to dryness. The product **2.31** (350 mg, 51% yield) was obtained via flash chromatography (hexane/acetone 20:1 to 5:1). The starting material **2.24** (120 mg, 24% yield) and its N,N'-di-Boc derivative **2.49** (70 mg, 15% yield) were also recovered.

2.31: **^{1}H NMR** (600 MHz, $CDCl_3$) δ 7.75 (s, 1H), 6.93 (s, 1H), 6.87 (s, 1H), 6.64 (s, 1H), 6.51 (s, 1H), 3.83 (br, 2H), 2.33 (s, 6H), 2.27 (s, 6H), 1.57 (s, 12H), 1.54 (s, 18H). **^{13}C NMR** (151 MHz, $CDCl_3$) δ 152.8, 137.3, 136.3, 133.8, 132.6, 132.2, 130.2, 129.7, 125.9, 120.1, 117.8, 116.3, 114.7, 80.6, 34.2, 31.9, 28.4, 21.4, 21.2. **IR (cm^{-1}):** 2359.5, 2160.1, 1736.4, 1558.7, 1540.7, 1507, 1229.4 1157.2. **HRMS** (ESI - TOF) m/z: calcd for $[C_{22}H_{28}N_2O_3 + H]^+$, 369.2100; found, 369.2120. mp: 54 ºC.

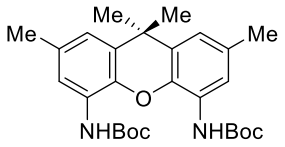

2.49: **^{1}H NMR** (500 MHz, $CDCl_3$) δ 7.76 (s, 2H), 6.89 - 6.86 (d, J = 7.5 Hz, 2H), 6.86 (s, 2H), 2.34 (s, 6H), 1.57 (s, 6H), 1.56 (s, 18H). **^{13}C NMR** (126 MHz, $CDCl_3$) δ 152.69, 137.09, 132.70, 129.72, 125.74, 120.23, 118.20, 80.57, 34.27, 31.87, 28.36, 21.42. **IR (cm^{-1}):** 1780, 1590.7, 1120.2. **HRMS** (ESI - TOF) m/z: calcd for $[C_{27}H_{36}N_2O_5 + H]^+$, 469.2702; found, 469.2717. mp: 71 ºC.

3b. ***Preparation of P(XBoc)$_2$ 2.32*****.** To a solution of **2.31** (368 mg, 1.00 mmol) in 5 mL CH_2Cl_2, a solution of freshly prepared **1.19** (335 mg, 0.500 mmol) in 10 mL acetonitrile was added at rt. After 30 min, TLC analysis indicated full conversion. The reaction was diluted with 40 mL of CH_2Cl_2 and washed with 20 mL saturated aqueous K_2CO_3. The organic layer was dried with Na_2SO_4 and rotary evaporated to dryness. The product was obtained as a reddish-orange powder (470 mg, 97% yield).**^{1}H NMR** (600 MHz, $CDCl_3$) δ 13.24 (s, 2H), 9.25 - 9.26 (d, J = 6Hz, 6H), 8.48 - 8.49 (d, J = 6Hz, 6H), 8.09 - 8.10 (m, 4H), 7.88 (s, 2H), 7.12 (s, 4H), 6.95 (s, 2H), 2.46 (s, 6H), 2.37 (s, 6H), 1.72(s, 12H), 1.55(s, 30H). **^{13}C NMR** (151 MHz, $CDCl_3$) δ 161.9, 151.8, 141.7, 140.5, 140.0, 137.2, 136.9, 133.2, 133.0, 131.9, 130.7, 130.4, 129.3, 126.4, 125.6, 122.3, 121.8, 119.4, 116.8, 34.7, 31.5, 27.4, 21.6, 21.5. **IR (cm^{-1}):** 1680.2, 1531, 1425.4, 1261.1, 1156.6, 750.8. **HRMS** (ESI - TOF) m/z: calcd for $[C_{58}H_{60}N_6O_8 + Na]^+$, 991.4365; found, 991.4370.

3c. ***Preparation of PX₂ 2.25.*** To a solution of **2.32** (97 mg, 0.10 mmol) in 20 mL CH_2Cl_2, 20 mL TFA was added. The reaction was left to stir for 30 minutes, at which time TLC analysis indicated full conversion. 10 mL saturated K_2CO_3 was added to the mixture, and the mixture was extracted with CH_2Cl_2 (20 mL × 3), dried with Na_2SO_4 and rotary evaporated to dryness. The residue was a light orange powder. (77 mg, 99% yield). **^{1}H NMR** data matched those of **2.25** obtained by the previously published method.[1]

3d. ***Preparation of {PX}₂ 2.30.*** To a mixture of **2.25** (77 mg, 0.10 mmol) and 20 mL CH_2Cl_2, **8** (69 mg, 0.10 mmol) in 5 mL acetonitrile was added slowly via syring pump over the course of 30 minutes. Then the reaction was left stirring for 1 h, at which time TLC analysis indicated full conversion. The mixture was quenched with 10 mL of saturated aqueous K_2CO_3 and extracted with CH_2Cl_2 (3×20 mL), dried with Na_2SO_4 and rotary evaporated to dryness. The residue was a light orange powder. (95 mg, 95% yield). 1H NMR (600 MHz, cdcl3) δ 12.21 (s, 4H), 8.29 - 8.30 (d, J = 6 Hz, 4H), 8.20 - 8.21 (d, J = 6 Hz, 4H), 7.73 (s, 4H), 7 .65 - 7.68 (t, J = 6 Hz, 4H), 7.22 (s, 4H), 2.45 (s, 12H), 1.26 (s, 12H). **MALDI-TOF** m/z: calcd. for $[C_{62}H_{48}N_8O_6 + H]^+$, 1001.378; found 1001.456.

2.4.5. Synthesis of macrocycle 2.38.

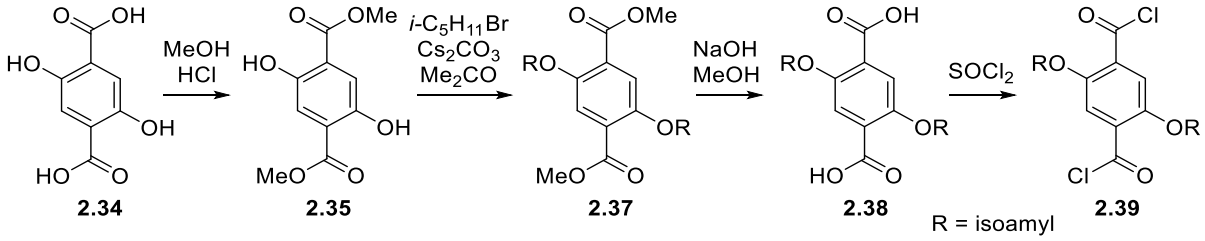

4a. Dimethyl 2,5-dihydroxyterephthalate 2.35. Prepared via a modified literature procedure.[35] A mixture of 2,5 - dihydroxyterephthalic acid (1.50 g, 7.57 mmol), 2 mL of conc. aqueous HCl, and 50 mL of MeOH was refluxed for 12 h. After cooling to room

temperature, the mixture was rotary evaporated to dryness to afford the crude product as a dark green solid (1.66 g, 97% yield) that was used in the next step without further purification. **^{1}H NMR** (600 MHz, CD_3CN) δ 10.07 (br, 2H), 7.69 (s, 2H), 4.27 - 4.29 (t, J = 6 Hz, 6H), 1.74 - 1.84 (m, 6H), 0.98 - 0.99 (d, J = 6 Hz, 12H). **^{13}C NMR** (151 MHz, CD_3CN) δ 165.6, 152.6, 124.5, 117.7, 70.3, 38.3, 25.9, 22.8. mp: 142 ^{o}C.

4b. Dimethyl 2,5-bis(isoamyloxy)terephthalate 2.37. A mixture of the crude **2.35** (1.66 g, 7.34 mmol), Cs_2CO_3 (11.96 g, 36.7 mmol), isoamyl bromide (2.20 mL, 18.4 mmol), and 50 mL acetone was refluxed for 18 h. After cooling to rt, the mixture was filtered and rotary evaporated to give the product as a yellow oil (2.53 g, 94% yield). **^{1}H NMR** (500 MHz, $CDCl_3$) δ 7.36 (s, 2H), 4.02 - 4.05 (t, J = 7.5 Hz, 2H), 3.90 (s, 3H), 1.81 - 1.89 (m, 2H), 1.68 - 1.72 (dd, J = 10 Hz, 4H), 0.95 - 0.96 (d, J = 5 Hz, 12H). **^{13}C NMR** (126 MHz, $CDCl_3$) δ 166.3, 151.8, 124.4, 116.6, 68.4, 52.2, 37.9, 25.1, 22.6. **IR (cm^{-1}):** 2955.1, 2359.8, 1737.3, 1457.1, 1383.1, 1206.6. **HRMS** (ESI - TOF) m/z: calcd for $[C_{20}H_{30}O_6 + Na]^{+}$, 389.1935; found, 389.1977.

4c. 2,5-Bis(isoamyloxy)terephthalic acid 2.38. A mixture of **2.37** (2.53 g, 6.90 mmol) and MeOH 10 mL was treated with aqueous NaOH (2.8 g, 69 mmol in 10 mL) and refluxed for 12 h. After cooling to room temperature, the mixture was acidified with HCl (37%) to pH 1 and diluted with CH_2Cl_2 (40 mL). The aqueous phase was extracted with CH_2Cl_2 (40 mL × 3) and the combined organic phase was washed with brine, dried with Na_2SO_4 and rotary evaporated to dryness. The residue was a white crystal (2.41 g, 90% yield). **^{1}H NMR** (600 MHz, CD_3CN) δ 10.69 (br, 2H), 7.69 (s, 2H), 4.27 - 4.29 (t, J = 6 Hz, 6H), 1.79 - 1.85 (m, 2H), 1.74 - 1.77 (dd, J = 6 Hz, 4H), 0.98 - 0.99 (d, 12H). **^{13}C NMR** (126 MHz, $CDCl_3$) δ 165.9, 152.9, 124.9, 118.7, 118.0, 70.6, 38.7, 26.2, 23.1. **IR (cm^{-1}):**

2953, 1720.5, 1382.2, 1195.6, 1000, 781.5, 737. **HRMS** (ESI - TOF) m/z: calcd for $[C_{18}H_{26}O_6 + Na]^+$, 361.1627; found, 361.1579.

4d. 2,5-Bis(isoamyloxy)terephthaloyl dichloride 2.39. A mixture of **2.38** (2.41 g, 6.21 mmol), $SOCl_2$ (2.26 mL, 31.05 mmol) and 40 mL CH_2Cl_2 was refluxed for 6 h. After cooling to room temperature, the mixture was rotary evaporated to dryness, resulting yellow green solid (2.31 g, 99% yield). **^{1}H NMR** (600 MHz, $CDCl_3$) δ 7.49 (s, 2H), 4.08 - 4.10 (t, J = 6 Hz, 4H), 1.84 - 1.90 (m, 2H), 1.71 - 1.74 (m, 4H), 0.96 - 0.97 (d, J = 6 Hz, 12H). **^{13}C NMR** (151 MHz, $CDCl_3$) δ 163.60, 151.09, 128.38, 116.99, 68.44, 37.55, 24.83, 22.49, 22.46.

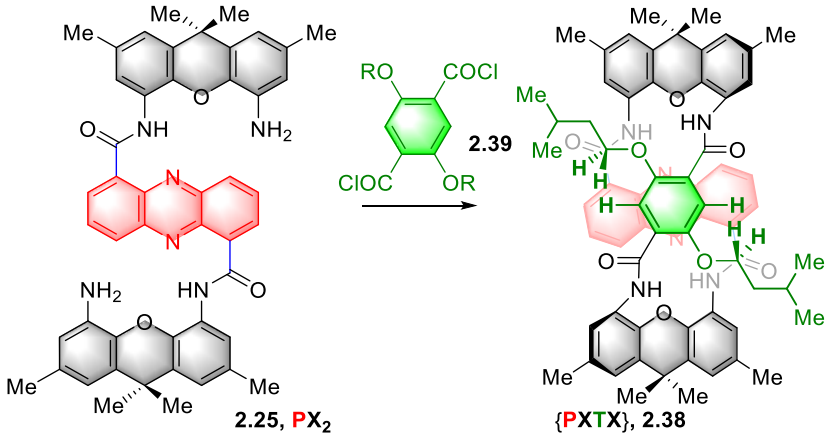

4e. Preparation of Macrocycle 24 from PX_2 2.25. To a solution of **2.25** (77 mg, 0.10 mmol) and Et_3N (42 µL, 0.3 mmol) in 5 mL CH_2Cl_2 stirring at rt was added acyl chloride **2.38** (38 mg, 0.10 mmol) in 2 mL CH_2Cl_2. After 30 min, the reaction mixture was washed with saturated aqueous K_2CO_3, then water, aqueous phase was extracted with CH_2Cl_2 and combined organic extracts were dried over Na_2SO_4. Rotary evaporation yielded an amber solid (100 mg, 94% yield). **^{1}H NMR** 12.92 (s, 2H), 9.97 (s, 2H), 9.09 - 9.10 (d, J = 6 Hz, 2H), 8.10 - 8.12 (d, J = 6 Hz, 2H), 7.97 - 7.99 (t, J = 6 Hz, 2H), 7.11 (s,

2H), 6.23 (s, 2H), 3.64 - 3.67 (dd, J = 6 Hz, 2H), 3.55 - 3.59 (dd, J = 6 Hz, 2H), 2.46 (s, 6H), 2.43 (s, 6H), 1.76 - 1.77 (d, 12H), 1.48 - 1.56 (m, 4H), 1.36 - 1.40 (m, 2H), 0.59 - 0.61 (t, J = 6 Hz, 12H). **^{13}C NMR** (151 MHz, $CDCl_3$) δ 161.63, 161.58, 149.19, 140.99, 139.89, 139.71, 137.56, 136.50, 133.17, 133.04, 133.01, 131.71, 129.91, 129.75, 129.08, 125.83, 125.63, 122.20, 121.59, 121.33, 119.14, 113.14., 68.28, 37.36, 34.68, 32.89, 31.30, 24.68, 22.50, 21.76, 21.61, 21.52. **IR (cm^{-1}):** 2000, 1987.8, 1634.7, 1570.1, 1407.2, 713.0. **MALDI-TOF** m/z: calcd for $[C_{66}H_{66}N_6O_8 + H]^+$, 1071.502; found, 1071.610**.**

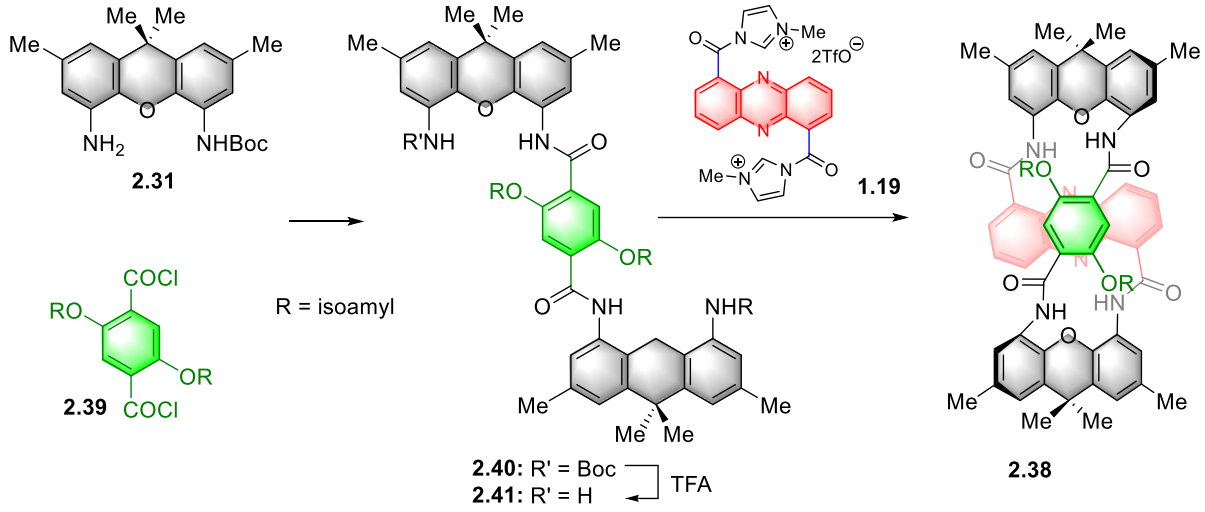

4f. Preparation of 2.40. To a solution of **2.31** (37 mg, 0.10 mmol) and 100 µL Et_3N in 5 mL CH_2Cl_2 stirring at rt was added a solution of acyl chloride **2.39** (19 mg, 0.05 mmol) in 5 mL CH_2Cl_2. After 1 h, the reaction mixture was washed with saturated aqueous K_2CO_3, then water, aqueous phase was extracted with CH_2Cl_2 and combined organic extracts were dried over Na_2SO_4. Rotary evaporation yielded white solid (90 mg, 85% yield). **^{1}H NMR** (500 MHz, $CDCl_3$) δ 10.64 (s, 2H), 8.17 (s, 2H), 8.10 (s, 2H), 7.96 (s, 2H), 7.20 (s, 2H), 7.04 (s, 2H), 6.90 (s, 2H), 4.46 - 4.49 (t, J = 5 Hz, 2H), 2.41 (s, 6H), 2.36 (s, 6H), 1.73 - 1.82 (m, 6H), 1.62 (s, 12H), 1.44 (s, 18H), 0.82 - 0.83(d, J = 5 Hz, 12H). **^{13}C**

NMR (126 MHz, $CDCl_3$) δ 161.72, 152.61, 151.24, 138.82, 136.69, 132.98, 132.82, 130.40, 130.13, 126.19, 125.76, 125.36, 121.74, 120.67, 119.41, 117.90, 117.25, 80.74, 70.04, 37.70, 34.61, 34.50, 31.53, 31.28, 28.45, 24.95, 22.59, 22.27, 21.51, 21.42. **IR (cm^{-1}):** 359.5, 1422.7, 1275.5, 750.1, 668.8. **HRMS** (ESI - TOF) m/z: calcd for $[C_{62}H_{78}N_4O_{10} + Na]^+$, 1061.5610, found 1061.5688.

4g. Preparation of TX_2 2.41. A solution of **2.40** (103 mg, 0.1 mmol) in 5 mL CH_2Cl_2 stirring at rt was treated with 5 mL TFA. After 30 min, the reaction mixture was diluted with 5 mL CH_2Cl_2 and quenched by slow addition of 5 mL saturated aqueous Na_2CO_3. The resulting mixture was extracted with CH_2Cl_2 (10 mL × 3) and the extracts were dried over Na_2SO_4. The mixture was rotary evaporated to yield amber solid (83 mg, >99% yield). **^{1}H NMR** (500 MHz, $CDCl_3$) δ 10.64 (s, 2H), 8.17 (s, 2H), 8.10 (s, 2H), 7.96 (s, 2H), 7.20 (s, 2H), 7.04 (s, 2H), 6.90 (s, 2H), 4.46 - 4.49 (t, J = 5 Hz, 2H), 2.41 (s, 6H), 2.36 (s, 6H), 1.73 - 1.82 (m, 6H), 1.62 (s, 12H), 1.44 (s, 18H), 0.82 - 0.83(d, J = 5 Hz, 12H). **^{13}C NMR** (126 MHz, $CDCl_3$) δ 161.72, 152.61, 151.24, 138.82, 136.69, 132.98, 132.82, 130.40, 130.13, 126.19, 125.76, 125.36, 121.74, 120.67, 119.41, 117.90, 117.25, 80.74, 70.04, 37.70, 34.61, 34.50, 31.53, 31.28, 28.45, 24.95, 22.59, 22.27, 21.51, 21.42. **HRMS** (ESI - TOF) m/z: calcd for $[C_{52}H_{62}N_4O_6 + H]^+$, 840.4776, found 893.4710. **IR (cm^{-1}):** 2360.41, 1738.30, 1542.30, 1449.50, 1217.53.

4h. Preparation of Macrocycle 2.38 from 2.41. To a solution of **2.41** (84 mg, 0.10 mmol) and 100 μL Et_3N in 5 mL CH_2Cl_2 stirring at rt a solution of **1.19** (70 mg, 0.10 mmol) in 5 mL CH_2Cl_2 was added dropwise. After 1 h, TLC indicated complete conversion. The reaction mixture was washed with saturated aqueous K_2CO_3, then water, aqueous phase was extracted with CH_2Cl_2 and combined organic extracts were dried over Na_2SO_4. Rotary

evaporation yielded white solid (99 mg, 93% yield). ^{1}H NMR spectrum was identical to that of **2.38** obtained from **2.25**.

2.4.6. Synthesis of interleafed oligomers.

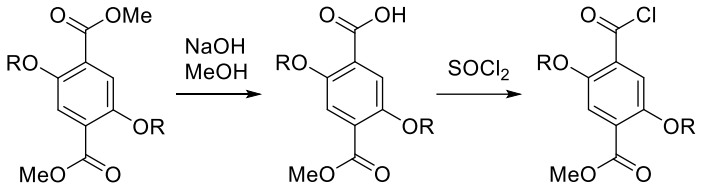

2.37 **2.38-OMe** **2.39-OMe**

5a. 4-carbomethoxy-2,5-bis(isoamyloxy)benzoic acid 2.38-OMe. A mixture of **2.37** (1.57 g, 4.3 mmol) prepared as described above, 20 mL MeOH, and aqueous KOH (0.28 g of 85% pellets, 4.3 mmol KOH in 5 mL H_2O) was stirred for 12 h at rt and monitored by TLC. Then the mixture was rotary evaporated to remove MeOH, acidified with 10 mL 1M HCl, and extracted with EtOAc (3×40 mL). The combined organic extract was dried over Na_2SO_4 and then evaporated to dryness. Flash chromatography (hexane/acetone 10:1 to 5:1) yielded the product as a yellow oil (864 mg, 57% yield). **^{1}H NMR** (500 MHz, $CDCl_3$) δ 7.71 (s, 2H), 7.41 (s, 2H), 4.22 - 4.24 (t, J = 7.5 Hz, 2H), 4.03 - 4.06 (t, J = 7.5 Hz, 2H), 3.88 (s, 3H), 1.74 - 1.84 (m, 4H), 1.65 - 1.69 (dd, J = 10 Hz, 2H), 0.92 - 0.97 (d, J = 9 Hz, 12H). **^{13}C NMR** (126 MHz, $CDCl_3$) δ 165.8, 164.5, 152.7, 150.5, 125.7, 121.1, 117.5, 115.7, 69.5, 68.1, 52.3, 37.7, 37.5, 25.0, 24.9, 22.4, 22.3. **IR (cm^{-1}):** 2955.9, 1739.5, 1419.0, 1214.0, 986.0. **HRMS** (ESI - TOF) m/z: calcd for $[C_{19}H_{28}O_6 + Na]^{+}$, 375.1778; found, 375.1734.

5b. 4-Carbomethoxy-2,5-bis(isoamyloxy)benzoyl chloride 2.39-OMe. A mixture of **2.38-OMe** (1.57 g, 4.30 mmol), $SOCl_2$ (1.57 mL, 21.5 mmol) and 40 mL CH_2Cl_2 was refluxed for 6 h. After cooling to room temperature, the mixture was rotary evaporated to dryness, to afford the product as a dark green oil (1.58 g, 99% yield). **^{1}H NMR** (600 MHz, $CDCl_3$) δ 7.52 (s,1H), 7.32 (s, 1H), 4.03 - 4.05 (m, 4H), 3.89 (s, 3H), 1.82 - 1.87 (m, 2H), 1.67 - 1.71 (m, 4H), 0.90 - 0.98 (m, 12H). **^{13}C NMR** (151 MHz, $CDCl_3$) δ 165.72, 163.34, 151.96, 151.03, 127.00, 125.73, 117.96, 115.82, 68.40, 68.11, 52.38, 52.36, 52.35, 52.33, 37.70, 37.58, 24.90, 24.75, 22.45, 22.38.

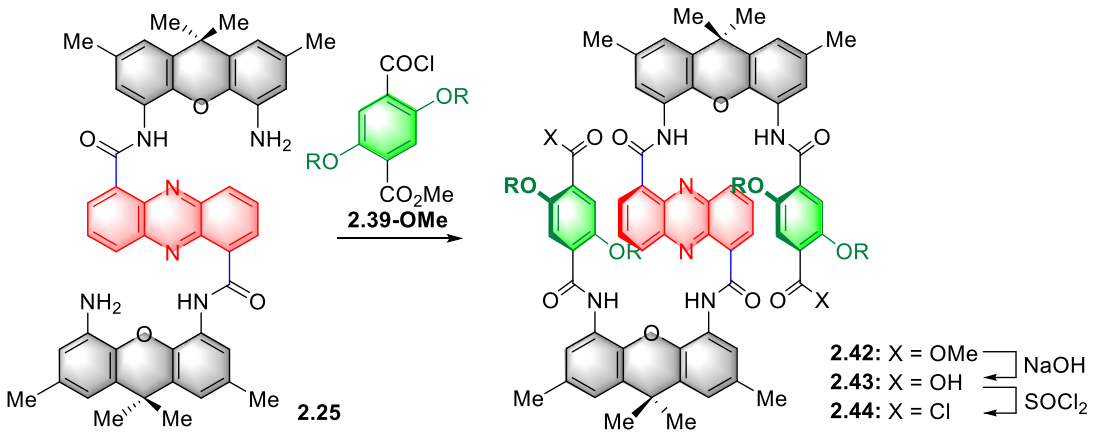

5c. Synthesis of P(XT)$_2$ Diester 2.42. To a suspension of **2.25** (300 mg, 0.400 mmol) in 10 mL CH_2Cl_2 stirring at rt was added Et_3N (168 µL, 0.300 mmol) followed by acyl chloride **27** (594 mg, 1.60 mmol) in 10 mL CH_2Cl_2. After 30 min, the reaction mixture was rotary evaporated to dryness, and the residue was washed with acetonitrile (10 mL × 3). The acetonitrile rinses were discarded. The remaining orange solid was dried (480 mg, 87% yield). **^{1}H NMR** (600 MHz, CD_2Cl_2) δ 13.07 (s, 2H), 9.78 (s, 2H), 8.99 - 9.00 (d, J = 6 Hz 2H), 8.33 (s, 2H), 8.15 - 8.18 (m, 4H), 7.91 - 7.94 (d, J = 6 Hz 2H), 7.16 (s, 2H), 7.13 (s, 2H), 6.66 (s, 2H), 5.45 (s, 2H), 3.99 - 4.02 (m, 4H), 3.73 - 3.76 (m, 2H), 3.18 (s, 3H),

2.92 - 2.96 (m, 2H), 2.74 - 2.77 (m, 2H), 2.52 (s, 6H), 2.41 (s, 6H), 1.87 - 1.93 (m, 4H), 1.75 - 1.81 (m, 14H), 1.30 - 1.37 (m, 4H), 1.15 - 1.18 (m, 2H), 1.00 - 1.06 (m, 12H). **^{13}C NMR** (151 MHz, CD_2Cl_2) δ 166.40, 161.95, 161.78, 152.31, 147.60, 140.86, 139.62, 139.54, 138.51, 136.11, 134.17, 133.21, 133.07, 131.43, 130.58, 130.26, 129.87, 126.58, 126.45, 125.79, 122.89, 122.71, 122.52, 122.34, 120.58, 115.18, 114.37, 69.52, 68.06, 54.36, 54.18, 54.00, 53.82, 53.64, 51.80, 38.61, 37.72, 37.63, 34.96, 33.80, 31.88, 25.69, 25.15, 23.53, 22.81, 22.63, 21.91, 21.83. **IR (cm^{-1}):** 2956.51, 1673.29, 1559.55, 1435.39, 1226.80, 1051.34. **HRMS** (ESI - TOF) m/z: calcd for $[C_{86}H_{98}N_6O_{14} + H]^+$, 1437.7057; found, 1437.7064.

5d. Synthesis of P(XT)$_2$ Diacid 2.43. A solution of TXPXT Diester **2.42** in 10 mL of 1,4-dioxane was mixed with a solution of KOH (99 mg of 85% pellets, 1.5 mmol) in aqueous MeOH (10 mL MeOH/1 mL H_2O). The mixture was heated to 60 ^oC for 12 h, at which time TLC analysis indicated full conversion. The mixture was rotary evaporated to dryness, acidified with 10 mL 1 M HCl and extracted with CH_2Cl_2 (20 mL × 3). The combined organic extract was dried over Na_2SO_4 and evaporated to dryness to give the product as an orange power (190 mg, 93% yield) that was used in the next step without further purification. **^{1}H NMR** (500 MHz, $CDCl_3$) δ 12.86 (s, 2H), 10.52 (s, 2H), 9.86 (s, 2H), 9.04 - 9.05 (d, J = 5 Hz, 2H), 8.41 (s, 2H), 8.15 (s, 2H), 8.13 - 8.15 (d, J = 5 Hz, 2H), 7.99 - 8.02 (t, J = 5 Hz, 2H), 7.13 (s, 2H), 6.76 (s, 2H), 5.85 (s, 2H), 4.30 - 4.31 (m, 2H), 3.93 - 3.96 (m, 2H), 3.01 - 3.04 (m, 2H), 2.91 - 2.99 (m, 2H), 2.49 (s, 6H), 2.43 (s, 6H), 1.70 - 1.90 (m, 18H), 1.25 - 1.37 (m, 6H), 1.16 - 1.21 (m, 2H), 1.01 - 1.03 (m, 12H), 0.47 - 0.50 (m, 12H). **^{13}C NMR** (126 MHz, $CDCl_3$) δ 163.41, 161.28, 160.47, 150.73, 148.34, 140.37, 139.00, 138.61, 137.71, 136.03, 134.03, 132.65, 131.55, 130.29, 129.97, 129.03,

126.69, 125.65, 125.33, 122.35, 122.14, 120.43, 119.56, 115.80, 113.77, 69.51, 69.29, 37.62, 36.93, 34.55,32.99, 32.86, 31.58, 29.66, 25.03, 24.53, 22.85, 22.40, 22.20, 21.62, 21.52. **IR (cm^{-1}):** 2955.5, 2360.1, 1667.7, 1624.1, 1548.7, 1433.9, 1266.7, 1219.7, 1049.5, 852.9, 752.4. **HRMS** (ESI-TOF) m/z: calcd for $[C_{84}H_{92}N_6O_{14} + Na]^+$, 1431.6569; found 1431.6920.

5d. Synthesis of P(XT)$_2$ Bis-Acyl chloride 2.44. A solution of diacid **2.43** (70 mg, 0.050 mmol) in 3 mL CH_2Cl_2 was treated with oxalyl chloride (42 μL, 0.5 mmol) and 2 μL of DMF (catalyst). The reaction was left at rt for 16 h and rotary evaporated. The dry residue was triturated with EtOAc (10 mL × 3). The solution was decanted from the sticky solids on the bottom of the flask, transferred into another flask and rotary evaporated to dryness to give **2.44** as an orange solid (68 mg, 97% yield) that was used in the next step without further purification. **^{1}H NMR** (500 MHz, $CDCl_3$) δ 12.98 (s, 2H), 9.88 (s, 2H), 9.05 - 9.07 (d, J = 5 Hz, 2H), 8.30 (s, 2H), 8.24 (s, 2H), 8.20 - 8.22 (d, J = 5 Hz, 2H), 7.99 - 8.00 (t, J = 5 Hz, 2H), 7.14 (s, 2H), 6.74 (s, 2H), 4.03 - 4.06 (m, 2H), 3.76 - 3.79 (m, 2H), 2.83 - 2.89 (m, 2H), 2.96 - 3.01 (m, 2H), 2.50 (s, 6H), 2.43 (s, 6H), 1.70 - 1.90 (m, 18H), 1.37 (m, 6H), 1.20 - 1.24 (m, 2H), 1.15 - 1.17 (m, 2H), 0.96 - 1.03 (m, 12H), 0.48 - 0.49 (m, 12H). **^{13}C NMR** (126 MHz, $CDCl_3$) δ 162.26, 160.99, 160.63, 152.23, 146.75, 140.31, 139.08, 138.94, 135.84, 133.64, 132.82, 132.72, 131.45, 129.54, 129.43, 127.30, 125.58, 125.33, 124.04, 122.23, 121.90, 120.04, 116.99, 115.47, 114.21, 53.40, 37.71, 37.56, 36.89, 34.53, 33.03, 24.88, 24.84, 24.54, 23.05, 22.46, 22.43, 22.13, 21.59, 21.52, 21.50.

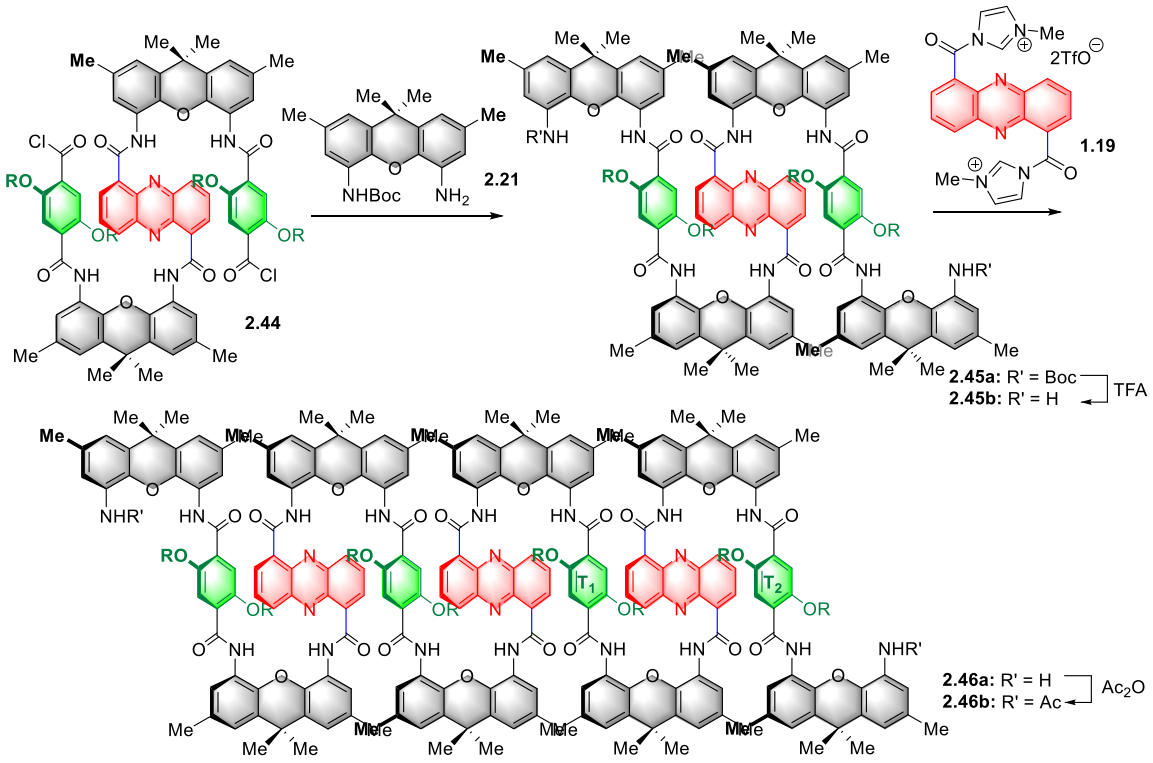

5e. Synthesis of P(XTXBoc)$_2$ 2.45a. A solution of P(XT)$_2$ Bis-Acyl chloride **2.44** (30 mg, 0.020 mmol) in 3 mL CH_2Cl_2 was added to a solution of **2.21** (17 mg, 0.060 mmol), Et_3N (13 µL, 0.09 mmol) and 2 mL CH_2Cl_2. After, 30 min, the reaction mixture was washed with saturated K_2CO_3, H_2O, aqueous phase extracted with CH_2Cl_2 and dried over Na_2SO_4. Chromatography with hexane: acetone 7:1 to 5:1 yielded the product as a light orange powder. (31 mg, 80% yield). **^{1}H NMR** (600 MHz, $CDCl_3$) δ 12.90 (s, 2H), 10.00 (s, 2H), 9.90 (s, 2H), 8.99 - 9.00 (d, J = 6 Hz, 2H), 8.43 - 8.45 (d, J = 6 Hz, 2H), 8.33 (s, 2H), 8.03 - 8.05 (t, J = 6 Hz, 2H), 7.81 - 7.83 (m, 4H), 7.11 - 7.13 (m, 4H), 6.96 (s, 2H), 6.94 (s, 2H), 6.84 (s, 2H), 6.75 (s, 2H), 6.14 (s, 2H), 4.31 - 4.33 (m, 2H), 4.22 - 4.26 (m, 2H), 2.89 - 2.91 (m, 2H), 2.46 (s, 6H), 2.30 (s, 6H), 2.14 (s, 6H), 1.97 - 1.99 (m, 4H), 1.90 (s, 6H), 1.85 (s, 6H), 1.63 (s, 6H), 1.53 (s, 6H), 1.47 (s, 6H), 1.17 (s, 18H), 0.47 - 0.51 (dd, J1 = 12 Hz, J2 = 6 Hz, 12 H). **^{13}C NMR** (151 MHz, $CDCl_3$) δ 161.75, 161.35, 161.02, 152.38, 149.97,

148.18, 140.36, 139.00, 138.30, 135.56, 134.38, 132.85, 132.72, 132.27, 131.29, 130.12, 130.01, 129.76, 129.13, 126.11, 126.05, 124.63, 124.48, 124.38, 123.84, 123.53, 122.13, 122.00, 121.84, 121.34, 119.92, 119.44, 115.20, 114.71, 80.54, 68.80, 68.45, 38.14, 36.78, 35.00, 34.45, 33.34, 29.82, 28.19, 25.28, 24.62, 22.79, 22.55, 22.36, 21.58, 21.49, 21.42. **IR (cm^{-1}):** 2958.1, 2360.2, 1672, 1623.9, 1551.0, 1427.6, 1224.8, 1153.2, 1004.3, 851.9, 751.7, 668.6.

5f. Preparation of intermediate 2.45b. Oligomer **2.45a** (21 mg, 0.010 mmol) was dissolved in 1 mL CH_2Cl_2 and treated with 1 mL trifluoracetic acid at rt. After 30 min, the mixture was diluted with 5 mL CH_2Cl_2 and quenched by slow addition of 5 mL saturated Na_2CO_3. The resulting mixture was extracted with CH_2Cl_2 (10 mL × 3) and the combined organic extract was dried with Na_2SO_4 and rotary evaporated to yield intermediate **2.45b** as an amber solid (19 mg, >99% yield), which was sufficiently pure for the next step. **^{1}H NMR** (500 MHz, $CDCl_3$) δ 12.94 (s, 2H), 9.93 (s, 2H), 8.99 (m, 2H), 8.43 - 8.45 (d, J = 6Hz, 2H), 8.26 (s, 2H), 8.04 (m, 2H), 7.91(s, 2H), 7.09 (m, 6H), 6.91 (s, 4H), 6.57 (s, 2H), 6.39 (s, 2H), 6.10 (s, 2H), 4.33 (m, 2H), 4.14 (m, 2H), 2.87 (m, 2H), 2.58 (m, 2H), 2.43 (s, 6H), 2.23 (s, 6H), 2.17 (s, 6H), 1.79 -1.84 (m, 12H), 1.53 - 1.59 (m, 27H), 0.98 (br, 15H), 0.47 (br, 12H). **^{13}C NMR** (126 MHz, $CDCl_3$) δ 161.75, 161.54, 161.30, 150.10, 148.38, 140.43, 139.08, 138.31, 136.27, 135.57, 135.57, 134.28, 132.87, 132.62, 132.54, 131.65, 131.26, 130.21, 129.72, 129.20, 125.78, 125.08, 124.97, 124.81, 123.21, 122.21, 121.74, 121.73, 120.85, 120.25, 115.36, 114.93, 114.26, 69.37, 68.62, 36.84, 34.39, 34.33, 32.80, 31.58, 30.28, 25.23, 24.62, 22.65, 22.51, 21.52, 21.19. **IR (cm^{-1}):** 2956.8, 2360.4, 1742.9, 1673.7, 1558.7, 1418.9, 1265.4, 1222.6, 752.6. **HRMS** (ESI - TOF) m/z: calcd for $[C_{118}H_{128}N_{10}O_{14} + H]^+$, 1910.9718; found, 1910.9717.

5f. Preparation of Oligomer 2.46a. Intermediate **2.45b** (70 mg, 0.037 mmol) was dissolved in 1ml $CHCl_3$ at reflux and treated with a solution of **1.19** (19 mg, 0.027 mmol) in 1 mL MeCN and added in small portions over 40 min. The mixture was kept at 70 ^oC for another hour. After cooling to rt, the mixture was washed with 1 mL saturated K_2CO_3, extracted with CH_2Cl_2 (5 mL × 3), and the organic extract dried over Na_2SO_4. The crude mixture was subjected to purification by preparative GPC using JAIGEL2HR column and one JAIGEL-2.5HR column in tandem. Fraction 5 was found to contain the pure product (20 mg, 27% yield). **^{1}H NMR** (600 MHz, $CDCl_3$, partial assignment due to complexity): δ 12.82 (s, 2H), 12.52 (s, 2H), 12.23 (s, 2H), 9.85 (s, 2H), 9.80 (s, 2H), 9.59 (s, 2H), 9.04 (s, 2H), 8.89 - 8.90 (m, 2H), 8.51 (m, 2H), 8.47 (m, 2H), 8.19 (m, 2H), 8.11 (m, 2H), 8.04 (m, 2H), 7.96 (m, 4H), 7.82 (m, 3H), 7.72 (s, 2H), 7.60 (m, 4H), 7.36 (s, 2H), 6.93 - 7.04 (m, 8H), 6.81 - 6.90 (m, 8H), 6.72 (s, 2H), 6.54 (s, 2H), 6.35 (s, 2H), 5.83 (s, 2H), 5.24 (s, 2H), 5.13 (s, 2H), 4.31 (m, 2H), 4.10 - 4.11 (m, 2H), 3.56 (m, 4H), 3.03 (m, 2H), 2.82 (m, 2H), 2.62 (m, 2H), **^{13}C NMR** (151 MHz, $CDCl_3$) δ 161.39, 161.30, 161.18, 160.96, 160.64, 160.46, 149.87, 148.21, 147.61, 147.38, 140.13, 139.66, 139.30, 139.13, 138.85, 138.63, 138.33, 138.15, 136.21, 135.50, 135.31, 134.25, 133.94, 133.59, 133.01, 132.57, 132.23, 132.11, 131.87, 131.52, 131.13, 131.01, 130.59, 130.22, 129.84, 129.55, 129.38, 129.18, 129.05, 128.36, 128.17, 125.76, 125.50, 125.16, 124.98, 124.71, 123.97, 123.70, 123.27, 122.58, 122.27, 122.11, 121.78, 121.66, 121.41, 120.36, 119.79, 115.23, 114.64, 114.16, 112.89, 111.92, 69.21, 68.50, 37.56, 37.05, 36.77, 36.40, 34.69, 34.24, 33.58, 33.45, 32.97, 31.06, 30.39, 29.93, 29.02, 25.27, 25.17, 24.38, 22.68, 22.47, 22.27, 21.88, 21.65, 21.48, 21.21, 21.15, 20.73, 20.54. **IR (cm^{-1}):** 2958.4, 2360.2, 1672.9, 1556.6, 1434.4, 1222.2, 751.3, 668.7. **MALDI-TOF** m/z: calcd for $[C_{250}H_{260}N_{22}O_{30} + H]^+$, 4050.957; found,

4051.465; $[C_{250}H_{260}N_{22}O_{30} + Na]^+$, 4072.939, found, 4073.675; $[C_{250}H_{260}N_{22}O_{30} + K]^+$, 4088.913, found, 4089.516.

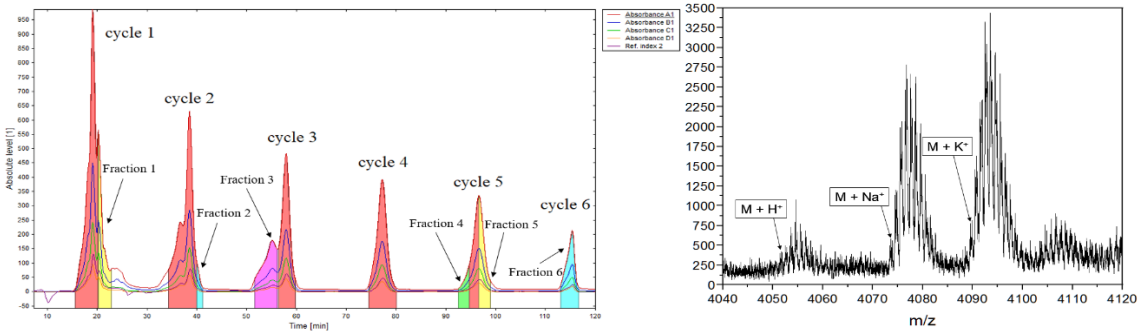

5g. Synthesis of Acetylated Oligomer 2.46b. Oligomer **2.46a** (20 mg, 4.9 nmol) was dissolved in 0.5 mL $CDCl_3$ and heated to 70 °C. Acetic anhydride (1 µL, 10 mmol) was added and the mixture was kept at 70 ℃ for 1 h, at which time ^{1}H NMR indicated complete conversion. The mixture was rotary evaporated to dryness to produce **2.46b** as an amber solid (20 mg, >99% yield). **^{1}H NMR** (600 MHz, $CDCl_3$, partial assignment due to complexity): δ 12.69 (s, 2H), 12.47 (s, 2H), 12.26 (s, 2H), 9.88 (s, 2H), 9.79 (s, 2H), 9.52 (s, 2H), 9.04 (s, 2H), 8.88 (m, 2H), 8.46 - 8.50 (m, 4H), 8.20 (s, 2H), 8.10 - 8.12 (d, J = 6 Hz, 2H), 8.04 (s, 2H), 7.95 - 7.98 (m, 4H), 7.88 (s, 2H), 7.74 - 7.77 (m, 4H), 7.56 - 7.59 (m, 6H), 7.49 (s, 2H), 7.33 (s, 2H), 7.29 (s, 2H), 7.23 (s, 2H), 7.13 - 7.17 (m, 4H), 7.07 (s, 2H), 7.01 (s, 2H), 6.97 (s, 2H), 6.94 (s, 2H), 6.91 (s, 2H), 6.85 (s, 4H), 6.78 (s, 2H), 6.70 (s, 2H), 5.91 (s, 2H), 5.23 (s, 2H), 5.13 (s, 2H), 4.32 (m, 4H), 4.10 - 4.11 (m, 4H). **^{13}C NMR** (151 MHz, $CDCl_3$) δ 167.73, 161.43, 161.13, 160.89, 160.59, 160.35, 149.95, 148.67, 147.67, 147.29, 139.60, 139.20, 139.04,

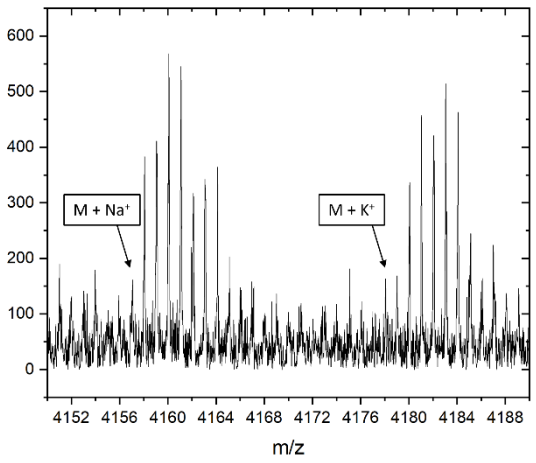

138.60, 138.33, 138.10, 137.85, 137.35, 135.52, 135.34, 133.76, 132.98, 132.69, 132.53, 132.31, 131.95, 131.07, 130.79, 130.09, 129.87, 129.63, 129.23, 129.01, 128.20, 125.72, 125.49, 125.28, 124.76, 124.30, 124.00, 123.35, 122.40, 122.20, 121.99, 121.51, 121.32, 120.70, 119.42, 114.73, 112.96, 112.04, 38.07, 37.12, 36.82, 36.40, 34.67, 34.41, 34.25, 33.46, 32.68, 31.92, 29.69, 29.35, 29.23, 28.93, 25.52, 25.27, 25.16, 25.07, 24.44, 24.07, 22.71, 22.40, 22.31, 22.22, 21.90, 21.50, 21.41, 21.21, 20.81, 20.65, 14.12. **IR (cm^{-1}):** 2374.3, 1698.4, 1575.8, 1435.2, 1224.7, 757.1, 671.2. **MALDI-TOF** m/z: calcd for $[C_{254}H_{264}N_{22}O_{32} + Na]^+$, 4156.960; found, 4157.086; $[C_{254}H_{264}N_{22}O_{32} + K]^+$, 4172.934, found, 4172.836.

2.4.7. Redox cycling using catalytic hydrogenation.

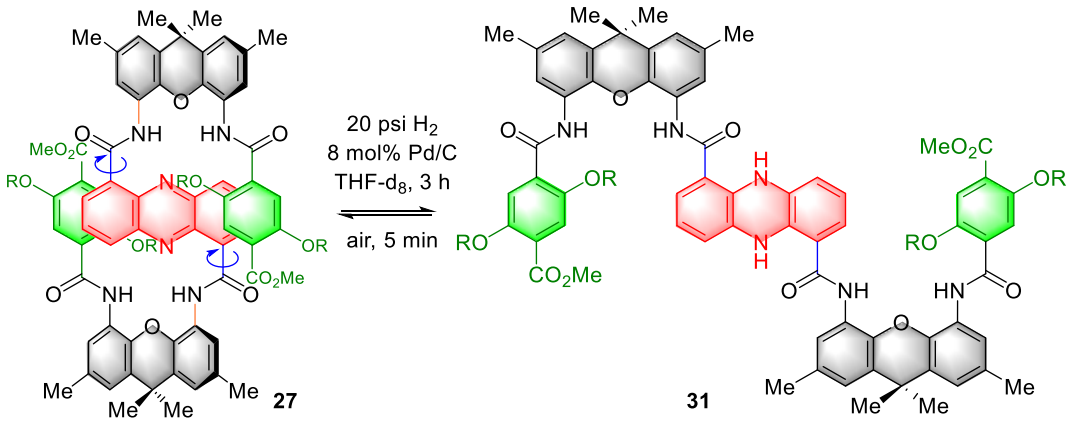

2.4.7a. Hydrogenation of P(XT)$_2$ Diester 2.42 to Dihydrophenazine 2.47. A 5 mm Wilmad quick pressure valve NMR tube was charged with TXPXT Diester **2.42** (42 mg, 0.030 mmol), dry 5% Pd/C (5 mg, 0.002 mmol), and 1 g of THF-d_8. The tube was purged with hydrogen 3 times, filled to 20 psi, and shaken by inverting it mechanically at ca. 6 revolutions per min. Reaction progress was monitored by ^{1}H NMR. After 3 h, complete consumption of the starting material was confirmed and the spectra of

dihydrophenazine **2.47** were recorded. The mixture was shaken in the same manner for another 24 h to confirm than no overreduction was taking place. **^{1}H NMR** (600 MHz, THF-d8) δ 10.24 (s, 2H), 9.31 (s, 2H), 8.78 (s, 2H), 8.24 (s, 2H), 7.73 (s, 2H), 7.62 (s, 2H), 7.17 (s, 2H), 7.15 (s, 2H), 7.07 (s, 2H), 7.08 (s, 2H), 6.64 - 6.65 (d, J = 6 Hz, 2H), 5.87 - 5.88 (d, J = 6 Hz, 2H), 5.67 - 5.70 (t, J = 6 Hz, 2H), 3.99 - 4.01 (t, J = 6 Hz, 4H), 3.84 - 3.96 (t, J = 6 Hz, 4H), 3.58 (s, 3H), 2.36 - 2.37 (d, J = 12Hz, 12H), 1.88 - 1.94 (m, 2H), 1.64 - 1.73 (m, 20H), 0.92 - 0.93 (d, J = 6Hz, 12H), 0.72 - 0.73 (d, J = 6Hz, 12H). **^{13}C NMR** (151 MHz, THF-d8) δ 204.89, 167.49, 166.61, 162.80, 153.44, 151.02, 141.90, 139.51, 138.35, 134.63, 133.32, 133.10, 132.16, 131.05, 127.80, 127.22, 126.54, 125.51, 124.17, 123.32, 121.66, 121.02, 120.36, 119.51, 117.73, 117.31, 117.13, 115.15, 112.74, 69.73, 67.86, 67.72, 67.57, 67.42, 67.28, 52.39, 46.32, 39.09, 38.81, 35.58, 31.98, 30.57, 23.10, 22.91.

2.4.7b. Aerial oxidation of Dihydrophenazine 2.47. The hydrogen pressure in the NMR tube (see above) was released and the mixture was allowed to come into contact with air for 1 min. The tube was inverted by hand and the progress of reoxidation was monitored by ^{1}H NMR. After 4 min, complete disappearance of the dihydrophenazine form **2.42** was confirmed and the spectrum of **2.42** was recorded.

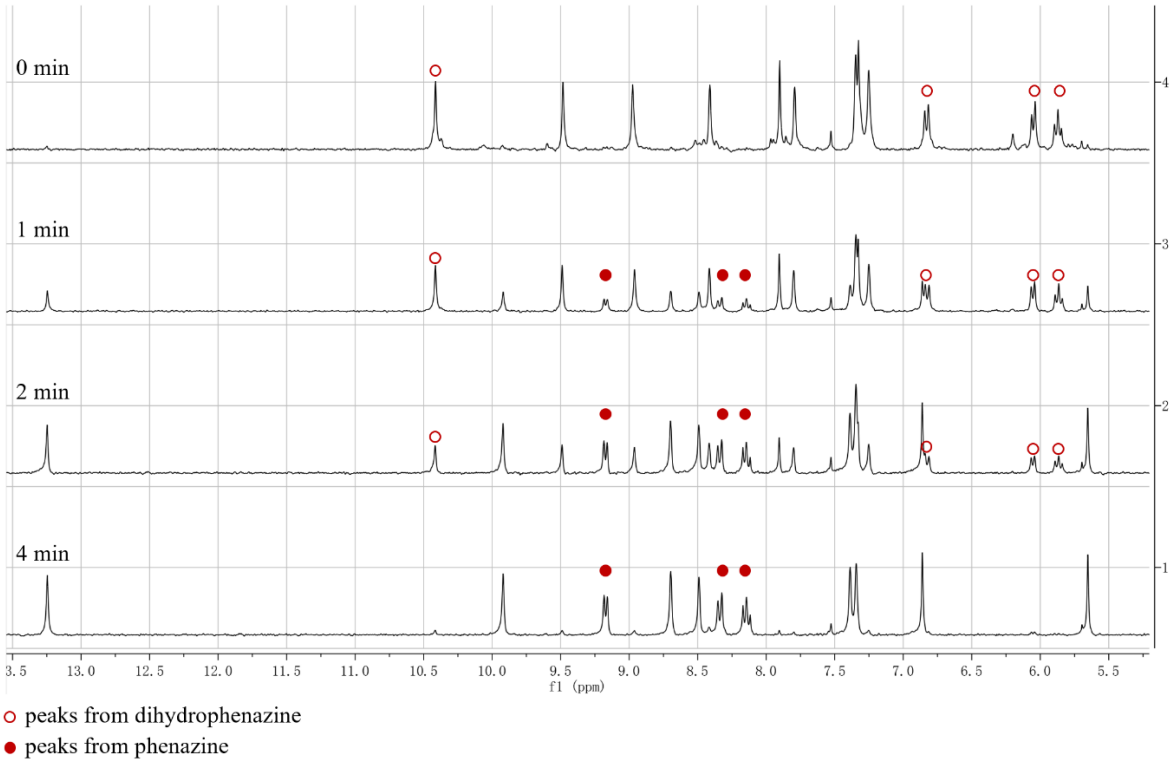

2.4.7c. Redox cycling. The hydrogenation (3 h) and reoxidation (4 min) described above were performed 10 times using the same sample in order to confirm that no decomposition products accumulate in the reaction mixture. The resulting spectra are shown in Figure 10 of the article.

Redox cycling of **2.42**:

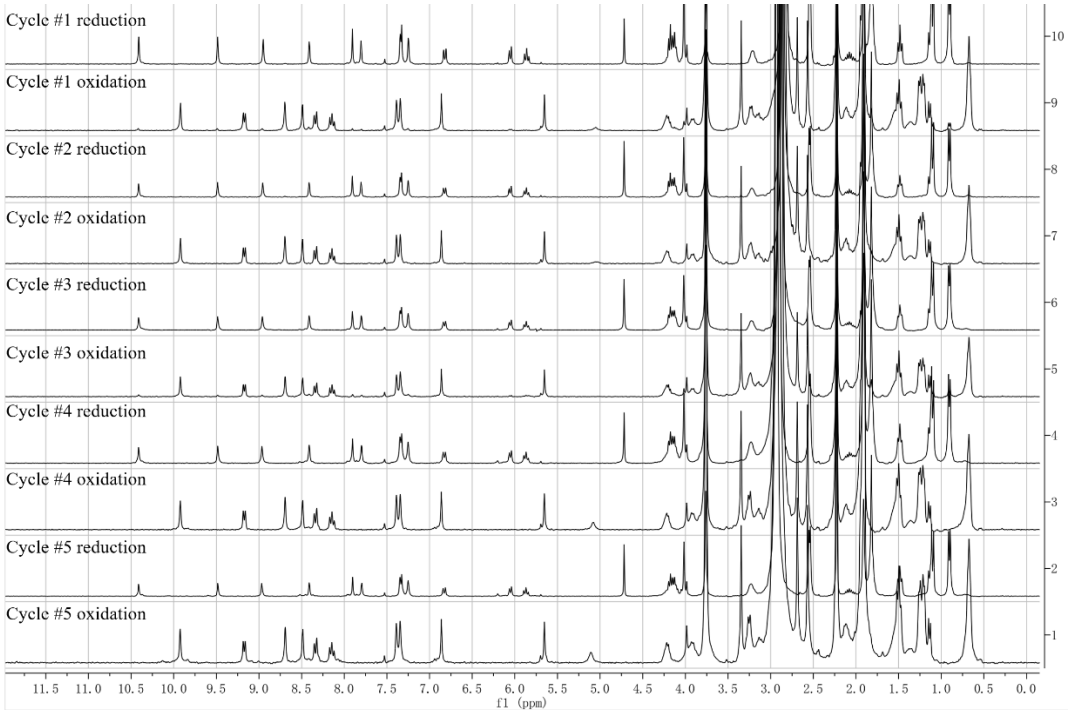

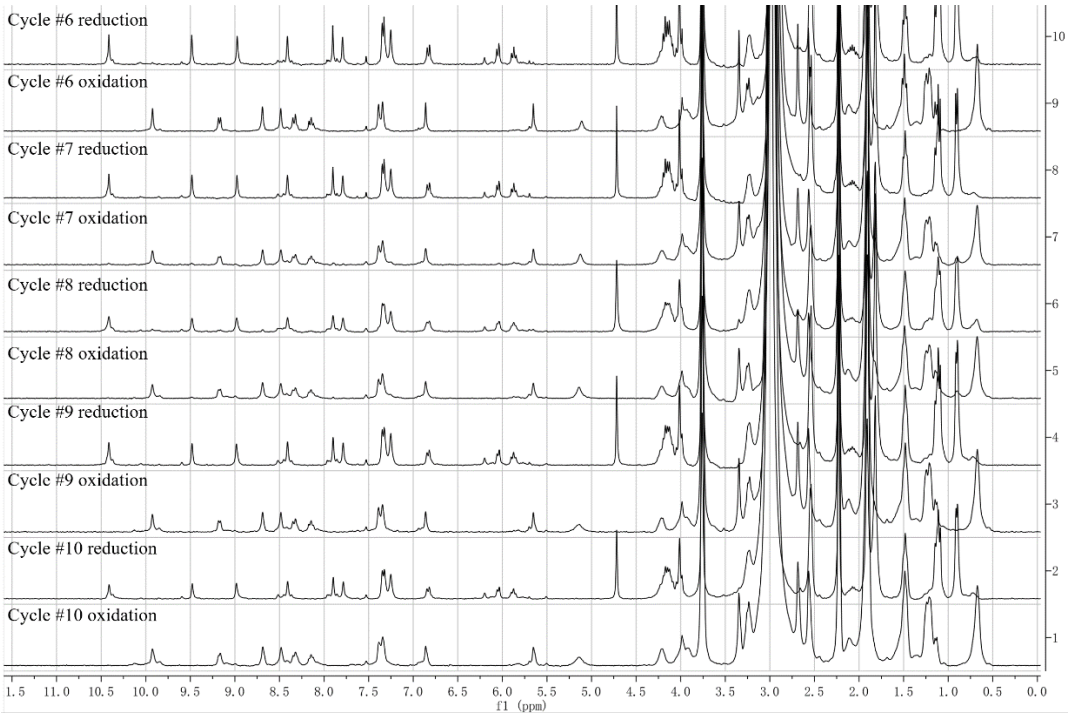

2.4.7d. Redox cycling of Oligomer 2.46b. A 5 mm Wilmad quick pressure valve NMR tube was charged with Oligomer **2.46b** (7 mg, 1.6 nmol), 5% Pd/C (1 mg, 0.0004 mmol) and 0.8 mL $CDCl_3$. Hydrogenation (12 h) and reoxidation (18 min) were performed in the same manner as described above. *NMR data for the reduced form of **2.46b**:* **^{1}H NMR** (600 MHz, $CDCl_3$) δ 0.75 (br, 36H), 1.25 (br, 10H), 2.03 (s, 4H), 2.17 (s, 4H), 2.28 - 2.37 (m, 30H), 3.98 - 4.02 (m, 8H), 4.27 (s, 4H), 5.35 (br, 6H), 5.89 (br, 6H), 6.31 (br, 6H), 6.94 - 7.04 (m, 12H), 7.77 - 7.85 (m, 10H), 7.93 (m, 2H), 8.00 - 8.11 (m, 8H), 8.19 (br, 2H), 9.02 (br, 2H), 10.32 (br, 2H), 10.50 (br, 2H). **^{13}C NMR** (151 MHz, $CDCl_3$) δ 1.03, 21.34, 21.38, 21.42, 21.51, 22.27, 22.33, 24.92, 25.05, 29.71, 31.36, 31.51, 34.54, 34.58, 37.70, 37.74, 37.78, 69.06, 71.73, 111.62, 111.79, 111.88, 114.25, 114.43, 114.58, 117.45, 117.73, 117.90, 119.34, 119.48, 119.77, 119.89, 120.44, 120.55, 120.76, 121.23, 121.43, 121.54, 121.66, 121.73, 122.10, 122.33, 124.92, 125.05, 125.14, 125.26, 125.36, 125.81, 126.98, 130.15, 130.37, 130.49, 132.59, 132.78, 132.84, 132.89, 132.95, 133.00, 133.07, 133.56, 133.67, 133.79, 137.24, 137.36, 137.42, 138.75, 139.39, 150.62, 150.88, 151.92, 161.53, 162.06, 162.13, 166.25, 166.42, 168.25.

Aerial oxidation of **2.48b**:

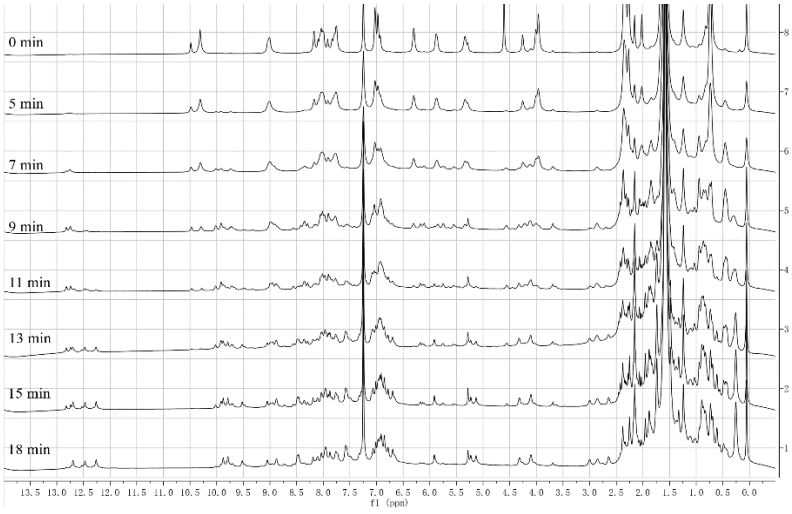

Redox cycling of **2.48b**:

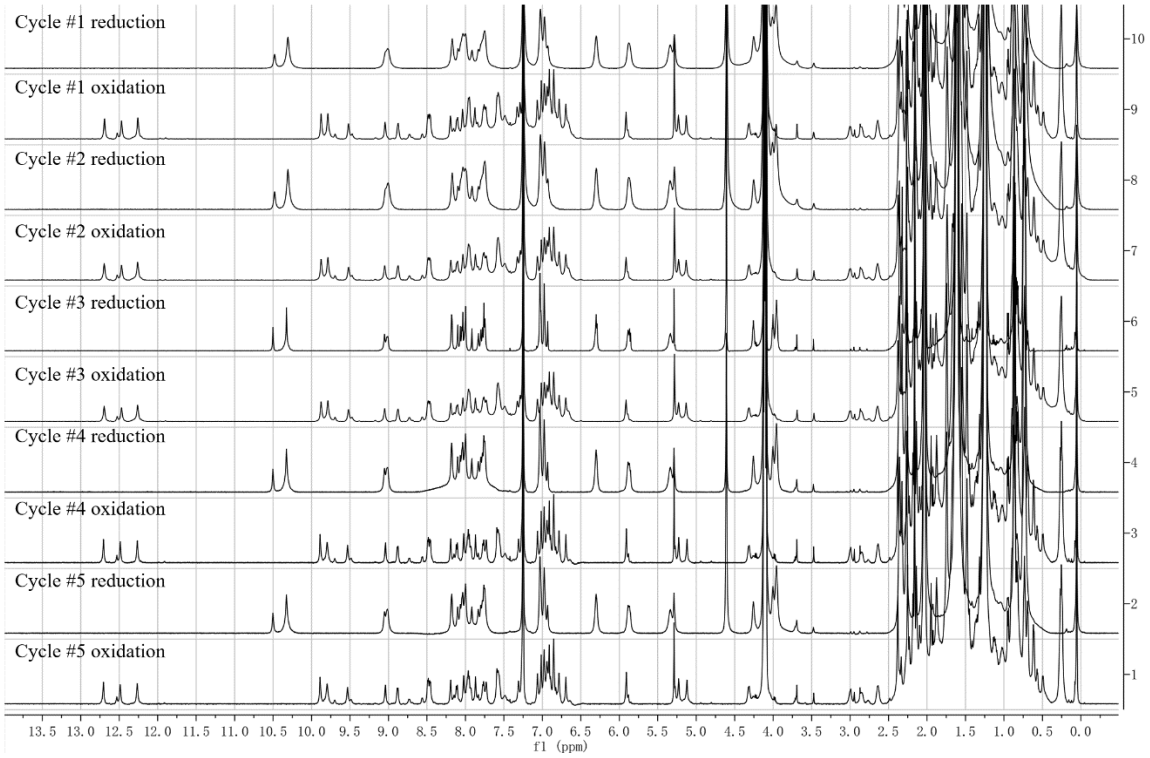

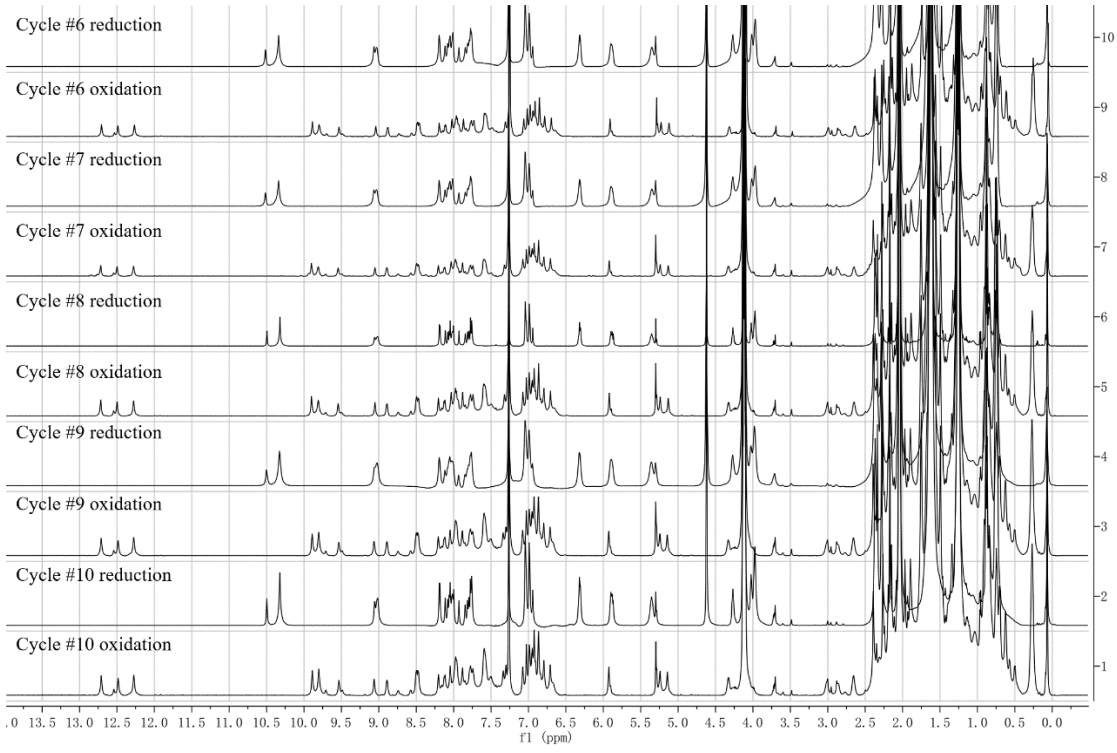

2.4.8. Electrochemical studies

2.4.8a. Cyclic voltammetry study. Cyclic voltammetric experiments were performed using a BAS 100B Electrochemical Analyzer in a conventional one-compartment three-electrode cell with glassy carbon as the working electrode, a platinum wire auxiliary electrode, and a Ag/AgCl reference electrode.

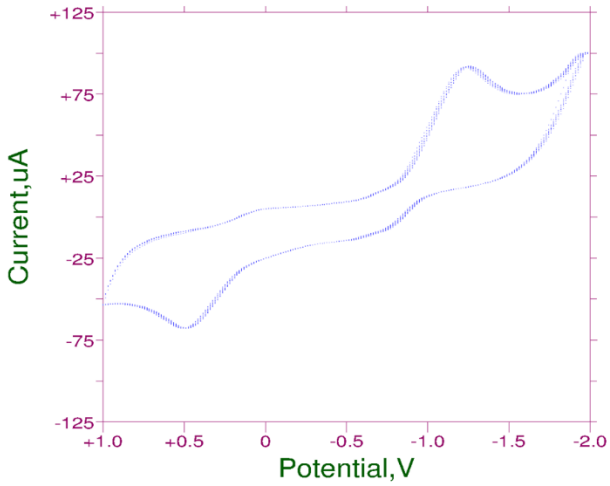

The surface of the working electrode was polished with filter paper immediately before use. The cell was flushed with argon before use and the measurements were conducted under an argon atmosphere at room temperature. The substrate (**27**, 7 mg, 0.005 mmol, 0.005 M concentration) and lithium perchlorate (21 mg, 0.2 mmol, 0.2 M concentration) were dissolved in 1 mL of a 4:1 mixture of HPLC grade chloroform and methanol degassed before use. Cyclic voltammograms were recorded at 250 mV/s sweep rate after 10 cycles. The overlaid voltammograms for cycles 10 through 40 (shown) indicate that the redox cycle was fully reversible.

2.4.8b. Bulk electrolysis

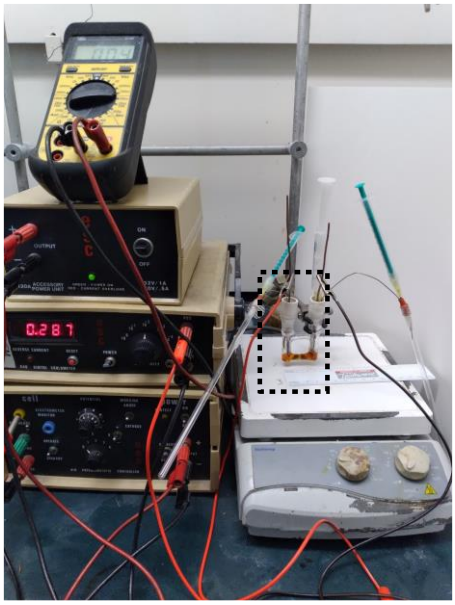

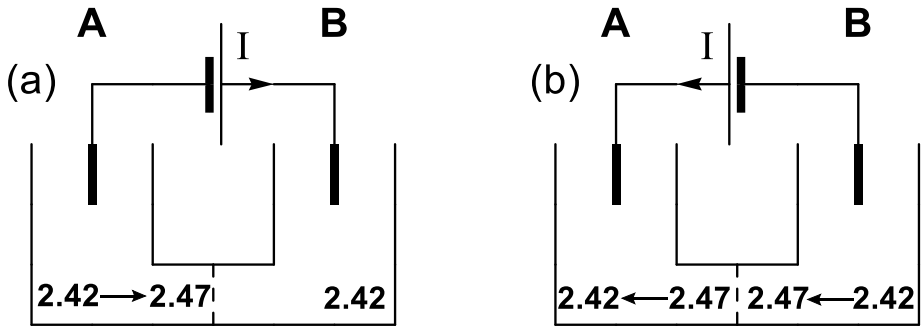

(a) A divided cell separated by a 5 μm glass frit was charged with anhydrous $MgSO_4$ (5 mg) and a solution of **2.42** (7 mg, 0.005 mmol), N_2H_4-H_2O (25 μL, 0.5 mmol), and $LiClO_4$ (10 mg, 0.1 mmol) in 0.5 mL of 4:1 v/v $CDCl_3$-CD_3OD mixture. Two NMR tubes were connected to each chamber via a cannula. The cell was equipped with graphite electrodes and purged thoroughly with N_2 using the freeze-pump-thaw technique. A constant current of 0.5 mA was passed through the cell until 5 Coulombs was reached. The contents of each chamber was transferred to each NMR tube by cannulation and analyzed by ^1H NMR. The solution from the cathodic chamber (**A**)

contained >95% dihydrophenazine **2.47**, while that from the anodic chamber (**B**) contained unchanged starting material **2.42**.

(b) The experiment was repeated as described above, except that after passing 5 Coulombs of current, the current was reversed and the same amount of charge was passed in the opposite direction. NMR analysis indicated that the contents of both chambers were also reversed.

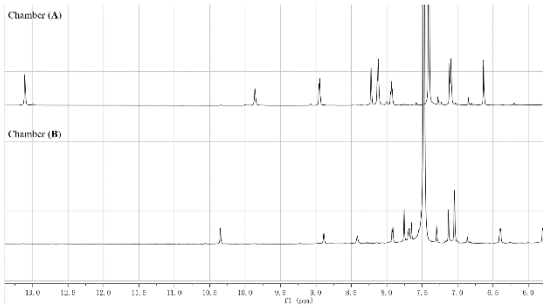

Part (a)

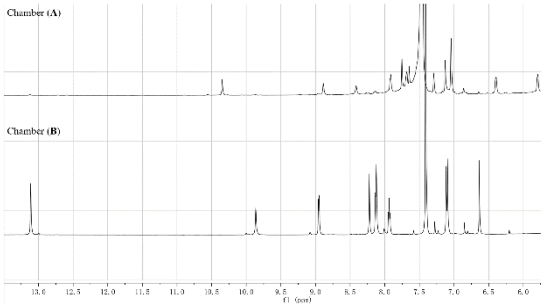

Part (b)

2.4.9. Computer modeling.

The conformations of oligomers **2.49**, **2.29/2.29-[H2]** and **2.46b/32b** were optimized by Molecular Mechanics MMFF calculations in gas phase using Spartan'20 software. All other structures shown below were obtained by geometry optimization performed at the B3LYP/6-31G* level of theory. [28]

2.4.9a. Probable geometry of macrocycles 2.30 and 2.38. Two possible diastereomers of cyclic dimer **2.30** were optimized at the B3LYP/6-31G* level of theory in gas phase. Diastereomer **2.30a** with the parallel arrangement of the amide groups was found to be less stable than the antiparallel **2.30b** (ca. 5.2 Kcal/mol). Analogously, both diastereomers of macrocycle **2.38** were modeled by their abbreviated structures **2.38a** and **2.38b** wherein the isoamyl side chains were replaced with methyl groups. In this case, the preference for the antiparallel diastereomer **2.38b** was even more pronounced (Figure S-1).

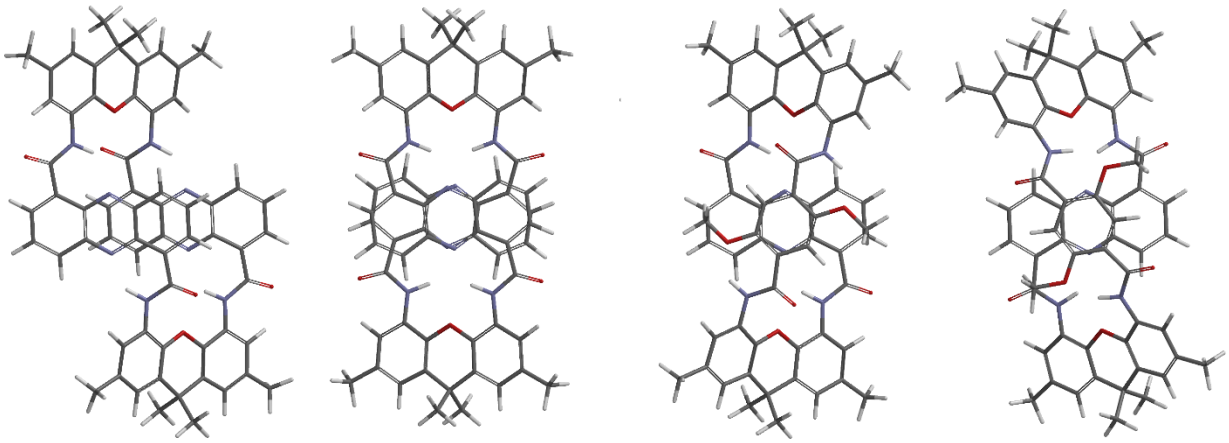

2.30a
5.2 Kcal/mol

2.30b
0 Kcal/mol

2.38a
8.5 Kcal/mol

2.38b
0 Kcal/mol

Figure 2-33. Top views of macrocycles **2.30** and **2.38.**

2.4.9b. Rotation barriers for the side arm flipping.

	$\Delta H_{(rel)}$, Kcal/mol*	
$\Theta_{C—N}$	**2.49**	**2.50**
−180 °	0.82	0.5
−160 °	0.14	0.12
−140 °	0.63	0.77
−120 °	1.62	2.2
−100 °	2.85	3.77
−80 °	2.51	4.48
−60 °	2.43	2.82
−40 °	3.47	4.16
−20 °	5.2	6.84
−10 °	6.25	8.0
0 °	7.19	9.01
10 °	6.25	7.92
20 °	5.3	6.72
40 °	3.17	4.13
60 °	2.34	2.89
80 °	2.65	4.57
100 °	2.88	3.83
120 °	1.75	2.23
140 °	0.64	0.7
160 °	0.21	0
180 °	0.62	0.36
$\Theta_{C—C}$	**2.49**	**2.50**
0 °	0.12	0.19
20 °	0.28	0.13
40 °	1.91	1.42
60 °	4.39	3.75
80 °	5.32	6.15
100 °	5.28	6.71
120 °	4.95	4.25
140 °	4.93	6.05
160 °	6.88	7.86
180 °	9.86	9.22
200 °	6.77	7.94
220 °	4.93	6.23
240 °	4.75	4.66
260 °	5.41	6.6
280 °	5.47	6.16
300 °	4.44	3.74
320 °	1.83	1.45
340 °	0.25	0.3
360 °	0.15	0.33

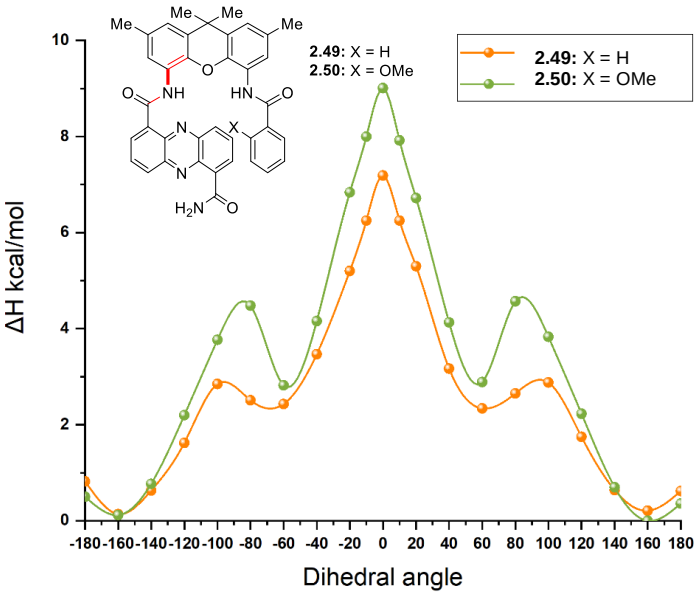

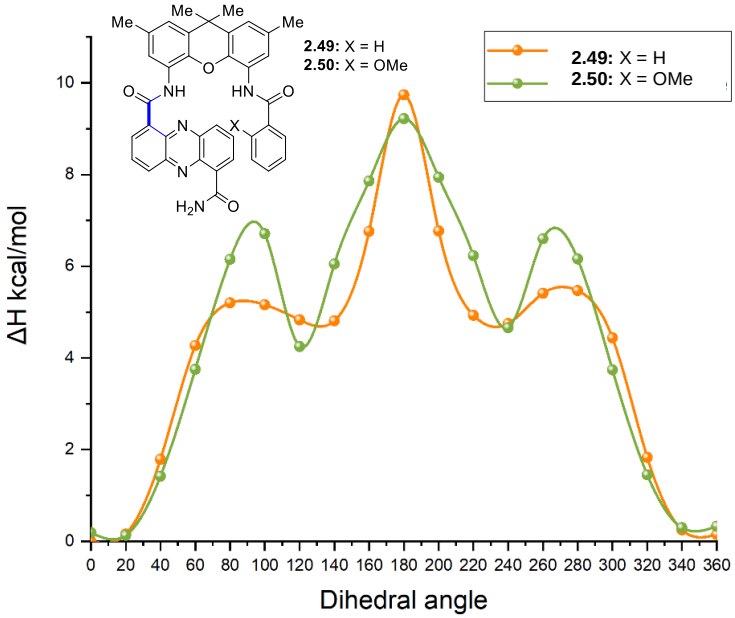

Figure 2-34. C—N and C—C bond rotation barrier.

Structures **2.49** and **2.50** were used as simplified one-arm analogues of compounds **2.27** and **2.42**, respectively. Their geometries were optimized at the B3LYP/6-31G* level of theory using a nonpolar solvent model. The dihedral angles of the C—N bonds highlighted in red were found to be ±163 °. The red bonds were then constrained at dihedral angles ranging from −180 °to +180 °at 20 degree intervals and re-optimized. Comparison of the resulting energy profiles is shown in Figure 2-34.

The dihedral angles of the C—C bonds highlighted in blue were found to be ±10 ° in the unconstrained models. Energy profiles for rotation about these bonds ranging from 0 °to 360 °are compared in Figure 2-34.

Available results suggest that the side arm flipping in **2.49** should occur more easily via C—N than C—C bond rotation (7.2 vs. 9.9 Kcal/mol rotation barriers), while for **2.50** both pathways are comparable (9.0 vs. 9.2 Kcal/mol, respectively).

The lower C—N bond rotation barrier in **2.49** relative to that in **2.50** is qualitatively consistent with the Gibbs free energies of the double flip experimentally determined for compounds **2.27** and **2.42** (10.9 and 17.0 Kcal/mol, respectively, see below).

2.4.9c. Estimation of relative elongation.

Model structures **2.51** and **2.52** (Figure 2-35) representing bis-acetamide terminated derivatives of **2.29** and its reduced form **2.29-[H_2]**, respectively, were minimized using Molecular Mechanics (MMFF). The three phenazine groups in **2.29** were parallel to each other. Distance measurements between several pairs of analogous atoms of the outer phenazine groups gave consistent values (7.3 ±0.1 Å). Similar measurements of

the reduced form, **2.29-[H_2]**, gave the distance of 15.5 ±1 Å. The relative elongation of all-phenazine oligomers of general structure **2.29-[H_2]** was thus estimated at ca. 110%.

Abbreviated structure of **2.46b** with isoamyl side chains replaced by methyl groups was minimized analogously. All phenazine and dialkoxyphenylene groups were predicted to adopt a parallel, skewed orientation as shown in Figure S-5. Distance measurements between several pairs of analogous atoms of the outermost dialkoxyphenylene groups gave consistent values (23.6 ±0.1 Å). Similar measurements of the reduced form, **2.48b**, gave a distance of ca. 35.2 Å (Figure 2-36). Based on these values, the relative elongation of interleafed oligomers represented by **2.46b** was estimated at ca. 50%.

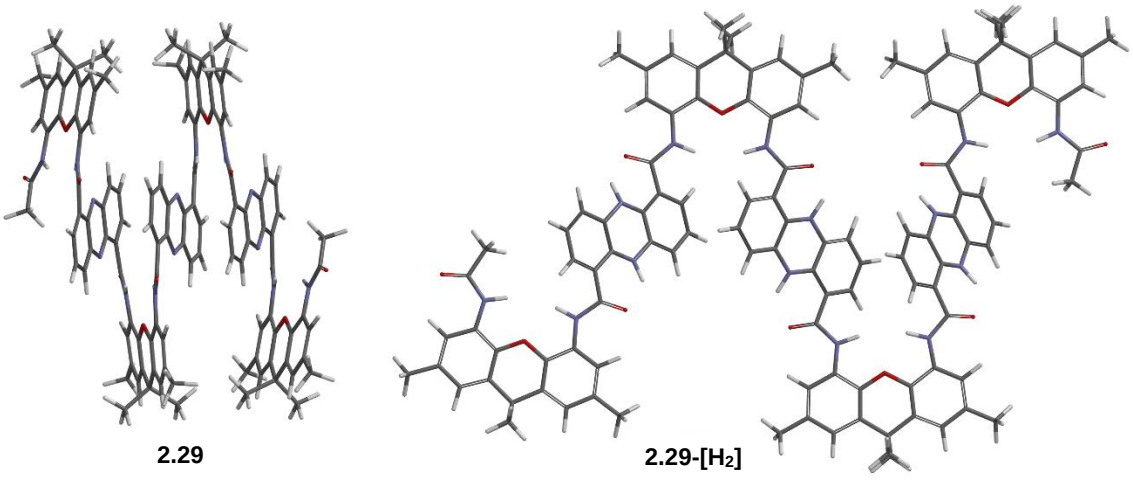

Figure 2-35. AcNH-terminated models of **2.29** and **2.29-[H_2].**

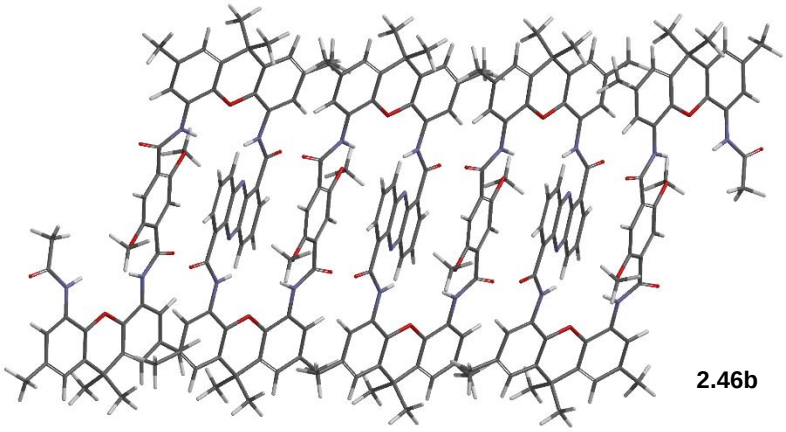

Figure 2-36. Abbreviated model of **2.46b.**

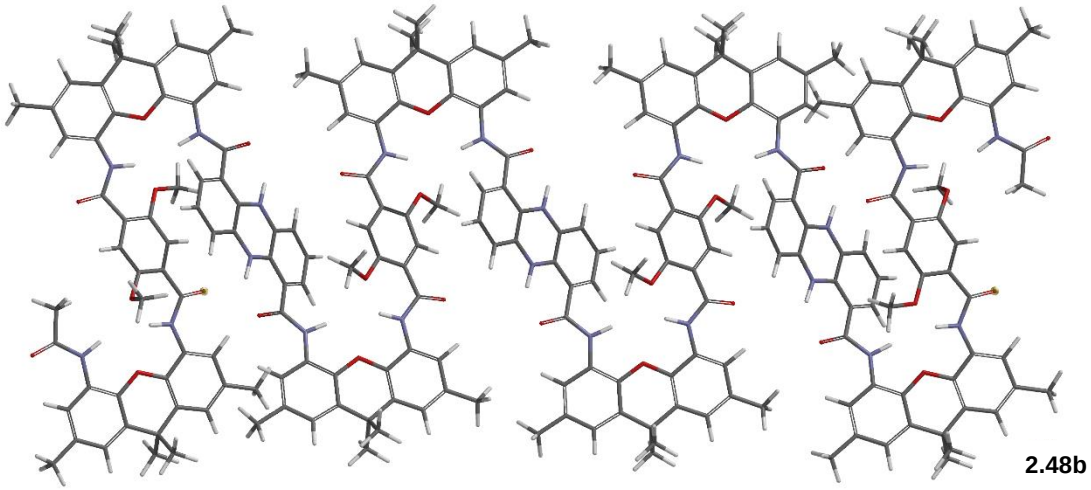

Figure 2-37. Abbreviated model of **2.48b.**

2.4.10. GIBBS FREE ENERGY OF THE DOUBLE FLIP.

The spectrum of **2.27** was recorded on a 300 MHz spectrometer in CD_2Cl_2 at the temperatures indicated below. At the lowest attainable temperature (–80 ℃) the eparation between the signals of **h** and **h′** was measured as: $\Delta\delta_{\mathbf{h/h'}} = 0.37$ ppm ($|\nu_{\mathbf{h}} - \nu_{\mathbf{h'}}| = 111$ Hz). At the coalescence temperature (– 42 ℃, $T_c = 231$ K), the rate of exchange is:[27]

$$k_{Tc} = 111 \text{ Hz} \times \pi/\sqrt{2} = 246 \text{ s}^{-1}$$

From the Eyring-Polanyi equation, $\Delta G^{\neq} = R \times T_c \times \ln [(k_B \times T_c)/(h \times k_{Tc})] =$

$= 8.314\ J \bullet mol^{-1} \bullet K^{-1} \times 231\ K \times \ln [(1.38\ 10^{-23}\ J \bullet K^{-1} \times 231\ K) / (6.63\ 10^{-34}\ J \bullet s \times 246\ s^{-1})] =$

= 45,516 J/mol = **10.9 Kcal/mol**

The spectrum of **2.42** was recorded on a 600 MHz spectrometer in toluene-d_8 at the temperatures indicated below. At the lowest attainable temperature (25 ℃) the separation between the signals of **Me^1** and **Me^2** was measured as: $\Delta\delta_{h/h'} = 0.03$ ppm ($|\nu_h - \nu_{h'}| = 18$ Hz). At the coalescence temperature (58 ℃, $T_c = 331$ K), the rate of exchange is:[27]

$k_{Tc} = 18\ Hz \times \pi/\sqrt{2} = 40\ s^{-1}$

From the Eyring-Polanyi equation, $\Delta G^{\neq} = R \times T_c \times \ln [(k_B \times T_c)/(h \times k_{Tc})] =$

$= 8.314\ J \bullet mol^{-1} \bullet K^{-1} \times 331\ K \times \ln [(1.38\ 10^{-23}\ J \bullet K^{-1} \times 331\ K) / (6.63\ 10^{-34}\ J \bullet s \times 40\ s^{-1})] =$

= 71198 J/mol = **17 Kcal/mol**

2.4.11. 1D NMR Spectrum

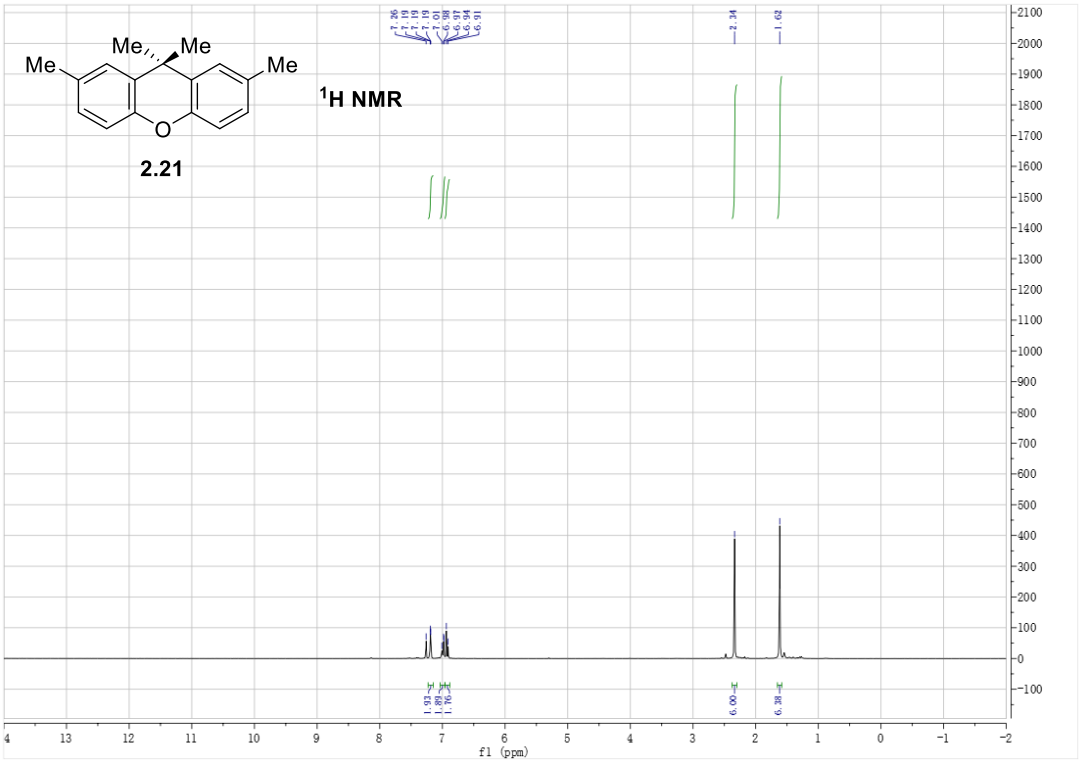

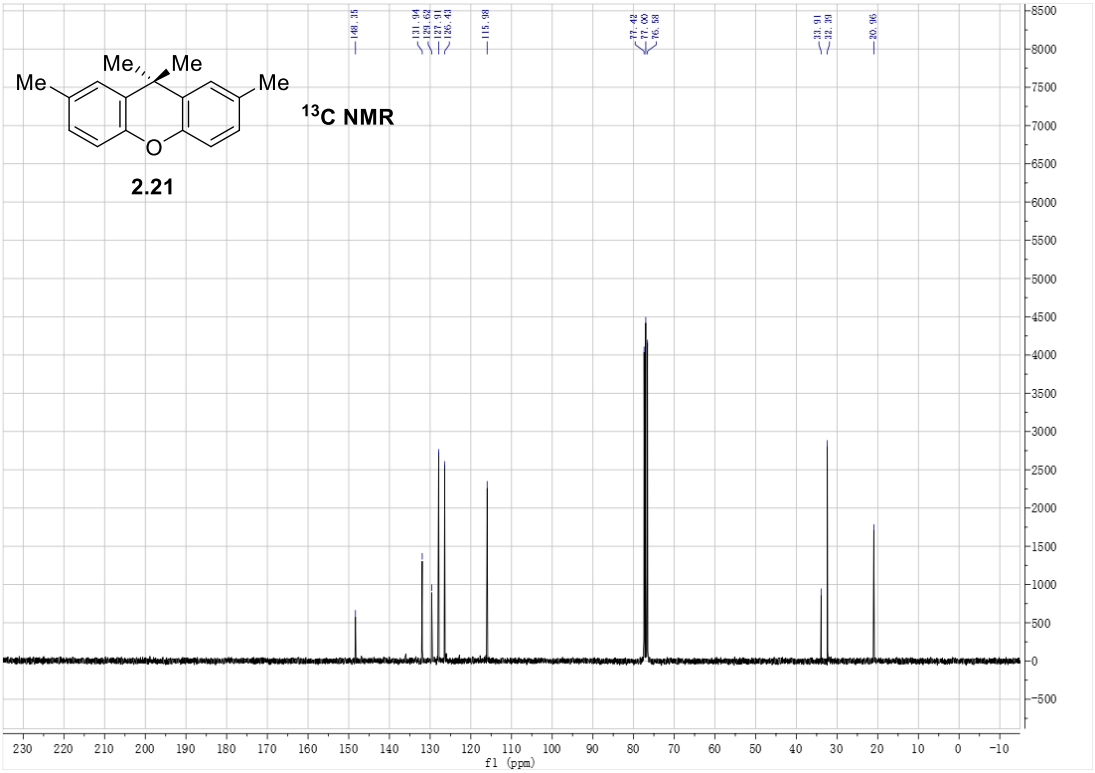

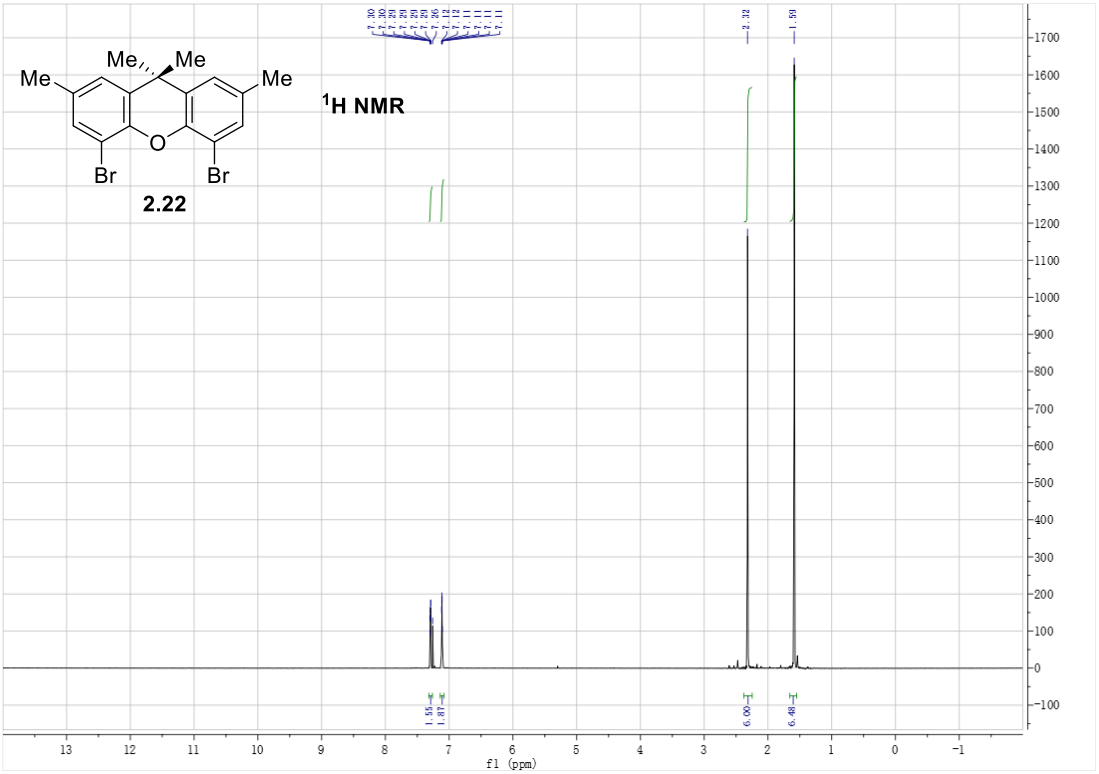
Me
Me
Me
Me
O
Br
Br
2.22
^{1}H NMR
f1 (ppm)

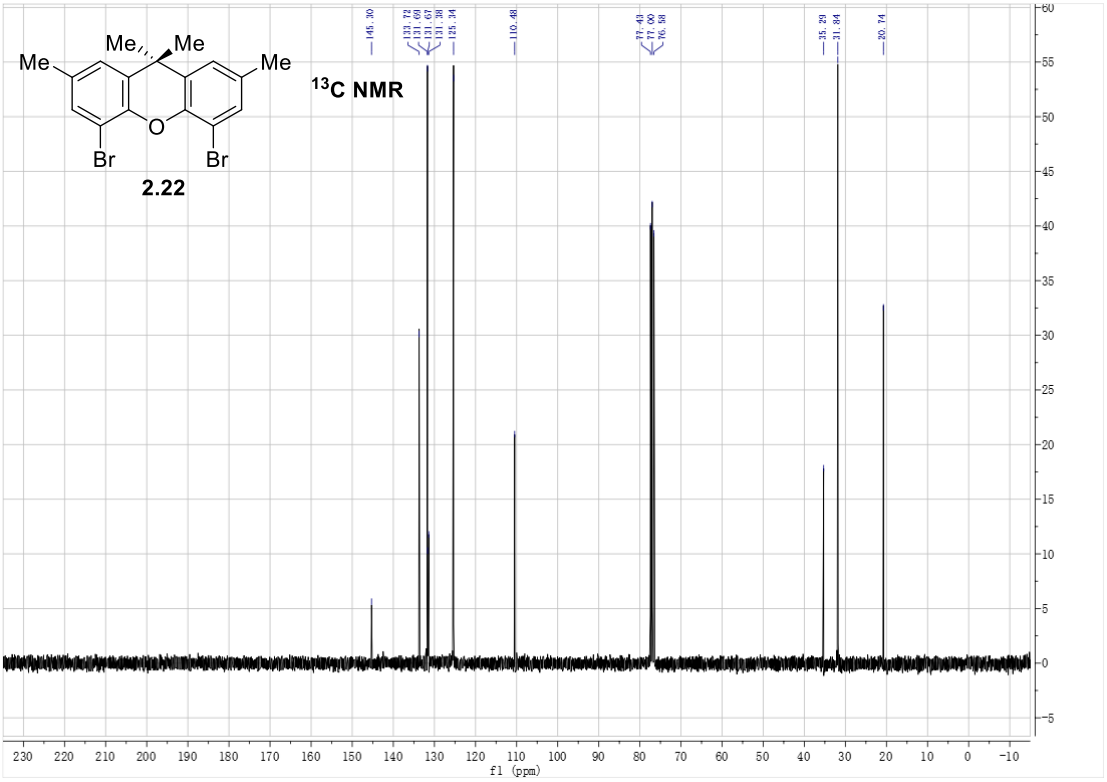
Me
Me
Me
Me
O
Br
Br
2.22
^{13}C NMR
f1 (ppm)

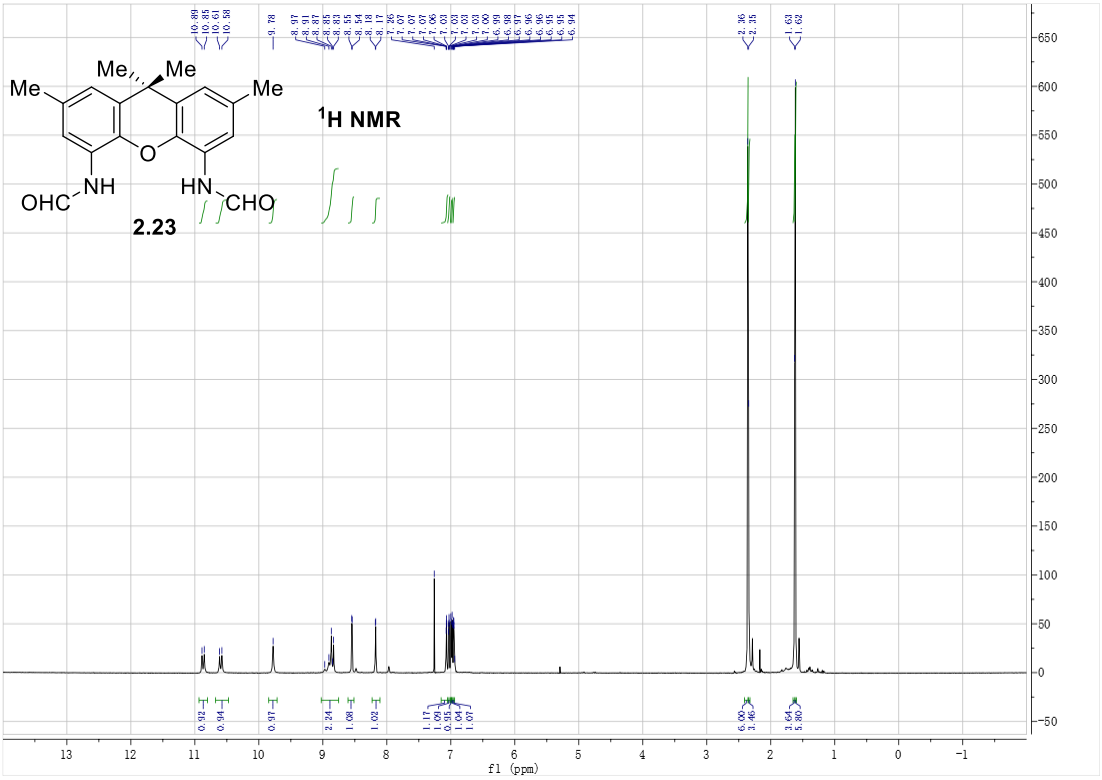
Me
Me
Me
Me
O
NH
HN
OHC
CHO
2.23
1H NMR
f1 (ppm)

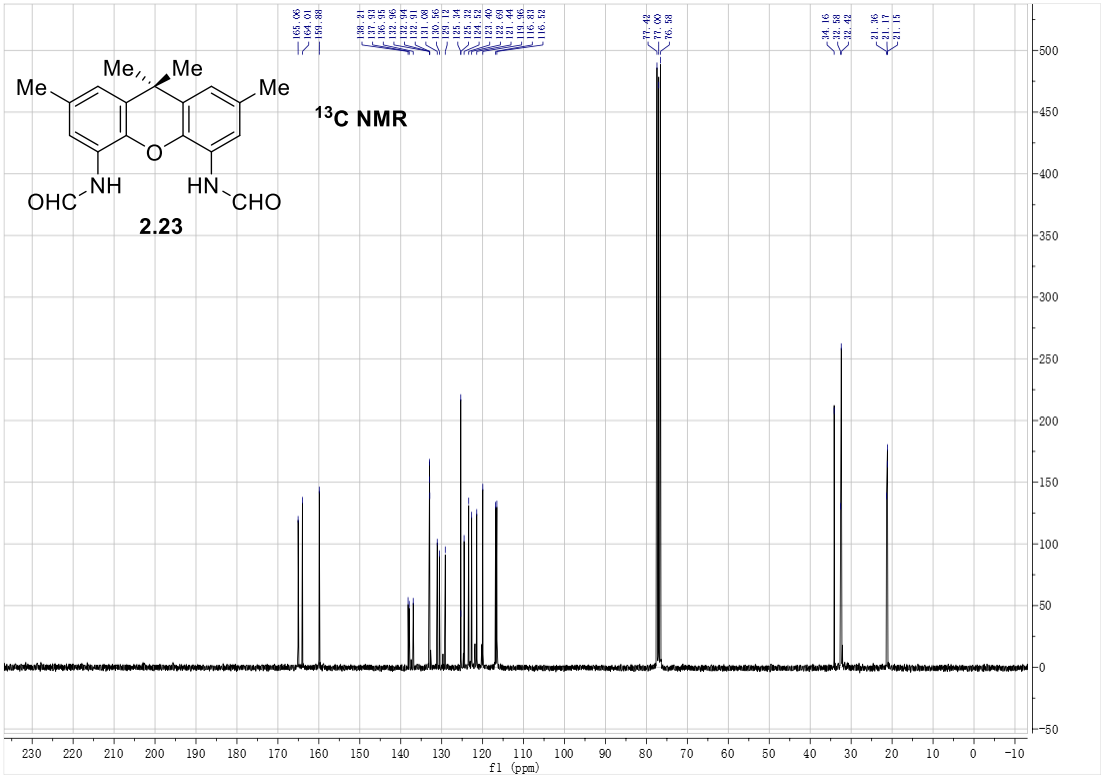
Me
Me
Me
Me
O
NH
HN
OHC
CHO
2.23
13C NMR
f1 (ppm)

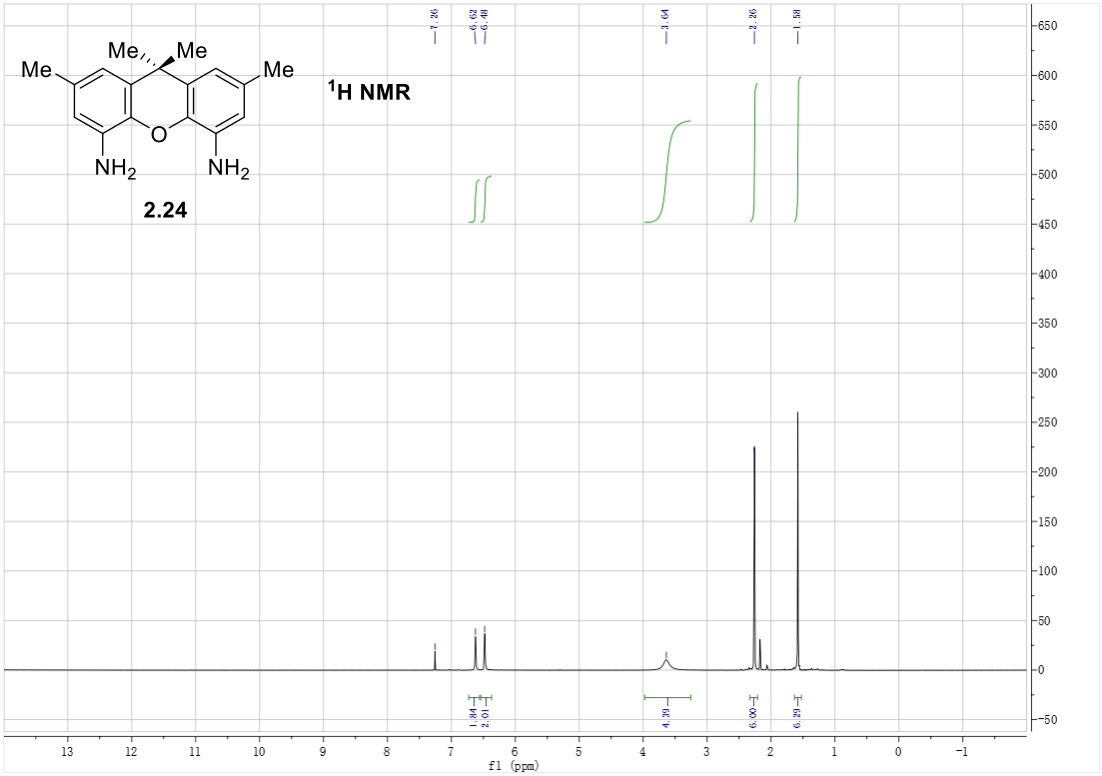
Me
Me
Me
Me
O
NH2
NH2
2.24
1H NMR
7.26
6.62
6.48
3.64
2.26
1.58
1.84
2.01
4.39
6.00
6.29
f1 (ppm)

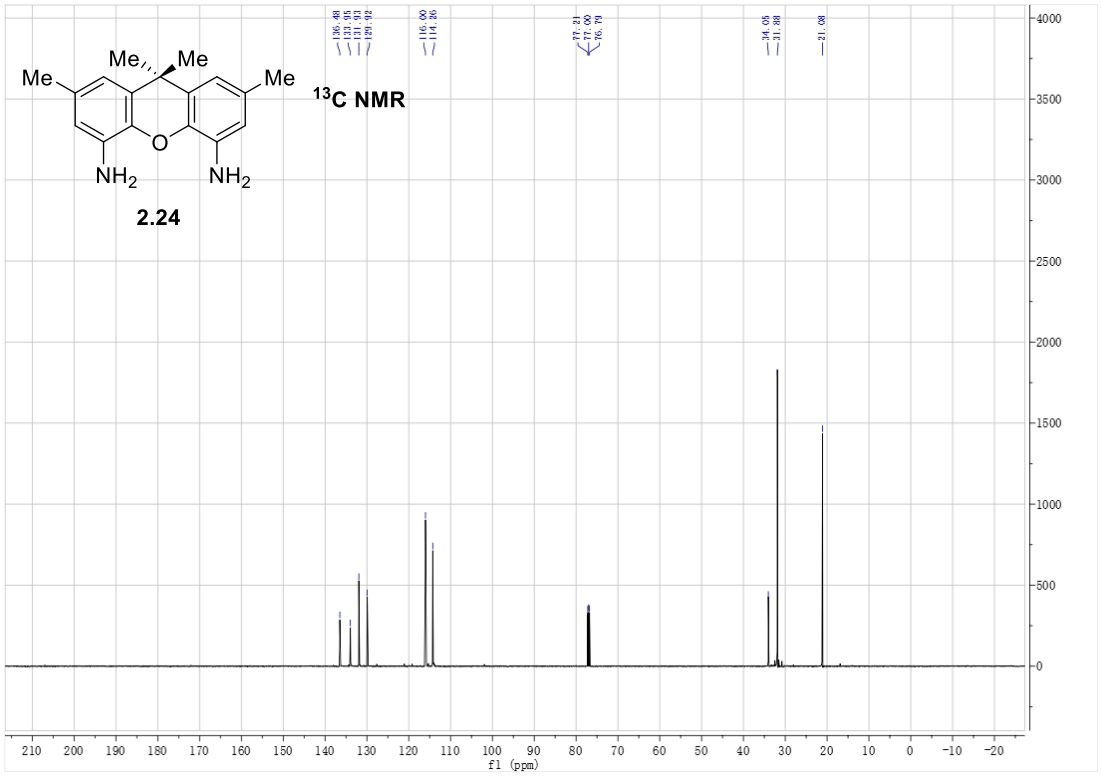
Me
Me
Me
Me
O
NH2
NH2
2.24
13C NMR
136.48
133.95
131.73
129.42
116.00
114.26
77.21
77.00
76.79
24.05
21.88
21.08
f1 (ppm)

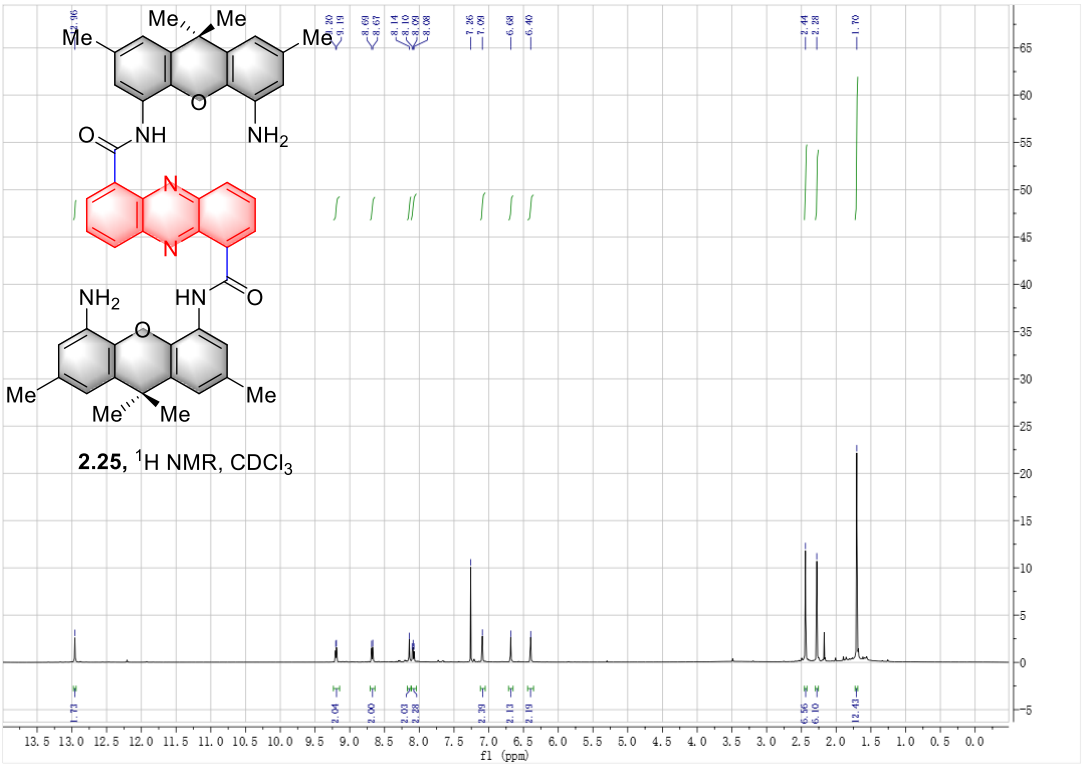
Me
Me
Me
Me
O
NH
NH2
N
N
NH2
HN
O
O
Me
Me
Me
Me
2.25, 1H NMR, CDCl3
f1 (ppm)

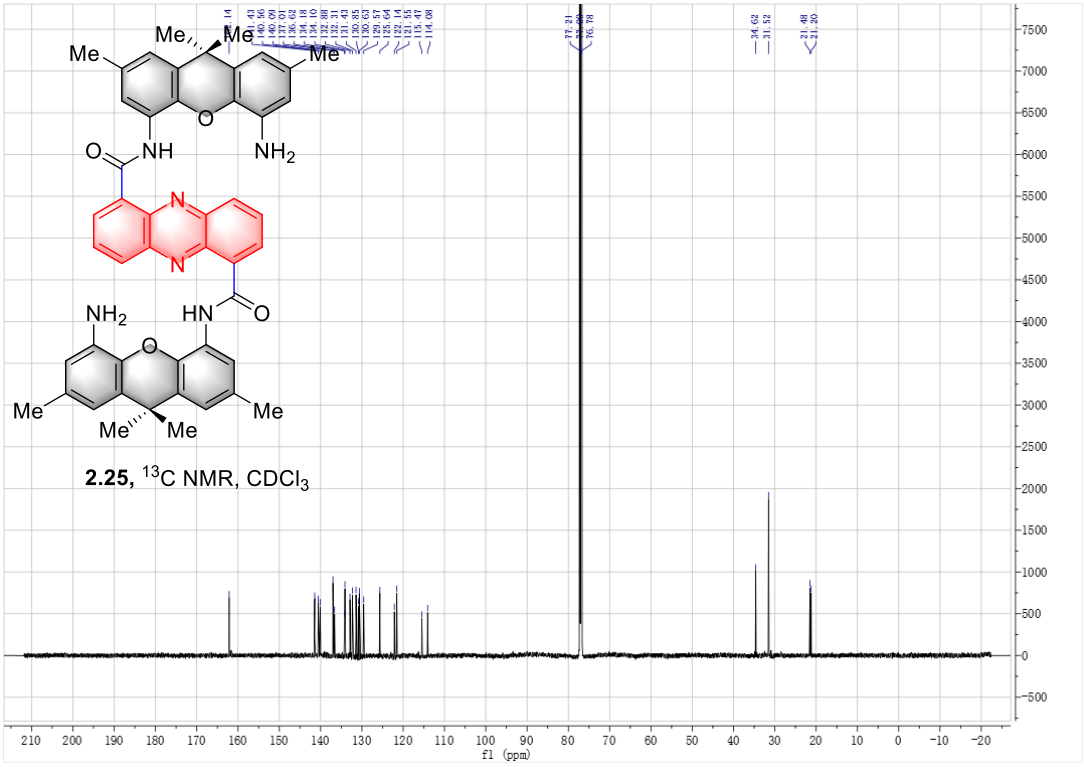
Me
Me
Me
Me
O
NH
NH2
N
N
NH2
HN
O
O
Me
Me
Me
Me
2.25, 13C NMR, CDCl3
f1 (ppm)

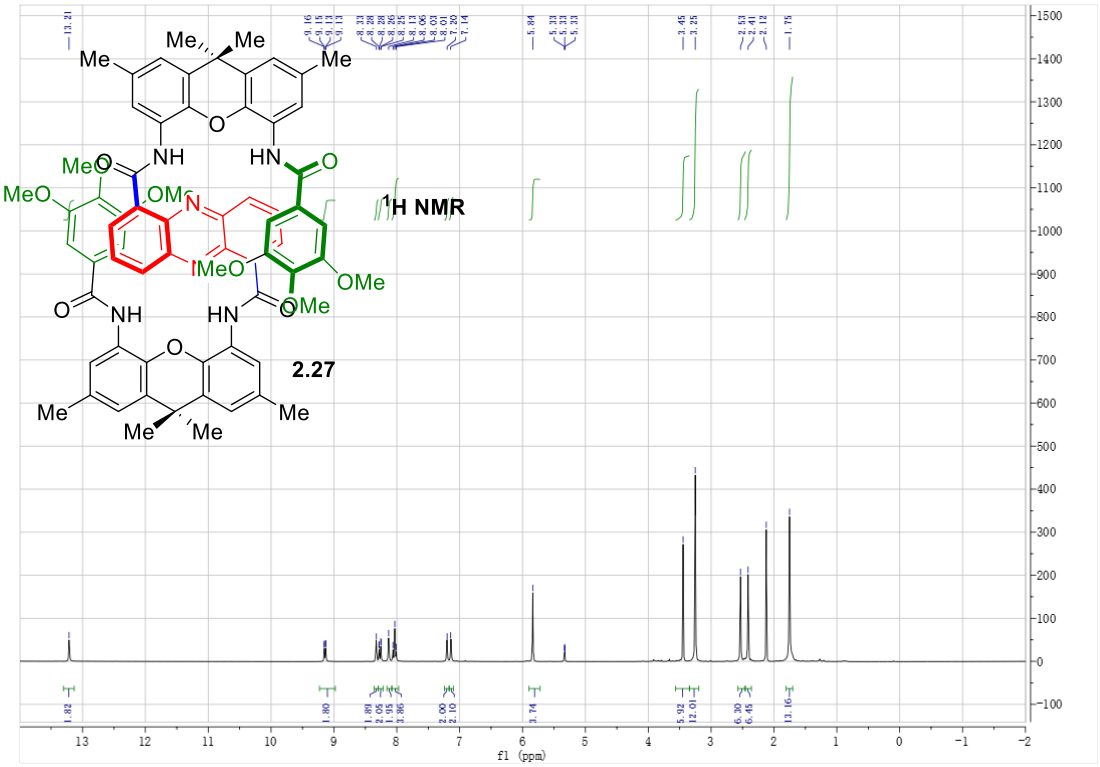
Me
Me
Me
Me
O
NH
HN
O
MeO
MeO
OMe
N
MeO
OMe
O
NH
HN
OMe
O
2.27
Me
Me
Me
Me
^{1}H NMR
f1 (ppm)

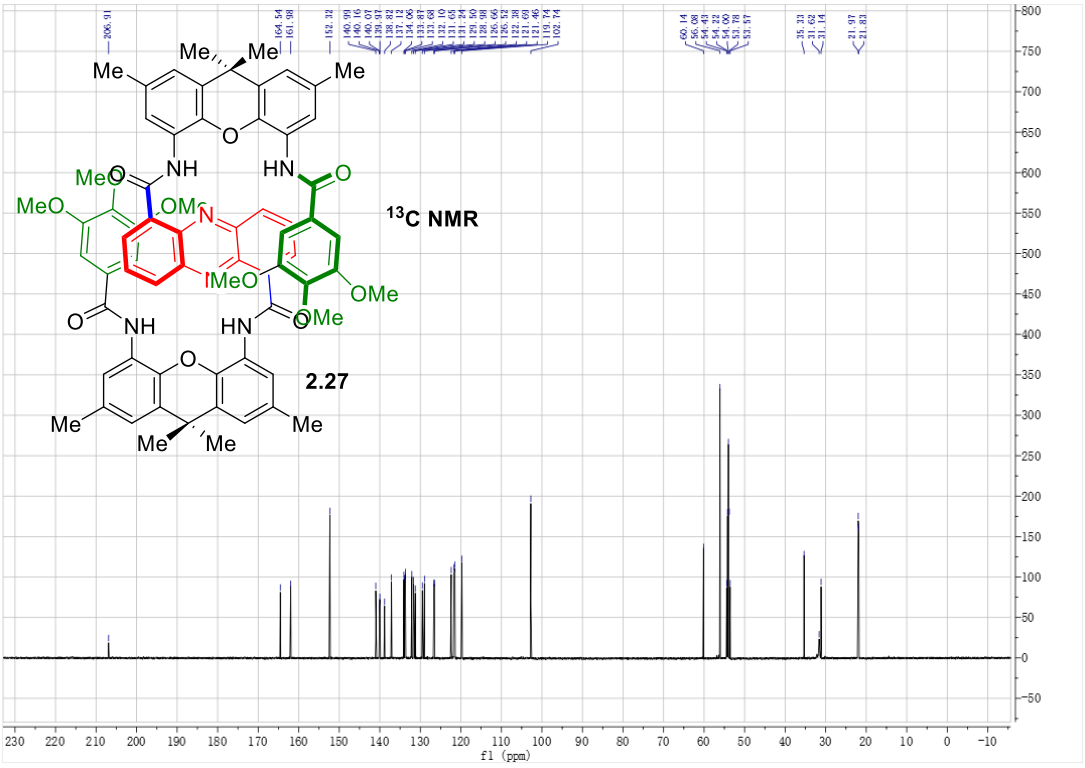
Me
Me
Me
Me
O
NH
HN
O
MeO
MeO
OMe
N
MeO
OMe
O
NH
HN
OMe
O
2.27
Me
Me
Me
Me
^{13}C NMR
f1 (ppm)

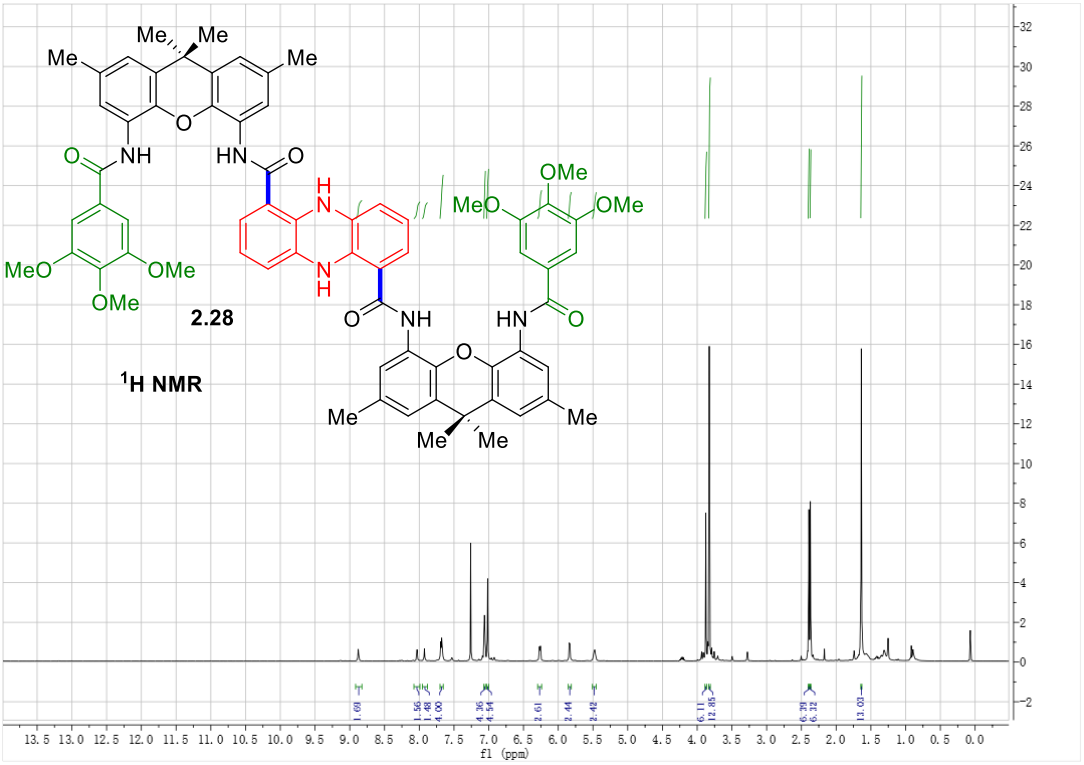

2.28 ^{13}C NMR

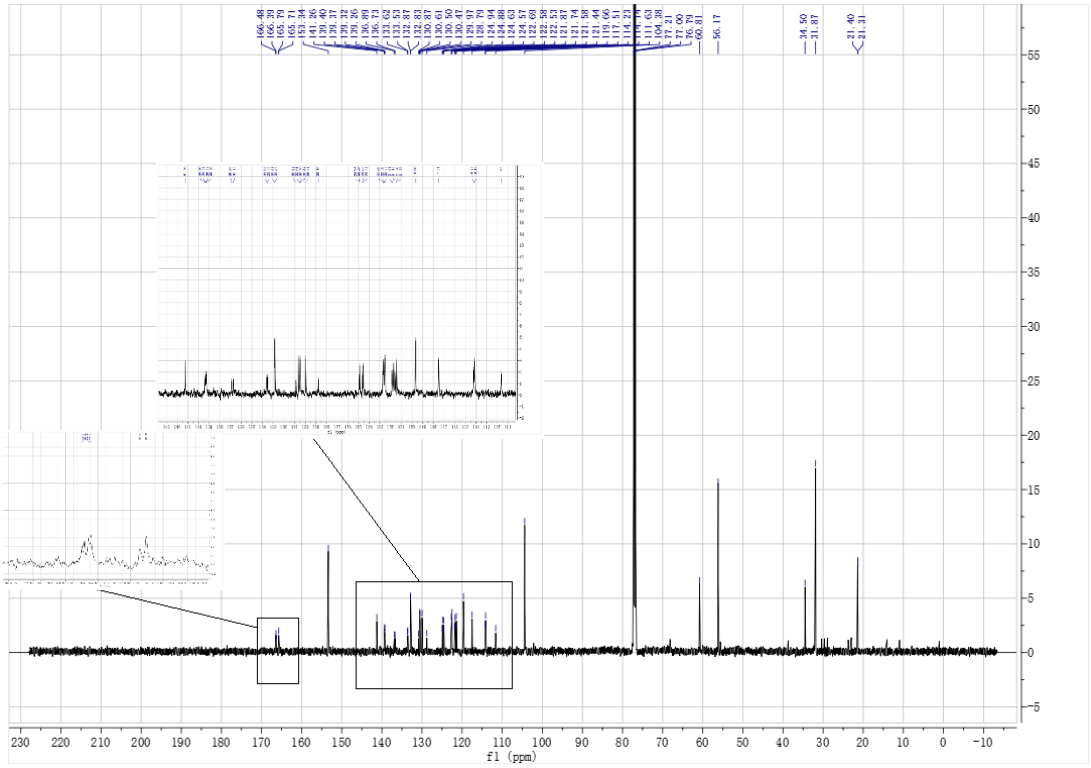

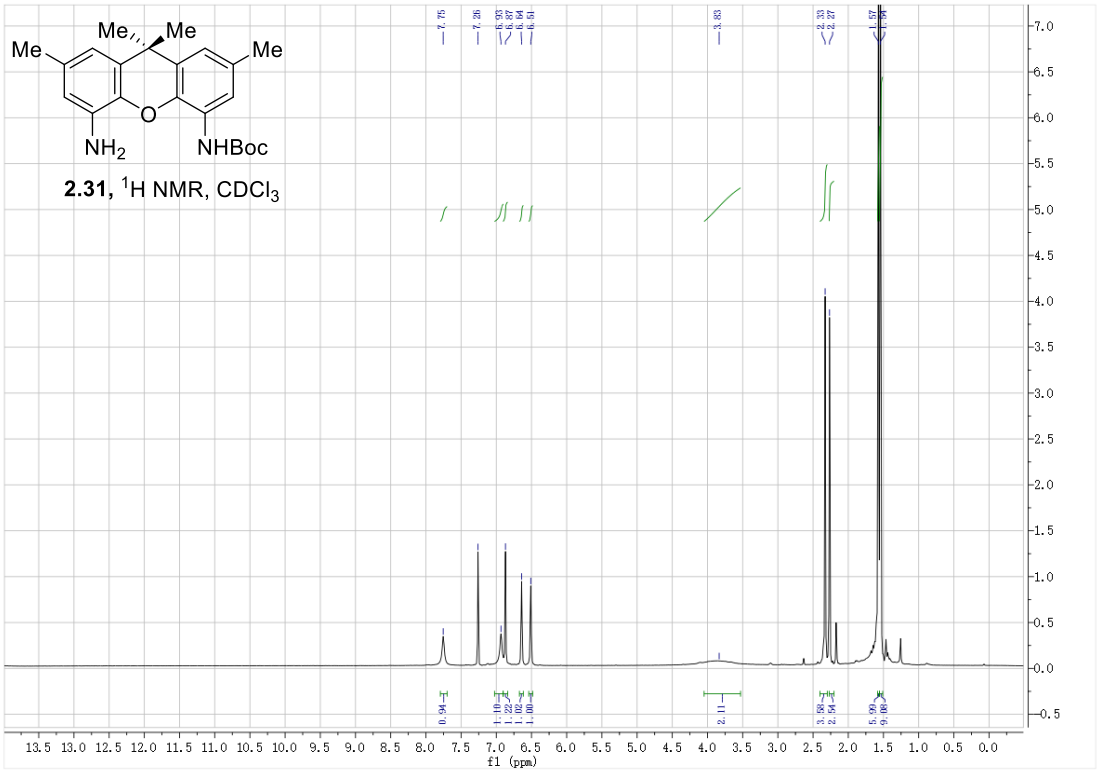
Me
Me
Me
Me
O
NH2
NHBoc
2.31, 1H NMR, CDCl3
f1 (ppm)

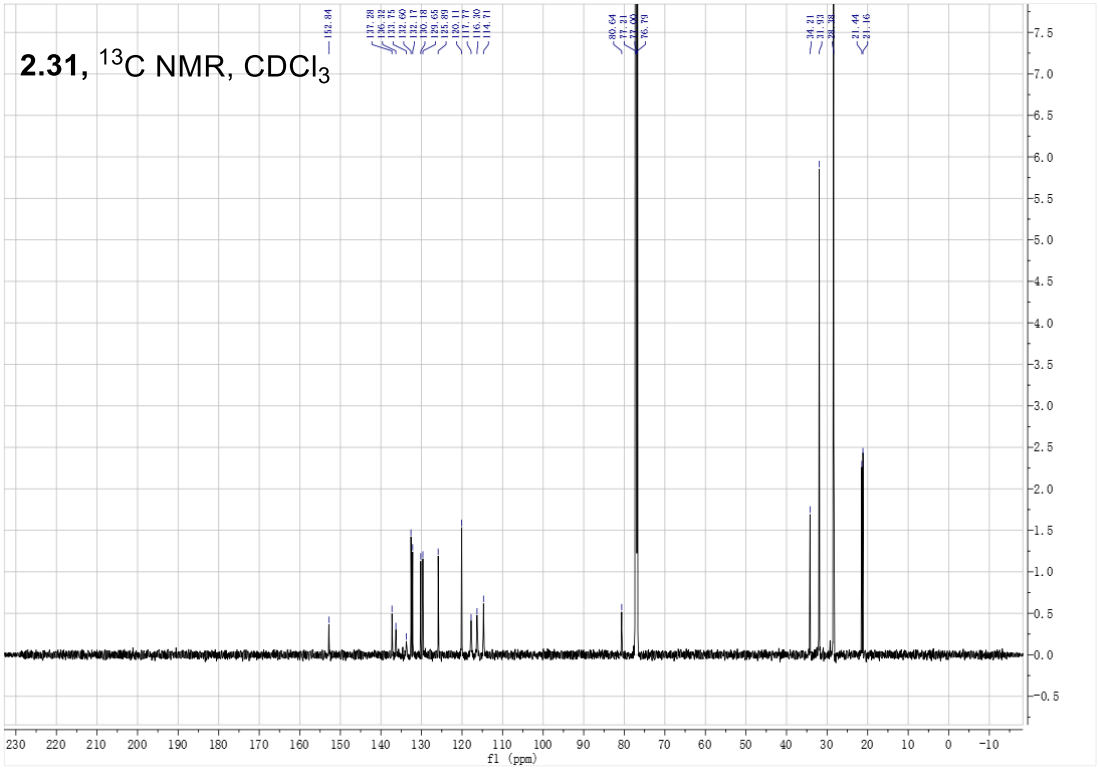
2.31, 13C NMR, CDCl3
f1 (ppm)

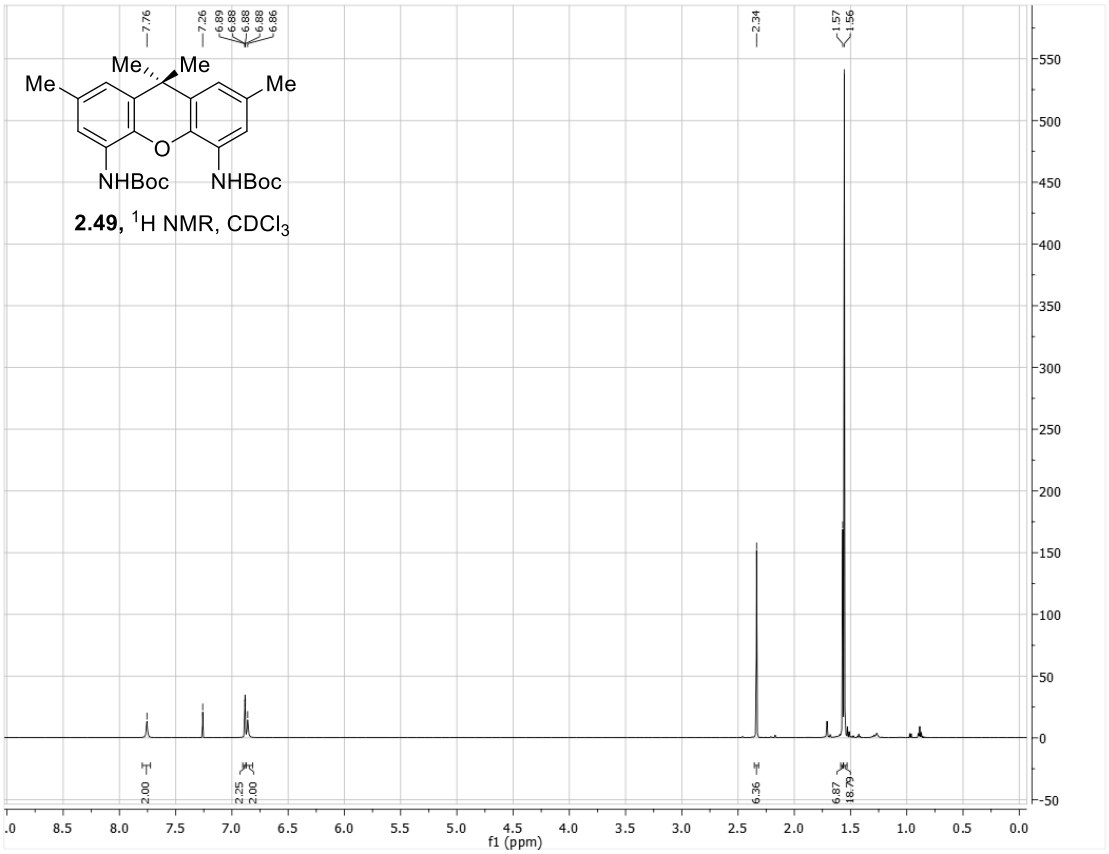

2.49, ^{1}H NMR, $CDCl_3$

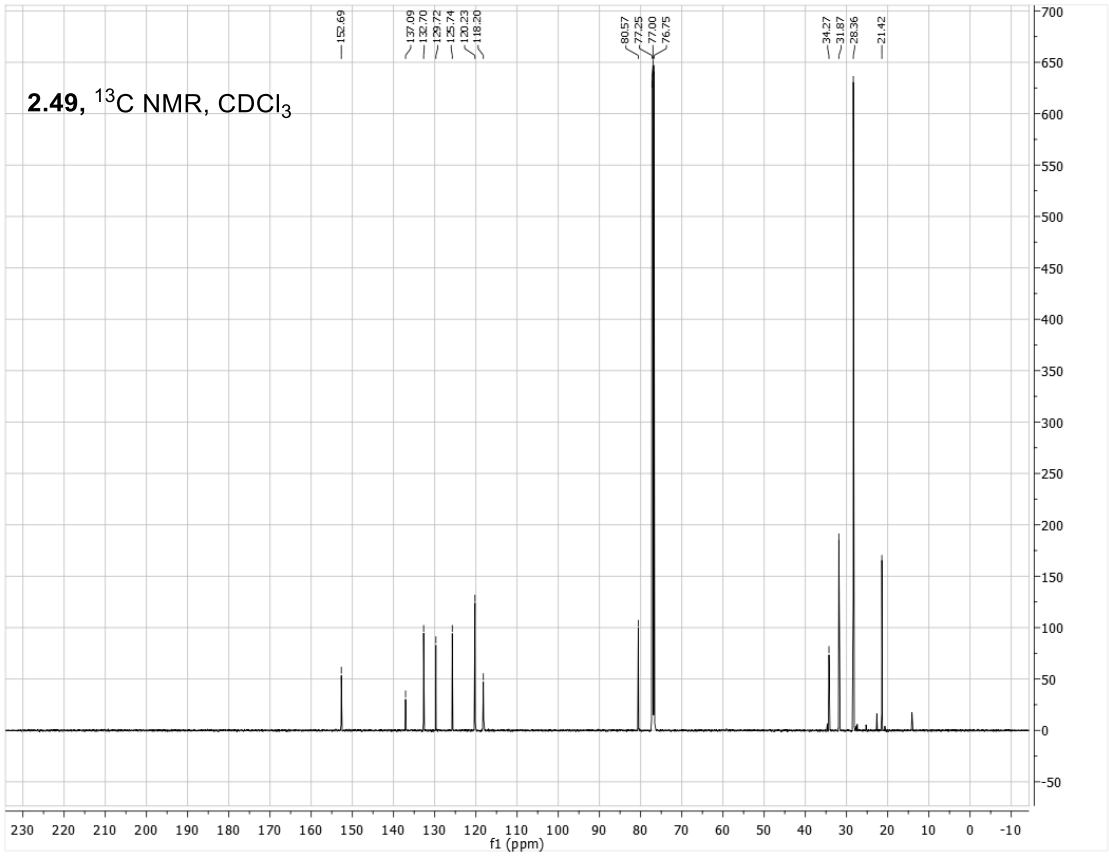

2.49, ^{13}C NMR, $CDCl_3$

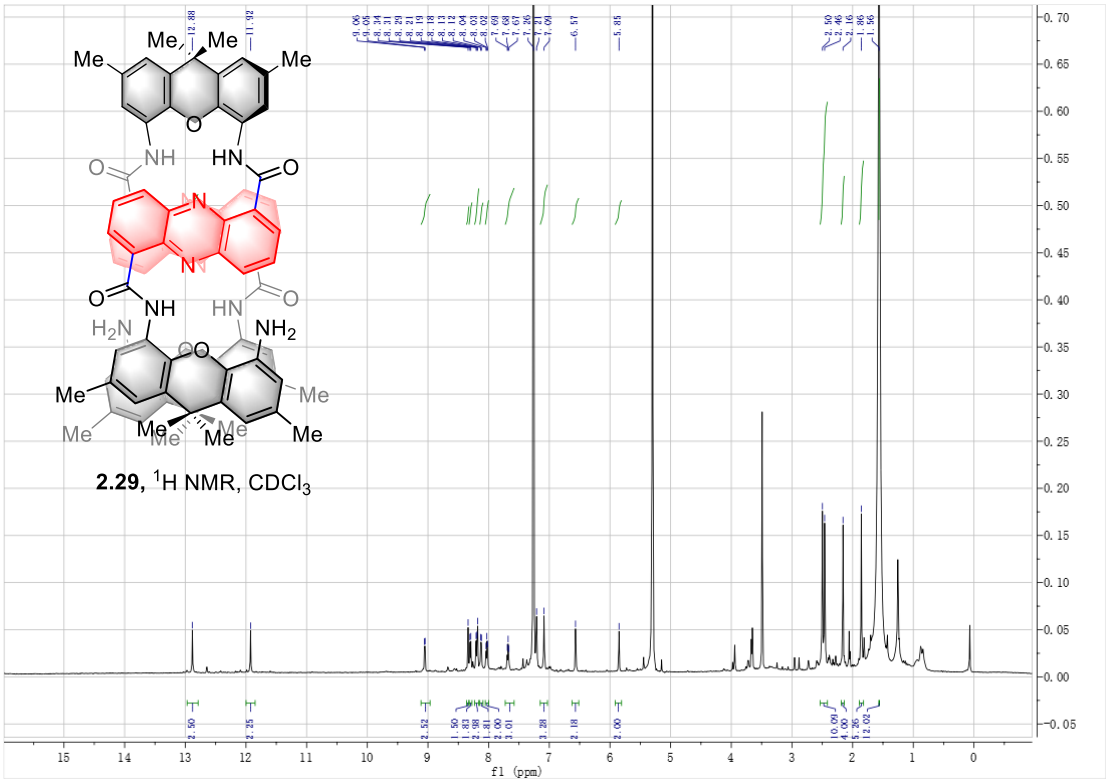
Me
Me
Me
Me
O
NH
HN
O
N
N
O
NH
HN
O
H2N
NH2
O
Me
Me
Me
Me
Me
Me
Me
Me
2.29, 1H NMR, CDCl3
f1 (ppm)

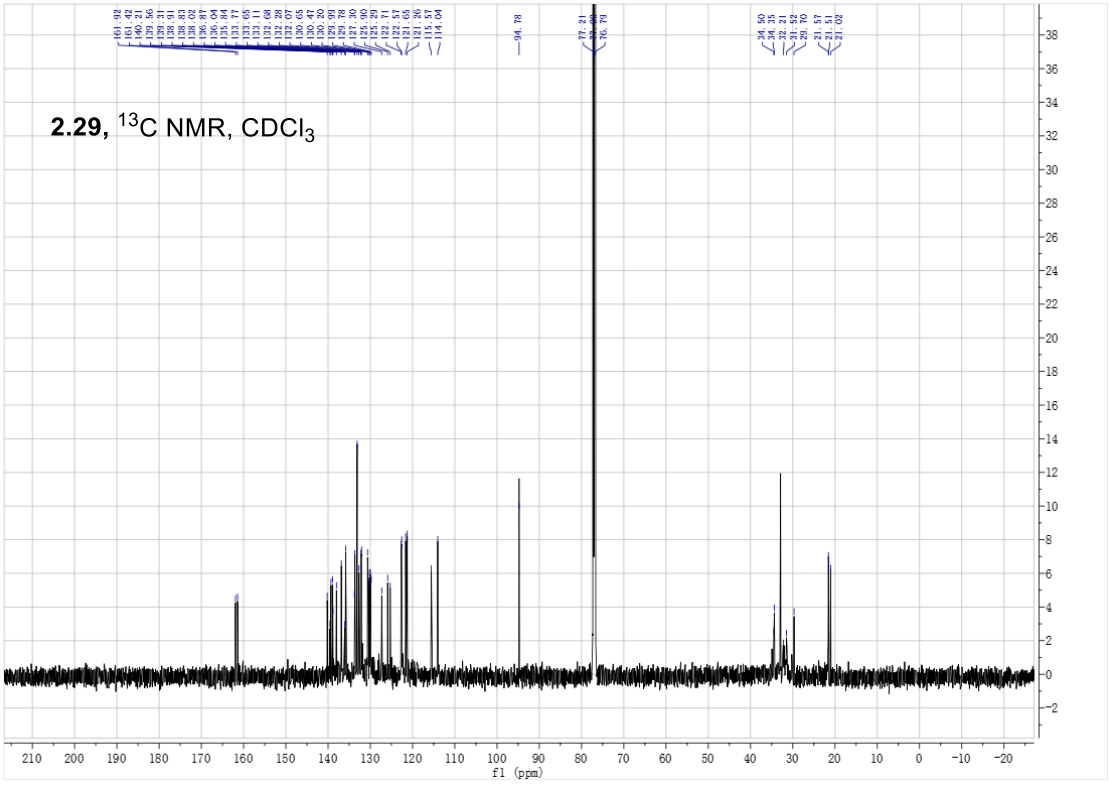
2.29, 13C NMR, CDCl3
f1 (ppm)

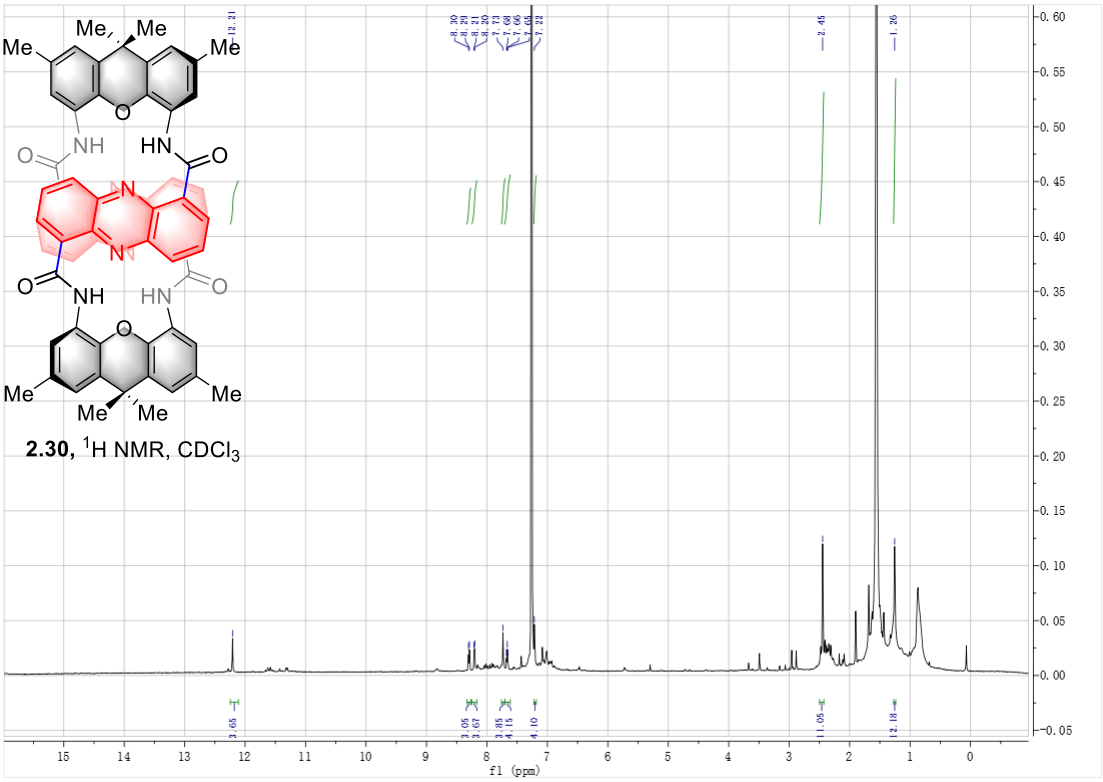
Me
Me
Me
O
NH
HN
O
O
N
N
O
NH
HN
O
O
Me
Me
Me
Me
2.30, 1H NMR, CDCl3
f1 (ppm)

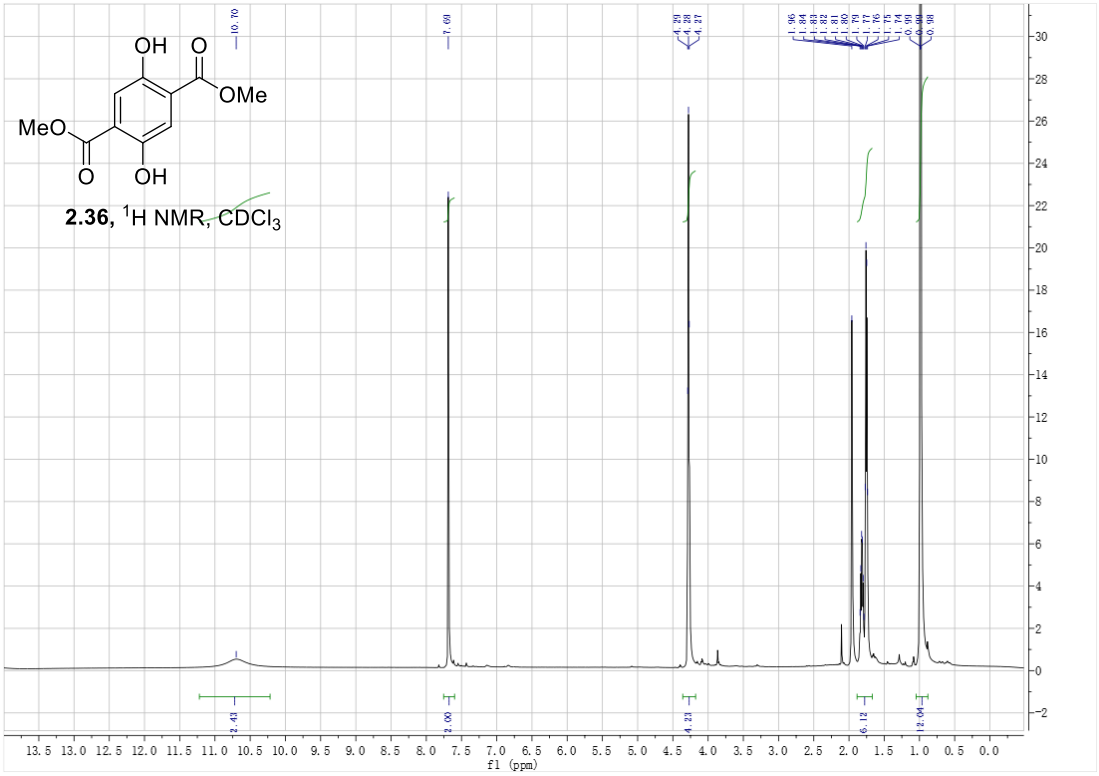
OH
O
OMe
MeO
O
OH
2.36, 1H NMR, CDCl3
f1 (ppm)

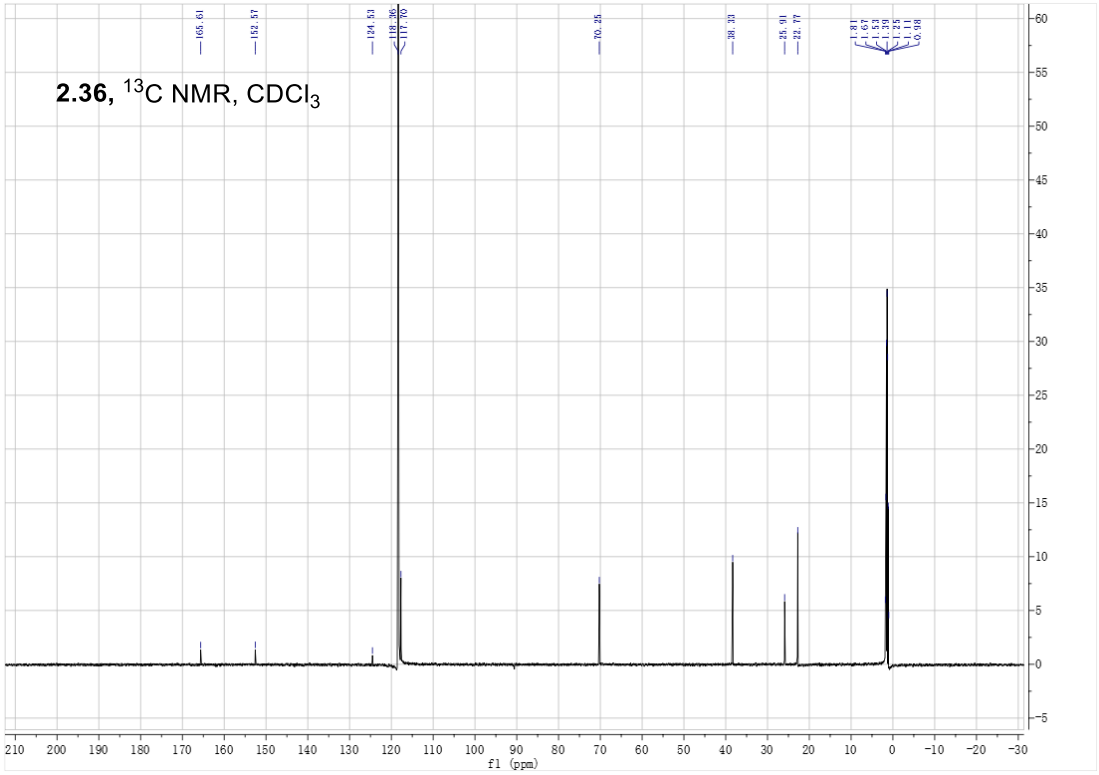
2.36, 13C NMR, CDCl3
f1 (ppm)

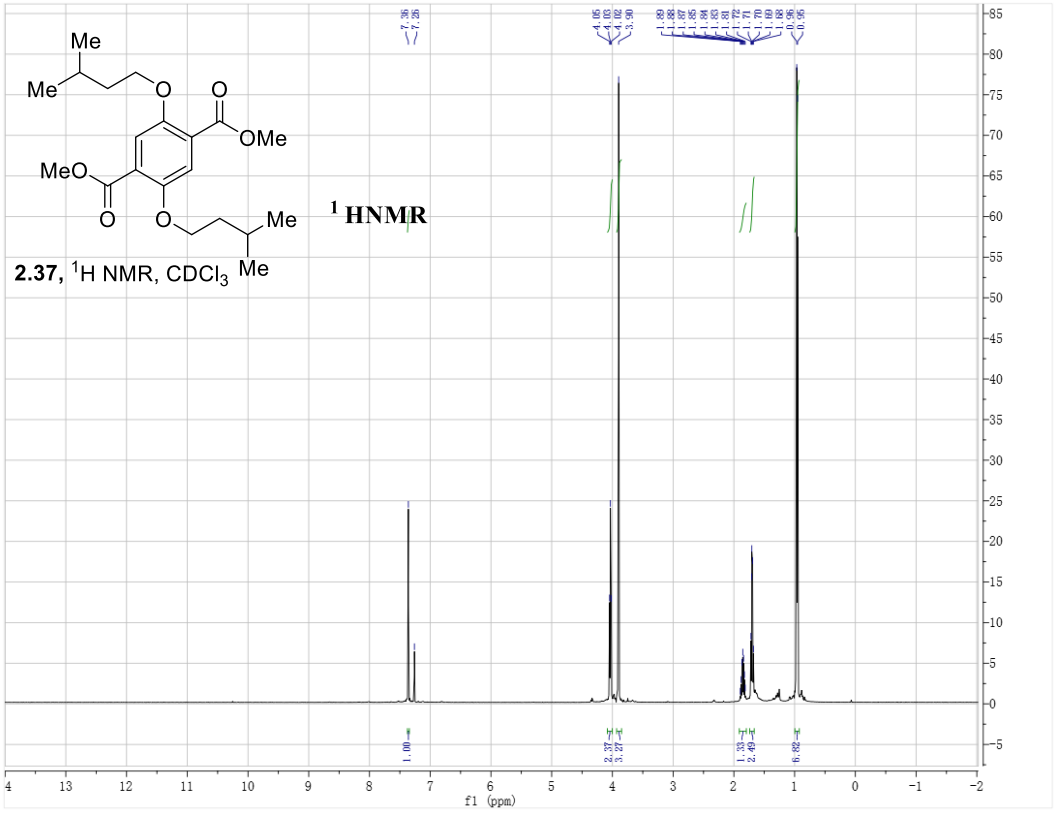
Me
Me
O
O
OMe
MeO
O
O
Me
Me
2.37, 1H NMR, CDCl3
1 HNMR
f1 (ppm)

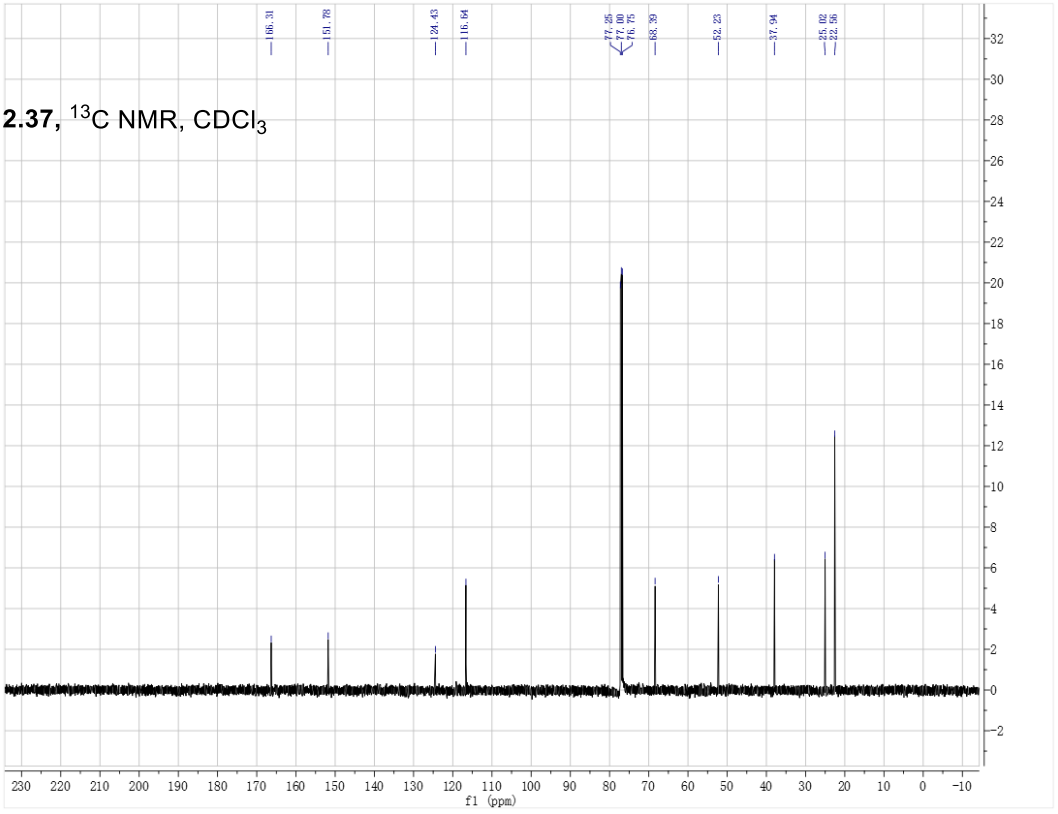
2.37, 13C NMR, CDCl3
f1 (ppm)

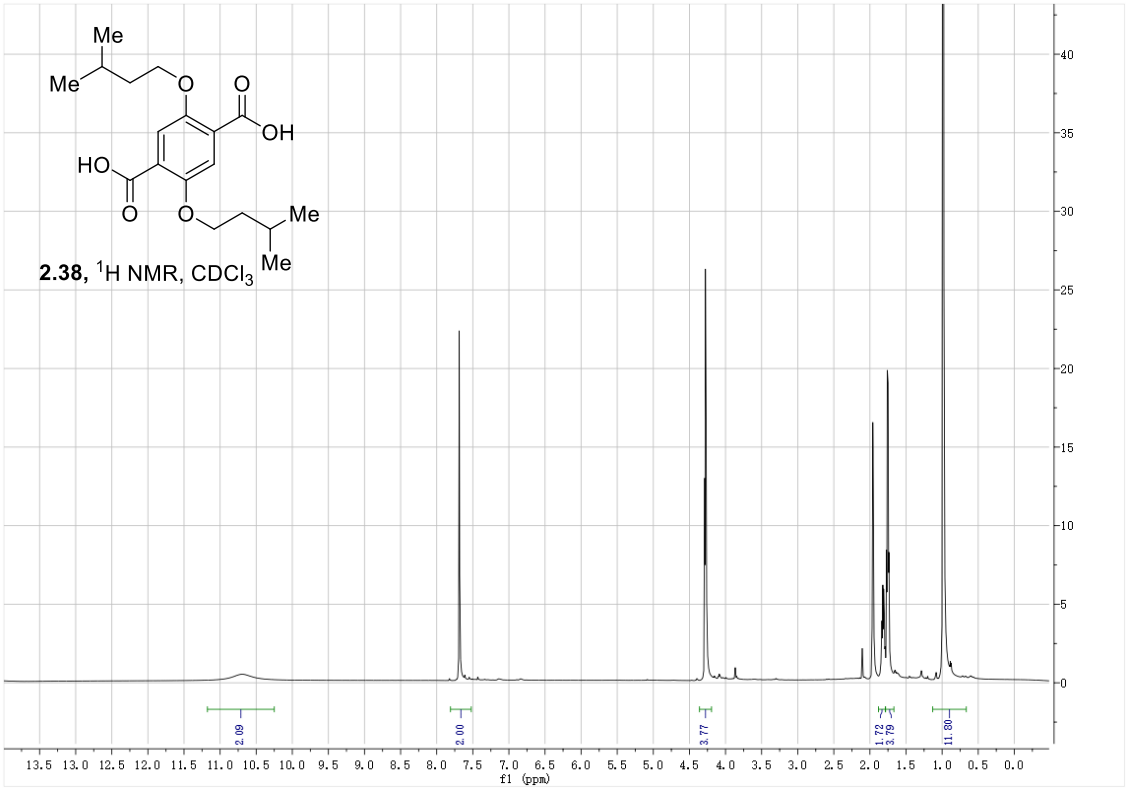
Me
Me
O
O
OH
HO
O
O
Me
Me
2.38, 1H NMR, CDCl3
2.09
2.00
3.77
1.72
3.79
11.60
f1 (ppm)

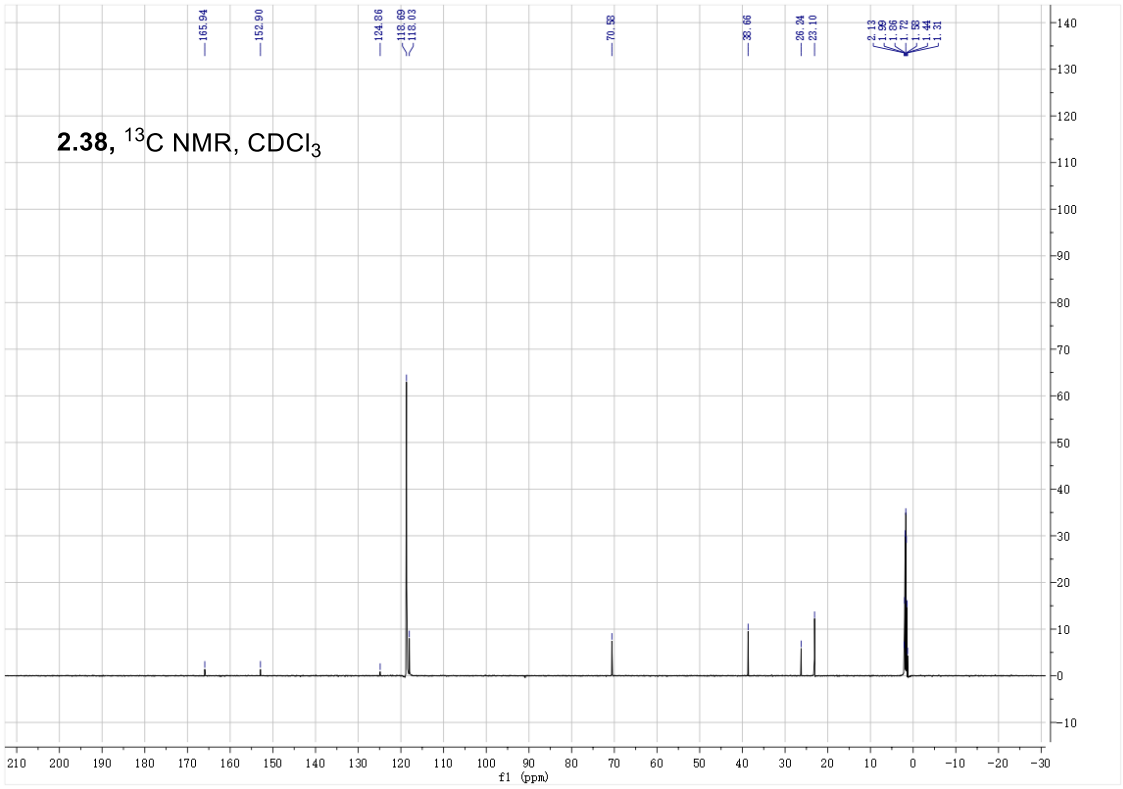
165.94
152.90
124.86
118.69
118.03
70.83
38.66
26.24
23.10
2.13
1.99
1.96
1.72
1.59
1.44
1.31
2.38, 13C NMR, CDCl3
f1 (ppm)

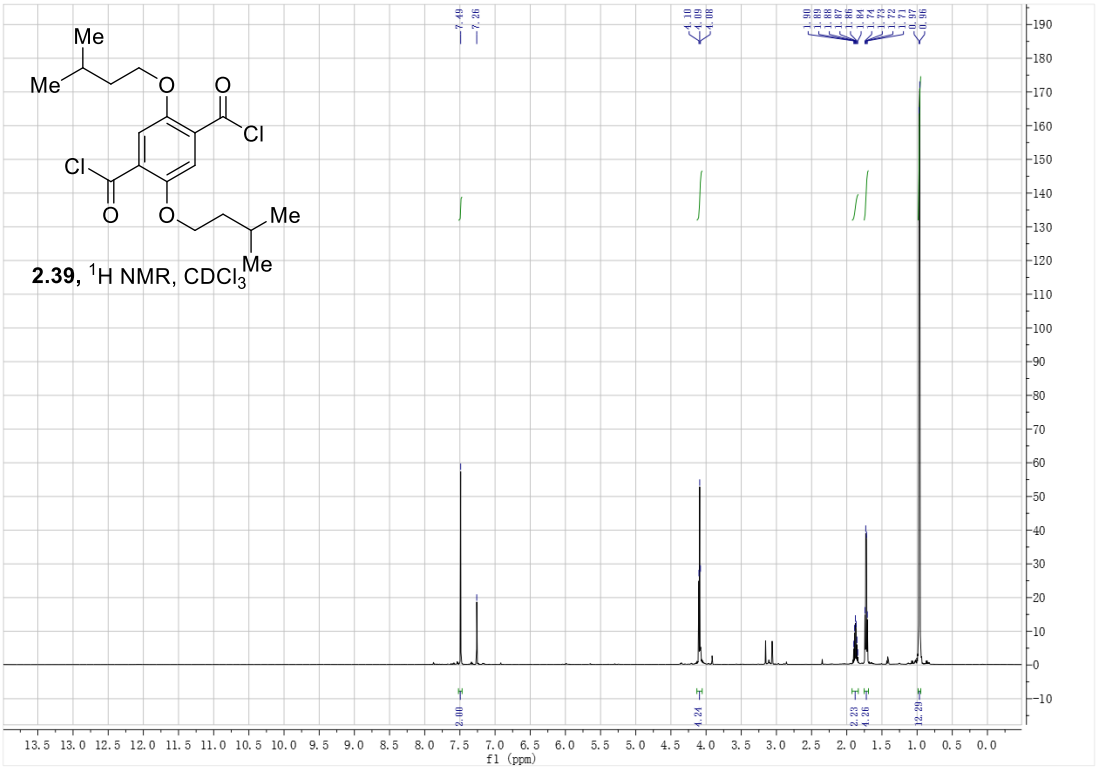
Me
Me
O
O
Cl
Cl
O
O
Me
Me
2.39, 1H NMR, CDCl3

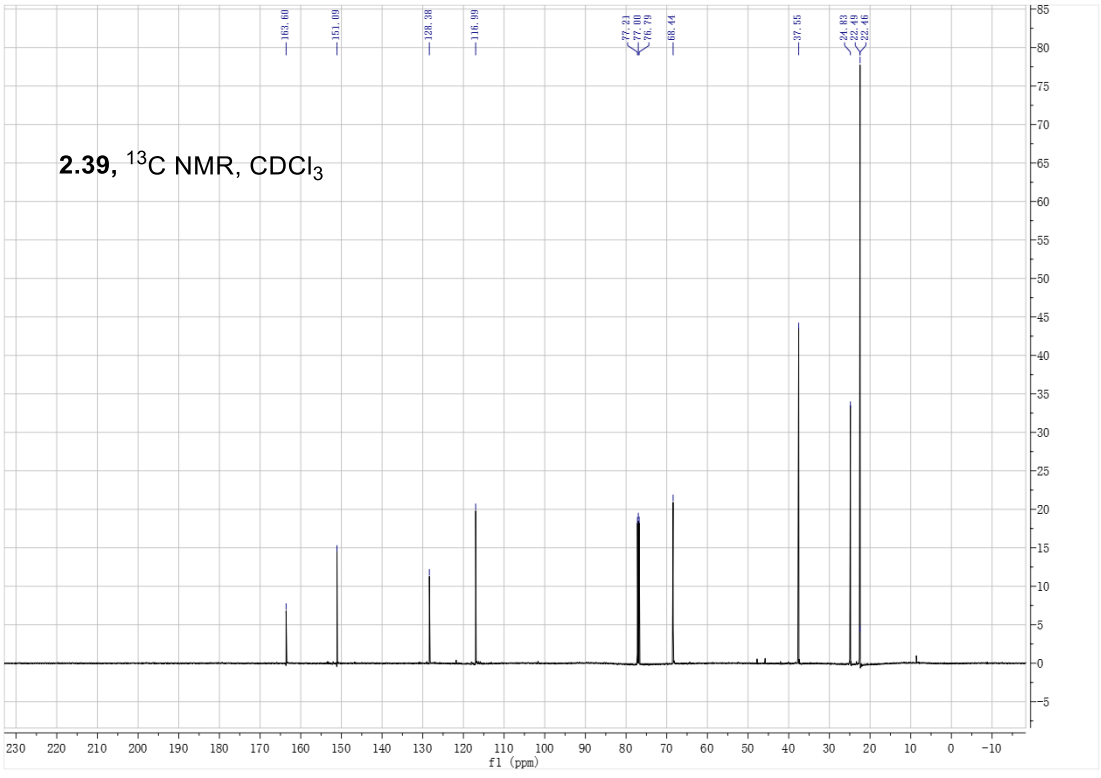
2.39, 13C NMR, CDCl3

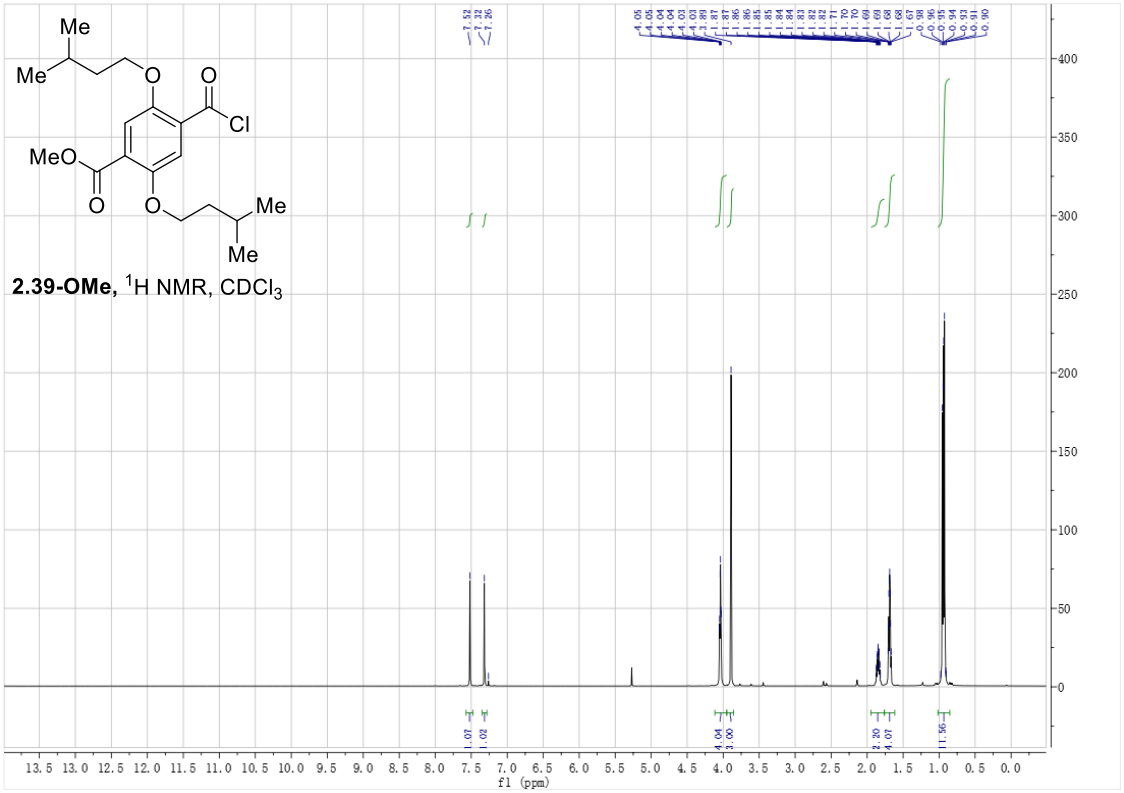
Me
Me
O
O
Cl
MeO
O
O
Me
Me
2.39-OMe, 1H NMR, CDCl3
f1 (ppm)

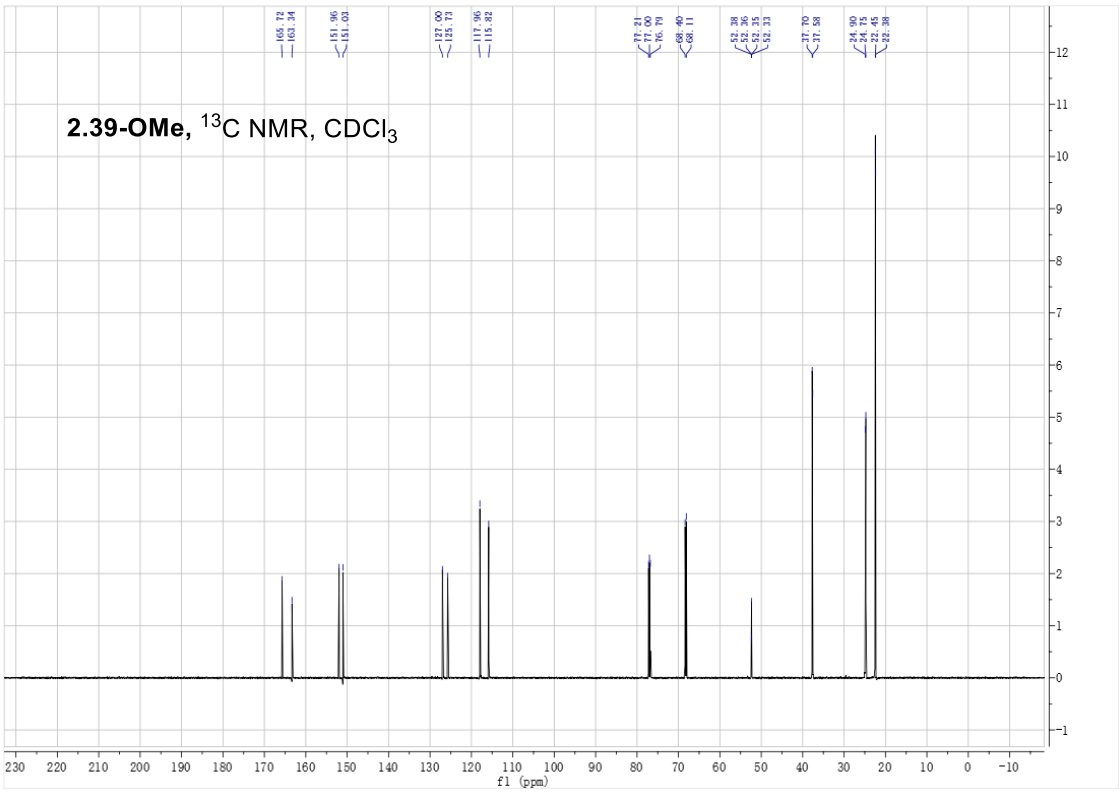
2.39-OMe, 13C NMR, CDCl3
f1 (ppm)

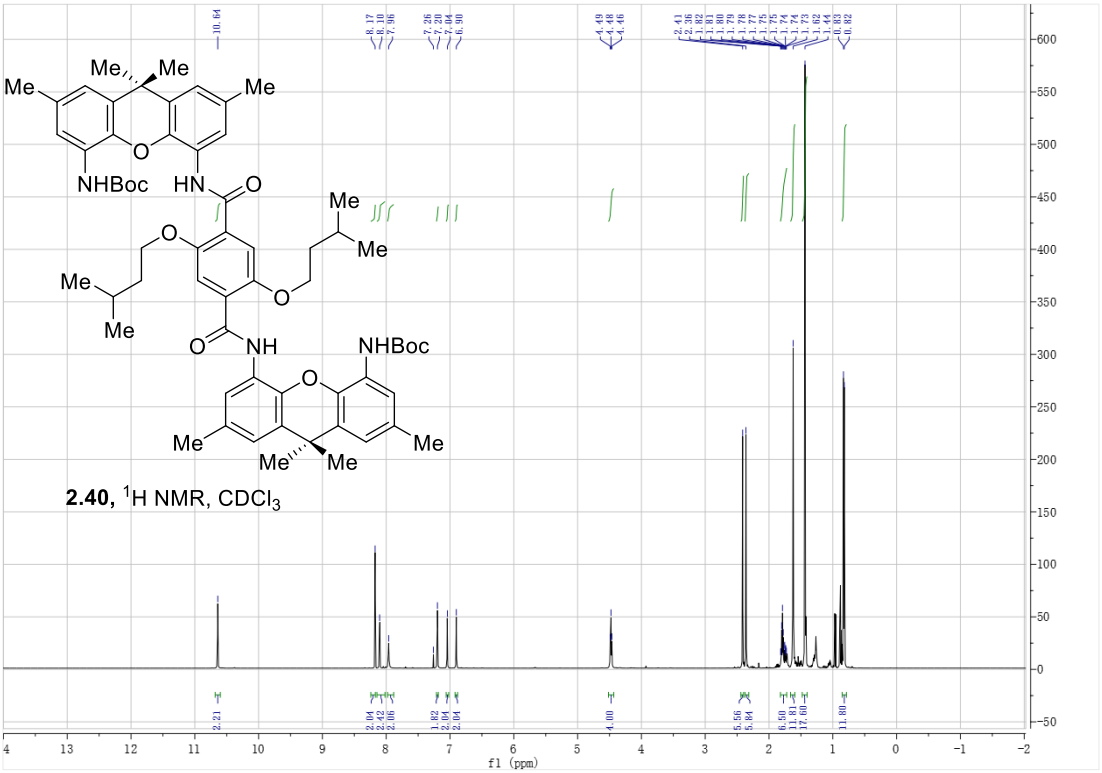

2.40, ^{1}H NMR, $CDCl_3$

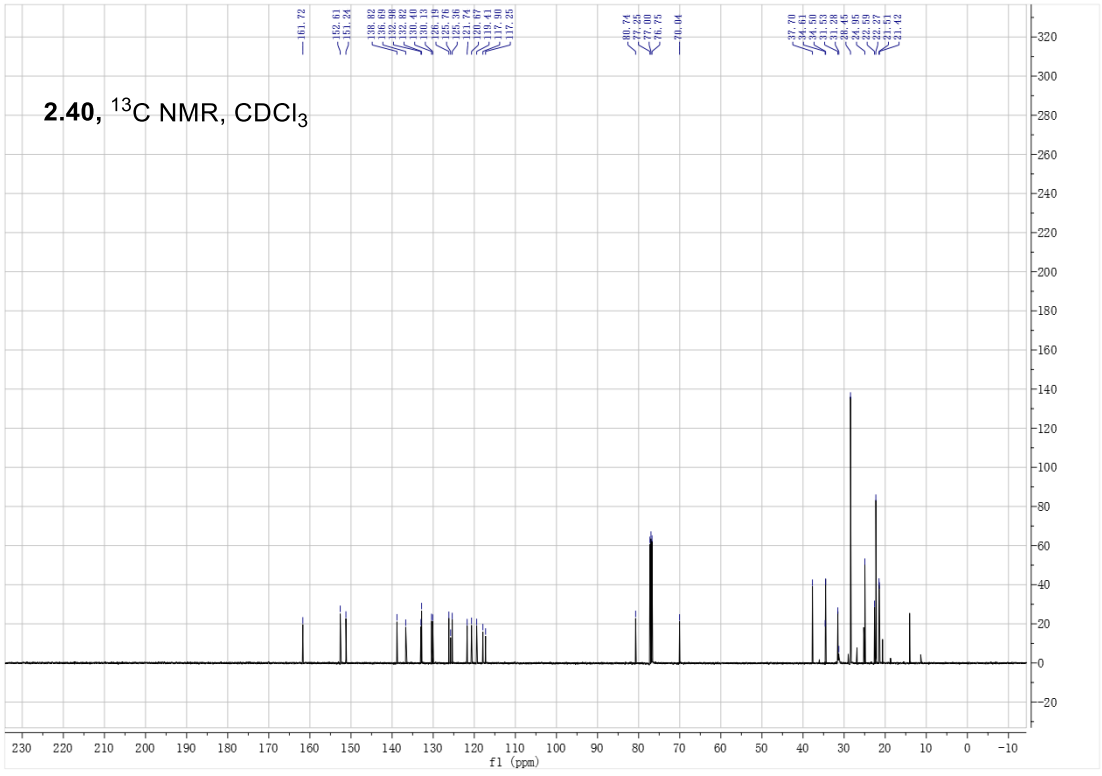

2.40, ^{13}C NMR, $CDCl_3$

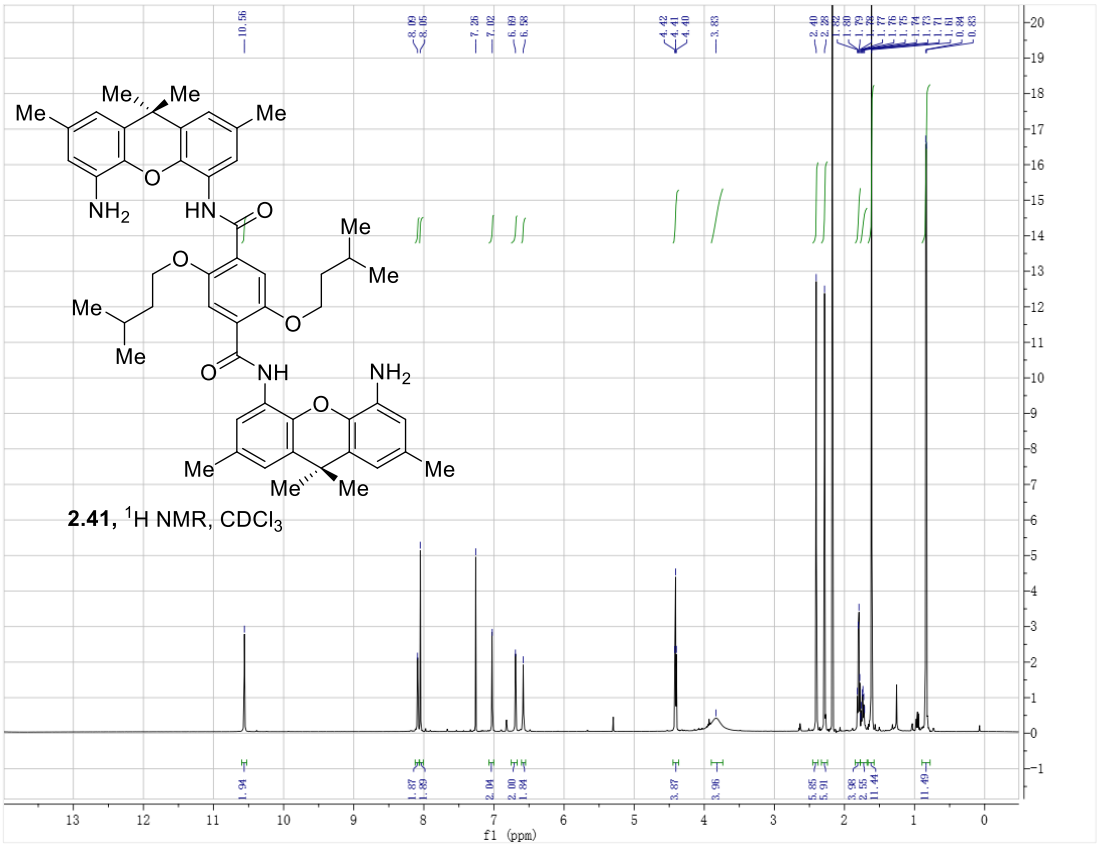

2.41, ^{1}H NMR, $CDCl_3$

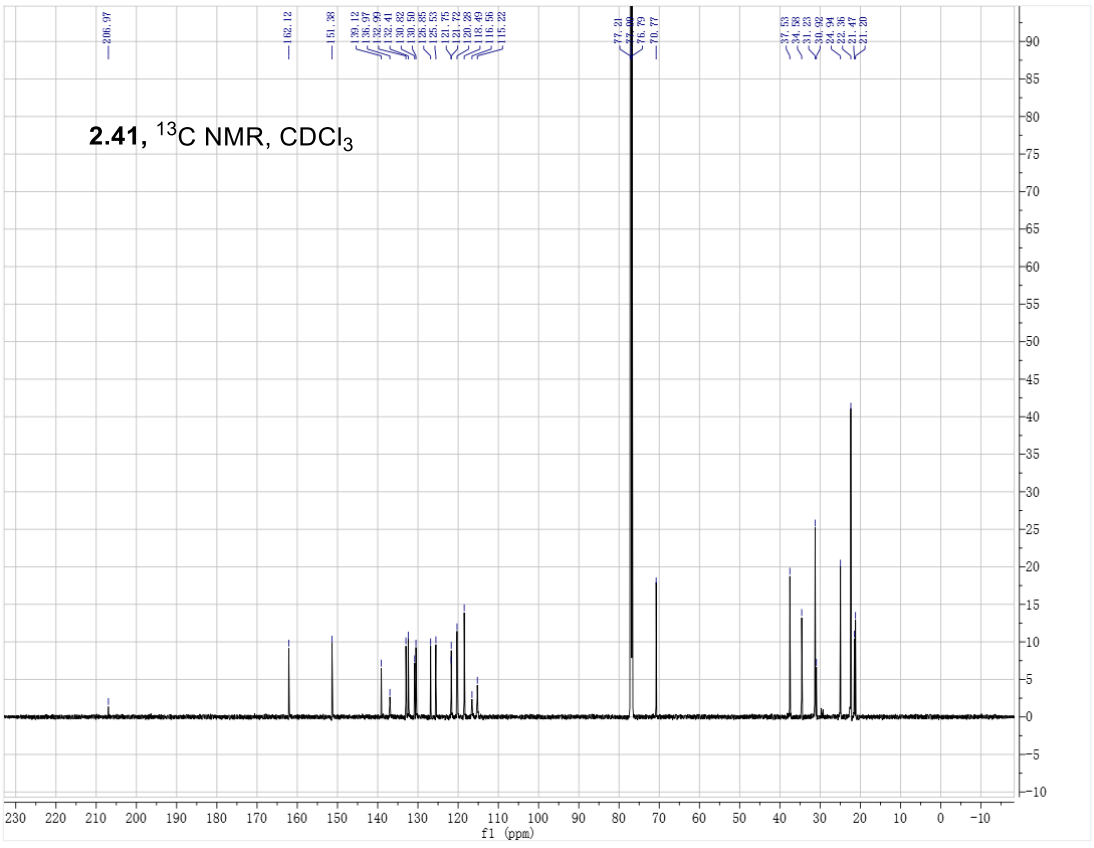

2.41, ^{13}C NMR, $CDCl_3$

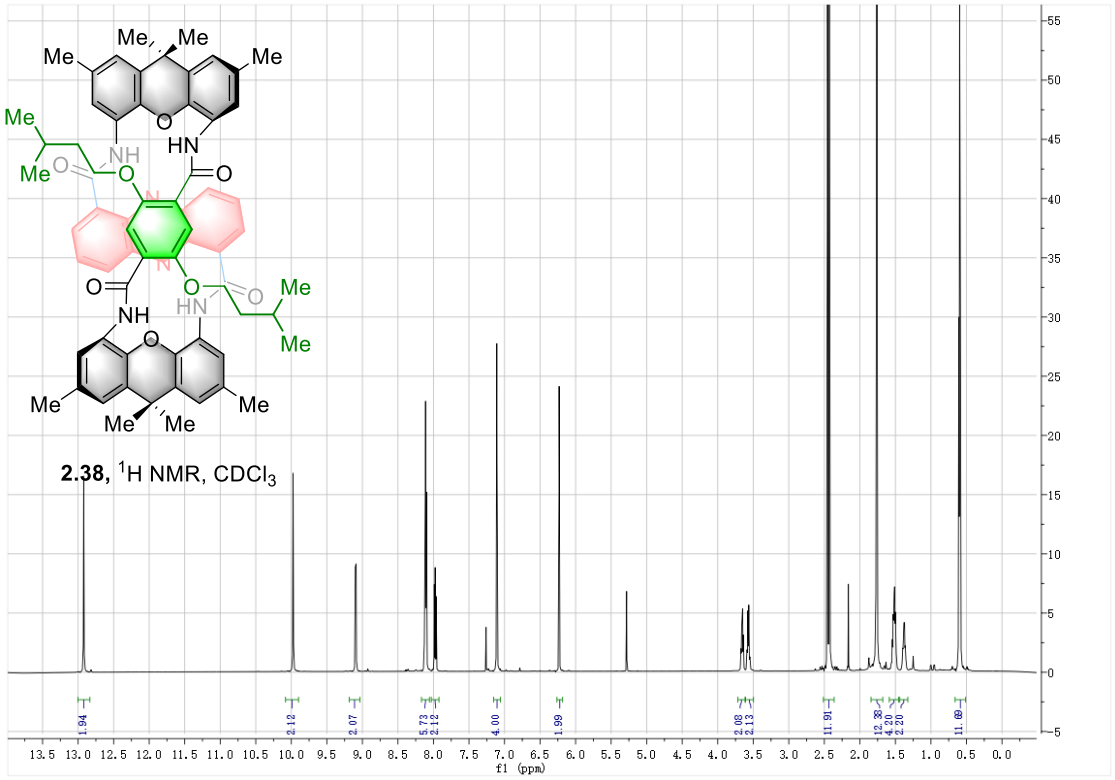
2.38, ^{1}H NMR, CDCl$_3$

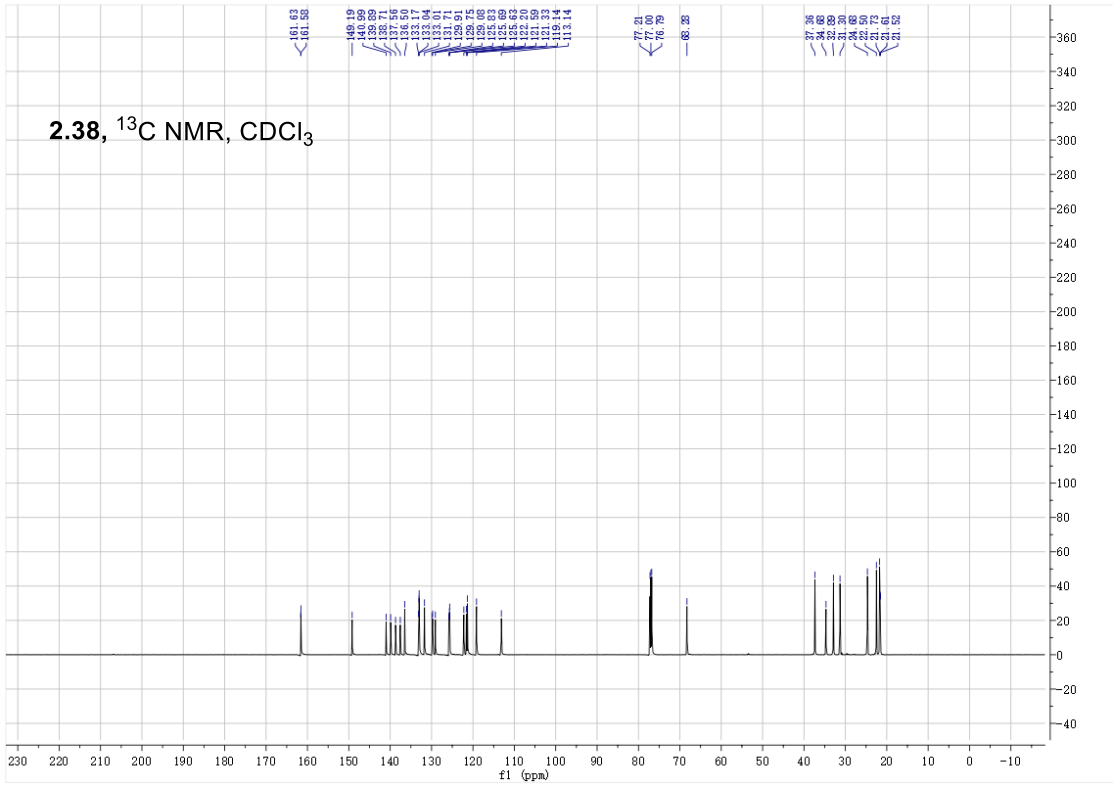
2.38, ^{13}C NMR, CDCl$_3$

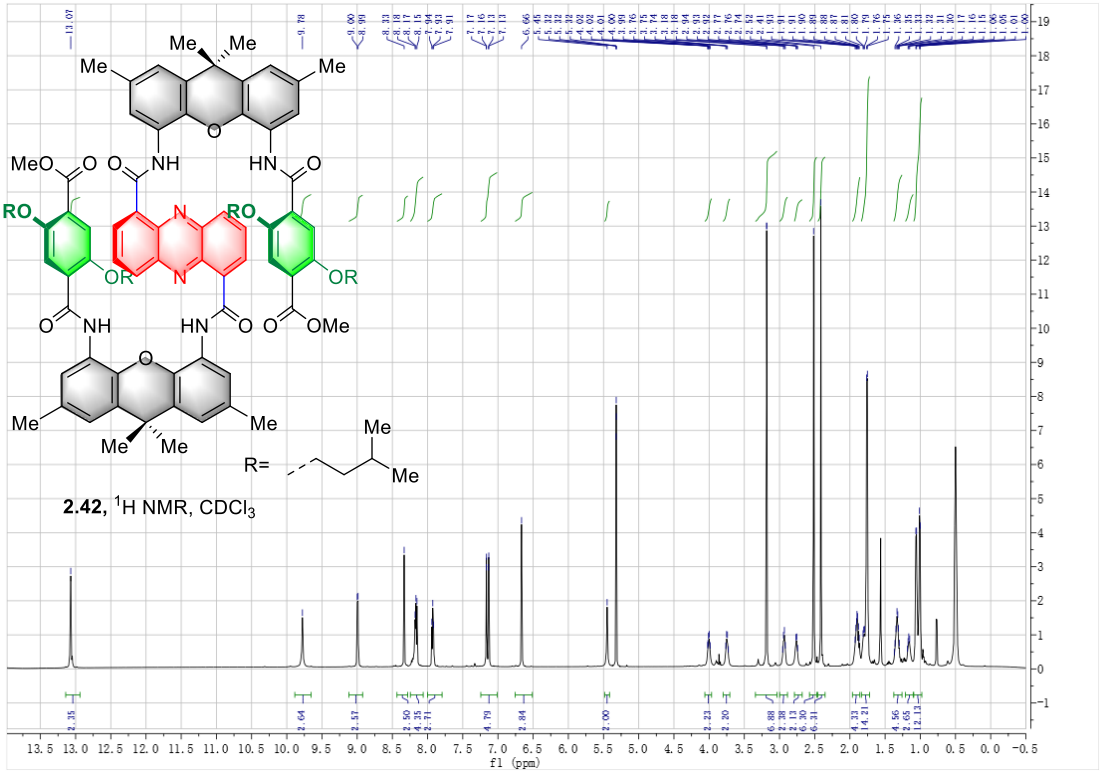
Me
Me
Me
Me
O
MeO
O
O
NH
HN
O
RO
RO
N
N
OR
OR
O
NH
HN
O
O
OMe
O
Me
Me
Me
Me
R=
Me
Me
2.42, 1H NMR, CDCl3
f1 (ppm)

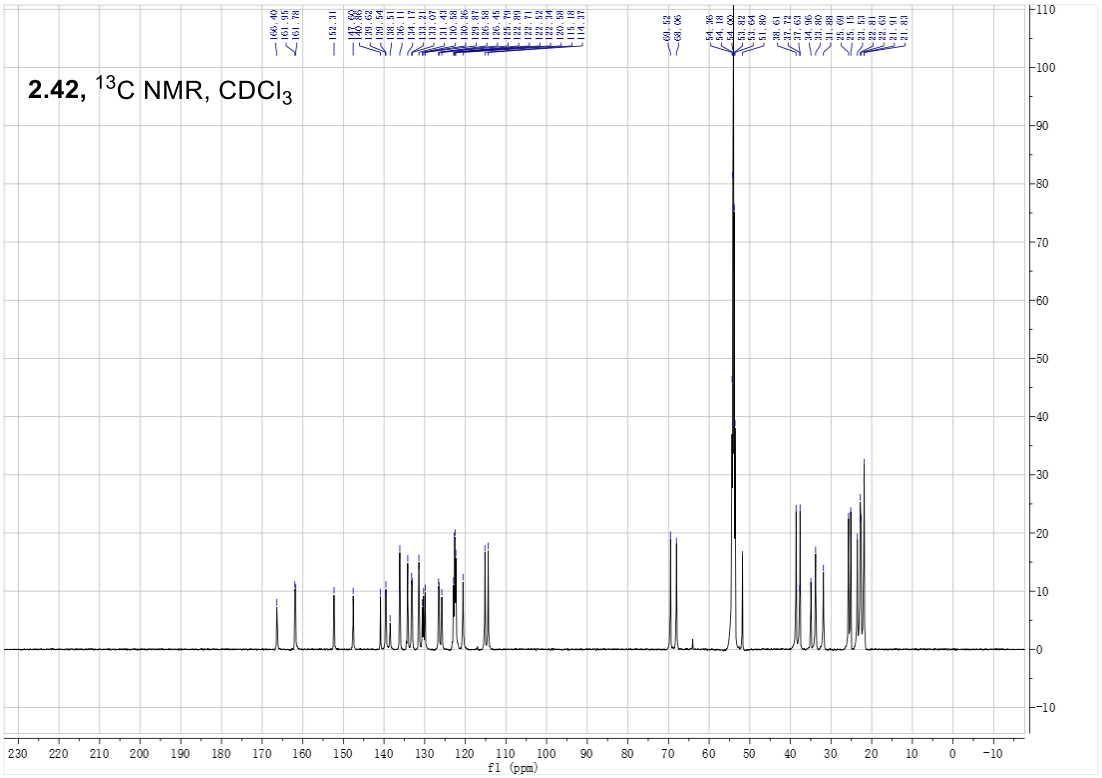
2.42, 13C NMR, CDCl3
f1 (ppm)

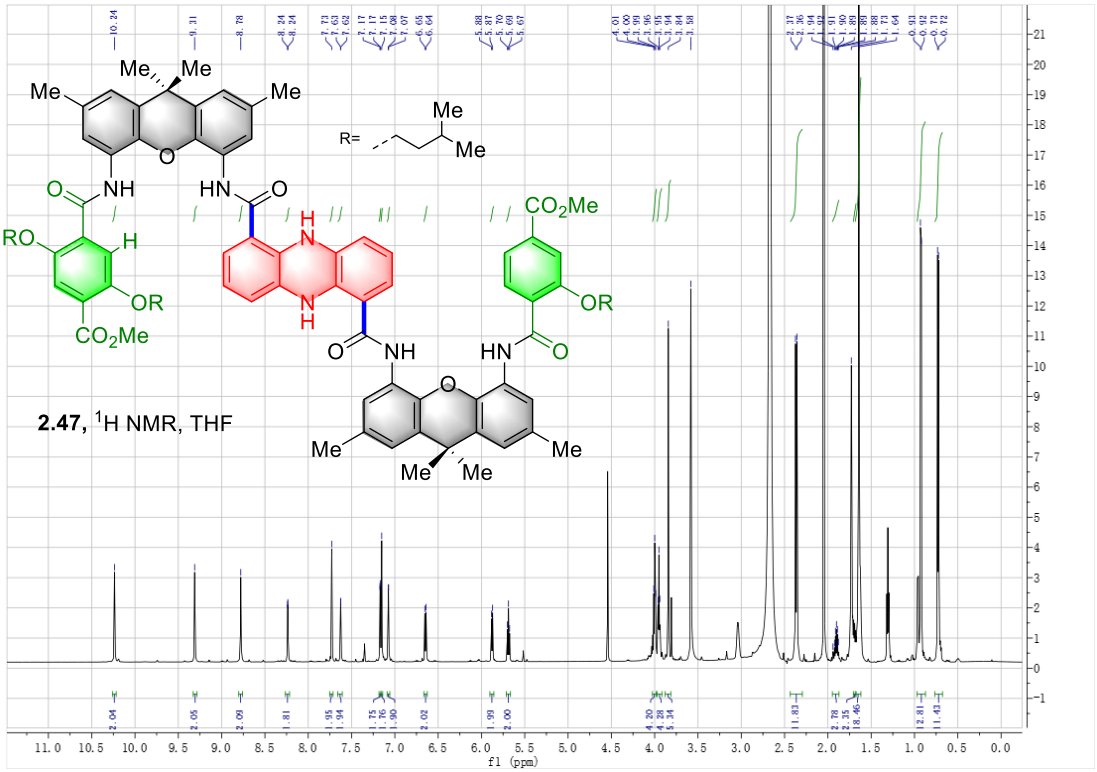
2.47, 1H NMR, THF
R=
Me
Me
Me
Me
Me
Me
Me
Me
O
NH
HN
O
RO
H
OR
CO2Me
CO2Me
OR
H
N
N
H
O
NH
HN
O
O
Me
Me
Me
Me
f1 (ppm)

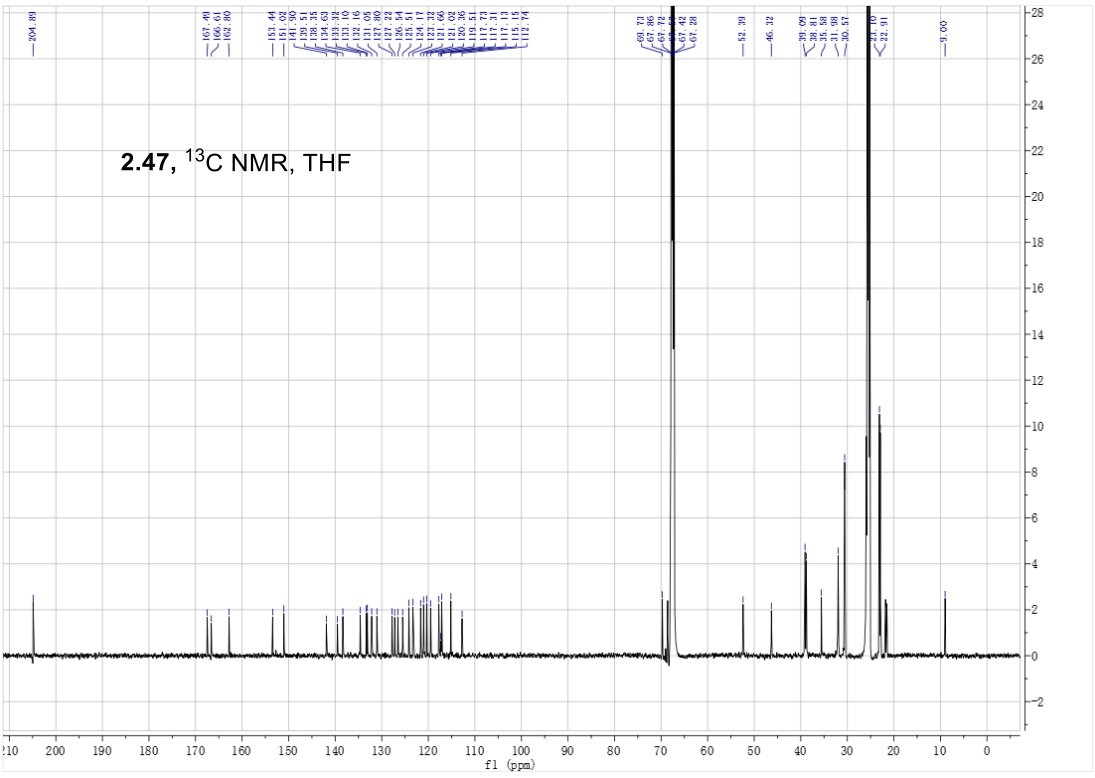
2.47, 13C NMR, THF
f1 (ppm)

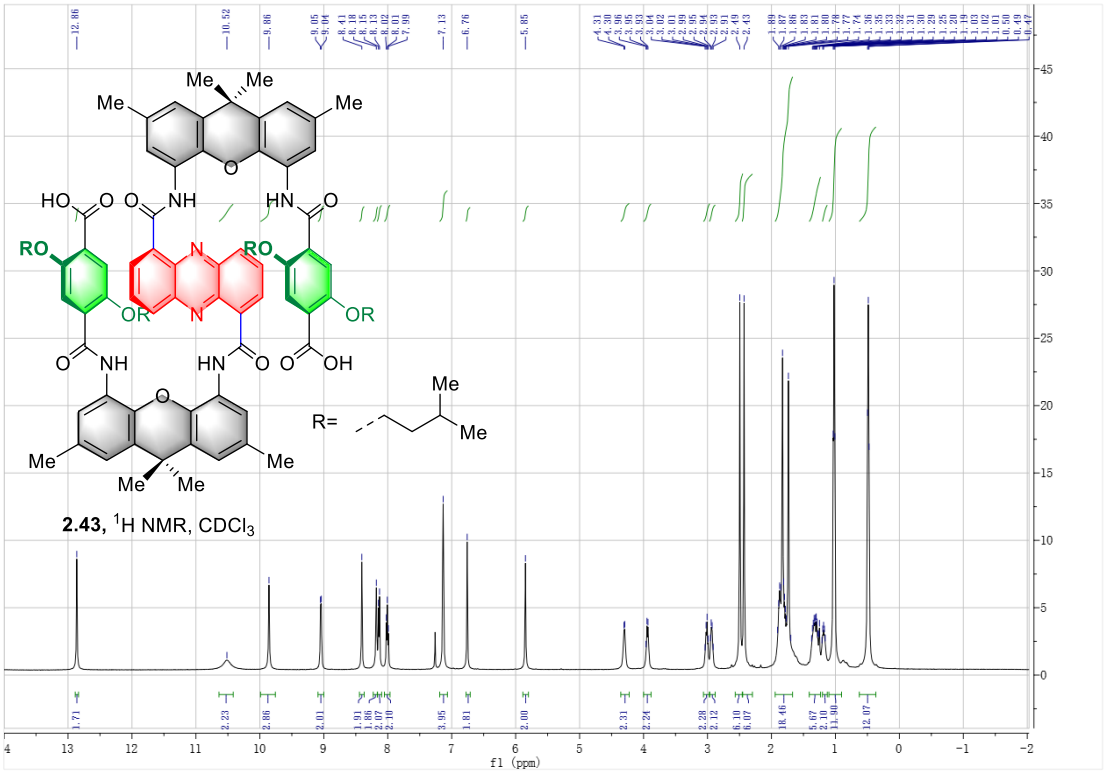
Me
Me
Me
Me
O
HO
O
O
NH
HN
O
RO
RO
N
N
OR
OR
O
NH
HN
O
O
OH
Me
R=
Me
Me
Me
Me
Me
2.43, ^{1}H NMR, CDCl$_3$
f1 (ppm)

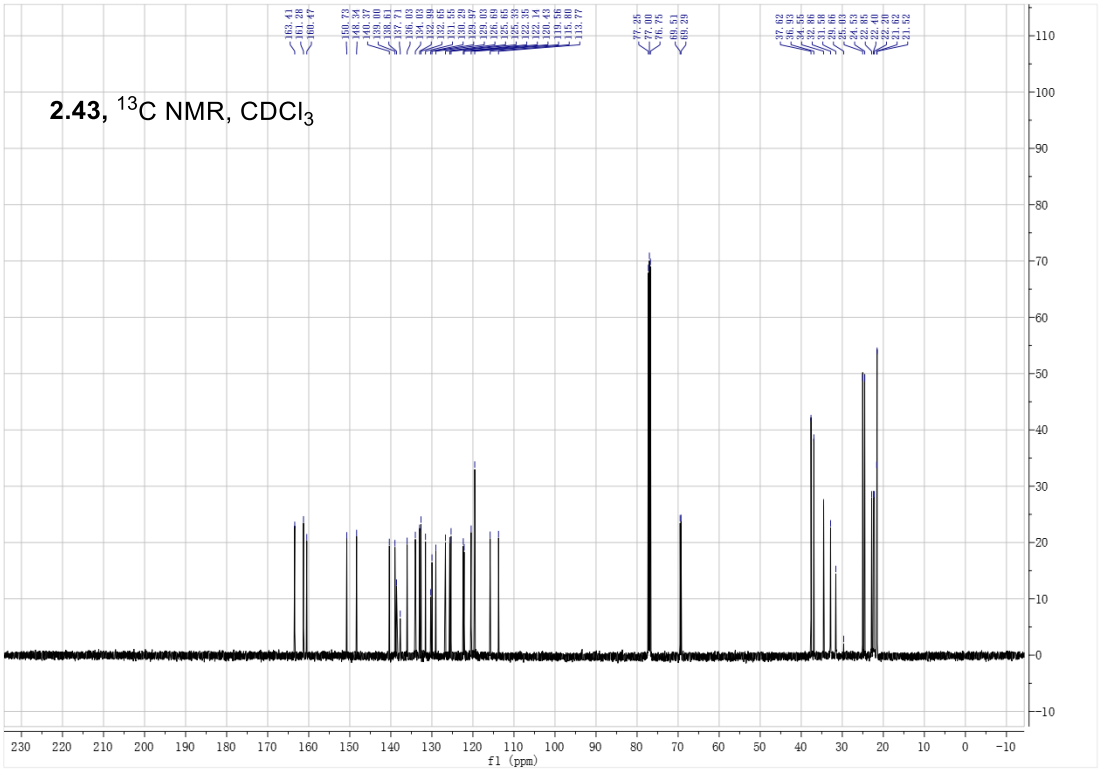
2.43, ^{13}C NMR, CDCl$_3$
f1 (ppm)

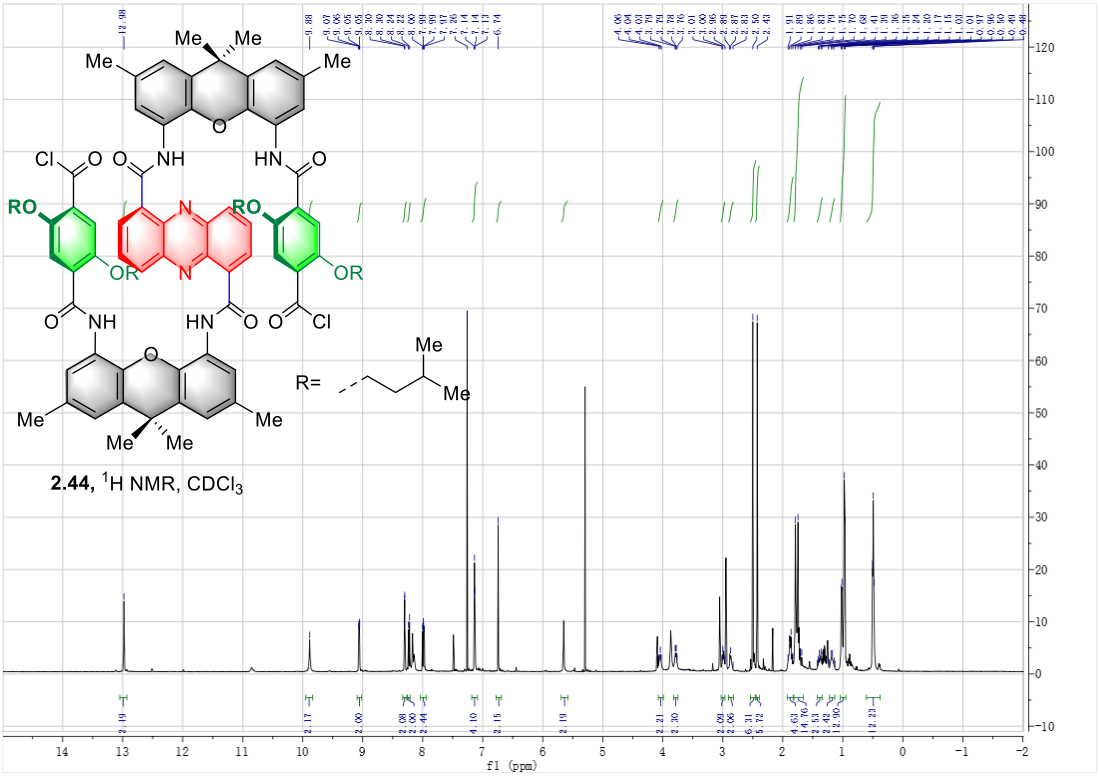
Me
Me
Me
Me
O
Cl
O
O
NH
HN
O
RO
RO
N
N
OR
OR
O
NH
HN
O
O
Cl
O
Me
Me
Me
Me
Me
R=
Me
2.44, ^{1}H NMR, CDCl$_3$
f1 (ppm)

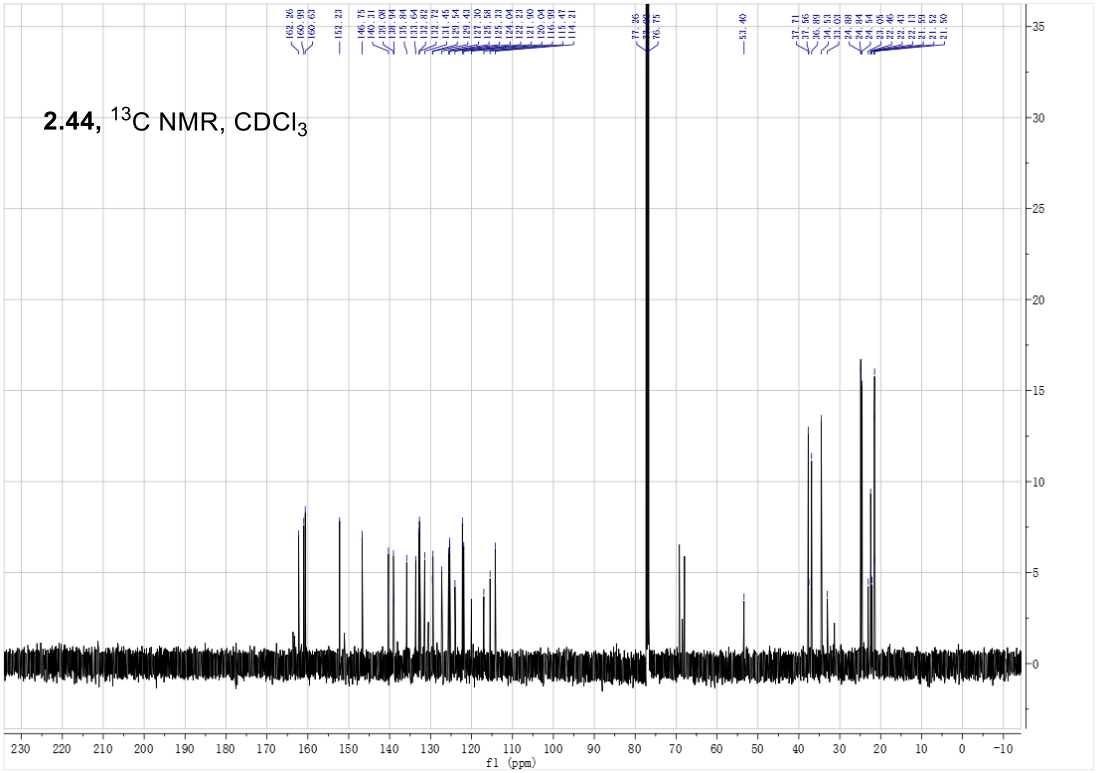
2.44, ^{13}C NMR, CDCl$_3$
f1 (ppm)

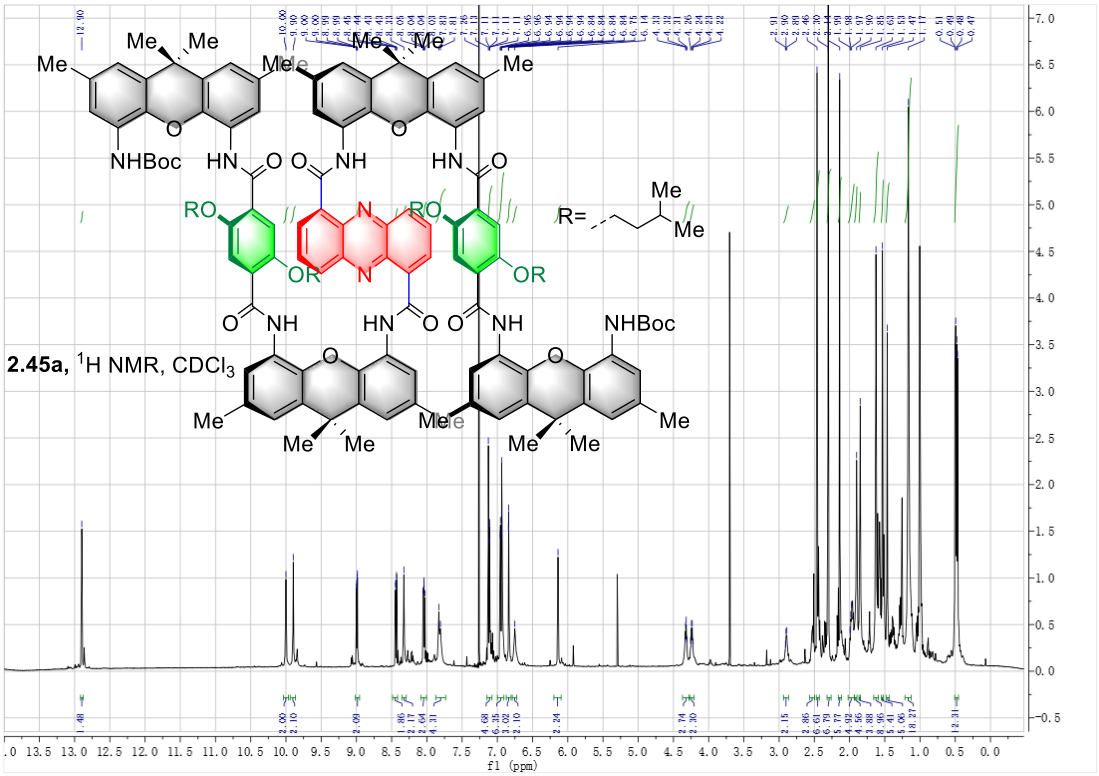
2.45a, ^{1}H NMR, CDCl$_3$
R=
f1 (ppm)

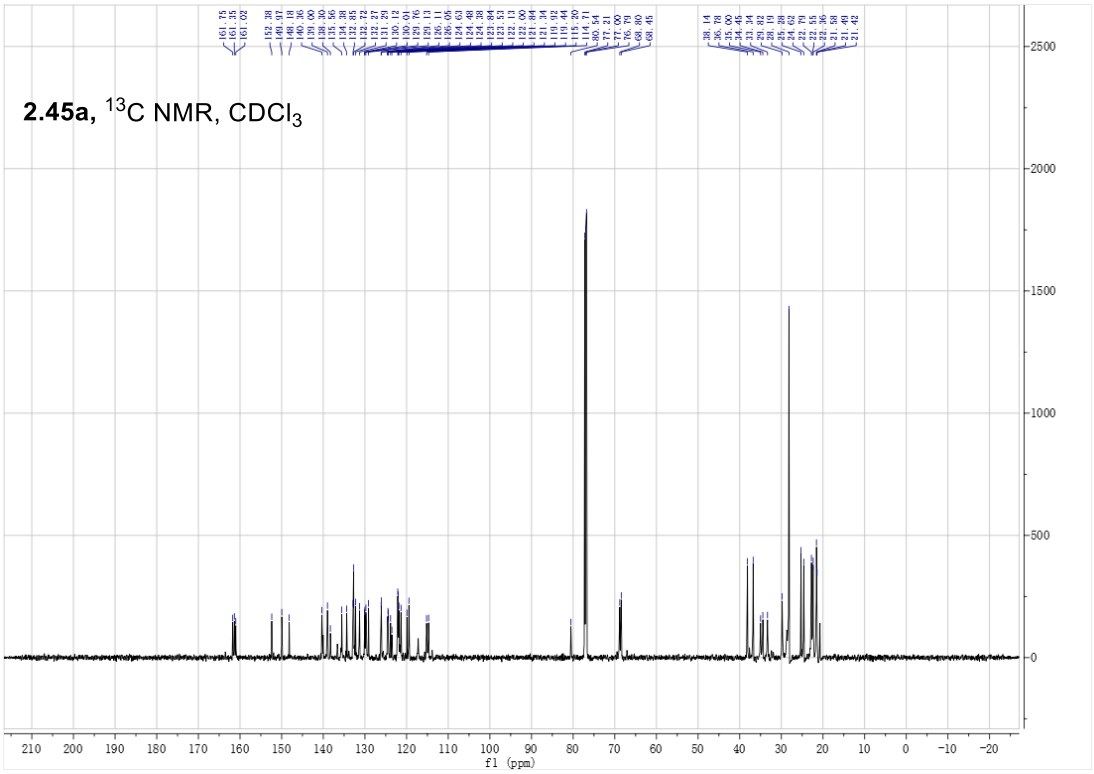
2.45a, ^{13}C NMR, CDCl$_3$
f1 (ppm)

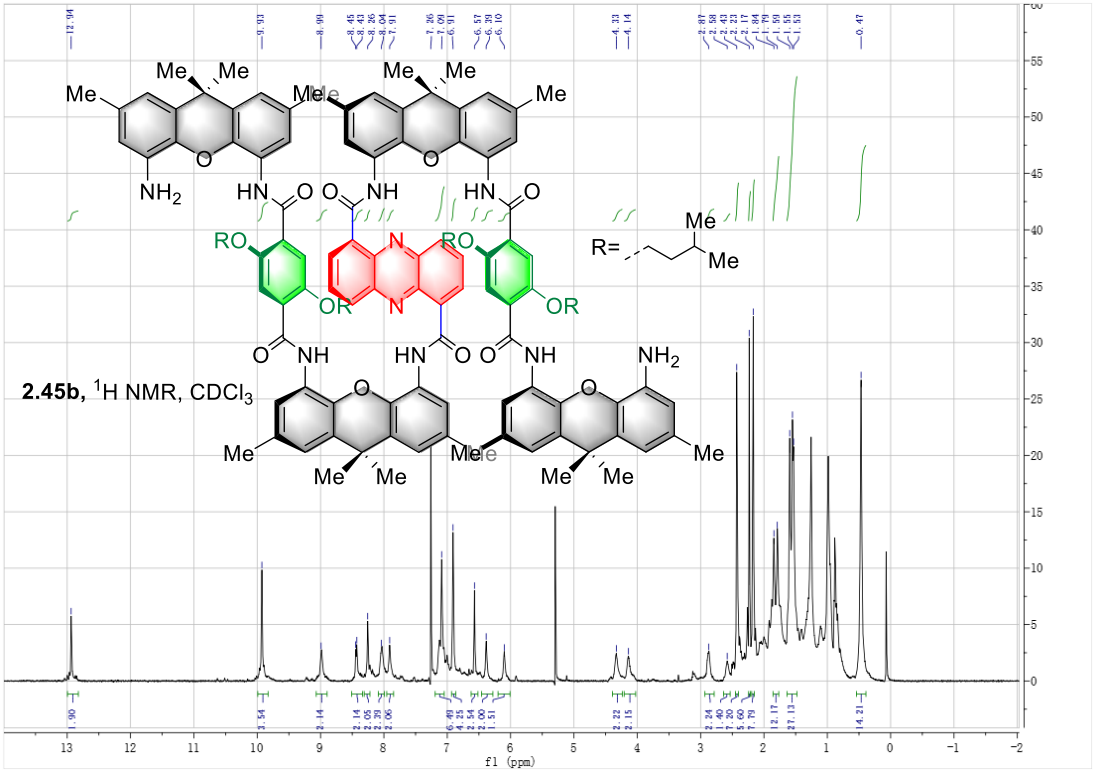
2.45b, ^{1}H NMR, CDCl$_3$
R=
f1 (ppm)

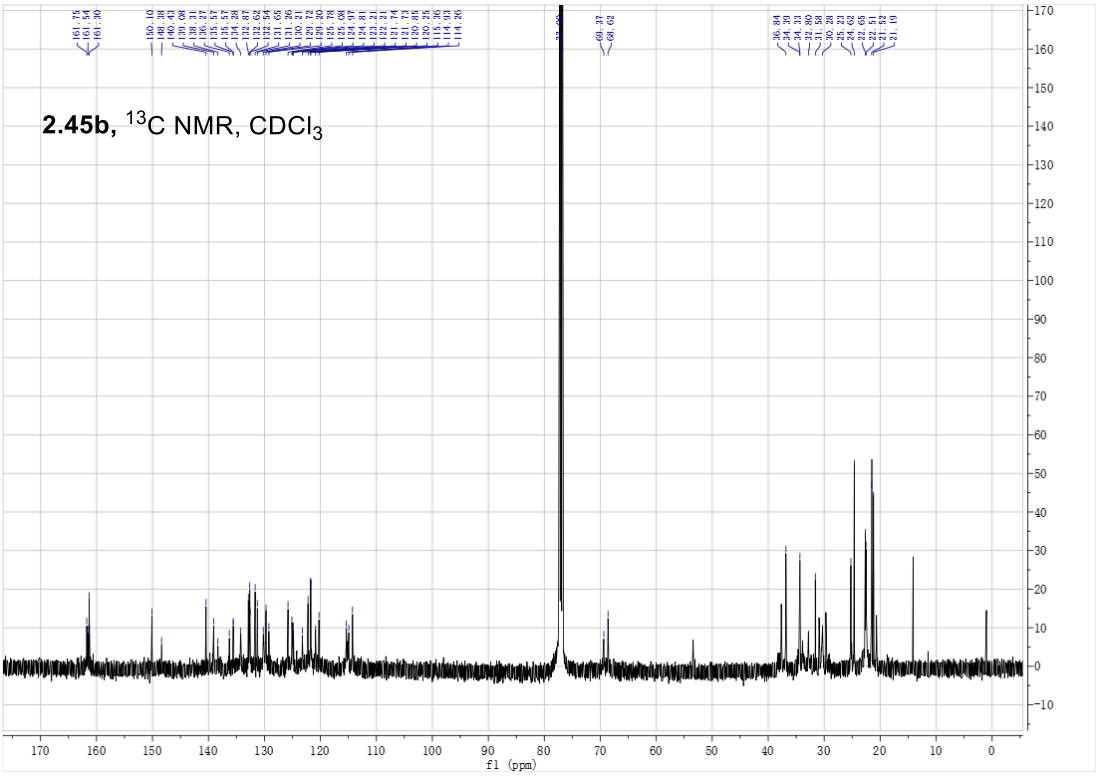
2.45b, ^{13}C NMR, CDCl$_3$
f1 (ppm)

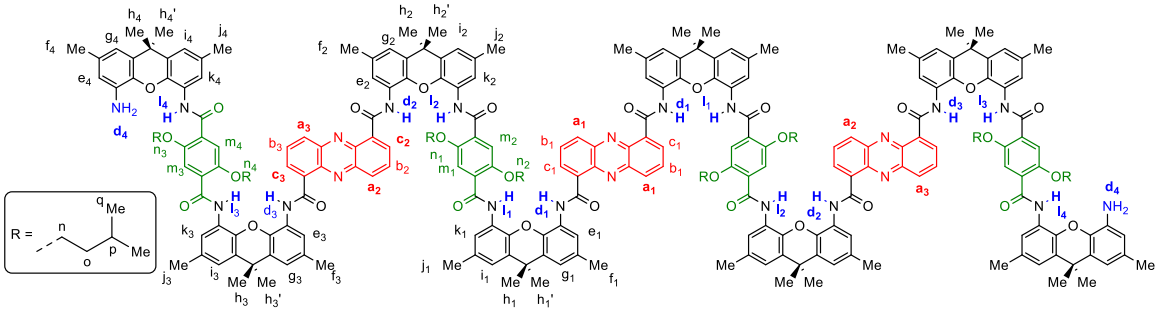

30a

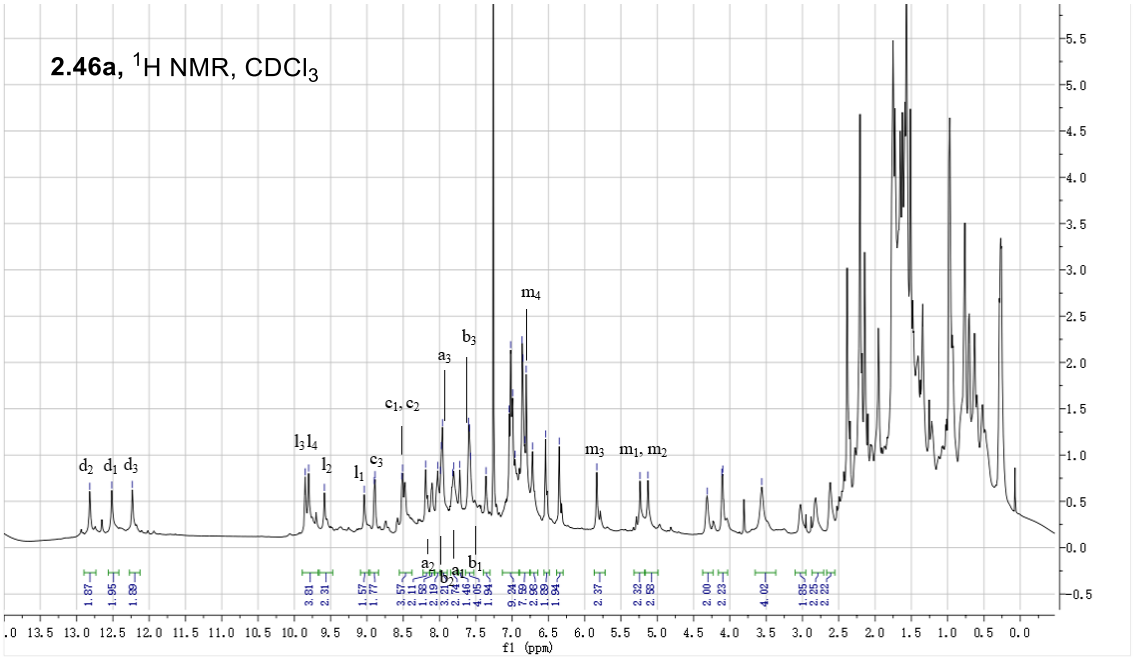
2.46a, 1H NMR, CDCl3
d2 d1 d3
l3 l4
l2
l1
c3
c1, c2
a3
b3
m4
m3
m1, m2
a2
a1
b2
b1
f1 (ppm)

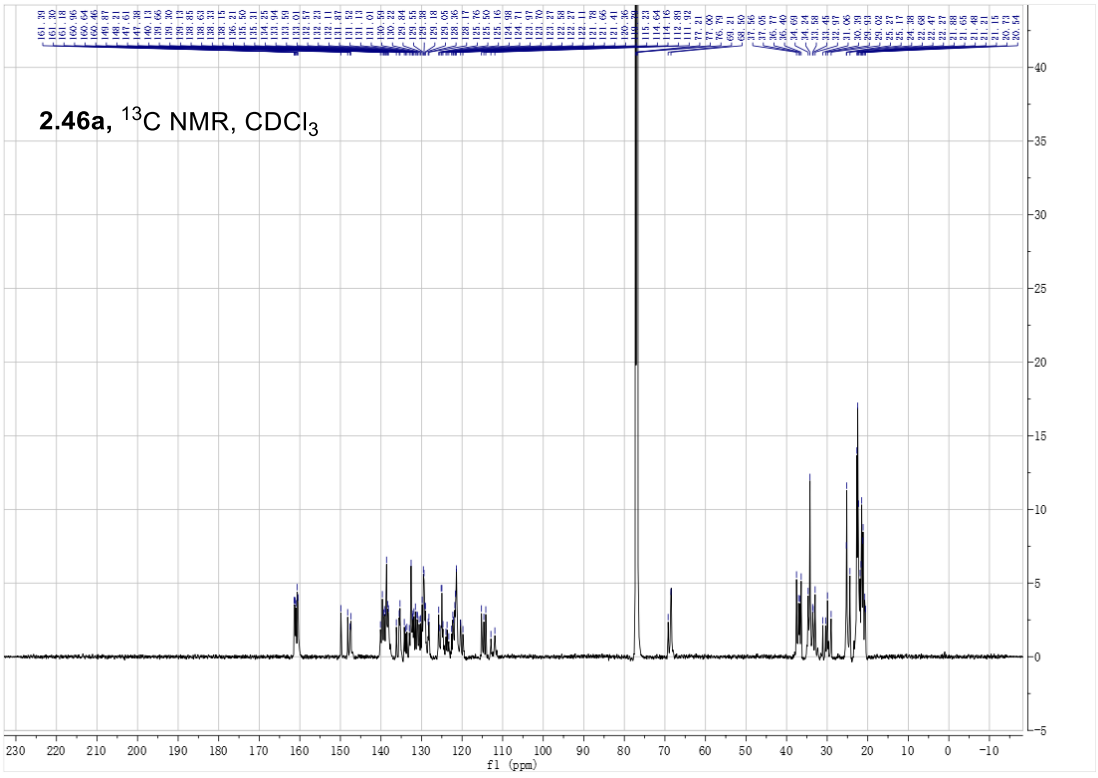
2.46a, 13C NMR, CDCl3
f1 (ppm)

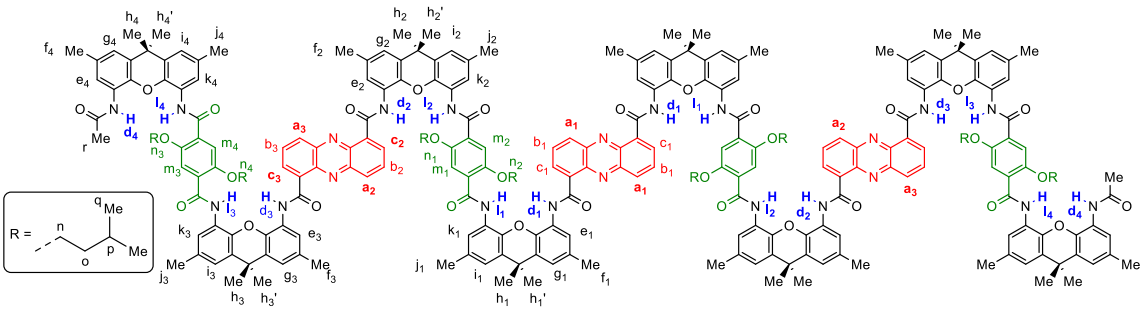

30b

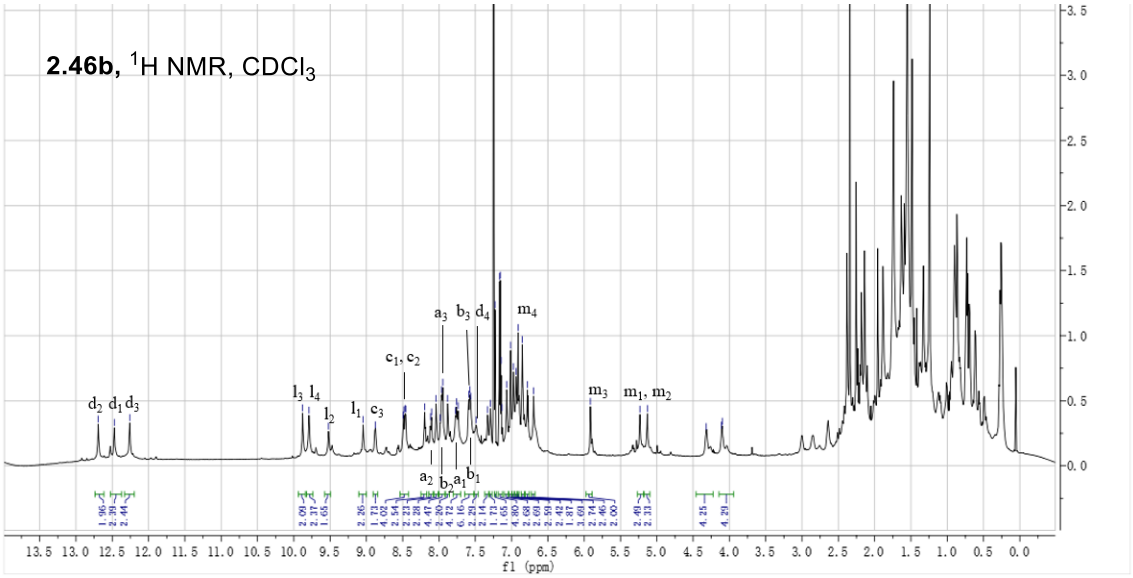
2.46b, 1H NMR, CDCl3
d2 d1 d3
l3 l4
l2
l1 c3
c1, c2
a3 b3 d4
m4
m3
m1, m2
a2 b2 a1 b1
f1 (ppm)

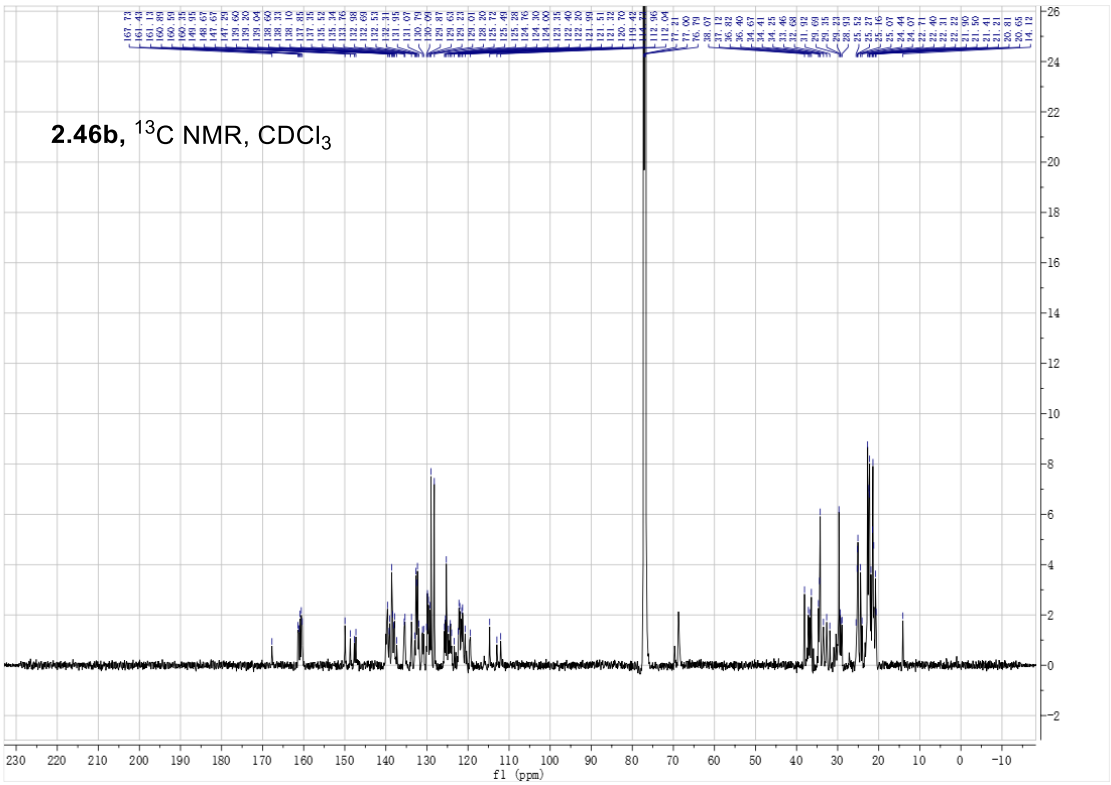
2.46b, 13C NMR, CDCl3
f1 (ppm)

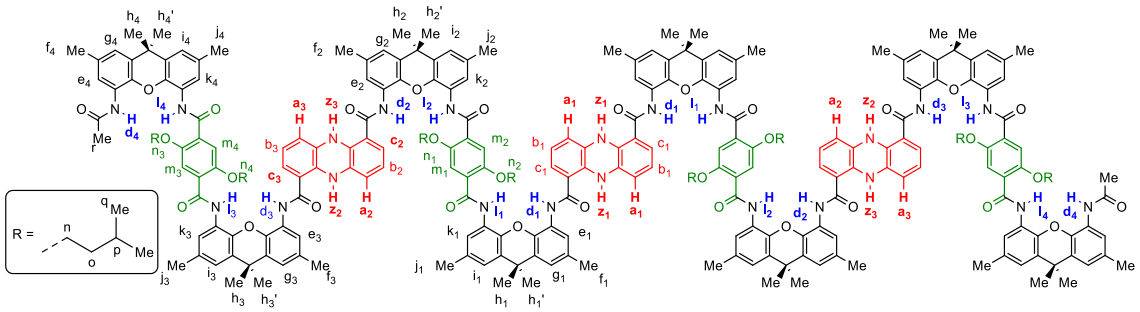
R =
32b

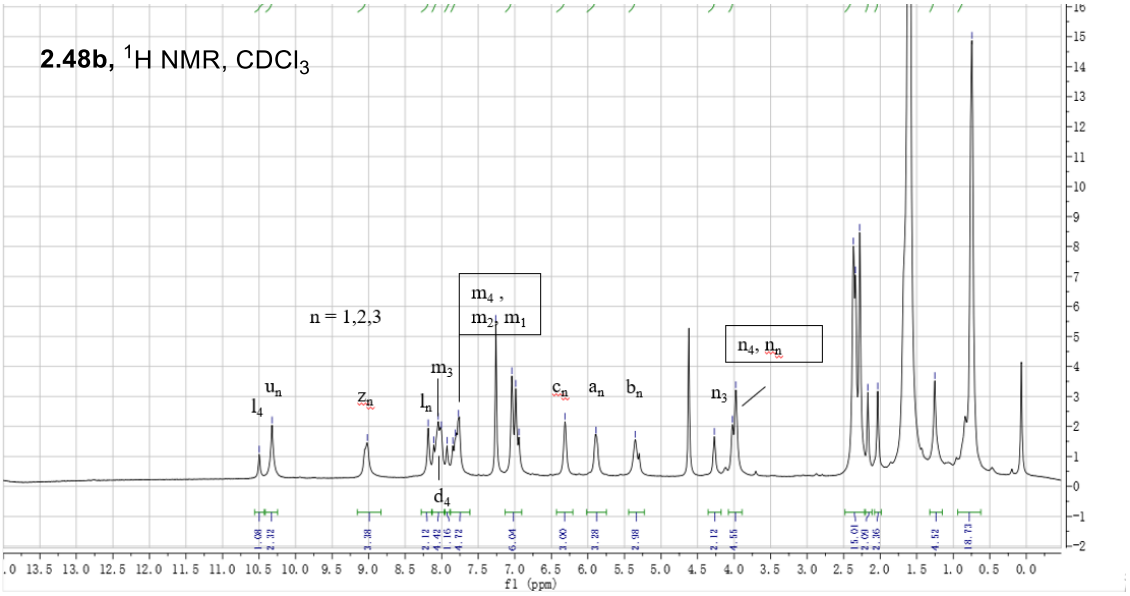
2.48b, 1H NMR, CDCl3
n = 1,2,3
m4 , m2, m1
m3
un
ln
zn
cn
an
bn
n3
n4, nn
d4
f1 (ppm)

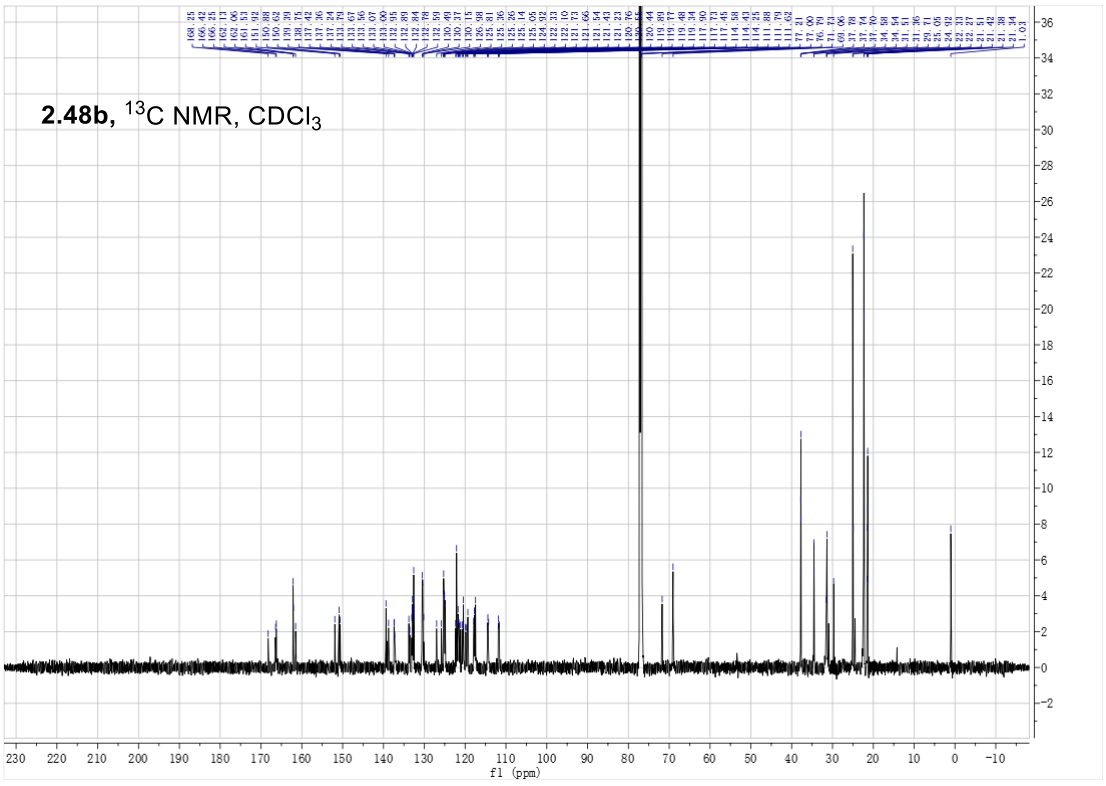
2.48b, 13C NMR, CDCl3
f1 (ppm)

2.4.12. 2D NMR Spectra.

NOESY Spectrum of **2.27**:

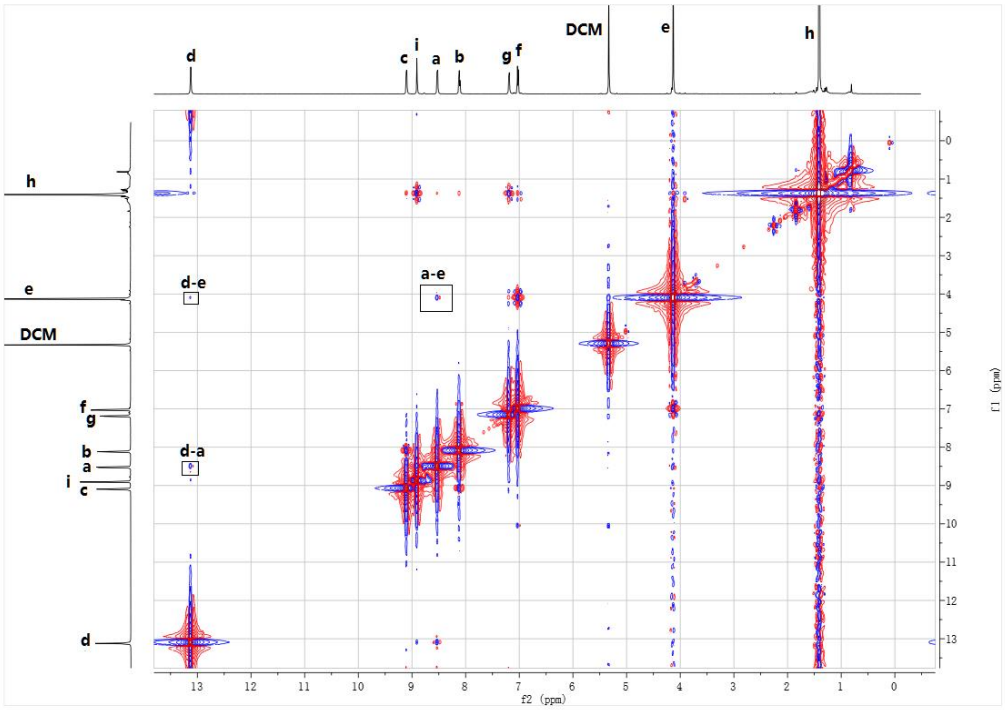

NOESY Spectrum of **2.28**

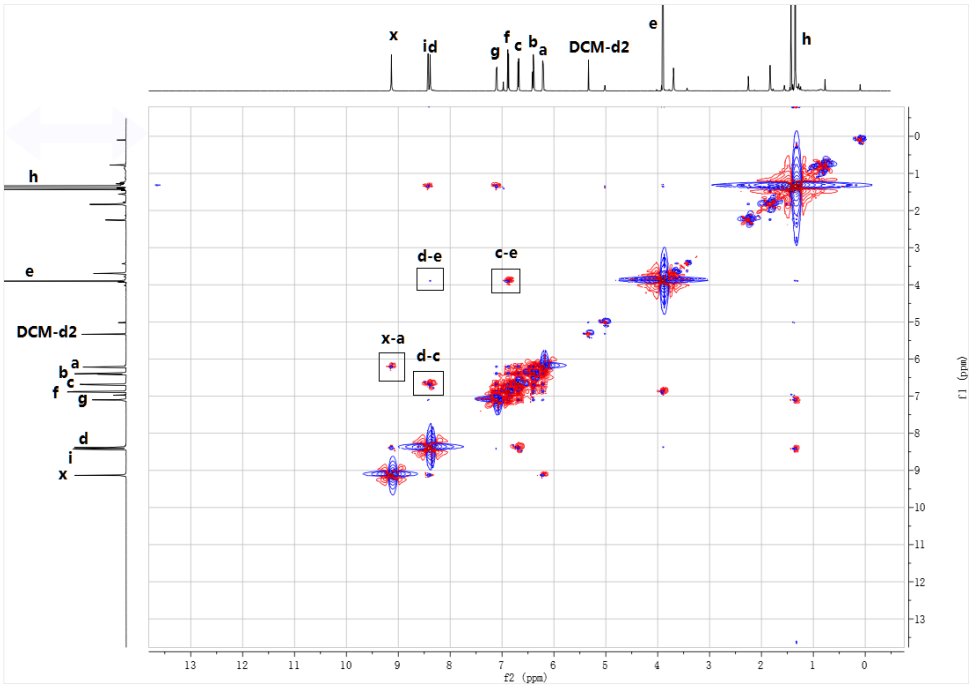

NOESY Spectrum of **2.27**

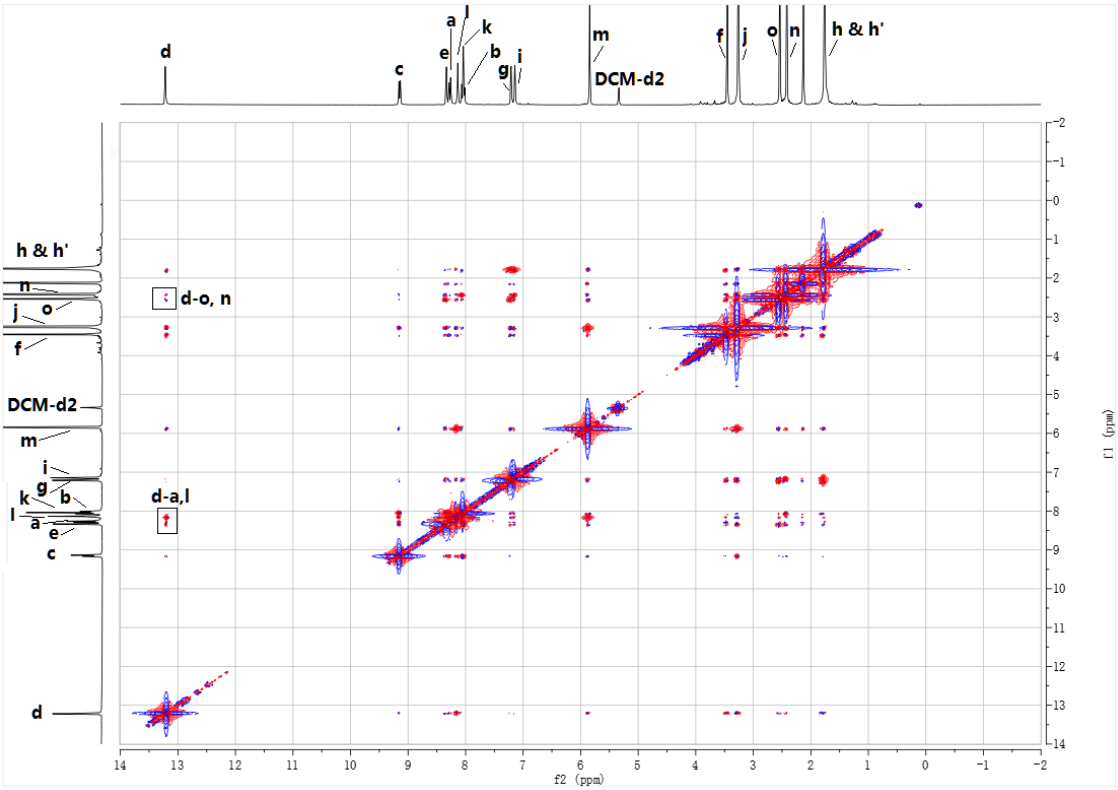

HMBC Spectrum of **2.27**

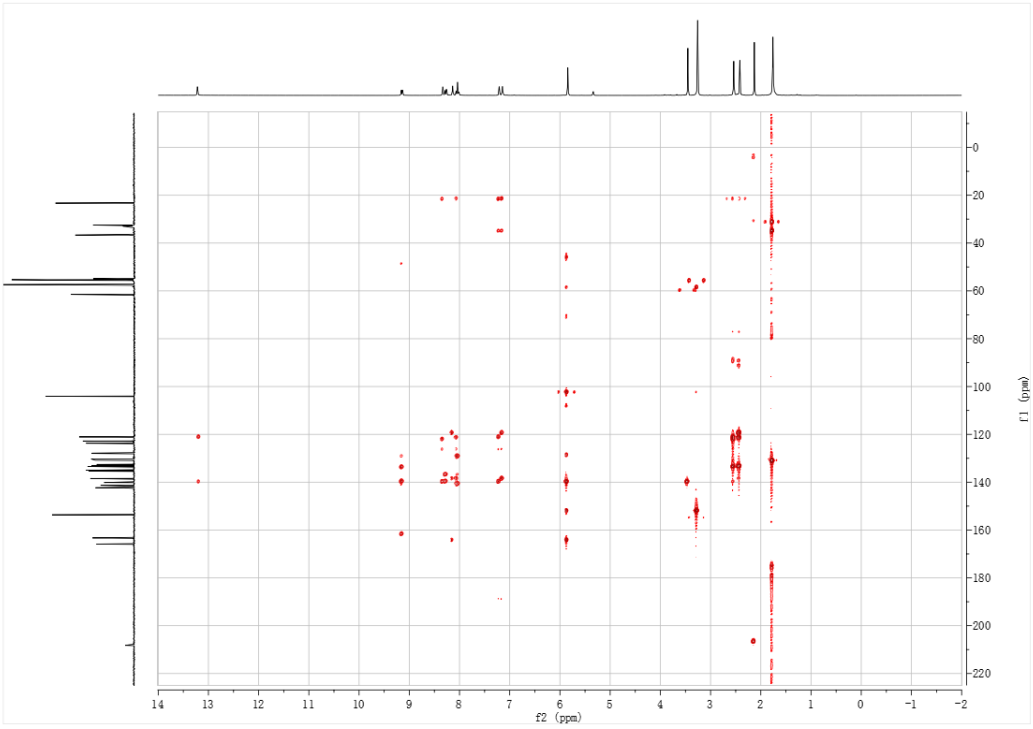

NOESY Spectrum of **2.28**

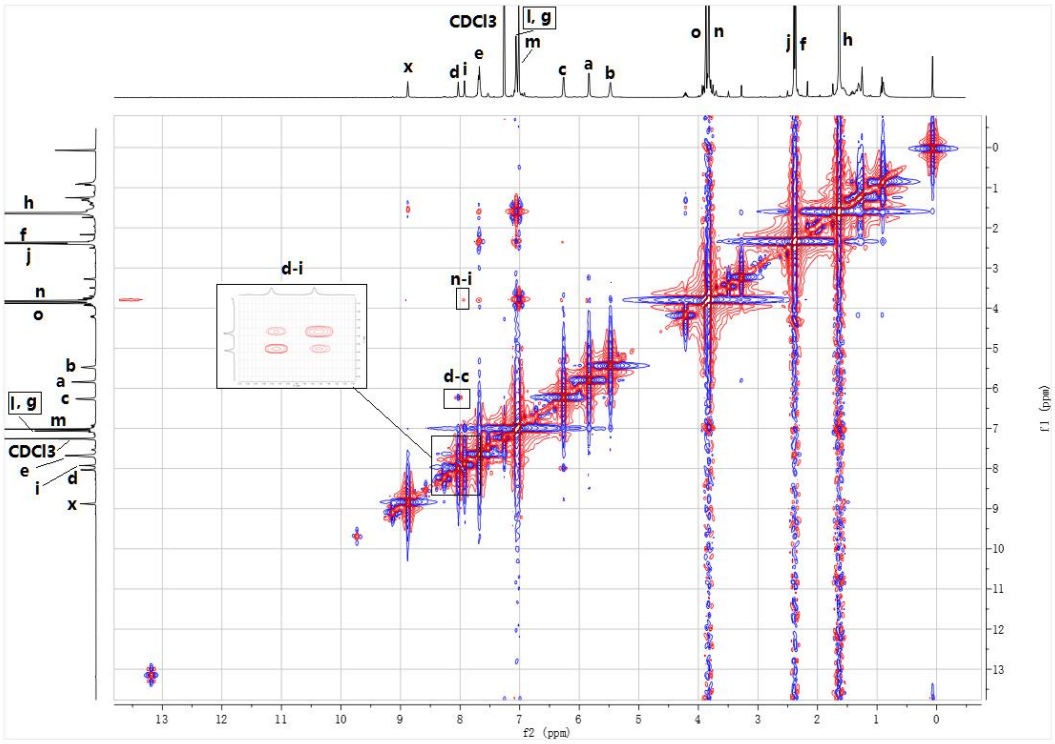

HSQC Spectrum of **2.28**

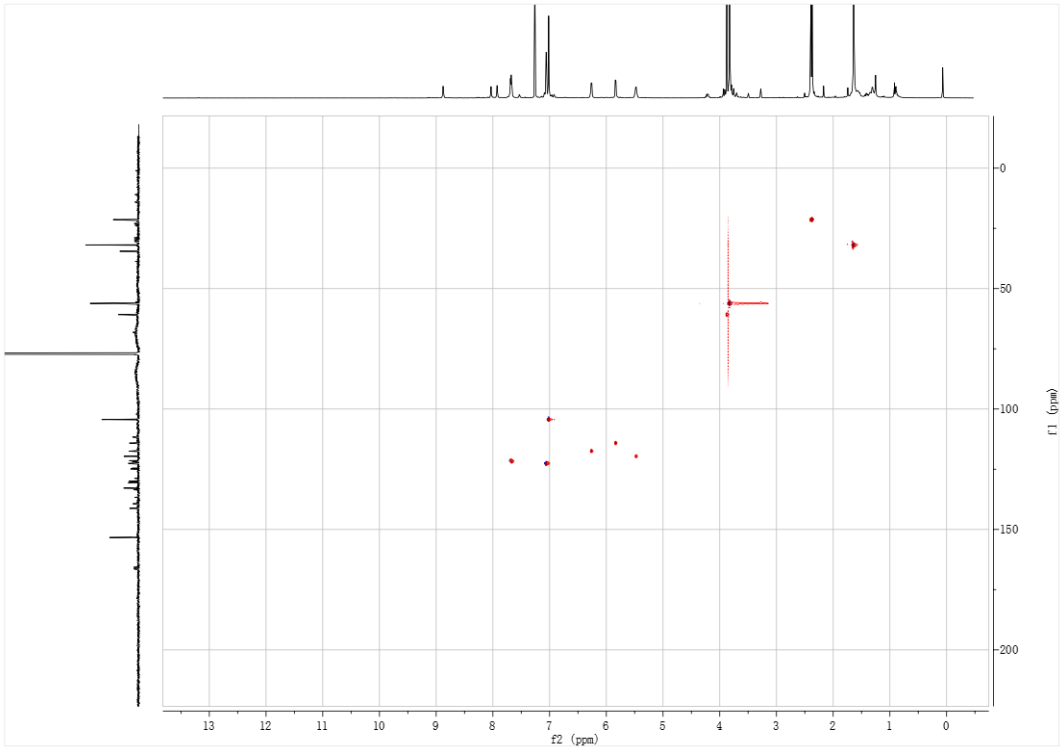

HMBC Spectrum of **2.28**

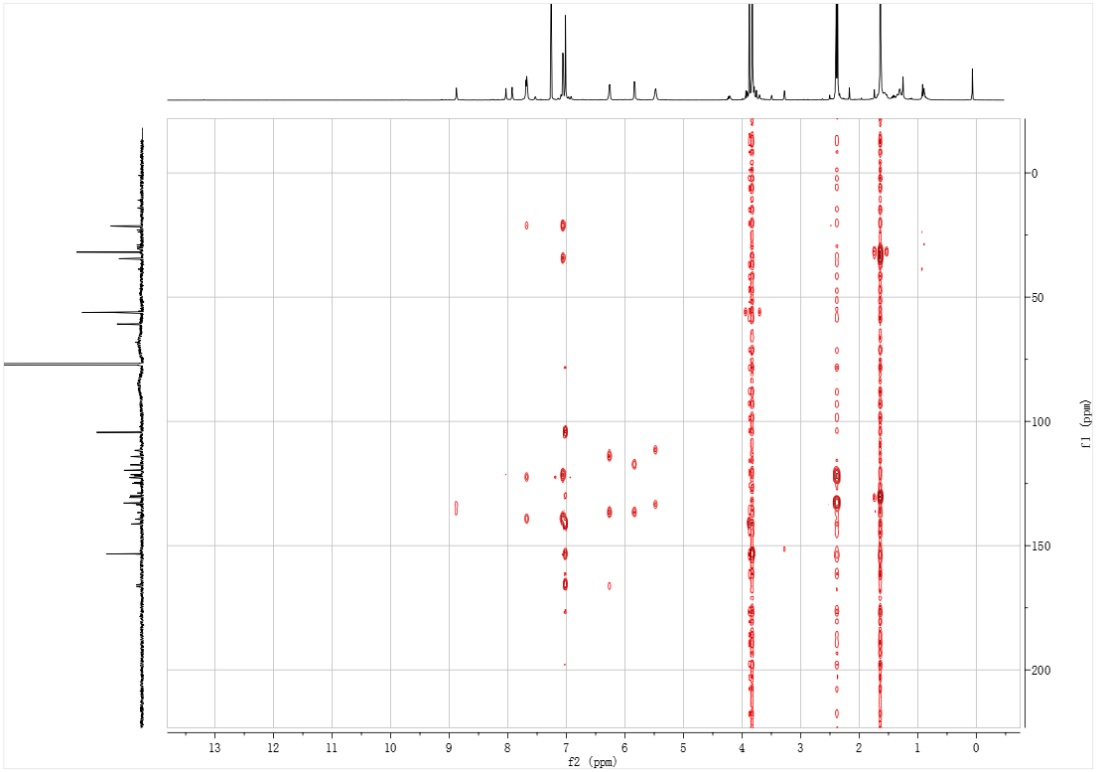

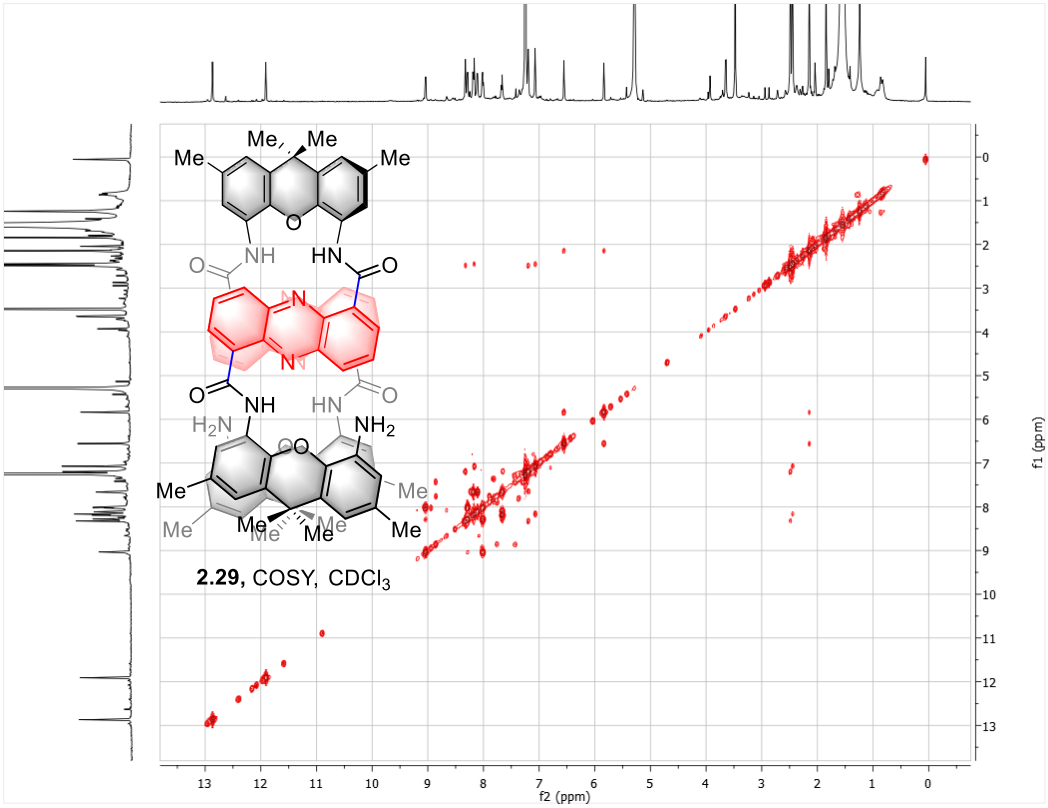
Me
Me
Me
Me
O
NH
HN
O
O
N
N
O
NH
HN
O
H2N
NH2
O
O
Me
Me
Me
Me
Me
Me
Me
Me
2.29, COSY, CDCl3
f2 (ppm)
f1 (ppm)

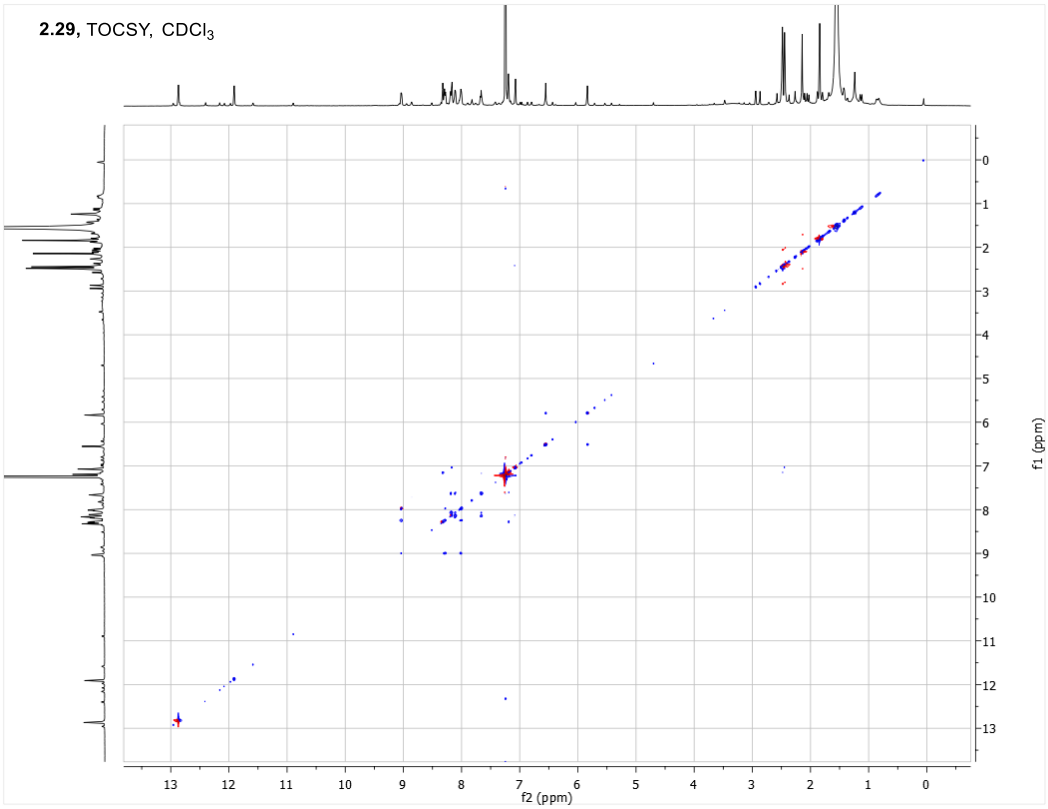
2.29, TOCSY, CDCl3
f2 (ppm)
f1 (ppm)

2.29, HSQC, $CDCl_3$

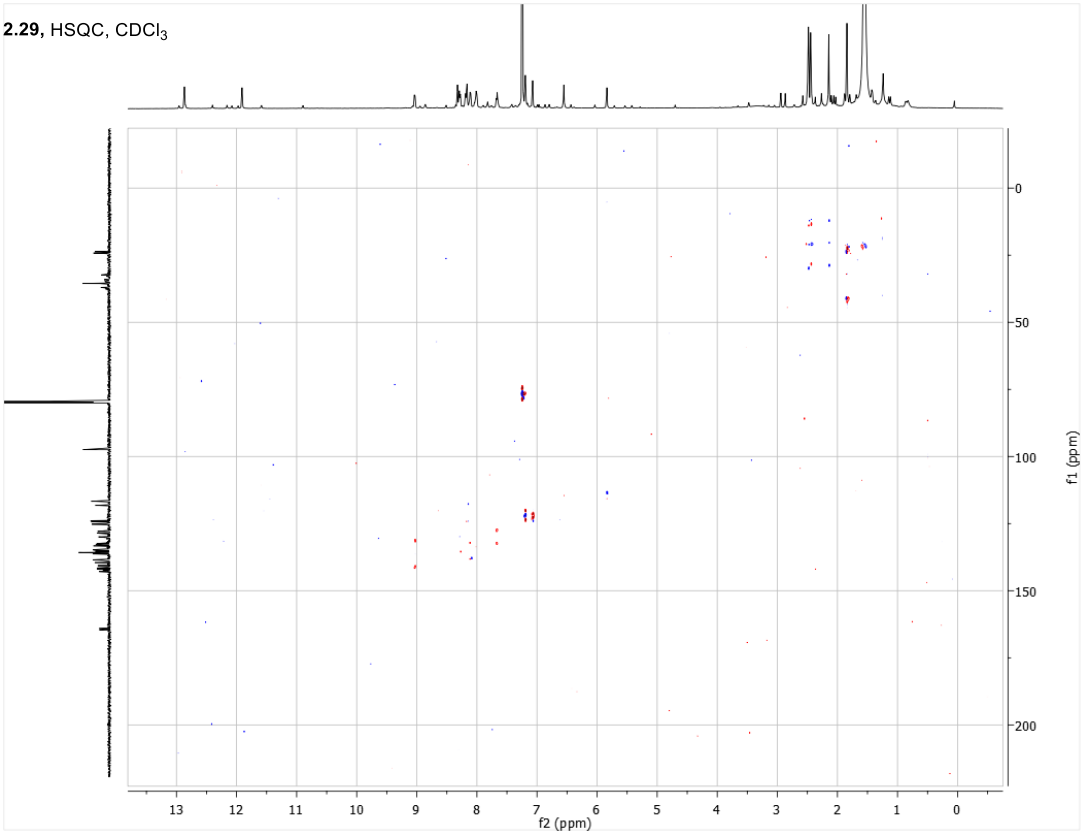

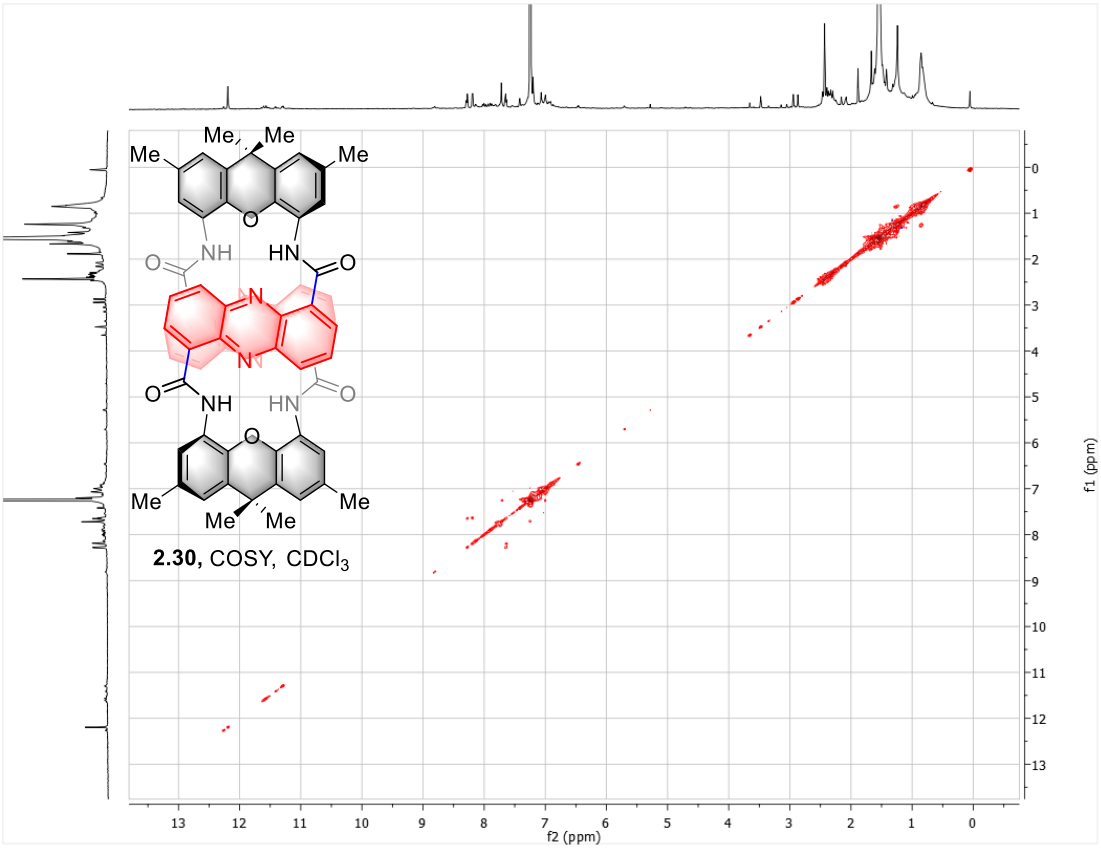

2.30, COSY, $CDCl_3$

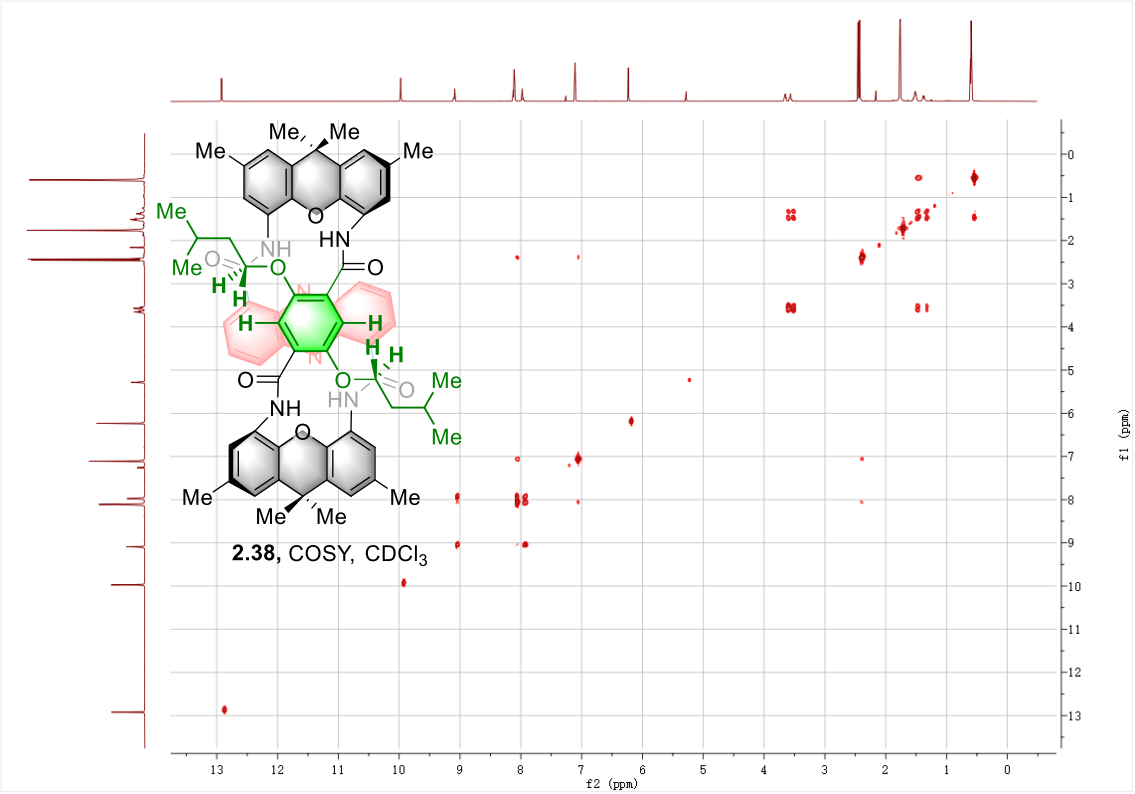

2.38, COSY, $CDCl_3$

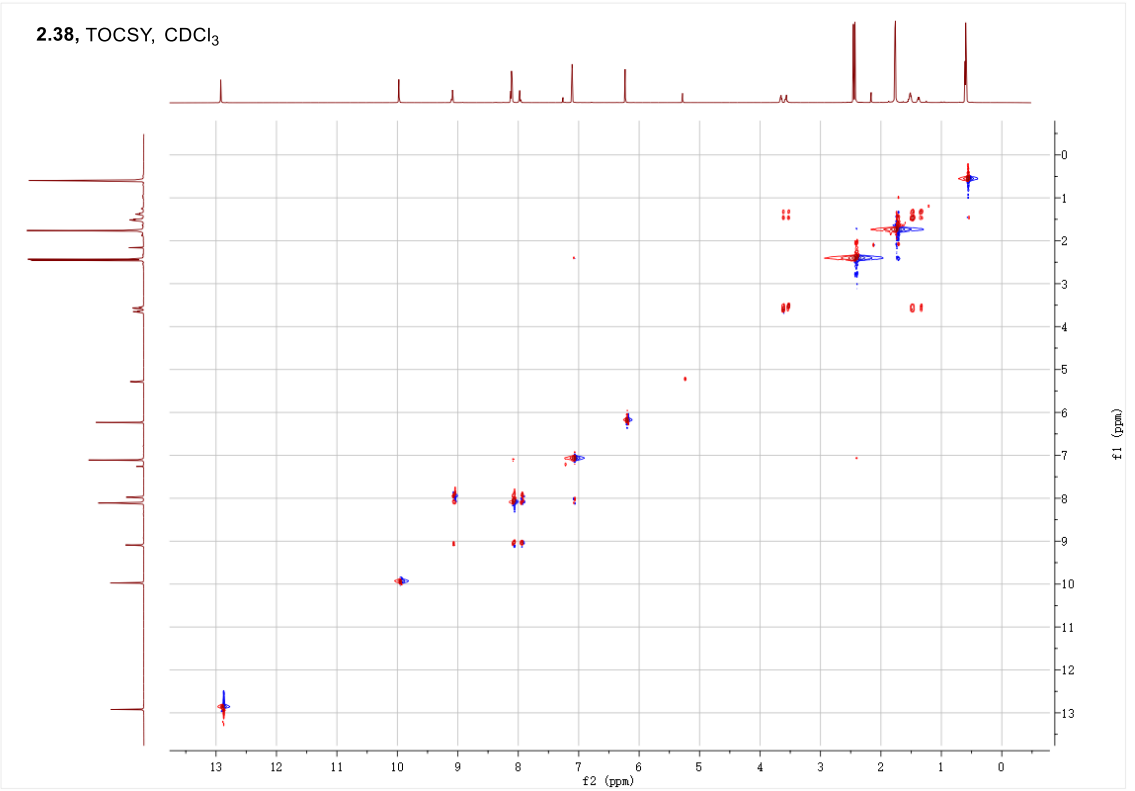

2.38, TOCSY, $CDCl_3$

2.38, NOESY, $CDCl_3$

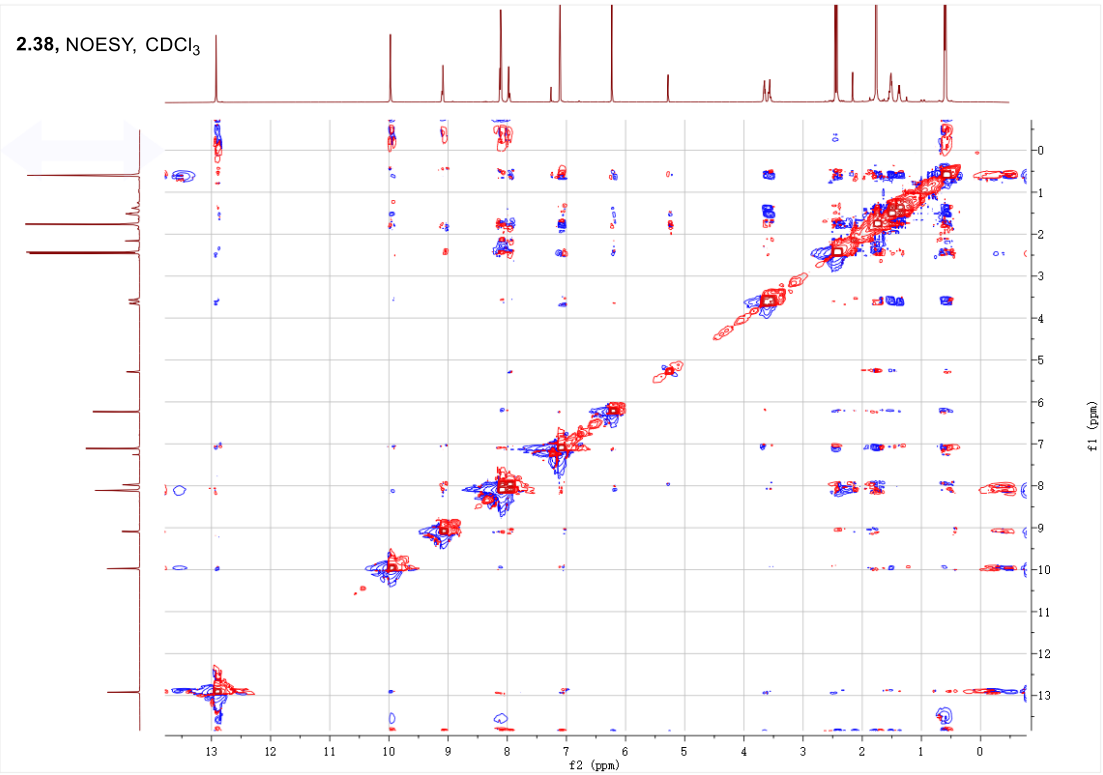

2.38, HSQC, $CDCl_3$

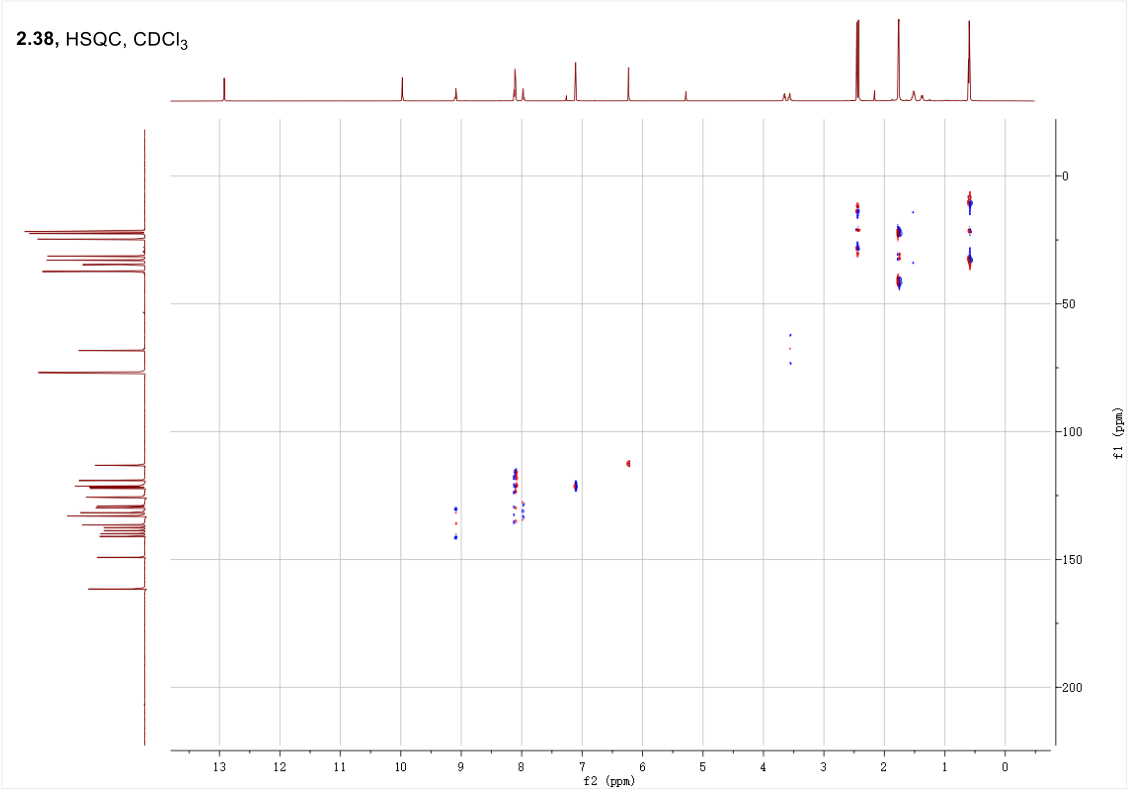

2.38, HMBC, $CDCl_3$

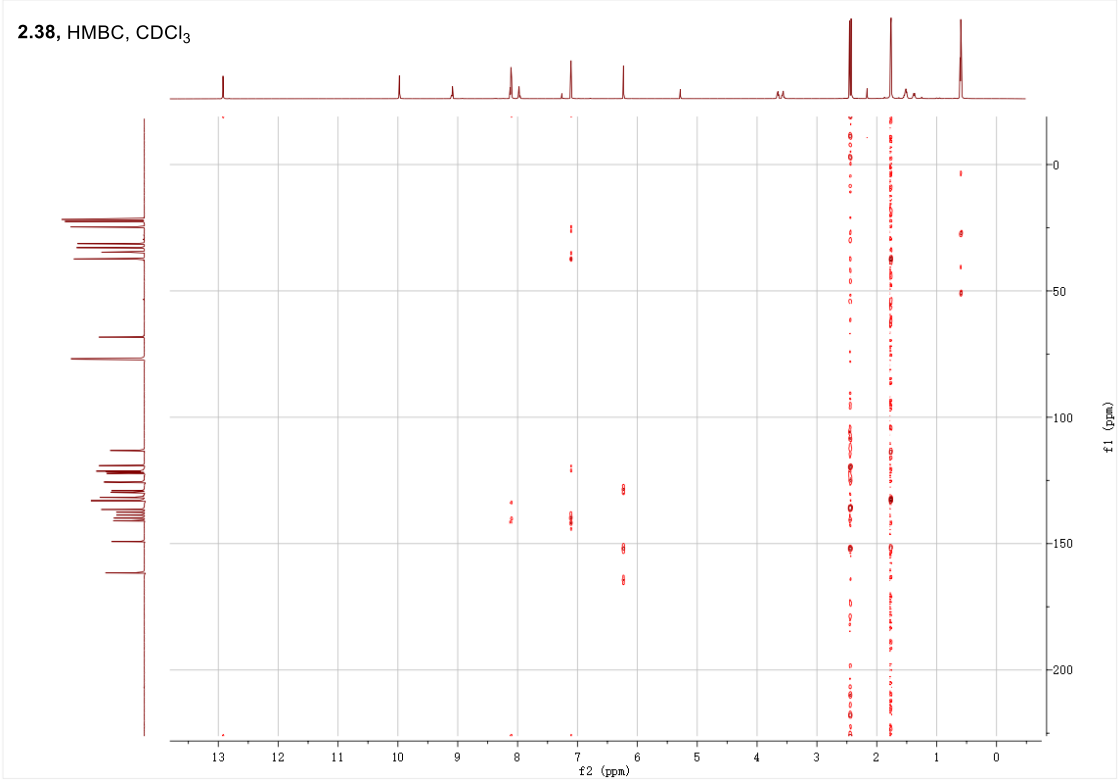

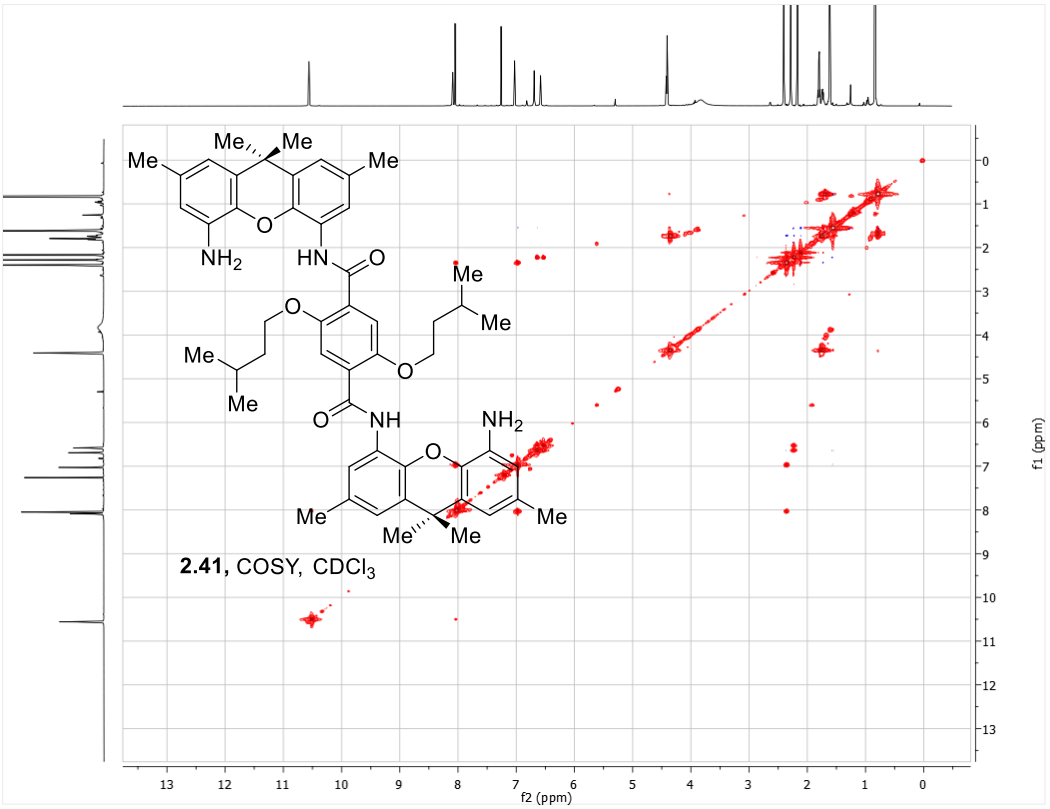

2.41, COSY, $CDCl_3$

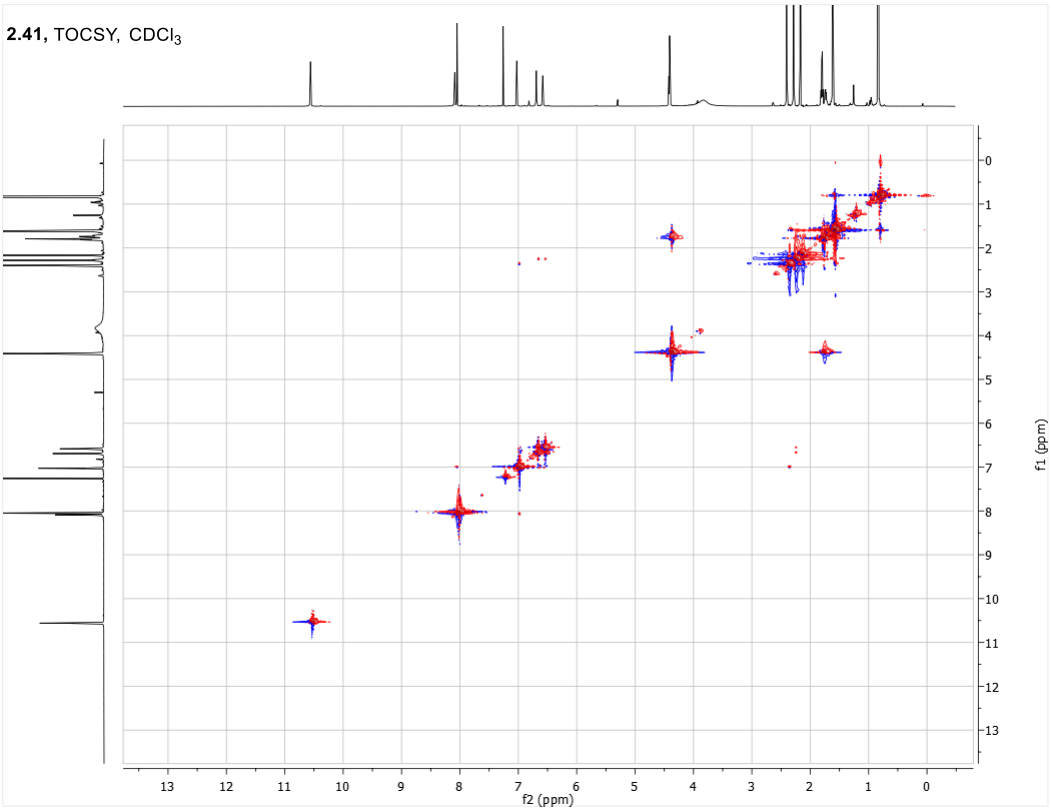

2.41, TOCSY, $CDCl_3$

2.41, NOESY, $CDCl_3$

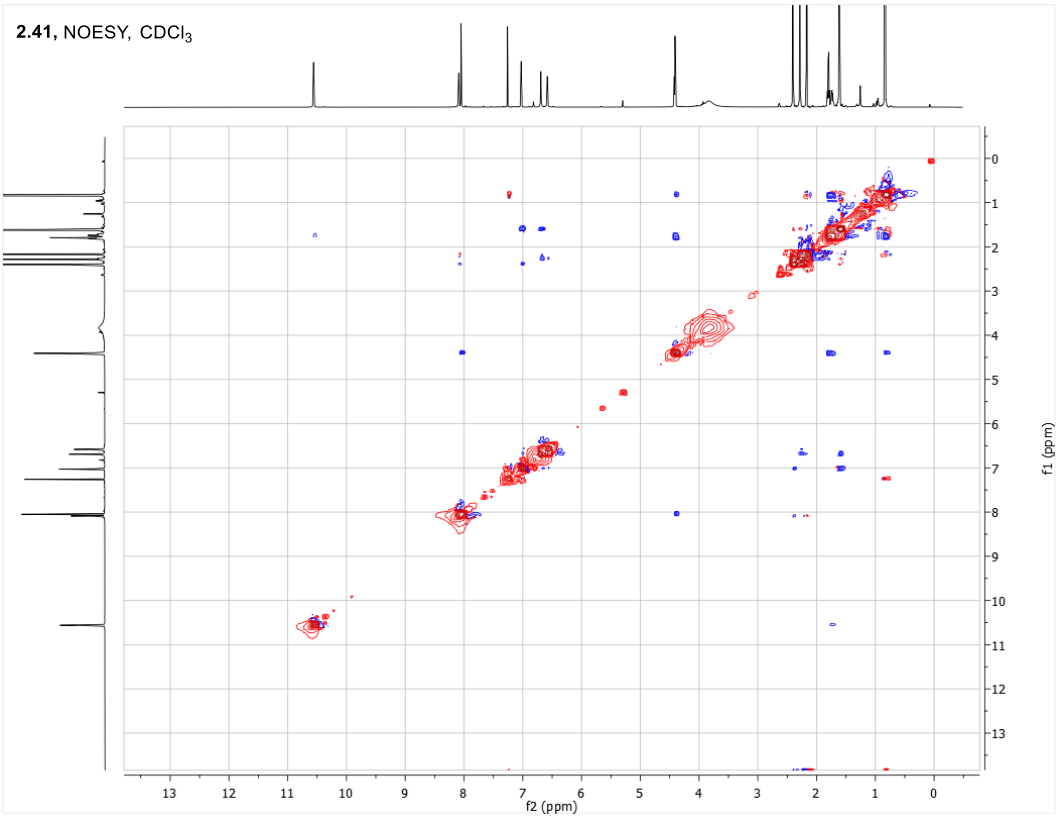

2.41, HSQC, $CDCl_3$

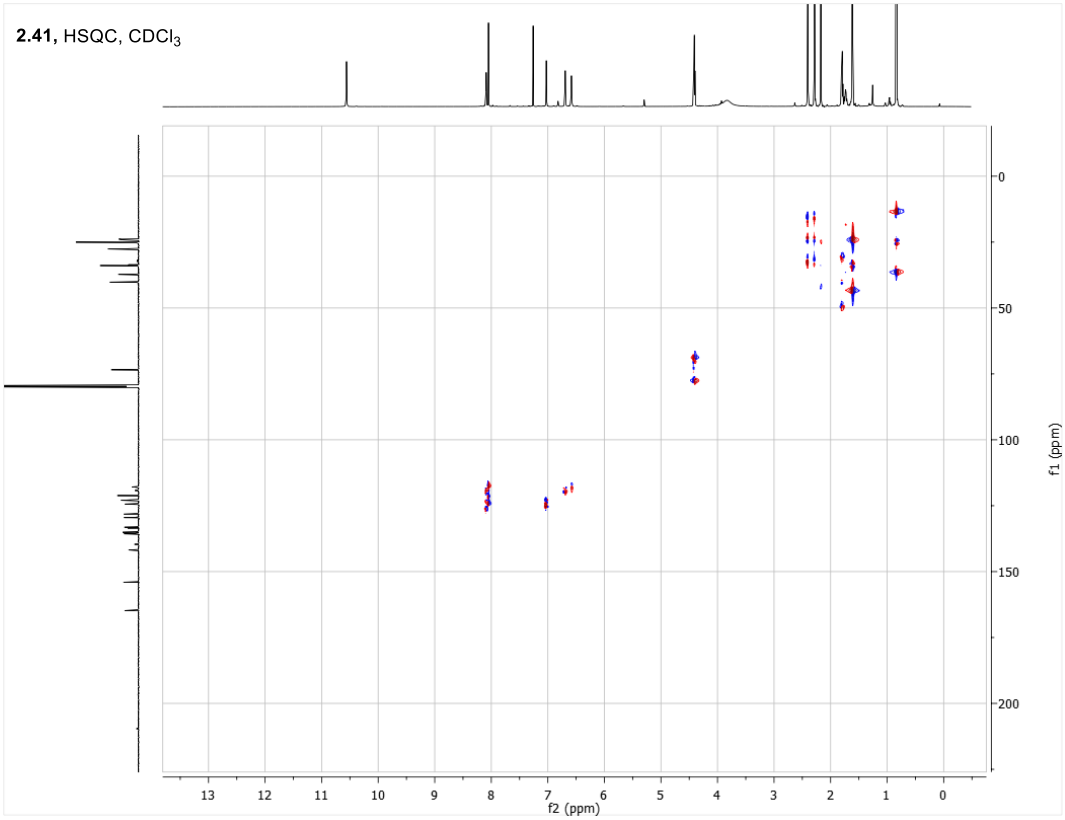

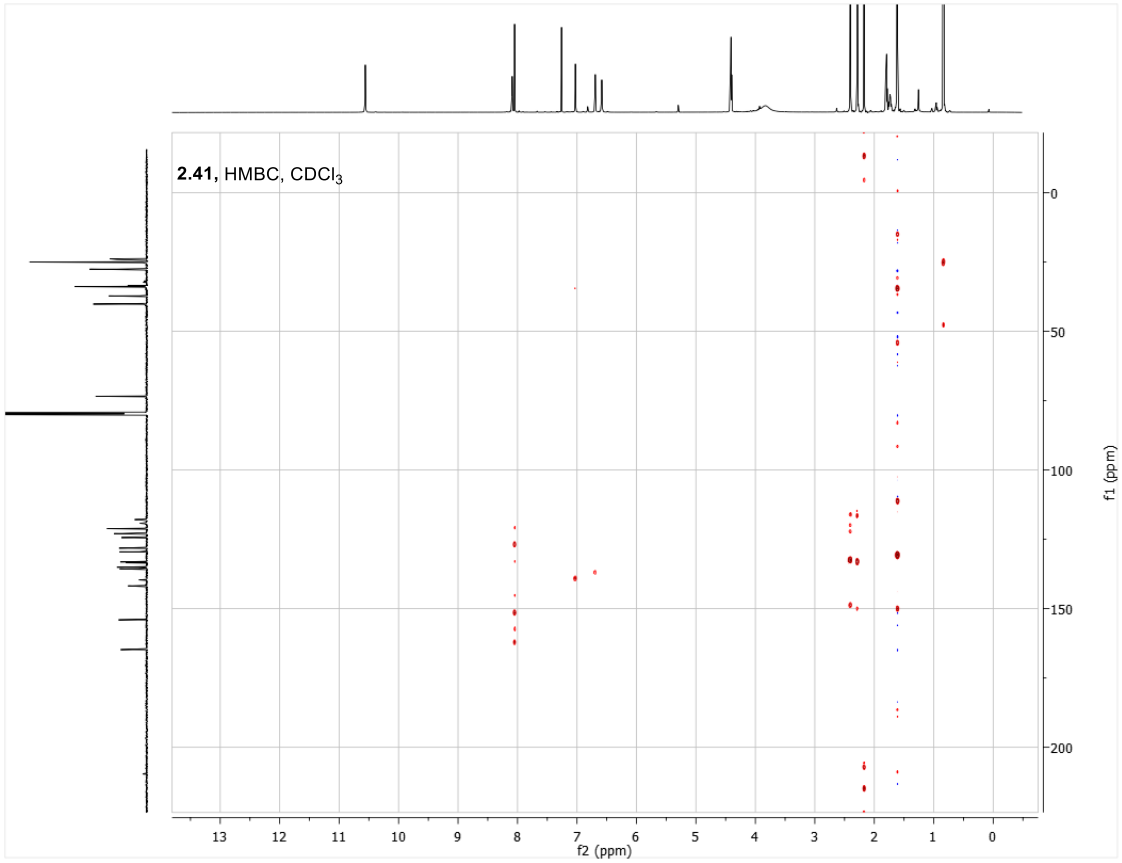
2.41, HMBC, CDCl3
f2 (ppm)
f1 (ppm)
13
12
11
10
9
8
7
6
5
4
3
2
1
0
0
50
100
150
200

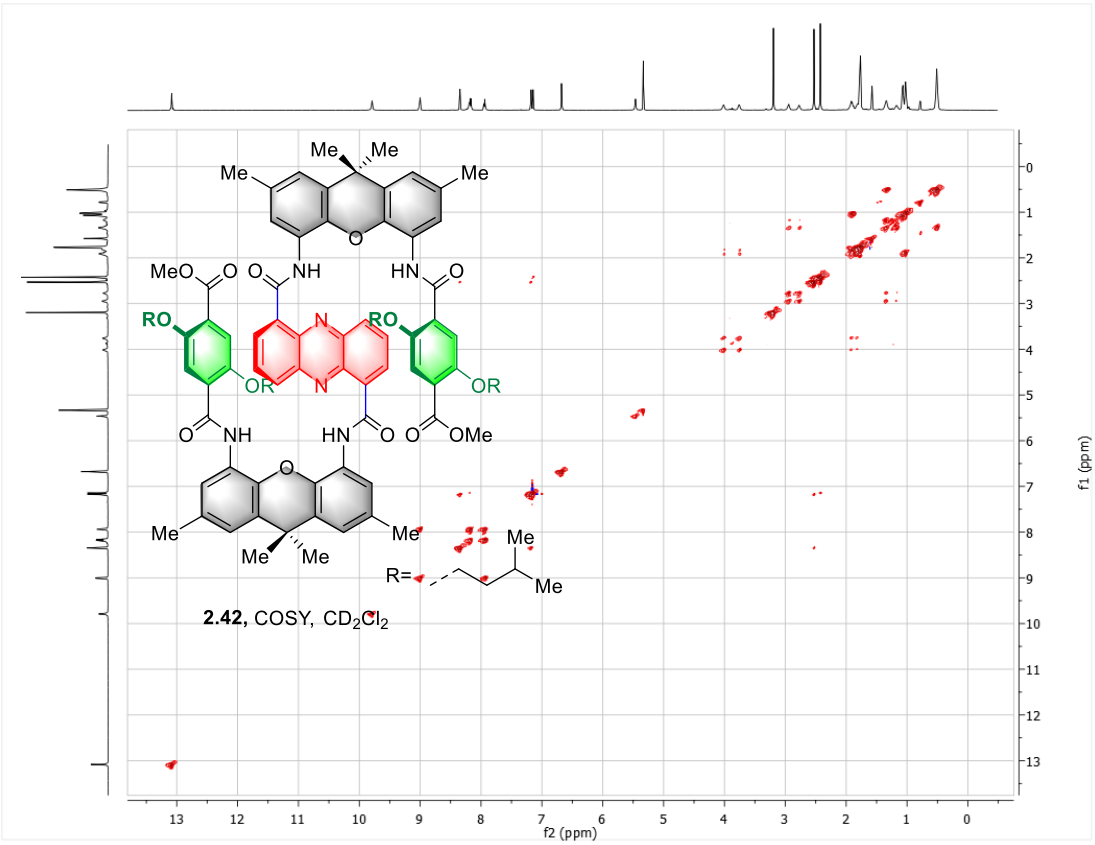

2.42, COSY, CD_2Cl_2

2.42, TOCSY, CD_2Cl_2

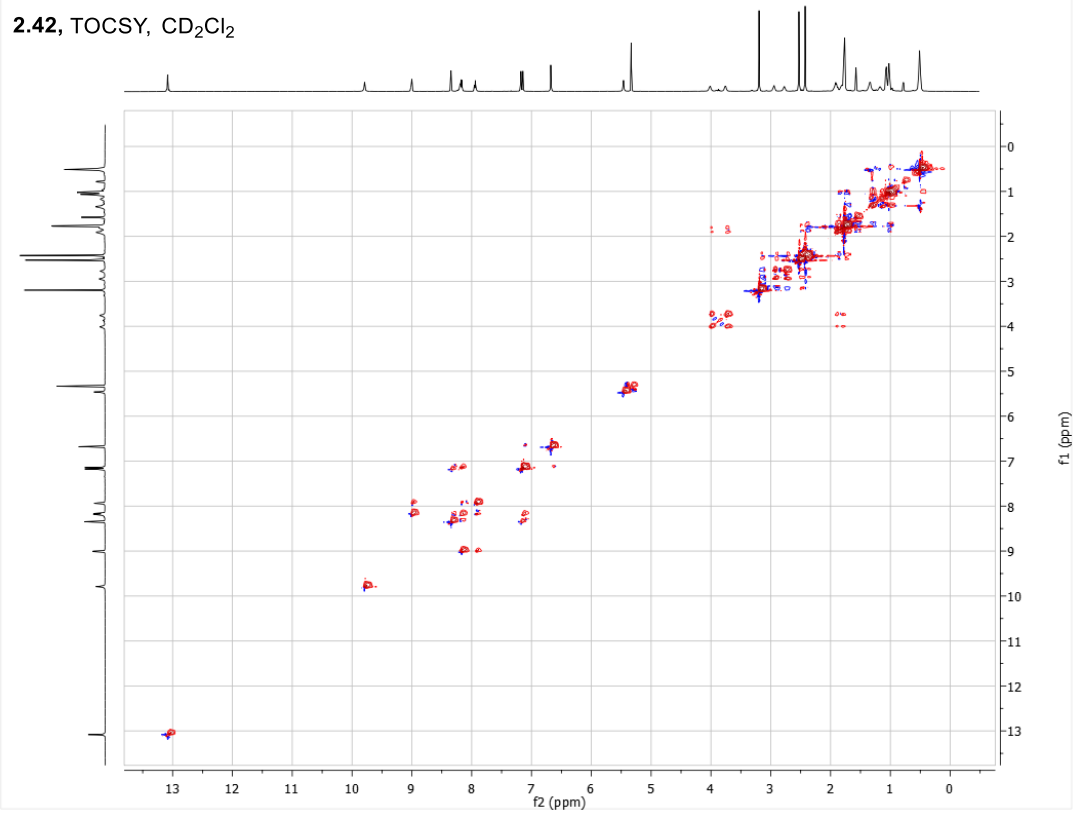

2.42, NOESY, CD_2Cl_2

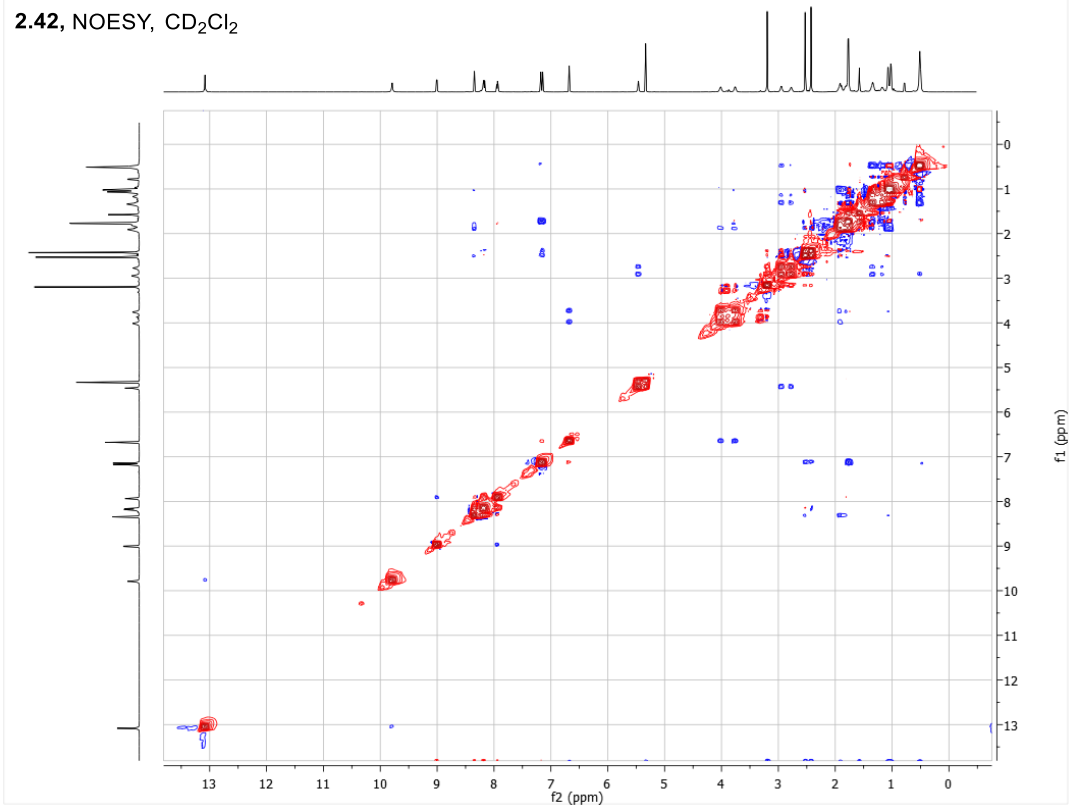

2.42, HSQC, CD_2Cl_2

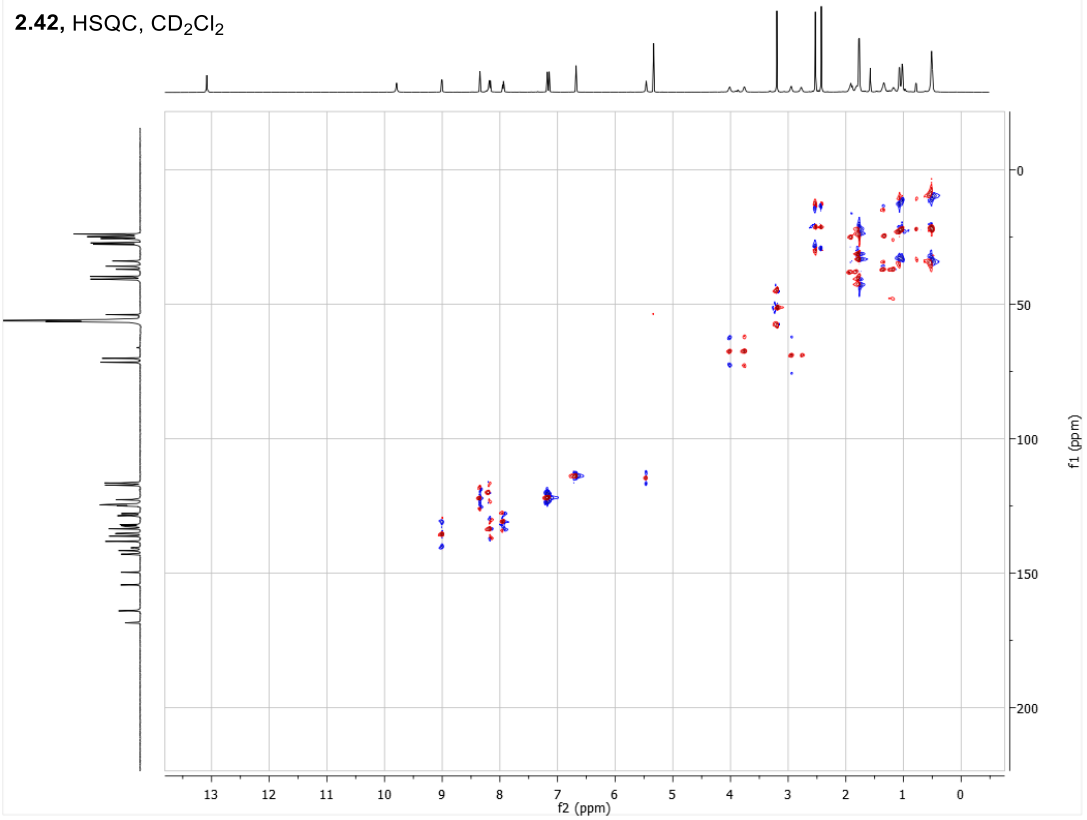

2.42, HMBC, CD_2Cl_2

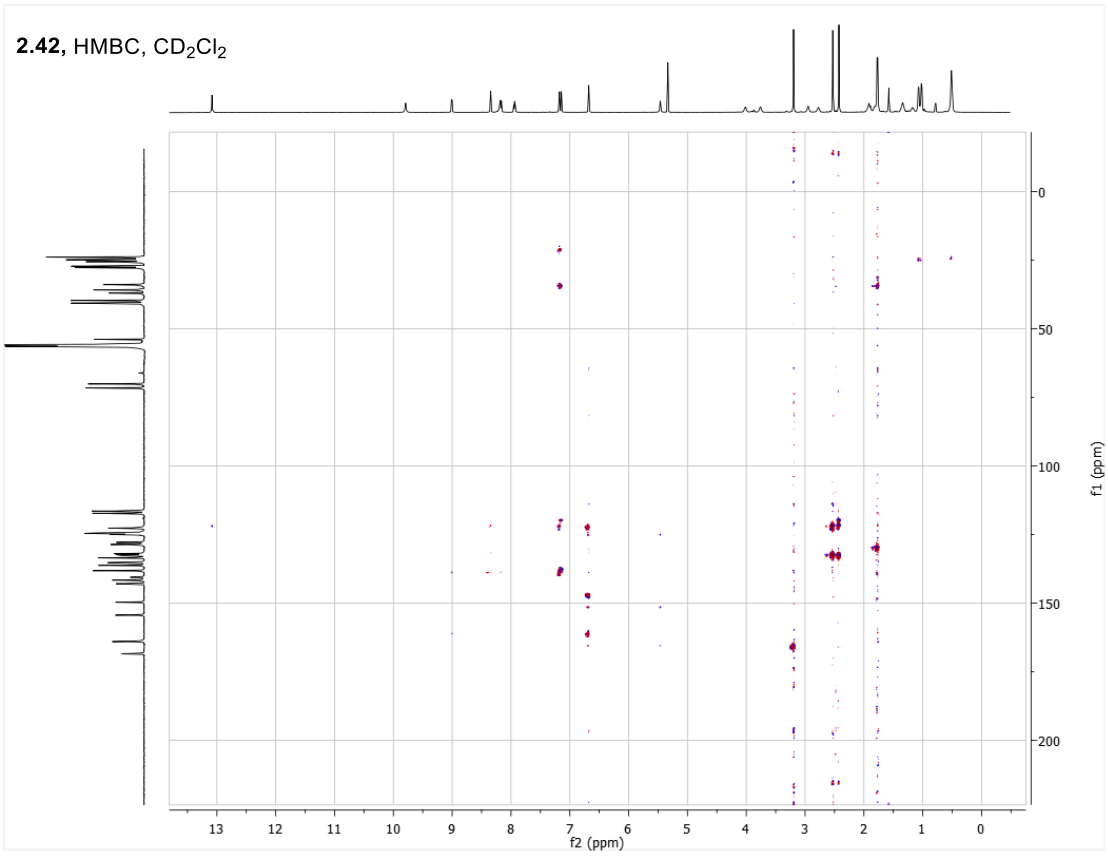

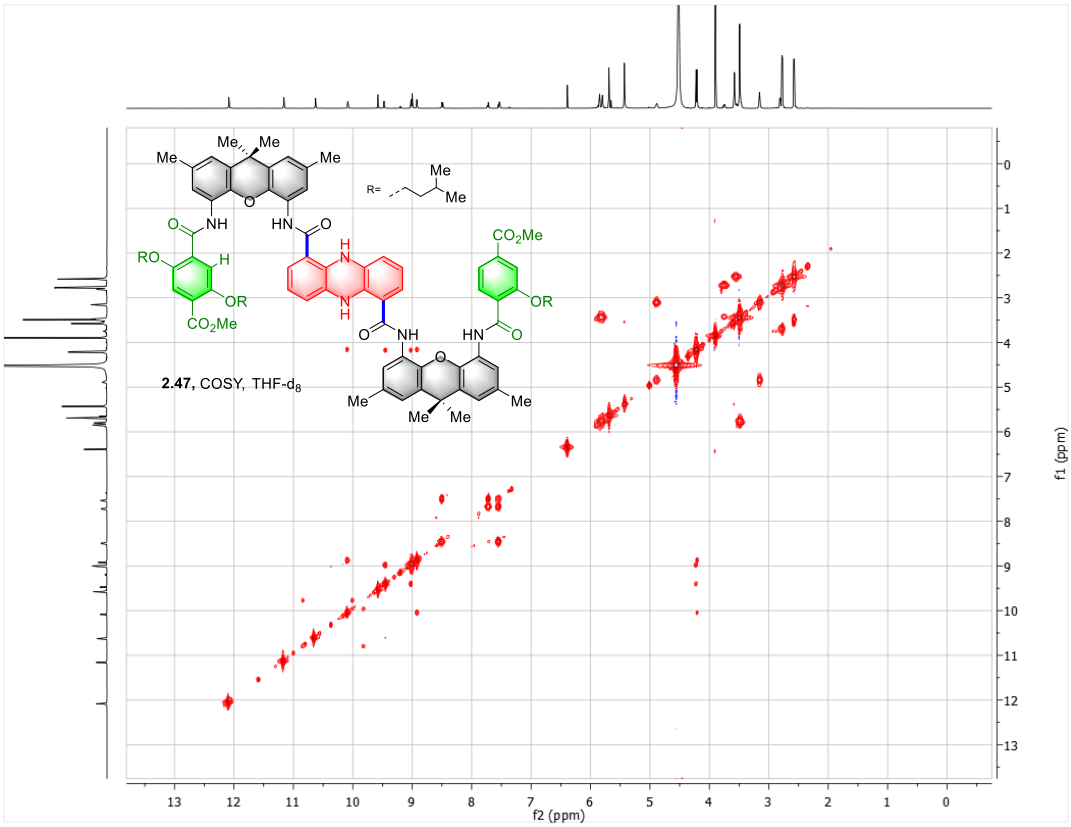
2.47, COSY, THF-d8
f2 (ppm)
f1 (ppm)

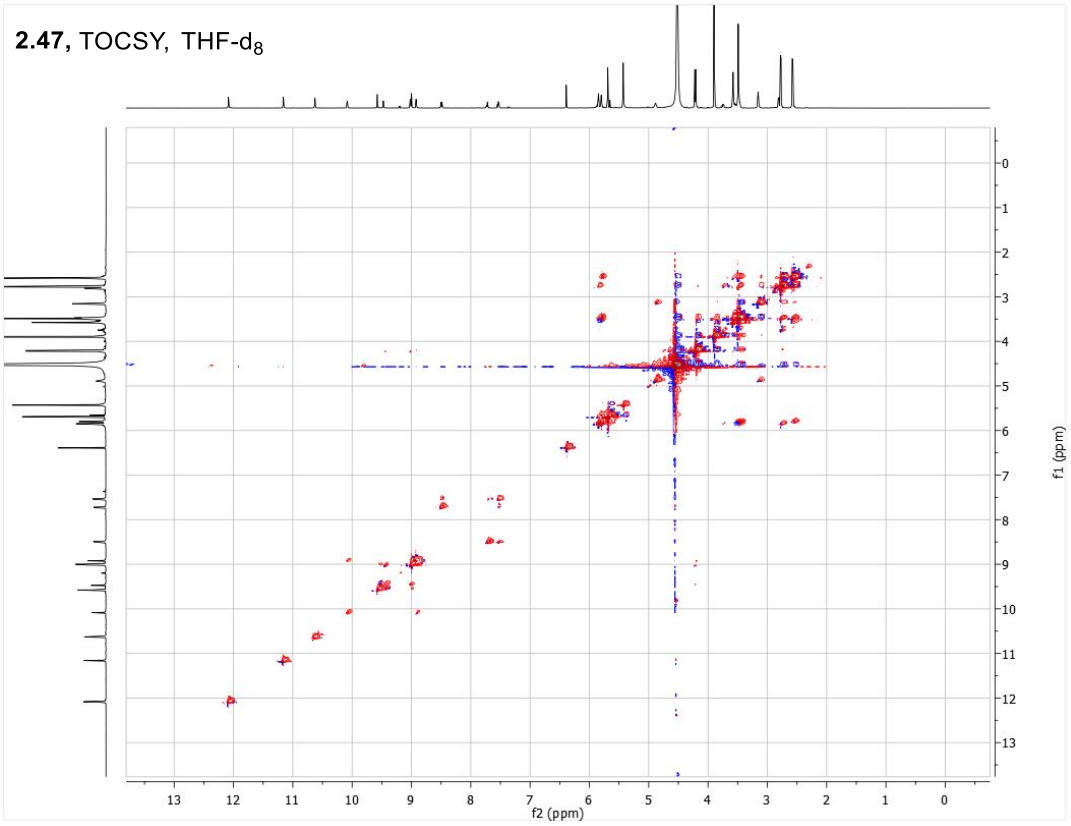
2.47, TOCSY, THF-d8
f2 (ppm)
f1 (ppm)

2.47, NOESY, THF-d_8

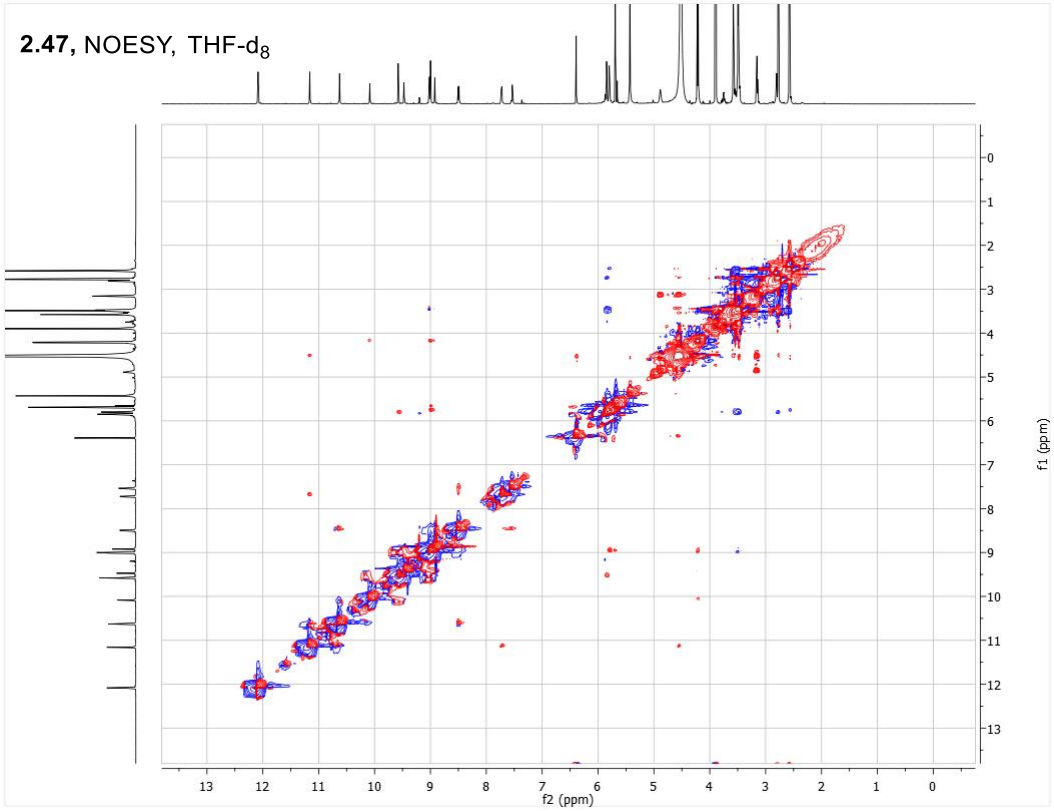

2.47, HSQC, THF-d_8

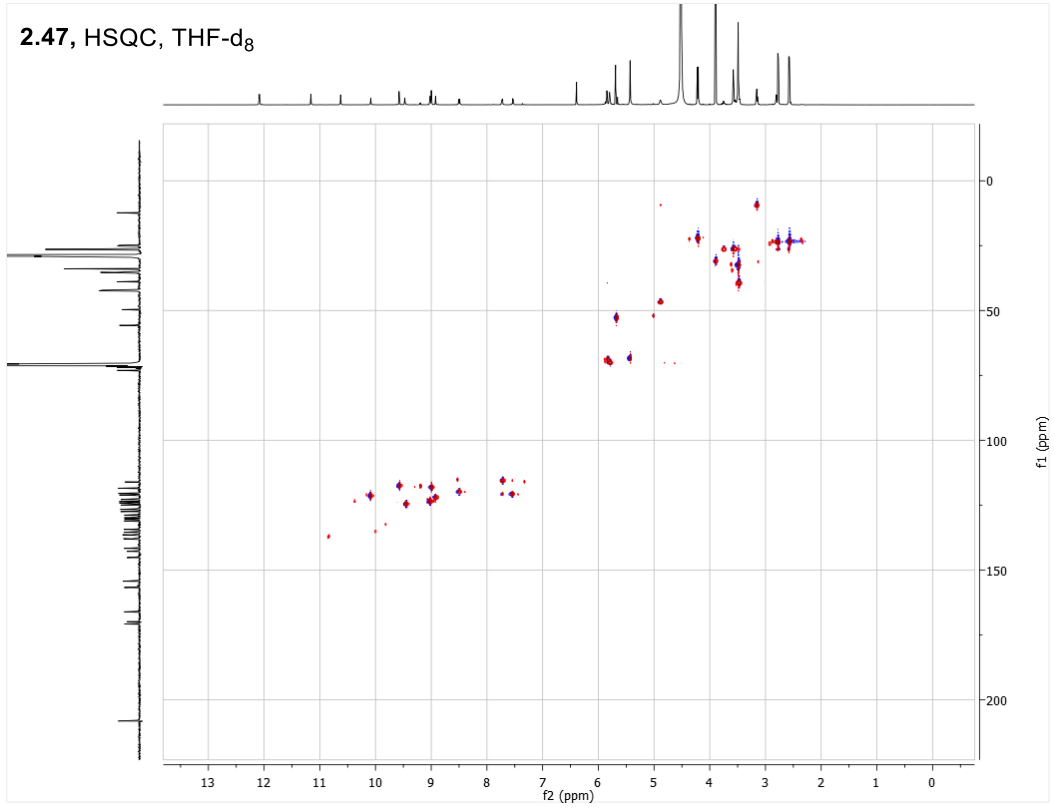

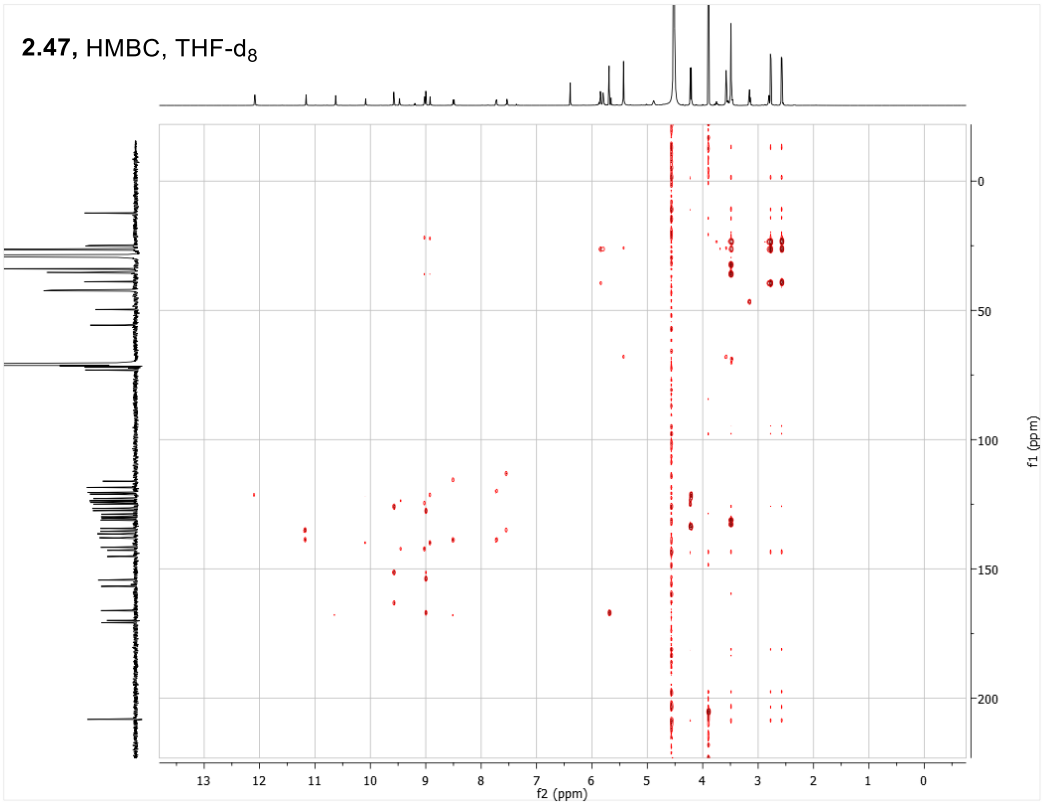
2.47, HMBC, THF-d8
0
50
100
150
200
f1 (ppm)
13
12
11
10
9
8
7
6
5
4
3
2
1
0
f2 (ppm)

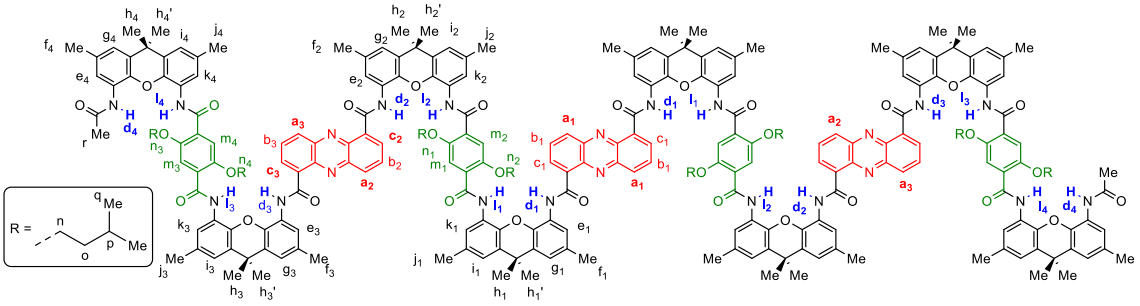

30b

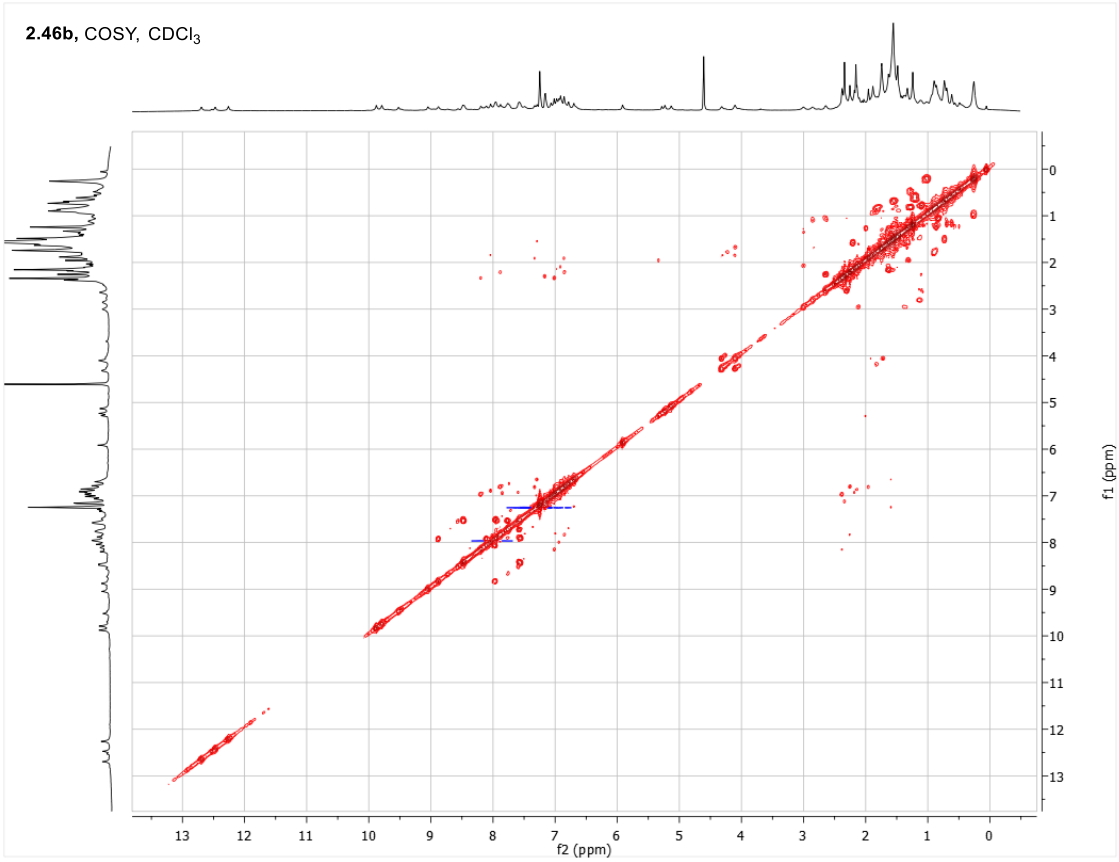

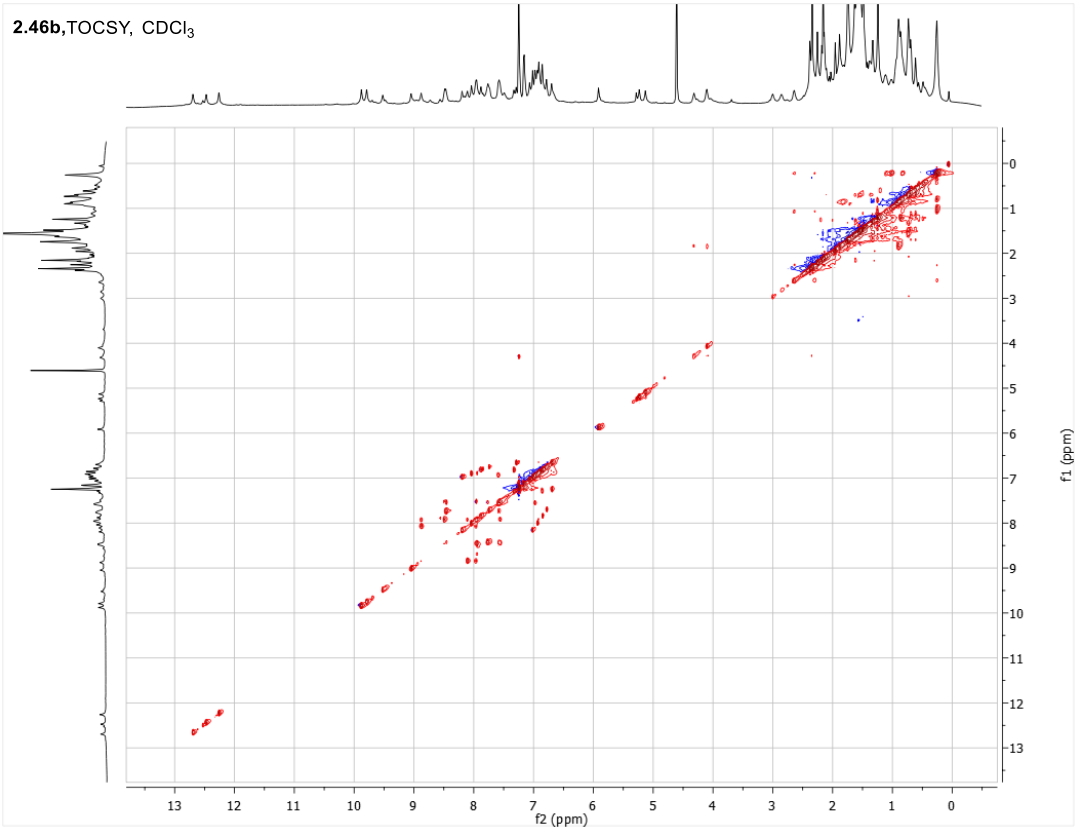
2.46b, TOCSY, CDCl3
f2 (ppm)
f1 (ppm)

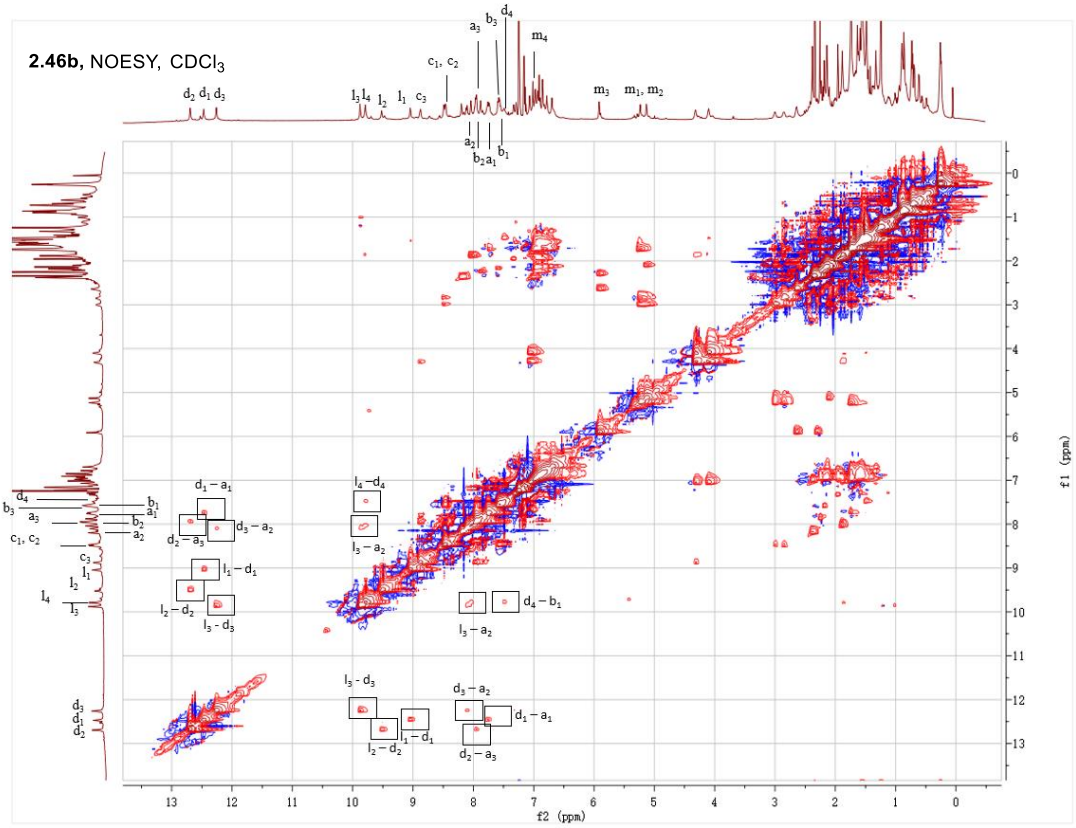
2.46b, NOESY, CDCl3
f2 (ppm)
f1 (ppm)

2.46b, HSQC, $CDCl_3$

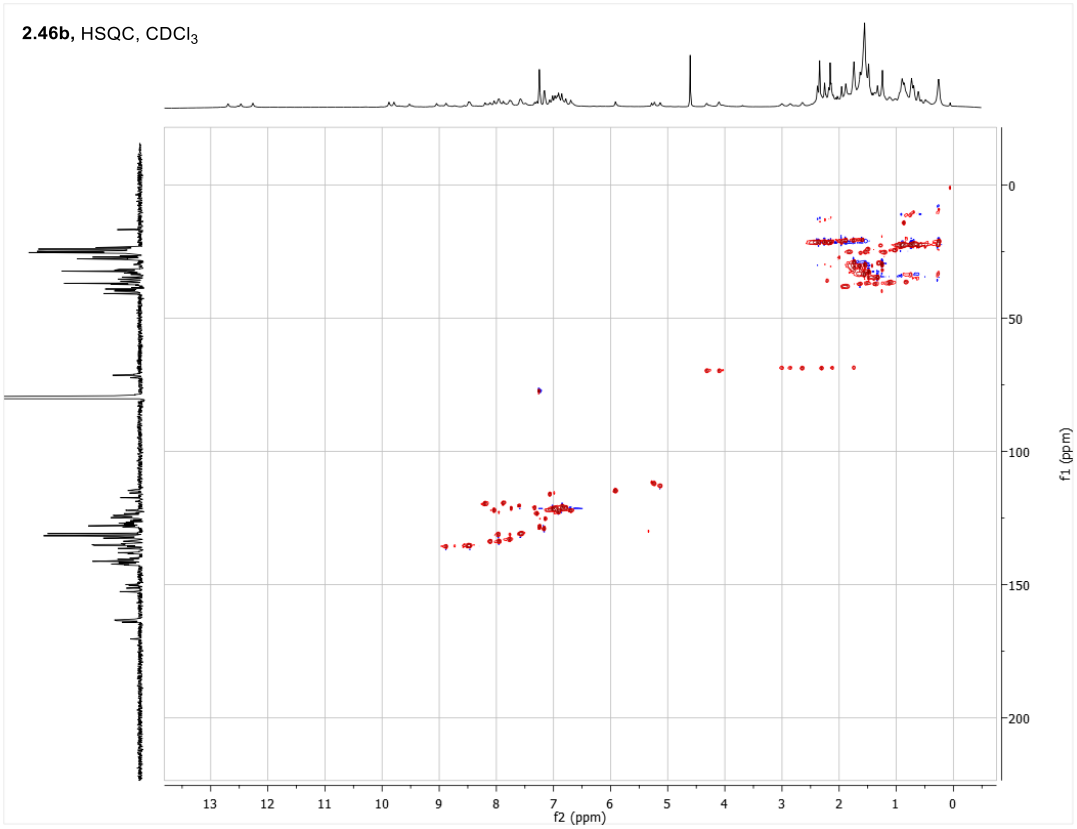

2.46b, HMBC, $CDCl_3$

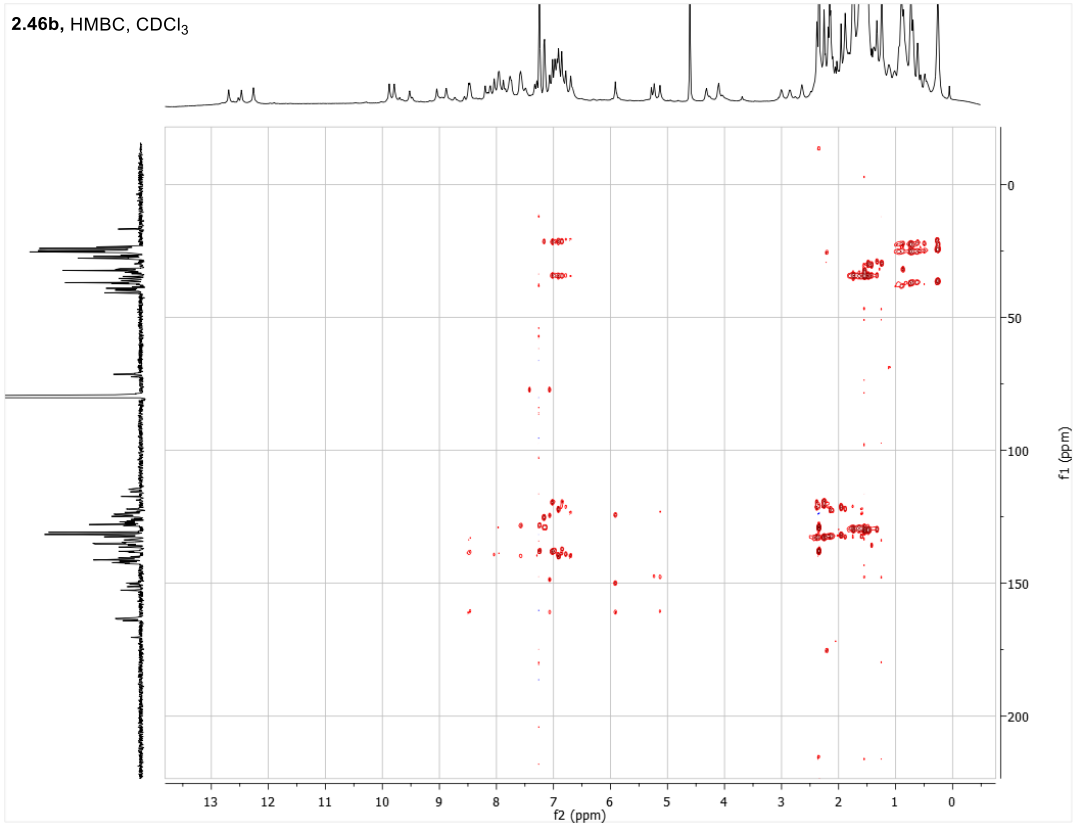

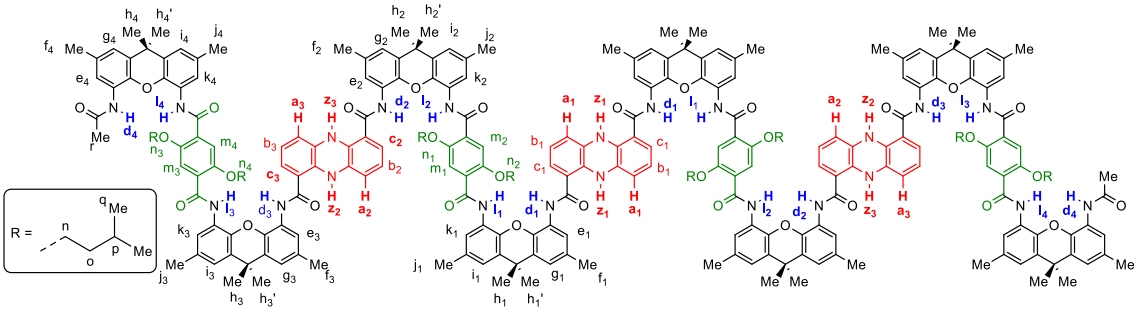

32b

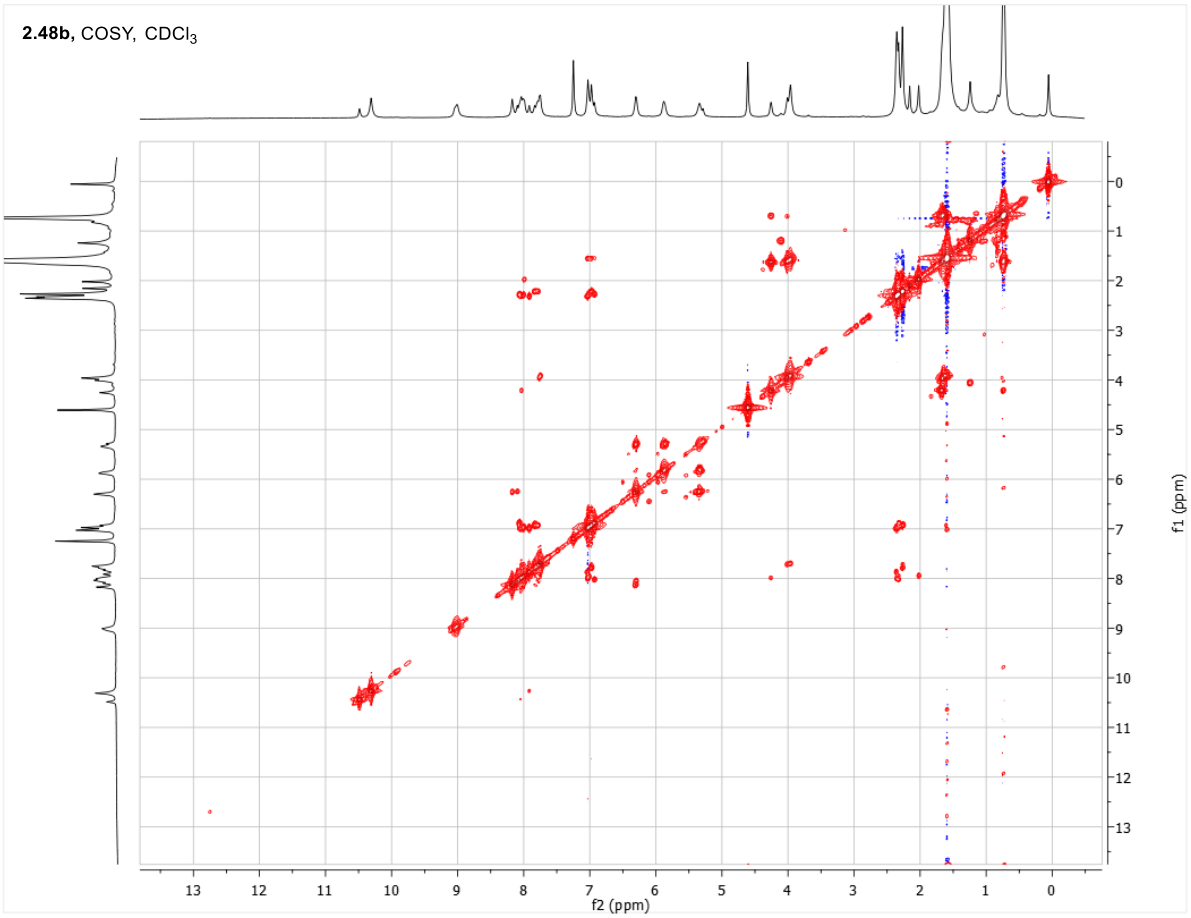

2.48b, TOCSY, $CDCl_3$

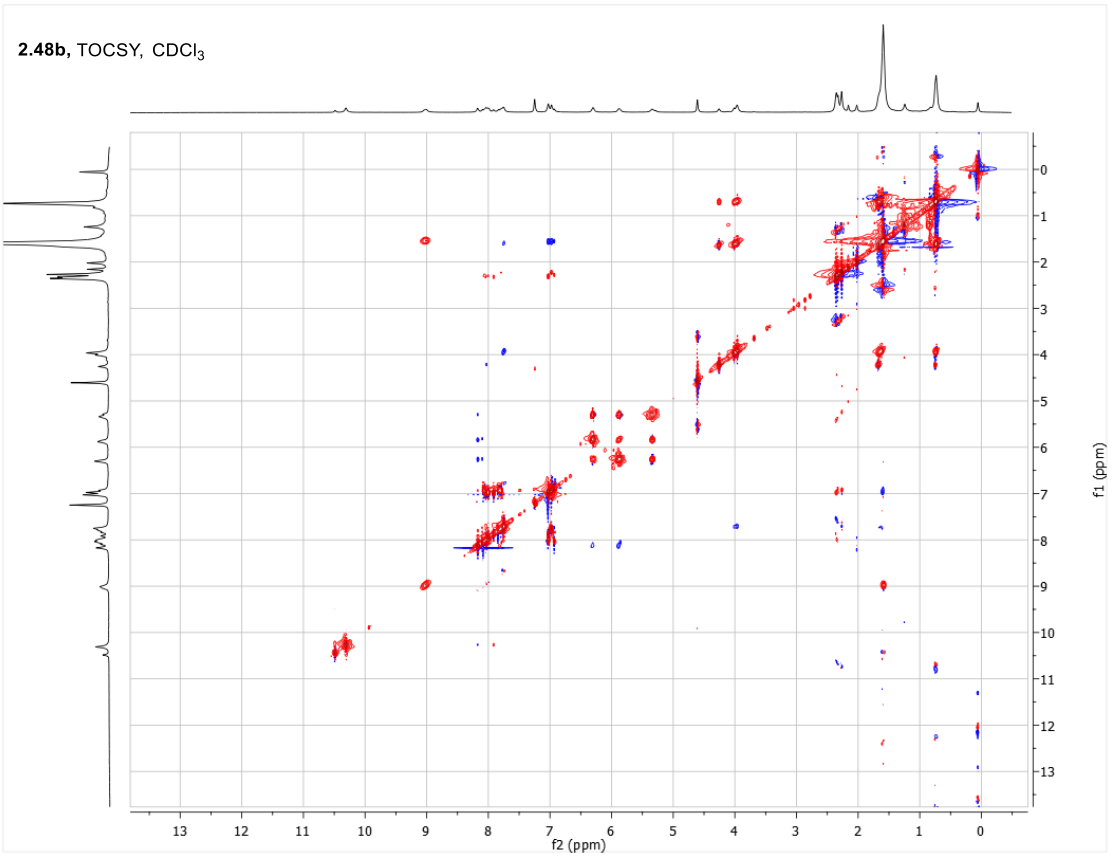

n = 1,2,3

2.48b, NOESY, $CDCl_3$

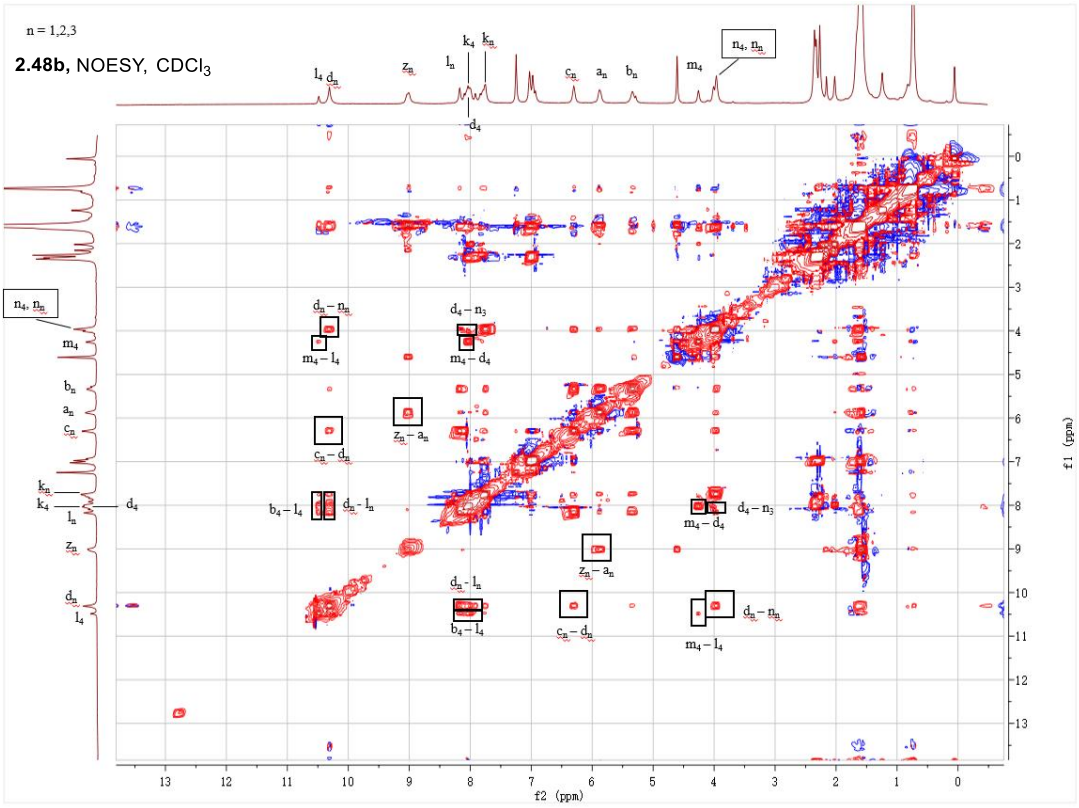

2.48b, HSQC, $CDCl_3$

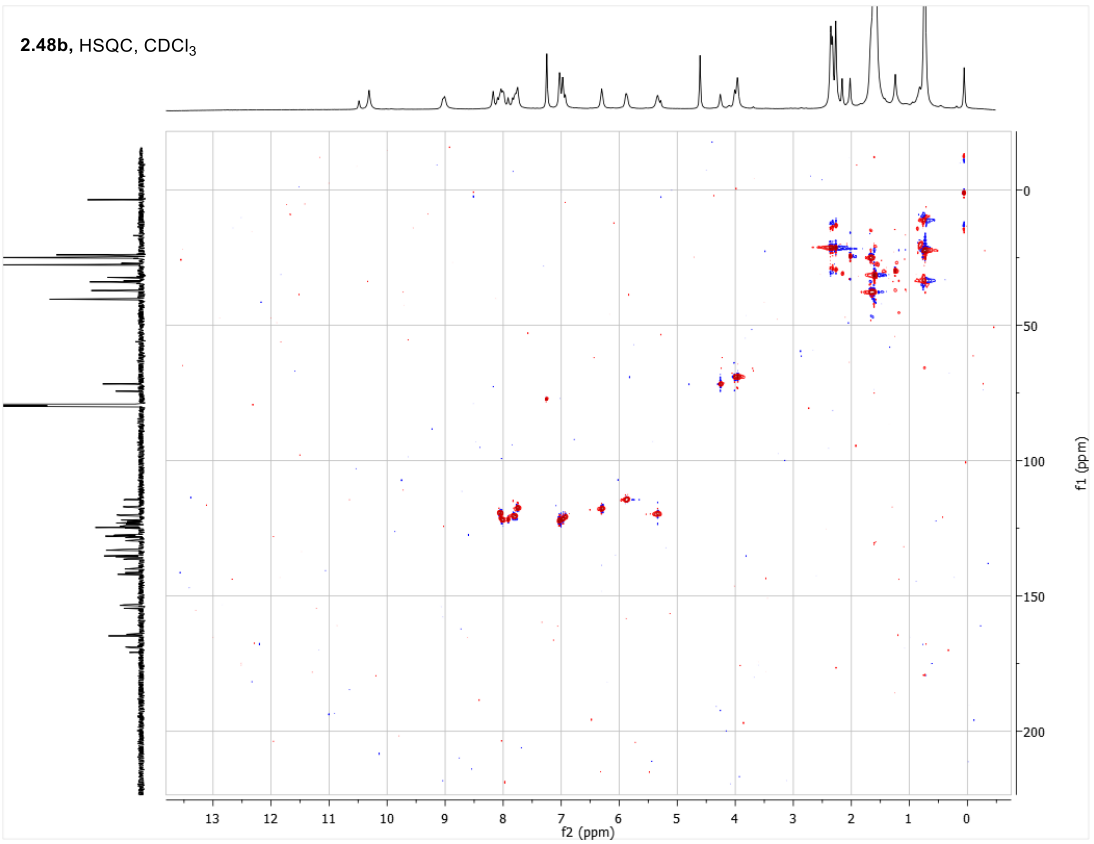

2.48b, HMBC, $CDCl_3$

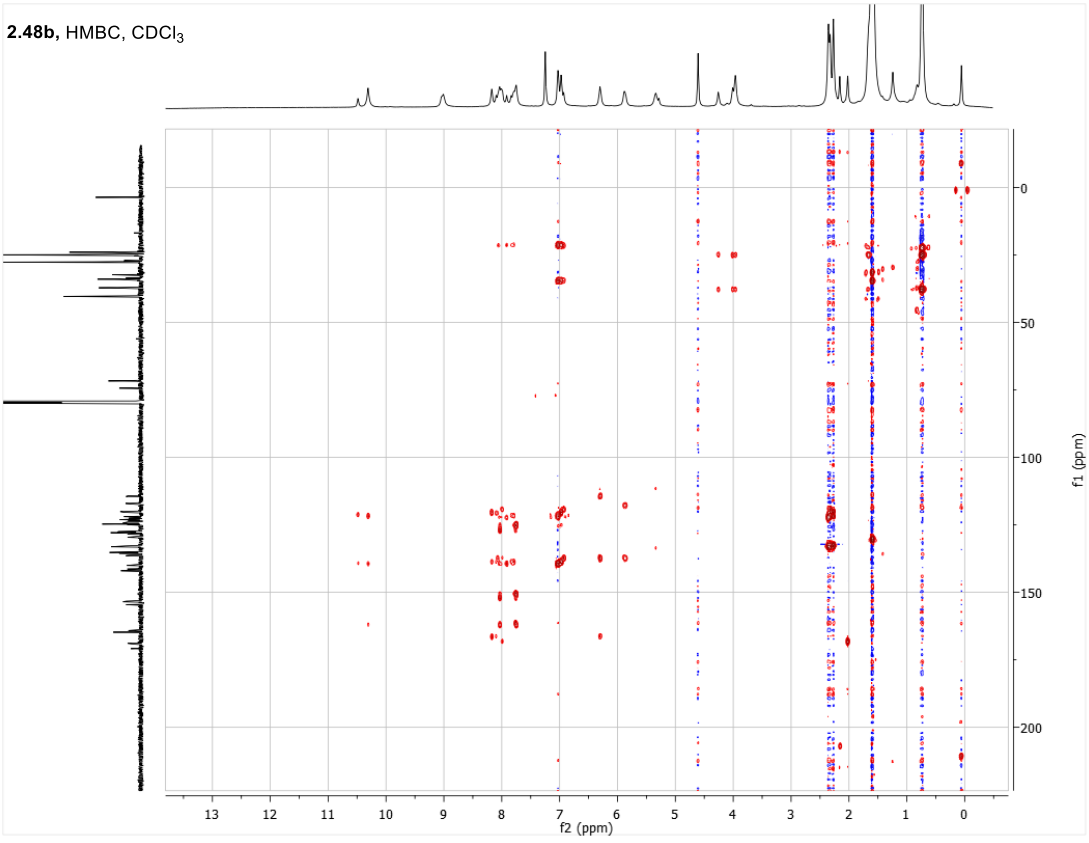

2.4.13. X-RAY CRYSTALLOGRAPHIC DATA FOR 12.

Table 2-1. Crystal data and structure refinement for vb7519.

Identification code	v7519/lt/Venture/Yin-Birman	
Empirical formula	C_{72} H_{68} Cl_{12} N_6 O_{12}	
Formula weight	1634.72	
Temperature	100(2) K	
Wavelength	1.54178 Å	
Crystal system	Triclinic	
Space group	P-1	
Unit cell dimensions	a = 9.3674(5) Å	= 102.300(3) °.
	b = 14.1728(7) Å	= 103.122(3) °.
	c = 15.4346(9) Å	= 107.338(3) °.
Volume	1816.04(17) $Å^3$	
Z	1	
Density (calculated)	1.495 Mg/m^3	
Absorption coefficient	4.740 mm^{-1}	
F(000)	842	
Crystal size	0.182 x 0.124 x 0.093 mm^3	
Theta range for data collection	3.084 to 68.314 °.	
Index ranges	$-11 \le h \le 11$, $-17 \le k \le 17$, $-18 \le l \le 18$	
Reflections collected	18610	
Independent reflections	6510 [R(int) = 0.0454]	

Completeness to theta = 67.679 °	97.9 %
Absorption correction	Semi-empirical from equivalents
Max. and min. transmission	0.5210 and 0.3976
Refinement method	Full-matrix least-squares on F^2
Data / restraints / parameters	6510 / 1 / 470
Goodness-of-fit on F^2	1.085
Final R indices [I>2sigma(I)]	R1 = 0.0904, wR2 = 0.2172
R indices (all data)	R1 = 0.1103, wR2 = 0.2348
Largest diff. peak and hole	0.788 and -0.494 e.$Å^{-3}$

Table 2-2. Atomic coordinates (x 104) and equivalent isotropic displacement parameters (Å2x 103) for vb7519. U(eq) is defined as one third of the trace of the orthogonalized Uij tensor.

	x	y	z	U(eq)
O(1)	1202(5)	3644(3)	5879(3)	37(1)
O(2)	2619(5)	5308(3)	7378(3)	32(1)
O(3)	5602(5)	5823(3)	8394(3)	35(1)
O(4)	7090(5)	2761(3)	7113(3)	42(1)
O(5)	5370(4)	1686(3)	3792(3)	29(1)
O(6)	936(5)	2336(3)	2074(3)	37(1)
N(1)	5569(5)	2116(3)	5593(3)	28(1)
N(2)	3198(5)	2323(3)	2993(3)	26(1)
N(3)	5075(5)	5954(3)	5530(3)	28(1)
C(1)	2719(6)	3817(4)	6352(4)	30(1)
C(2)	3463(7)	4713(4)	7119(4)	29(1)
C(3)	5015(7)	4951(4)	7671(4)	29(1)
C(4)	5808(7)	4290(4)	7441(4)	29(1)
C(5)	5053(7)	3401(4)	6677(4)	28(1)
C(6)	3516(6)	3161(4)	6130(4)	28(1)
C(7)	381(7)	2722(5)	5138(5)	41(2)
C(8)	3004(8)	6255(5)	7138(4)	37(1)
C(9)	7153(8)	6088(5)	9019(4)	40(1)
C(10)	5996(7)	2738(4)	6493(4)	31(1)

C(11)	6258(6)	1425(4)	5251(4)	25(1)
C(12)	7046(6)	963(4)	5803(4)	28(1)
C(13)	7654(6)	252(4)	5403(4)	29(1)
C(14)	7447(6)	-2(4)	4455(4)	30(1)
C(15)	6667(6)	446(4)	3879(4)	27(1)
C(16)	6496(7)	247(4)	2843(4)	30(1)
C(17)	5021(7)	409(4)	2350(4)	29(1)
C(18)	4148(7)	-73(4)	1417(4)	32(1)
C(19)	2904(7)	179(4)	978(4)	32(1)
C(20)	2531(7)	971(4)	1499(4)	32(1)
C(21)	3370(7)	1458(4)	2422(4)	28(1)
C(22)	4589(6)	1164(4)	2853(4)	27(1)
C(23)	6114(6)	1175(4)	4300(4)	27(1)
C(24)	8489(7)	-241(5)	6011(4)	33(1)
C(25)	7945(7)	1060(5)	2738(4)	35(1)
C(26)	6451(8)	-846(5)	2393(4)	39(1)
C(27)	2002(8)	-343(5)	-44(4)	40(1)
C(28)	2078(7)	2731(4)	2772(4)	28(1)
C(29)	2344(6)	3756(4)	3464(4)	27(1)
C(30)	1153(7)	4123(4)	3277(4)	31(1)
C(31)	1204(7)	5078(4)	3835(4)	31(1)
C(32)	2499(6)	5666(4)	4584(4)	27(1)
C(33)	3799(6)	5341(4)	4806(4)	26(1)

C(34)	6271(6)	5635(4)	5746(4)	26(1)
C(1S)	6571(7)	3240(5)	455(4)	36(1)
C(2S)	9765(8)	7018(5)	1765(5)	43(2)
Cl(1)	8406(2)	3094(1)	817(1)	44(1)
Cl(2)	5062(2)	2135(1)	456(1)	43(1)
Cl(3)	6240(2)	3379(1)	-676(1)	50(1)
Cl(4)	10785(2)	8055(1)	1438(1)	50(1)
Cl(5)	9650(2)	5824(1)	1072(1)	52(1)
Cl(6)	7835(2)	6998(2)	1689(2)	54(1)
Cl(6')	8460(30)	7270(20)	2370(20)	54(1)

Table 2-3. Bond lengths [Å] and angles [ᵒ] for vb7519.

O(1)-C(1)	1.363(7)	C(19)-C(27)	1.507(8)	C(4)-C(3)-C(2)	119.3(5)
O(1)-C(7)	1.404(7)	C(20)-C(21)	1.369(8)	C(5)-C(4)-C(3)	119.8(5)
O(2)-C(2)	1.376(6)	C(20)-H(20)	0.9500	C(5)-C(4)-H(4)	120.1
O(2)-C(8)	1.434(7)	C(21)-C(22)	1.406(8)	C(3)-C(4)-H(4)	120.1
O(3)-C(3)	1.343(7)	C(24)-H(24A)	0.9800	C(4)-C(5)-C(6)	121.1(5)
O(3)-C(9)	1.438(7)	C(24)-H(24B)	0.9800	C(4)-C(5)-C(10)	115.8(5)
O(4)-C(10)	1.221(7)	C(24)-H(24C)	0.9800	C(6)-C(5)-C(10)	123.1(5)
O(5)-C(23)	1.385(6)	C(25)-H(25A)	0.9800	C(1)-C(6)-C(5)	119.5(5)
O(5)-C(22)	1.387(6)	C(25)-H(25B)	0.9800	C(1)-C(6)-H(6)	120.2
O(6)-C(28)	1.217(7)	C(25)-H(25C)	0.9800	C(5)-C(6)-H(6)	120.2
N(1)-C(10)	1.371(7)	C(26)-H(26A)	0.9800	O(1)-C(7)-H(7A)	109.5
N(1)-C(11)	1.403(7)	C(26)-H(26B)	0.9800	O(1)-C(7)-H(7B)	109.5
N(1)-H(1)	0.8800	C(26)-H(26C)	0.9800	H(7A)-C(7)-H(7B)	109.5
N(2)-C(28)	1.354(7)	C(27)-H(27A)	0.9800	O(1)-C(7)-H(7C)	109.5
N(2)-C(21)	1.423(6)	C(27)-H(27B)	0.9800	H(7A)-C(7)-H(7C)	109.5
N(2)-H(2)	0.8800	C(27)-H(27C)	0.9800	H(7B)-C(7)-H(7C)	109.5
N(3)-C(34)	1.330(7)	C(28)-C(29)	1.523(7)	O(2)-C(8)-H(8A)	109.5
N(3)-C(33)	1.339(7)	C(29)-C(30)	1.364(8)	O(2)-C(8)-H(8B)	109.5
C(1)-C(6)	1.390(8)	C(29)-C(34)#1	1.442(8)	H(8A)-C(8)-H(8B)	109.5
C(1)-C(2)	1.399(8)	C(30)-C(31)	1.422(8)	O(2)-C(8)-H(8C)	109.5
C(2)-C(3)	1.407(8)	C(30)-H(30)	0.9500	H(8A)-C(8)-H(8C)	109.5

C(3)-C(4)	1.396(8)	C(31)-C(32)	1.361(8)	H(8B)-C(8)-H(8C)	109.5
C(4)-C(5)	1.390(8)	C(31)-H(31)	0.9500	O(3)-C(9)-H(9A)	109.5
C(4)-H(4)	0.9500	C(32)-C(33)	1.423(7)	O(3)-C(9)-H(9B)	109.5
C(5)-C(6)	1.391(8)	C(32)-H(32)	0.9500	H(9A)-C(9)-H(9B)	109.5
C(5)-C(10)	1.497(7)	C(33)-C(34)#1	1.436(7)	O(3)-C(9)-H(9C)	109.5
C(6)-H(6)	0.9500	C(1S)-Cl(3)	1.766(6)	H(9A)-C(9)-H(9C)	109.5
C(7)-H(7A)	0.9800	C(1S)-Cl(2)	1.771(6)	H(9B)-C(9)-H(9C)	109.5
C(7)-H(7B)	0.9800	C(1S)-Cl(1)	1.771(6)	O(4)-C(10)-N(1)	122.4(5)
C(7)-H(7C)	0.9800	C(1S)-H(1S)	1.0000	O(4)-C(10)-C(5)	121.3(5)
C(8)-H(8A)	0.9800	C(2S)-Cl(4)	1.740(7)	N(1)-C(10)-C(5)	116.4(5)
C(8)-H(8B)	0.9800	C(2S)-Cl(5)	1.758(7)	C(12)-C(11)-	
C(8)-H(8C)	0.9800	C(2S)-Cl(6')	1.769(12)	C(23)	118.7(5)
C(9)-H(9A)	0.9800	C(2S)-Cl(6)	1.775(7)	C(12)-C(11)-N(1)	123.4(5)
C(9)-H(9B)	0.9800	C(2S)-H(2S)	1.0000	C(23)-C(11)-N(1)	117.8(4)
C(9)-H(9C)	0.9800	C(1)-O(1)-C(7)	117.4(4)	C(11)-C(12)-	
C(11)-C(12)	1.392(7)	C(2)-O(2)-C(8)	113.2(4)	C(13)	120.1(5)
C(11)-C(23)	1.399(8)	C(3)-O(3)-C(9)	118.2(4)	C(11)-C(12)-H(12)	120.0
C(12)-C(13)	1.399(7)	C(23)-O(5)-C(22)	116.5(4)	C(13)-C(12)-H(12)	120.0
C(12)-H(12)	0.9500	C(10)-N(1)-C(11)	127.0(5)	C(14)-C(13)-	
C(13)-C(14)	1.383(8)	C(10)-N(1)-H(1)	116.5	C(12)	119.7(5)
C(13)-C(24)	1.501(7)	C(11)-N(1)-H(1)	116.5	C(14)-C(13)-	
C(14)-C(15)	1.396(8)	C(28)-N(2)-C(21)	127.2(5)	C(24)	121.2(5)
C(14)-H(14)	0.9500	C(28)-N(2)-H(2)	116.4	C(12)-C(13)-	

C(15)-C(23)	1.395(7)	C(21)-N(2)-H(2)	116.4	C(24)	119.1(5)
C(15)-C(16)	1.526(8)	C(34)-N(3)-C(33)	118.9(5)	C(13)-C(14)-C(15)	121.9(5)
C(16)-C(17)	1.525(8)	O(1)-C(1)-C(6)	124.4(5)	C(13)-C(14)-H(14)	119.0
C(16)-C(26)	1.541(7)	O(1)-C(1)-C(2)	115.5(5)	C(15)-C(14)-H(14)	119.0
C(16)-C(25)	1.563(8)	C(6)-C(1)-C(2)	120.1(5)	C(23)-C(15)-C(14)	117.2(5)
C(17)-C(18)	1.387(8)	O(2)-C(2)-C(1)	119.5(5)	C(23)-C(15)-C(16)	118.5(5)
C(17)-C(22)	1.399(7)	O(2)-C(2)-C(3)	120.1(5)	C(14)-C(15)-C(16)	124.1(5)
C(18)-C(19)	1.392(8)	C(1)-C(2)-C(3)	120.2(5)	C(17)-C(16)-C(15)	109.3(4)
C(18)-H(18)	0.9500	O(3)-C(3)-C(4)	125.7(5)	C(17)-C(16)-C(26)	111.1(5)
C(19)-C(20)	1.416(8)	O(3)-C(3)-C(2)	115.0(5)	C(15)-C(16)-C(26)	111.6(5)
				C(17)-C(16)-C(25)	107.8(4)
				C(15)-C(16)-C(25)	108.5(5)
				C(26)-C(16)-C(25)	108.4(5)

		C(18)-C(17)-C(22) 117.2(5) C(18)-C(17)-C(16) 124.9(5)
C(22)-C(17)-C(16) 117.7(5) C(17)-C(18)-C(19) 122.6(5) C(17)-C(18)-H(18) 118.7 C(19)-C(18)-H(18) 118.7 C(18)-C(19)-C(20) 118.8(5) C(18)-C(19)-C(27) 121.2(5) C(20)-C(19)-C(27) 119.9(5) C(21)-C(20)-C(19) 119.9(5) C(21)-C(20)-H(20) 120.1 C(19)-C(20)-H(20) 120.1 C(20)-C(21)-C(22) 119.9(5) C(20)-C(21)-N(2) 124.9(5) C(22)-C(21)-N(2) 115.0(5) O(5)-C(22)-C(17) 122.0(5) O(5)-C(22)-C(21) 116.4(4) C(17)-C(22)-C(21) 121.6(5) O(5)-C(23)-C(15) 121.5(5) O(5)-C(23)-C(11) 116.2(4) C(15)-C(23)-C(11) 122.3(5)	C(16)-C(25)-H(25B) 109.5 H(25A)-C(25)-H(25B) 109.5 C(16)-C(25)-H(25C) 109.5 H(25A)-C(25)-H(25C) 109.5 H(25B)-C(25)-H(25C) 109.5 C(16)-C(26)-H(26A) 109.5 C(16)-C(26)-H(26B) 109.5 H(26A)-C(26)-H(26B) 109.5 C(16)-C(26)-H(26C) 109.5 H(26A)-C(26)-H(26C) 109.5 H(26B)-C(26)-H(26C) 109.5 C(19)-C(27)-H(27A) 109.5 C(19)-C(27)-H(27B) 109.5	C(32)-C(31)-C(30) 119.2(5) C(32)-C(31)-H(31) 120.4 C(30)-C(31)-H(31) 120.4 C(31)-C(32)-C(33) 120.8(5) C(31)-C(32)-H(32) 119.6 C(33)-C(32)-H(32) 119.6 N(3)-C(33)-C(32) 119.2(5) N(3)-C(33)-C(34)#1 121.0(5) C(32)-C(33)-C(34)#1 119.8(5) N(3)-C(34)-C(33)#1 120.1(5) N(3)-C(34)-C(29)#1 121.6(5) C(33)#1-C(34)-C(29)#1 118.3(5)

C(13)-C(24)-H(24A) 109.5	H(27A)-C(27)-	Cl(3)-C(1S)-Cl(2) 110.2(3)
C(13)-C(24)-H(24B) 109.5	H(27B) 109.5	Cl(3)-C(1S)-Cl(1) 109.6(3)
H(24A)-C(24)-	C(19)-C(27)-H(27C) 109.5	Cl(2)-C(1S)-Cl(1) 109.0(3)
H(24B) 109.5	H(27A)-C(27)-	Cl(3)-C(1S)-H(1S) 109.3
C(13)-C(24)-H(24C) 109.5	H(27C) 109.5	Cl(2)-C(1S)-H(1S) 109.3
H(24A)-C(24)-	H(27B)-C(27)-	Cl(1)-C(1S)-H(1S) 109.3
H(24C) 109.5	H(27C) 109.5	Cl(4)-C(2S)-Cl(5) 112.1(4)
H(24B)-C(24)-	O(6)-C(28)-N(2) 124.3(5)	Cl(4)-C(2S)-
H(24C) 109.5	O(6)-C(28)-C(29) 120.6(5)	Cl(6') 114.8(10)
C(16)-C(25)-H(25A) 109.5	N(2)-C(28)-C(29) 115.1(5)	Cl(5)-C(2S)-
	C(30)-C(29)-	Cl(6') 128.3(11)
	C(34)#1 119.0(5)	Cl(4)-C(2S)-Cl(6) 110.0(4)
	C(30)-C(29)-C(28) 114.8(5)	Cl(5)-C(2S)-Cl(6) 109.4(4)
	C(34)#1-C(29)-	Cl(4)-C(2S)-H(2S) 108.4
	C(28) 126.2(5)	Cl(5)-C(2S)-H(2S) 108.4
	C(29)-C(30)-C(31) 122.9(5)	Cl(6)-C(2S)-H(2S) 108.4
	C(29)-C(30)-H(30) 118.5	
	C(31)-C(30)-H(30) 118.5	

Symmetry transformations used to generate equivalent atoms:

#1 -x+1,-y+1,-z+1

Table 2-4. Anisotropic displacement parameters (Å2x 103) for vb7519. The anisotropic displacement factor exponent takes the form: -2 2[h2 a*2U11 + ... + 2 h k a* b* U12]

	U11	U22		
	U33	U23	U13	U12
O(1)	26(2)	32(2)	49(2)	
	1(2)	6(2)	16(2)	
O(2)	32(2)	23(2)	46(2)	
	8(2)	15(2)	14(2)	
O(3)	36(2)	29(2)	36(2)	
	1(2)	4(2)	16(2)	
O(4)	51(3)	42(2)	36(2)	
	2(2)	3(2)	33(2)	
O(5)	33(2)	22(2)	33(2)	
	6(2)	6(2)	16(2)	
O(6)	30(2)	33(2)	39(2)	
	2(2)	0(2)	16(2)	
N(1)	27(2)	25(2)	32(2)	
	9(2)	7(2)	14(2)	
N(2)	33(2)	22(2)	27(2)	
	4(2)	7(2)	19(2)	
N(3)	30(2)	23(2)	35(2)	
	10(2)	12(2)	15(2)	
C(1)	25(3)	27(3)	40(3)	

	10(2)	13(2)	12(2)
C(2)	31(3)	25(3)	37(3)
	10(2)	13(2)	17(2)
C(3)	31(3)	25(3)	36(3)
	10(2)	14(2)	14(2)
C(4)	30(3)	31(3)	33(3)
	13(2)	10(2)	17(2)
C(5)	34(3)	26(3)	30(3)
	11(2)	11(2)	17(2)
C(6)	31(3)	24(3)	32(3)
	10(2)	11(2)	13(2)
C(7)	28(3)	36(3)	52(4)
	3(3)	7(3)	14(3)
C(8)	44(3)	32(3)	48(3)
	16(3)	19(3)	24(3)
C(9)	44(4)	31(3)	39(3)
	5(2)	1(3)	19(3)
C(10)	37(3)	27(3)	35(3)
	12(2)	11(2)	19(2)
C(11)	25(3)	15(2)	36(3)
	9(2)	7(2)	10(2)
C(12)	27(3)	21(2)	38(3)
	11(2)	11(2)	11(2)

C(13)	29(3)	21(2)	45(3)
	16(2)	15(2)	13(2)
C(14)	27(3)	19(2)	46(3)
	8(2)	14(2)	11(2)
C(15)	26(3)	17(2)	41(3)
	8(2)	11(2)	12(2)
C(16)	31(3)	24(3)	40(3)
	8(2)	14(2)	17(2)
C(17)	32(3)	21(3)	42(3)
	11(2)	16(2)	14(2)
C(18)	38(3)	23(3)	38(3)
	6(2)	16(2)	16(2)
C(19)	33(3)	22(3)	38(3)
	6(2)	11(2)	12(2)
C(20)	34(3)	29(3)	38(3)
	11(2)	7(2)	18(2)
C(21)	34(3)	23(3)	33(3)
	9(2)	13(2)	16(2)
C(22)	31(3)	23(3)	32(3)
	10(2)	13(2)	14(2)
C(23)	27(3)	16(2)	39(3)
	5(2)	9(2)	11(2)
C(24)	37(3)	33(3)	43(3)

	17(2)	17(3)	23(3)
C(25)	33(3)	36(3)	39(3)
	13(2)	9(2)	16(3)
C(26)	50(4)	28(3)	40(3)
	4(2)	11(3)	25(3)
C(27)	47(4)	31(3)	39(3)
	4(2)	7(3)	20(3)
C(28)	31(3)	22(3)	34(3)
	9(2)	13(2)	13(2)
C(29)	27(3)	24(3)	34(3)
	10(2)	12(2)	13(2)
C(30)	27(3)	27(3)	39(3)
	9(2)	6(2)	13(2)
C(31)	29(3)	28(3)	38(3)
	8(2)	11(2)	14(2)
C(32)	31(3)	25(3)	32(3)
	9(2)	14(2)	17(2)
C(33)	34(3)	20(2)	31(3)
	11(2)	15(2)	15(2)
C(34)	28(3)	22(2)	36(3)
	12(2)	16(2)	16(2)
C(1S)	38(3)	30(3)	39(3)
	12(2)	13(3)	11(3)

C(2S)	44(4)	41(3)	47(4)
	15(3)	9(3)	20(3)
Cl(1)	42(1)	43(1)	50(1)
	10(1)	13(1)	22(1)
Cl(2)	46(1)	30(1)	54(1)
	10(1)	22(1)	11(1)
Cl(3)	51(1)	44(1)	45(1)
	18(1)	7(1)	10(1)
Cl(4)	51(1)	42(1)	62(1)
	22(1)	21(1)	16(1)
Cl(5)	47(1)	38(1)	63(1)
	7(1)	10(1)	16(1)
Cl(6)	48(1)	65(1)	75(2)
	38(1)	32(1)	33(1)
Cl(6')	48(1)	65(1)	75(2)
	38(1)	32(1)	33(1)

Table 2-5. Hydrogen coordinates (x 104) and isotropic displacement parameters (Å2x 10 3) for vb7519.

	x	y	z	U(eq)
H(1)	4777	2155	5187	33
H(2)	3897	2626	3551	32
H(4)	6862	4447	7804	35
H(6)	3015	2554	5608	33
H(7A)	914	2714	4660	62
H(7B)	-696	2683	4866	62
H(7C)	351	2127	5370	62
H(8A)	2635	6099	6458	56
H(8B)	4148	6623	7370	56
H(8C)	2493	6692	7422	56
H(9A)	7914	6174	8672	60
H(9B)	7173	5533	9302	60
H(9C)	7429	6737	9510	60
H(12)	7171	1131	6452	33
H(14)	7846	-495	4188	36
H(18)	4410	-595	1063	38
H(20)	1699	1163	1209	39
H(24A)	8521	34	6657	50
H(24B)	7927	-993	5793	50
H(24C)	9566	-84	5981	50

H(25A)	7989	1761	3017	53
H(25B)	7843	951	2074	53
H(25C)	8913	978	3055	53
H(26A)	7386	-942	2740	58
H(26B)	6437	-926	1744	58
H(26C)	5503	-1367	2408	58
H(27A)	2711	-509	-378	60
H(27B)	1564	124	-299	60
H(27C)	1145	-982	-118	60
H(30)	250	3722	2752	37
H(31)	345	5303	3686	37
H(32)	2535	6301	4964	33
H(1S)	6582	3872	898	43
H(2S)	10331	7114	2428	52

Table 2-6. Torsion angles [º] for vb7519.

C(7)-O(1)-C(1)-C(6)	2.3(8)	C(26)-C(16)-C(17)-C(22)	156.6(5)
C(7)-O(1)-C(1)-C(2)	-176.4(5)	C(25)-C(16)-C(17)-C(22)	-84.8(6)
C(8)-O(2)-C(2)-C(1)	-105.8(6)	C(22)-C(17)-C(18)-C(19)	0.9(8)
C(8)-O(2)-C(2)-C(3)	80.0(6)	C(16)-C(17)-C(18)-C(19)	-173.3(5)
O(1)-C(1)-C(2)-O(2)	4.2(8)	C(17)-C(18)-C(19)-C(20)	1.1(9)
C(6)-C(1)-C(2)-O(2)	-174.5(5)	C(17)-C(18)-C(19)-C(27)	178.6(6)
O(1)-C(1)-C(2)-C(3)	178.3(5)	C(18)-C(19)-C(20)-C(21)	-1.2(9)
C(6)-C(1)-C(2)-C(3)	-0.4(8)	C(27)-C(19)-C(20)-C(21)	-178.7(6)
C(9)-O(3)-C(3)-C(4)	-3.2(8)	C(19)-C(20)-C(21)-C(22)	-0.7(9)
C(9)-O(3)-C(3)-C(2)	176.8(5)	C(19)-C(20)-C(21)-N(2)	174.1(5)
O(2)-C(2)-C(3)-O(3)	-5.2(8)	C(28)-N(2)-C(21)-C(20)	8.6(9)
C(1)-C(2)-C(3)-O(3)	-179.3(5)	C(28)-N(2)-C(21)-C(22)	-176.3(5)
O(2)-C(2)-C(3)-C(4)	174.7(5)	C(23)-O(5)-C(22)-C(17)	-25.8(7)
C(1)-C(2)-C(3)-C(4)	0.7(8)	C(23)-O(5)-C(22)-C(21)	156.3(5)
O(3)-C(3)-C(4)-C(5)	179.2(5)	C(18)-C(17)-C(22)-O(5)	179.3(5)
C(2)-C(3)-C(4)-C(5)	-0.7(8)	C(16)-C(17)-C(22)-O(5)	-6.1(8)
C(3)-C(4)-C(5)-C(6)	0.6(8)	C(18)-C(17)-C(22)-C(21)	-2.9(8)
C(3)-C(4)-C(5)-C(10)	-179.5(5)	C(16)-C(17)-C(22)-C(21)	171.8(5)
O(1)-C(1)-C(6)-C(5)	-178.3(5)	C(20)-C(21)-C(22)-O(5)	-179.2(5)
C(2)-C(1)-C(6)-C(5)	0.3(8)	N(2)-C(21)-C(22)-O(5)	5.5(7)
C(4)-C(5)-C(6)-C(1)	-0.4(8)	C(20)-C(21)-C(22)-C(17)	2.8(8)
C(10)-C(5)-C(6)-C(1)	179.7(5)	N(2)-C(21)-C(22)-C(17)	-172.5(5)

C(11)-N(1)-C(10)-O(4) 1.0(9)	C(22)-O(5)-C(23)-C(15) 27.7(7)
C(11)-N(1)-C(10)-C(5) -179.4(5)	C(22)-O(5)-C(23)-C(11) -151.6(5)
C(4)-C(5)-C(10)-O(4) 24.0(8)	C(14)-C(15)-C(23)-O(5) 178.0(5)
C(6)-C(5)-C(10)-O(4) -156.1(6)	C(16)-C(15)-C(23)-O(5) 2.4(8)
C(4)-C(5)-C(10)-N(1) -155.6(5)	C(14)-C(15)-C(23)-C(11) -2.8(8)
C(6)-C(5)-C(10)-N(1) 24.4(8)	C(16)-C(15)-C(23)-C(11)-178.4(5)
C(10)-N(1)-C(11)-C(12) 26.0(8)	C(12)-C(11)-C(23)-O(5) -177.7(5)
C(10)-N(1)-C(11)-C(23) -155.2(5)	N(1)-C(11)-C(23)-O(5) 3.5(7)
C(23)-C(11)-C(12)-C(13) -1.1(8)	C(12)-C(11)-C(23)-C(15) 3.0(8)
N(1)-C(11)-C(12)-C(13) 177.7(5)	N(1)-C(11)-C(23)-C(15) -175.8(5)
C(11)-C(12)-C(13)-C(14) -1.0(8)	C(21)-N(2)-C(28)-O(6) 8.4(9)
C(11)-C(12)-C(13)-C(24)-179.6(5)	C(21)-N(2)-C(28)-C(29) -170.8(5)
C(12)-C(13)-C(14)-C(15) 1.2(8)	O(6)-C(28)-C(29)-C(30) 5.7(8)
C(24)-C(13)-C(14)-C(15)179.8(5)	N(2)-C(28)-C(29)-C(30) -175.1(5)
C(13)-C(14)-C(15)-C(23) 0.7(8)	O(6)-C(28)-C(29)-C(34)#1-172.2(5)
C(13)-C(14)-C(15)-C(16)176.0(5)	N(2)-C(28)-C(29)-C(34)#17.0(8)
C(23)-C(15)-C(16)-C(17)-31.3(7)	C(34)#1-C(29)-C(30)-C(31)-0.7(8)
C(14)-C(15)-C(16)-C(17)153.4(5)	C(28)-C(29)-C(30)-C(31)-178.7(5)
C(23)-C(15)-C(16)-C(26)-154.7(5)	C(29)-C(30)-C(31)-C(32) 0.7(9)
C(14)-C(15)-C(16)-C(26) 30.0(7)	C(30)-C(31)-C(32)-C(33) 0.7(8)
C(23)-C(15)-C(16)-C(25) 86.0(6)	C(34)-N(3)-C(33)-C(32) 178.5(5)
C(14)-C(15)-C(16)-C(25)-89.3(6)	C(34)-N(3)-C(33)-C(34)#1-1.4(8)
C(15)-C(16)-C(17)-C(18)-152.9(5)	C(31)-C(32)-C(33)-N(3) 177.9(5)

C(26)-C(16)-C(17)-C(18)-29.2(8)	C(31)-C(32)-C(33)-C(34)#1-2.2(8)
C(25)-C(16)-C(17)-C(18) 89.4(6)	C(33)-N(3)-C(34)-C(33)#11.4(8)
C(15)-C(16)-C(17)-C(22) 33.0(6)	C(33)-N(3)-C(34)-C(29)#1-177.9(5)

Symmetry transformations used to generate equivalent atoms:

#1 -x+1,-y+1,-z+1

Table 2-7. Hydrogen bonds for vb7519 [Å and °].

D-H...A	d(D-H)	d(H...A)	d(D...A)	<(DHA)
N(2)-H(2)...N(3)#1	0.88	2.00	2.716(6)	137.8
C(8)-H(8B)...O(3)	0.98	2.52	3.051(7)	113.9
C(9)-H(9B)...Cl(3)#2	0.98	2.92	3.833(7)	154.5
C(12)-H(12)...O(4)	0.95	2.35	2.878(7)	114.8
C(20)-H(20)...O(6)	0.95	2.29	2.890(7)	120.4
C(1S)-H(1S)...O(2)#1	1.00	2.50	3.315(7)	138.3
C(1S)-H(1S)...O(3)#1	1.00	2.63	3.364(7)	130.3
C(2S)-H(2S^a)...O(4)#3	1.00	2.30	2.946(8)	121.4

Symmetry transformations used to generate equivalent atoms:

#1 -x+1,-y+1,-z+1 #2 x,y,z+1 #3 -x+2,-y+1,-z+1

Projection view with 30% probability ellipsoids- solvent molecules omitted for clarity:

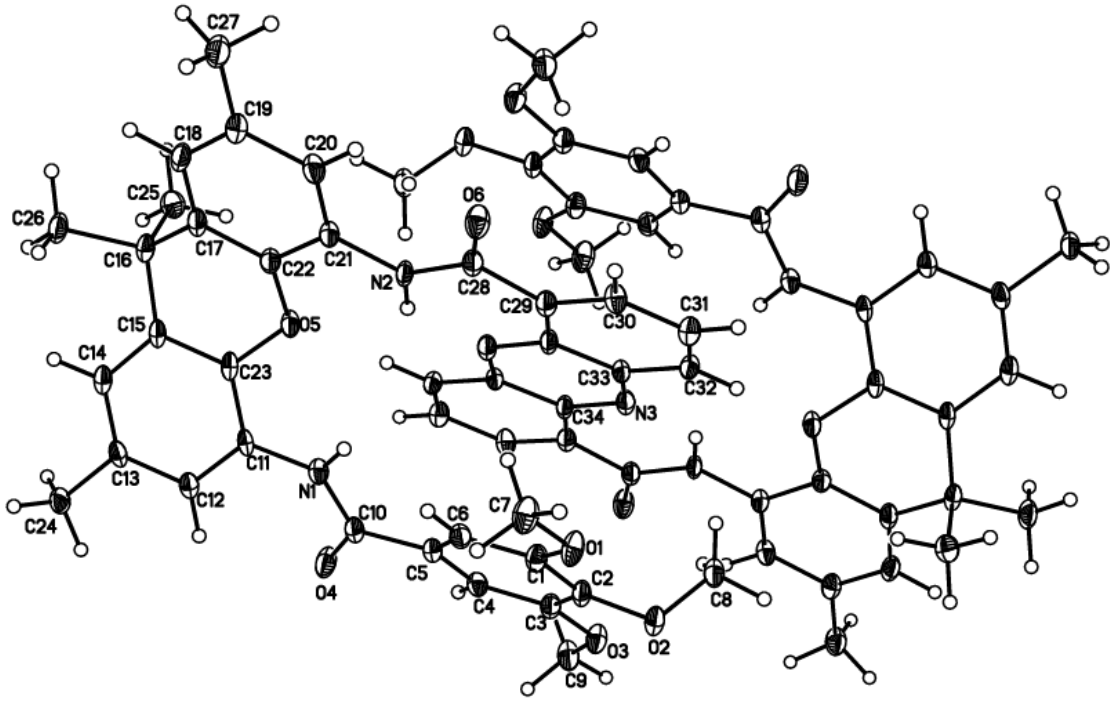

2.5. References

1. (a) Gellman, S. H., Foldamers: A Manifesto. *Acc. Chem. Res.* **1998,** *31*, 173-180. (b) Appella, D. H.; Christianson, L. A.; Klein, D. A.; Powell, D. R.; Huang, Xi.; Barchi, J. J.; Gellman, Samuel H. Residue-based control of helix shape in β-peptide oligomers. *Nature* **1997**, *387*, 381-384. (c)

2. Hill, D. J.; Mio, M. J.; Prince, R. B.; Hughes, T. S.; Moore, J. S., A Field Guide to Foldamers. *Chem. Rev.* **2001**, *101*, 3893-4011.

3. Yashima, E.; Maeda, K.; Iida, H.; Furusho, Y.; Nagai, K., Helical Polymers: Synthesis, Structures, and Functions. *Chem. Rev.* **2009,** *109*, 6102-6211. (c) Zhang, D.-W.; Zhao, X.; Hou, J.-L.; Li, Z.-T., Aromatic Amide Foldamers: Structures, Properties, and Functions. *Chem. Rev.* **2012,** *112*, 5271-5316.

4. Zhang, D.-W.; Zhao, X.; Hou, J.-L.; Li, Z.-T., Aromatic Amide Foldamers: Structures, Properties, and Functions. *Chem. Rev.* **2012,** *112*, 5271-5316.

5. Hamuro, Y.; Geib, S. J.; Hamilton, A. D. *Angew. Chem., Int. Ed. Engl.* **1994**, *33*, 446.

6. Prest. J. P.; Prince, R. B.; and Moore, J. S., Supramolecular Organization of Oligo(m-phenylene ethynylene)s in the Solid-State. *J. Am. Chem. Soc.* **1999**, *121*, 5933-5939.

7. Zhang, Z-X.; Moore, J. S.; Zang, L., Reversible Dispersion and Release of Carbon Nanotubes Using Foldable Oligomers. *J. Am. Chem. Soc.* **2010**, *132*, 14113-14117.

8. Berl, V.; Huc, I.; Khoury, R.; Lehn, J-M., Helical molecular programming. Folding of oligopyridine-dicarboxamides into molecular single helices, *Chem. Eur. J.* **2001**, *7*, 2798-2809.

9. Jiang, H.; Le ́ger, J-M., Huc, I., Aromatic δ-Peptides, *J. Am. Chem. Soc.* **2003**, *125*, 3448-3449.

10. Li, X.; Qi, T.; Srinivas, K.; Massip, S.; Maurizot, V.; Huc, I., Synthesis and multibromination of nanosized helical aromatic amide foldamers via segment-doubling condensation, *Org. Lett.* **2016**, *18*, 1044-1047.

11. Srinivas, K.; Huc, I., Remote substituent effects and regioselective enhancement of electrophilic substitutions in helical aromatic oligoamides. *J. Am. Chem. Soc.* **2008**, *130*, 13210-13211.

12. (a) Hua, J.; Huc, I., Switching of chiral induction in helical aromatic oligoamides using solid state− solution state equilibrium. *J. Am. Chem. Soc.* **2004**, *126*, 1034-1035. (b) Delsuc, N.; Kawanami, T.; Lefeuvre, J.; Shundo, A.; Ihara, H.; Takafuji, M.; Huc, I.; Kinetics of helix handedness inversion: folding and unfolding in aromatic amide oligomers, *ChemPhysChem*. **2008**, *9*, 1882-1890.

13. (a) Lautrette, G.; Kauffmann, B.; Ferrand, Y.; Aube, C.; Chandramouli, N.; Dubreuil, D.; Huc, I., Structure elucidation of host-guest complexes of tartaric and malic acids by quasi-racemic crystallography, *Angew. Chem. Int. Ed.* **2013**, *52*, 11517-11520. (b) Ziach, K.; Huc, I., Single helically folded aromatic oligoamides that mimic the charge surface of double-stranded B-DNA. *Nature Chemistry*, **2018**, *10*, 511-518.

14. Hou, J-L.; Li, Z-T., Hydrogen bonded oligohydrazide foldamers and their recognition for saccharides. *J. Am. Chem. Soc.* **2004**, *126*, 12386-12394.

15. Zhao, H-Q.; Zeng, H-Q., Chiral crystallization of aromatic helical foldamers via complementarities in shape and end functionalities. *Chem. Sci.* **2012**, *3*, 2042-2046.

16. (a) Jimenez, M. C.; Dietrich-Buchecker, C.; Sauvage, J.-P. Towards´ Synthetic Molecular Muscles: Contraction and Stretching of a Linear Rotaxane Dimer. *Angew. Chem., Int. Ed.* **2000**, *39*, 3284-3287. (b) Jimenez-Molero, M.; Dietrich-Buchecker, C.; Sauvage, J.-P. Chemically Induced Contraction and Stretching of a Linear Rotaxane Dimer. *Chem. Eur. J.* **2002**, *8*, 1456-1466. (c) Jimenez-Molero, M. C.; Dietrich-Buchecker, C.; Sauvage, J.-P. Towards Artificial Muscles at the Nanometric Level. *Chem. Commun.* **2003**, 1613-1616.

17 . Barboiu, M.; Lehn, J-M., Dynamic chemical devices: Modulation of contraction/extension molecular motion by coupled-ion binding/pH change-induced structural switching. *PNAS*, **2002**, *99*, 5201-5206.

18. Badjic, J. D.; Balzani, V.; Credi, A.; Silvi, S.; Stoddart, J. F. A´ Molecular Elevator. *Science*, **2004**, *303*, 1845-1849.

19. Tsuda, S.; Aso, Y.; Kaneda, T., Linear Oligomers Composed of a Photochromically Contractible and Extendable Janus [2]Rotaxane. *Chem. Commun.* **2006**, 3072-3074.

20. Li, S.; Taura, D.; Hashidzume, A.; Harada, A., Light-Switchable Janus [2]Rotaxanes Based on α-Cyclodextrin Derivatives Bearing Two Recognition Sites Linked with Oligo(Ethylene Glycol). *Chem. Asian. J.* **2010**, *5*, 2281-2289.

21. Bruns, C. J.; Stoddart, F., Rotaxane-Based Molecular Muscles. *Acc. Chem. Res.* **2014**, *47*, 2186-2199.

22. Greene, A. F.; Danielson, M. K.; Delawder, A. O.; Liles, K. P.; Li, X.; Natraj, A.; Wellen, A.; Barnes, J. C. Redox-Responsive Artificial Molecular Muscles: Reversible Radical Based Self-Assembly for Actuating Hydrogels. *Chem. Matter.* **2017**, *29*, 9498-9508.

23. Liles, K. P.; Greene, A. F.; Danielson, M. K.; Colley, N. D.; Wellen, A.; Fisher, J. M.; Barnes. J. C., *Macromol. Rapid Commun.* **2018**, *39*, 1700781.

24 . Nakahata, M.; Takashima, Y.; Hashidzume, A.; Harada, A. Redox-Generated Mechanical Motion of a Supramolecular Polymeric Actuator Based on Host–Guest Interactions. *Angew. Chem. Int. Ed.* **2013**, *52*, 5731-5735.

25. Herwig, J.; Bohnen, H.; Skutta, P.; Sturm, S.; Van Leeuwen, P. W. N. M.; Bronger, R. Novel diphosphines and a method for their production. WO2002068434A1, 2002.

26. For a general procedure, see: Komati, R.; Jursic, B. S., Ligand free open air copper (II) mediated aryl formamidation and amination of aryl halides. *Tetrahedron Lett.* **2014**, *55*, 1523-1527.

27. Gasparro, F. P.; Kolodny, N. H., NMR determination of the rotational barrier in N, N-dimethylacetamide. A physical chemistry experiment. *J. Chem. Educ.* **1977,** *54*, 258-261.

28. Holmes, R. J.; Abrahams, B. F.; Murray, V.; Denny, W. A.; McFadyen, W. D., A 2D hydrogen-bonded network constructed from large organic dications. *J. Mol. Struct.* **2010,** *975*, 186-189.

29. see experimental part.

30. (a) Becke, A. D., Density-functional thermochemistry. III. The role of exact exchange. *J. Chem. Phys.* **1993,** *98*, 5648-52. (b) Lee, C.; Yang, W.; Parr, R. G., Development of the Colle-Salvetti correlation-energy formula into a functional of the electron density. *Phys. Rev. B: Condens. Matter* **1988,** *37*, 785-789.

31. The lengths of tris-phenazine oligomer **2.19** and its reduced form **2.19-[H_2]** were 7.4 and 15.8 Å, respectively, as estimated by Molecular Mechanics (MMFF). The lengths of

tris-phenazine oligomer **2.46b** and its reduced form **2.48b** were 23.6 and 39.4 Å. See Supporting Information for details.

32. Yin, J.; Khalilov, A. N.; Muthupandi, P.; Ladd, R.; Birman, V. B., Phenazine-1,6-dicarboxamides: redox-responsive molecular switches. *J. Am. Chem. Soc.* **2020,** *142*, 60-63.

33. see experimental part.

34. For examples of *meso*-helical foldamers, see (a) Maurizot, V.; Dolain, C.; Leydet, Y.; Leger, J.-M.; Guionneau, P.; Huc, I., Design of an Inversion Center between Two Helical Segments. *J. Am. Chem. Soc.* **2004,** *126*, 10049-10052. (b) Hu, H.-Y.; Xiang, J.-F.; Chen, C.-F., Conformationally constrained aromatic oligoamide foldamers with supersecondary structure motifs. *Org. Biomol. Chem.* **2009,** *7*, 2534-2539. (c) Wechsel, R.; Raftery, J.; Cavagnat, D.; Guichard, G.; Clayden, J., The meso Helix: Symmetry and Symmetry-Breaking in Dynamic Oligourea Foldamers with Reversible Hydrogen-Bond Polarity. *Angew. Chem., Int. Ed.* **2016,** *55*, 9657-9661

35. Helal, A.; Nguyen, H. L.; Al-Ahmed, A.; Cordova, K. E.; Yamani, Z. H., An Ultrasensitive and Selective Metal-Organic Framework Chemosensor for Palladium Detection in Water. *Inorg. Chem.* **2019,** *58*, 1738-1741.

Chapter 3: Second generation of phenazine-based interleafed foldamers as redox-responsive molecular muscles

3.1 Design and synthesis of the second generation of phenazine based interleafed foldamer

We have presented our first generation of phenazine based interleafed foldamers in Chapter 2 (Figure 3-1). It behaved as intended as a redox responsive molecular actuator with high efficiency. However, from the point of view of a synthetic chemist, its synthesis was not straightforward. With this in mind, we sought to come up with a streamlined design of a phenazine based interleafed foldamer that would behave the same way, but be easier to synthesize (Figure 3-2).

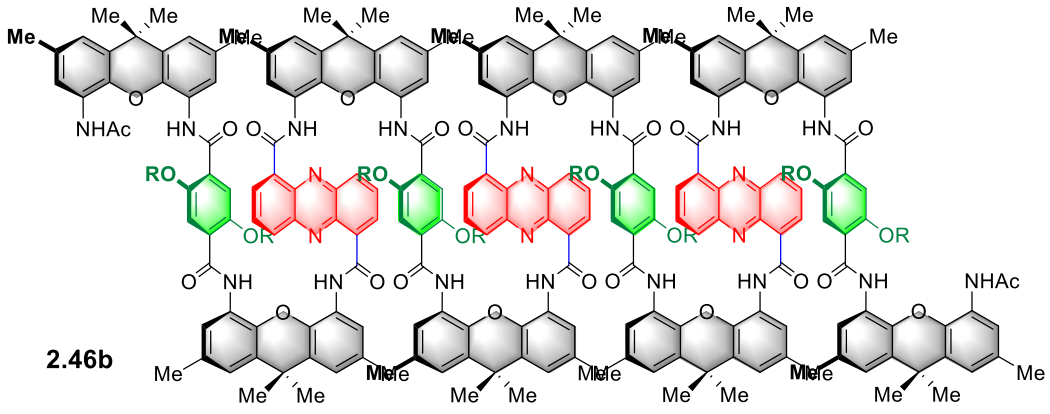

Figure 3-1. First generation of phenazine based interleafed foldamer.

In foldamer **2.46b**, the butterfly coil was composed of S-shaped phenazine units and Z-shaped linkers composed of two xanthenes linked by a terephthalamide moiety. With the assistance of computational modeling, we should be able to find other linker that has similar Z-shaped geometry. Indeed, 2,4-diphenylthiazole-based linker in **3.01** adopts a Z-shaped geometry with two amino groups almost parallel to each other. This linker requires shorter synthetic route, and has four alkyl groups to increase its solubility. To our knowledge, diarylazole derivatives in foldamer design have not been reported before.[1]

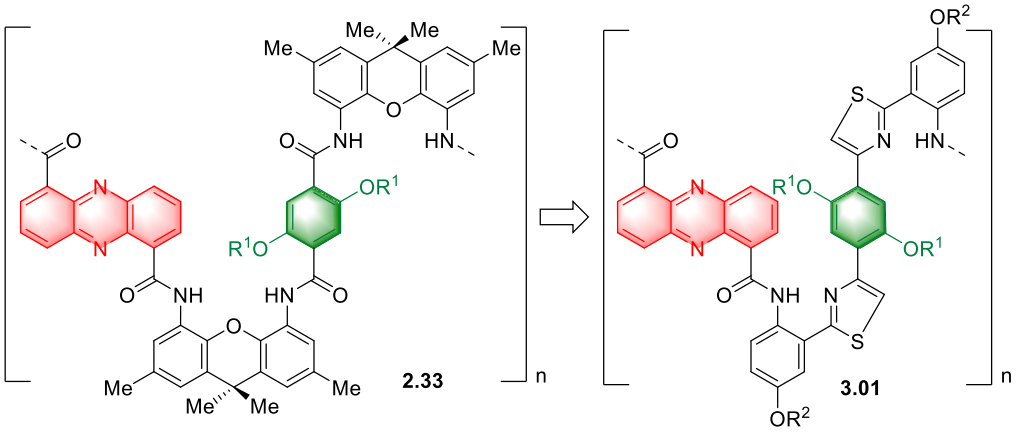

Figure 3-2. Stream-lined design with a bis-thiazole Z-shaped linkers.

A convergent strategy was employed in the synthesis of linker **3.13**, which relied on Hantzsch thiazole synthesis[2] between **3.06** and **3.11**. Some details regarding the synthesis of these building blocks are discussed below. Synthesis of thioamide **3.06** started from the known ester **3.02**. Like in other Williamson ether syntheses in Chapter 2, ground Cs_2CO_3 worked best. Vigorous stirring was also necessary to secure consistent quantitative yields. Base hydrolysis of **3.03** only gave 20% of **3.04.** Fortunately, lithium iodide removed the methyl ester to give acid **3.04** in 91% yield. To remove the methylpyridinium iodide formed as a by-product, it is advisable to wash the post workup mixture with 3M HCl 5 times until the aqueous layer becomes colorless.

Conversion of **3.04** to acyl imidazolide followed by addition of ammonia hydroxide gave **3.05** in 90% yield. Its conversion to the desired thioamide 3.06 was carried out with Lawesson's reagent in 80% yield. The other coupling partner, bis-chloroketone **3.11,** can be synthesized from **3.07** in three steps. Etherification of **3.08** required nitrogen protection to obtain high yields. In fact, when dealing with scale larger than 10 mmol, it is recommended to cool the ethanolic solution of **3.07** and isoamyl bromide to −78 ℃ and degas it three times under vacuum before introducing NaOH. Incomplete removal of air will result in a dark solution and a diminished yield. The bromination of **3.08** was relatively straightforward. Aqueous saturated Na_2SO_3 was used to remove excess bromine. The crude **3.09** can be further purified via recrystallization in hexane to result a pristine white powder. In the following step, **3.09** was lithiated twice to give **3.09-Li**. If Weinreb amide **3.10** was added to **3.09-Li** directly, only 17% yield of **3.11** was obtained. It was surmised that **3.09-Li** was so basic that it deprotonated the Weinreb amide. We reasoned that switching from lithium to magnesium and reversing the order of addition would solve this problem. Therefore, $MgBr_2 \cdot Et_2O$ was prepared by dissolving magnesium strip in 1,2-dibromoethane in ether.[3] After generating **3.09-Li**, eight equivalents of $MgBr_2 \cdot Et_2O$ was added at −78 ℃. White precipitation was formed instantly. After stirring for 30 min, **3.09-Mg** was cannulated to **3.10** at −40 ℃ over the course of 30 min. Upon complete addition, the mixture was allowed to warm up to room temperature over the course of 4 h. The desired **3.11** was obtained in 78% yield on a 10 mmol scale. Refluxing **3.06** and **3.11** in ethanol produced hand, bis-thiazole **3.12** in 80% yield. Its reduction to the diamine linker **3.13,** however, proved tricky. When **3.12** was hydrogenated by Pd/C under the same conditions as **1.12** in Chapter 1, no reaction occurred. We surmised that sulfurous impurities in **3.11,** evident by their foul smell but invisible by NMR or TLC, poisoned the palladium catalyst. Therefore, Raney nickel was used to the reduction of the nitro groups to

give **3.13** in an excellent yield as a bright yellow odorless solid after chromatography. It is advisable to store **3.13** under nitrogen. It's also worth mentioning that **it** has good solubility in acetone, ethyl acetate, dichloromethane, chloroform, dimethylformamide, and moderate solubility in hexane.

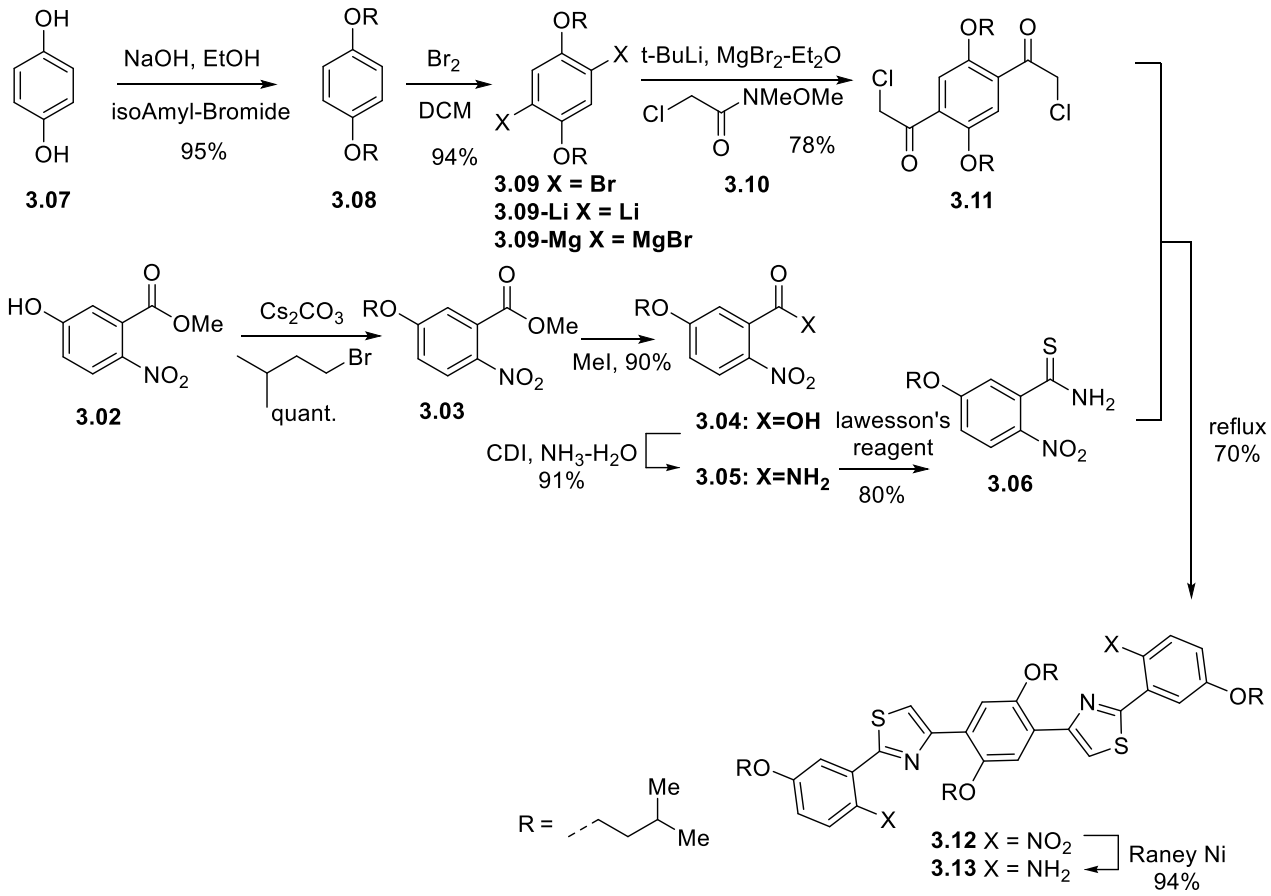

Figure 3-3. Synthesis of Z-shaped linker **3.13**.

With **3.13** in hand, we explored its reaction towards **1.19**. Interestingly, two macrocycles were obtained with a 2.3:1 ratio in a high yield after chromatography. No oligomer or other side product was detected. Both macrocycles exhibited good solubility in organic solvents like dichloromethane, chloroform, acetone and dimethylformamide. However, they were still not soluble in acetonitrile or methanol. ^{1}H NMR and 2D NMR studies were carried out to determine

their conformation. Structure of **3.14a** and **3.14b** were assigned based on differences in nOe effects. DFT calculations in gas phase indicated that **3.14b is** favored over **3.14a** by 5 kCal/mol.

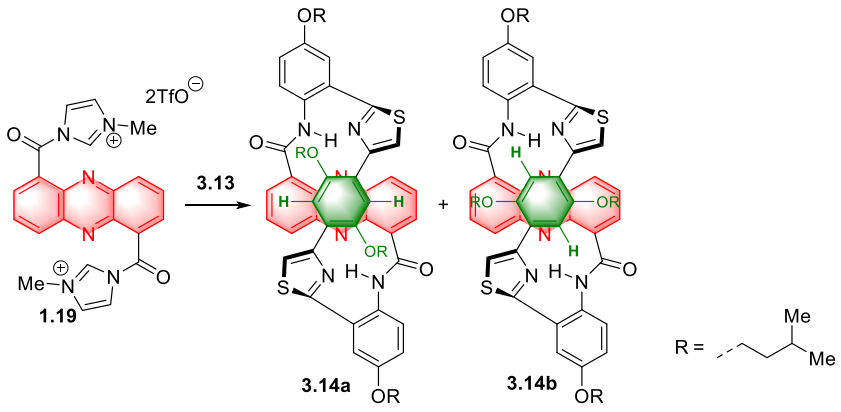

Figure 3-4. Synthesis of macrocycle **3.14.**

To avoid macrocyclization, protection/deprotection strategy was used again. Di-tert-butyl dicarbonate was our first choice. The reaction between **3.13** and Boc_2O did not proceed at all at room temperature, but at 60 ℃ gave a nearly statistical mixture of the mono- (**3.15**) and bis-protected (**3.16**) products along with the unreacted starting material **3.13**. Fortunately, all three compounds could be separated by chromatography and the bis-protected **3.16** was recycled by treating it with 50% TFA in CH_2Cl_2. It should be noted that **3.13** was not stable under strongly acidic conditions, therefore it is recommended to keep acid exposure within 30 min.

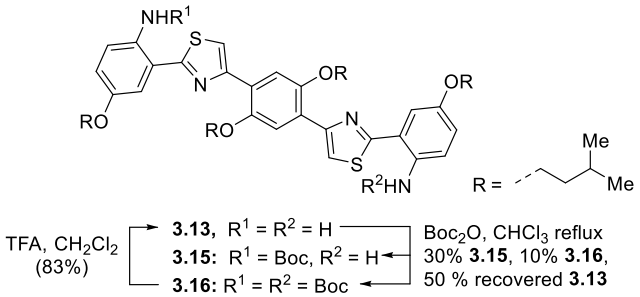

Figure 3-5. Protection of **3.13**.

The protected linker **3.15** was then reacted with **1.19** at reflux to deliver **3.16** in 90% yield. Treatment with 50% TFA in CH_2Cl_2 resulted in **3.17** in 95% yield. When **3.17** was treated with excess of **1.19** at 120 ℃, polymerization was observed. According to MALDI analysis, this mixture contained oligomers up to 9 phenazines. However, the mixture could not be separated by chromatography or GPC. Therefore, we decided to obtain specific oligomers via a protection group controlled synthesis. Boc-protection of **3.17** was achieved at 110 ℃ in 1,4-dioxane overnight. Mono protected **3.18** was isolated via chromatography in 35% yield with 60% recovery of **3.17**, which amounts to 88% yield based on recovered starting material. Reaction between **3.18** and **1.19** was smooth at high temperature in a sealed tube. The resulting **3.19** can be purified via chromatography with 80% isolated yield. A brief treatment of **3.19** with 50% TFA in CH_2Cl_2 gave **3.20** in quantitative yield. Unfortunately, although **3.20** was essentially pure by ^{1}H NMR, its complete purification via chromatography was very difficult. Therefore, the crude **3.20** was used as is in the next step. A mixture of **3.20** and **1.19** was heated to 120 ℃ in a sealed tube overnight and quenched with excess Ac_2O. The resulting mixture was purified via Gel permeation chromatography to give **3.20** in 14% yield.

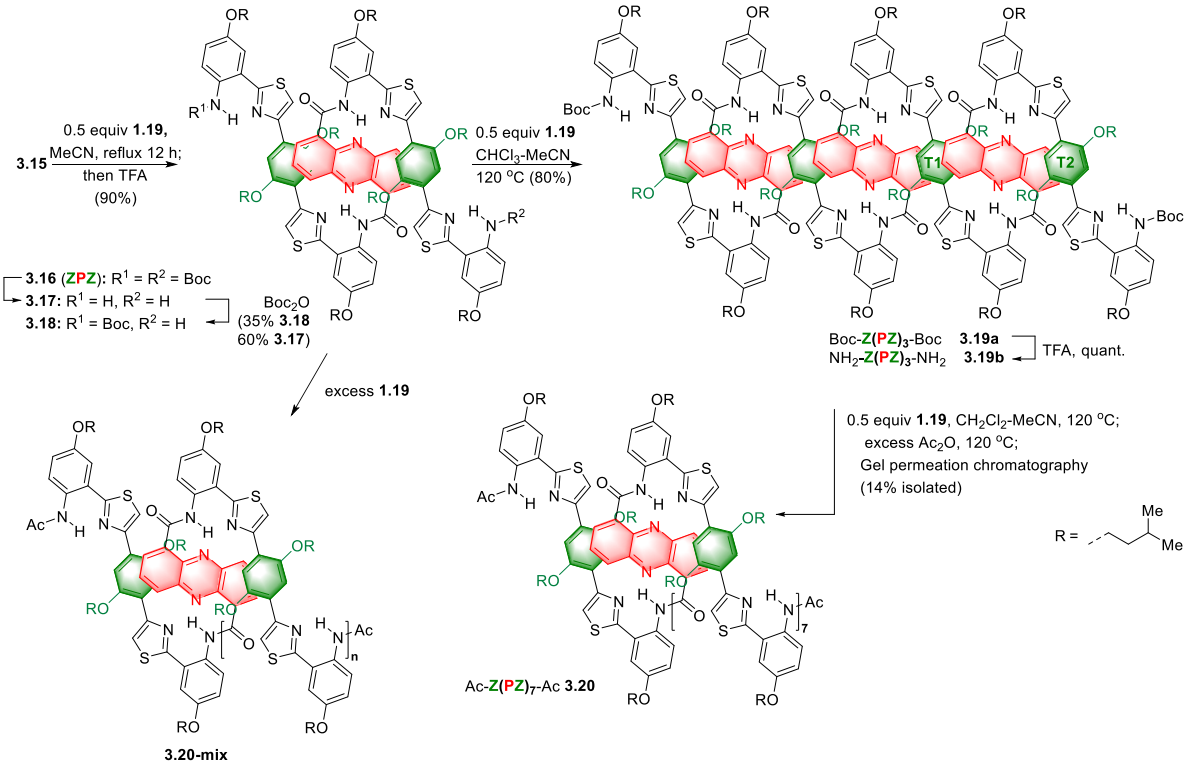

Figure 3-6. Synthesis of **3.20**.

By analogy with the 1st-generation oligomers such as **2.46b** discussed in Chapter 2, shielding effects were also evident in the 2,5-dialkoxy-p-phenylene groups present in the new series of foldamers and macrocycles (Figure 3-7). Both the aromatic protons and the α-protons on the isoamyl side chains were shifted upfield significantly compared to the parent compound **3.13** (ca. 6 ppm vs 7.23 ppm, ca.3 ppm vs 4 ppm). The aromatic protons in **3.14a** were shifted upfield slightly more than those in **3.14b** (6.51 ppm vs 6.64 ppm), while shielding effects on α-protons were reversed (3 ppm/3.3 ppm in **3.14a** vs 2.9 ppm/3.4 ppm in **3.14b**). Such subtle differences can be explained based on the relative orientation of the 2,5-dialkoxy-p-phenylene and the phenazine rings (Figure 3.4). For **3.19a** and **3.20**, the *ortho*-protons in the 'inner' 2,5-dialkoxy-p-phenylene groups T_1 displayed larger shielding effects than the 'outer' protons, due to shielding from two phenazine rings. In heptamer **3.20,** the aromatic and α-protons on the "inner" 2,5-dialkoxy-p-

phenylene groups were not resolved, but presented themselves together as broad peaks at 5.83 and 2.23 ppm, respectively. Overall, these observations were fully consistent with the expected folded structures of oligomers **3.19** and **3.20**.

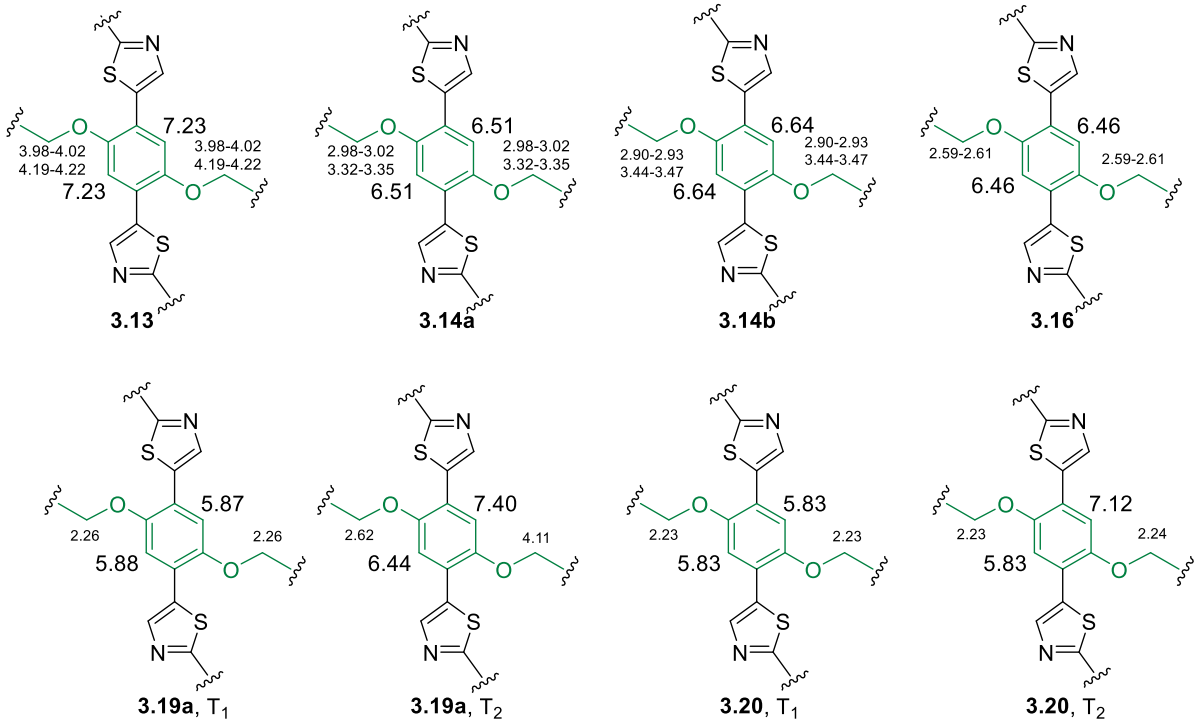

Figure 3-7. Shielding effects.

Next, we studied the chemical redox on **3.19a** and **3.20**. Like other oligomers in Chapter 2, reduction was achieved over Pd/C in a valved NMR tube. In both cases, complete conversion towards dihydrophenazine was observed. It is impressive that heterogeneous catalyst Pd/C was still very effective in the reduction of **3.19a** or **3.20,** which took only 3 hours, similar to other oligomers in Chapter 2. Aero oxidation was enough to revert them back to phenazine. Reduction and oxidation was repeated on **3.19a** for three times and on **3.20** for 10 times. No side-product or decay in catalytic activity was observed.

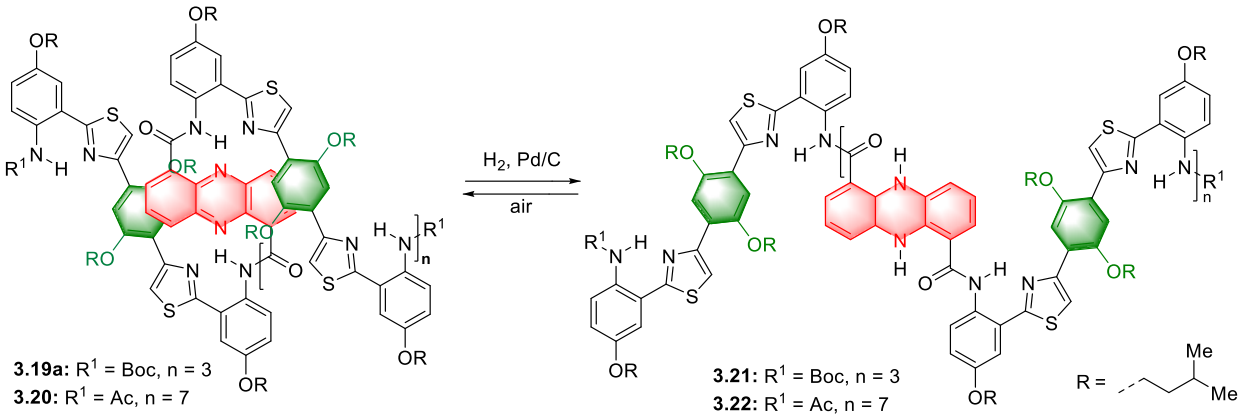
H2, Pd/C
air
3.19a: R1 = Boc, n = 3
3.20: R1 = Ac, n = 7
3.21: R1 = Boc, n = 3
3.22: R1 = Ac, n = 7
R =
Me
Me

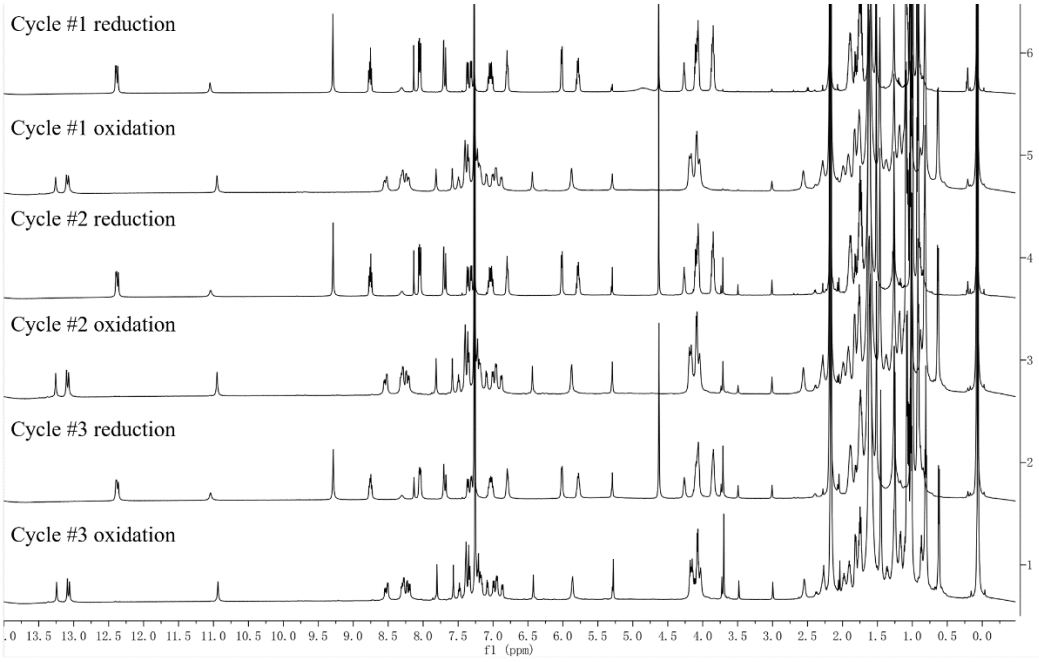
Cycle #1 reduction
Cycle #1 oxidation
Cycle #2 reduction
Cycle #2 oxidation
Cycle #3 reduction
Cycle #3 oxidation
f1 (ppm)

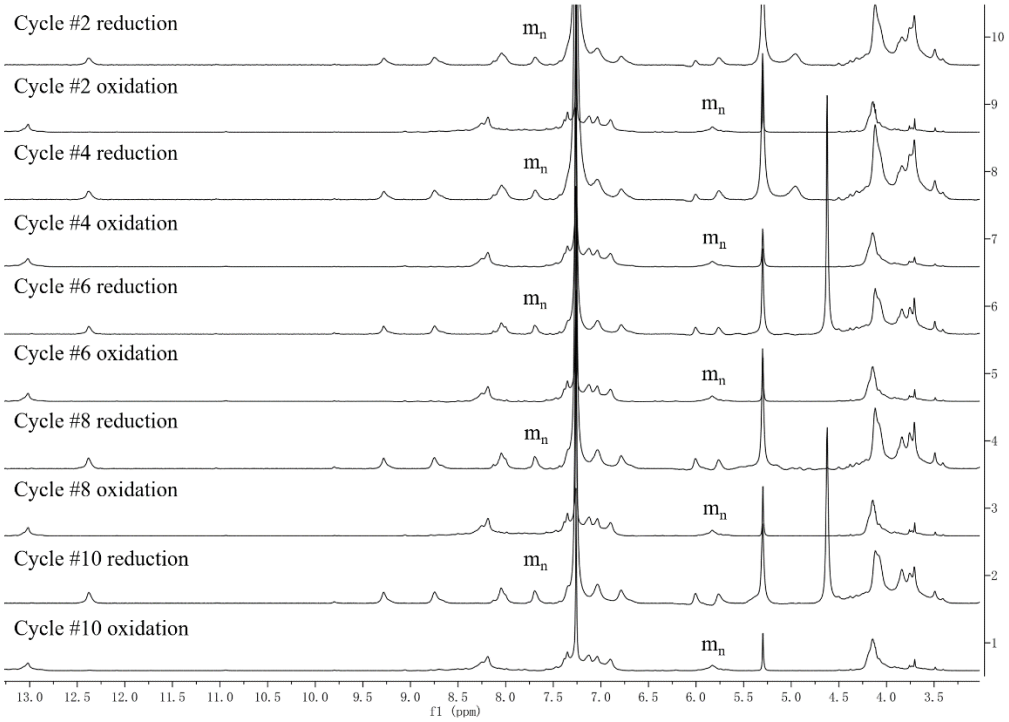

Figure 3-8. Chemical reduction on oligomer **3.19a** and **3.20**.

Electrochemical redox was also explored on **3.19a**. The reduction was done in a divided cell with tetrabutylammonium tetrafluoroborate as electrolyte. N_2H_4-H_2O was also presented on each side of the cell as sacrificial reductant. In the first around (Figure 3-9 (a)), **3.19a** was completely reduced in cell A while remained intact in cell B. When the current was reversed with exactly same amount of charge passing through the cell (Figure 3-9 (a)), **3.19a** in cell B was reduced in the meanwhile, **3.21** in cell A was oxidized cleanly. Such reversible process demonstrated its capability was chemical/electrochemical redox responsive molecular actuators.

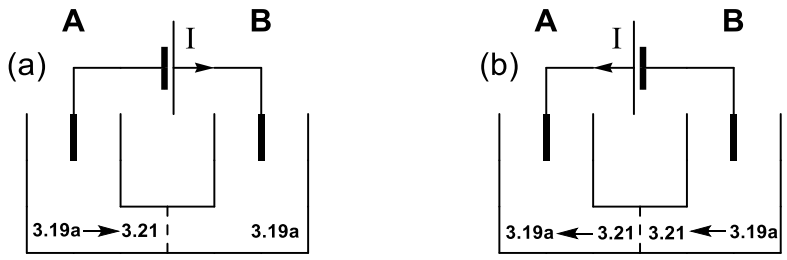

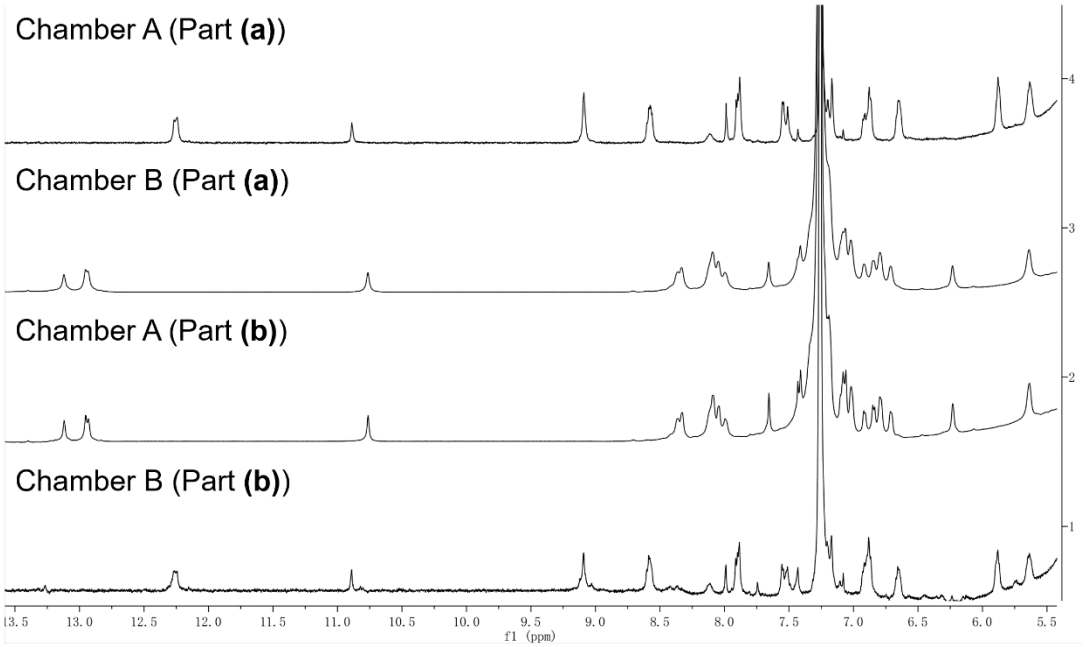

Figure 3-9. Bulk electrolysis of **3.19a**.

We used computational modeling of our oligomers for their confirmation and sizes. Diffusion NMR (DOSY) was also utilized to assist size estimation.[4] According to DOSY, macrocycle **3.14a** and **3.14b** have exactly the same size of 1.1 nm, comparable to our calculation (see Experimental part 3.3.7). Oligomer **3.19a** has been studied as well and was estimated to be 2 nm in hydrodynamic radius, which was also comparable to our model. More interestingly, relative elongation of **3.19a** and **3.20** upon reduction was also estimated by DOSY to be ca. 50% and 30%, also similar to our computational studies.

3.2 Conclusion

In Chapters 1-3, we have described our efforts towards a novel class of foldamers that function as redox-responsive molecular actuators. We started with the de novo design of

phenazine-1,6-dicarboxyamides as redox responsive molecular switches. In Chapter 2, we incorporated this molecular switch into our first generation interleafed phenazine based foldamer **2.46b**. In Chapter 3, we have presented our second-generation design of this new class of foldamers. It represents a major improvement in terms of synthesis, being scalable and highly convergent. This new Z-shaped linker **3.15** has enabled us to access longer oligomers directly or via a step-growth polymerization. Good solubility of all **3.15**-based macrocycles and foldamers obtained so far bodes well for their further study and future applications. Second generation oligomers **3.19a** and **3.20** have demonstrated excellent stability in chemical or electrochemical redox cycling. Computer modeling supported by DOSY studies estimate the maximum relative elongation of these foldamers at ca. 40-50%. Although it may seem modest, it is on par with the many rotaxane-based designs explored by other groups.[5]

Where do we go from here? There is always room for improvement in the basic design of our foldamer backbone. To this end, my lab mate Ruth Son has developed a dibenzofuran linker that gives better elongation upon reduction.

What we presented here is just the beginning of our effort towards molecular muscles and engines. Our ultimate goal is to develop a soft material that would extend and contract in response to electric current. We need to self-assemble our foldamers into an ordered state in hydrogel. This could be accomplished by attaching foldamers end-to-end and side-to-side.

End-to-end linkage could be achieved by a metal chelated junction shown in Figure 3-21. Chelation ligand such as **3.22** can be attached to the end of our oligomer **3.19b** via amide bonds. Upon chelation to metal ions such as Copper, 8-hydroxyquinoline rings are expected to overlap with the adjacent aryl groups, giving a butterfly-coiled polymer. Additional chelation groups such as N-hydroxy-2-pyridone, 3-hydroxy-4-pyridone and metals ions also need to be explored.

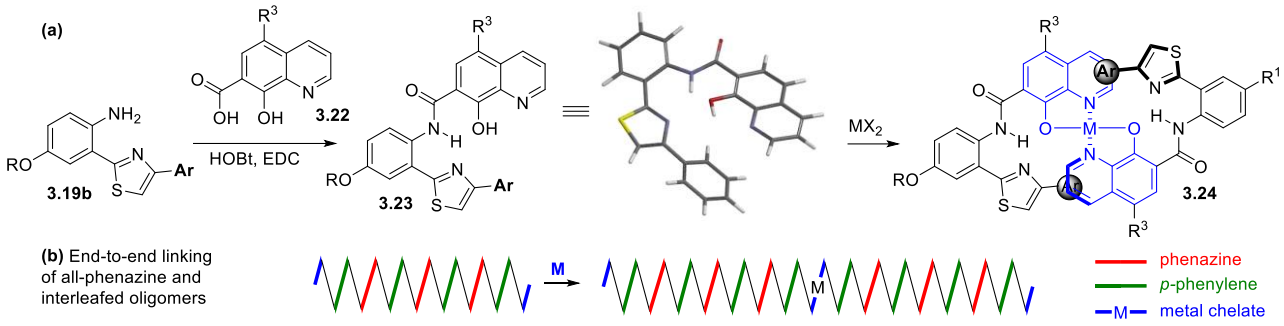

Figure 3-10. Metal chelation junction.

Side-by-side interactions can be promoted by linking the side chain on oligomers. We could use side chains with terminal double bond. The dihydroxylation on such double bond would create diols that could be linked via boron bridge.

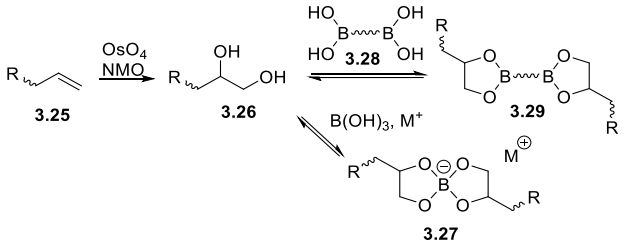

Figure 3.11. Potential side chain linkage.

Some alternative strategies for achieving alignment of oligomers involve the use self-complimentary hydrogen bonding arrays, such as SCUBAs (Self-Complementary Urea-Based Arrays) currently explored by my lab mate Ruth Son.

Besides efforts towards bulk materials, there are also many other interesting directions worth pursuing. Future researchers could explore the rate of the switching of our molecular switch via cyclic voltammetry. It would be interesting to measure the relative elongation of this redox

process by attaching florescent groups at the terminal. The force and work throughout this redox process is also very interesting and should not be neglected.

3.3 Experimental

3.3.1. General

All reagents were obtained commercially and used as received unless specified otherwise. All reactions were carried out under argon, unless noted otherwise. Hydrogenations were carried out by first charging the reaction vessel with solid starting materials and palladium catalyst, then purging with argon, then adding the reaction solvents, and finally purging the vessel with hydrogen. ***Note:*** *mixtures of organic vapors or hydrogen with air have been observed to ignite spontaneously*

upon contact with an active palladium catalyst. Solvents used for chromatography were ACS or HPLC grade. Reactions were monitored by thin layer chromatography (TLC) and by 1H NMR. Uniplate HLF (250 μm) silica gel plates were used for TLC analyses. Flash column chromatography was performed over Sorbent Technologies silica gel (40-63 mm). ^{1}H, ^{13}C and ^{19}F NMR spectra were recorded on a Mercury 300 MHz spectrometer and DD2 500 MHz and 600 MHz Agilent spectrometers. The chemical shifts are reported as δvalues (ppm) relative to TMS using the residual $CHCl_3$ peak (7.26 ppm) as the reference. Melting points were measured on a Stuart SMP10 melting point apparatus. High-Resolution mass spectral analyses were performed at Washington University MS Center on a Bruker MaXis QTOF mass spectrometer using Electrospray Ionization (ESI) and Atmospheric Pressure Chemical Ionization (APCI) methods. Infrared spectrums were recorded on a Bruker Alpha Platinum-ATR spectrophotometer. Preparative gel permeation chromatography (GPC) analyses were performed on Japan Analytical Industry LaboACE instrument with one JAIGEL2HR column and one JAIGEL-2.5HR column in tandem, running with chloroform ($CHCl_3$) at 10 mL/min. To conduct the electrochemical reactions, a preparative reaction setup from Electrolytica was used. The equipment is comprised of an AC/DC converter (model 420A), a digital coulometer (model 640), a potentio/galvanostatic controller, and an ammeter. All the electrochemical reactions conducted in this paper were run under constant current conditions. Cyclic voltammetry apparatus was based on BAS100W application. Matrix assisted laser desorption/ionization time-of-flight mass spectrometry (MALDI-TOF-MS) was recorded on a Bruker Solaris 12T FT-MS; samples were prepared using 2,5-dihydroxybenzoic acid, 3,5-dimethoxy-4-hydroxyciinamic acid or α-Cyano-4-hydroxycinnamic acid matrices.

3.3.2. Synthesis of Linker 3.13 and its derivatives

3.3.2a. Preparation of Bis-chloroketone 3.11.

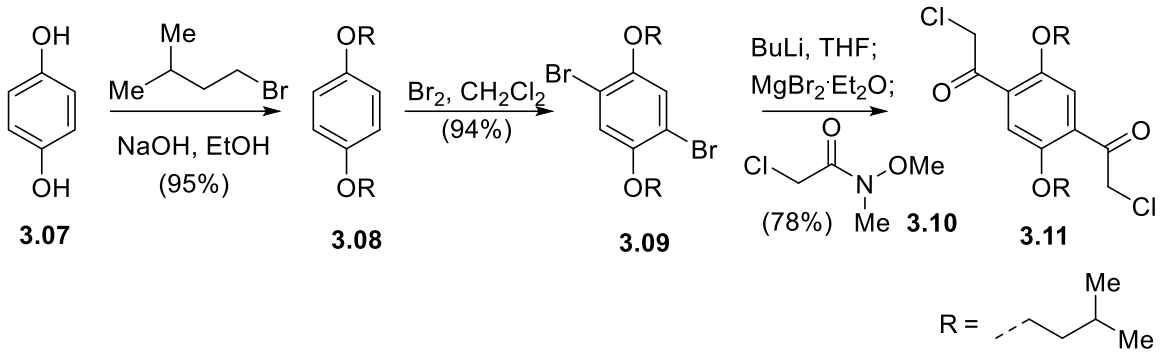

1,4-Di(isoamyloxy)benzene 3.08. A 250 mL flask equipped with a stir bar and an addition funnel was purged with nitrogen and charged with hydroquinone (4.4 g, 40 mmol) and NaOH (4 g, 100 mmol). Ethanol (100 mL) was added via syringe. The mixture was degassed three times using the freeze-pump-thaw technique and brought to reflux. Isoamyl bromide (12 mL, 100 mmol) was added dropwise over 2 h. Reflux was continued overnight at which point TLC indicated completion. The mixture was cooled to rt and concentrated via rotary evaporation. The residue was partitioned between 200 mL of water and 200 mL of hexanes. The aqueous layer was extracted with hexanes 3 times. The combined organic phase was washed with saturated aqueous K_2CO_3, dried over $NaSO_4$ and concentrated. The resulting solid was recrystallized from hexanes to afford the product as white cubic crystals (9.5 g, 95 % yield). **^{1}H NMR** (600 MHz, $CDCl_3$) δ 6.82 (s, 4H), 3.94 - 3.92 (t, 4H), 1.85 - 1.80 (m, 2H), 1.67 - 1.64 (m 4H), 0.96 - 0.95 (d, J = 6 Hz, 6H). **^{13}C NMR** (151 MHz, $CDCl_3$) δ 153.18, 115.36, 67.00, 38.14, 25.05, 22.61. **IR** (cm^{-1}).2952.0, 2927.5, 2867.7, 1506.1, 1473.5, 1390.0, 1221.4, 821.0, 740.0. **m. p.** 65 ℃. **MS**: HR-ESI calculated for [$C_{16}H_{26}O_2$ + H^+]: 251.2011, found 251.2003.

1,4-Dibromo-2,5-di(isoamyloxy)benzene 3.09. A solution of **3.08** (7.5 g, 30 mmol) in 100 mL of DCM was cooled to 0 ℃ and treated with bromine (3.4 mL ,66 mmol) added slowly with

magnetic stirring. After stirring for 2 h, the reaction mixture was washed with 50 mL of saturated Na_2SO_3, then 100 mL of 1M NaOH, dried over Na_2SO_4, and rotary evaporated. The residue was recrystallized from hexanes to yield white crystals. (11.5 g, 94% yield). **^{1}H NMR** (600 MHz, $CDCl_3$) δ 7.09 (s, 2H), 3.99 - 3.96 (t, J = 9 Hz, 4H), 1.90 - 1.85 (m, 2H), 1.72 - 1.68 (m, 4H), 0.98 - 0.96 (d, 6H). **^{13}C NMR** (151 MHz, $CDCl_3$) δ 150.06, 118.36, 111.07, 68.68, 37.82, 25.02, 22.57. **IR** (cm $^{-1}$). 2953.4, 2869.6, 2360.2, 1498.0, 1366.8, 1213.9, 1065.8, 843.1. **m. p.** 132 ℃. **MS**: HR-ESI calculated for [$C_{16}H_{24}Br_2O_2 + H^+$]: 407.0221, found 407.0230.

1,4-Di(chloroacetyl)-2,5-di(isoamyloxy)benzene 3.09. A solution of **3.08** (4.08 g, 10 mmol) in 70 mL of dry THF was cooled to −78 °C and treated with *t*-BuLi in pentane (33 mL, 1.2 M, 40 mmol) added dropwise. The mixture turned yellow instantly and was kept at −78 °C for 2 h. A solution of $MgBr_2$ in Et_2O[6] (1.16 M, 45 mmol) was added at the same temperature. The color disappeared and white precipitation was observed. After another 2 h, the suspension was transferred at a moderate speed via a polyethylene cannula to a stirring solution of Weinreb amide **3.10**[7] (6.87g, 50 mmol) in 40 mL THF at −40 °C. Upon completion of the cannulation, the mixture was allowed to slowly warm up to rt and stirred for additional 4 h, then quenched with 1M HCl, diluted with EtOAc, dried over Na_2SO_4 and rotary evaporated to dryness. Recrystallization from methanol gave a yellow solid (3.4 g 403.34, 78% yield). **^{1}H NMR** (600 MHz, $CDCl_3$) δ 7.45 (s, 2H), 4.77 (s, 4H), 4.15 - 4.10 (t, J = 15 Hz, 4H), 1.83 - 1.72 (m, 6H), 1.00 - 0.98 (d, J = 6 Hz, 12H). **^{13}C NMR** (151 MHz, $CDCl_3$) δ 192.08, 152.05, 129.05, 114.73, 114.73, 77.42, 77.00, 76.57, 68.05, 50.70, 37.82, 25.26, 22.54. **IR** (cm $^{-1}$). 3341.3, 2958.8, 2359.6, 1653.8, 1382.2, 1213.7, 1005.7, 715.1. **m. p.** 152 ℃. **MS**: HR-ESI calculated for [$C_{20}H_{28}Cl_2O_4 + H^+$]: 403.1442, found 403.1437.

3.3.2b. Preparation of Thioamide 7.

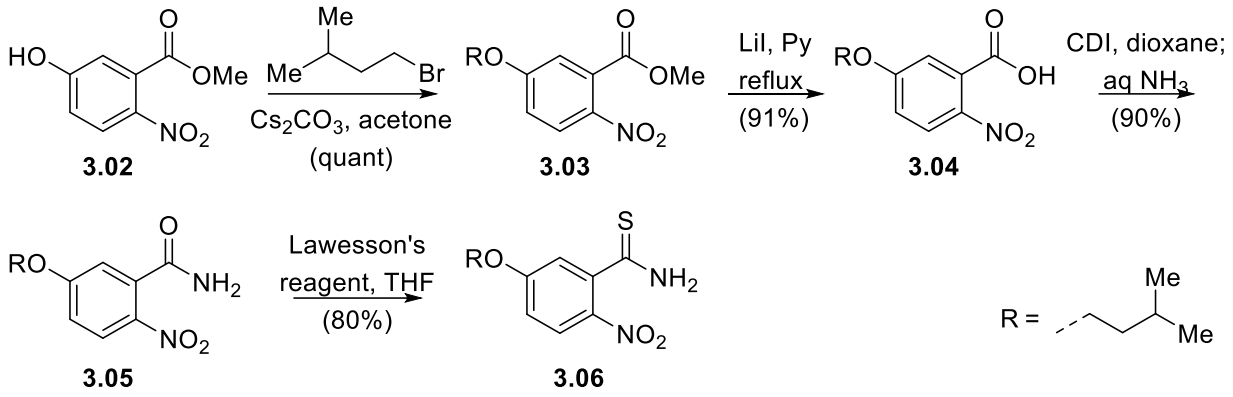

Methyl 5-isoamyloxy-2-nitrobenzoate 3.03. A mixture of methyl 5-hydroxy-2-nitrobenzoate **3.02**[8] (9.86 g, 50 mmol), isoamyl bromide (7.2 mL, 60 mmol), and Cs_2CO_3 (19.5 g, 60 mmol) in 100 mL of acetone was refluxed overnight, filtered, diluted with ethyl acetate, washed with saturated aqueous K_2CO_3, dried over Na_2SO_4, rotary evaporated to dryness, and purified via recrystallization from Et_2O. The product was a yellow solid (13.4 g, >99% yield). **^{1}H NMR** (600 MHz, $CDCl_3$) δ 8.04 - 8.02 (d, J = 12 Hz, 1H), 7.03 (d, J = 6 Hz, 1H) 7.01 - 6.99 (dd, J_1 = 12 Hz, J_2 = 6 Hz, 1H), 4.09 - 4.07 (t, J = 6 Hz, 2H), 3.93 (s, 3H), 1.84 - 1.80 (m, 1H), 1.73 - 1.69 (m, 2H), 0.97 - 0.96 (d, J = 6 Hz, 6H). **^{13}C NMR** (151 MHz, $CDCl_3$) δ 166.56, 162.96, 139.56, 131.12, 126.58, 115.95, 114.38, 67.56, 53.69, 53.21, 37.39, 24.85, 22.35. **IR** (cm^{-1}) 3356.0, 2360.8, 1710.6, 1583.3, 1518.3, 1438.3, 1315.9, 1062.6, 876.3. **m. p.** 75 ℃. **MS**: HR-ESI calculated for [$C_{13}H_{17}NO_5 + H^+$]: 268.1185, found 268.1181.

5-Isoamyloxy-2-nitrobenzoic acid 3.04. A mixture of **3.03** (5.34 g, 20 mmol) and lithium iodide (7.98 g, 60 mmol) in 100 mL pyridine was heated to reflux for 3 h and evaporated to dryness and diluted with EtOAc. The solution was washed with 3M HCl, dried over Na_2SO_4 and rotary evaporated. The residue was recrystallized from acetone to give the product as a white solid (4.61 g, 91% yield). **^{1}H NMR** (500 MHz, $CDCl_3$) δ 11.37 (br, 1H), 8.01 - 7.99 (d, J = 10 Hz, 1H), 7.18 - 7.17 (d, J = 5 Hz, 1H), 7.06 - 7.03 (dd, J_1 = 5 Hz, J_2 = 10 Hz, 1H), 4.12 - 4.11 (t, J = 2.5 Hz, 3H),

4.09 (s, 3H), 1.85 - 1.81 (m, 1H), 1.74 - 1.70 (m, 2H), 0.98 - 0.96 (d, *J* = 5 Hz, 6H). **^{13}C NMR** (126 MHz, $CDCl_3$) δ 171.48, 162.86, 139.92, 129.76, 126.64, 116.71, 114.76, 67.75, 37.45, 24.92, 22.42. **IR** (cm $^{-1}$).2956.6, 2361.0, 1734.7, 1583.7, 1518.5, 1341.1, 1247.4, 1065.8, 756.2. **m. p.** 195 ℃. **MS**: HR-ESI calculated for [$C_{12}H_{15}NO_5$ + H^+]: 254.1028, found 254.1032.

5-Isoamyloxy-2-nitrobenzamide 3.05. A solution of **3.04** (2.53 g, 10 mmol) and 1,1'-carbonyldiimidazole (1.78 g, 11 mmol) in 100 mL of 1,4-dioxane was stirred at rt for 2 h, cooled to 0 ℃, and treated with ammonia hydroxide (2 mL, 14.8 M solution, 29.6 mmol) added dropwise. The mixture was heated to reflux for 1 h, cooled to rt, rotary evaporated to dryness and the residue redissolved in EtOAc. The solution was washed with 1 M HCl, dried over Na_2SO_4 and rotary evaporated. The resulting solid was recrystallized from acetone to give the product as white crystals (2.27 g, 90% yield). **^{1}H NMR** (500 MHz, $CDCl_3$) δ 8.04 - 8.02 (d, *J* = 10 Hz, 1H), 7.03 - 7.02 (d, *J* = 5 Hz, 1H), 7.01 - 6.99 (dd, J_1 = 10 Hz, J_2 = 5 Hz, 1H), 4.09 - 4.07 (t, *J* = 5 Hz, 2H), 3.93 (s, 1H) 1.85 - 1.80 (m, 1H), 1.73 - 1.69 (dd, *J* = 5 Hz, 2H), 0.97 - 0.96 (d, *J* = 5 Hz, 6H). **^{13}C NMR** (126 MHz, $CDCl_3$) δ 166.68, 163.01, 139.69, 131.23, 126.67, 116.08, 114.39, 67.63, 53.34, 37.48, 24.94, 22.45. **IR** (cm $^{-1}$)2956.1, 2360.2, 1738.5, 1585.4, 1521.0, 1340.8, 1299.3, 1240.0, 1066.8, 833.9. **m. p.** 270 - 274 ℃. **MS**: HR-ESI calculated for [$C_{12}H_{16}N_2O_4$ + H^+]: 253.1188, found 253.1190.

5-Isoamyloxy-2-nitrothiobenzamide 3.06. A suspension of **3.05** (2.52 g, 10 mmol) and Lawesson's reagent (2.8 g, 404.47, 7 mmol) in 100 mL THF was heated to reflux overnight, cooled to rt, diluted with EtOAc, washed with 3M HCl, saturated aqueous K_2CO_3, dried over Na_2SO_4, and rotary evaporated to dryness. The residue was purified by chromatography (30% acetone in hexanes) to afford the product as a yellow solid (2.15 g, 268.33, 80% yield). **^{1}H NMR** (500 MHz, $CDCl_3$) δ 8.05 - 8.03 (d, *J* = 10 Hz, 1H), 6.93 - 6.90 (m, 2H), 4.09 - 4.06 (t, *J* = 5 Hz, 2H), 1.85 -

1.80 (m, 1H), 1.72 - 1.67 (dd, *J* = 5 Hz, 2H), 0.97 - 0.96 (d, *J* = 5 Hz, 6H). **^{13}C NMR** (126 MHz, $CDCl_3$) δ 201.53, 163.17, 140.30, 137.27, 127.36, 115.13, 113.84, 67.65, 37.50, 24.91, 22.46. **IR** (cm $^{-1}$) 2955.5, 1579.5, 1513.7, 1336.0, 1244.0, 1070.4, 863.0. **MS**: HR-ESI calculated for [$C_{12}H_{16}N_2O_3S + H^+$]: 269.0960, found 269.0962.

3.3.2c. Preparation of Linker 8.

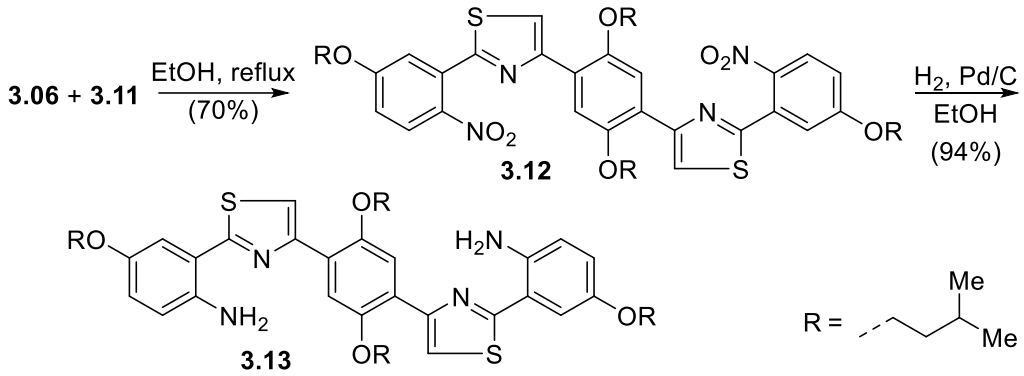

Bis-Thiazole 3.12. A solution of **3.11** (2.02 g, 5 mmol) and **3.06** (2.68 g, 10 mmol) in 50 mL of EtOH was refluxed overnight, rotary evaporated to dryness, and the residue was diluted with ethyl acetate. The solution was washed with aqueous K_2CO_3, dried over $MgSO_4$ and evaporated. The residue was purified by chromatoraphy (10% → 40% acetone in hexanes) to afford the product as yellow solids (2.91 g, 70% yield). **^{1}H NMR** (500 MHz, $CDCl_3$) δ 8.20 (s, 2H), 7.96 (s, 2H), 7.87 - 7.85 (d, *J* = 10 Hz, 2H), 7.22 - 7.21 (d, *J* = 5 Hz, 2H), 7.01 - 6.99 (dd, J_1 = 5 Hz, J_2 = 10 Hz, 2H), 4.25 - 4.22 (t, *J* = 5 Hz, 4H), 4.13 - 4.10 (t, *J* = 5 Hz, 4H), 1.94 - 1.82 (m, 8H), 1.75 - 1.71 (dd, *J* = 5 Hz, 4H), 1.03 - 0.98 (dd, *J* = 5 Hz, 24H). **^{13}C NMR** (126 MHz, $CDCl_3$) δ 161.51, 159.73, 152.10, 150.45, 142.14, 130.04, 126.50, 122.56, 119.00, 116.90, 114.98, 113.74,

67.47, 67.41, 38.37, 37.63, 25.44, 24.98, 22.73, 22.51. **IR** (cm $^{-1}$) 2955.9, 2360.0, 2341.6, 1530.2, 1206.1, 689.0. **MS**: HR-ESI calculated for [$C_{44}H_{54}N_4O_8S_2$ + H^+]: 831.3461, found 831.3465.

Linker 3.13. A suspension of bis-thiazole **3.12** (2.91 g, 3.5 mmol) and Raney nickel (1 g, wet with water) in 100 mL of 1,4-dioxane was shaken under 40 psi of hydrogen in a Parr shaker apparatus for 12 h. The mixture was filtered through Celite, diluted with EtOAc, washed with brine, and rotary evaporated to dryness. The residue was purified by chromatography (5% → 30% acetone in hexanes) to give the product (2.54 g, 94% yield) as a yellow solid. **^{1}H NMR** (500 MHz, $CDCl_3$) δ 8.01 (s, 2H), 7.93 (s, 2H), 7.23 - 7.22 (d, J = 5 Hz, 2H), 6.89 - 6.78 (dd, J_1 = 5 Hz, J_2 = 10 Hz, 4H), 5.94 (br, 4H), 4.22 - 4.19 (t, J = 5 Hz, 4H), 4.02 - 3.99 (t, J = 5 Hz, 4H), 1.93 - 1.81 (m, 8H), 1.72 - 1.68 (m., 4H), 1.02 - 0.99 (dd, J = 5 Hz, 24H). **^{13}C NMR** (126 MHz, $CDCl_3$) δ 166.66, 150.89, 150.76, 150.37, 139.61, 133.70, 122.84, 118.76, 118.30, 116.56, 115.88, 114.21, 113.61, 67.50, 67.28, 38.25, 38.13, 25.36, 25.01, 22.70, 22.63. **IR** (cm $^{-1}$) 2955.3, 2359.9, 1507.0, 1251.5, 1204.3, 1062.7. **m. p. MS**: HR-ESI calculated for [$C_{44}H_{58}N_4O_4S_2$ + H^+]: 771.3977, found 771.3972.

3.3.2d. Preparation of Mono-Boc protected Linker 9.

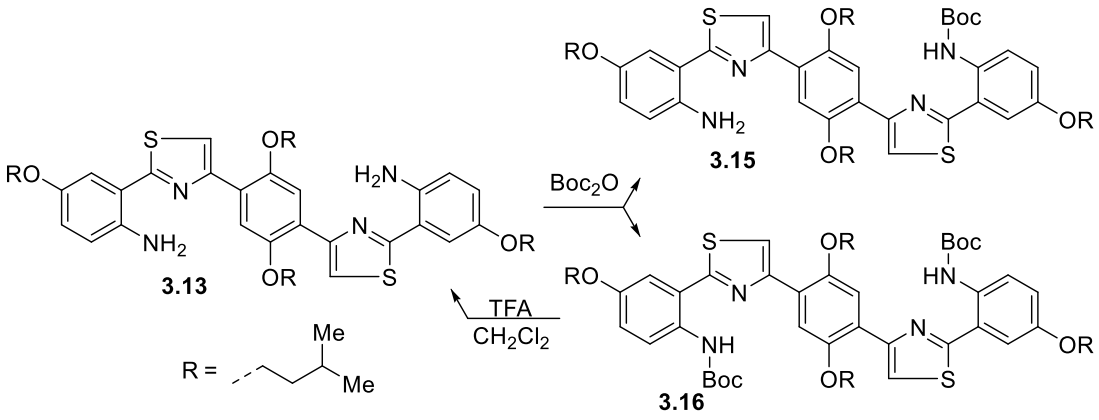

Boc-protection of Linker 3.13. To a solution of **3.13** (1.20 g, 1.5 mmol) in 5 mL $CHCl_3$ was added Boc_2O (163 mg, 0.75 mmol) and refluxed for 4 h. The mixture was quenched with 2 mL of ammonium hydroxide and extracted with CH_2Cl_2. The organic phase was dried over Na_2SO_4, and rotary evaporated to dryness. The residue was purified by chromatography (10% →30% acetone in hexanes) to **3.16** (146 mg, 10% yield) followed by **3.15** (392 mg, 30% yield) and **3.13** (0.60 g, 60% recovery).

3.15: ^{1}H NMR (600 MHz, $CDCl_3$) δ 11.05 (s, 2H), 8.29 (br, 1H), 8.06 (s, 1H), 8.01 (s, 1H), 7.99 (s, 1H), 7.92 (s, 1H), 7.25 (s, 1H), 7.21 (s, 1H), 6.99 - 6.97 (d, J = 12 Hz, 1H), 6.87 - 6.85 (d, J = 12 Hz, 1H), 6.79 - 6.77 (d, J = 12 Hz, 1H), 5.93 (br, 2H), 4.26 - 4.24 (t, J = 6 Hz, 2H), 4.21 - 4.19 (t, J = 6 Hz, 2H), 4.03 - 4.01 (t, J = 6 Hz, 2H), 4.00 - 3.97 (t, J = 6 Hz, 2H), 1.90 - 1.81 (m, 8H), 1.49 (s, 9H), 1.01 - 0.97 (m, 24H). **^{13}C NMR** (151 MHz, $CDCl_3$) δ 166.73, 165.84, 153.89, 153.61, 151.04, 150.78, 150.73, 150.46, 139.45, 130.77, 123.38, 122.42, 121.27, 120.58, 118.81, 118.41, 117.02, 116.92, 116.15, 114.64, 114.30, 114.07, 113.45, 68.10, 67.50, 67.34, 66.91, 38.41, 38.31, 38.02, 28.43, 25.41, 25.04, 22.81, 22.72, 22.64. **IR** (cm^{-1}) 2956.7, 2361.2, 1512.1, 1252.1, 1203.6, 1063.1. **MS**: HR-ESI calculated for [$C_{49}H_{66}N_4O_6S_2$+ Na^+]: 893.4321, found 893.4324.

3.16: **^{1}H NMR** (600 MHz, $CDCl_3$) δ 11.05 (s, 2H), 8.30 (br, 2H), 8.11 (s, 1H), 8.01 (s, 1H), 7.27 - 7.26 (d, J = 5 Hz, 2H), 7.00 - 6.98 (dd, J = 5 Hz, 2H), 4.30 - 4.27 (t, J = 7.5 Hz, 4H), 4.05 - 4.02 (t, J = 7.5 Hz, 4H), 1.93 - 1.82 (m, 8H), 1.73 - 1.69 (m, 4H), 1.51 (s, 18H), 1.02 - 0.98 (dd, J = 5 Hz, 24H). **^{13}C NMR** (126 MHz, $CDCl_3$) δ 165.86, 153.89, 153.58, 151.00, 150.74, 130.72, 121.27, 120.57, 117.24, 116.88, 114.66, 113.72, 80.03, 67.98, 66.88, 38.42, 38.00, 28.43, 25.43, 25.01, 22.83, 22.62. **IR** (cm^{-1}) 2957.8, 2362.6, 1514.5, 1253.4, 1205.1, 1064.2. **MS**: HR-ESI calculated for [$C_{54}H_{74}N_4O_8S_2$+ Na^+]: 993.4846, found 993.4847.

Recovery of Linker 3.13. Bis-Boc derivative **3.16** (320 mg, 0.33 mmol) was dissolved in 2 mL of 1:1 mixture of TFA and DCM. After 30 min at rt, the reaction mixture was quenched with 5 mL of aqueous K_2CO_3, washed with brine, dried over $MgSO_4$ and concentrated via rotary evaporation. Linker **3.13** (211 mg, 83% yield) was recovered by flash chromatography (10% →40% acetone in hexanes).

3.3.3. Synthesis of Macrocycle 3.14

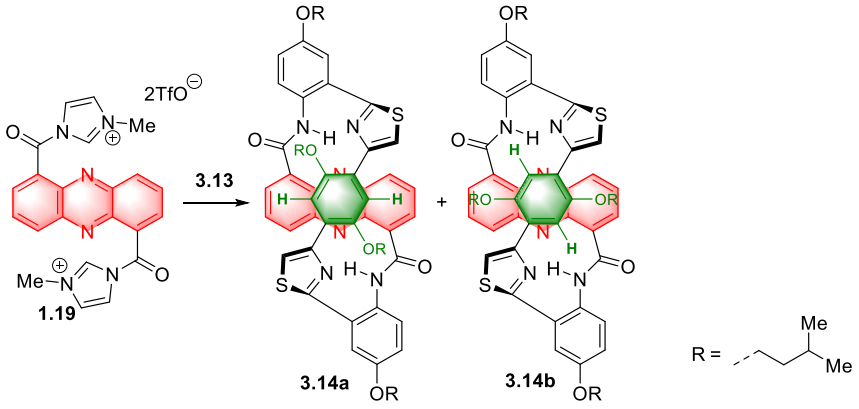

Macrocycle 3.14: A solution of **3.13** (154 mg, 2 mmol) in 1 mL $CHCl_3$ was added to a solution of **1.19** (139 mg, 2 mmol) in 1 mL MeCN and stirred at rt for 1 h. The mixture was rotary evaporated to dryness and purified by chromatography (10% → 30% acetone in hexanes) to afford, in order of elution, major (**3.14a,** 133mg, 65%) and minor (**3.14b,** 57 mg, 28%) diastereomers as orange solids.

3.14a: ^{1}H NMR (500 MHz, $CDCl_3$) δ 13.18 (s, 2H), 8.63 - 8.59 (dd, J_1 = 5 Hz, J_2 = 10 Hz, 4H), 7.73 - 7.71 (t, J = 7.5 Hz, 2H), 7.57 - 7.55 (d, J = 10 Hz, 2H), 7.51 (s, 2H), 7.36 (d, J = 5 Hz, 2H), 7.13 - 7.11 (dd, J = 5 Hz), 6.64 (s, 2H), 4.14 - 4.12 (t, J = 5 Hz, 4H), 3.47 - 3.44 (dd, J = 5 Hz, 2H), 2.93 - 2.90 (dd, J = 5 Hz, 2H), 1.94 - 1.90 (m, 2H), 1.79 - 1.75 (dd, J = 5 Hz, 4H), 1.70 - 1.64 (m, 2H), 1.55 - 1.50 (m, 2H), 1.47 - 1.41 (m, 2H), 1.03 - 1.02 (d, J = 5 Hz, 12H), 0.94 - 0.92

(dd, J = 5 Hz, 12H). **^{13}C NMR** (126 MHz, $CDCl_3$) δ 164.15, 163.91, 155.75, 150.80, 148.51, 141.43, 139.77, 133.55, 133.14, 132.81, 130.00, 129.67, 125.20, 123.93, 122.64, 116.71, 116.25, 114.72, 112.35, 66.96, 66.45, 38.12, 37.97, 25.24, 25.05, 23.03, 22.62, 22.55. **IR** (cm^{-1}) 2923.3, 2868.5, 2360.0, 2341.3, 750.9. **MS**: HR-ESI calculated for [$C_{58}H_{62}N_6O_6S_2 + Na^+$]: 1025.4069, found 1025.4074.

3.14b: ^{1}H NMR (500 MHz, $CDCl_3$) δ 13.09 (s, 2H), 8.48 - 8.46 (d, *J* = 10 Hz, 2H), 8.43 - 8.42 (d, *J* = 10 Hz, 2H), 8.28 - 8.26 (d, *J* = 10 Hz, 2H), 7.70 - 7.67 (t, *J* = 7.5, 2H), 7.40 (s, 2H), 7.36 - 7.35 (d, *J* = 5 Hz, 2H), 7.13 - 7.11 (dd, *J* = 5 Hz), 6.51 (s, 2H), 4.13 - 4.11 (t, *J* = 7.5 Hz, 3H), 3.35 - 3.32 (dd, *J* = 5 Hz, 2H), 3.02 - 2.98 (dd, *J* = 5 Hz, 2H), 1.94 - 1.89 (m, 2H), 1.78 - 1.74 (dd, *J* = 5 Hz, 2H), 1.38 - 1.34 (m, 2H), 1.15 - 1.11 (m, 2H), 1.03 - 1.02 (d, J = 5 Hz, 12H), 0.72 - 0.70 (dd, J = 5 Hz, 12H). **^{13}C NMR** (126 MHz, $CDCl_3$) δ 165.11, 164.99, 156.19, 152.04, 150.12, 141.95, 140.59, 133.86, 133.18, 133.06, 129.78, 129.70, 126.58, 125.73, 124.50, 116.38, 116.05, 115.27, 115.10, 68.30, 66.90, 37.95, 37.67, 25.03, 24.91, 22.61, 22.39. **IR** (cm^{-1}) 2924.4, 2360.2, 2341.6, 750.3, 668.8. **MS**: HR-ESI calculated for [$C_{58}H_{62}N_6O_6S_2 + Na^+$]: 1025.4069, found 1025.4068.

3.3.4. Synthesis of interleafed oligomers

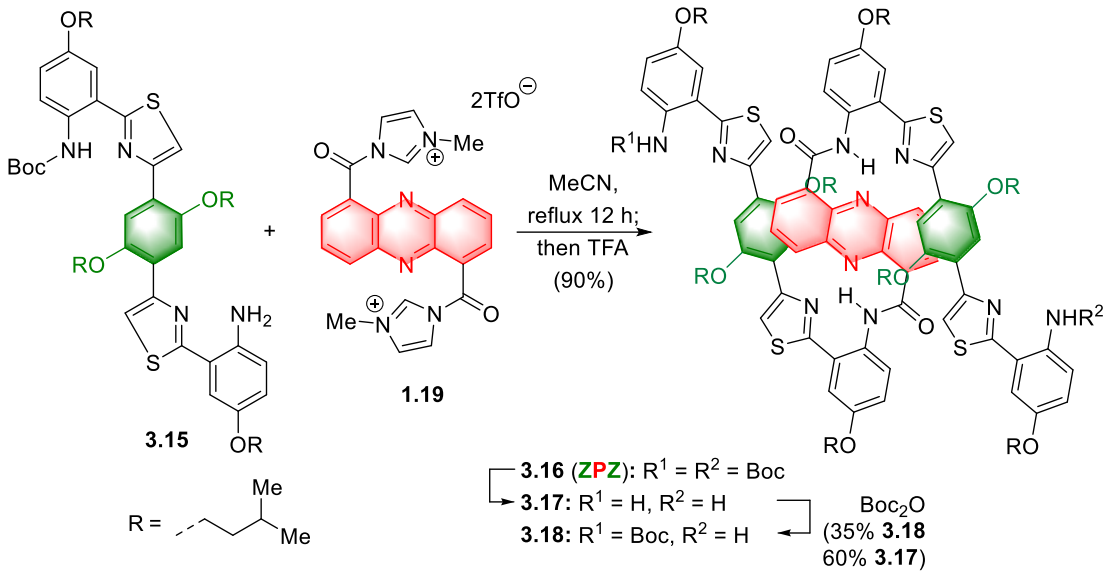

***3.3.4a. Preparation of ZPZ-Di-Boc* 3.16.** A mixture of **1.19** (87 mg, 0.1 mmol) in 0.5 mL $CHCl_3$ was added **3.15** (35 mg, 0.05 mmol) in 0.5 mL MeCN and heated to reflux for 1 h. Upon cooling to room temperature, the mixture was diluted with 5 mL CH_2Cl_2, washed with aqueous K_2CO_3, dried over $MgSO_4$ and rotary evaporated to dryness. The residue purified via chromatography (2% →10% acetone in hexanes) to afford **3.16** (94 mg, 95% yield) as a red solid.

3.16: ^{1}H NMR (500 MHz, $CDCl_3$) δ 13.33 (s, 2H), 10.99 (s, 2H), 8.64 - 8.62 (d, J = 10 Hz, 2H), 8.51 - 8.50 (d, J = 5 Hz, 2H), 8.32 (br, 2H), 7.89 (s, 2H), 7.66 (s, 2H), 7.62 - 7.59 (dd, J = 7.5 Hz, 2H), 7.43 - 7.40 (m, 6H), 7.25 - 7.24 (d, J = 5Hz, 2H), 7.04 - 7.02 (d, J = 10 Hz,2H), 6.94 - 6.92 (d, J = 10 Hz,2H), 6.46 (s, 2H), 4.11 - 4.09 (t, J = 5Hz, 12H), 2.61 - 2.59 (d, J = 5Hz, 4H), 2.00 - 1.91 (m, 8H), 1.87 - 1.83 (m, 4H), 1.80 - 1.75 (m, 8H), 1.40 - 1.32 (m, 6H), 1.14 - 1.13 (d, J = 5 Hz, 12H), 1.06 - 1.04 (d, J = 6 Hz, 24H), 0.72 - 0.71 (d, J = 6 Hz, 12H). ^{13}C NMR (126 MHz, $CDCl_3$) δ 165.63, 164.42, 162.24, 155.16, 153.81, 153.59, 151.25, 150.26, 149.42, 148.65, 140.97, 139.20, 134.01, 132.81, 131.74, 130.86, 129.97, 129.30, 124.12, 123.20, 122.43, 121.42, 121.22, 120.80, 117.48, 117.33, 116.44, 116.27, 115.35, 114.99, 114.03, 112.24, 111.86, 67.05, 66.93, 66.87, 38.65, 38.14, 38.04, 28.43, 25.52, 25.07, 24.90, 23.01, 22.66. **IR** (cm $^{-1}$) 2955.6, 2930.1,

2360.3, 2342.0, 1525.7, 1162.7, 1013.8, 751.3. **MS**: HR-ESI calculated for [$C_{112}H_{136}N_{10}O_{14}S_4$ + H^+]: 1973.9198, found 1973.9206.

3.3.4b. Deprotection of 3.16: A solution of **3.16** (94 mg, 0.48 mmol) in 1 mL CH_2Cl_2 was treated 1 mL TFA for 30 min. The reaction mixture was poured into 3 mL of 3 mL of saturated aqueous K_2CO_3 and extracted with CH_2Cl_2. The organic phase was dried over Na_2SO_4 and concentrated by rotary evaporation. The residue was purified by chromatography (10% →30% acetone in hexanes) to afford **3.17** as a dark-red solid (80 mg, 95 % yield).

3.3.4c. One-pot Preparation of 3.18. A solution of **3.15** (348 mg, 0.5 mmol) in 1 mL of MeCN was added to a solution of **1.19** (871 mg, 1 mmol) in 1 mL of $CHCl_3$. The reaction mixture was heated to reflux for 12 h, cooled to rt, and treated with 1 mL of TFA. After 30 min, the mixture was poured into 3 mL of saturated aqueous K_2CO_3 and extracted with CH_2Cl_2. The organic phase was dried over Na_2SO_4 and concentrated by rotary evaporation. The residue was purified by chromatography (10% →30% acetone in hexanes) to afford the product as a dark-red solid (1.59 g, 90 % yield).

3.17: **^{1}H NMR** (600 MHz, $CDCl_3$) δ 13.31 (s, 2H), 8.62 - 8.61 (d, J = 6 Hz, 2H), 8.46 - 8.44 (d, J = 12 Hz, 2H), 7.80 (s, 2H), 7.60 - 7.59 (d, J = 6 Hz, 2H), 7.57 (s, 2H), 7.34 - 7.31 (m, 6H), 7.14 - 7.13 (d, J = 6 Hz, 2H), 6.92 - 6.90 (dd, J = 6 Hz, 2H), 6.87 - 6.85 (d, J = 6 Hz, 2H), 6.69 - 6.67 (dd, J = 6 Hz, 2H), 6.41 (s, 2H), 6.12 (br, 2H), 4.03 - 4.00 (m, 8H), 3.97 - 3.95 (t, J = 6 Hz, 4H), 2.62 - 2.60 (t, J = 6 Hz, 4H), 1.93 - 1.87 (m, 6H), 1.80 - 1.77 (m, 4H), 1.75 - 1.71 (m, 10H), 1.41 - 1.36 (m, 2H), 1.24 - 1.21 (m, 4H), 1.08 - 1.06 (d, J = 6 Hz,12H), 1.03 - 1.01 (dd, J = 6 Hz, 24H), 0.72 - 0.71 (d, J = 6 Hz,12H). **^{13}C NMR** (151 MHz, $CDCl_3$) δ 166.50, 164.31, 162.21, 155.10, 151.26, 151.02, 150.20, 148.94, 148.72, 140.85, 139.54, 139.14, 133.78, 132.84, 131.65, 129.84, 129.28, 124.05, 123.22, 122.57, 120.88, 118.63, 118.48, 117.29, 117.13, 116.01, 115.35,

114.34, 111.95, 111.73, 67.35, 66.78, 66.47, 66.43, 38.39, 38.28, 38.02, 37.96, 25.46, 25.10, 25.07, 24.94, 22.83, 22.71, 22.67, 22.61. **IR** (cm^{-1}) 2954.7, 2929.5, 2869.4, 2360.3, 2342.3, 1502.9, 750.5. **MS**: HR-ESI calculated for [$C_{102}H_{120}N_{10}O_{10}S_4+H^+$]: 1773.8150, found 1773.8157.

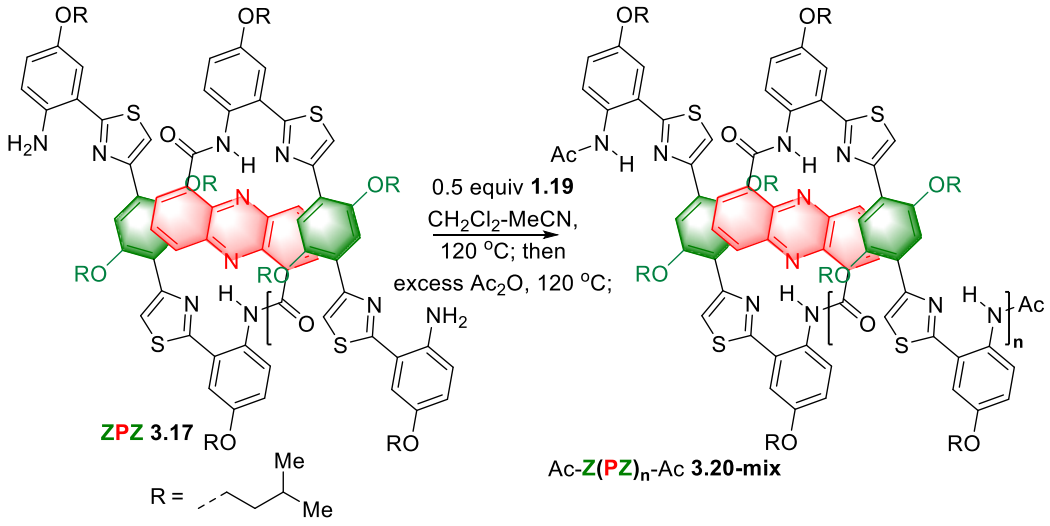

3.3.4d. Oligomerization. In a pressure tube with **3.17** (89 mg, 0.05 mmol in 1 mL $CHCl_3$, **1.19** (70 mg, 0.1 mmol in 1 mL MeCN) was added and the mixture was heated at 80 ℃ for 2 h. Upon cooling the mixture to rt, an aliquot was analyzed by NMR and found to contain unreacted **3.17**. Additional **1.19** (70 mg, 0.1 mmol in 1 mL MeCN) was introduced. Addition of **1.19** was repeated in 2 h and the mixture was left stirring overnight at 80 ℃. The mixture was cooled, rotary evaporated to dryness. The residue suspended in 3 mL of acetic anhydride and heat at 120 ℃ for 12 h. Upon cooling to rt, the mixture was diluted with CH_2Cl_2, washed with saturated aqueous K_2CO_3, dries over $MgSO_4$ and rotary evaporated to dryness to give the product mixture as an orange solid. The residue was analyzed by HNMR and MALDI. 5P: MALDI calc. [$C_{338}H_{372}N_{34}O_{36}S_{12}$ + H^+], 5867.505, found 5866.768; calc. [$C_{338}H_{372}N_{34}O_{36}S_{12}$ + Na^+], 5889.487, found 5888.987. 7P: MALDI calc. [$C_{454}H_{496}N_{46}O_{48}S_{16}$ + Na^+], 7894.321, found 7895.263. 9P:

MALDI calc. [$C_{570}H_{620}N_{58}O_{60}S_{20}$+ H^+], 9877.174, found 9877.169; calc. [$C_{570}H_{620}N_{58}O_{60}S_{20}$+ Na^+], 9899.156, found 9899.223.

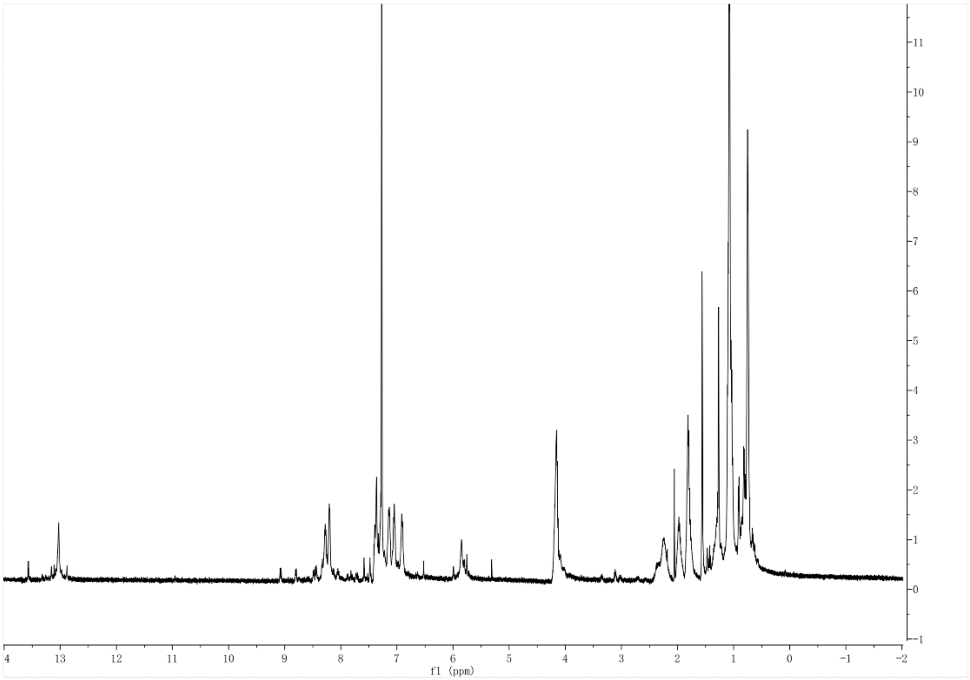

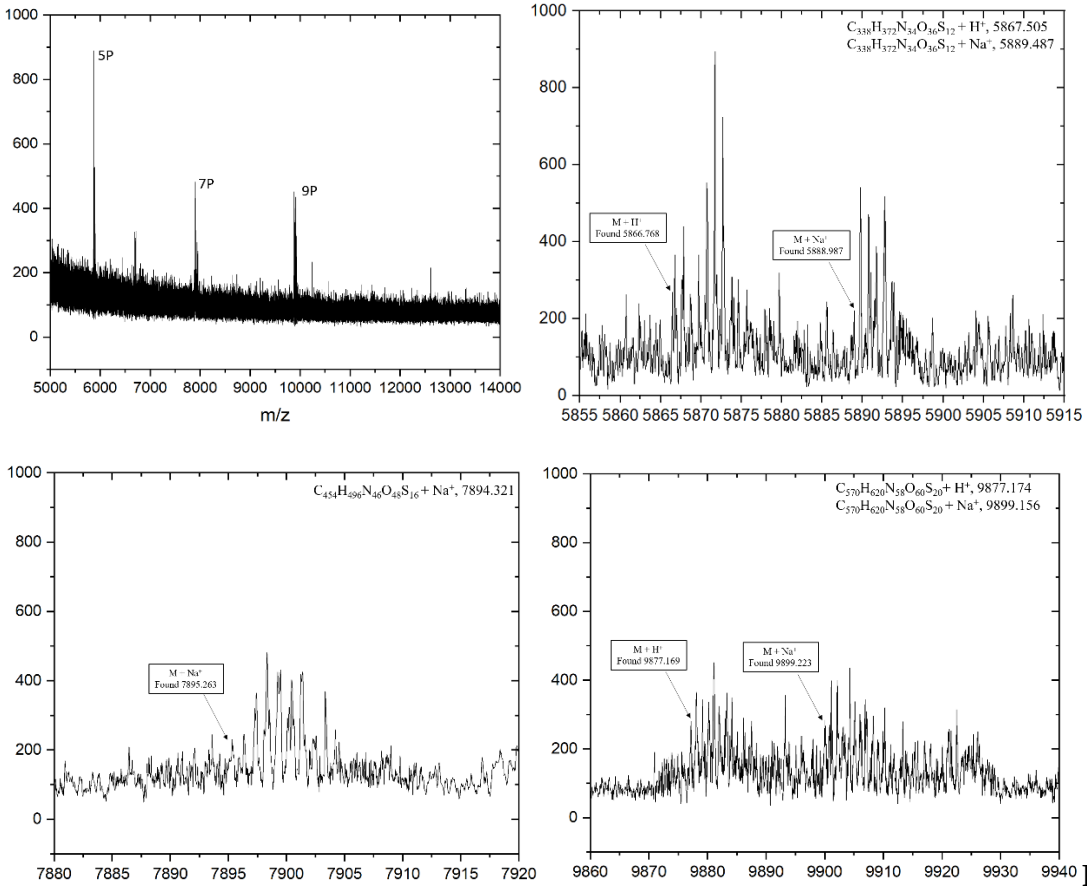

Figure 3-12. HNMR and MALDI of **3.20-mix**.

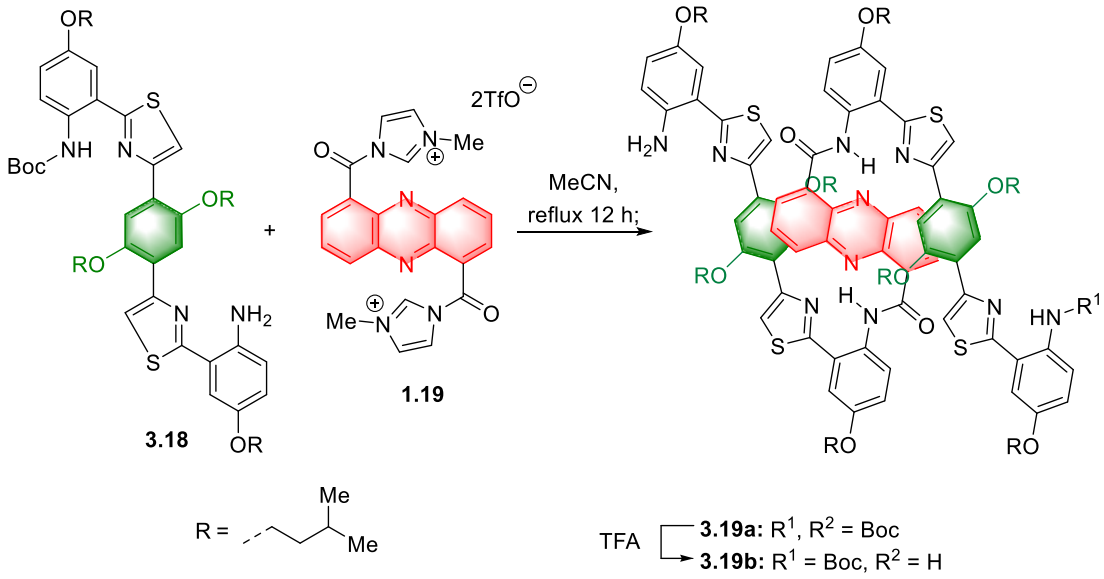

3.3.4e. One-pot preparation of Boc-ZPZ 3.18. The reaction was carried out as described above for **13** (See 4a) except that the crude mixture was treated with TFA for only 90 s. Chromatography delivered **3.18** (750 mg, 40 % yield) followed by **3.17** (532 mg, 30 % yield).

3.3.4f. Preparation of 3.18 by mono-protection of 3.17. A solution of **3.17** (355 mg, 0.2 mmol) and Boc_2O (43.6 mg, 0.2 mmol) in 5 mL 1,4-dioxane was refluxed for 10 h. The mixture was quenched with 2 mL of ammonium hydroxide and extracted with CH_2Cl_2. The organic phase was dried over Na_2SO_4, and rotary evaporated to dryness. The residue was purified by chromatography (10% →30% acetone in hexanes) to give **3.18** (131 mg, 35% yield) followed by **3.17** (213 mg, 60 % recovery).

3.18: **^{1}H NMR** (600 MHz, $CDCl_3$) δ 13.37 (s, 1H), 13.25 (s, 1H), 10.95 (s, 1H), 8.67 - 8.65 (d, J = 6 Hz, 1H), 8.58 - 8.54 (dd, J = 6 Hz, 2H), 8.39 - 8.38 (d, J = 6 Hz, 1H), 8.30 (br, 1H), 7.85 (s, 1H), 7.79 (s, 1H), 7.63 (s, 1H), 7.62 - 7.60 (t, J = 6 Hz, 1H), 7.57 (s, 1H), 7.55 - 7.53 (t, J = 6 Hz, 1H), 7.38 - 7.32 (m, 6H), 7.25 - 7.23 (d, J = 6 Hz, 1H), 7.10 - 7.09 (d, J = 6 Hz, 1H), 7.00 - 6.97 (m, 2H), 6.91 - 6.89 (d, J = 6 Hz, 1H), 6.84 - 6.83 (d, J = 6 Hz, 1H), 6.59 - 6.57 (d, J = 6 Hz, 1H), 6.49 (s, 1H), 6.33 (s, 1H), 5.93 (br, 2H), 4.10 - 4.04 (m, 6H), 4.02 - 3.95 (m, 6H), 2.59 - 2.57 (t, J = 6 Hz, 4H), 1.95 - 1.86 (m, 7H), 1.82 - 1.79 (m, 5H), 1.76 - 1.70 (m, 8H), 1.47 (s, 9H), 1.09 - 1.08 (d, J = 6 Hz, 12H), 1.03 - 1.01 (m, 24H), 0.71 - 0.68 (dd, 12H). **^{13}C NMR** (151 MHz, $CDCl_3$) δ 166.59, 165.60, 164.43, 164.30, 162.20, 155.10, 153.79, 153.58, 151.27, 151.20, 150.81, 150.26, 150.17, 149.48, 148.81, 148.70, 148.66, 140.99, 140.82, 139.96, 139.20, 139.11, 134.02, 133.71, 132.85, 132.77, 131.93, 131.47, 130.85, 130.19, 129.61, 129.42, 129.14, 124.40, 123.75, 123.30, 123.05, 122.58, 122.37, 121.42, 121.34, 120.81, 120.61, 118.52, 118.42, 117.45, 117.35, 117.28, 116.88, 116.44, 116.31, 115.94, 115.85, 115.37, 115.32, 114.97, 114.28, 112.27, 112.06, 111.89, 111.46, 67.33, 67.08, 66.91, 66.87, 66.73, 66.61, 66.36, 38.60, 38.40, 38.29, 38.13, 38.02, 37.94,

29.68, 28.42, 25.48, 25.10, 25.06, 24.91, 22.97, 22.84, 22.71, 22.66, 22.60. **IR** (cm $^{-1}$) 2956.5, 2360.9, 2341.8, 874.8. **IR** (cm $^{-1}$) 2956.5, 2929.7, 2360.9, 2341.8, 1529.9, 874.8. **MS**: HR-ESI calculated for [$C_{107}H_{128}N_{10}O_{12}S_4$ + H^+]: 1873.8674, found 1873.8664.

3.3.4g. Controlled preparation of Z(PZ)$_3$ 3.19a.

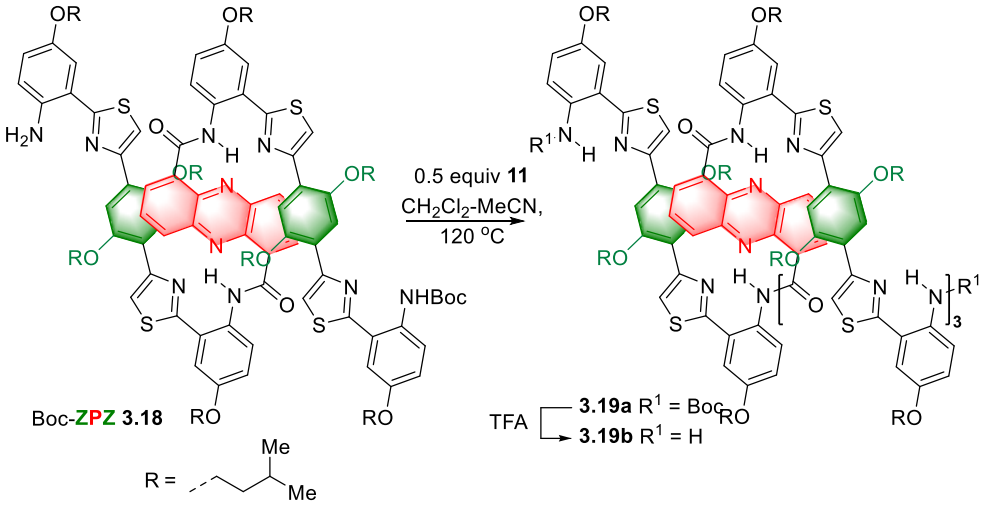

3.3.4h. Preparation of Boc-Z(PZ)$_3$Boc 3.19a. A solution of **3.18** (187 mg, 0.1 mmol) and **1.19** (35 mg, 0.05 mmol) in a mixture of 1 mL $CHCl_3$ and 1 mL MeCN was heated at 120 ℃ in a sealed pressure tube overnight. Upon cooling, the mixture was rotary evaporated to dryness and the residue washed with MeCN five times and purified by chromatography (5% →20% acetone in hexanes) to give the product as an orange solid (160 mg, 80% yield). **^{1}H NMR** (600 MHz, $CDCl_3$) δ 13.25 (s, 2H), 13.10 (s, 2H), 13.07 (s, 2H), 10.95 (s, 2H), 8.56 - 8.55 (d, J = 6 Hz, 2H), 8.52 - 8.51 (d, J = 6 Hz, 2H), 8.33 - 8.30 (d, J = 6 Hz, 2H), 8.30 - 8.28 (d, J = 6 Hz, 2H), 8.25 - 8.23 (d, J = 6 Hz, 2H), 8.22 - 8.20 (d, J = 6 Hz, 2H), 7.81 (s, 2H), 7.58 (s, 2H), 7.50 - 7.48 (t, J = 6 Hz, 2H), 7.41 - 7.39 (m, 6H), 7.36 - 7.35 (m, 6H),7.25 - 7.24 (m, 4H), 7.23 - 7.16 (m, 8H), 7.10 - 7.08 (d, J = 6 Hz, 2H), 7.01 - 6.99 (d, J = 6 Hz, 2H), 6.96 - 6.94 (d, J = 6 Hz, 2H), 6.89 - 6.87 (d, J = 6 Hz, 2H), 6.44 (s, 2H), 5.88 (s, 2H), 5.87 (s, 2H), 4.20 - 4.15 (m, 8H), 4.10 - 4.07 (dd, J = 6 Hz, 8H),

4.05 - 4.03 (m, 4H), 2.57 - 2.54 (m, 4H), 2.28 (m, 4H), 2.04 - 1.89 (m, 8H), 1.84 - 1.80 (m, 8H), 1.79 - 1.73 (m, 12H), 1.46 (s, 18H), 1.39 - 1.35 (m, 6H), 1.30 - 1.23 (m, 6H), 1.20 - 1.16 (m, 10H), 1.14 - 1.01 (m, 72H), 0.83 - 0.81 (dd, J = 6 Hz, 24H), 0.64 - 0.63 (d, J = 6 Hz, 12H). **^{13}C NMR** (151 MHz, $CDCl_3$) δ 165.61, 164.30, 164.19, 164.12, 162.14, 162.10, 162.03, 155.20, 155.14, 155.09, 153.81, 153.58, 151.19, 150.28, 150.18, 149.45, 148.69, 147.41, 140.86, 140.58, 140.50, 139.04, 138.87, 138.74, 133.72, 133.45, 132.77, 132.30, 131.69, 131.11, 130.83, 130.18, 129.92, 129.67, 129.35, 128.92, 128.86, 124.28, 124.03, 123.84, 123.50, 123.37, 123.07, 122.42, 121.38, 121.25, 120.79, 120.73, 117.52, 117.38, 116.47, 116.35, 116.10, 116.01, 115.52, 115.37, 115.19, 115.15, 114.95, 112.34, 111.94, 110.32, 67.08, 66.92, 66.87, 66.55, 65.76, 65.71, 38.57, 38.31, 38.28, 38.16, 38.13, 38.03, 37.91, 29.69, 28.41, 25.47, 25.12, 25.07, 25.04, 24.83, 22.99, 22.97, 22.80, 22.75, 22.69, 22.66, 22.61, 22.53. **IR** (cm^{-1}) 2954.8, 2925.1, 2869.0, 1723.5, 1528.9, 1500.0, 1260.1, 1014.1, 750.0. **MS**: MALDI-TOF calculated for [$C_{228}H_{260}N_{22}O_{26}S_8$ + H^+]: 3978.754, found 3979.124.

3.3.4i. Deprotection of 3.19a. A stirring solution of **3.19a** (126 mg, 0.03 mmol) in 2 mL of CH_2Cl_2 was treated with 2 mL of TFA for 10 min at rt and poured into 10 mL of saturated aqueous K_2CO_3. The mixture was extracted with CH_2Cl_2, organic phase washed with NaCl, dried over $MgSO_4$ and rotary evaporated to dryness. The residue was washed by MeCN. Oligomer **3.19b** (102 mg, 90% yield) was obtained as a red solid that was sufficiently pure for the next step.

Partial assignment due to complexity: **^{1}H NMR** (500 MHz, $CDCl_3$) δ 13.24 (s, 2H), 13.18 (s, 2H), 13.09 (s, 2H), 8.58 - 8.56 (d, J = 12 Hz, 2H), 8.43 - 8.42 (d, J = 6 Hz, 2H), 8.32 - 8.29 (dd, J = 6 Hz, 4H), 8.25 - 8.23 (t, J = 6 Hz, 4H), 7.77 (s, 2H), 7.57 - 7.53 (dd, J = 12 Hz, 2H), 7.51 (s, 2H), 7.40 - 7.39 (dd, J= 6 Hz, 2H), 7.36 - 7.32 (m, 8H), 7.24 - 7.08 (m, 14H), 6.96 - 6.89 (m, 6H), 6.66 - 6.64 (dd, J = 6 Hz, 2H), 6.30 (s, 2H), 5.85 (s, 2H), 5.83 (s, 2H), 4.19 - 4.17 (t, J = 6 Hz, 4H),

4.11 - 4.03 (m, 12H), 3.98 - 3.95 (t, J = 12 Hz, 4H). **^{13}C NMR** (126 MHz, $CDCl_3$) δ 166.08, 164.20, 164.02, 162.26, 162.04, 155.09, 151.12, 150.32, 150.13, 148.88, 148.55, 147.37, 140.71, 140.54, 140.48, 138.85, 138.72, 133.63, 133.48, 132.68, 132.46, 132.29, 131.99, 131.33, 129.86, 129.76, 129.40, 128.91, 128.70, 123.90, 123.10, 120.82, 120.78, 120.77, 118.12, 117.56, 117.50, 117.41, 117.34, 117.34, 116.28, 116.02, 115.47, 115.29, 115.10, 114.36, 111.79, 111.48, 110.29, 38.21, 38.13, 38.01, 37.81, 29.70, 25.42, 25.07, 24.83, 22.98, 22.94, 22.82, 22.75, 22.71, 22.66, 22.52. **m.p.** > 300 ℃.

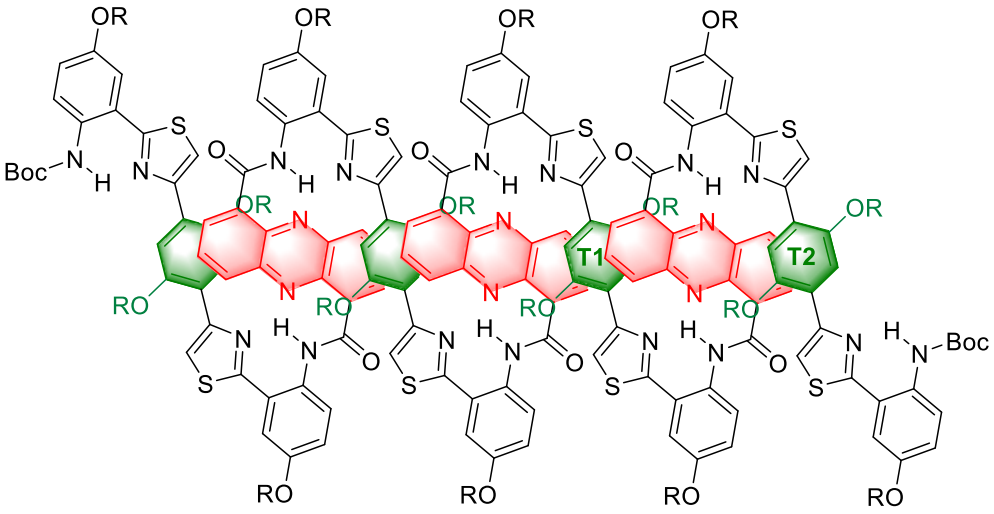

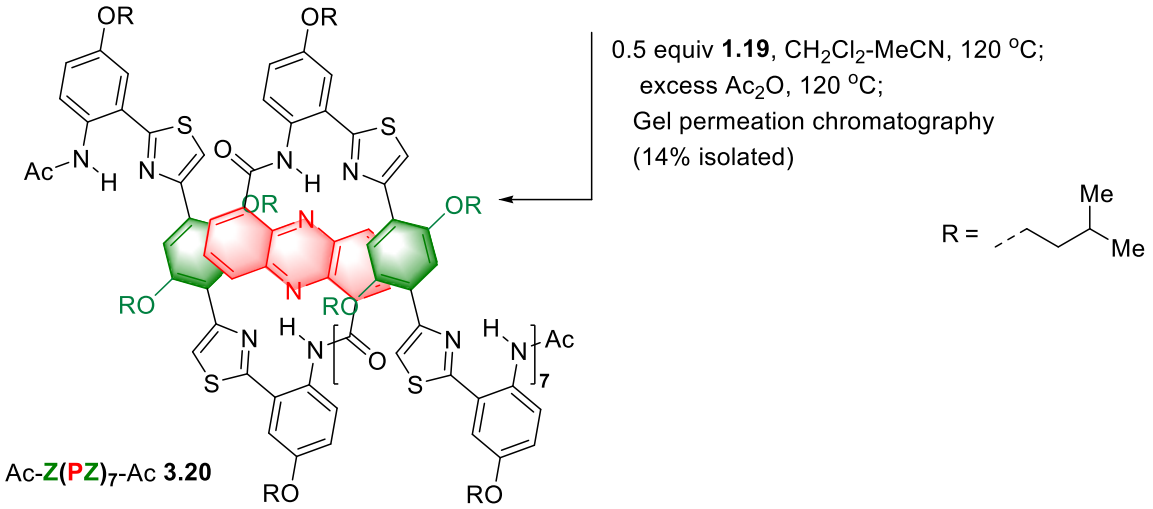

3.3.4j. Preparation of AcZ(PZ)$_7$Ac 3.20. A solution of **3.19b** (75 mg, 0.02 mmol) and **1.19** (10 mg, 0.015 mmol) in a mixture of 2 mL CH_2Cl_3 and 2 mL MeCN was heated at 120 ℃ in a sealed pressure tube overnight. Upon cooling, the mixture was rotary evaporated to dryness, the residue suspended in 3 mL of acetic anhydride and heated at 120 ℃ for 12 h. The mixture was cooled to rt, diluted with CH_2Cl_2, washed with saturated K_2CO_3, dried over $MgSO_4$ and rotary evaporated to dryness. The residue was purified by GPC (0.75% EtOH in $CHCl_3$). Heptamer **3.20** was isolated as a dark-orange solid (22 mg, 14% yield).

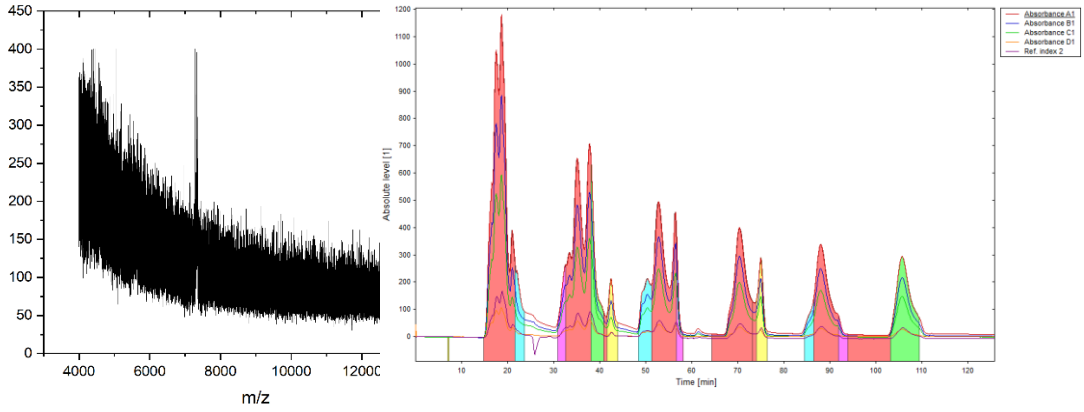

Figure 3-13. MALDI and GPC traces of **3.20**.

Partial assignment due to complexity. **^{1}H NMR** (600 MHz, $CDCl_3$) δ 13.02 (s, 14H), 8.26 - 8.18 (m, 28H), 7.39 - 7.28 (m, 18H), 7.12 - 6.89 (m, 48H), 5.83 (m, 14H). **^{13}C NMR** (151 MHz, $CDCl_3$) δ 164.04, 162.00, 155.11, 150.26, 147.39, 140.47, 138.71, 133.41, 132.28, 129.86, 128.89, 123.99, 120.80, 117.51, 116.08, 115.32, 110.39, 94.76, 66.92, 65.71, 38.16, 29.71, 25.11, 25.00, 22.90, 22.74. **IR** (cm $^{-1}$) 2953.4, 2926.1, 2826.9, 1667.9, 1530.4, 1500.2, 1184.2, 749.6, 682.4. MALDI-TOF calc. for [$C_{454}H_{496}N_{46}O_{48}S_{16}$+$Na^+$]: 7894.321, found 7894.241.

3.3.5. Redox cycling by catalytic hydrogenation

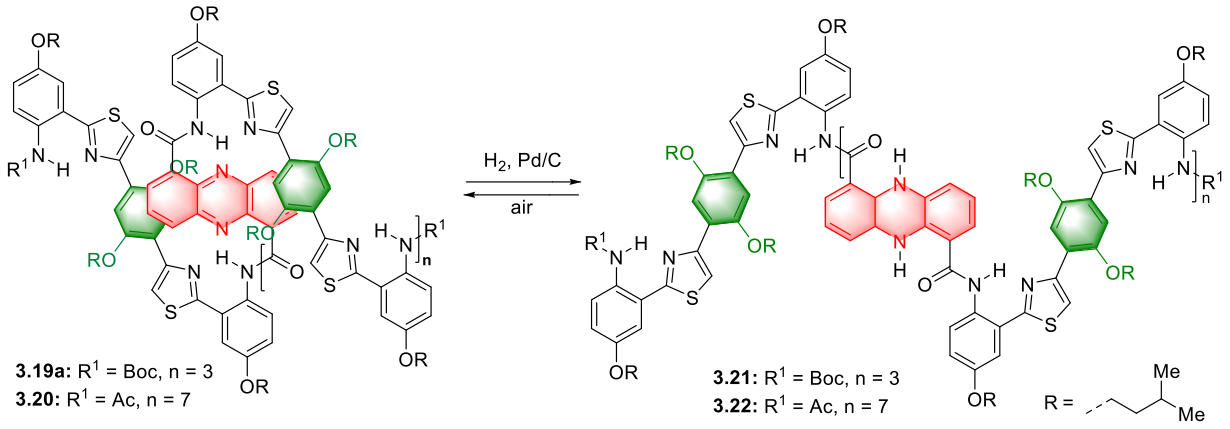

3.3.5a. Reduction of Oligomer 3.19a. A 5 mm Wilmad quick pressure valve NMR tube was charged with **3.19a** (4 mg, 2 nmol), dry 10% Pd/C (0.5 mg, 0.2 nmol), and 0.5 mL $CDCl_3$, purged with hydrogen 10 times and shaken under 20 psi of hydrogen by inverting it mechanically at ca. 6 revolutions per min. Reaction progress was monitored by ^{1}H NMR. After 3 h, complete consumption of the starting material was confirmed and the spectra of dihydrophenazine **3.21** were recorded. No further changes in the spectrum were observed on longer exposure to hydrogen.

^{1}H NMR (600 MHz, $CDCl_3$) δ 12.40 - 12.37 (m, 6H), 11.05 (s, 6H), 9.29 (s, 6H), 8.78 - 8.74 (dd, J = 6 Hz, 6H), 8.31 (br, 2H), 8.13 (s, 2H), 8.06 - 8.03 (dd, J = 6 Hz, 8H), 7.71 - 7.68 (m, 6H), 7.38 - 7.35 (dd, J = 6 Hz, 4H), 7.32 - 7.29 (dd, J = 6 Hz, 4H), 7.07 - 7.00 (m, 8H), 6.81 - 6.78 (m, 6H), 6.03 - 6.01 (d, J = 6 Hz, 6H), 5.81 - 5.76 (m, 6H), 4.28 - 4.25 (m, 4H), 4.12 - 4.05 (m, 16H), 3.88 - 3.84 (m, 12H), 1.91 - 1.88 (m, 16H), 1.78 -1.72 (m, 32H), 1.04 - 0.99 (m, 60H),

0.94 - 0.91 (m, 36H). **^{13}C NMR** (151 MHz, $CDCl_3$) δ 167.45, 166.34, 165.92, 154.81, 153.97, 153.62, 151.28, 150.96, 150.40, 150.03, 137.49, 133.79, 130.73, 130.24, 122.51, 122.35, 121.95, 121.62, 121.37, 120.70, 119.98, 119.77, 117.76, 117.52, 116.95, 116.69, 114.87, 114.74, 114.01, 113.82, 112.73, 94.77, 68.06, 67.34, 66.92, 38.47, 38.00, 30.94, 29.71, 28.47, 25.48, 25.39, 25.04, 22.83, 22.72, 22.64.

3.3.5b. Aerial oxidation of reduced oligomer 3.21. The hydrogen pressure in the NMR tube (see above) was released and the mixture was allowed to come into contact with air for 2 min. The tube was inverted mechanically and the progress of reoxidation was monitored by ^{1}H NMR (see diagnostic peaks below). After 18 h, complete disappearance of the dihydrophenazine form **3.21** and clean recovery of **3.19a** were confirmed.

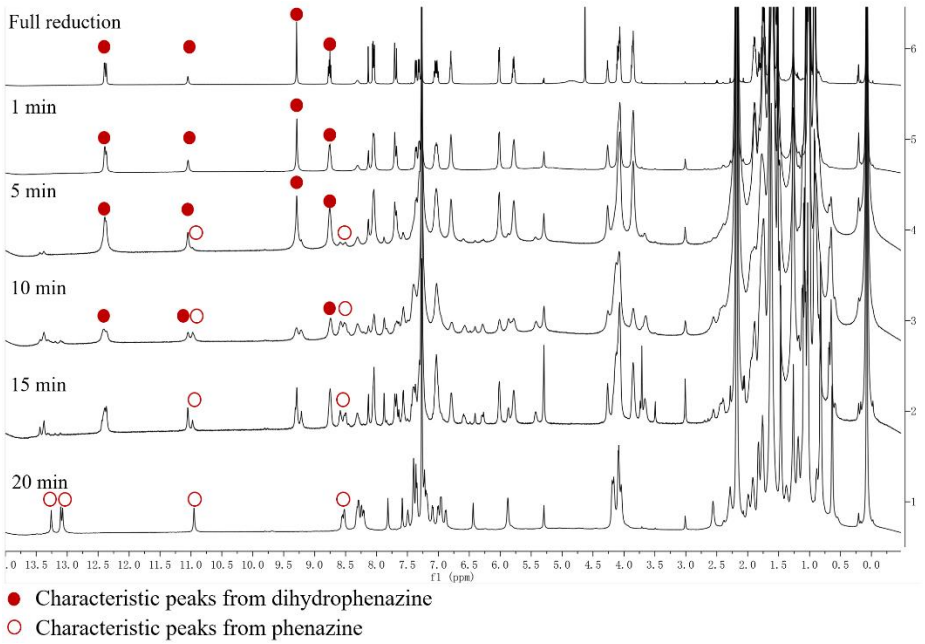

Figure 3-14. Arial oxidation of **3.21**.

3.3.5c. Redox cycling of 3.19a. The above steps were repeated 3 times. The stacked specta are shown below.

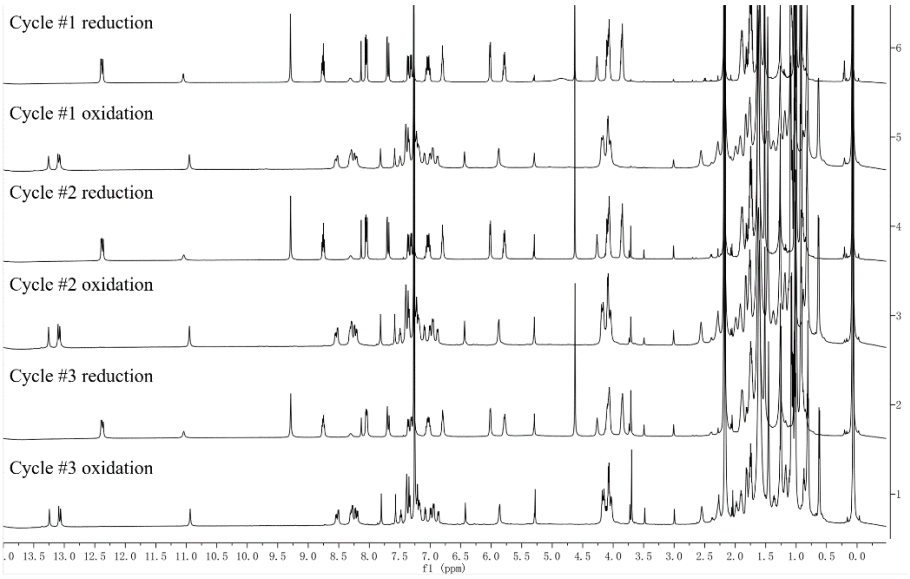

Figure 3-15. Redox cycling of **3.19a.**

***3.3.5d*. Redox cycling of 3.20.** The hydrogenation-reoxidation were performed as described above using **3.20 (**5 mg, 0.6 nmol) and dry 10% Pd/C (0.1 mg, 0.4 nmol). The resulting spectra are shown below.

3.20: 1H NMR (600 MHz, $CDCl_3$) δ 12.32 (s, 14H), 9.27 (s, 20H), 8.71 (s, 20H), 8.13 (s, 2H), 8.06 - 8.05 (m, 16H), 7.70 (m, 18H), 7.04 (m, 18H), 6.80 (m, 20H), 6.00 (m, 14H), 5.78 (m, 14H).

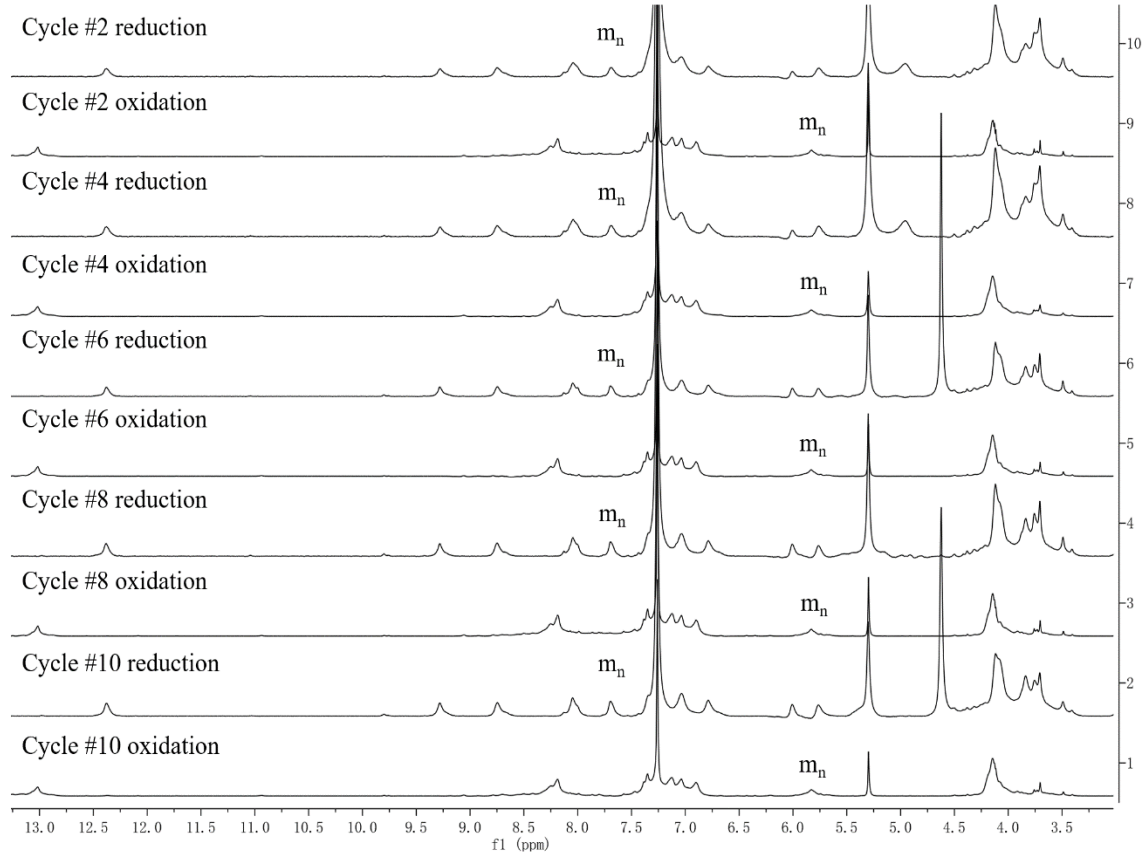
Cycle #2 reduction
Cycle #2 oxidation
Cycle #4 reduction
Cycle #4 oxidation
Cycle #6 reduction
Cycle #6 oxidation
Cycle #8 reduction
Cycle #8 oxidation
Cycle #10 reduction
Cycle #10 oxidation
m_n
f1 (ppm)

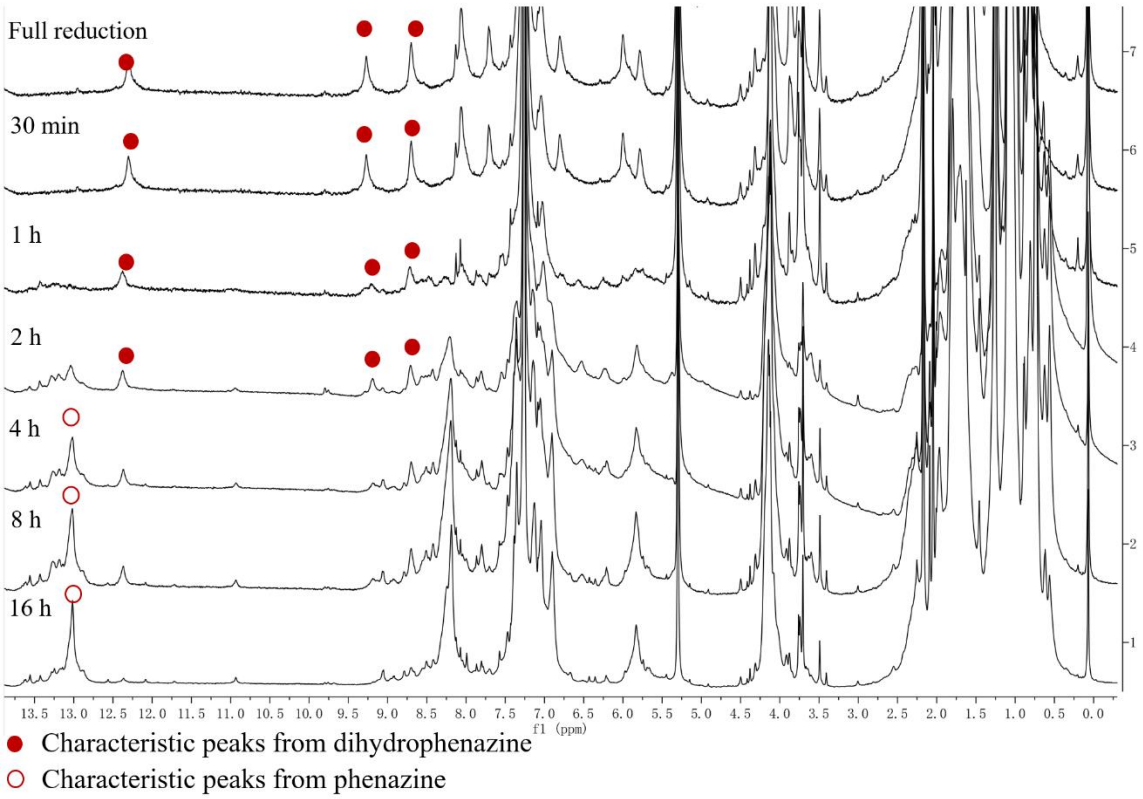
Full reduction
30 min
1 h
2 h
4 h
8 h
16 h
f1 (ppm)
Characteristic peaks from dihydrophenazine
Characteristic peaks from phenazine

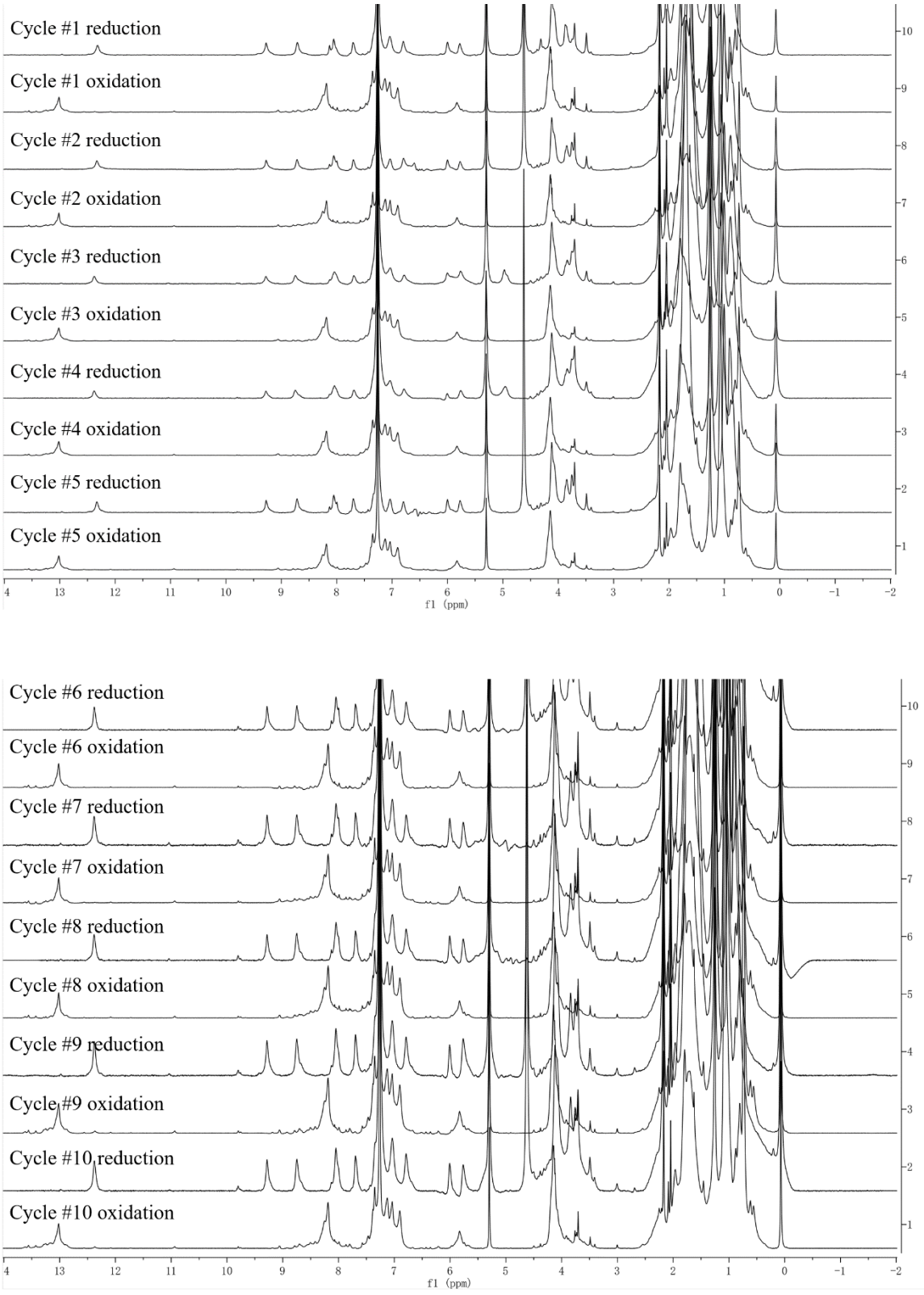

Figure 3-14. Redox cycling of **3.20.**

3.3.6. Electrochemical studies.

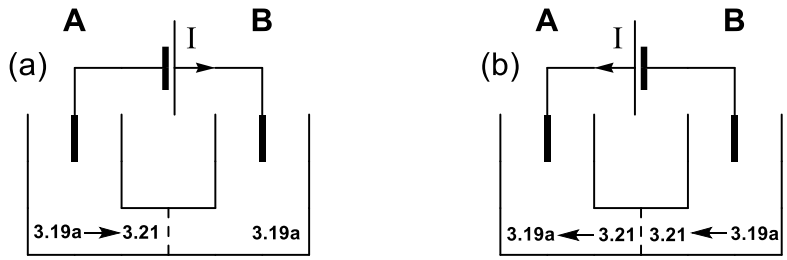

Figure 3-17. Bulk electrolysis of **3.19a.**

(a) A divided cell separated by a 5 μm glass frit was charged with anhydrous $MgSO_4$ (2 mg) and a solution of **3.19a** (10 mg, 0.0025 mmol), N_2H_4-H_2O (13 μL, 0.25 mmol), and *t*-Bu_4NBF_4 (16 mg, 0.05 mmol) in 0.5 mL of 4:1 v/v $CDCl_3$-CD_3OD mixture. Two NMR tubes were connected to each chamber via a cannula. The cell was equipped with graphite electrodes and purged thoroughly with N_2 using the freeze-pump-thaw technique. A constant current of 0.4 mA was passed through the cell until 2.5 Coulombs was reached. The contents of each chamber was transferred to each NMR tube by cannulation and analyzed by ^1H NMR. The solution from the cathodic chamber (**A**) contained >95% dihydrophenazine **3.20**, while that from the anodic chamber (**B**) contained unchanged starting material **3.19a**.

(b) The experiment was repeated as described above, except that after passing 2.5 Coulombs of current, the current was reversed and the same amount of charge was passed in the opposite direction. NMR analysis indicated that the contents of both chambers were also reversed.

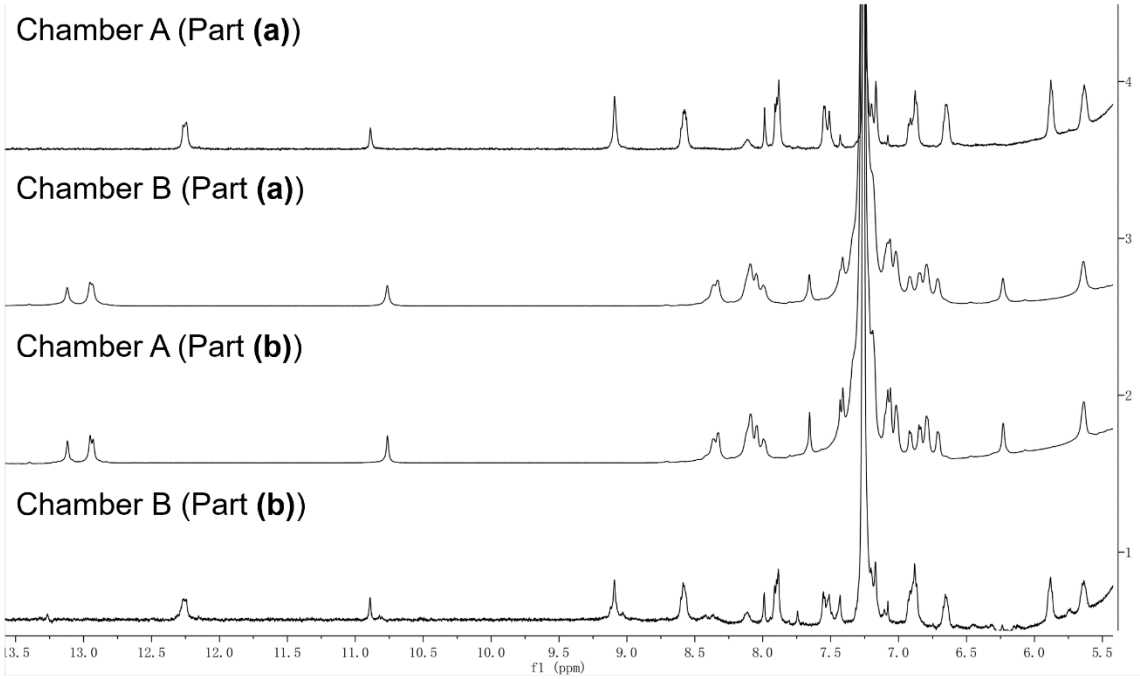

Figure 3-16. Electrochemical studies on **3.19a.**

3.3.7. Size estimation by computational and DOSY studies.

The conformations of oligomers **3.19a, 3.21, 3.20 and 3.22** were optimized by Molecular Mechanics MMFF calculations in gas phase using Spartan'20 software. All other structures shown below were obtained by geometry optimization performed at the B3LYP/6-31G* level of theory. [9]

3.3.7a. DFT calculations of two possible conformation of macrocycle 3.14.

There are two possible isomers of **3.14** have been studies by DFT calculation at B3LYP/6-31G* level with isoamyl side chains replaced by methyl groups. Macrocycle **3.14a'** was ca. 5 kcal/mol lower in energy than **3.14b'**. With length ca. 1.8nm and a height between phenazine and terephthaly ring ca. 0.4 nm, **3.14a'** and **3.14b'** have the same size.

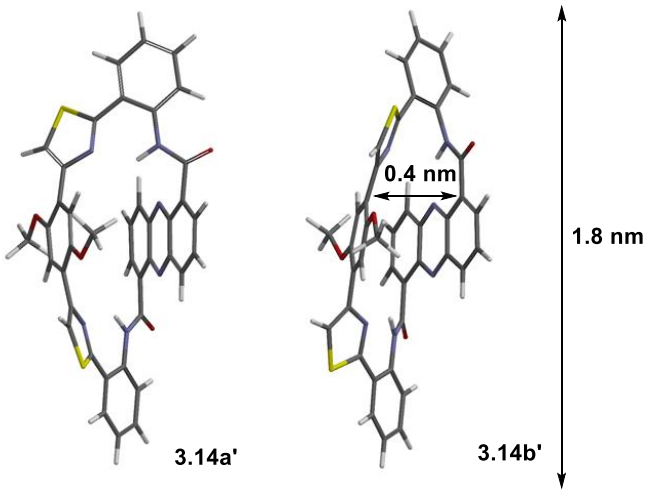

Figure 3-19. DFT calculations of **3.14a/b.**

3.3.7b. DOSY of 3.14a and 3.14b.

TMSS (Tetrakis(trimethylsilyl)silane) was used as reference sample for all DOSY studies.[4] According to Einstein-stock equation, the diameter of **3.14a/b** is:

$$R_{3.14a/b} = (D_{TMSS} / D_{3.14a/b}) \times R_{TMSS}$$

$$= (9.99 \times 10^{-9}\ m^{-2}/s / 7.11 \times 10^{-9}\ m^{-2}/s) \times 0.80\ nm$$

$$= 1.12\ nm.$$

DOSY of TMSS

D = 9.99 x 10^{-9} m^{-2}/s

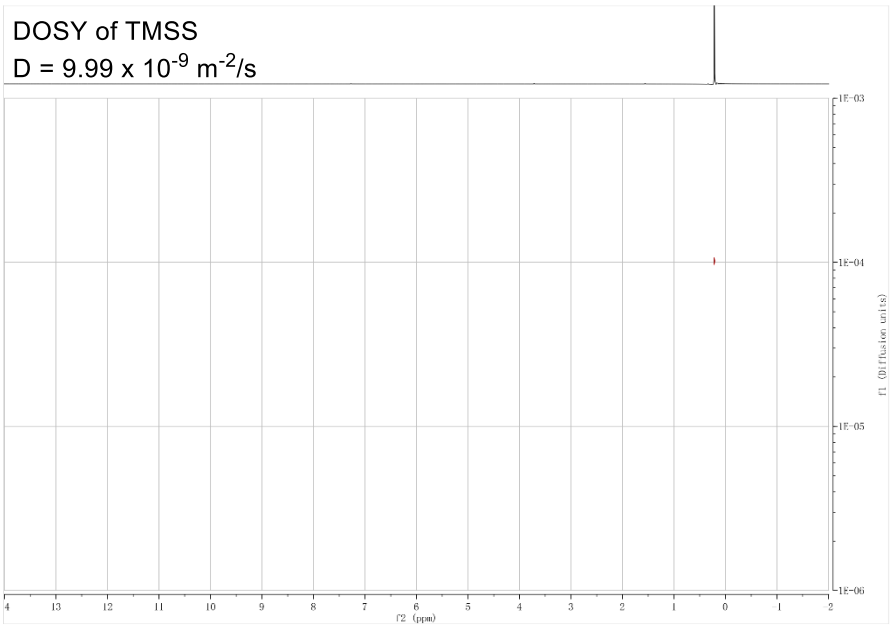

DOSY of **3.14a**

D = 7.11 x 10^{-9} m^{-2}/s

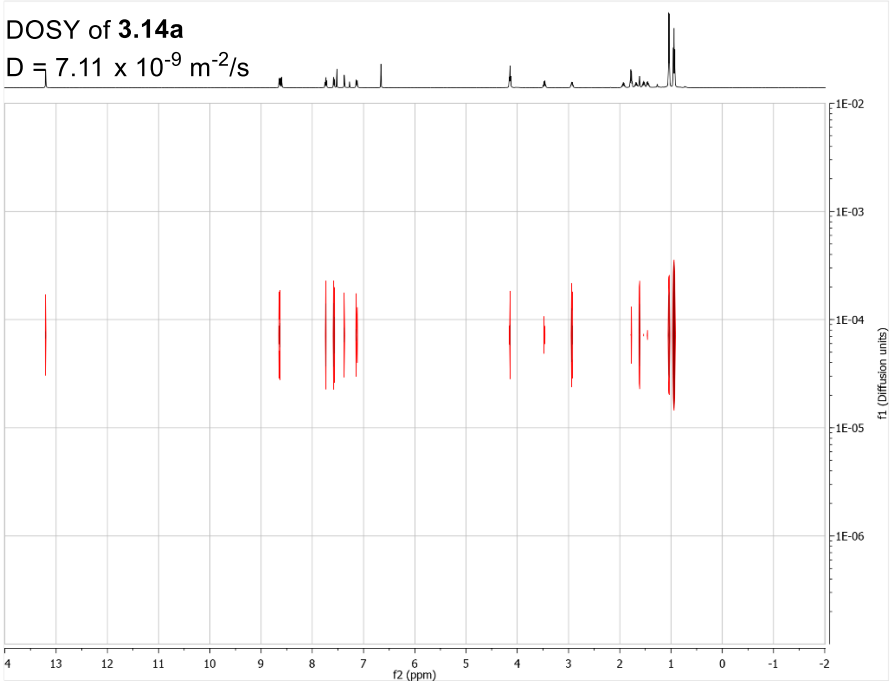

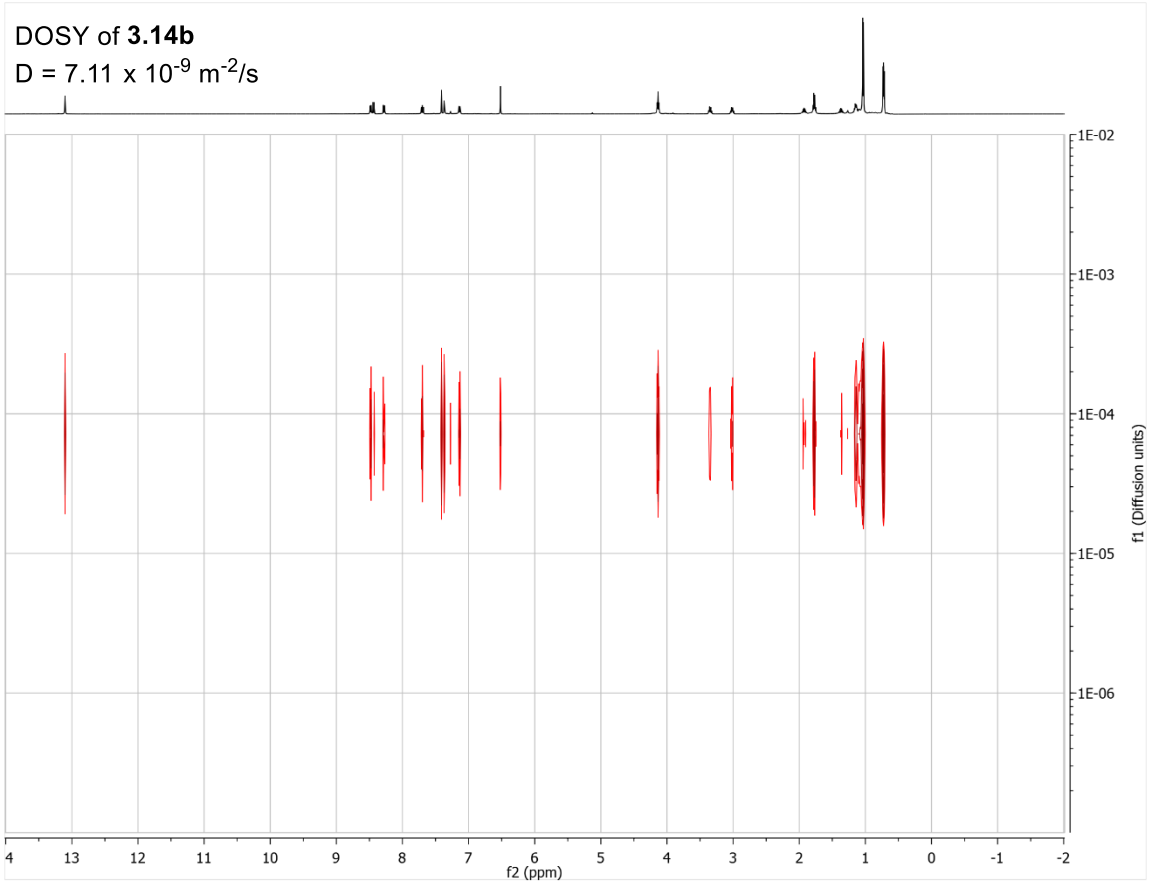

Figure 3-20. DOSY spectrum of **3.14a/b.**

3.3.7c. Estimation of sizes and relative elongation by calculation.

The structure of oligomer **3.19a** was simplified with isoamyl side chains replaced by methyl groups and minimized with Molecular Mechanics MMFF calculations in gas phase. All phenazine and dialkoxyphenylene groups in **3.19a'** were predicted to adopt a parallel, skewed orientation as shown in Figure 3-19. Distance between several pairs of analogous atoms of the outermost dialkoxyphenylene groups is ca. 2.3 nm, while the distance between the terminal Boc group is ca. 2.9 nm. While for **3.21'**, the distance between several pairs of analogous atoms of the outermost dialkoxyphenylene groups is ca. 3.6 nm and the terminal Boc group is ca. 4.6 nm. This gave a relative elongation of ca. 60%.

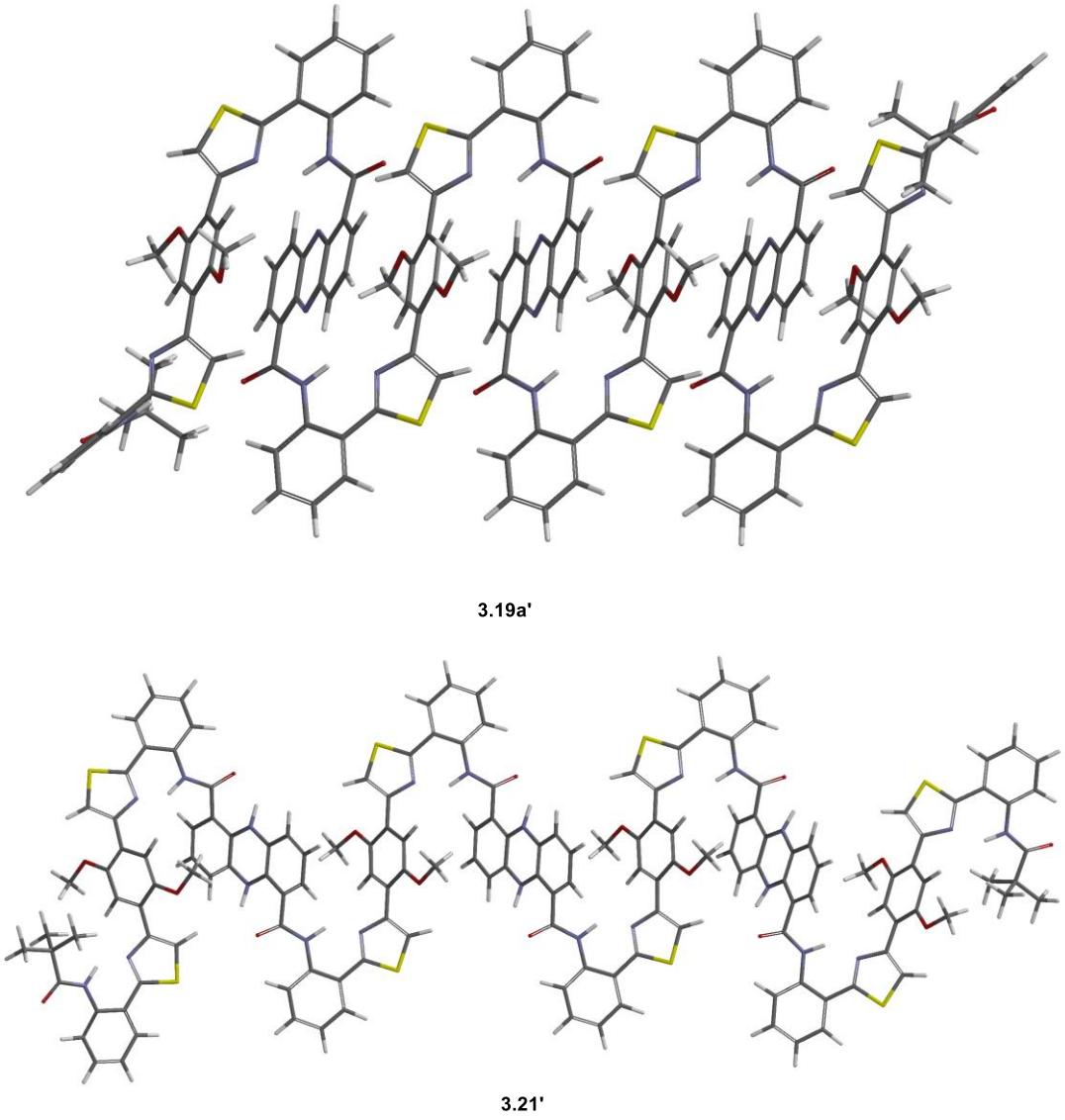

Figure 3-21. Computational model of **3.19a** and **3.21**.

On the other hand, DOSY estimated the diameter of **3.19a** to be:

$$\mathbf{R}_{3.19a} = (D_{TMSS} / D_{3.19a}) \times R_{TMSS}$$

$$= (9.99 \times 10^{-9}\ m^{-2}/s / 3.91 \times 10^{-9}\ m^{-2}/s) \times 0.80\ nm$$

$$= 2.04\ nm.$$

$\mathbf{R}_{3.20} = (D_{TMSS} / D_{3.21}) \times R_{TMSS}$

$= (9.99 \times 10^{-9}\ m^{-2}/s / 2.66 \times 10^{-9}\ m^{-2}/s) \times 0.80\ nm$

$= 3.00\ nm.$

This gave a relative elongation of ca. 50%, comparable to our calculation.

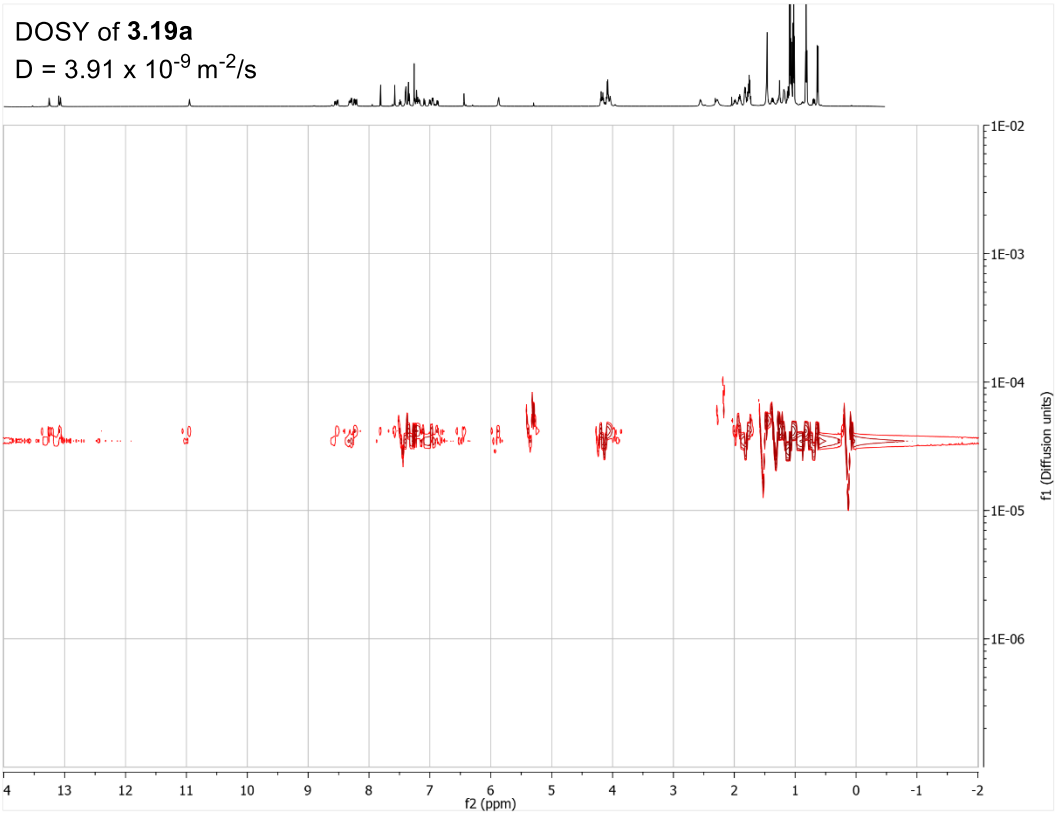

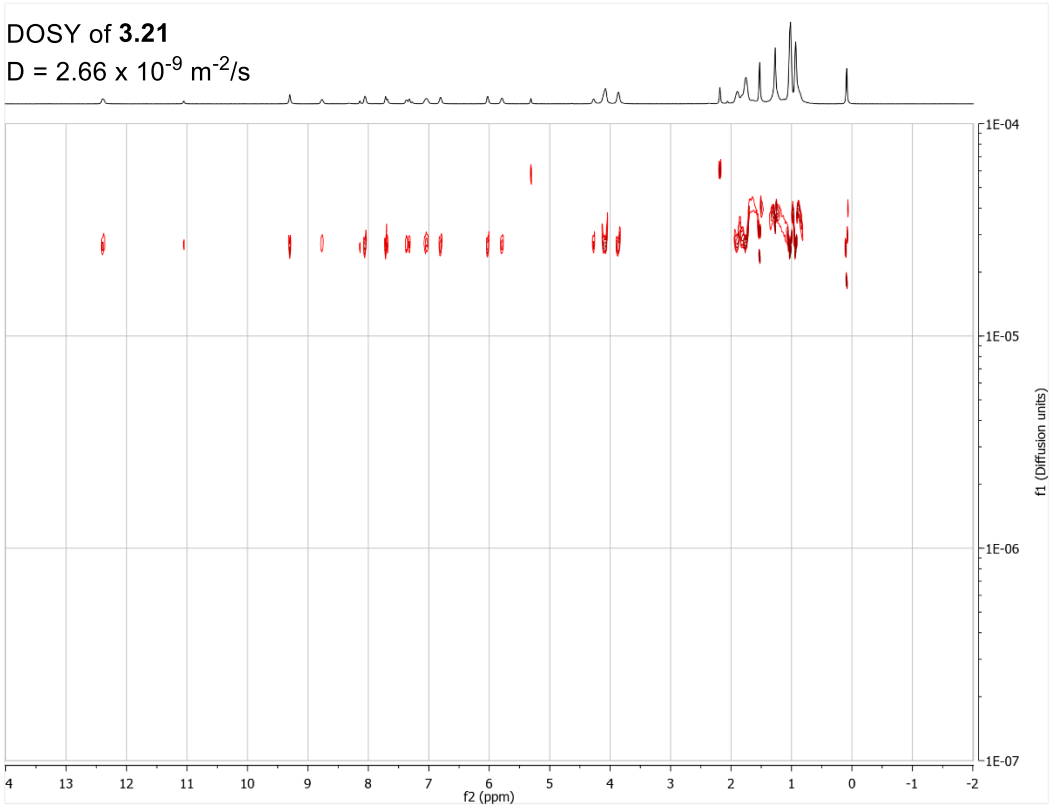

Figure 3-20. DOSY spectrum of **3.19a** and **3.21**.

DOSY estimated the diameter of **3.20** and **3.22** to be:

$\mathbf{R}_{3.20} = (D_{TMSS} / D_{3.20}) \times R_{TMSS}$

$= (9.99 \times 10^{-9}\ m^{-2}/s / 1.46 \times 10^{-10}\ m^{-2}/s) \times 0.80\ nm$

$= 5.47\ nm.$

$\mathbf{R}_{3.22} = (D_{TMSS} / D_{3.22}) \times R_{TMSS}$

$= (9.99 \times 10^{-9}\ m^{-2}/s / 1.12 \times 10^{-9}\ m^{-2}/s) \times 0.80\ nm$

$= 7.14\ nm.$

This gave a relative elongation of ca. 30%, comparable to our calculation.

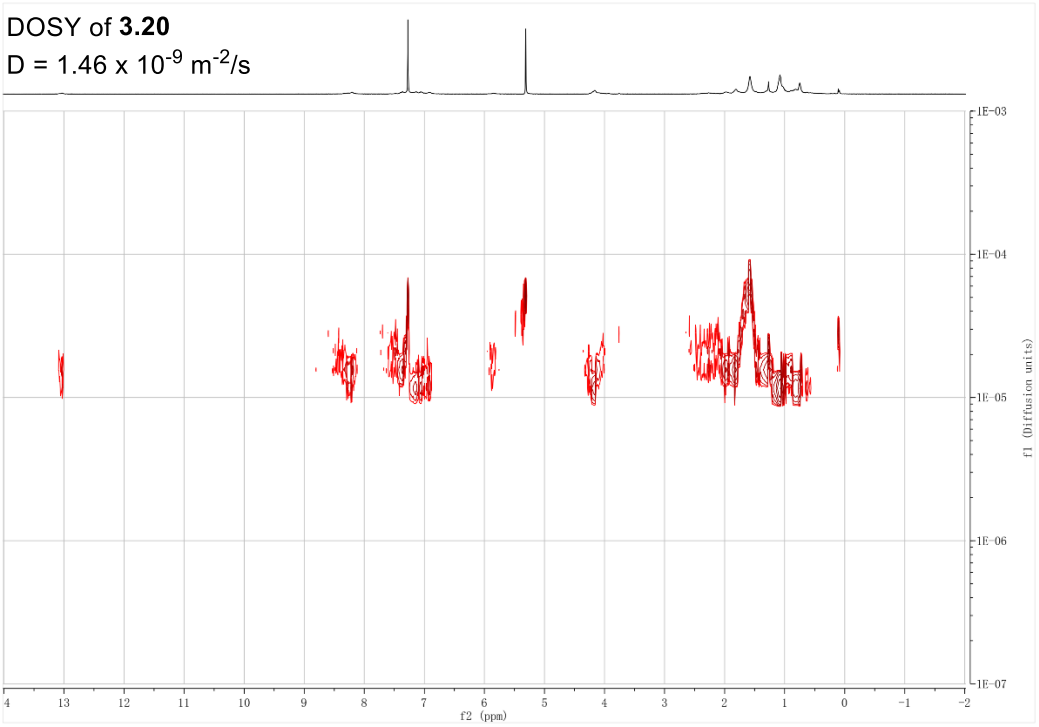

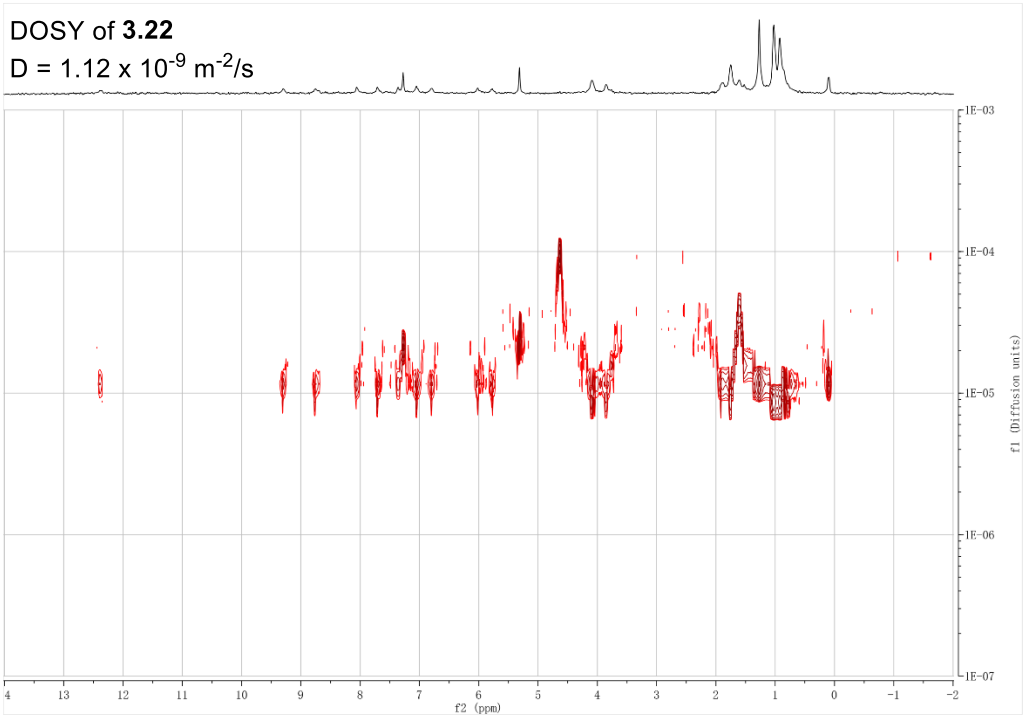

3.3.8. 1D NMR

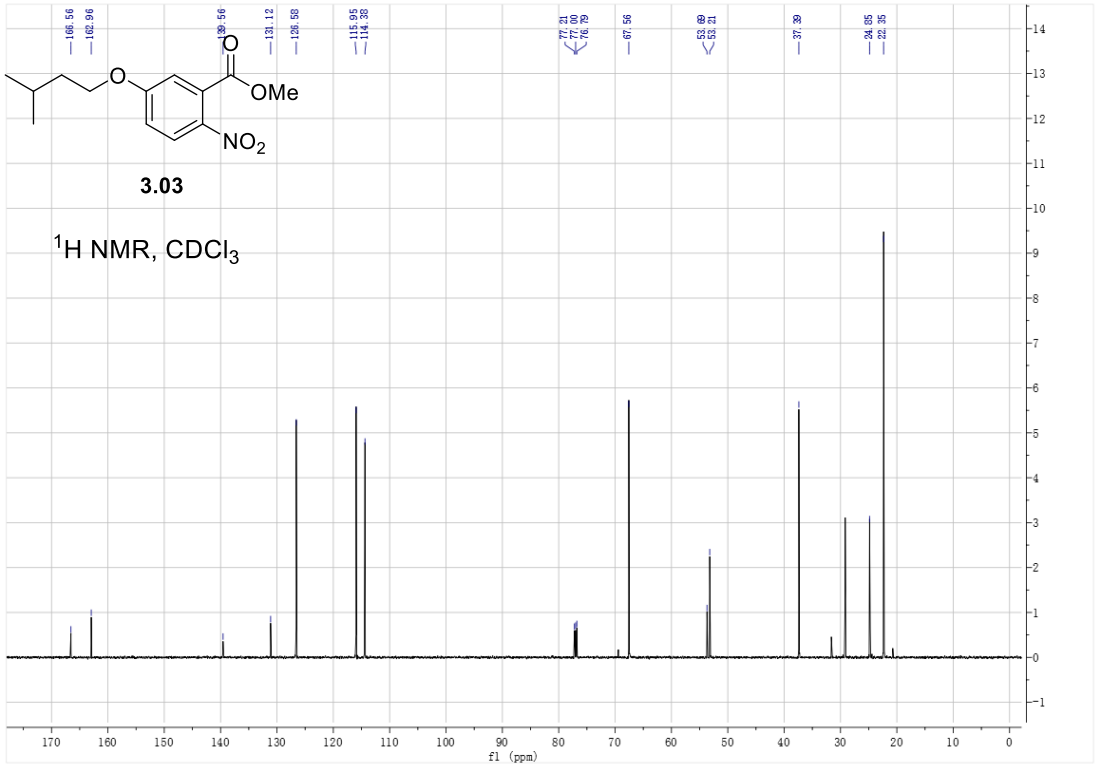
166.56
162.96
139.56
131.12
126.58
115.95
114.38
77.21
77.00
76.79
67.56
53.69
53.21
37.39
24.85
22.35
O
O
OMe
NO2
3.03
1H NMR, CDCl3
f1 (ppm)

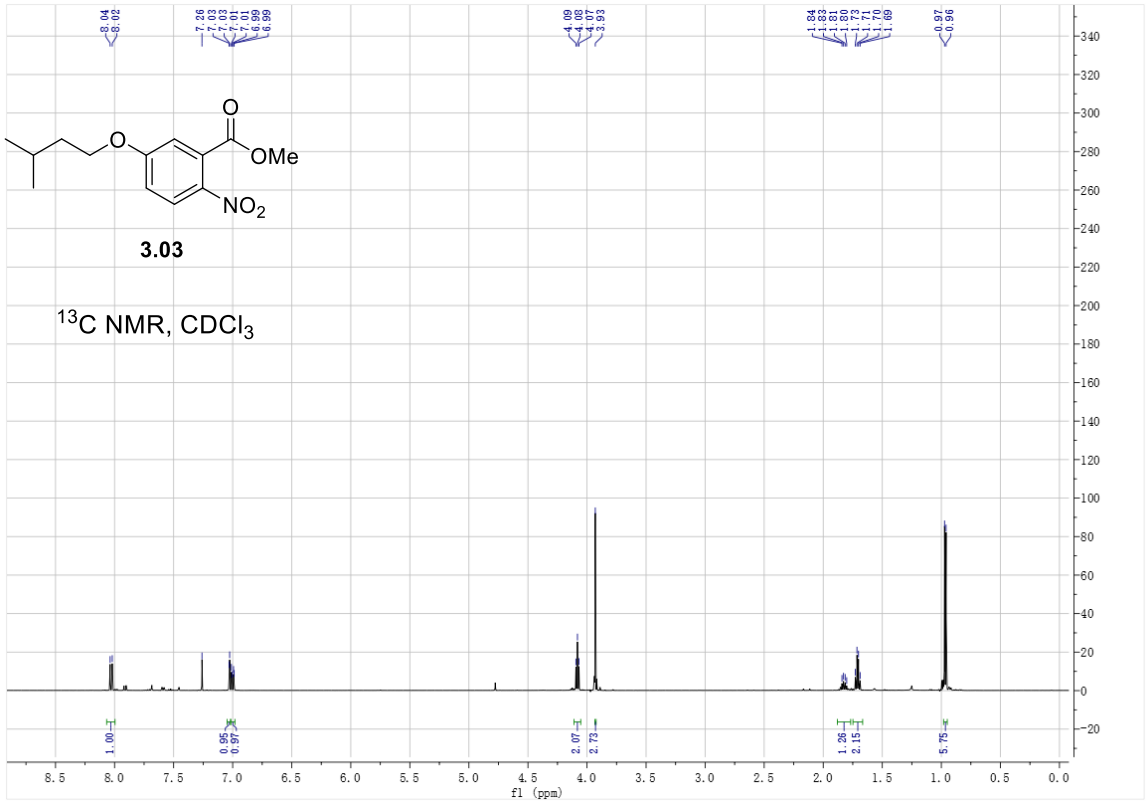
8.04
8.02
7.26
7.03
7.03
7.01
7.01
6.99
6.99
4.09
4.08
4.07
4.07
3.93
1.84
1.83
1.81
1.80
1.73
1.71
1.70
1.69
0.97
0.96
O
O
OMe
NO2
3.03
13C NMR, CDCl3
1.00
0.95
0.97
2.07
2.73
1.26
2.15
5.75
f1 (ppm)

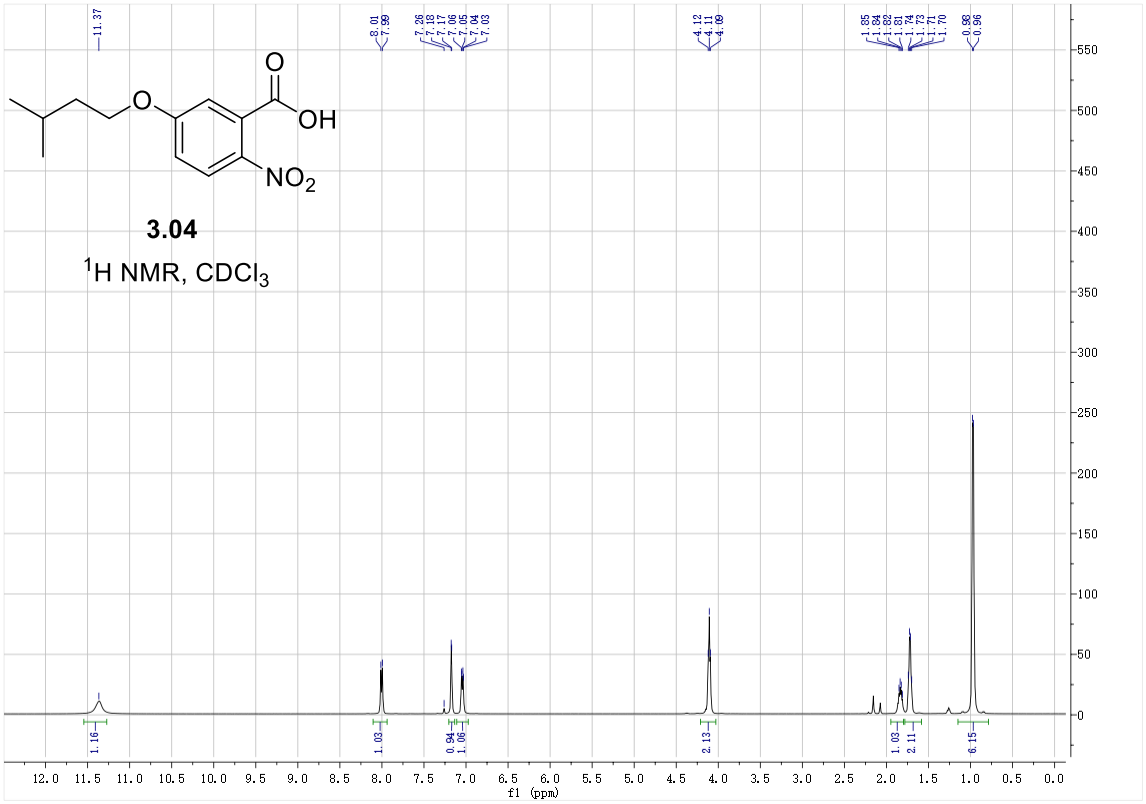
O
O
OH
NO2
3.04
1H NMR, CDCl3
f1 (ppm)

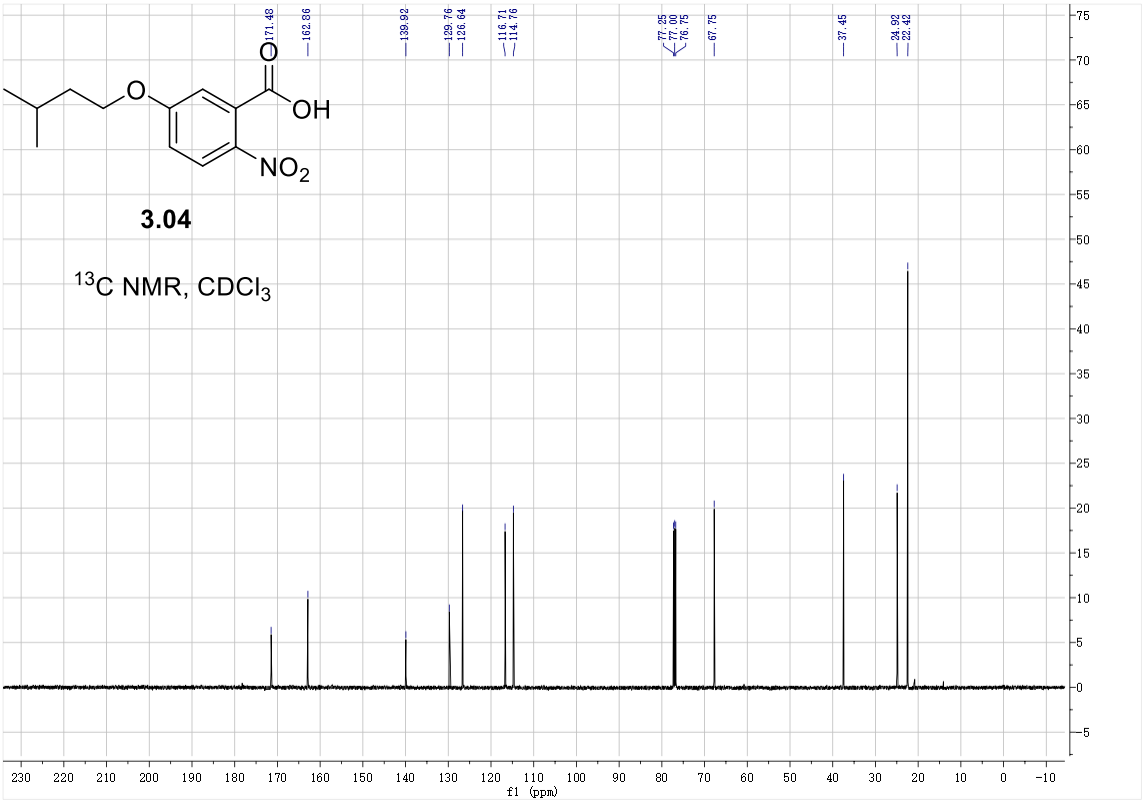
O
O
OH
NO2
3.04
13C NMR, CDCl3
f1 (ppm)

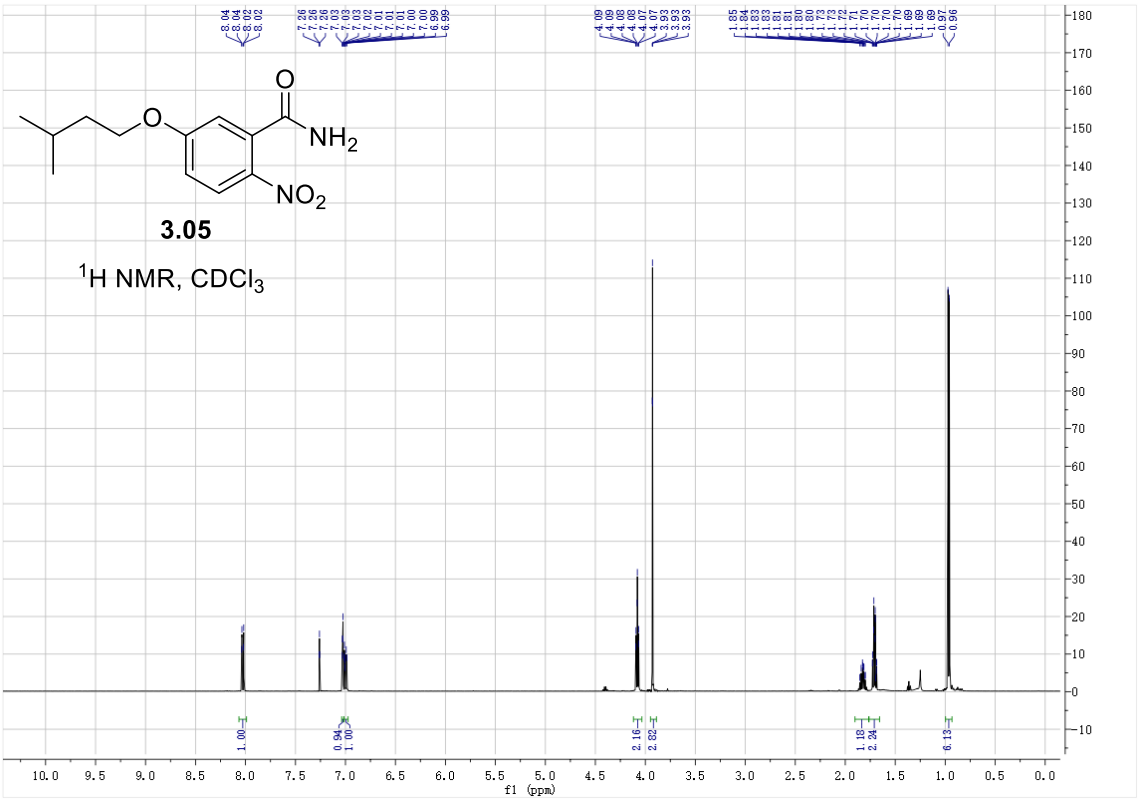
3.05
^{1}H NMR, $CDCl_3$
f1 (ppm)

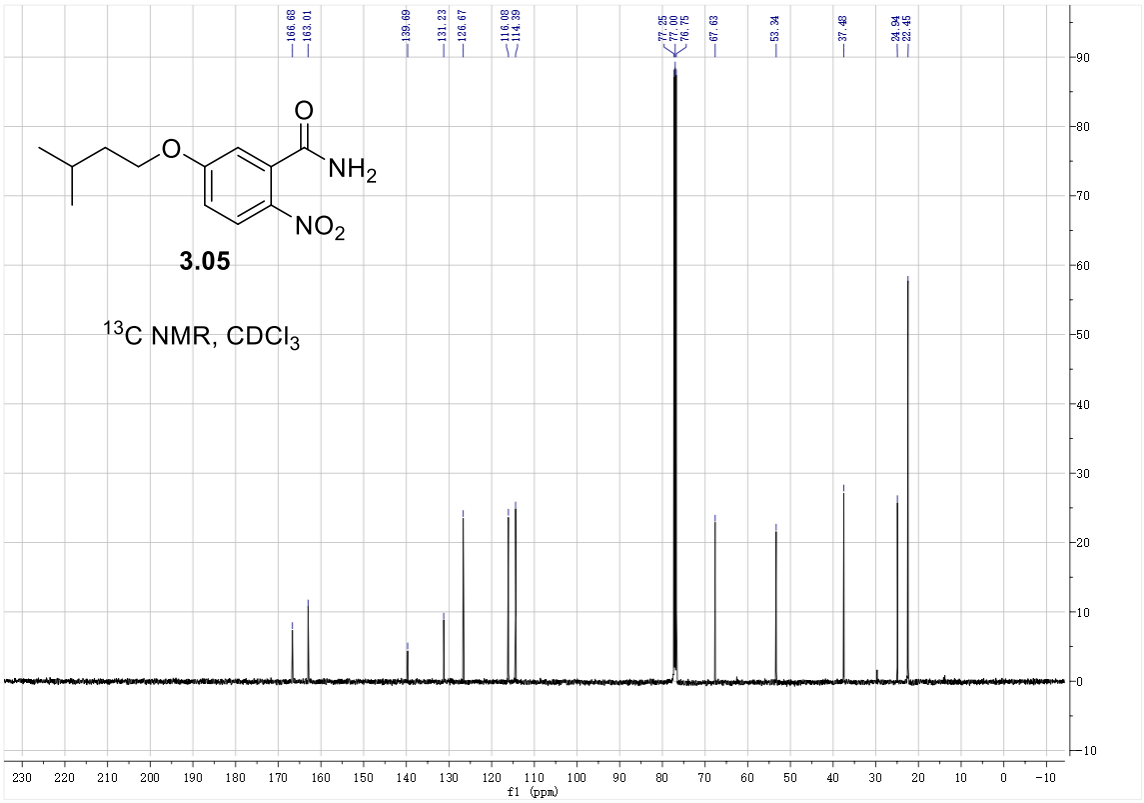
3.05
^{13}C NMR, $CDCl_3$
f1 (ppm)

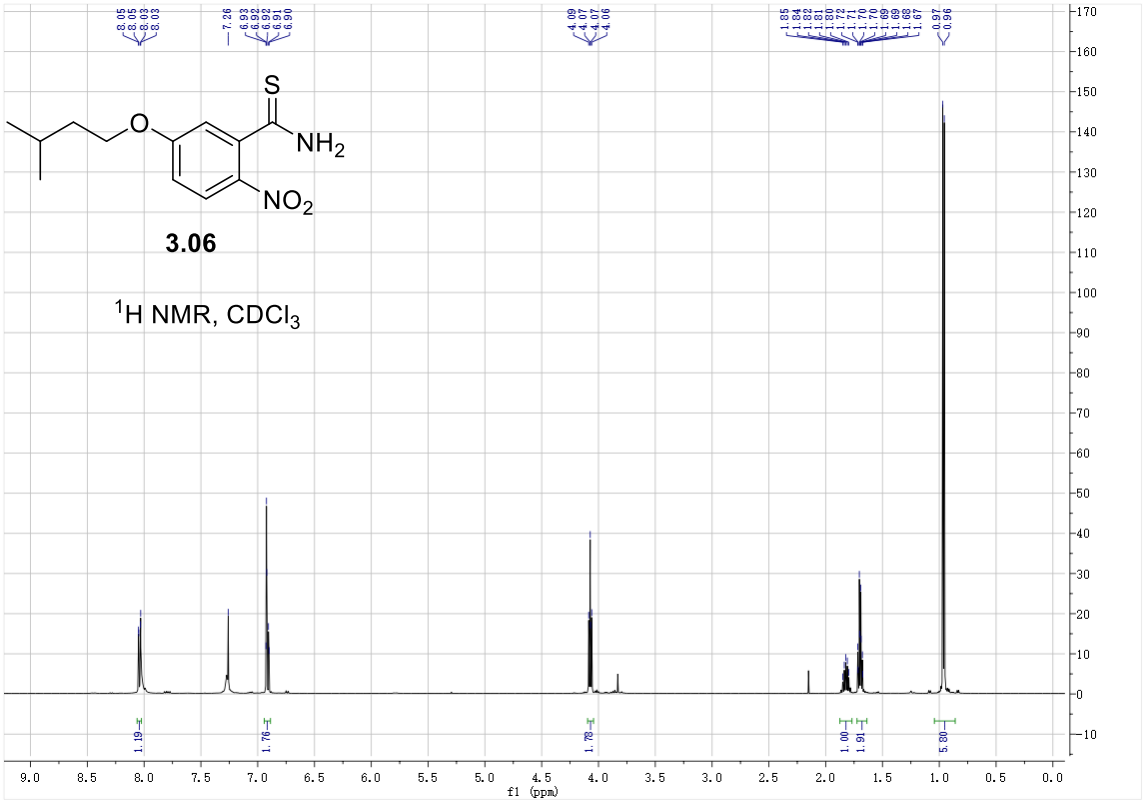
S
O
NH2
NO2
3.06
1H NMR, CDCl3
f1 (ppm)

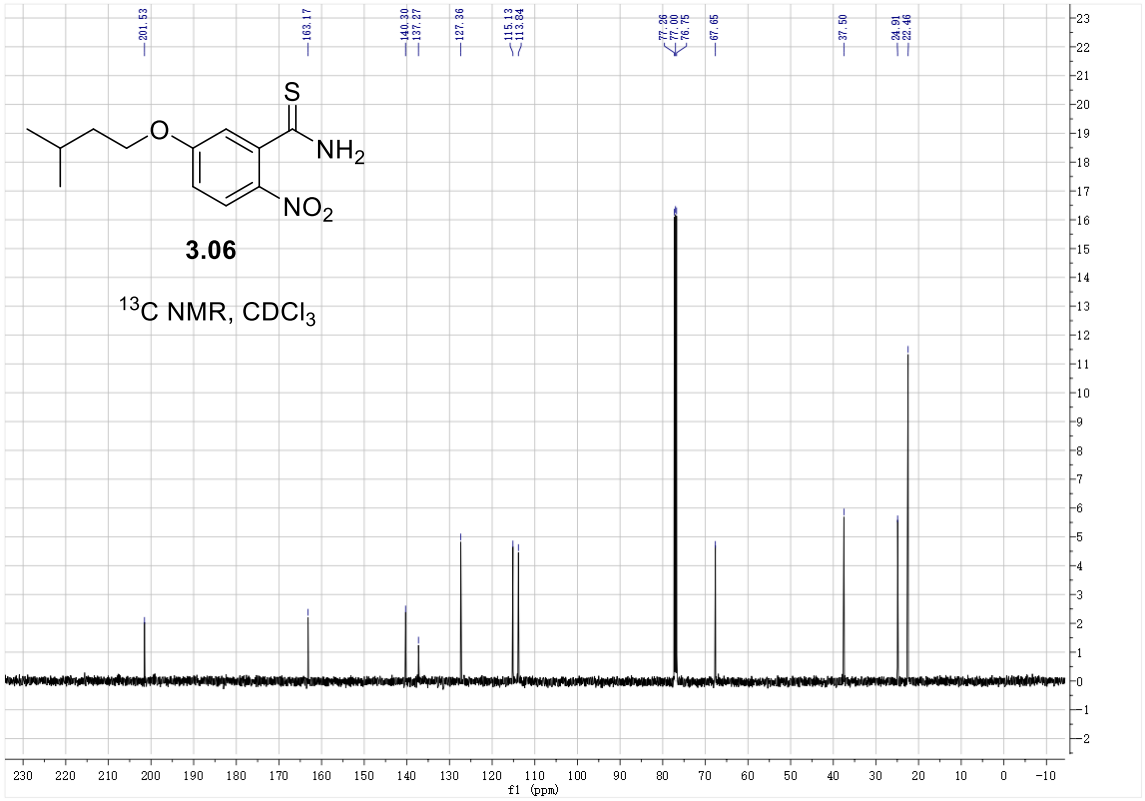
S
O
NH2
NO2
3.06
13C NMR, CDCl3
f1 (ppm)

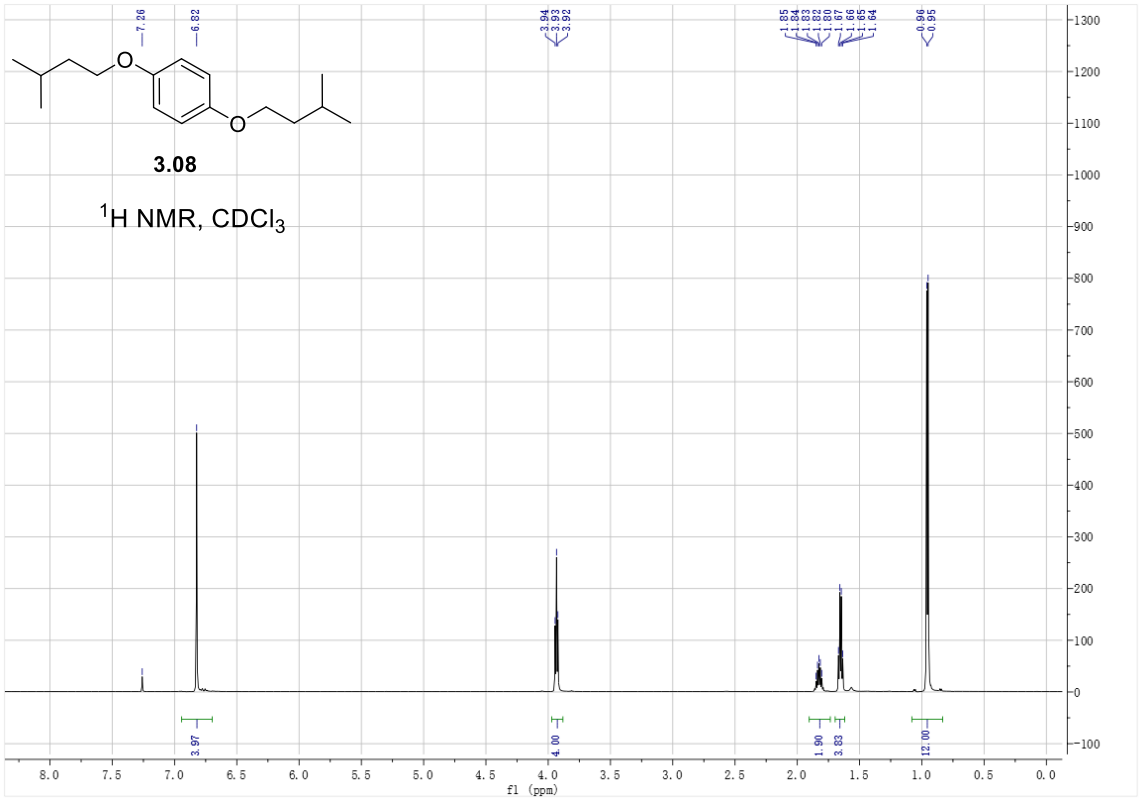
7.26
6.82
3.94
3.93
3.92
1.85
1.84
1.83
1.82
1.80
1.67
1.66
1.65
1.64
0.96
0.95
O
O
3.08
^{1}H NMR, CDCl$_3$
3.97
4.00
1.90
3.83
12.00
f1 (ppm)

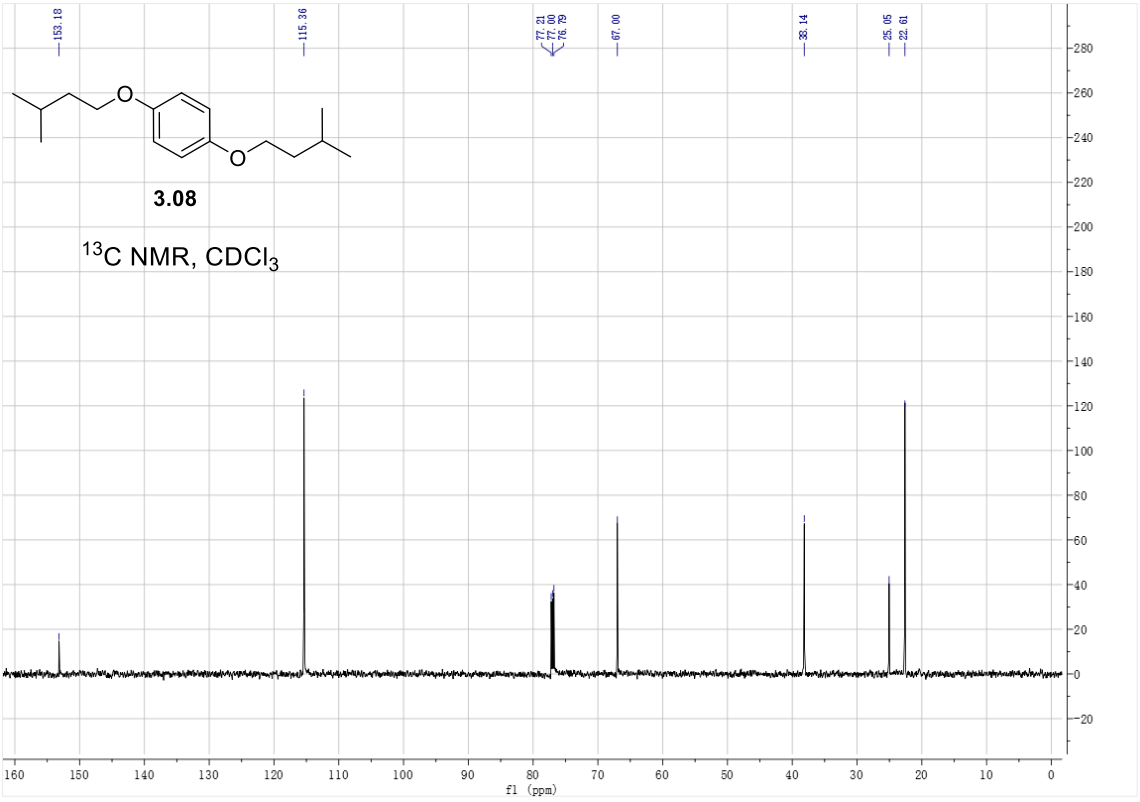
153.18
115.36
77.21
77.00
76.79
67.00
38.14
25.05
22.61
O
O
3.08
^{13}C NMR, CDCl$_3$
f1 (ppm)

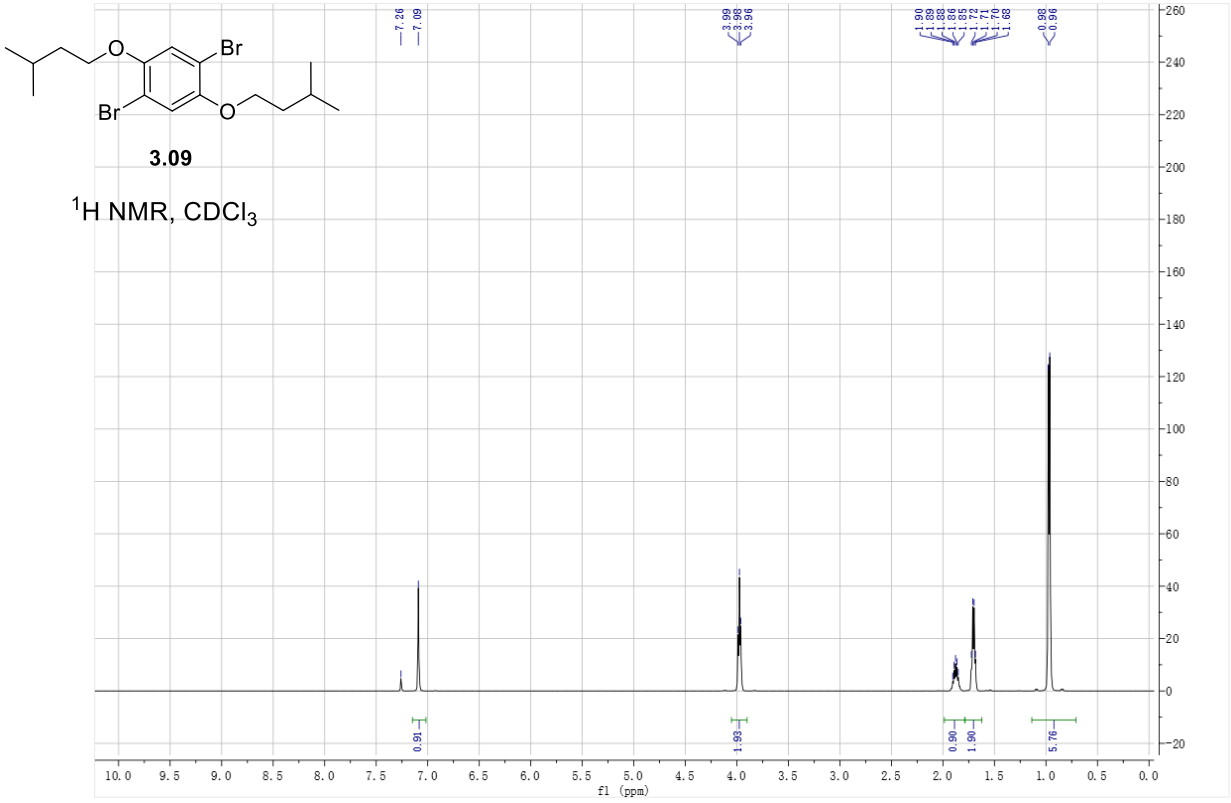
Br
O
Br
O
3.09
1H NMR, CDCl3
7.26
7.09
3.99
3.98
3.96
1.90
1.89
1.88
1.86
1.85
1.72
1.71
1.70
1.68
0.98
0.96
0.91
1.93
0.90
1.90
5.76
f1 (ppm)

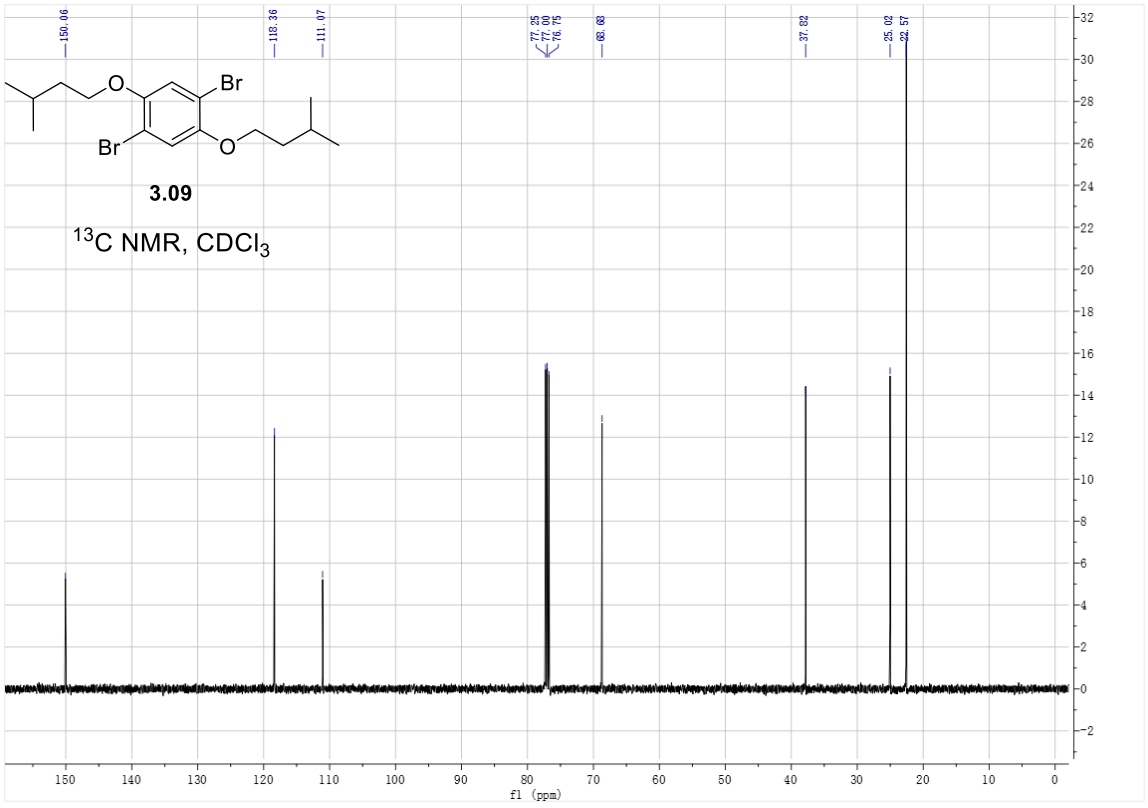
Br
O
Br
O
3.09
13C NMR, CDCl3
150.06
118.36
111.07
77.25
77.00
76.75
68.88
37.82
25.02
22.57
f1 (ppm)

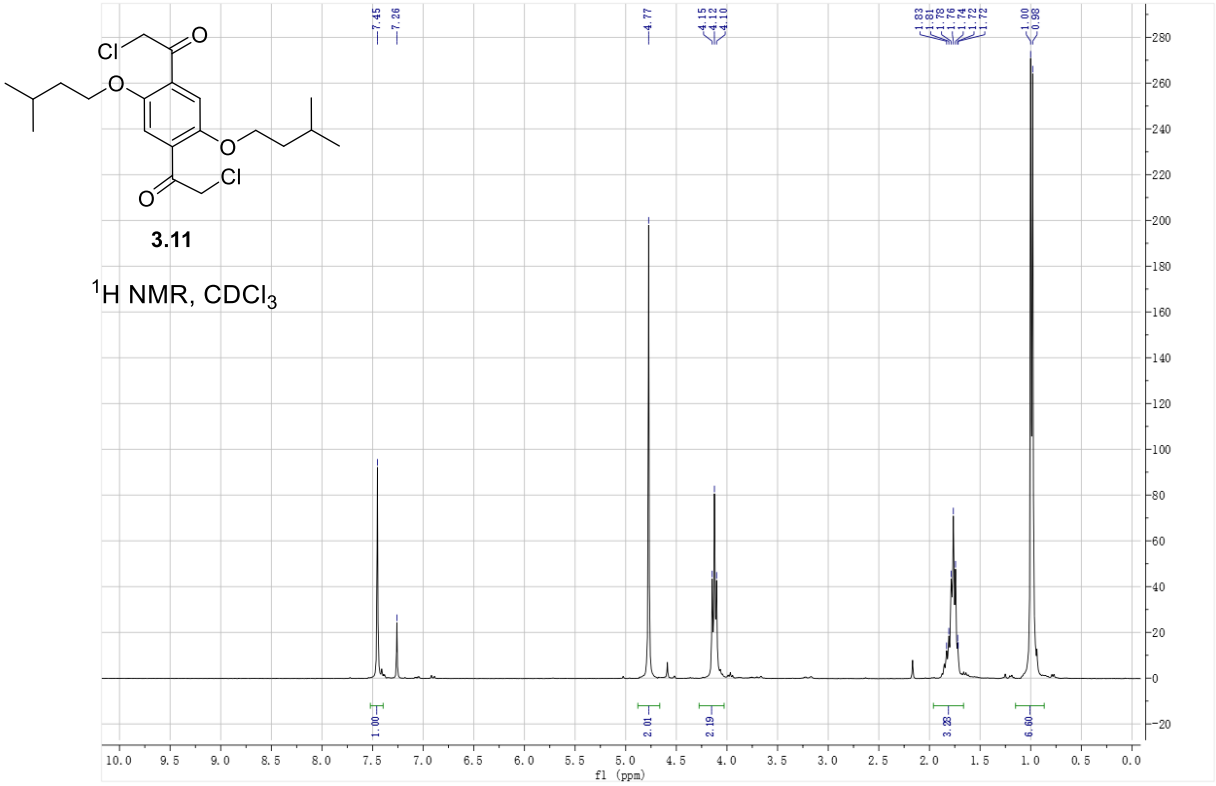
Cl
O
O
O
Cl
O
3.11
1H NMR, CDCl3
7.45
7.26
4.77
4.15
4.12
4.10
1.83
1.81
1.78
1.76
1.74
1.72
1.72
1.00
0.98
1.00
2.01
2.19
3.23
6.60
f1 (ppm)

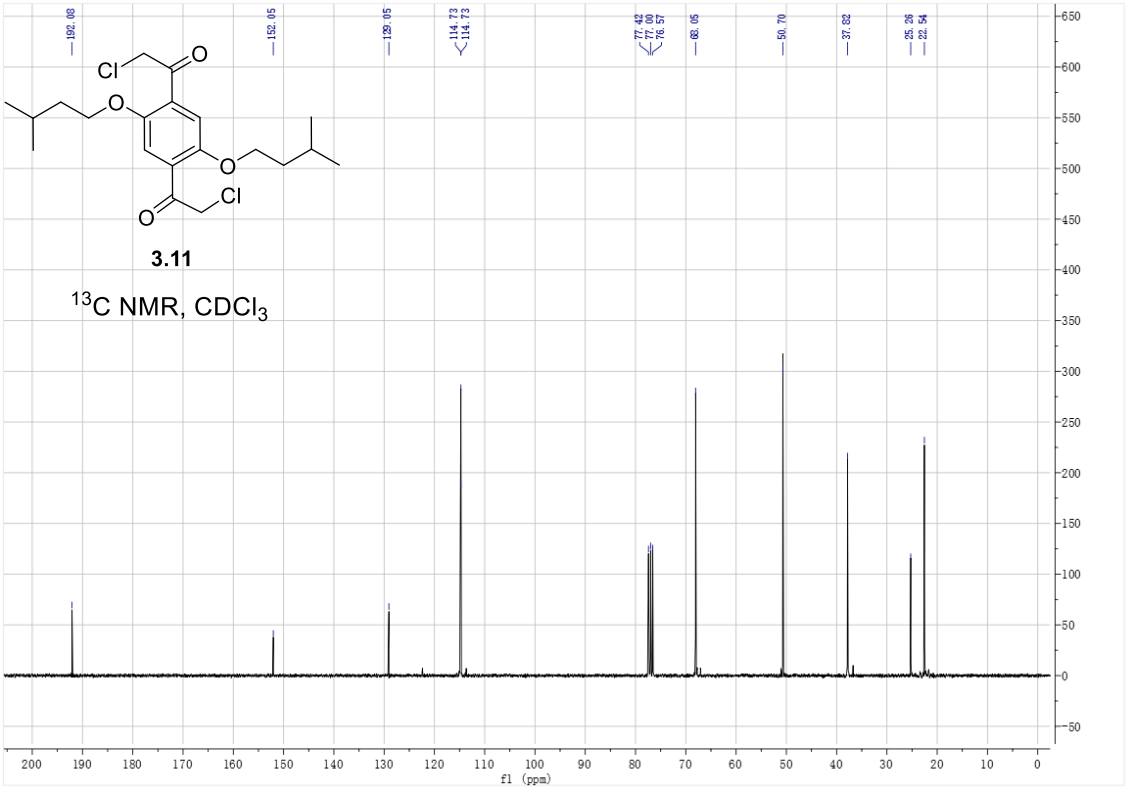
Cl
O
O
O
Cl
O
3.11
13C NMR, CDCl3
192.08
152.05
129.05
114.73
114.73
77.42
77.00
76.57
68.05
50.70
37.82
25.26
22.54
f1 (ppm)

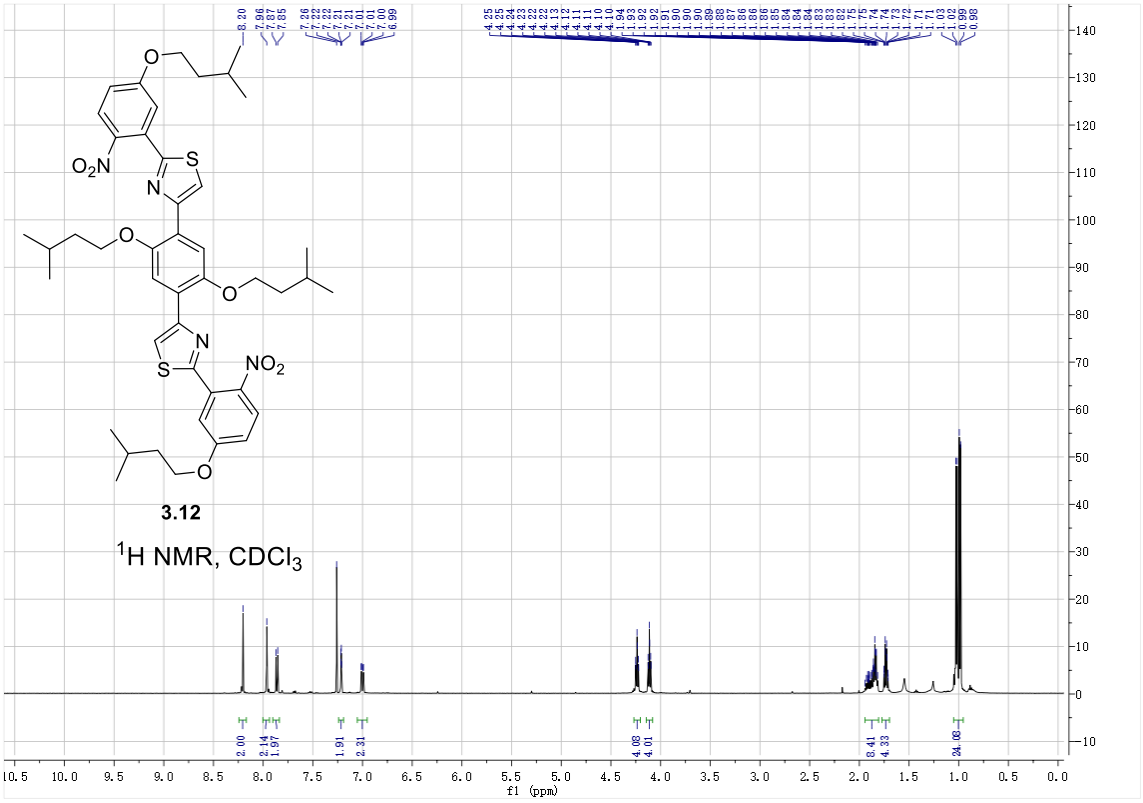
3.12
^{1}H NMR, CDCl$_3$
f1 (ppm)

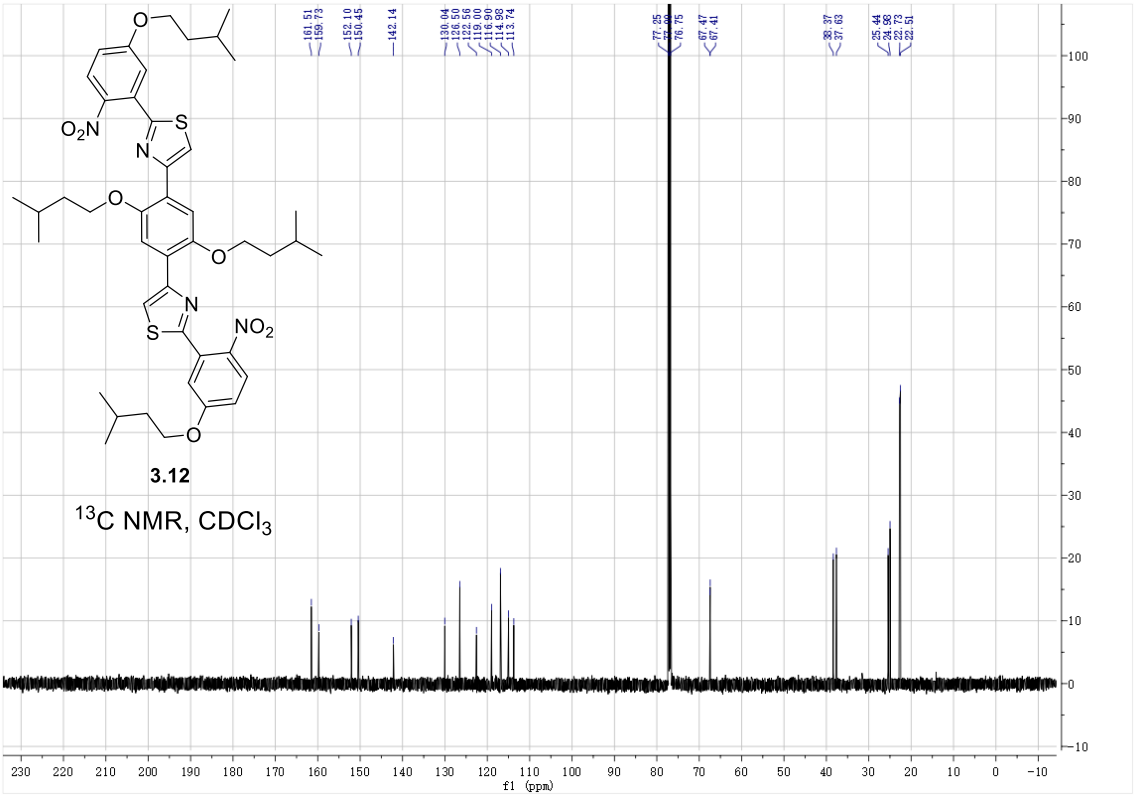
3.12
^{13}C NMR, CDCl$_3$
f1 (ppm)

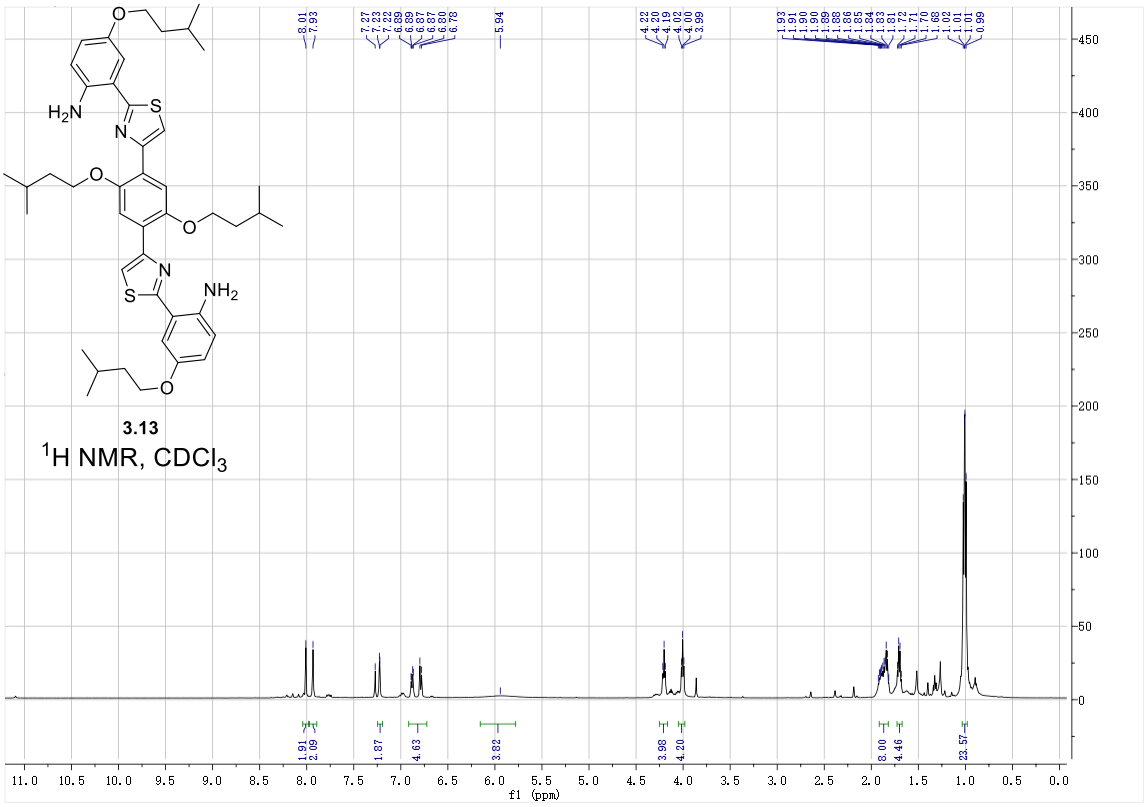
3.13
1H NMR, CDCl3
f1 (ppm)

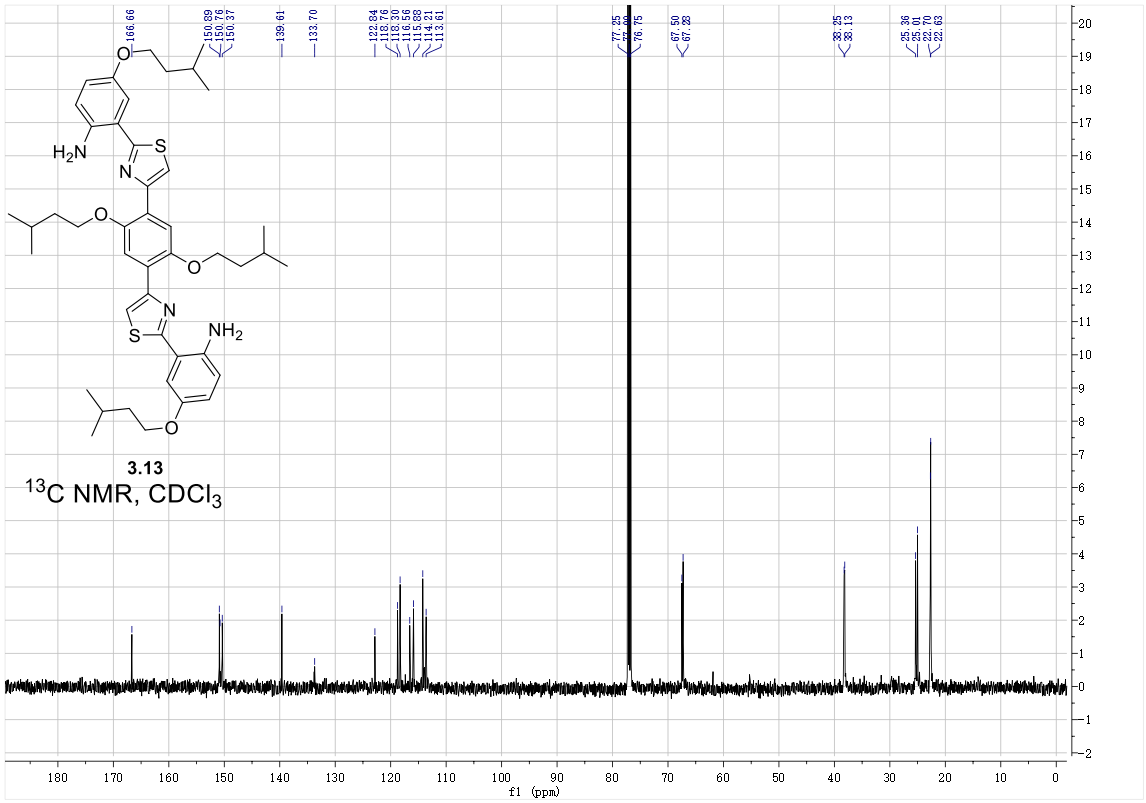
3.13
13C NMR, CDCl3
f1 (ppm)

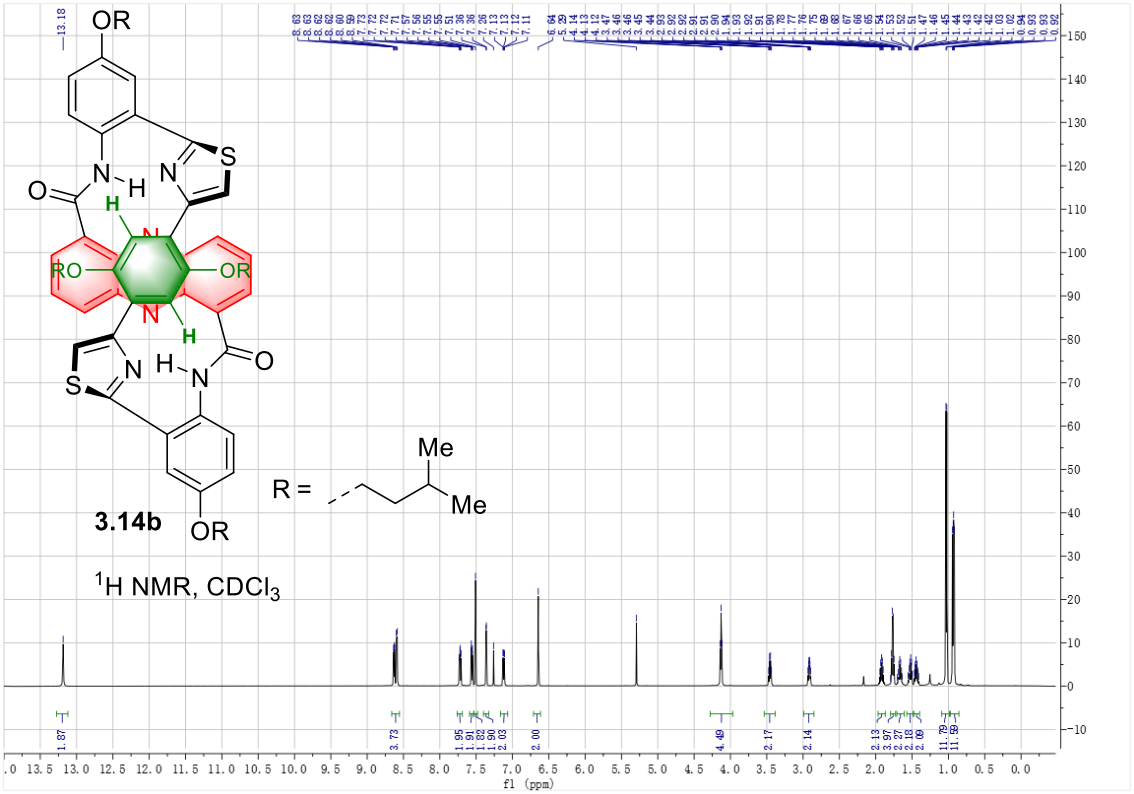
OR
RO
OR
OR
3.14b
R =
Me
Me
^{1}H NMR, CDCl$_3$
f1 (ppm)

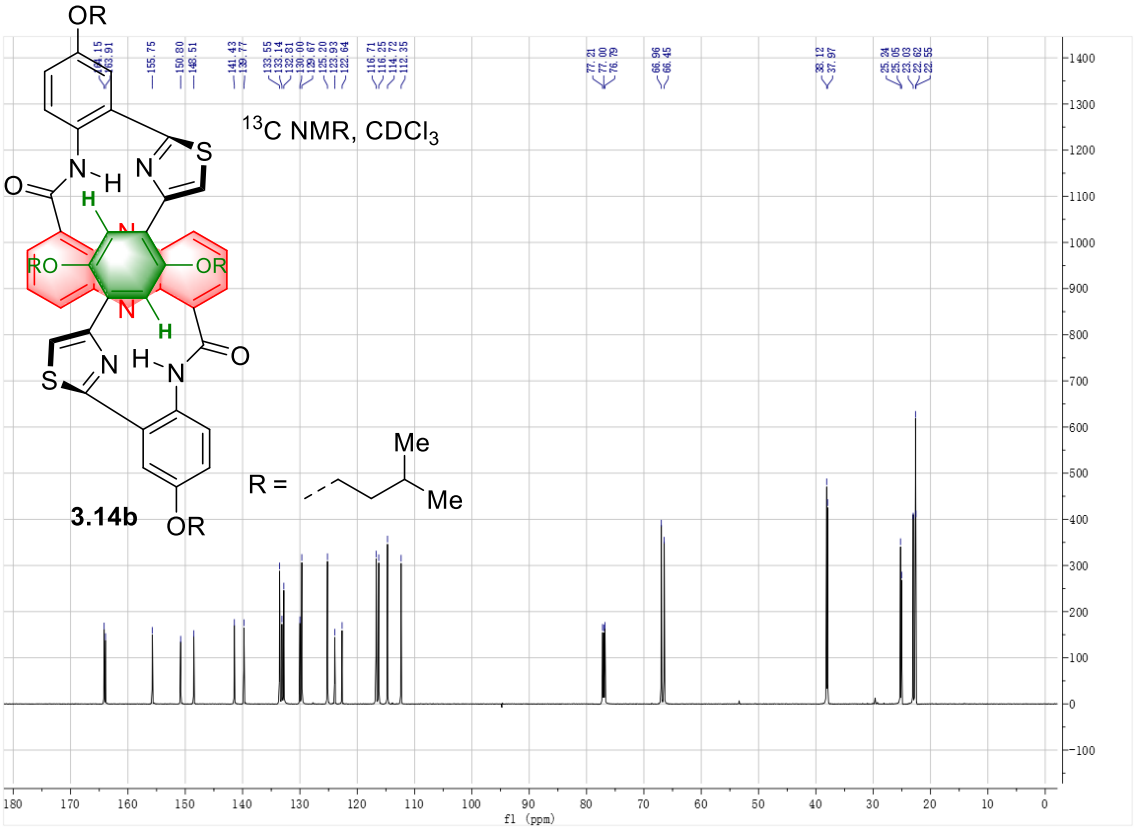
OR
RO
OR
OR
3.14b
R =
Me
Me
^{13}C NMR, CDCl$_3$
f1 (ppm)

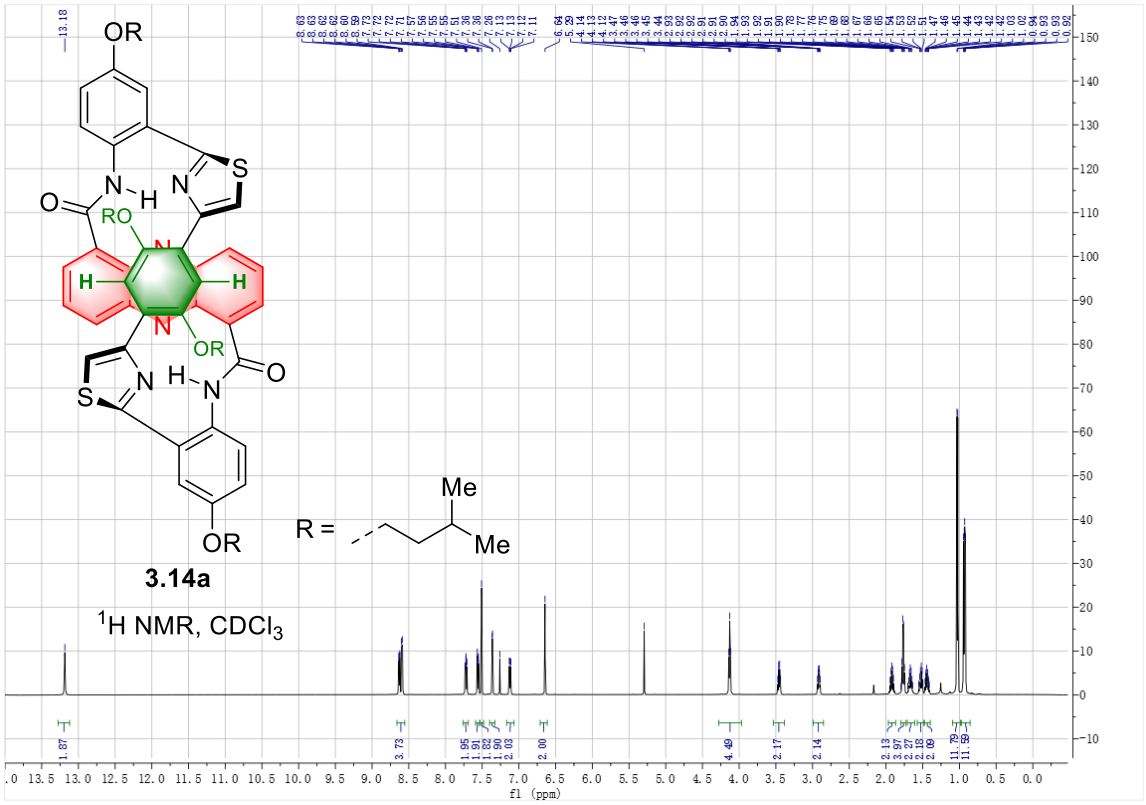
OR
RO
OR
R =
Me
Me
3.14a
^{1}H NMR, CDCl$_3$
f1 (ppm)

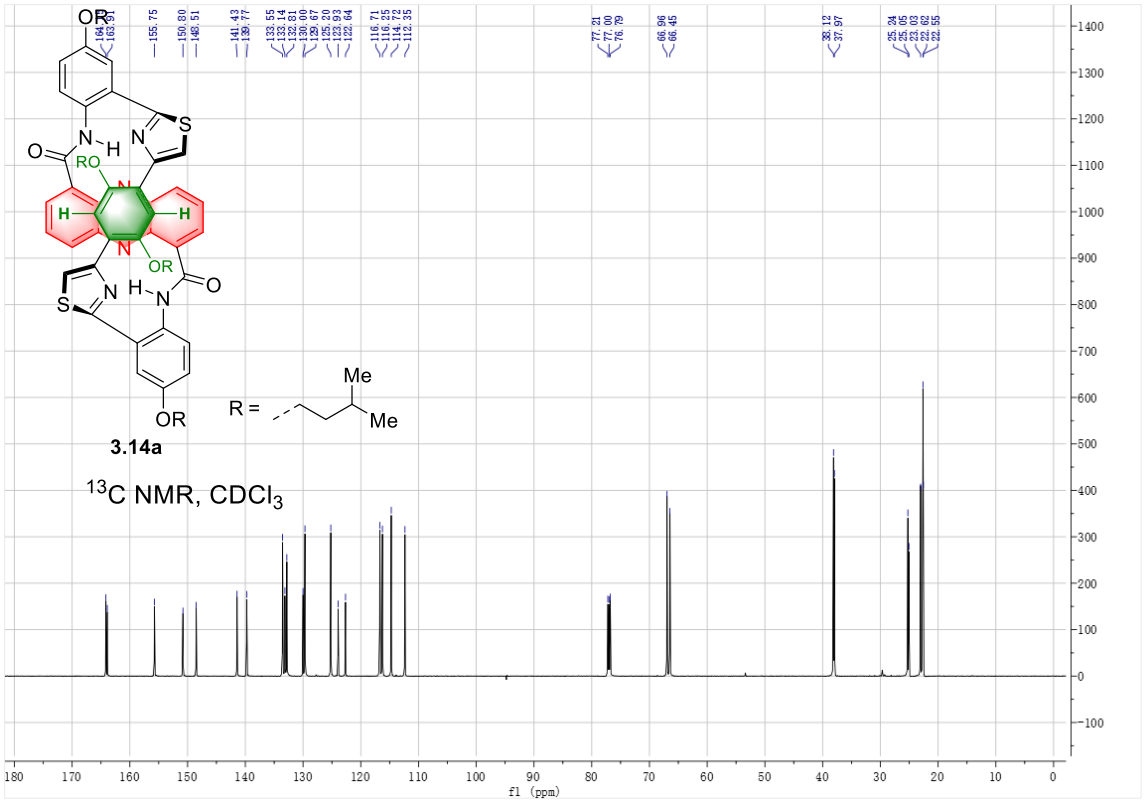
OR
RO
OR
R =
Me
Me
3.14a
^{13}C NMR, CDCl$_3$
f1 (ppm)

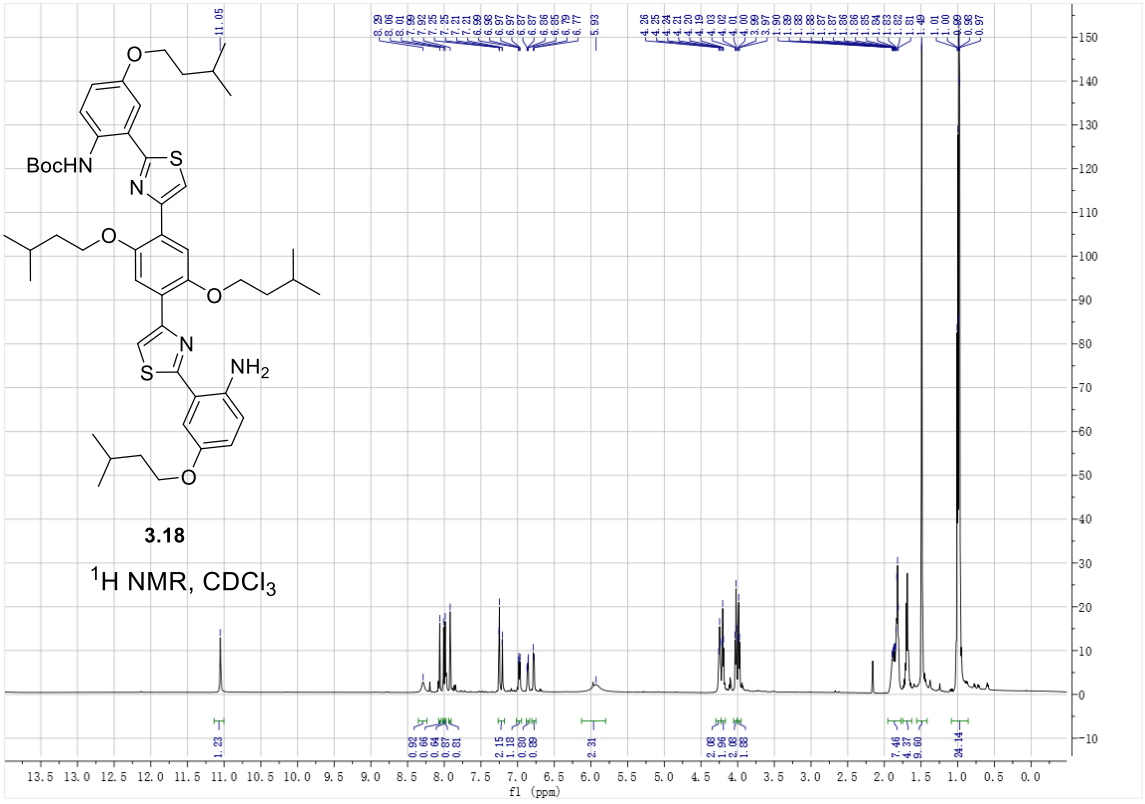
BocHN
NH2
3.18
1H NMR, CDCl3

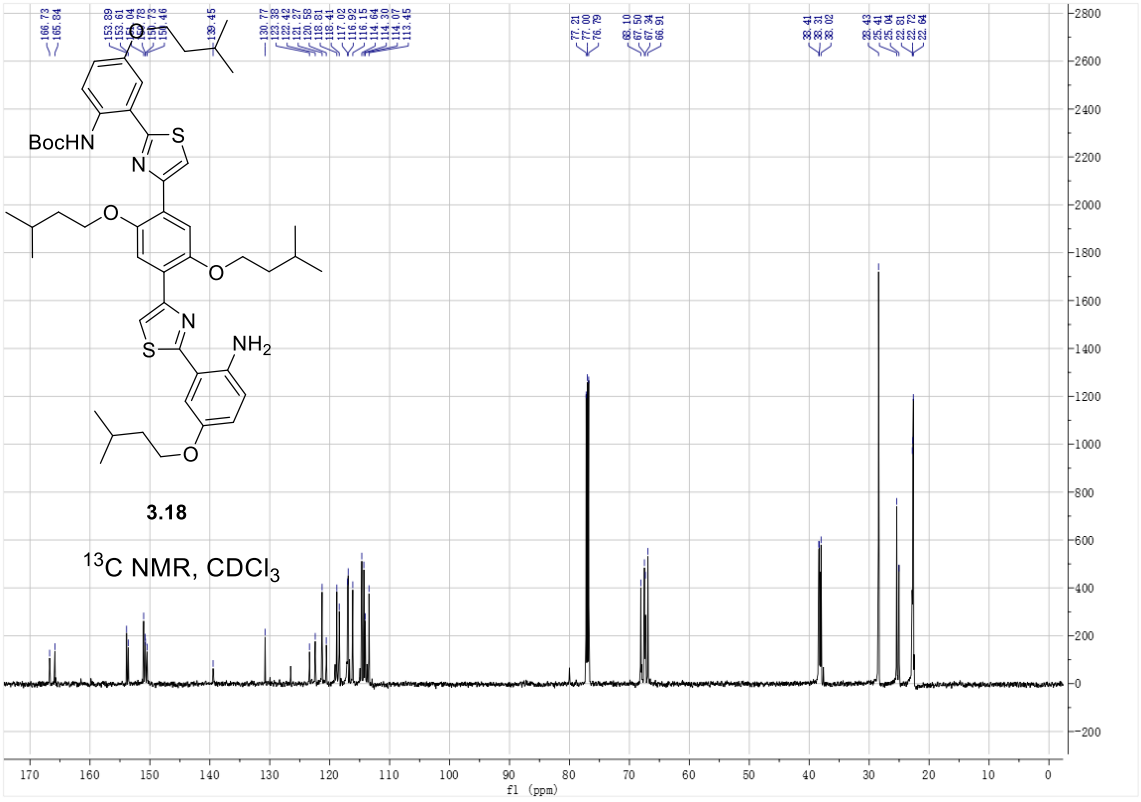
BocHN
NH2
3.18
13C NMR, CDCl3

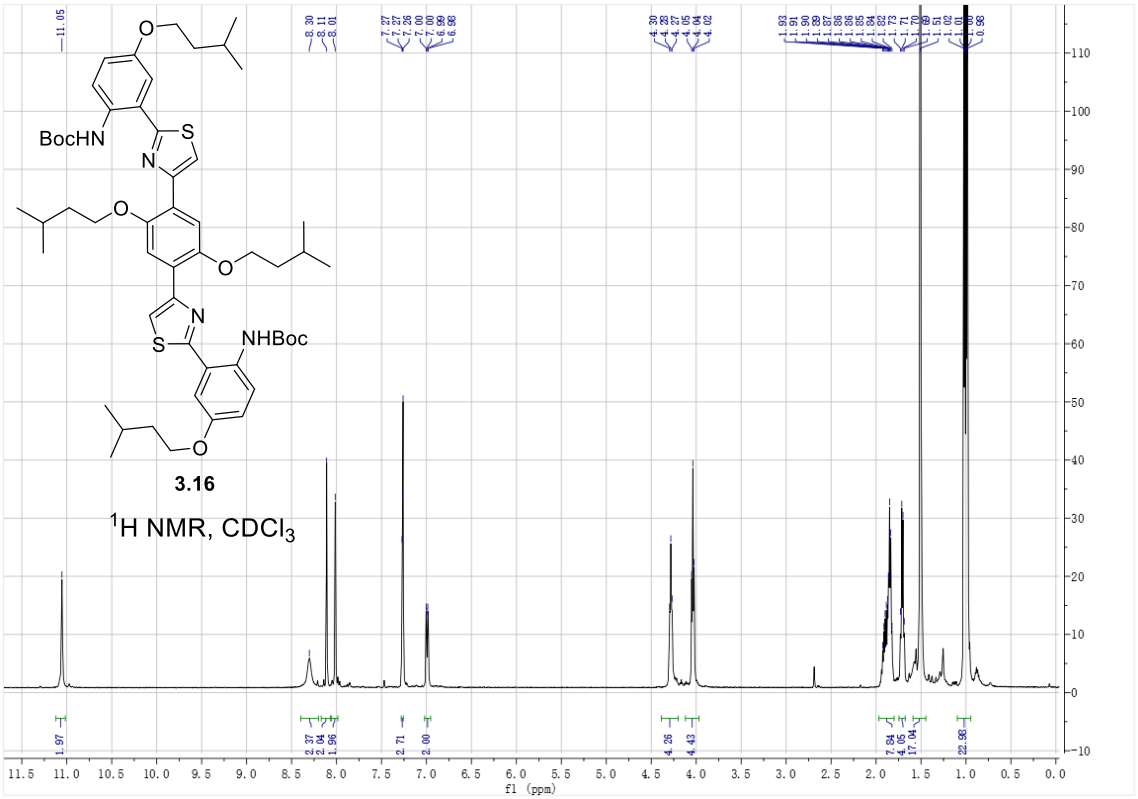
BocHN
NHBoc
3.16
^{1}H NMR, CDCl$_3$
f1 (ppm)

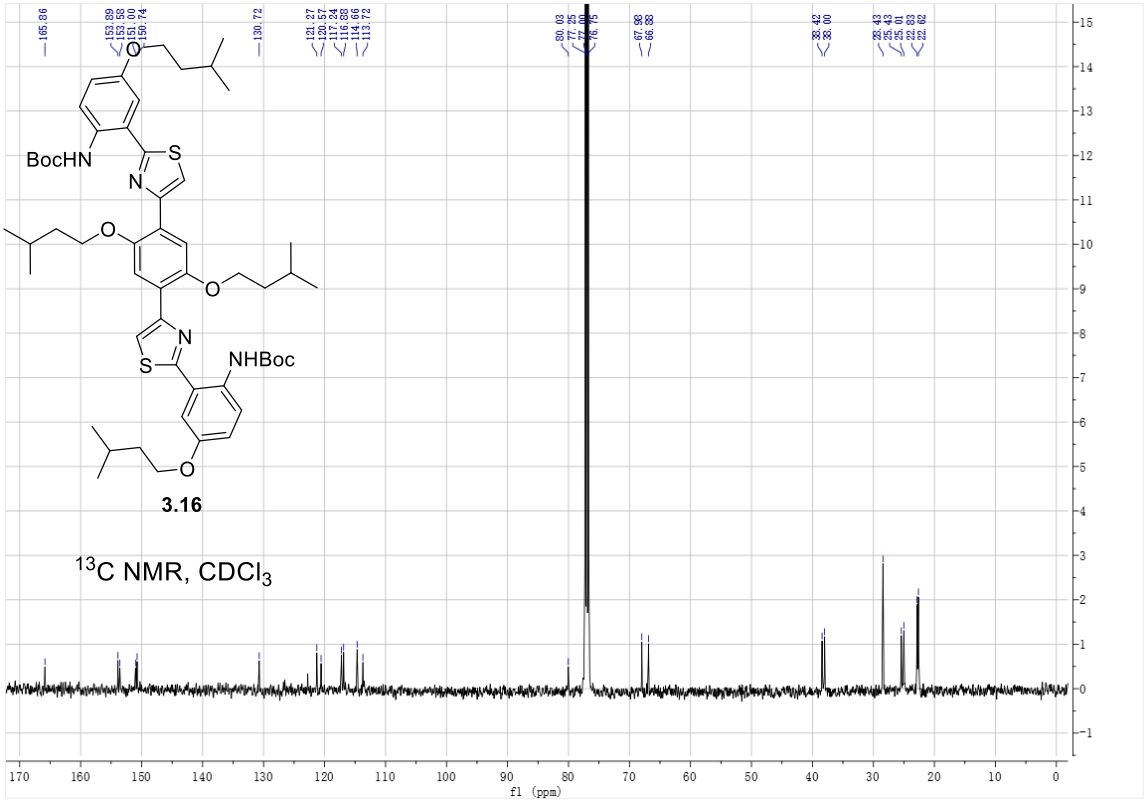
BocHN
NHBoc
3.16
^{13}C NMR, CDCl$_3$
f1 (ppm)

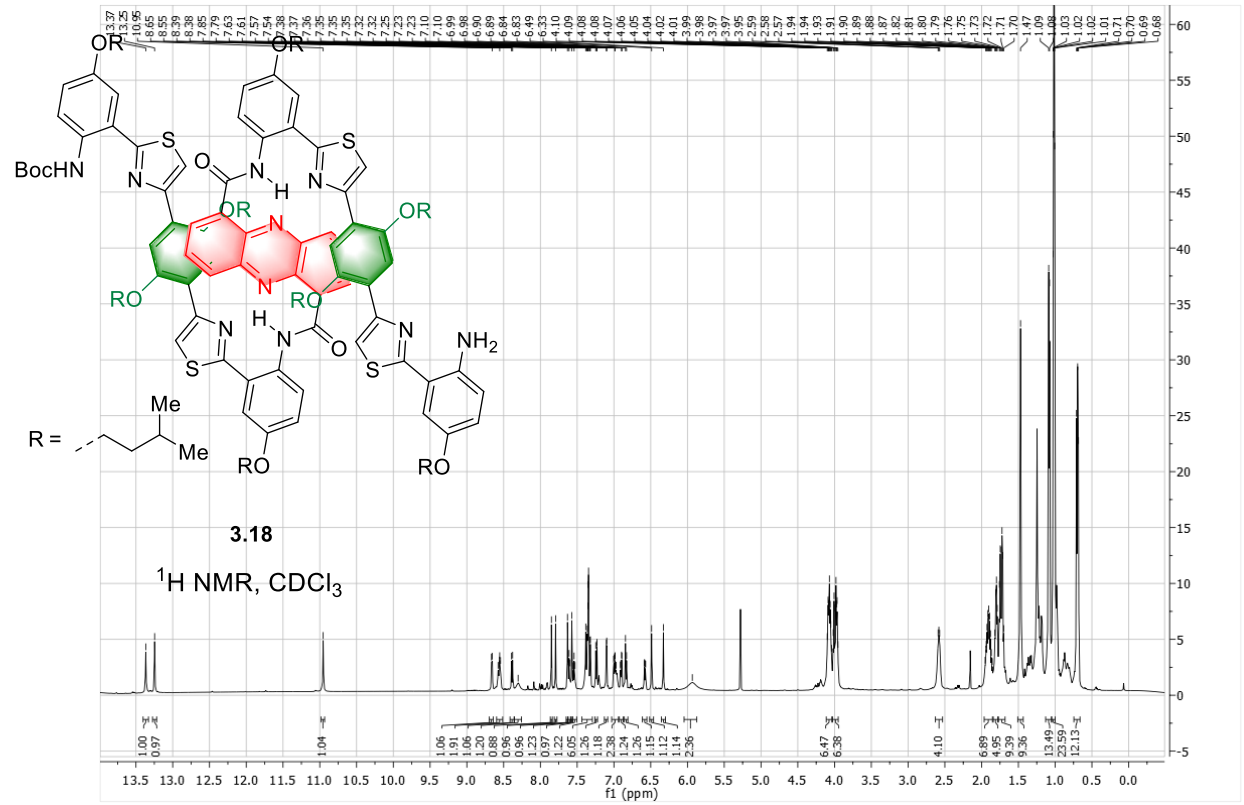
OR
BocHN
S
N
O
N
H
RO
NH2
Me
Me
R =
3.18
1H NMR, CDCl3
f1 (ppm)

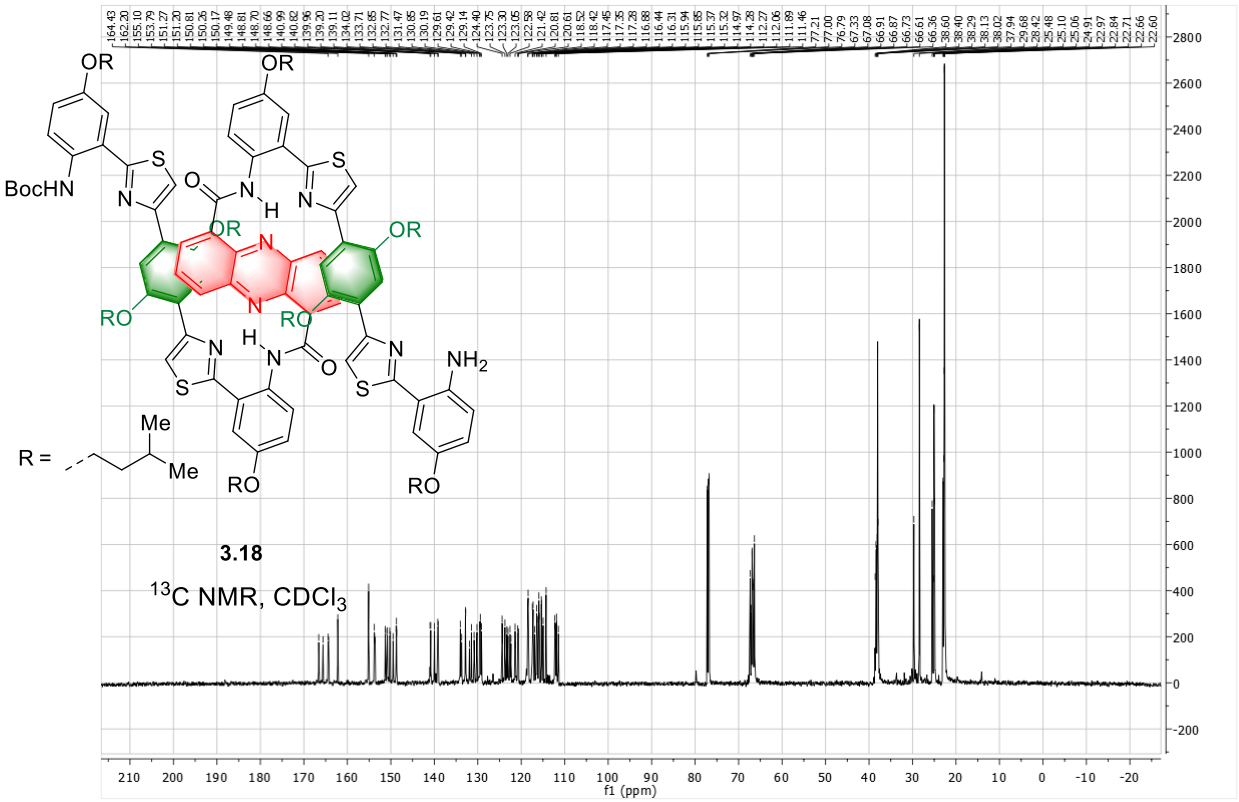
OR
BocHN
S
N
O
N
H
RO
NH2
Me
Me
R =
3.18
13C NMR, CDCl3
f1 (ppm)

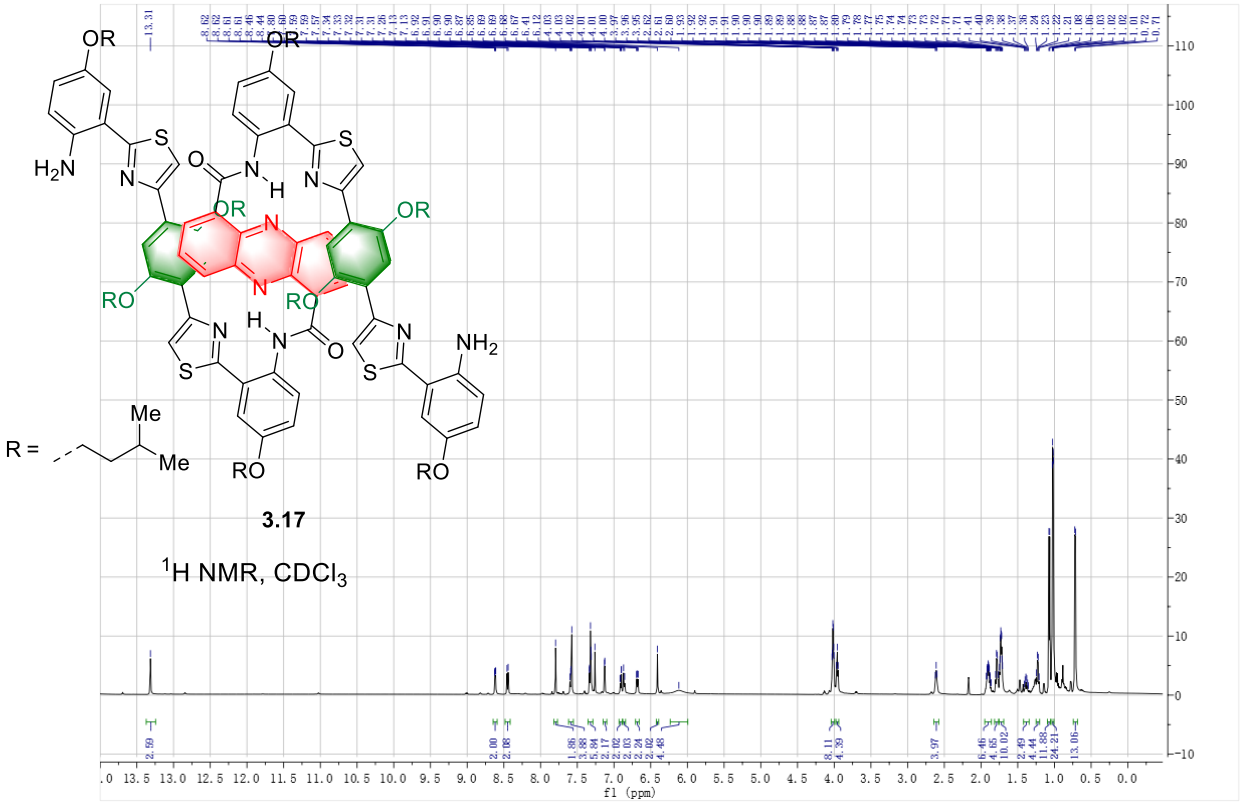
OR
OR
H2N
S
N
O
N
H
OR
N
OR
RO
RO
N
H
N
O
N
NH2
S
S
Me
R =
Me
RO
RO
3.17
1H NMR, CDCl3
fl (ppm)

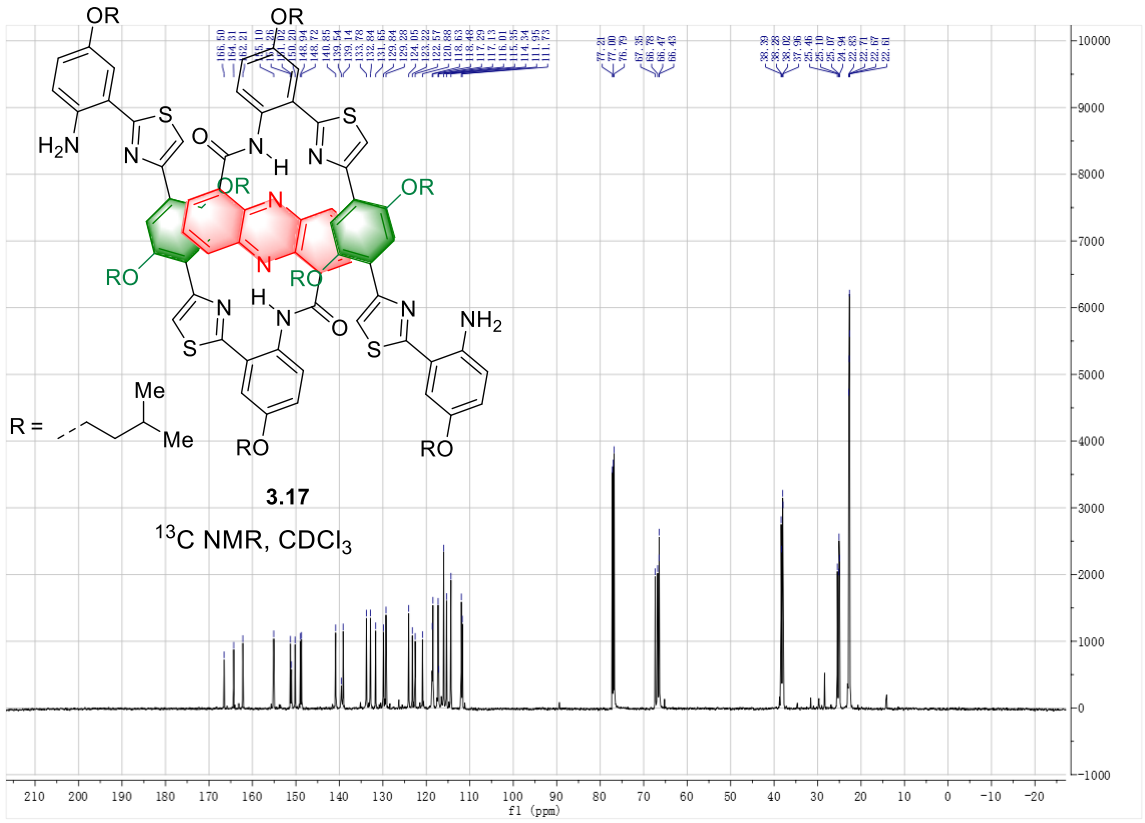
OR
OR
H2N
S
N
O
N
H
OR
N
OR
RO
RO
N
H
N
O
N
NH2
S
S
Me
R =
Me
RO
RO
3.17
13C NMR, CDCl3
fl (ppm)

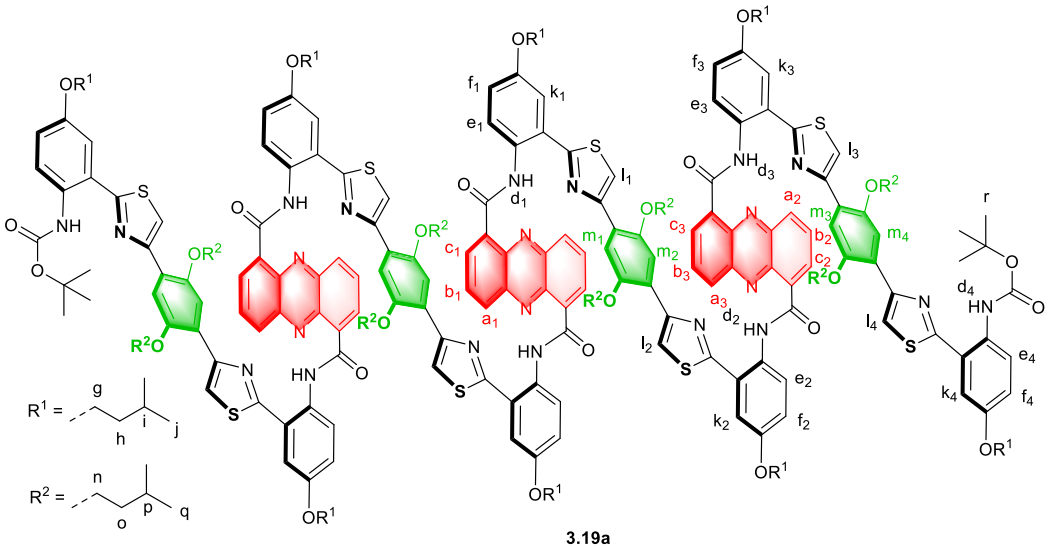

3.19a

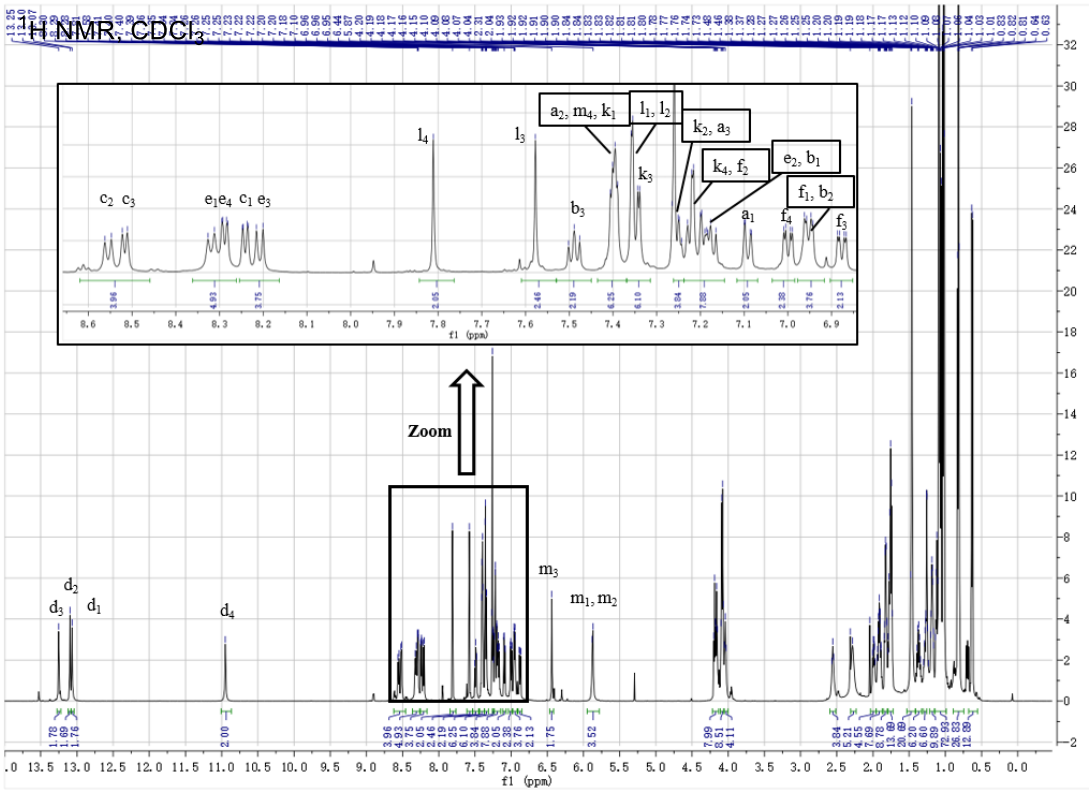

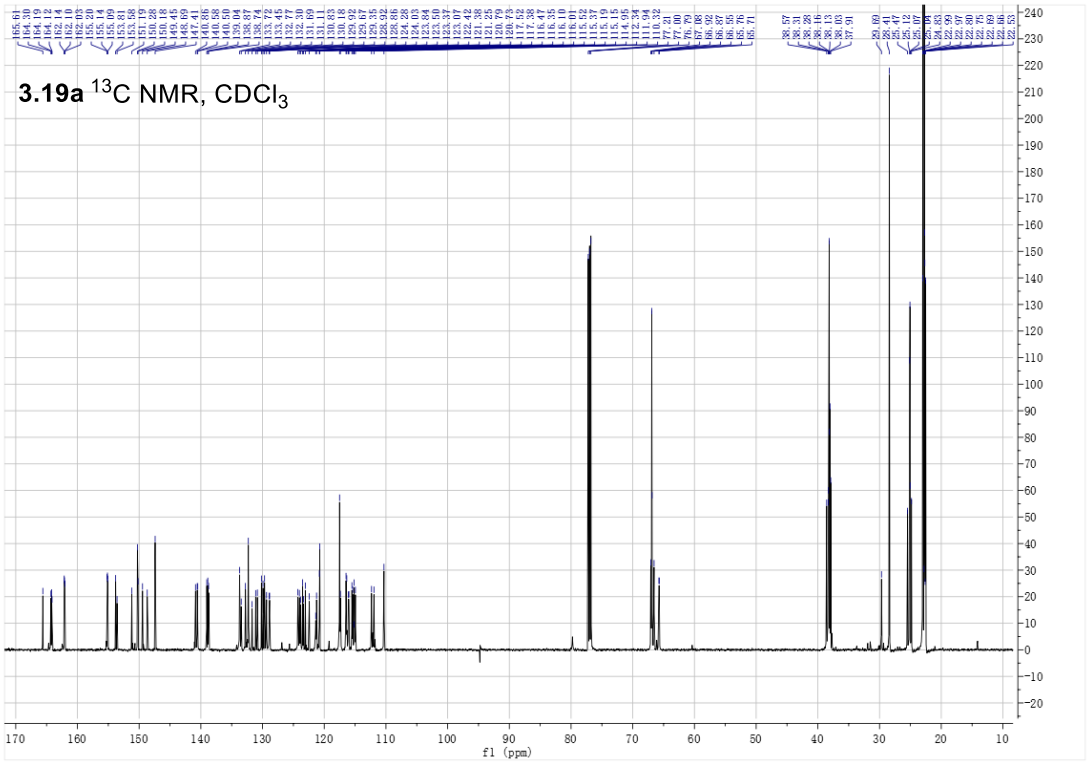
3.19a ^{13}C NMR, CDCl$_3$
f1 (ppm)

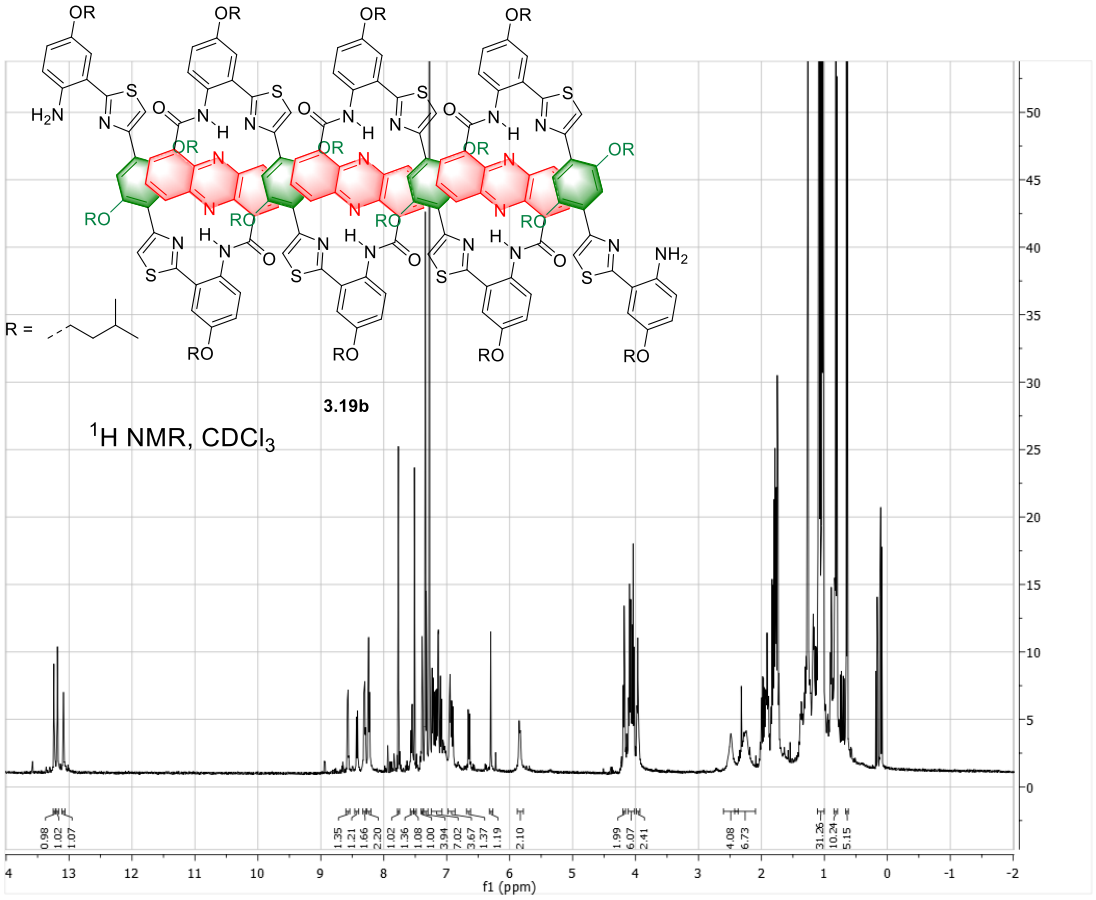
R =
3.19b
^{1}H NMR, CDCl$_3$
f1 (ppm)

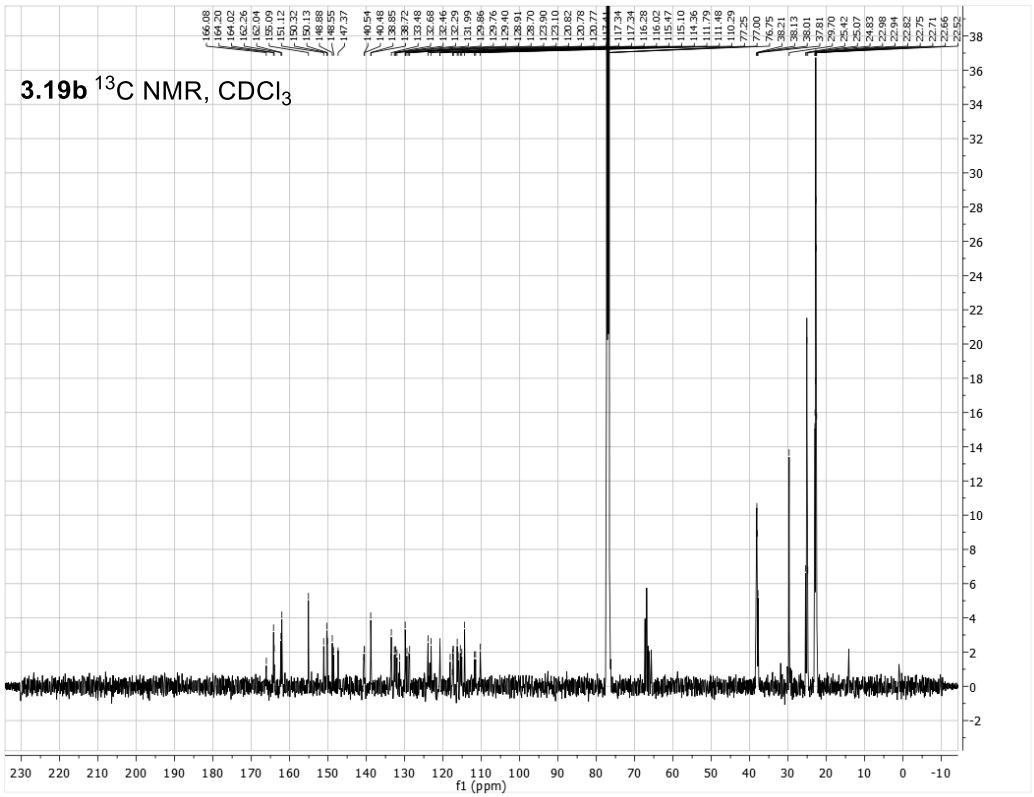
3.19b ^{13}C NMR, CDCl$_3$
f1 (ppm)

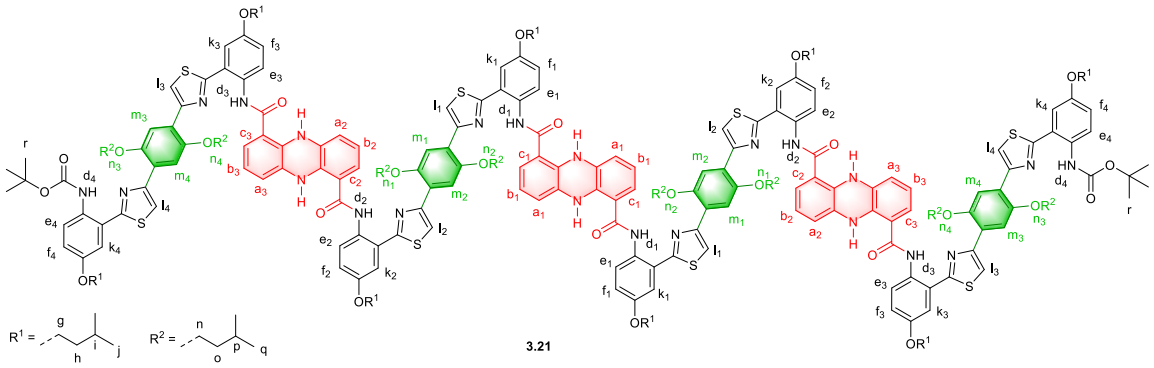

3.21

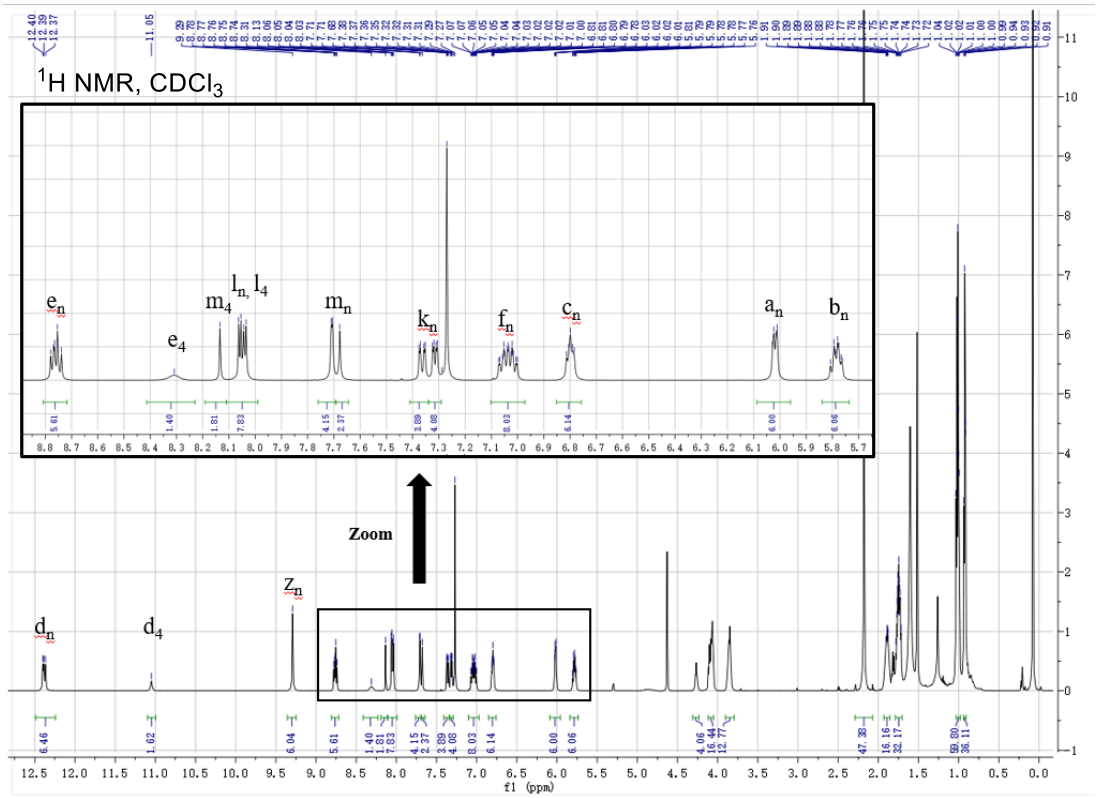

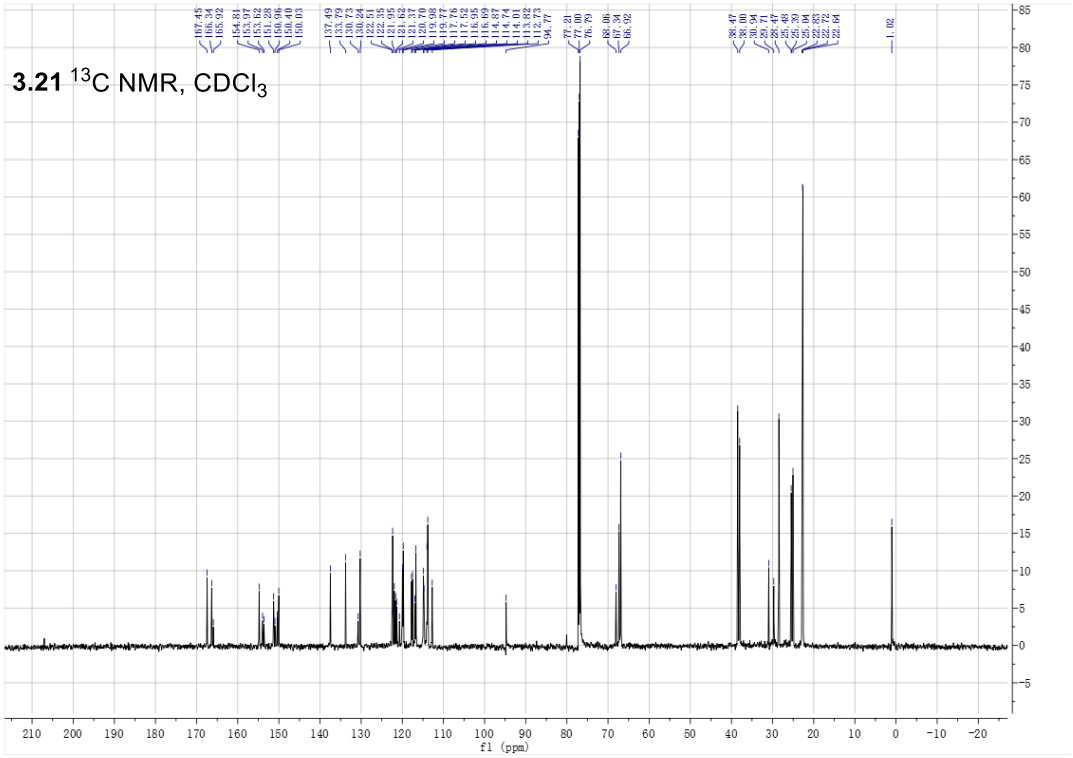
3.21 13C NMR, CDCl3
f1 (ppm)

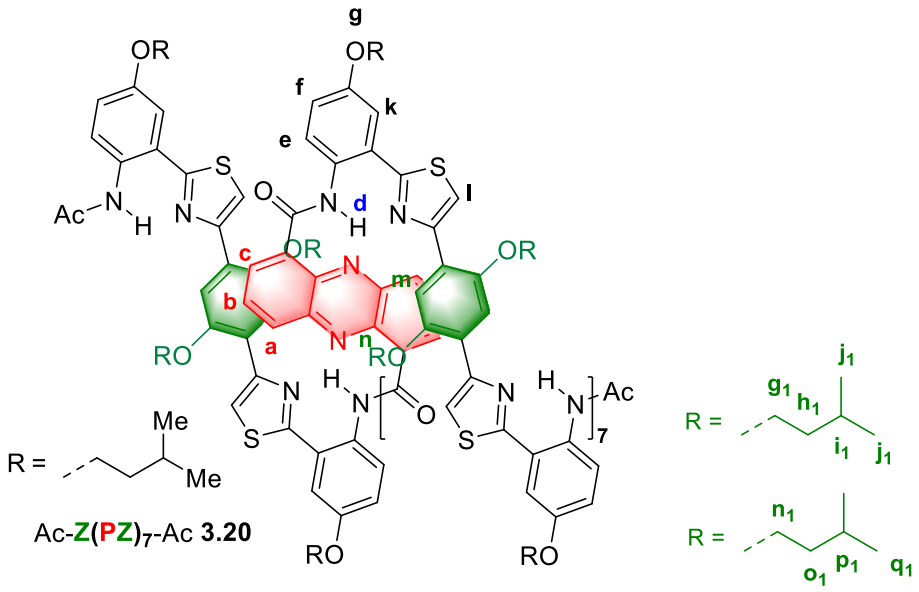
g
OR
OR
f
k
e
S
S
O
N
d
H
N
N
l
Ac
N
H
c
OR
N
OR
m
b
a
N
n
RO
RO
H
N
N
H
N
Ac
O
S
S
7
RO
RO
Me
R =
Me
Ac-Z(PZ)7-Ac 3.20
j1
g1
h1
R =
i1
j1
n1
R =
o1
p1
q1

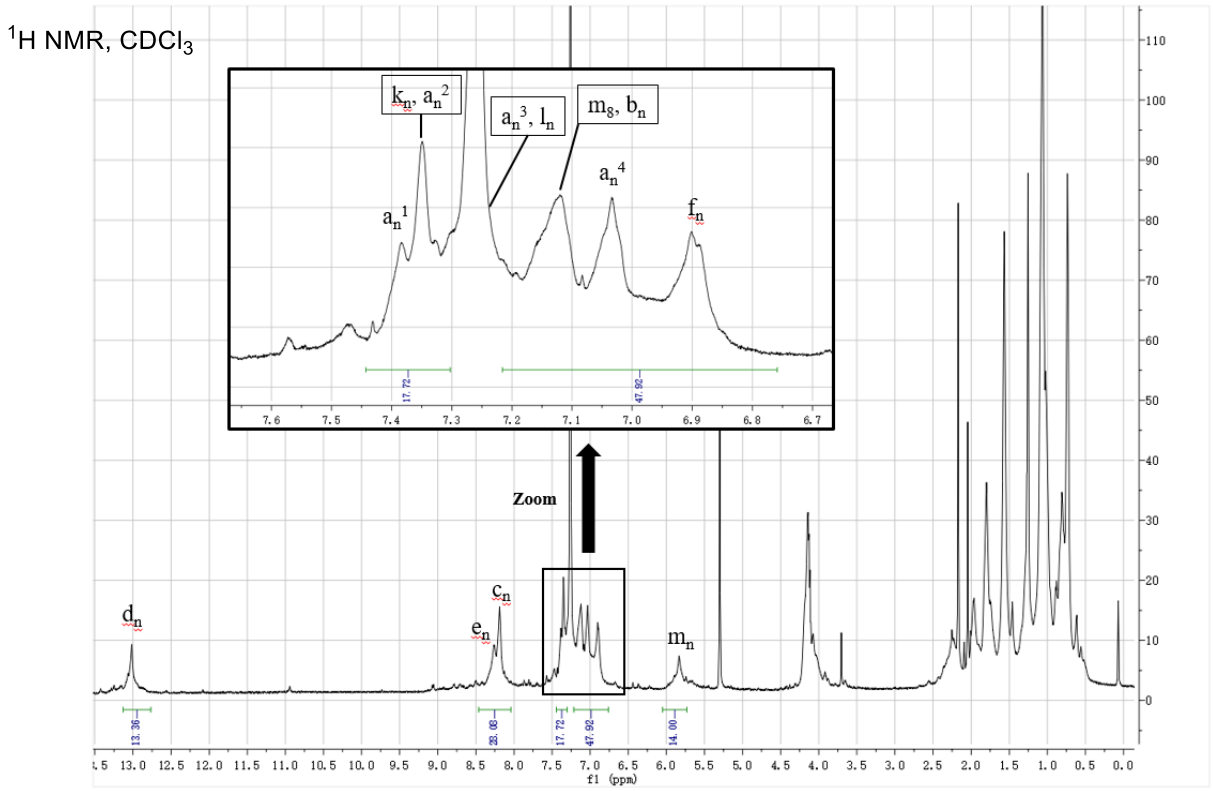
1H NMR, CDCl3
kn, an2
an3, ln
m8, bn
an4
an1
fn
Zoom
dn
en
cn
mn
f1 (ppm)

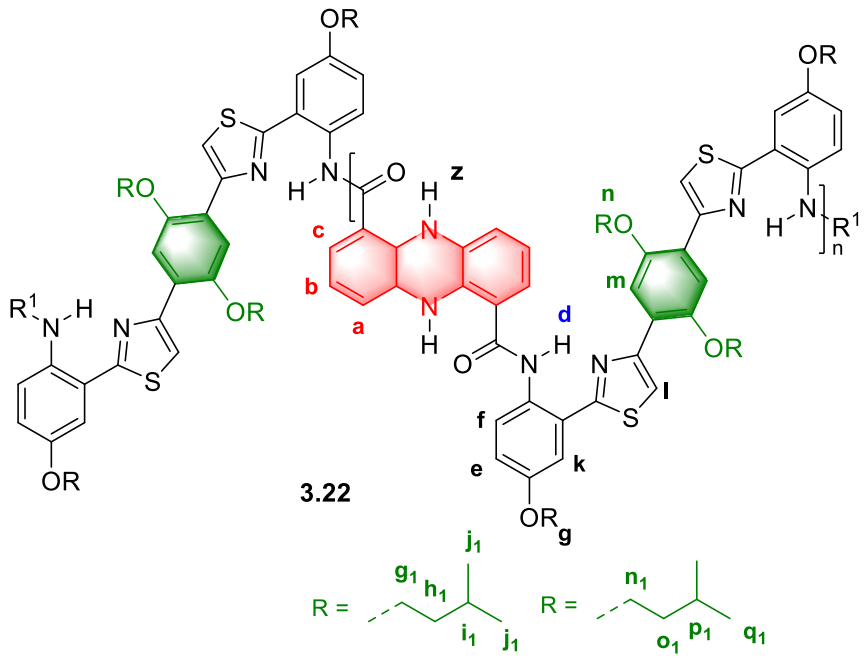
OR
RO
OR
OR
S
N
H
N
O
H
z
c
b
a
N
H
N
H
d
O
N
H
N
S
l
f
e
k
OR
g
n
RO
m
OR
OR
S
N
H
N
R1
n
R1
N
H
N
S
OR
3.22
j1
g1
h1
i1
j1
R =
n1
o1
p1
q1
R =

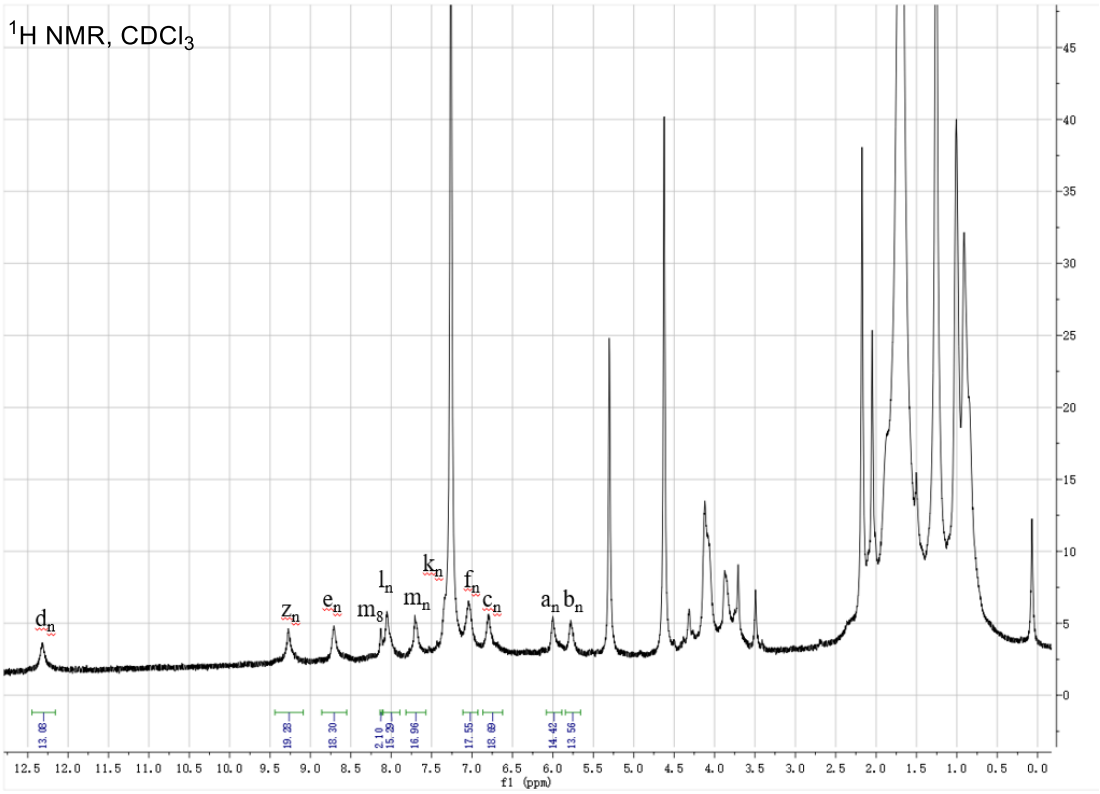
1H NMR, CDCl3
dn
zn
en
ms
ln
mn
kn
fn
cn
an
bn
45
40
35
30
25
20
15
10
5
0
13.00
19.23
18.30
2.10
15.29
16.96
17.55
18.69
14.43
13.56
12.5 12.0 11.5 11.0 10.5 10.0 9.5 9.0 8.5 8.0 7.5 7.0 6.5 6.0 5.5 5.0 4.5 4.0 3.5 3.0 2.5 2.0 1.5 1.0 0.5 0.0
f1 (ppm)

3.3.9. 2D NMR

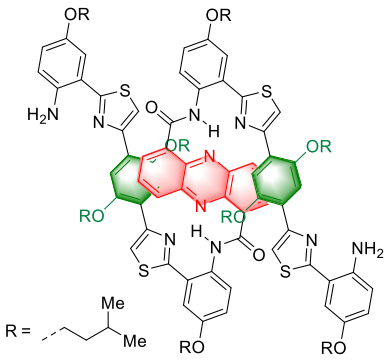

3.17

NOESY, $CDCl_3$

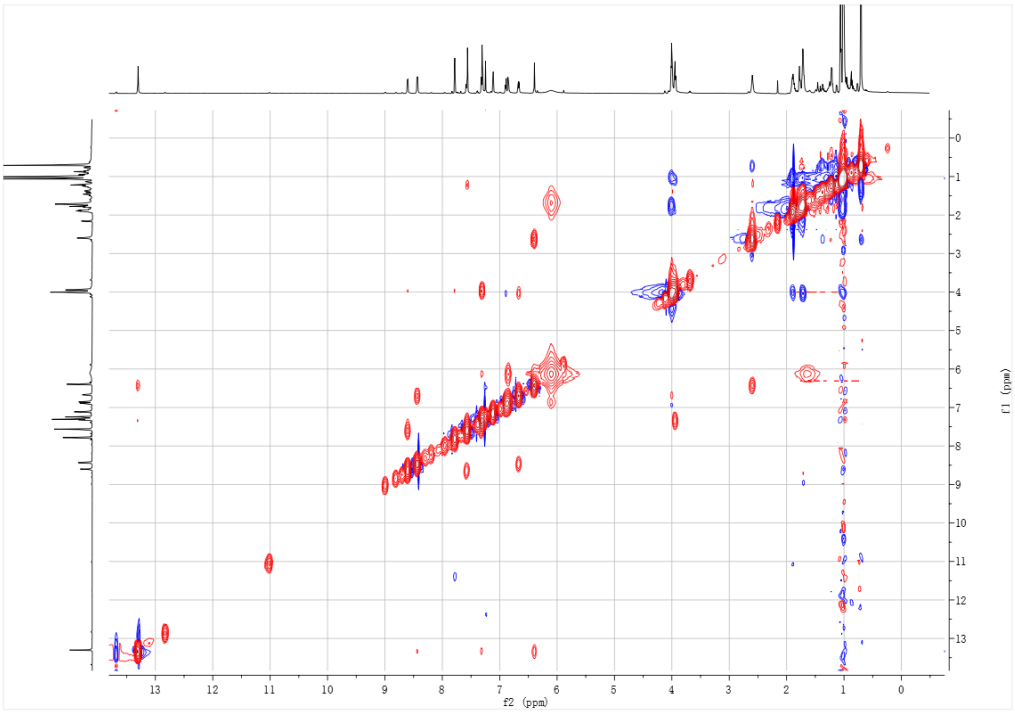

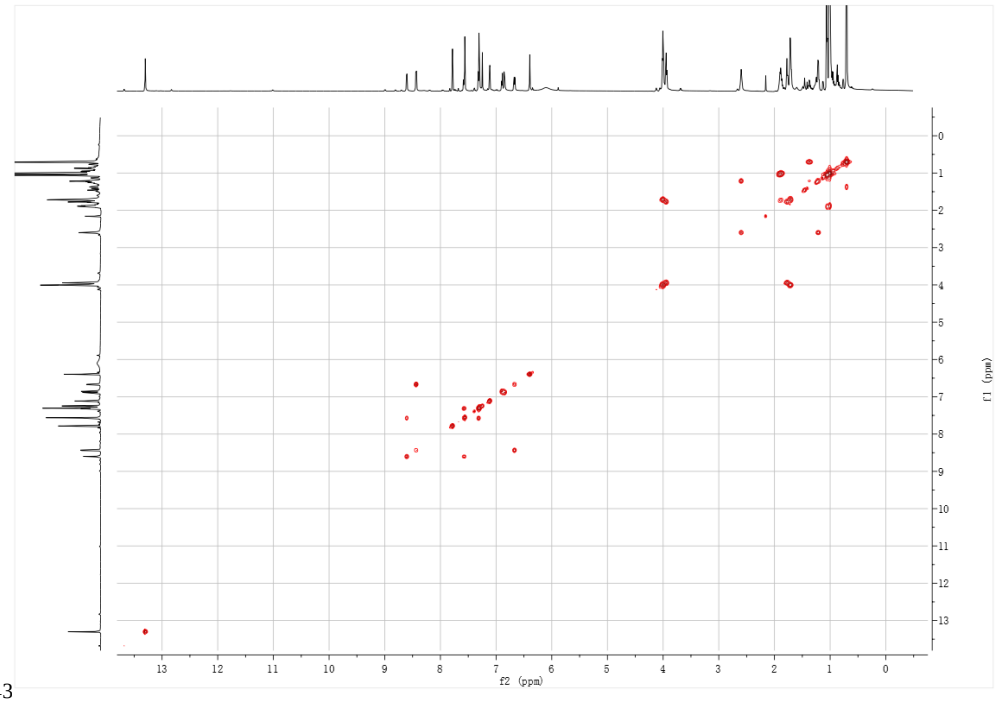

COSY, $CDCl_3$

TCOSY, $CDCl_3$

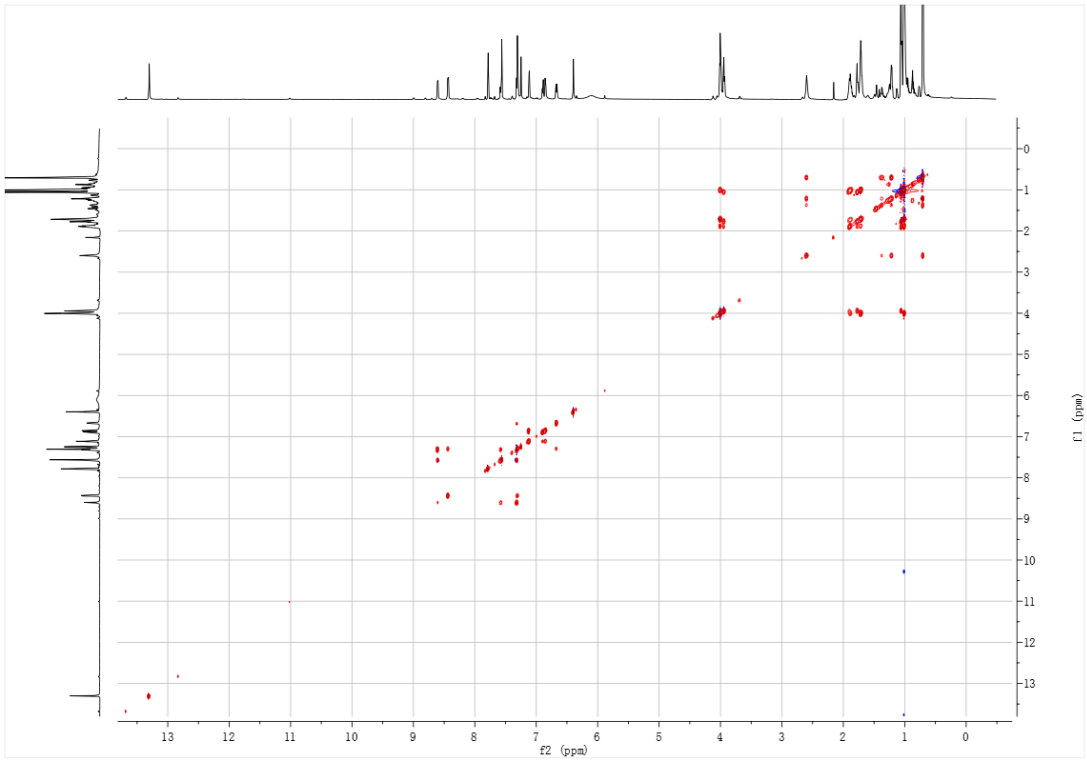

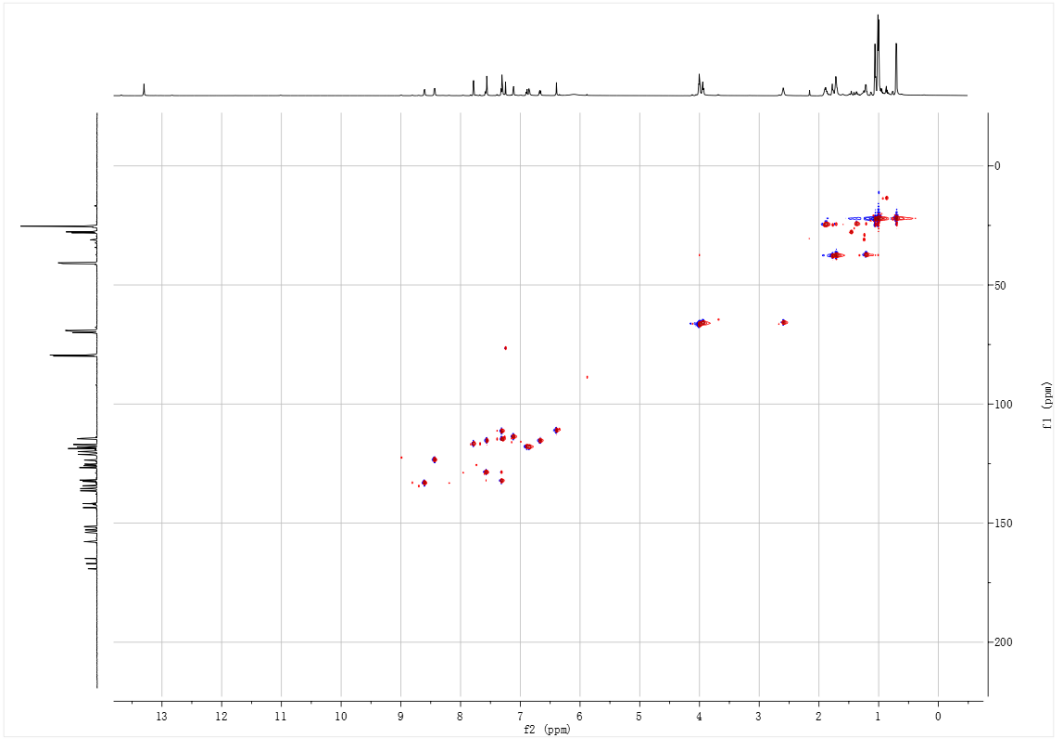

HSQC, CDCl

HMBC, $CDCl_3$

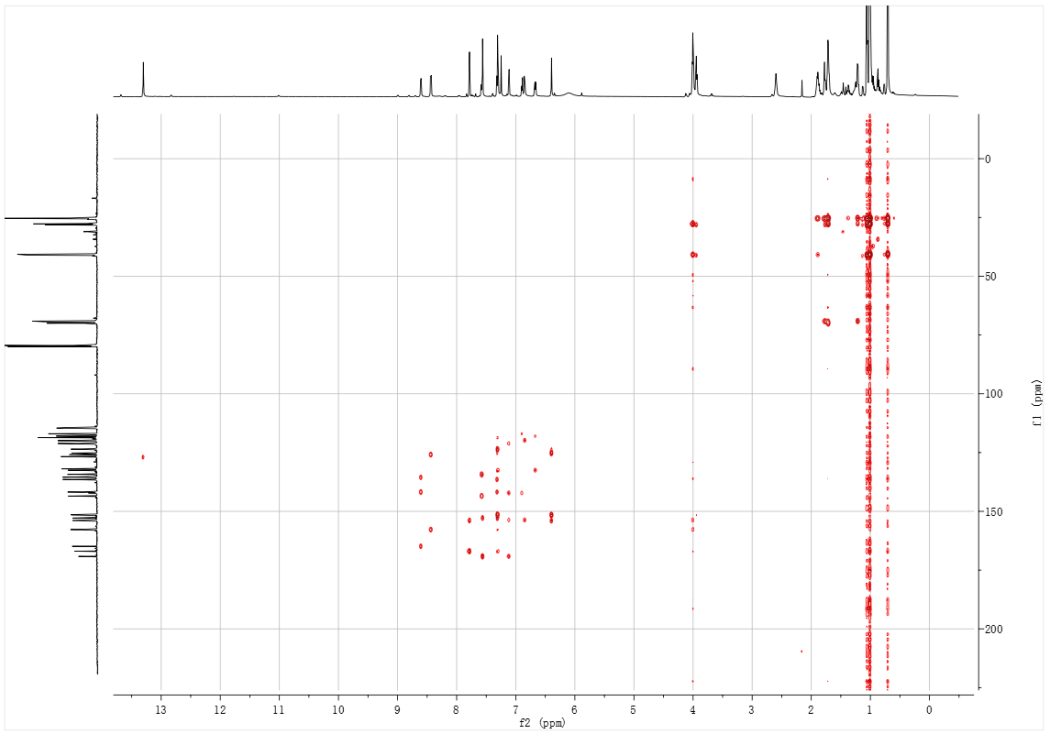

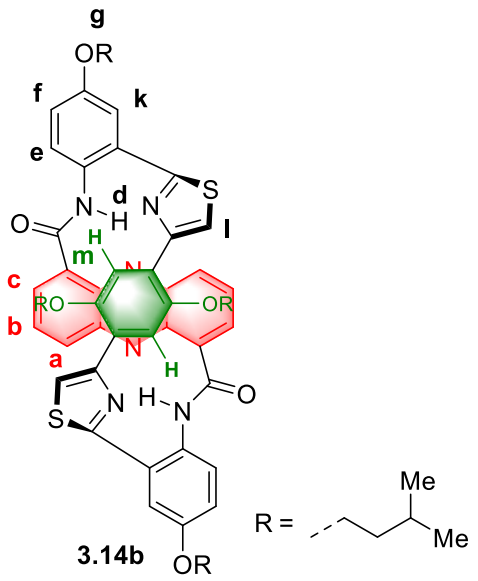
g
OR
f
k
e
d
N
H
S
N
l
O
H
m
c
RO
OR
b
a
N
H
S
N
H
N
O
3.14b
OR
R =
Me
Me

NOESY, $CDCl_3$

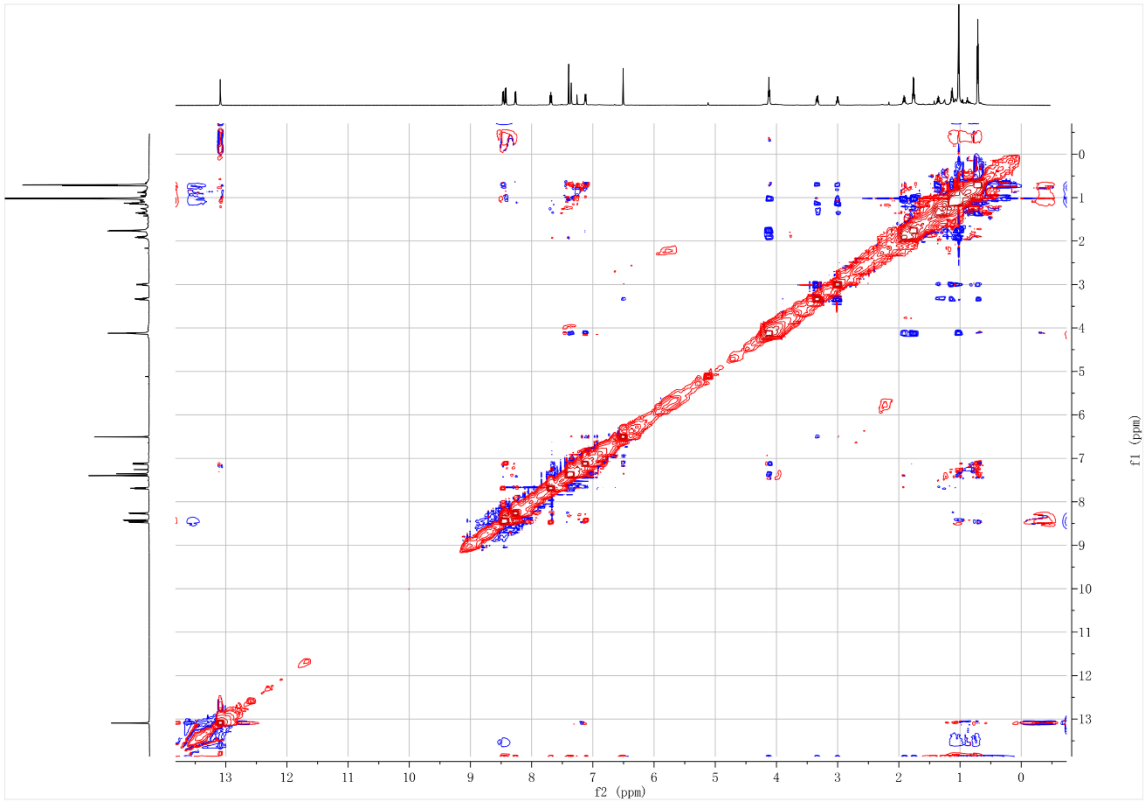
f2 (ppm)
f1 (ppm)

COSY, $CDCl_3$

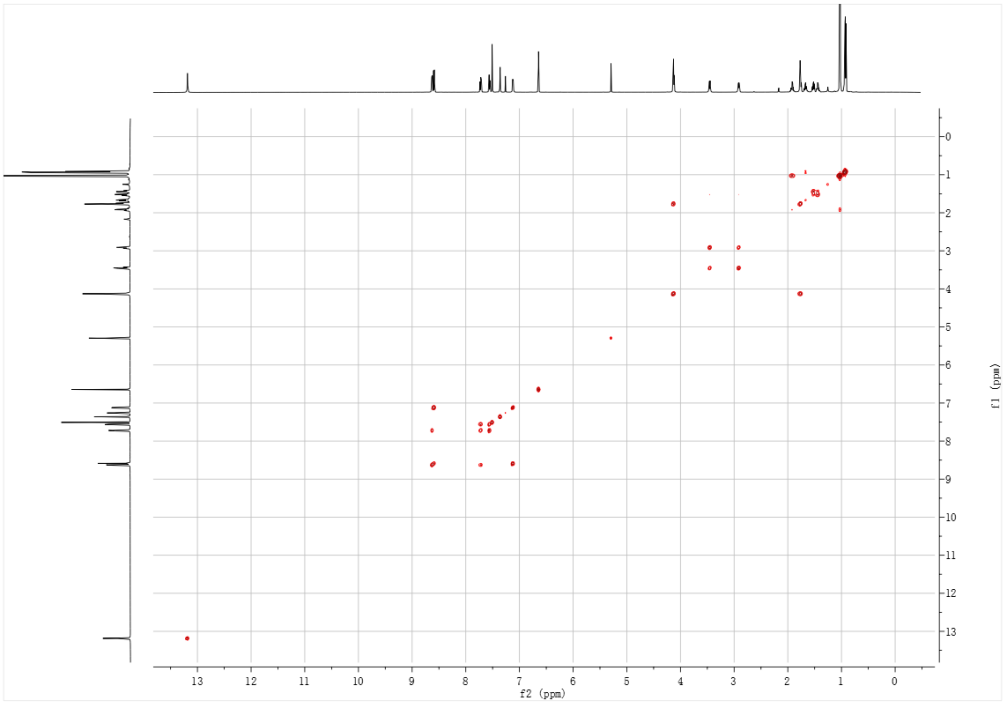

TCOSY, $CDCl_3$

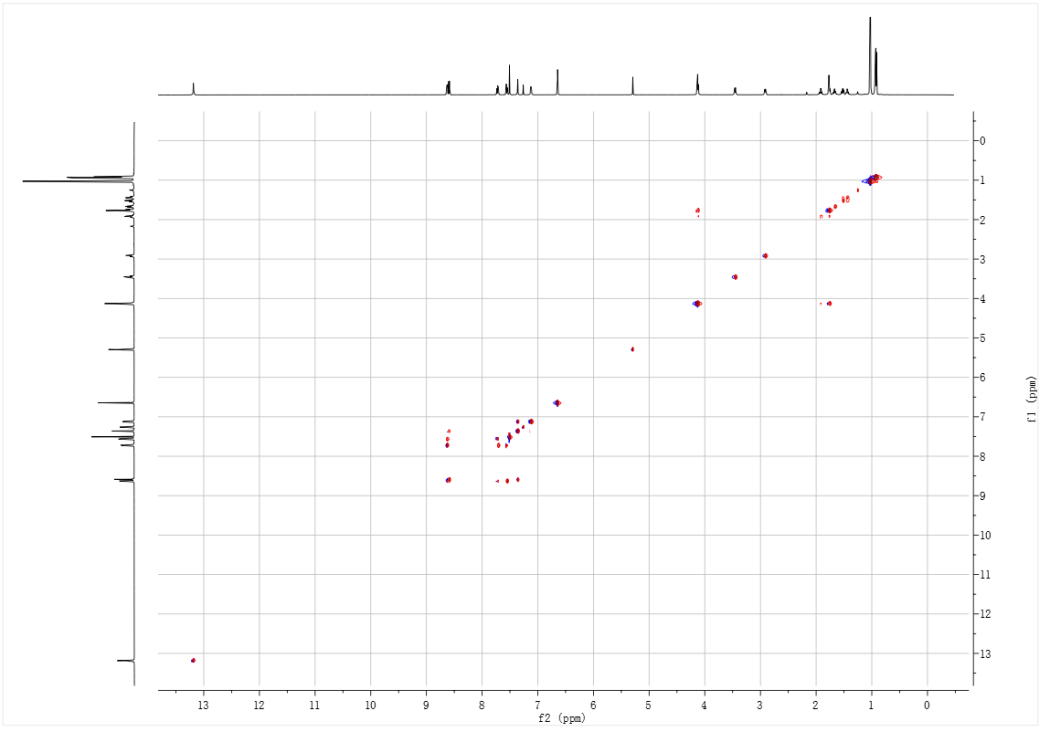

HSQC, $CDCl_3$

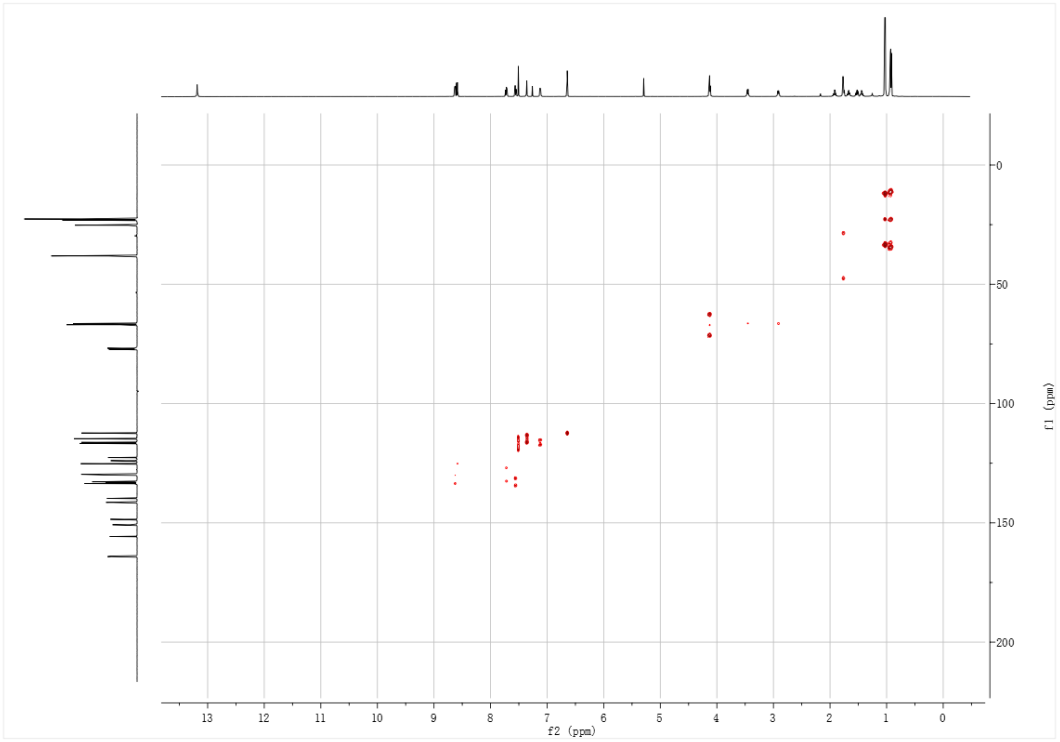

HMBC, $CDCl_3$

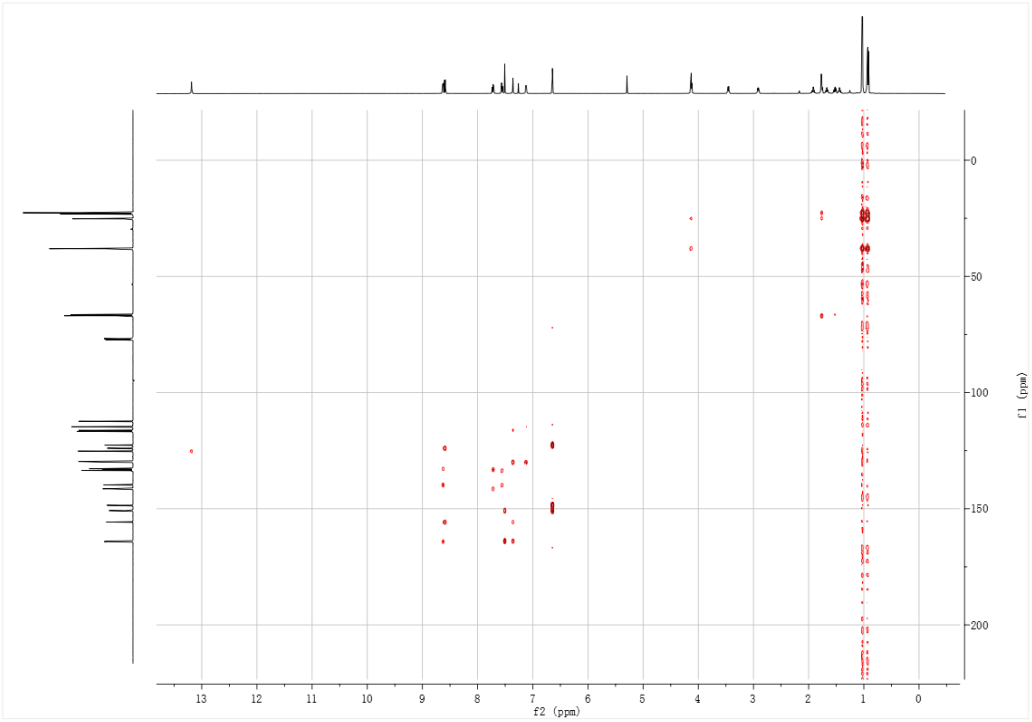

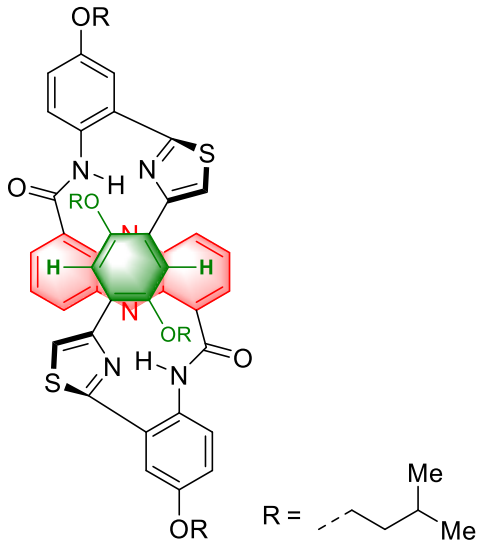

3.14a

NOESY, $CDCl_3$

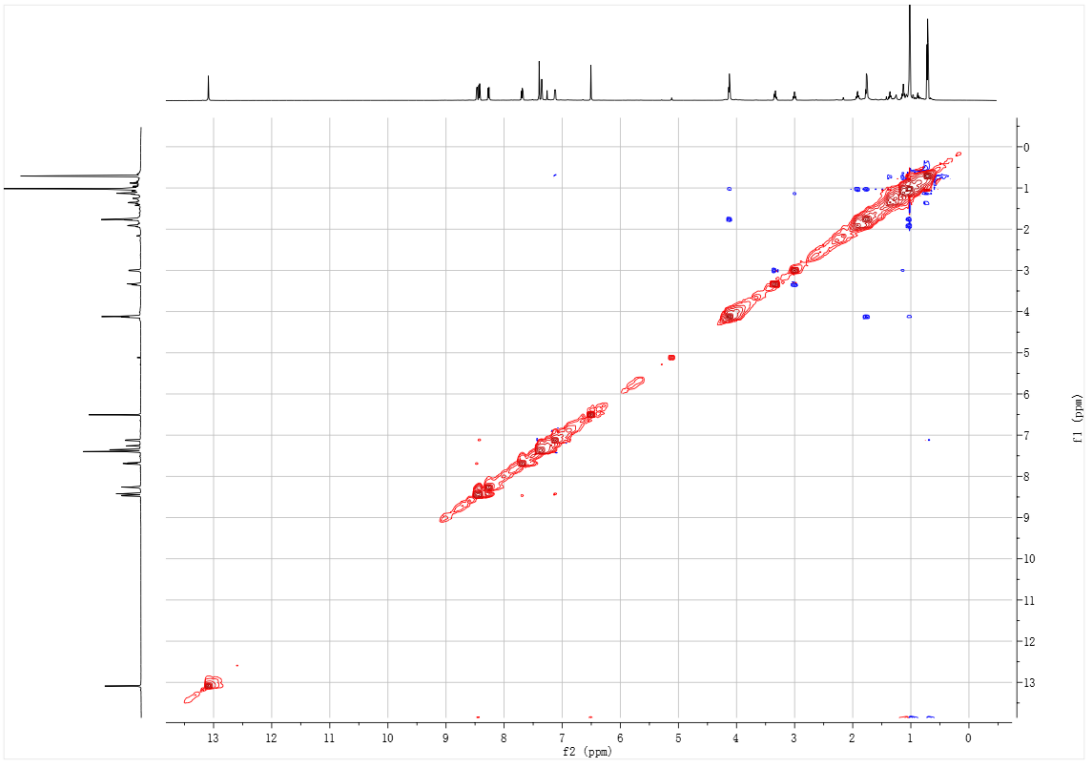

COSY, $CDCl_3$

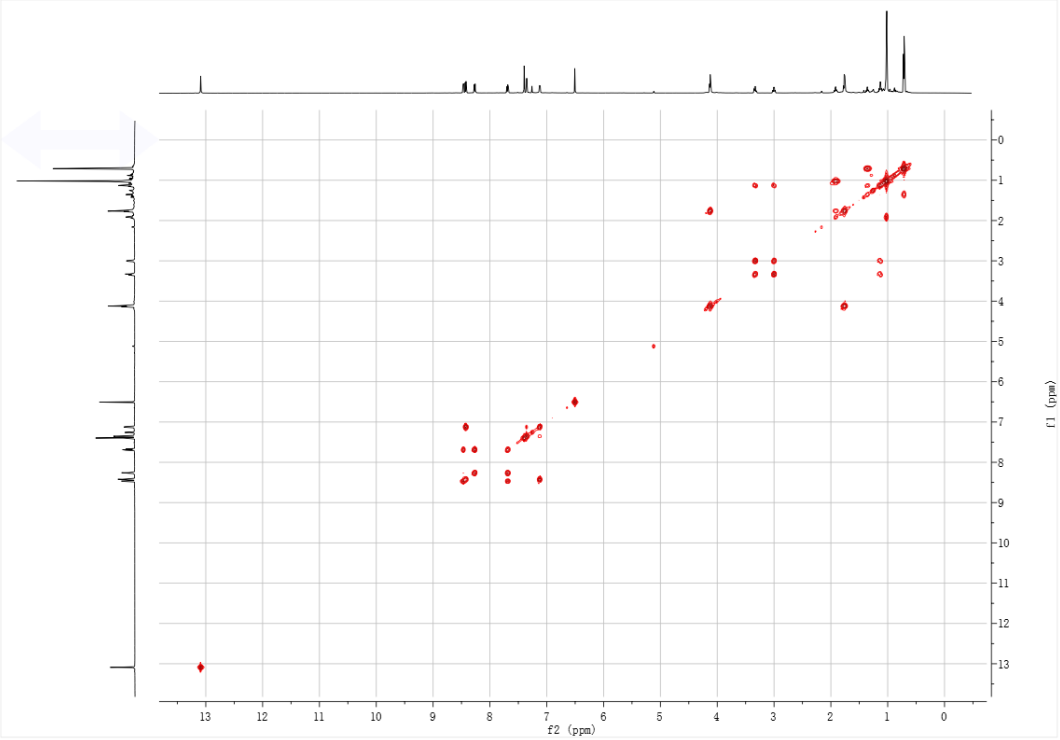

TCOSY, $CDCl_3$

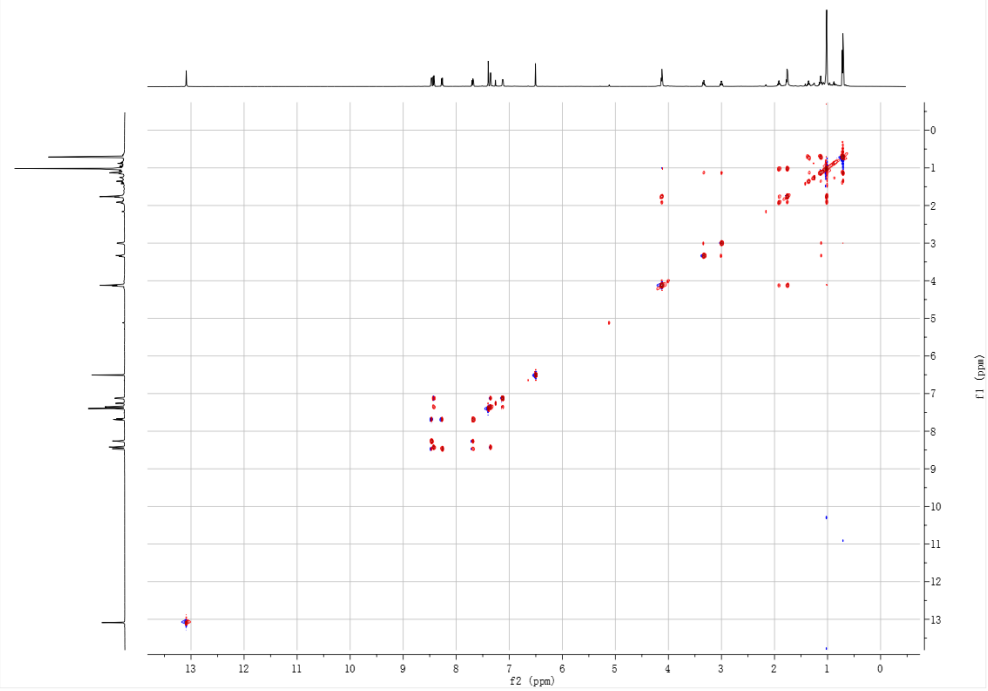

HSQC, $CDCl_3$

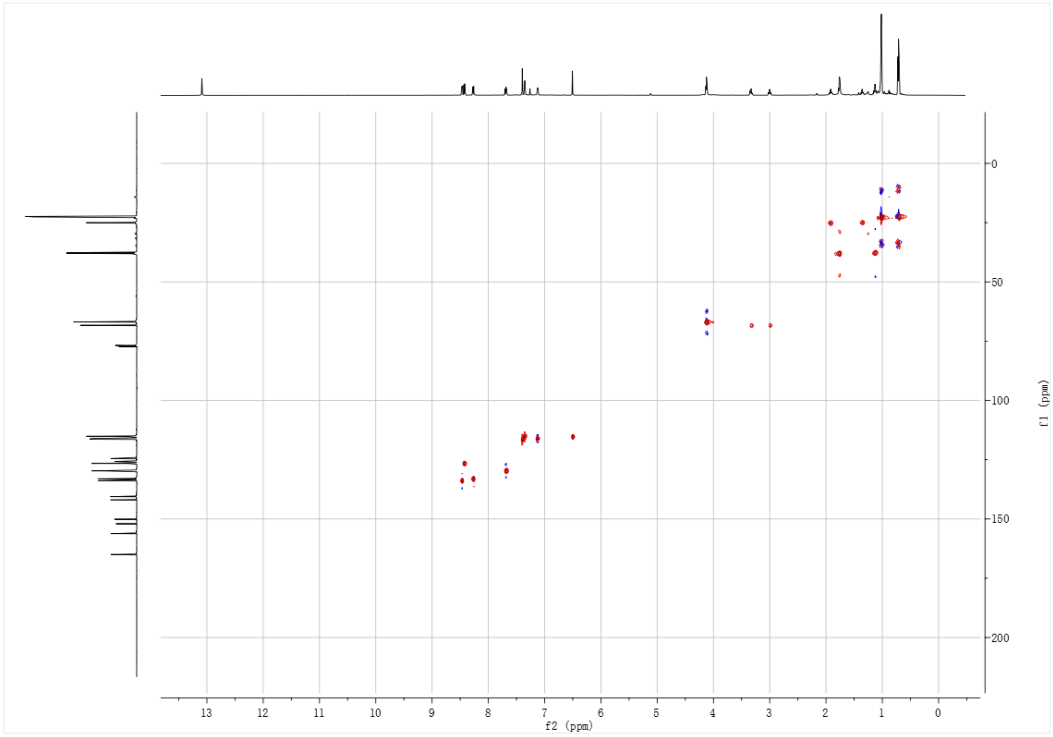

HMBC, $CDCl_3$

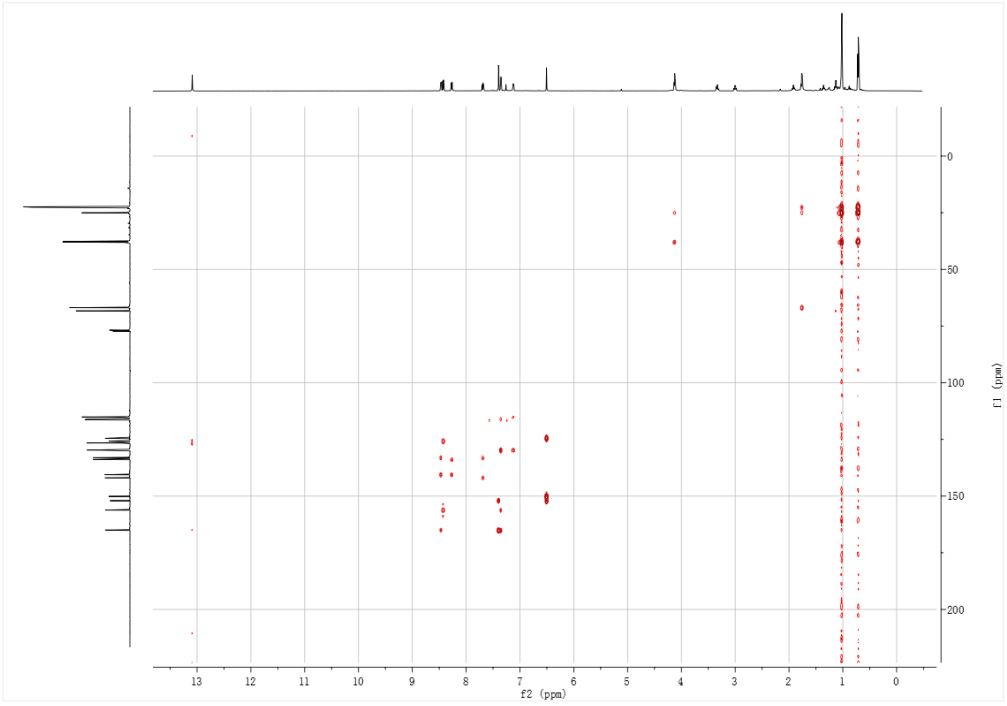

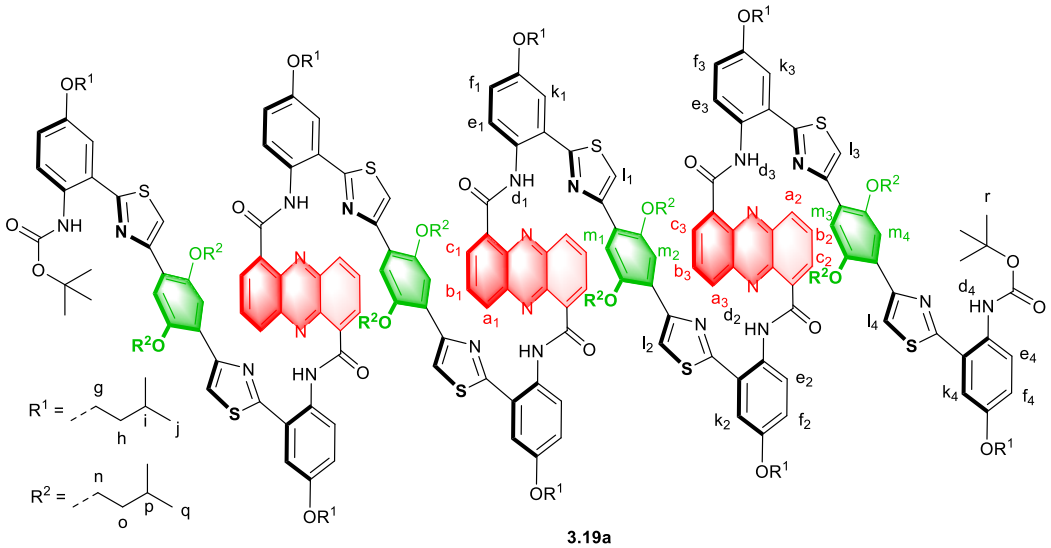

3.19a

NOESY, $CDCl_3$

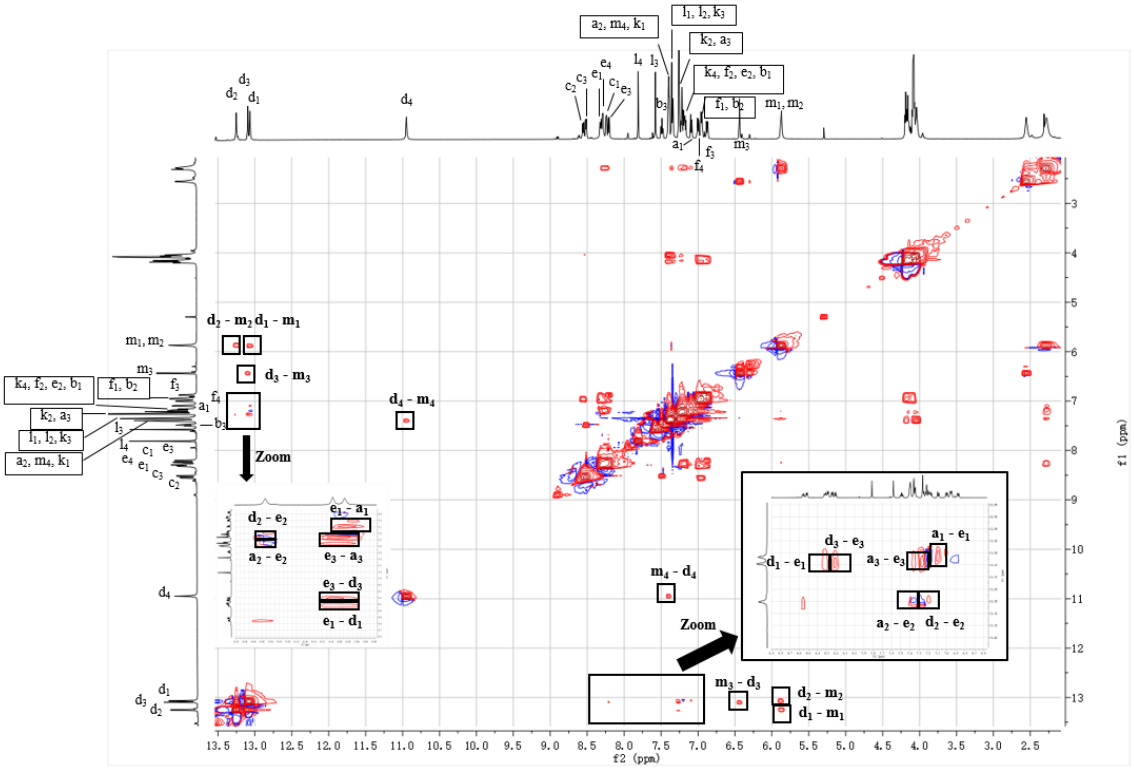

COSY, $CDCl_3$

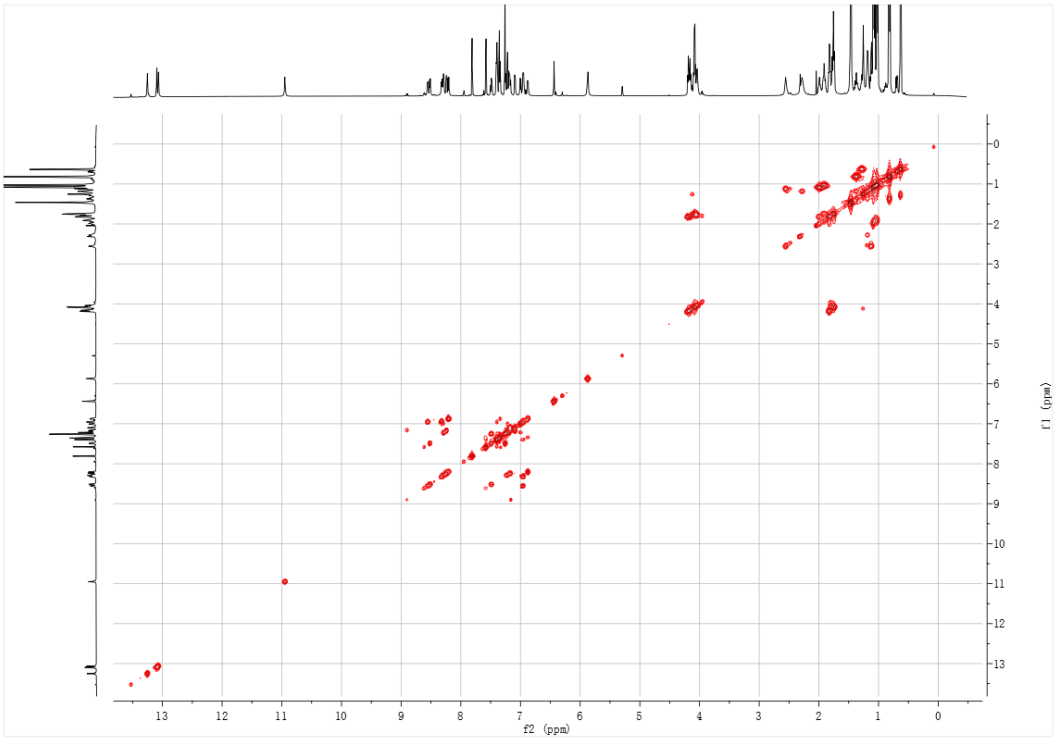

TCOSY, $CDCl_3$

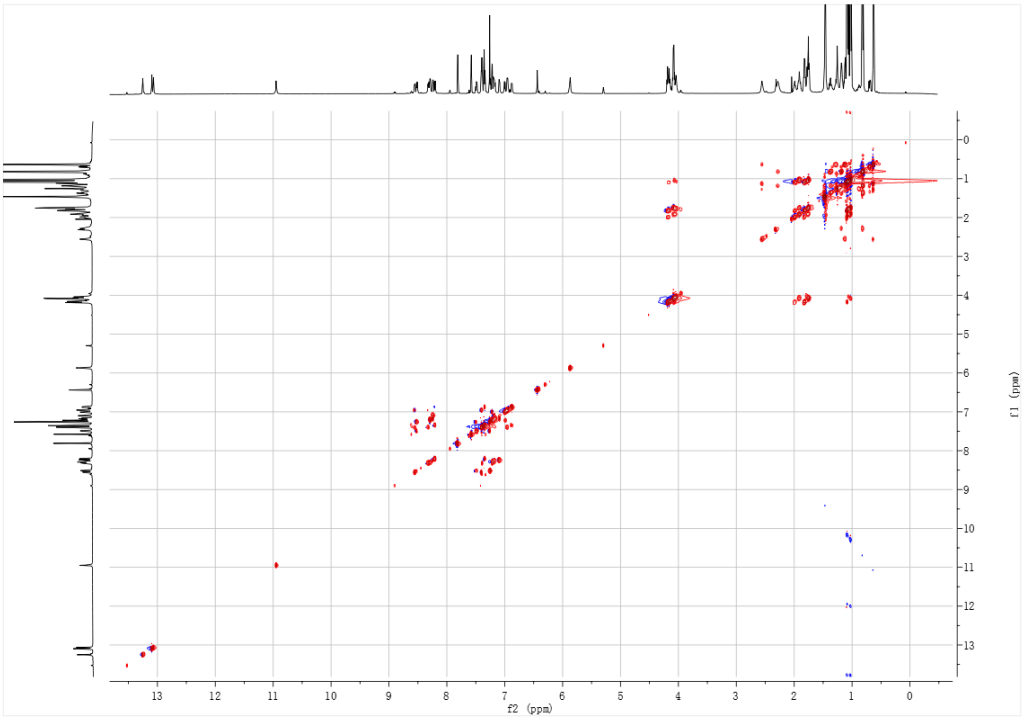

HSQC, $CDCl_3$

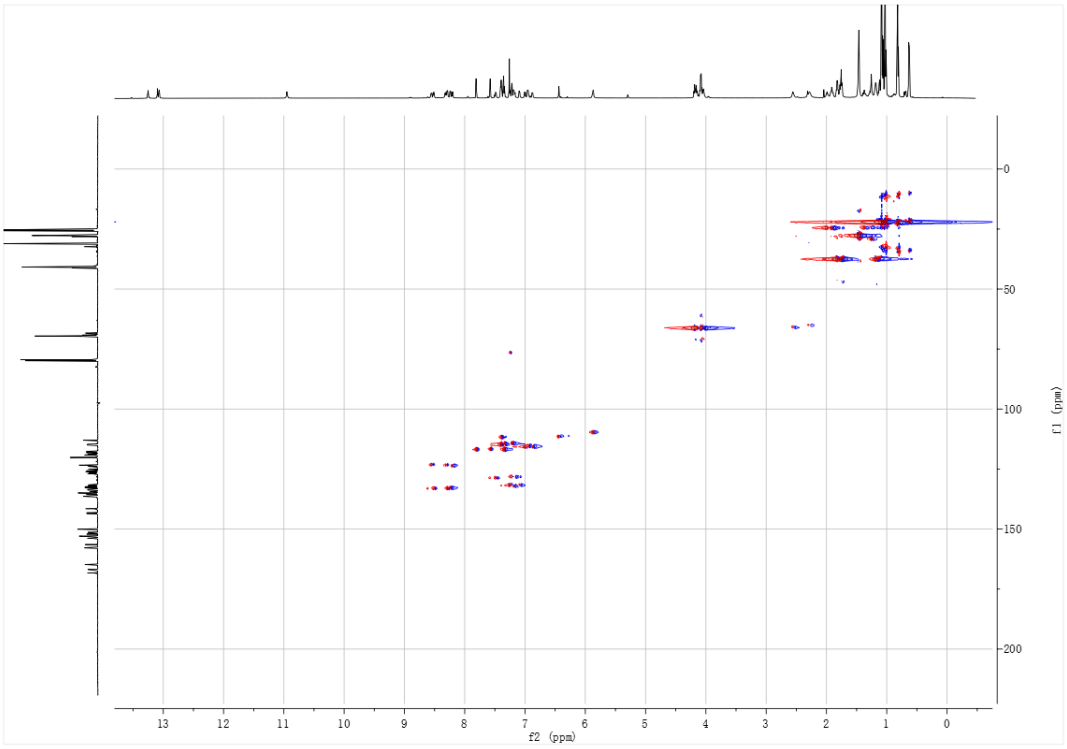

HMBC, $CDCl_3$

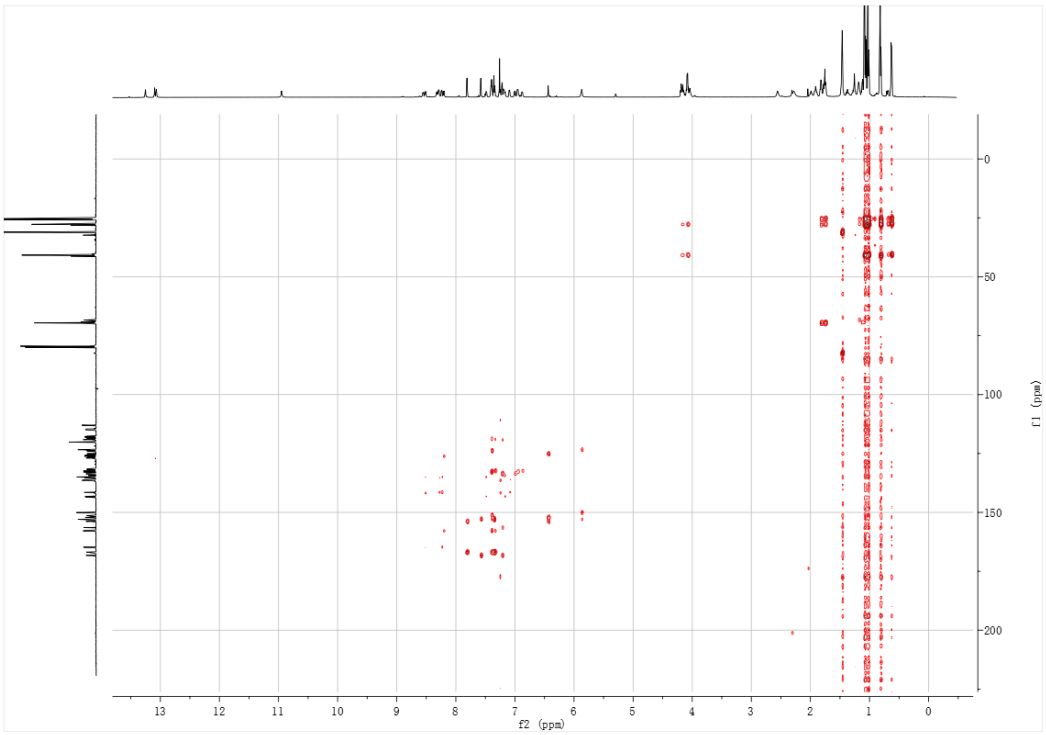

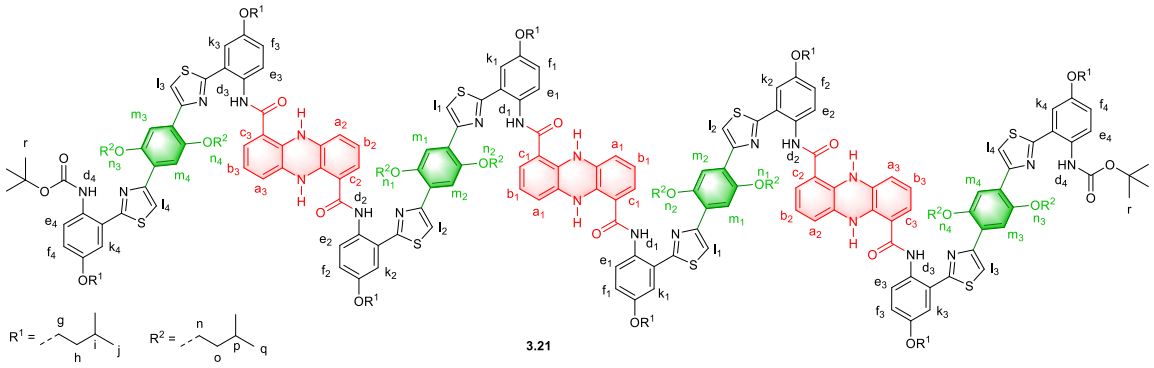

NOESY, $CDCl_3$

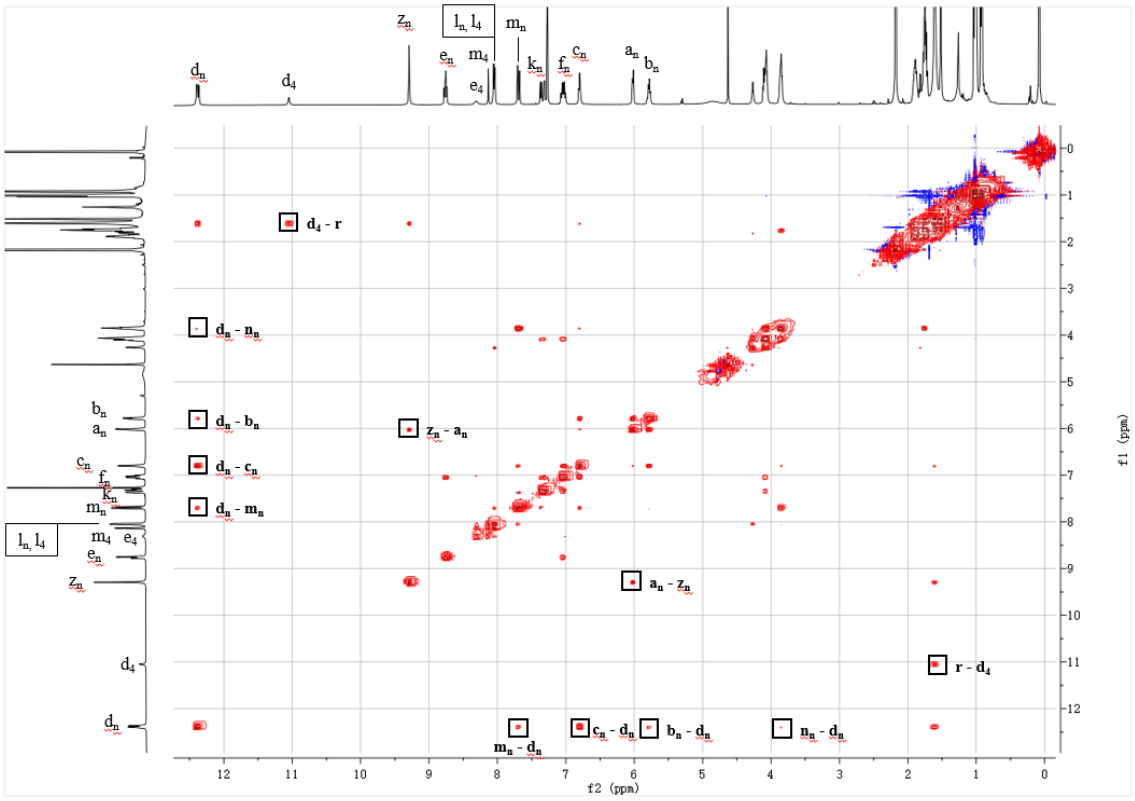
z_n
l_n, l_4
m_n
d_n
d_4
e_n
m_4
e_4
k_n
f_n
c_n
a_n
b_n
d_4 - r
d_n - n_n
d_n - b_n
z_n - a_n
d_n - c_n
d_n - m_n
a_n - z_n
r - d_4
m_n - d_n
c_n - d_n
b_n - d_n
n_n - d_n
f2 (ppm)
f1 (ppm)

COSY, $CDCl_3$

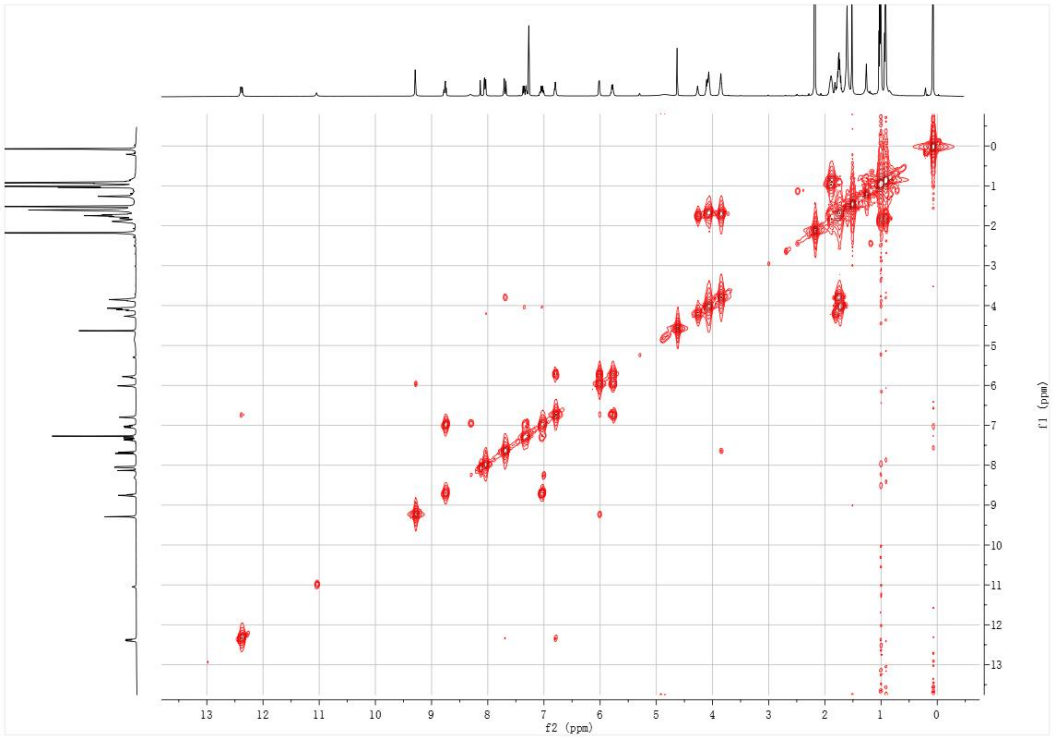

TCOSY, $CDCl_3$

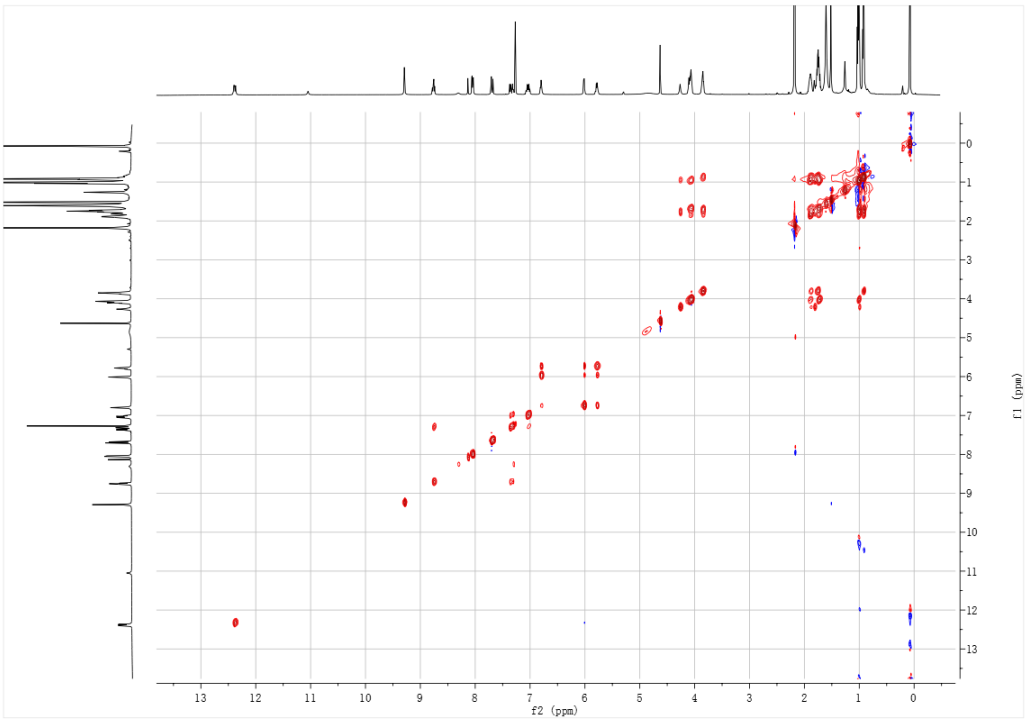

HSQC, $CDCl_3$

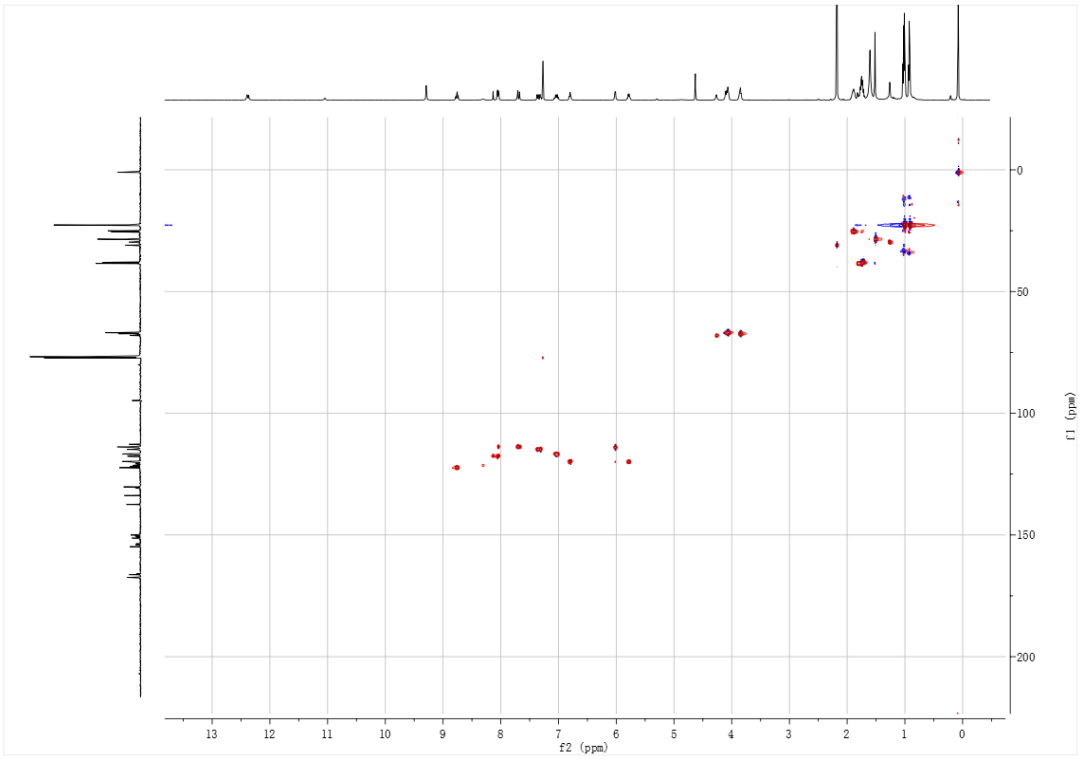
0
50
100
150
200
f1 (ppm)
13
12
11
10
9
8
7
6
5
4
3
2
1
0
f2 (ppm)

HMBC, $CDCl_3$

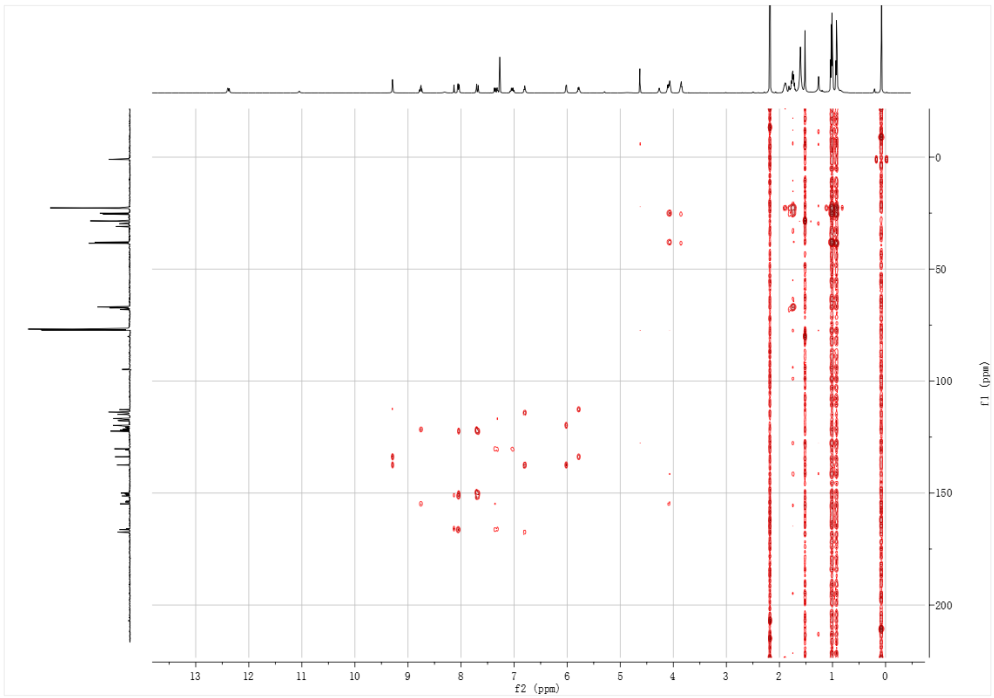
0
50
100
150
200
f1 (ppm)
13
12
11
10
9
8
7
6
5
4
3
2
1
0
f2 (ppm)

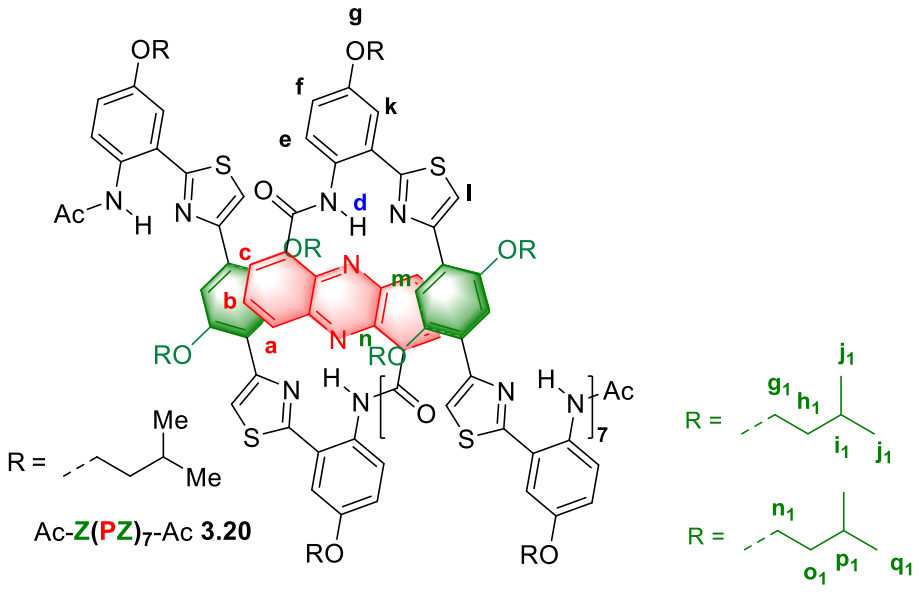

NOESY, $CDCl_3$

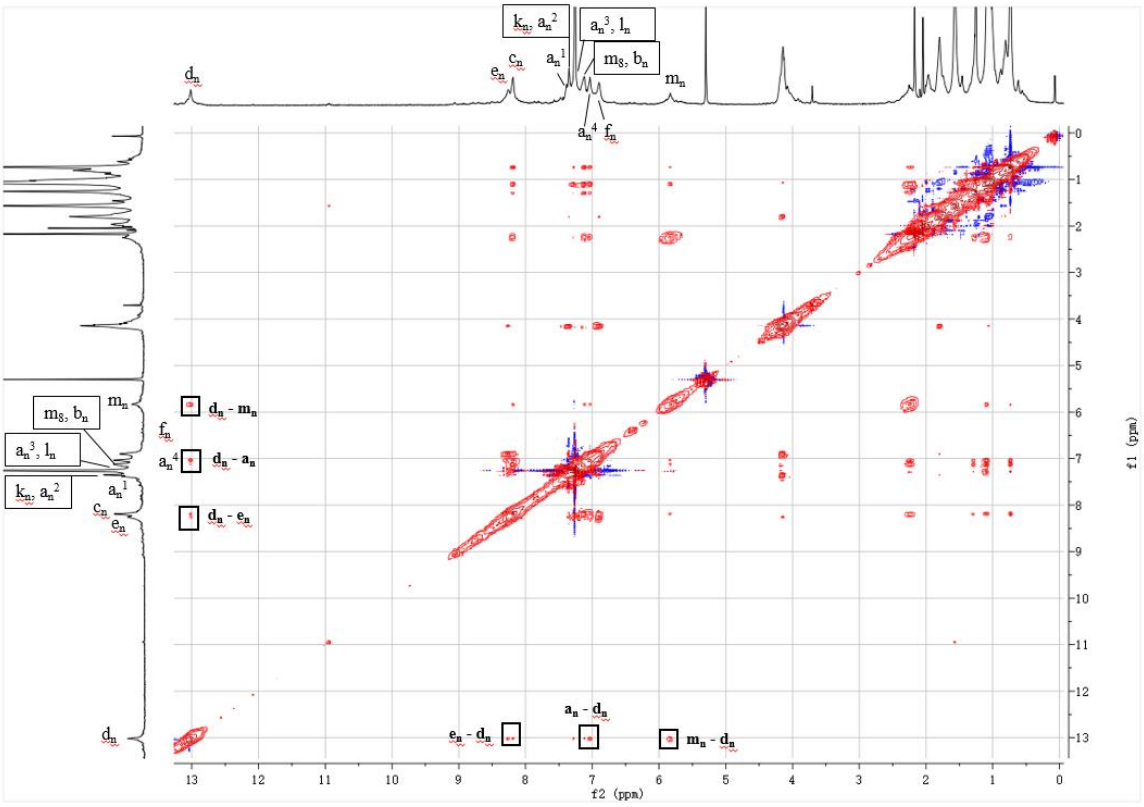

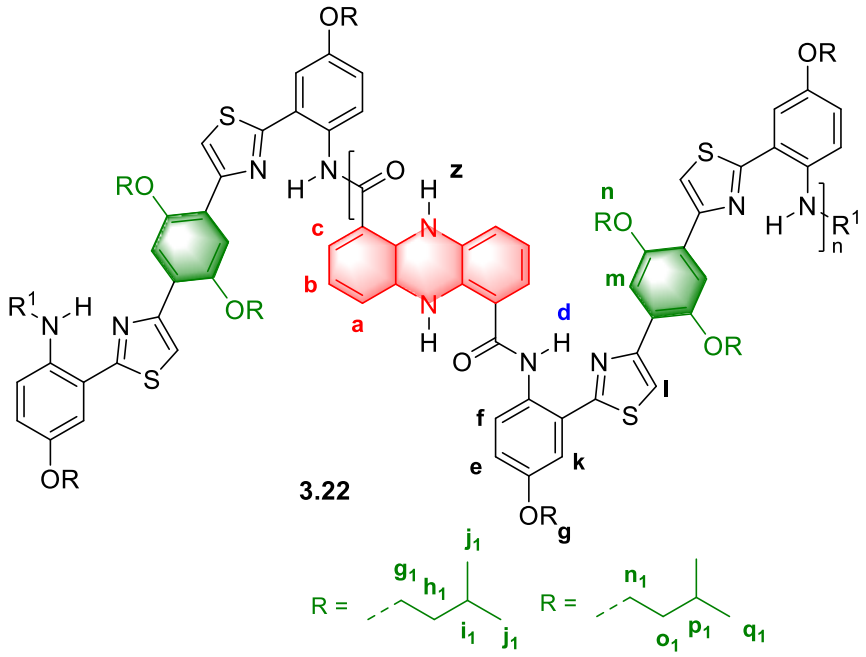
OR
RO
OR
OR
R1
H
N
S
N
H
N
O
z
c
b
a
d
n
RO
m
OR
OR
R1
n
f
e
k
l
OR
g
3.22
j1
g1
h1
i1
j1
R =
n1
o1
p1
q1
R =

NOESY, $CDCl_3$

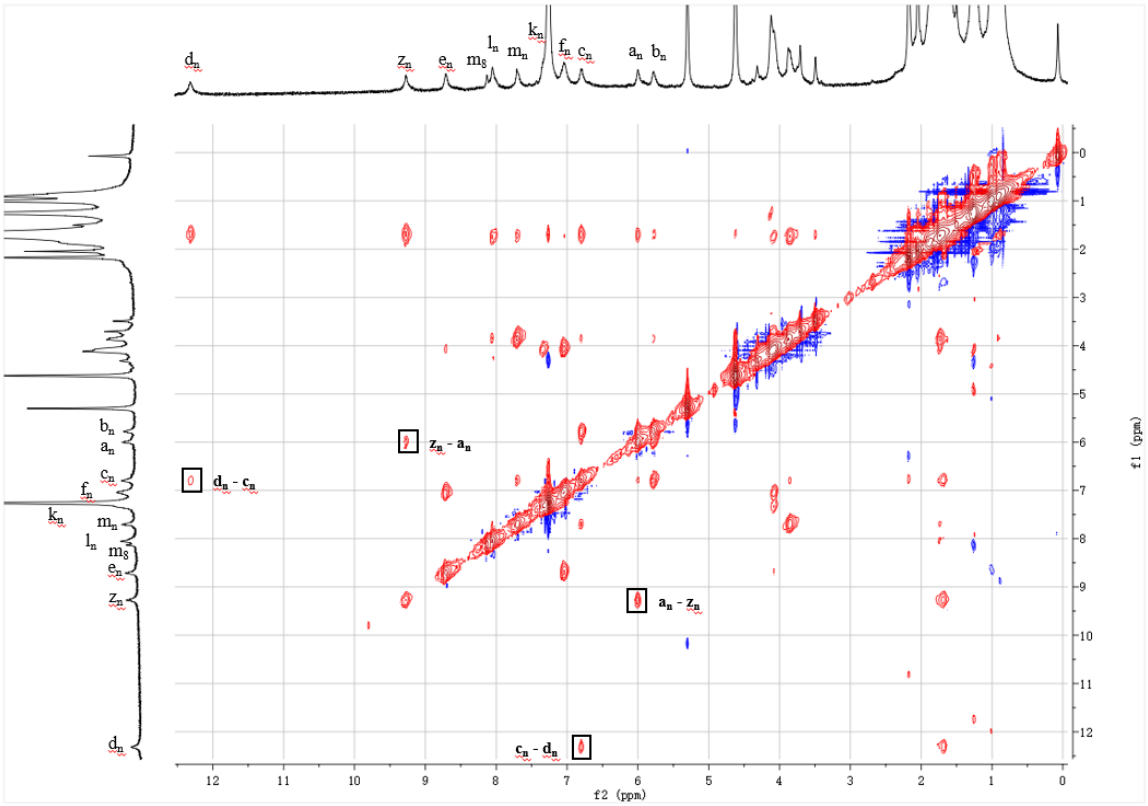
dn
zn
en
mg
ln
mn
kn
fn
cn
an
bn
dn - cn
zn - an
an - zn
cn - dn
f2 (ppm)
f1 (ppm)

3.4 References

1. For review of aromatic foldamers: (a) Zhang, D.-W.; Zhao, X.; Hou, J.-L.; Li, Z.-T., Aromatic Amide Foldamers: Structures, Properties, and Functions. *Chem. Rev.* **2012,** *112*, 5271-5316. (b) Koehler, V.; Roy, A.; Huc, I.; Ferrand, Y. Foldaxanes: Rotaxane-like Architectures from Foldamers. *Acc. Chem. Res.* **2022**, *55*, 7, 1074-1085.

2. Hantzsch, A. Weber, J. H. Über Verbindungen des Thiazols (Pyridins der Thiophenreihe) *Chem. Dtsch. Ber. Ges.* **1887,** *20,* 3118.

3. Freshly prepared from Mg and 1,2-dibromoethane in Et2O. See Footnote 43 in: Danishefsky, S. J.; Pearson, W. H.; Harvey, D. F.; Maring, C. J.; Springer, J. P., Chelation-controlled facially selective cyclocondensation reactions of chiral alkoxy aldehydes: syntheses of a mouse androgen and of a carbon-linked disaccharide. *J. Am. Chem. Soc.* **1985,** *107,* 1256-68.

4. (a) Macchioni, A.; Ciancaleoni, G.; Zuccaccia, C.; Zuccaccia, D. Determining accurate molecular sizes in solution through NMR diffusion spectroscopy. *Chem. Soc. Rev.***, 2008**, *37*, 479-489. (b) Avram L, Cohen Y. Diffusion NMR of molecular cages and capsules. *Chem Soc Rev.* **2015**, *44*(2):586-602. (c) Evans R. The interpretation of small molecule diffusion coefficients: Quantitative use of diffusion-ordered NMR spectroscopy. *Prog Nucl Magn Reson Spectrosc.* **2020**, *117*:33-69.

[5]. Bruns, C. J.; Stoddart, F., Rotaxane-Based Molecular Muscles. *Acc. Chem. Res.* **2014**, *47*, 2186-2199.

6. Freshly prepared from Mg and 1,2-dibromoethane in Et2O. See Footnote 43 in: Danishefsky, S. J.; Pearson, W. H.; Harvey, D. F.; Maring, C. J.; Springer, J. P.,

Chelation-controlled facially selective cyclocondensation reactions of chiral alkoxy aldehydes: syntheses of a mouse androgen and of a carbon-linked disaccharide. *J. Am. Chem. Soc.* **1985,** *107,* 1256-68.

7. Freshly prepared using procedure described in: Shen, Z.; Khan, H., A.; Dong, V. M. Rhodium-catalyzed carbonyl hydroacylation: an enantioselective approach to lactones. *J. Am. Chem. Soc.* **2008**, *130*, 10, 2916-2917.

8. Prepared from 5-chloro-2-nitrobenoic acid as previously described: (a) Bertrand, H.; Guillot, R.; Teulade-Fichou, M.-P.; Fichou, D., Synthesis, Properties, and Remarkable 2 D Self-Assembly at the Liquid/Solid Interface of a Series of Triskele-Shaped 5,11,17-Triazatrinaphthylenes (TrisK). *Chem. - Eur. J.* **2013,** *19,* 14654-14664. (b) Morin, M. D.; Wang, Y.; Jones, B. T.; Su, L.; Surakattula, M. M. R. P.; Berger, M.; Huang, H.; Beutler, E. K.; Zhang, H.; Beutler, B.; Boger, D. L., Discovery and Structure-Activity Relationships of the Neoseptins: A New Class of Toll-like Receptor-4 (TLR4) Agonists. *J. Med. Chem.* **2016,** *59* (10), 4812-4830.

9. (a) Becke, A. D., Density-functional thermochemistry. III. The role of exact exchange. *J. Chem. Phys.* **1993,** *98,* 5648-52. (b) Lee, C.; Yang, W.; Parr, R. G., Development of the Colle-Salvetti correlation-energy formula into a functional of the electron density. *Phys. Rev. B: Condens. Matter* **1988,** *37,* 785-789.

Chapter 4: Kinetic Resolution of cyclic hydroxamic acids via enantioselective catalytic O-acylation

4.1 Application and synthesis of hydroxamic acids

Chiral cyclic hydroxamic acids and their derivatives have extensive applications. For example, **4.1** - **4.3** showed interesting pharmacological properties (Figure 4-1). Two enantiomers of **4.1**, an indoleamine 2,3-dioxygenase inhibitor, showed drastically different IC_{50}.[1] Avibactam is a β-lactamase inhibitor,[2] approved by the FDA in 2015 in combination with Ceftazidime for the treatment of severe Gram-negative bacteria infections. Cyclic hydroxamic acid **4.2**[3] is a calcium antagonist, which can be used for treatment of nervous system diseases. Meanwhile, other hydroxamic acids and their derivatives have found applications in synthetic chemistry (Figure 4-2(a)). Bode *et al.*[4] used chiral hydroxamic acid **4.6** as co-catalysts for kinetic resolution of secondary amines, especially disubstituted piperidines,[5] and assignment of absolute configuration of amines. Furthermore, Rychnovsky *et al.*[6] used Bode's hydroxamic acid derivatives to assign the absolute configuration of cyclic amines (Figrue 4-2 (b)).

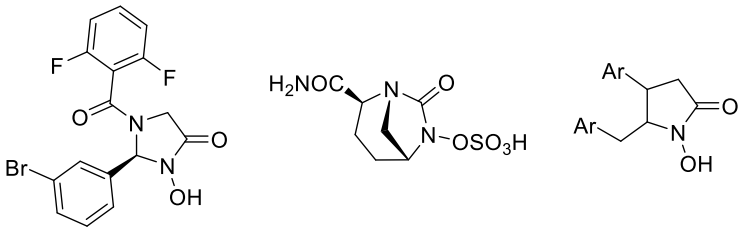

4.1, NTRC-3883-0, IDO1 inhibitor

4.2, Avibactam, β–lactamase inhibitor

4.3, Calcium antagonists

Figure 4-1. Pharmacological applications of hydroxamic acids.

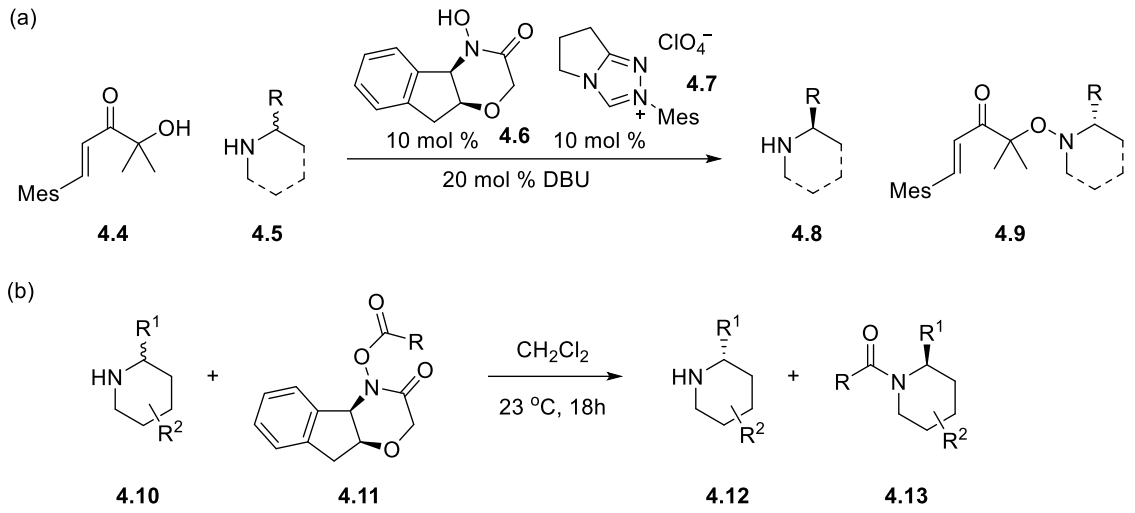

Figure 4-2. Applications of hydroxamic acids in organic synthesis.

Synthesis of achiral hydroxamic acids is well developed (Figure 4-3). Acylnitroso intermediate **4.15** generated *in situ* from oxidation of **4.14** reacted with intermolecular and intramolecular double bonds to deliver hydroxamic acids (Eq.1).[7] Jeffery *et al.*[8] developed series of cycloadditions to generate cyclic hydroxamic acids with good yield and diasteroselectivity. Typically, aza-oxyallyl cation **4.19** generated in situ from α-halohydroxamate **4.17** was heated with dienes or aldehyde **4.18** in 1,1,1,3,3,3-Hexafluoro-2-propanol (HFIP) (Eq.2). King *et al.*[9] developed ring-expansion through –NOH insertion on α-hydroxy C-nitroso species **4.21** to make cyclic hydroxamic acids (Eq.3). An interesting ring expansion was reported by Yamada *et al.*[10] Irradiation of **4.24** with a low-pressure mercury lamp generated nitronate anions **4.25** which underwent photorearrangement, resulted complete retention of stereochemistry (Eq.4). Castagnoli-Cushman reaction [11] provides another access (Eq.5). Furthermore, Sato and Chida *et al.*[12] produced a class of cyclic hydroxamic acid **4.30** via reduction of oxime **4.30** (Eq.6).

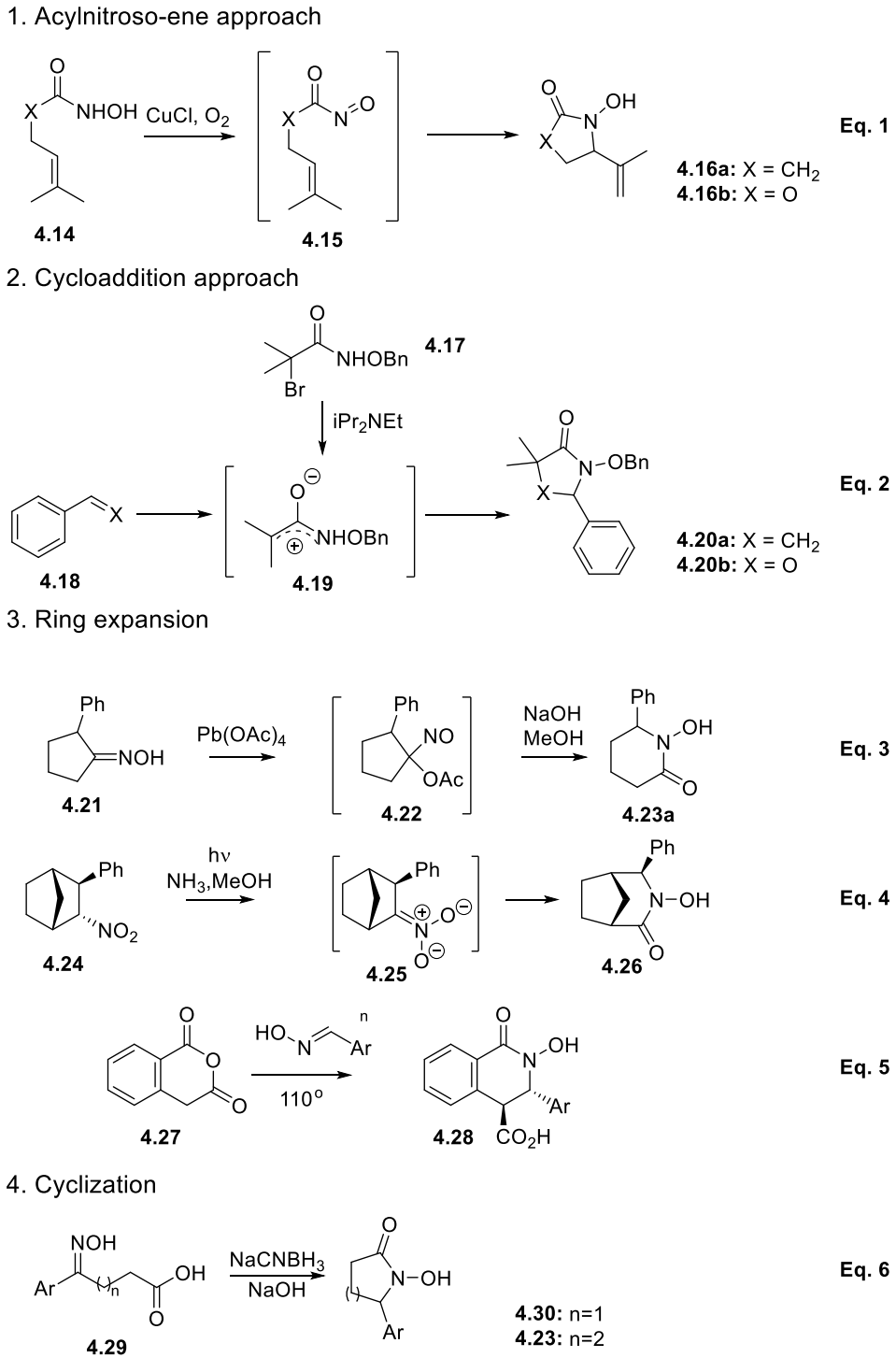

Figure 4-3. Racemic synthesis of hydroxamic acids.

On the other hand, there are only a few asymmetric catalysis methods available for cyclic hydroxamic acids (Figure 4-4). In 2012, Hamada *et al.* reported an aza-Michael-Michael tandem

reaction between **4.31** and **4.32** through iminium catalysis by **4.33** with high enantioselectivity (Eq.1).[13] Later, Helmchen *et al.* accomplished similar transformation via iridium catalyzed oxidation of **4.35** followed by ring-closing metathesis (Eq.2).[14] Recently, Kim and Jung *et al.* enabled the first asymmetric [4+3]-cycloaddition of δ-hydroxy α,β-unsaturated carbonyls **4.39** through bifunctional catalysis to prepare 1,4-oxazepanes **4.42** in one step, with good yield and high enantioselectivity (Eq.3).[15]

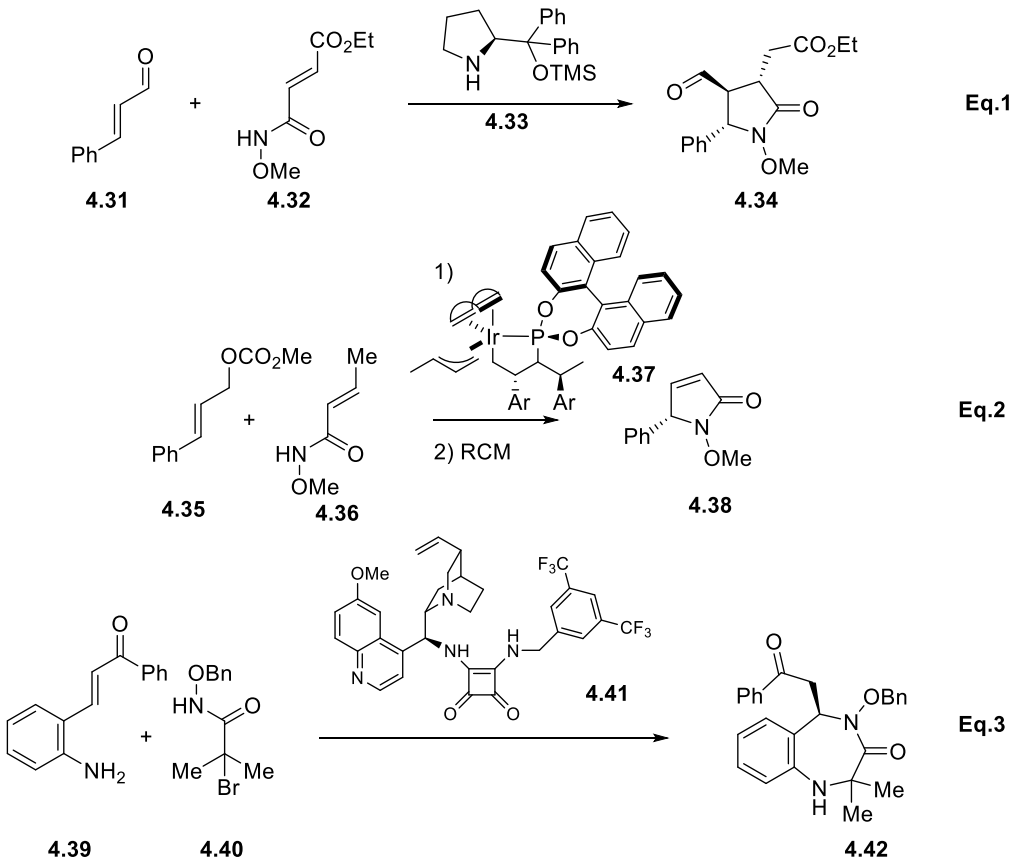

Figure 4-4. Asymmetric synthesis of hydroxamic acids.

In addition, chiral pool provides another synthetic route (Figure 4-5). Honda, *et al.*[16] explored the condensation between chiral amino acid derivatives **4.43** and keto acid **4.44** to form bicyclic hydroxamic acids **4.45**. This method is effective with substituents on amino acids varying

from alkyl to aromatic groups (Eq.1). Meanwhile, Bode *et al.*[17] started with chiral amino alcohol **4.46**. After first cyclization with ethyl-chloro acetate to deliver **4.48**, subsequent bromination and oxidation delivered chiral hydroxamic acid **4.49**, which was further converted to their co-catalysts in kinetic resolution of secondary amines.

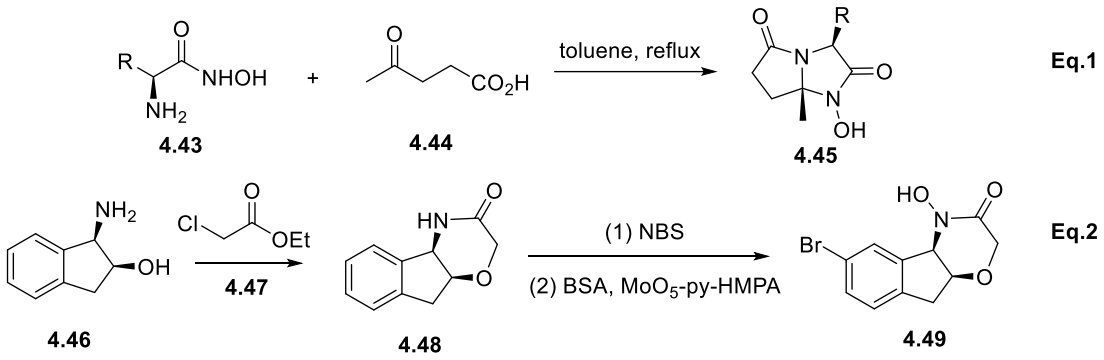

Figure 4-5. Chiral pool synthesis of hydroxamic acids.

However, none of these methods are sufficiently general. Besides, it would be hard to render racemic synthesis mentioned above asymmetric. With easy availability of racemic hydroxamic acids, kinetic resolution would be an attractive addition to existing examples.

4.2 Applications of Amidine-Based Catalysts

From 2003 to 2009, our group developed series of amidine-based catalysts, or ABCs (Figure 4-6), which are among the most easily accessible enantioselective acyl transfer catalysts reported to date. One of the first applications of ABCs is the kinetic resolution of secondary alcohols **4.55** (Figure 4-7).[18] This process is highly efficient for substrates bearing a π-system adjacent to the hydroxyl group, such as benzylic, allylic, and propargylic secondary alcohols and 2-substituted cycloalkanols (Eq.1). ABCs were also studied by many other groups. For example in 2013, Shiina *et al* [19] reposted kinetic resolution of racemic 2-hydroxy-γ-butyrolactones **4.61**

with diphenylacetic acid with pivalic anhydride and *(R)*-BTM. They explored 12 substrates with selectivity factor up to 1000 (Eq.2). ABCs are also used for the kinetic resolution of 4-aryl-oxazolidinones 4.62, which gives selectivity factor up to 200 (Figure 4-6).[20] Later, kinetic resolutions of β-lactams and thiolactams **4.64-4.67** were achieved with easy reaction conditions and high selectivities.[21]

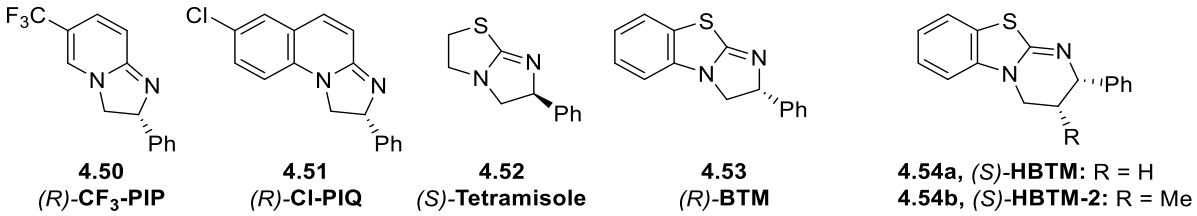

Figure 4-6. Amidine-Based Catalysts (ABCs).

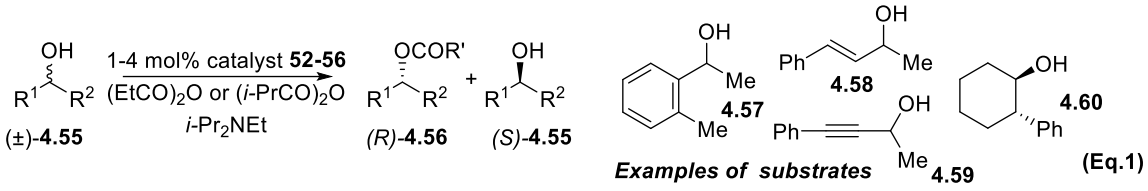

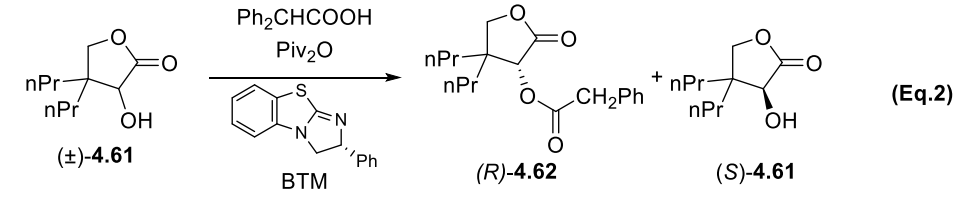

Figure 4-7. Kinetic resolution of secondary alcohols.

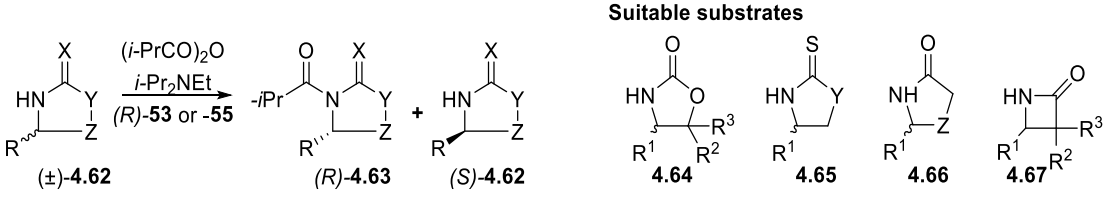

Figure 4-8. Kinetic resolution via enatioselective N-acylation.

Besides kinetic resolution, electro-rich ABCs can found applications in tandem reactions.[22]

Cyclic hydroxamic acids are structural similarity to 2-oxazolidinones **4.64** and 2-substituted cycloalkanols **4.66**, albeit it slightly more acid. It's surprising that there is no precedent of enantioselective acylation on hydroxamic acids. Hence, we decided to explore the possibility of chiral recognition between ABCs and cyclic hydroxamic acids.

4.3 Optimization of kinetic resolution on cyclic hydroxamic acids

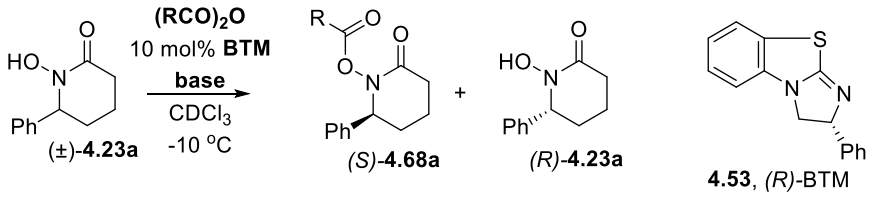

Figure 4-9. Initial results obtained by Matthew Straub.

My former lab mate, Matthew Straub, initially tested the kinetic resolution of 1-hydroxy-6-phenylpiperidin-2-one using isobutyric anhydride as acyl donor and (R)-BTM as catalysts, which had previously worked well for benzylic alcohols[18] and (thio)lactams[21] (Figure 4-9). At −10 ℃, this process is highly efficient, with selectivity factor up to 60. This is a very promising result. With his pending graduation, I decided to continue on this direction. However, his synthetic route to racemic hydroxamic acids was hard to follow. Through literature search, we found out that pyrrolidinone analogues can be obtained from corresponding ketoacids in one pot. Decision was made to start with this class of substrates (Figure 4-10).

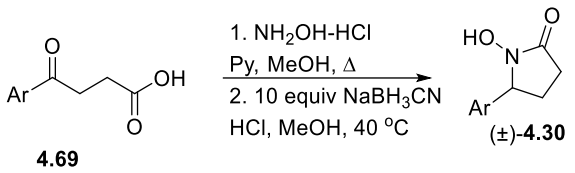

Figure 4-10. One pot synthesis of N-hydroxy pyrrolidinones.

The exploration of reaction conditions started with enantioselective acylation with isobutyric anhydride and Hünig's base in the presence of BTM, inspired by Matthew Straub (Table 4-1). However, only modest enantioselectivity was observed in this reaction (entry 1). This might be due to the background acylation through the anion of the hydroxamic acid substrate. Gratifyingly, omission of the base resulted in a practically useful selectivity factor (entry 2). Acylation with propionic anhydride resulted lower selectivity factor (entry 3). Benzoic anhydride was unreactive at this condition (entry 4). Different temperatures were explored and −10 ℃ is the most practical condition (entry 5 and entry 6). Lower the concentration by half seems no effect on selectivity (entry 7). Other class of amidine-based catalysts were tested, only to be less effective (entry 8 and entry 9). Polar and none-polar solvents were examined, which confirmed chloroform as best solvent in this case (entry 10-12). Each reaction was run in parallel to reduce experimental error and selectivity factors were calculated as average. And a few details are needed to keep consistent s values. Since this reaction is quite fast. It is recommended to cool the mixture to −10 ℃ before adding isobutyric anhydride. Isobutyric anhydride at the end of the reaction couldn't be fully removed by quenching with water. Therefore, concentration of the crude mixture will result in racemic acylation. It is recommended to load the crude mixture directly on the silica gel for purification. At that time, it was quite upsetting to me that the best selective factors were much lower than those obtained by Matthew Straub (22 vs 60). Since we don't have access to his

substrate **4.23** to verify those numbers, we have to assume that all this was because of the substrate differences and I have been doing everything correctly.

Table 4-1. Optimization on kinetic resolution of **4.30a**.

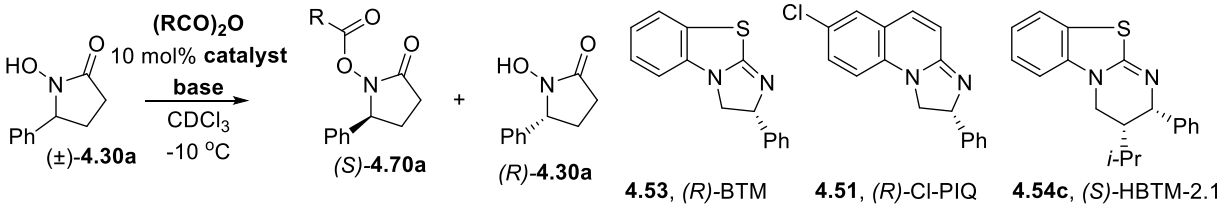

entry	catalyst	R	base	solvent	temp ℃	time h	ee_P %	ee_{SM} %	C %	S	C_{avg} %	S_{avg}
1	**4.53**	*i*-Pr	*i*-Pr_2NEt	$CDCl_3$	−10	1.0	64	46	58	5	54	4
							46	45	50	4		
2	**4.53**	*i*-Pr	none	$CDCl_3$	−10	2.0	75	82	48	23	47	23
							70	84	46	23		
3	**4.53**	Et	none	$CDCl_3$	−10	1.3	50	70	58	6	58	6
							47	65	58	5		
4	**4.53**	Ph	none	$CDCl_3$	−10	3.0	ND	ND	0	0	0	ND
							ND	ND	0	0		
5	**4.53**	*i*-Pr	none	$CDCl_3$	25	1.5	65	75	46	14	44	16
							57	82	41	18		
6	**4.53**	*i*-Pr	none	$CDCl_3$	−45	4.5	61	83	42	20	43	22
							68	85	44	23		
7[a]	**4.53**	*i*-Pr	none	$CDCl_3$	−45	8.0	73	82	47	22	44	23
							60	85	41	23		
8	**4.51**	*i*-Pr	none	$CDCl_3$	−10	2.0	48	60	44	6	41	7
							41	70	37	8		
9	**4.54c**	*i*-Pr	none	$CDCl_3$	−10	2.0	39	78	33	12	37	9
							42	61	41	6		
10	**4.53**	*i*-Pr	none	THF	−10	2.0	68	78	47	16	49	14
							73	69	51	12		
11	**4.53**	*i*-Pr	none	PhMe	−10	2.0	50	75	40	11	43	12
							64	75	46	13		
12	**4.53**	*i*-Pr	none	MeCN	−10	2.0	47	78	38	13	39	15
							54	82	40	17		
12	**4.53**	*i*-Pr	none	Me_2CO	−10	2.0	80	65	55	11	52	10
							62	65	49	9		

[a] Performed at 0.1 M concentration of the substrate. All other entries performed at 0.2 M concentration of the substrates.

4.4 Kinetic resolution of cyclic hydroxamic acids

With the optimized conditions in hand, we proceeded with N-hydroxy-2-pyrrolidone substrates with variation of the aryl groups (Table 4-2). Addition of methyl groups on aryl ring did not have much of an effect on the enantioselectivity. (entry 2 and 3 vs. 1). Electron-donating groups such as methoxy substituted at *para*- or *meta*-positions will enhance the enantioselectivity moderately (entries 4 and 5). However, such group in *ortho*-position was apparently detrimental, probably due to hindrance (entry 6). Electron rich rings 1-naphthyl (**4.30g**), 2-furyl (**4.30h**) and 2-thienyl (**4.30i**) analogues produced respectable s-values (entries 7-9), while substrate **4.30j**, without aromatic moiety, resulted virtually no selectivity under the standard conditions (entry 10). Cation-π interactions between the substrate and the N-acylated ABC catalysts was observed in previous studies, and was proved to be important in this study.

para-halogenated substrates **4.30k** and **4.30l** were confusing in the beginning. *p*-bromophenyl derivative **4.30l** produced a selectivity factor of 12, but its p-chlorophenyl counterpart **4.30k** gave a selectivity factor of 54, even better than other eletron-rich derivatives. Since **4.30k** and **4.30l** were sterically and electronically similar, we surmised that this outcome might be due to differences in solubility between enantiopure **4.30k** and its racemate. If the unreacted *(R)*- **4.30k** crystallized out of the reaction mixture during the KR while (±)-**4.30k** remained in solution, it should result in an apparent enhancement of enantioselectivity. To eprevent recrystallization, this procedure was repeated under more dilute conditions similar to **4.30l**. Indeed, the selectivity factor dropped to 12.

Table 4-2. Kinetic resolution of **4.30**.

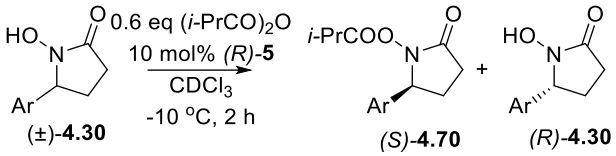

entry	#	Ar	% conv	s
1	**4.30a**		44	23
2	**4.30b**	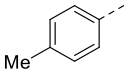	56	23
3	**4.30c**	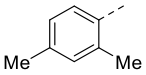	55	25
4	**4.30d**	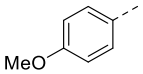	54	41
5	**4.30e**	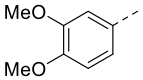	57	32
6	**4.30f**	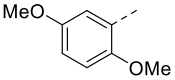	40	12
7	**4.30g**	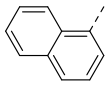	54	33
8	**4.30h**		55	40
9	**4.30i**		58	51
10	**4.30j**		32%	1.3
11	**4.30k**	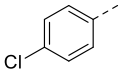	54 54[a]	54 12[a]
12	**4.30l**	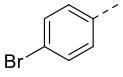	57[a]	12[a]

Standard conditions: See Table 4-1. [a] Carried out at 0.08 M substrate concentration for 4 h

Table 4-3. Racemic synthesis and kinetic resolution of **4.23**.

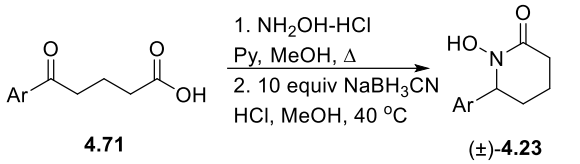

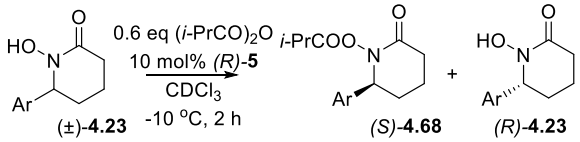

entry	#	Ar	% conv	s
1	**4.23a**		52	82
2	**4.23b**	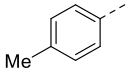	52	60
3	**4.23c**	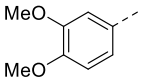	52	73
4	**4.23d**	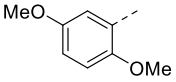	51	26
5	**4.23e**		51	96

Standard conditions: See Table 4-1. [a] Carried out at 0.08 M substrate concentration for 4 h

Next, N-hydroxy-2-piperidones **4.23** (Table 3) were examined. Similar condensation procedure mentioned in Figure 4-10 was utilized to access **4.23**. It was a relief to see that the *s* value of **4.23a** was even better than Matthew Straub's (82 vs 60) after optimization shown in Table 4-1. Throughout all five substrates, the enantioselectivities were higher than their five-membered counterparts while the influence of the aryl groups were similar. para-bromophenyl derivative was examined, but the selectivity factor was not determined due to failure in separation of enantiomers via HPLC.

Finally, the synthesis and resolution of N-hydroxy-4-thiazolidinones **4.75** was explored (Figure 4-11). We initially took the procedure involving simple reflux of **4.72**, **4.74** and

hydroxylamine (Eq.1).[23] However, very little conversion to **4.76** was observed on ^{1}H NMR. There has been a report of a one-pot three component synthesis of **4.78** with the assistance of DCC (Eq.2).[24] Inspired by structural similarity between **4.76** and **4.78**, I reasoned that similar protocol might be useful. (Eq.3). Indeed, **4.76** was isolated with up to 50 % yield (Eq.3). 4.73 was generated *in situ* before added **4.74** and later EDC in one pot. EDC was used instead of DCC for easy purification. It is worth mentioning that lack of easy methods to render this transformation enantioselective makes KR the most attractive option for these pharmacologically relevant [25] compounds in enantioenriched form.

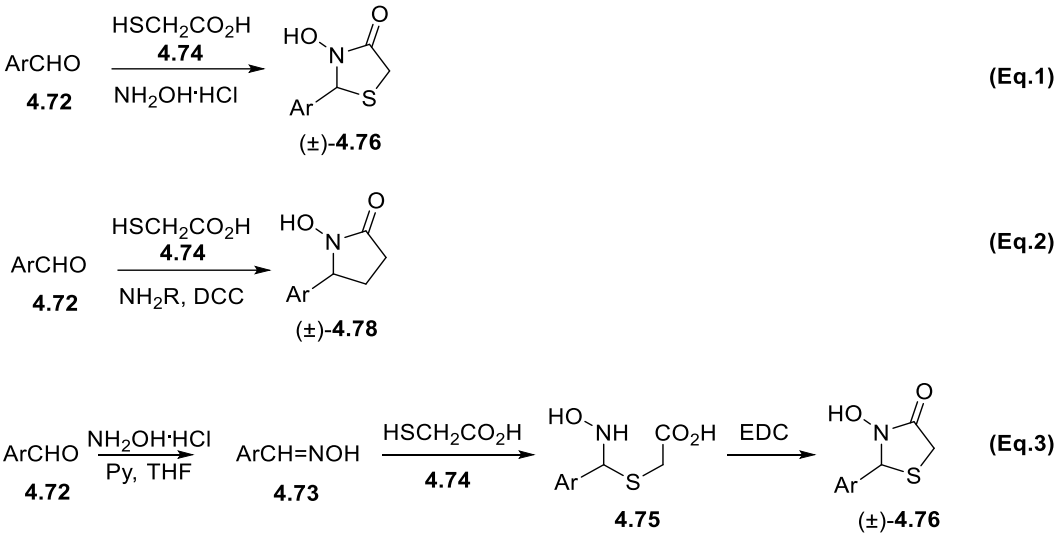

Figure 4-11. Synthesis of **4.76**.

When **4.76** was treated under our kinetic resolution protocol, most of the substrates tested resulted in synthetically useful s-values (Table 4-4). Veratryl derivative **4.76d** produced the most impressive result of this study (entry 4). Since we knew concentration might influence the true selectivity factors, as shown in Table 4-2 entry 11 and 12, we used lower concentrations for these N-hydroxy-4-thiazolidinones because of their poor solubility. 2-pyridyl and para-chlorophenyl

derivatives were also prepared, but the selectivity factors were not determined due to failure in separation of enantiomers via HPLC.

Table 4-4. KR of **4.76.**

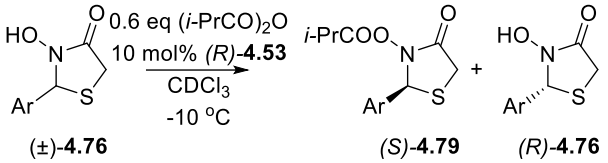

(±)-**4.76** *(S)*-**4.79** *(R)*-**4.76**

entry	#	Ar	[M][a]	time h	% conv	s
1	**4.76a**		0.085	2.5	53	45
2	**4.76b**	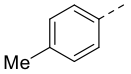	0.085	2.5	50	54
3	**4.76c**	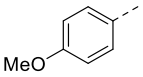	0.085	2.5	51	37
4	**4.76d**	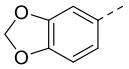	0.03	5	48	102
5	**4.76e**	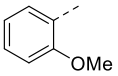	0.085	2.5	47	36
6	**4.76f**	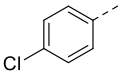	0.017	10	57	10
7	**4.76g**	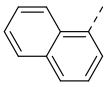	0.03	6.5	51	30
8	**4.76h**	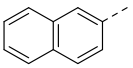	0.03	6.5	46	35

[a] Final concentration of the substrate.

This methodology remained effective in larger scale. Under 10 mmol scale (1.77 g), the resolution of (±)-**4.30a** resulted in good isolated yields and an s-value of 20 (Figure 4-12), similar to that obtained on exploratory scale (cf. Table 4-2, entry 1).

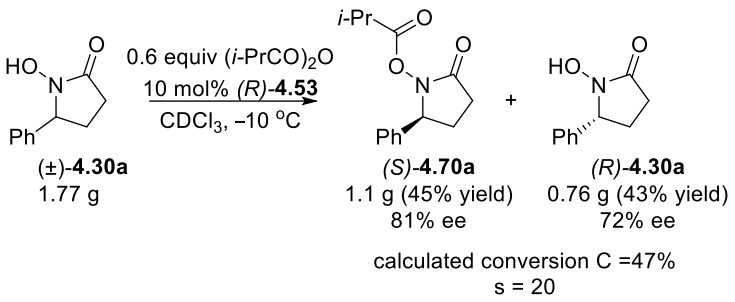

Figure 4-12. KR of (±)-**4.30a** on 10 mmol scale.

In conclusion, we have developed the first acylative kinetic resolution of cyclic hydroxamic acids. This methodology offers an attractive alternative to existing approaches because of easy availability of the requisite racemic starting materials and reagents under simple reaction procedures. In the studies of KR of benzylic alcohols[18] and (thio)lactams[21], we noticed the π-cation interactions between substrate and catalysts are vital. In this study, we also saw the importance of an aromatic group, preferably an electron rich one. π-system exists beyond aromatic groups, such as alkene and alkynes. Our undergraduate student Julian Liao is currently exploring this direction.

4.5 Experimental

All reagents were obtained commercially and used as received unless specified otherwise. Catalysts **4.53**,[26] **4.51**,[27] and **4.54c**[28] were prepared as previously described. Deuterated chloroform, deuterated acetone, deuterated acetonitrile, deuterated toluene, and deuterated tetrahydrofuran were used as the reaction medium. Solvents used for chromatography were ACS or HPLC grade, as appropriate. Reactions were carried out under inert atmosphere and monitored by 1 H NMR. Uniplate HLF (2 μm) silica gel plates were used for TLC analyses. Flash column chromatography was performed over Sorbent Technologies silica gel (40-63 mm). HPLC analyses were performed on a Shimadzu LC system using Chiralcel OD-H and Chiralpak AS-H analytical chiral stationary phase columns (4.6x250 mm, Chiral Technologies, Inc.) with UV detectors at 254 nm and 204 nm, as appropriate, with a flow rate of 1.0 mL/min. ^{1}H and ^{13}C NMR spectra were recorded on DD2 500 MHz Agilent spectrometers and 600 MHz Agilent spectrometers. The chemical shifts are reported as δ values (ppm) relative to TMS using residual $CHCl_3$ peak as the reference (7.26 ppm for 1 H NMR, 77.16 ppm for ^{13}C NMR). Melting points were measured on a Stuart SMP10 melting point apparatus. High-Resolution mass spectral analyses were performed at Washington University MS Center on a Bruker MaXis QTOF mass spectrometer using Electrospray Ionization (ESI). Infrared spectra were recorded on a Bruker Alpha Platinum-ATR. Optical rotations were determined on a Rudolph Autopol III polarimeter.

4.5.1 Synthesis of racemic substrates.

4.5.1a. Preparation of N-hydroxy-2-pyrrolidones 8 and N-hydroxy-2-piperidones 10.

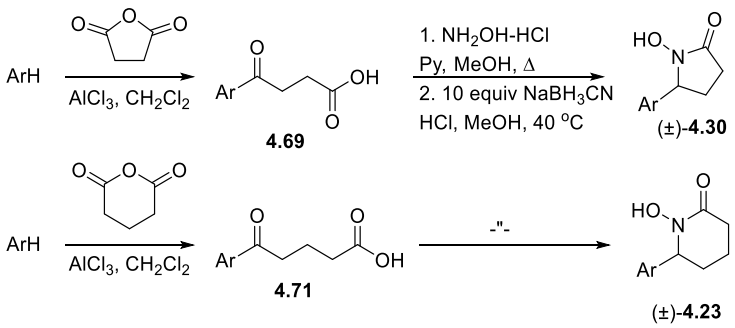

All racemic N-hydroxy-2-pyrrolidones **4.30**[29] and N-hydroxy-2-piperidones **4.23**[30] were prepared from the corresponding 4- and 5-ketoacids, respectively, as described in the literature. Most of the requisite ketoacids were known compounds obtainable commercially or via Friedel-Crafts acylation of arenes with succinic or glutaric anhydride, respectively. In the case of 1-nathyl and 2,5-dimethyl derivatives, Friedel-Crafts acylation produced other region isomers, which were hard to separate. Therefore, those ketoacids were obtained from the corresponding aromatic magnesium bromide and glutaric anhydride.[31]

In a round bottom flasked purged with nitrogen, aromatic bromide (20 mmol), magnesium turnings (30 mmol) quickly washed with 1 HCl and dried, was suspended in 50 mL dry THF heated with a heat gun till reflux. The mixture will keep reflux until solution turned dark and less heat was generated. Then the reaction was heated to 80 ℃ for another 30 min, cooled to -78 ℃ and cannulated to glutaric anhydride (22 mmol). Upon completion, the reaction was allowed to slowly warm up to 0 ℃. 20 mL 1M HCl was added slowly, and the mixture was extracted with ethyl acetate, washed with NaCl, dried over $MgSO_4$ and concentrated by rotary evaporation. The residue was purified via silica gel with 5% to 25% acetone in hexane.

Characterization of previously unreported compounds is given in Section 5.

4.5.2b. Preparation of N-hydroxy-4-thiazolidinones 4.76.

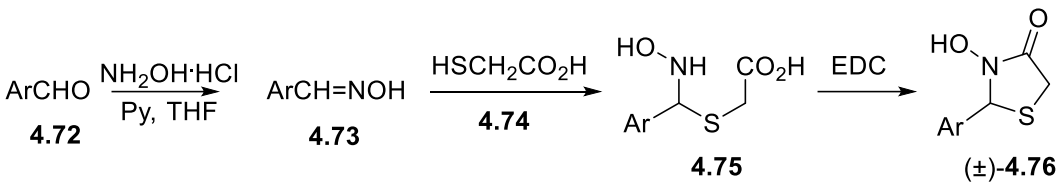

4.72 **4.73** **4.74** **4.75** (±)-**4.76**

A modified literature procedure was followed.[26] A mixture of an aromatic aldehyde (10 mmol), hydroxylammonium chloride (1.38 g, 20 mmol), pyridine (1.6 mL, 20 mmol) and THF (30 mL) was refluxed for 2 h. The mixture was cooled to rt and treated with 2-mercaptoacetic acid (2.76 g, 2.1 mL, 30 mmol) added slowly. After 1 h, EDC (15 mmol) was added to the mixture and the reaction was left stirring for 2 hours. The reaction mixture was diluted with 50 mL of EtOAc, washed with 1M HCl (3×50 mL), saturated K_2CO_3 (3×50 mL) and again with 1M HCl (3×50 mL). Upon drying with Na_2SO_4, the crude mixture was rotary-evaporated to dryness and purified via flash chromatography (hexane to acetone 10:1). Characterization of previously unreported compounds is given in Section 5.

4.5.2 Optimization studies.

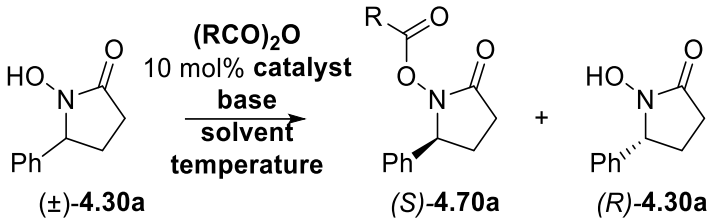

Figure 4-13. Optimization of reaction conditions

4.5.2a. Optimized procedure (Entry 2, Table 4-5): A solution of substrate (±)-**4.30a** (30 mg, 0.169 mmol, final concentration ca. 0.19 M) in 0.85 mL of $CDCl_3$ stirring magnetically with 10 mg of anhydrous Na_2SO_4 at −10 °C was treated sequentially with *(R)*-**4.53** (55 μL of 0.3 M stock solution in $CDCl_3$, 0.017 mmol, 0.10 equiv) and isobutyric anhydride (16 μL, 0.10 mmol, 0.60 equiv). The reaction progress was monitored by ^{1}H NMR. After reaching ca. 50% conversion (2 h), the reaction mixture was quenched with 1 M aqueous HCl and extracted with CH_2Cl_2. The extract was dried over Na_2SO_4 and added directly to a silica gel column pre-wetted with hexanes. The solvent was passed through the column using compressed air. The column was air dried before eluent (5% acetone in hexanes) was applied and chromatography continued (5→40%, acetone in hexanes).* The product was isolated as a colorless oil. The unreacted starting material was recovered as a white solid. Both were analyzed by chiral stationary phase HPLC (see Section 5). The reported % conversion **C** and selectivity factor **S** were calculated according to Kagan's equations:[32]

* Concentrating the reaction mixture in the usual manner before chromatography is not advisable, as it leads to unselective acylation of the starting material with excess anhydride and therefore lowers enantiomeric enrichment.

$C=ee_{SM}/(ee_P+ee_{SM})$, wherein **ee_P** is the enantiomeric excess of the acylated product and **ee_{SM}** is the enantiomeric excess of the unreacted substrate (expressed as fractions).

$S = \ln[(1-C)(1-ee_{SM})]/\ln[(1-C)(1+ee_{SM})]$.

Other experiments summarized in Table 4-5 were performed analogously except as specified in each case.

3b. Scaled-up procedure

The above procedure was scaled up to 10 mmol (1.77 g) of substrate (±)-**4.30a** using 53 mL chloroform, 100 mg Na_2SO_4 1 mmol catalyst *(R)*-**4.53**, and 6.0 mmol (0.95 mL) of isobutyric anhydride. The product was isolated in 45% yield (1.10 g) with 81% ee. The unreacted starting material was recovered in 43% yield (760 mg) with 72% ee.

4.5.3 Substrate scope

Kinetic resolution of all substrates was performed according to the optimized procedure shown in Section 3, except as specified in each case.

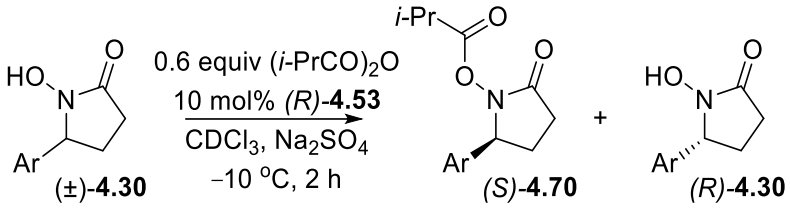

Table 4-5. KR of N-hydroxy-2-pyrrolidones

entry	substrate	Ar	eeSM %	eeP %	C %	S	Cavg %	Savg
1	4.30b	4-methylphenyl	95	73	56	23	56	23
			92	75	56	22		
2	4.30c	2,4-dimethylphenyl	94	76	55	26	55	25
			91	77	54	24		
3	4.30d	4-methoxyphenyl	96	84	53	44	41	53
			94	83	53	38		
4	4.30e	3,4-dimethoxyphenyl	99	72	58	32	57	32
			98	76	56	32		
5	4.30f	2,5-dimethoxyphenyl	48	79	38	14	40	12
			52	73	42	11		
6	4.30g	1-naphthyl	97	80	55	35	33	54
			92	81	53	31		
7	4.30h	2-furyl	98	82	55	42	55	40
			97	81	54	39		
8	4.30i	2-thienyl	90	91	50	65	51	58
			91	88	51	50		
9	4.30j	methyl	2	13	13	1.3	17	1.2
			1	4	20	1.1		
10	4.30k	4-chlorophenyl	98	85	54	57	54	54
			98	84	54	51		
11 a	4.30k	4-chlorophenyl	79	61	56	10	54	12
			77	72	52	14		
12 a	4.30l	4-bromophenyl	84	67	56	13	57	13
			86	63	58	12		

[a] Performed at 0.1 M concentration of the substrate; 4 h reaction time.

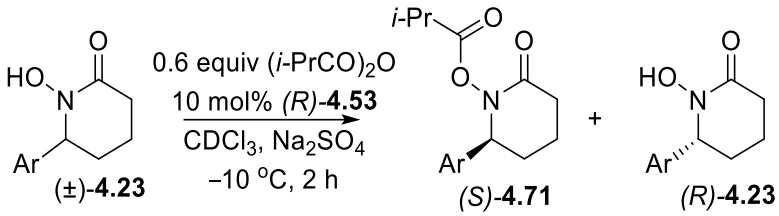

Table 4-6. KR of N-hydroxy-2-piperidones

entry	substrate	Ar	ee_{SM} %	ee_P %	C %	S	C_{avg} %	S_{avg}
1	**4.23a**	phenyl	98	89	53	81	52	82
			96	91	51	83		
2	**4.23b**	4-methylphenyl	95	88	52	61	52	60
			93	89	51	59		
3	**4.23c**	3,4-dimethoxyphenyl	95	91	51	79	52	73
			96	89	52	67		
4	**4.23d**	2,5-dimethoxyphenyl	83	84	50	29	51	26
			85	80	52	24		
5	**4.23e**	2-furyl	97	92	51	98	51	96
			94	93	50	94		

Performed at 0.2 M concentration of the substrate; 2 h reaction time.

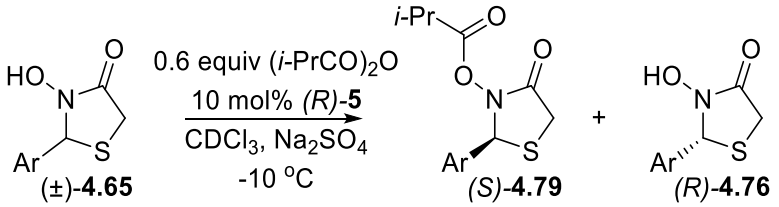

Table 4-8. KR of N-hydroxy-4-thiazolidones

entry	substrate	Ar	time, h	ee_{SM} %	ee_P %	C %	S	C_{avg} %	S_{avg}
1[a]	**4.65a**	phenyl	2.5	95	86	52	48	53	45
				96	83	54	42		
2[a]	**4.65b**	4-methylphenyl	2.5	94	89	51	60	50	54
				86	89	49	48		
3[a]	**4.65c**	4-methoxyphenyl	2.5	89	85	51	38	51	38
				90	85	52	37		
4[b]	**4.65d**	3,4-(methylene-dioxy)-phenyl	5	85	95	47	100	48	103
				92	94	49	105		
5[a]	**4.65e**	2-methoxyphenyl	2.5	75	89	46	39	47	36
				80	86	48	32		
6[c]	**4.65f**	4-chlorophenyl	10	85	56	60	9	57	10

				75	65	54	10		
7[b]	**4.65g**	1-naphthyl	6.5	89	83	52	32	51	30
				85	82	51	27		
8[b]	**4.65h**	2-naphthyl	6.5	70	89	44	38	46	35
				80	86	48	33		

[a] Performed at 0.085 M concentration of the substrate. [b] Performed at 0.03 M concentration of the substrate. [c] Performed at 0.017 M concentration of the substrate.

4.5.4 Characterization of new compounds

HPLC analysis. All hydroxamic acids **4.30**, **4.23**, and **4.76** listed below were converted into the corresponding O-isobutyryl derivatives to facilitate HPLC analysis of their enantiomeric composition. Typically, a hydroxamic acid (0.10 mmol), isobutyric anhydride (25 μL, 0.15 mmol) and DMAP (1 mg, 0.01 mmol) were dissolved in 1 mL chloroform. The reaction mixture was stirred at room temperature for 30 min, quenched with 1 M HCl, washed with saturated NaCl, extracted by CH_2Cl_2, dried over Na_2SO_4 and concentrated via rotary evaporation. The residue was purified by flash chromatography (hexane to acetone 10:1).

Absolute configuration: Unreacted **4.30a** and **4.23a** recovered from KR (see Table 4-5, entry 2 and Table 4-7, entry 1, respectively) were converted into the corresponding O-methyl derivatives by treatment with MeI and K_2CO_3 in acetone. Both Me-**4.30a** and Me-**4.23a** thus obtained displayed a positive sign of optical rotation and thus were assigned *(R)*-configuration by correlation with the literature data.[28] The configuration of other compounds was assigned by analogy.

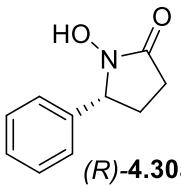

(R)-**4.30a**

Racemate is a known compound prepared as described[29] in 35% yield. **^{1}H NMR** (500 MHz, $CDCl_3$) δ 9.34 (br, 1H), 7.41 - 7.38 (m, 2H), 7.33 - 7.29 (m, 3H), 4.85 - 4.83 (t, *J* = 5 Hz, 1H), 2.58 - 2.43 (m, 3H), 1.95 - 1.87 (m, 1H). **^{13}C NMR** (125 MHz, $CDCl_3$): 171.4, 139.7, 128.9, 128.1, 126.3, 63.7, 27.3, 26.1. **IR** (cm^{-1}): 3113, 2872, 1674. **MS**: HR-ESI calculated for $[C_{10}H_{11}NO_2+H]^+$: 178.0868, found: 178.0873.; **m.p.** 129-132 ℃. *(R)*-**8a** was isolated in 47% yield and 70% ee (Table 4-5, entry 2a). $[\alpha]_D^{22}$= +35 °(c=1.00, acetone).

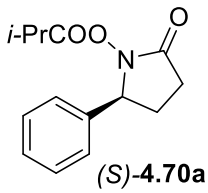

(S)-**4.70a**

Isolated in 36% yield and 84% ee (Table 4-5, entry 2a): **^{1}H NMR** (600 MHz, $CDCl_3$) δ 7.38 - 7.36 (m, 2H), 7.34 - 7.31 (m, 2H), 4.88 - 4.85 (t, *J* = 6 Hz), 2.62 - 2.51 (m, 4H), 2.06 – 2.00 (m, 1H), 1.09 - 1.05 (dd, *J* = 6 Hz, 6H). **^{13}C NMR** (151 MHz, $CDCl_3$): δ 174.0, 171.1, 138.7, 128.8, 128.4, 126.6, 62.8, 31.8, 27.1, 26.8, 18.6. **IR** (cm^{-1}): 3153, 2951, 1709, 1630. **MS**: HR-ESI calculated for $[C_{14}H_{17}NO_3+H]^+$: 248.1287, found: 248.1276; **HPLC** (7.5% isopropanol/hexanes, AS-H): *(S)* enantiomer: 16.7 min; *(R)* enantiomer: 27.2 min; $[\alpha]_D^{22}$= −29 °(c=1.00, acetone).

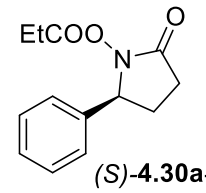

(S)-**4.30a**-Et

Isolated in 43% yield and 50% ee (Table 4-5, entry 3a): **^{1}H NMR** (500 MHz, $CDCl_3$) δ 7.40 - 7.36 (m, 2H), 7.35 - 7.31 (m, 2H), 4.90 - 4.87 (t, *J* = 65 Hz), 2.62 - 2.52 (m, 3H), 2.43 – 2.29 (m, 2H), 2.04 - 1.95 (m, 1H), 1.10 - 1.07 (dd, *J* = 5 Hz, 6H). **^{13}C NMR** (126 MHz, $CDCl_3$): δ 171.3, 171.2, 138.8, 128.8, 128.4, 126.5, 62.8, 27.0, 24.9, 8.7. **IR** (cm^{-1}): 2986, 2946, 1816, 1791, 1734, 1461, 1417, 1347, 1252. MS: HR-ESI calculated for $[C_{13}H_{15}NO_3+H]^+$: 234.1130, found: 234.1111. **HPLC** (7.5% isopropanol/hexanes, AS-H): *(S)* enantiomer: 18.2 min; *(R)* enantiomer: 30.0 min; 50% ee; $[\alpha]_D^{22}$= −12 °(c=1.00, acetone).

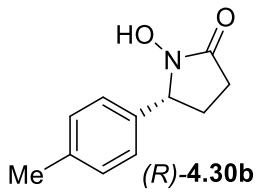

(R)-**4.30b**

Racemate was prepared in 35% yield. **^{1}H NMR** (600 MHz, $CDCl_3$) δ 7.21 - 7.18 (m, 4H), 4.80 - 4.78 (t, *J* = 6 Hz, 1H), 2.57 - 2.42 (m, 3H), 2.35(s, 3H), 1.94 - 1.89 (m, 1H). **^{13}C NMR** (151 MHz, $CDCl_3$): δ 171.2, 138.0, 136.6, 129.6, 126.2, 63.4, 27.3, 26.1, 21.1. **IR** (cm^{-1}): 3143, 2925, 1683, 1493, 1150. **MS**: HR-ESI calculated for $[C_{11}H_{13}NO_2+H^+]$: 214.0844, found, 214.0833.; **m.p.** 138-141 ℃. *(R)*-**8b** was isolated in 47% yield and 95% ee (Table 4-6, entry 1a). $[\alpha]_D^{22}$= +61 °(c=1.00, acetone).

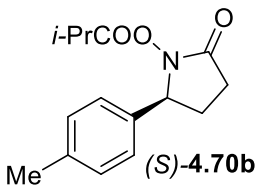

(S)-**4.70b**

Isolated in 53% yield and 74% ee (Table 4-6, entry 1a): **^{1}H NMR** (500 MHz, $CDCl_3$) δ 7.32 - 7.26 (m, 4H), 4.83 - 4.81 (t, *J* = 5 Hz, 1H), 2.53 - 2.48 (m, 4H), 2.32 - 2.25 (m, 3H), 1.98 - 1.91 (m, 1H), 1.02 - 1.00 (t, *J* = 5 Hz, 3H). **^{13}C NMR** (151 MHz, $CDCl_3$): δ 171.1, 171.0, 138.5, 128.6, 128.2, 126.3, 62.6, 28.4, 26.8, 24.7. **IR** (cm^{-1}): 2986, 2946, 1816, 1791, 1734, 1461. **MS**: HR-ESI calculated for [$C_{15}H_{19}NO_3$+Na^+]: 284.1263, found, 284.1251. **HPLC** (7.5% isopropanol/hexanes, AS-H): *(S)* enantiomer: 13.5 min; *(R)* enantiomer: 22.0 min; $[\alpha]_D^{22}$= −54 °(c=1.00, acetone).

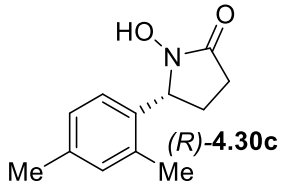

(R)-**4.30c**

Racemate was prepared in 39% yield. **^{1}H NMR** (500 MHz, $CDCl_3$) δ 9.37 (br, 1H), 7.09 - 7.02 (dd, *J* = 5 Hz, 2H), 5.16 - 5.06 (m, 1H), 2.56 - 2.48 (m, 3H), 2.35 (s, 3H), 2.31 (s, 3H), 1.86 - 1.81 (m, 1H). **^{13}C NMR** (126 MHz, $CDCl_3$): δ 171.3, 137.4, 136.1, 131.7, 130.7, 128.3, 125.4, 60.5, 29.7, 24.7, 21.1, 18.5. **IR** (cm^{-1}): 2977, 1785, 1734. **MS**: HR-ESI calculated for [$C_{12}H_{15}NO_2$+H^+]: 206.1181, found, 206.1171.; **m.p.** 142-144 ℃. *(R)*-**8c** was isolated in 37% yield and 94% ee (Table 4-6, entry 2a). $[\alpha]_D^{22}$= +89 °(c=1.00, acetone).

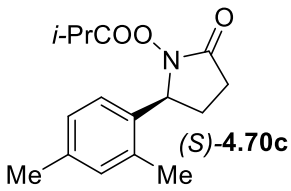

(S)-**4.70c**

Isolated in 55% yield and 76% ee (Table 4-6, entry 2a): **^{1}H NMR** (500 MHz, $CDCl_3$) δ 7.17 (s, 1H), 7.05 - 7.04 (d, *J* = 5 Hz, 1H), 7.02 - 7.01 (d, *J* = 5 Hz, 1H), 5.15 - 5.12 (t, *J* = 5 Hz, 1H), 2.64 - 2.53 (m, 4H), 2.32 (s, 3H), 2.26 (s, 3H), 1.92 - 1.88 (m, 1H), 1.17 - 1.08 (m, 6H). **^{13}C NMR** (126 MHz, $CDCl_3$): δ 174.17, 171.09, 136.58, 136.17, 131.95, 130.61, 128.51, 125.98, 59.27, 31.87, 26.71, 21.08, 18.76, 18.61. **IR** (cm^{-1}): 2920, 1677, 1457. **MS**: HR-ESI calculated for [$C_{16}H_{21}NO_3$+Na^+]: 298.1419, found, 298.1407. **HPLC** (1% isopropanol/hexanes, OD-H): *(S)* enantiomer: 30.3 min; *(R)* enantiomer: 37.6 min; $[\alpha]_D^{22}$= −41 °(c=1.00, acetone).

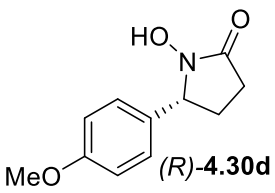

(R)-**4.30d**

Racemate was prepared in 28% yield. **^{1}H NMR** (500 MHz, $CDCl_3$) δ 9.37 (br, 1H), 7.09 - 7.02 (dd, *J* = 5 Hz, 2H), 5.16 - 5.06 (m, 1H), 2.56 - 2.48 (m, 3H), 2.35 (s, 3H), 2.31 (s, 3H), 1.86 - 1.81 (m, 1H). **^{13}C NMR** (126 MHz, $CDCl_3$): δ 171.3, 137.4, 136.1, 131.7, 130.7, 128.3, 125.4, 60.5, 29.7, 24.7, 21.1, 18.5. **IR** (cm^{-1}): 2977, 1785, 1734. **MS**: HR-ESI calculated for [$C_{11}H_{13}NO_3$+H^+]: 208.0974, found, 208.0967.; **m.p.** 152-155 ℃. *(R)*-**8d** was isolated in 44% yield and 96% ee (Table 4-6, entry 3a). $[\alpha]_D^{22}$= +76 °(c=1.00, acetone).

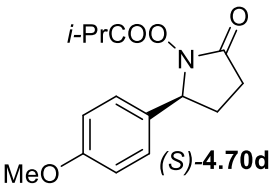

(S)-**4.70d**

Isolated in 50% yield and 84% ee (Table 4-6, entry 3a): **^{1}H NMR** (600 MHz, $CDCl_3$) δ 7.25 - 7.23 (d, *J* = 5 Hz, 2H), 6.90 - 6.88 (d, *J* = 5 Hz, 2H), 4.82 - 4.80 (t, *J* = 5 Hz, 1H), 3.80 (s, 1H), 2.61 - 2.48 (m, 3H), 2.05 - 2.18 (m, 1H), 1.09 - 1.06 (m, 6H). **^{13}C NMR** (151 MHz, $CDCl_3$): δ 173.97, 170.92, 159.68, 130.42, 128.02, 114.10, 62.38, 55.28, 31.82, 27.18, 26.78, 18.68. **IR** (cm^{-1}): 2977, 1784, 1731, 1541. **MS**: HR-ESI calculated for [$C_{15}H_{19}NO_4$+H^+]: 278.1392, found, 278.1391. **HPLC** (5% isopropanol/hexanes, OD-H): *(S)* enantiomer: 30.3 min; *(R)* enantiomer: 37.6 min; $[\alpha]_D^{22}$= −54 ° (c=1.00, acetone).

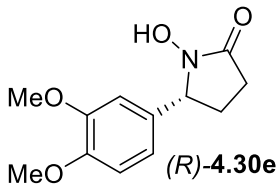

(R)-**4.30e**

Racemate was prepared in 37% yield. **^{1}H NMR** (500 MHz, $CDCl_3$) δ 9.38 (br, 1H), 7.23 - 7.21 (d, *J* = 5 Hz, 2H), 6.93 - 6.91 (d, *J* = 5 Hz, 2H), 4.79 - 4.76 (t, *J* = 5 Hz, 1H), 3.81 (s, 3H), 2.56 - 2.41 (m, 3H), 1.93 - 1.88 (m, 1H). **^{13}C NMR** (126 MHz, $CDCl_3$): δ 171.2, 159.5, 131.6, 127.6, 114.3, 63.1, 55.3, 27.4, 26.2. **IR** (cm^{-1}): 2908, 1683, 1515, 1248. **MS**: HR-ESI calculated for [$C_{12}H_{15}NO_4$+H^+]: 238.1079, found, 238.1065; **m.p.** 153-155 ℃. *(R)*-**8e** was isolated in 47% yield and 99% ee (Table 4-6, entry 4a). $[\alpha]_D^{22}$= +94 °(c=1.00, acetone).

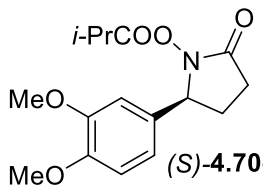

(*S*)-**4.70e**

Isolated in 50% yield and 72% ee (Table 4-6, entry 4a): **^{1}H NMR** (600 MHz, $CDCl_3$) δ 7.25 - 7.23 (d, *J* = 5 Hz, 2H), 6.90 - 6.88 (d, *J* = 5 Hz, 2H), 4.82 - 4.80 (t, *J* = 5 Hz, 1H), 3.88 (s, 3H), 3.87 (s, 3H), 2.61 - 2.48 (m, 3H), 2.05 - 2.18 (m, 1H), 1.09 - 1.06 (m, 6H). **^{13}C NMR** (151 MHz, $CDCl_3$): δ 173.99, 171.12, 149.33, 149.07, 130.97, 119.32, 110.93, 109.17, 77.25, 77.00, 76.75, 62.80, 55.93, 55.89, 31.84, 27.25, 26.94, 18.71, 18.65. **IR** (cm^{-1}): 2972, 1784, 1731. **MS**: HR-ESI calculated for [$C_{16}H_{21}NO_5$+Na^+]: 330.1317, found, 330.1297. **HPLC** (7.5% isopropanol/hexanes, OD-H): *(R)* enantiomer: 25.1 min; *(S)* enantiomer: 32.5 min; $[\alpha]_D^{22}$= −30 °(c=1.00, acetone).

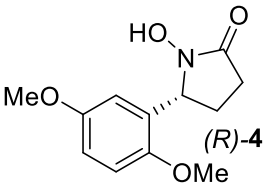

(*R*)-**4.30f**

Racemate was prepared in 42% yield. **^{1}H NMR** (600 MHz, $CDCl_3$) δ 10.34 (br, 1H), 6.86 (s, 1H), 6.80 - 6.75 (m, 2H), 5.15 -5.13 (t, *J* = 6 Hz, 1H), 3.76 - 3.75 (d, 6H), 2.53 - 2.36 (m, 3H), 1.81 - 1.77 (m, 1H). **^{13}C NMR** (126 MHz, $CDCl_3$): δ 171.76, 153.61, 150.80, 128.90, 113.30, 112.21, 111.67, 77.21, 77.00, 76.79, 58.86, 55.78, 55.59, 27.03, 24.28. **IR** (cm^{-1}): 1683, 1503, 1220. **MS**: HR-ESI calculated for [$C_{12}H_{15}NO_4$+H^+]: 260.0899, found, 260.0884; **m.p.** 164-**4.79**8 ℃. *(R)*-**8f** was isolated in 45% yield and 48% ee (Table 4-6, entry 5a). $[\alpha]_D^{22}$= +13 °(c=1.00, acetone).

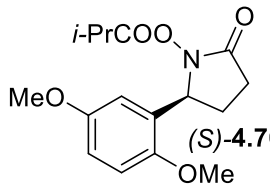

(*S*)-**4.70f**

Isolated in 51% yield and 79% ee (Table 4-6, entry 5a): **^{1}H NMR** (500 MHz, $CDCl_3$) δ 6.91 - 6.90 (d, *J* = 5 Hz, 2H), 6.80 - 6.79 (d, *J* = 5 Hz, 2H), 5.22 - 5.19 (t, *J* = 5 Hz, 1H), 3.77 (s, 3H), 3.75 (s, 3H), 2.64 - 2.47 (m, 4H), 1.94 - 1.86 (m, 1H), 1.14 - 1.08 (m, 6H). **^{13}C NMR** (126 MHz, $CDCl_3$): δ 173.89, 171.72, 153.70, 151.09, 128.04, 113.77, 112.30, 111.71, 57.55, 55.87, 55.71, 31.81, 26.77, 24.74, 18.65, 18.62. **IR** (cm^{-1}): 1784, 1735, 1503, 1466, 1221. **MS**: HR-ESI calculated for [$C_{16}H_{21}NO_5$+Na^+]: 330.1317, found, 330.1301. **HPLC** (5% isopropanol/hexanes, OD-H): *(R)* enantiomer: 15.5 min; *(S)* enantiomer: 17.1 min; $[\alpha]_D^{22}$= −43 °(c=1.00, acetone).

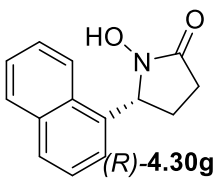

(R)-**4.30g**

Racemate was prepared in 28% yield. **^{1}H NMR** (500 MHz, $CDCl_3$) δ 7.95 - 7.90 (dd, *J* = 10 Hz, 2H), 7.84 - 7.82 (d, *J* = 10 Hz, 1H), 7.59 - 7.49 (m, 4H), 5.74 - 5.71 (t, *J* = 7.5 Hz), 2.86 - 2.82 (m, 1H), 2.10 - 2.02 (m, 3H), 1.17 - 1.15 (m, 1H), 1.07 - 1.05 (dd, *J* = 5 Hz, 6H). **^{13}C NMR** (126 MHz, $CDCl_3$): 174.17, 171.32, 134.41, 133.90, 130.39, 129.10, 128.42, 126.49, 125.84, 125.55, 122.76, 122.15, 59.38, 31.88, 30.88, 26.61, 25.95, 18.72, 18.56. **IR** (cm^{-1}): 3160, 2894, 1679. **MS**: HR-ESI calculated for [$C_{14}H_{13}NO_2$+H^+]: 228.1025, found, 228.1021; **m.p.** 170-176 ℃. *(R)*-**8g** was isolated in 48% yield and 94% ee (Table 4-6, entry 6a). $[\alpha]_D^{22}$= +132 °(c=1.00, acetone).

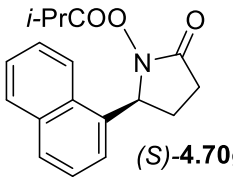

(S)-**4.70g**

Isolated in 52% yield and 80% ee (Table 4-6, entry 6a): **^{1}H NMR** (600 MHz, $CDCl_3$) δ 9.99 (br, 1H), 7.92 - 7.90 (d, *J* = 6 Hz, 2H), 7.83 - 7.81 (d, *J* = 9 Hz, 1H), 7.56 - 7.49 (m, 4H), 5.70 - 5.68 (t, *J* = 6 Hz, 1H), 2.80 - 2.74 (m, 1H), 2.61 - 2.51 (m, 2H), 2.03 - 1.97 (m, 1H). **^{13}C NMR** (151 MHz, $CDCl_3$): δ 174.17, 171.32, 134.41, 133.90, 130.39, 129.10, 128.42, 126.49, 125.84, 125.55, 122.76, 122.15, 59.38, 31.88, 30.88, 26.61, 25.95, 18.72, 18.56. **IR** (cm^{-1}): 2978, 1782, 1733. **MS**: HR-ESI calculated for [$C_{18}H_{19}NO_3$+H^+]: 298.1443, found, 298.1443. **HPLC** (5% isopropanol/hexanes, OD-H): *(S)* enantiomer: 17.9 min; *(R)* enantiomer: 19.6 min; $[\alpha]_D^{22}$= −51 °(c=1.00, acetone).

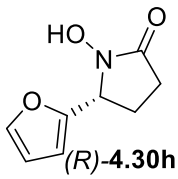

(R)-**4.30h**

Racemate was prepared in 25% yield. **^{1}H NMR** (500 MHz, $CDCl_3$) δ 7.41 (s, 1H), 6.35 - 6.34 (dd, *J* = 5 Hz, 1H), 6.32 - 6.31 (d, *J* = 5 Hz, 1H), 4.92 - 4.90 (t, *J* = 5 Hz, 1H), 2.70 - 2.60 (m, 2H), 2.54 - 2.45 (m, 2H), 2.39 - 2.32 (m, 1H), 1.19 - 1.16 (dd, *J* = 5 Hz, 6H). **^{13}C NMR** (126 MHz, $CDCl_3$): δ 173.93, 170.26, 150.60, 143.18, 110.34, 109.00, 55.57, 31.87, 29.69, 26.69, 22.11, 18.85, 18.68. **IR** (cm^{-1}): 3123, 2878, 1674, 746. **MS**: HR-ESI calculated for [$C_8H_9NO_3$+H^+]: 168.0661, found, 168.0650; **m.p.** 145 ℃ (dec). *(R)*-**8h** was isolated in 45% yield and 98% ee (Table 4-6, entry 7a). $[\alpha]_D^{22}$= +48 °(c=1.00, acetone).

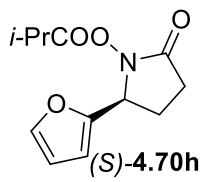

(S)-**4.70h**

Isolated in 53% yield and 82% ee (Table 4-6, entry 7a): **^{1}H NMR** (500 MHz, $CDCl_3$) δ 9.40 (br, 1H), 7.40 (s, 1H), 6.40 - 6.39 (d, *J* = 5 Hz, 1H), 6.36 - 6.35 (d, *J* = 5Hz, 1H), 4.86 - 4.83 (t, *J* = 5 Hz, 1H), 2.63 - 2.56 (m, 1H), 2.45 - 2.35 (m, 2H), 2.26 - 2.17 (m, 1H). **^{13}C NMR** (126 MHz, $CDCl_3$): δ 170.8, 151.3, 142.8, 110.5, 108.7, 76.8, 56.9, 27.1, 21.9. **IR** (cm^{-1}): 2925, 1791, 1733, 1717, 1070. **MS**: HR-ESI calculated for [$C_{12}H_{15}NO_4$+Na^+]: 260.0899, found, 260.0884. **HPLC** (7.5% isopropanol/hexanes, AS-H): *(S)* enantiomer: 27.1 min; *(R)* enantiomer: 47.4 min; $[\alpha]_D^{22}$= −30° (c=1.00, acetone).

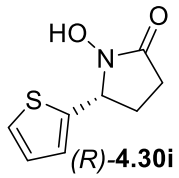

(R)-**4.30i**

Racemate was prepared in 34% yield. **^{1}H NMR** (600 MHz, $CDCl_3$) δ 9.44 (br, 1H), 7.30 - 7.29 (d, *J* = 6 Hz, 1H), 7.09 - 7.08 (d, *J* = 6 Hz, 1H), 7.00 - 6.98 (t, *J* = 6 Hz, 1H), 5.07 - 5.05 (t, *J* = 6 Hz, 1H), 2.60 - 2.51 (m, 2H), 2.47 - 2.41 (m, 1H), 2.14 - 2.09 (m, 1H). **^{13}C NMR** (151 MHz, $CDCl_3$): δ 170.84, 142.59, 126.92, 126.12, 125.49, 59.21, 27.26, 26.04. **IR** (cm^{-1}): 3103, 2869, 1677. **MS**: HR-ESI calculated for [$C_8H_9NO_2S$+H^+]: 184.0432, found, 184.0413.; **m.p.** 155 ℃ (dec). *(R)*-**8i** was isolated in 41% yield and 90% ee (Table 4-6, entry 8a). $[\alpha]_D^{22}$= +84 °(c=1.00, acetone).

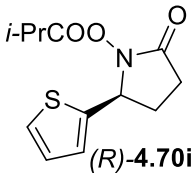

(R)-**4.70i**

Isolated in 55% yield and 91% ee (Table 4-6, entry 8a): **^{1}H NMR** (500 MHz, $CDCl_3$) δ 7.31 - 7.30 (d, *J* = 5 Hz, 1H), 7.03 - 7.02 (dd, *J* = 5 Hz, 1H), 6.97 - 6.95 (d, *J* = 5 Hz, 1H), 5.14 - 5.12 (t, *J* = 5 Hz, 1H), 2.67 - 2.49 (m, 4H), 2.25 - 2.16 (m, 1H), 1.15 - 1.11 (m, 6H). **^{13}C NMR** (126 MHz, $CDCl_3$): δ 173.92, 170.26, 141.67, 126.72, 126.38, 125.91, 58.13, 31.83, 26.99, 26.82, 18.71, 18.61. **IR** (cm^{-1}): 2977, 1785, 1733, 1069. **MS**: HR-ESI calculated for [$C_{12}H_{15}NO_3S$+Na^+]: 276.0670, found, 276.0664. **HPLC** (7.5% isopropanol/hexanes, AS-H): *(S)* enantiomer: 28.7 min; *(R)* enantiomer: 51.0 min; $[\alpha]_D^{22}$= −40 ° (c=1.00, acetone).

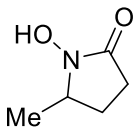

4.30j

Racemate was prepared in 34% yield. Oil. **^{1}H NMR** (600 MHz, $CDCl_3$) δ 9.67 (br, 1H), 3.87 - 3.83 (m, 1H), 2.43 - 2.33 (m, 2H), 2.25 - 2.22 (m, 1H), 1.33 - 1.32 (d, *J* = 6 Hz, 3H). **^{13}C NMR** (151 MHz, $CDCl_3$): δ 170.38, 55.43, 27.22, 23.93, 19.00. **IR** (cm^{-1}): 3132, 2974, 1681, 1060. **MS**: HR-ESI calculated for [$C_5H_9NO_2$+Na^+]: 138.0530, found, 138.0529; Isolated after attempted KR in 62% yield and <3% ee (Table 4-6, entry 9a). $[\alpha]_D^{22}$= 0 °(c=1.00, acetone).

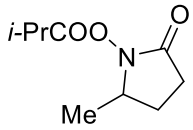

4.70j

Isolated in 32% yield and 13% ee (Table 4-6, entry 9a): **^{1}H NMR** (600 MHz, $CDCl_3$) δ 3.88 - 3.83 (m, 1H), 2.56 - 2.50 (m, 1H), 2.12 - 2.07 (m, 1H), 1.91 - 1.85 (m, 1H), 1.80 - 1.70 (m, 2H), 1.29 - 1.27 (dd, 6H). **^{13}C NMR** (151 MHz, $CDCl_3$): δ 173.94, 57.50, 32.98, 32.09, 31.82, 18.87, 18.81. **IR** (cm^{-1}): 2977, 1786, 1728, 1072. **MS**: HR-ESI calculated for [$C_9H_{15}NO_3$+H^+]: 208.0950, found, 208.0941. HPLC (5% isopropanol/hexanes, AS-H): *(S)*-enantiomer: 17.4 min; *(R)*-enantiomer: 28.7 min; $[\alpha]_D^{22}$= −2° (c=1.00, acetone).

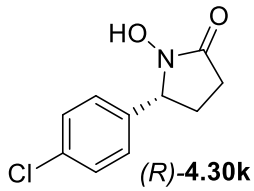

(R)-**4.30k**

Racemate was prepared in 37% yield. **^{1}H NMR** (500 MHz, $CDCl_3$) δ 9.58 (br, 1H), 7.38 - 7.36 (d, *J* = 5 Hz, 2H), 7.25 - 7.23 (d, *J* = 5Hz, 2H), 4.82 - 4.79 (dd, *J* = 5 Hz, 1H), 2.57 - 2.43 (m, 3H), 1.91 - 1.82 (m, 1H). **^{13}C NMR** (126 MHz, $CDCl_3$) δ 171.5, 138.2, 134.0, 129.1, 127.7, 63.0, 27.3, 26.1. **IR** (cm^{-1}): 3375, 2850, 1661. **MS**: HR-ESI calculated for [$C_{10}H_{10}ClNO_2$+H^+]: 212.0478, found, 212.0471.; **m.p.** 145 ℃ (dec). *(R)*-**8k** was isolated in 53% yield and 98% ee (Table 4-6, entry 10a).; $[\alpha]_D^{22}$= +69 ° (c=1.00, acetone).

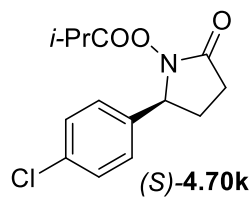

(S)-**4.70k**

Isolated in 55% yield and 85% ee (Table 4-6, entry 10a): **^{1}H NMR** (600 MHz, $CDCl_3$) δ 3.88 - 3.83 (m, 1H), 2.56 - 2.50 (m, 1H), 2.12 - 2.07 (m, 1H), 1.91 - 1.85 (m, 1H), 1.80 - 1.70 (m, 2H), 1.29 - 1.27 (dd, 6H). **^{13}C NMR** (151 MHz, $CDCl_3$): δ 173.94, 57.50, 32.98, 32.09, 31.82, 18.87, 18.81. **IR** (cm^{-1}): 2977, 1786, 1728, 1072. **MS**: HR-ESI calculated for [$C_{14}H_{16}ClNO_3$+Na^+]: 304.0716, found, 304.0707. **HPLC** (5% isopropanol/hexanes, AS-H): *(S)* enantiomer: 27.5 min; *(R)* enantiomer: 36.4 min; 85% ee; $[\alpha]_D^{22}$= −65 °(c=1.00, acetone).

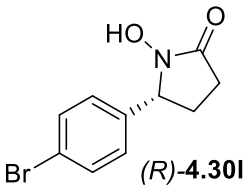

(R)-**4.30l**

Racemate was prepared in 34% yield. **^{1}H NMR** (500 MHz, $CDCl_3$) δ 9.42 (br, 1H), 7.53 - 7.51 (d, *J* = 5 Hz, 2H), 7.19 - 7.18 (d, *J* = 5 Hz), 4.80 - 4.77 (t, *J* = 5 Hz), 2.57 - 2.43 (m, 3H), 1.91 - 1.84 (m, 1H). **^{13}C NMR** (126 MHz, $CDCl_3$) δ 171.5, 138.7, 132.1, 128.1, 122.1, 63.1, 27.3, 26.0. IR (cm^{-1}): 2903, 1678, 1066, 1008. **MS**: HR-ESI calculated for [$C_{10}H_{10}BrNO_2$+Na^+]: 277.9793, found, 277.9753.; **m.p.** 170 ℃ (dec). *(R)*-**8l** was isolated in 41% yield and 84% ee (Table 4-6, entry 12a). $[\alpha]_D^{22}$= +67 °(c=1.00, acetone).

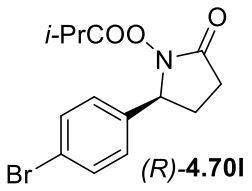

(R)-**4.70l**

Isolated in 54% yield and 67% ee (Table 4-6, entry 12a): **^{1}H NMR** (500 MHz, $CDCl_3$) δ 7.51 - 7.49 (d, *J* = 5 Hz, 2H), 7.22 - 7.20 (d, *J* = 5 Hz, 2H), 4.84 - 4.81 (t, *J* = 5 Hz, 1H), 2.63 - 2.50 (m, 4H), 2.00 -1.93 (1H), 1.12 - 1.08 (m, 6H). **^{13}C NMR** (126 MHz, $CDCl_3$) δ 173.94, 171.06, 137.82, 131.98, 128.32, 122.35, 62.28, 31.85, 27.01, 26.74, 18.68, 18.66. **IR** (cm^{-1}): 2978, 1785, 1733, 1490, 1070. **MS**: HR-ESI calculated for [$C_{14}H_{16}BrNO_3$+Na^+]: 348.0211, found, 348.0203. **HPLC** (5% isopropanol/hexanes, AS-H): *(S)* enantiomer: 22.9 min; *(R)* enantiomer: 30.6 min; $[\alpha]_D^{22}$= −24 °(c=1.00, acetone).

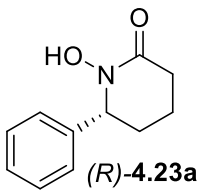

(R)-**4.23a**

Racemate is a known compound prepared as described[5] in 34% yield. **^{1}H NMR** (500 MHz, $CDCl_3$) δ 8.57 (br, 1H), 7.39 - 7.37 (m, 2H), 7.32 - 7.31 (d, *J* = 5 Hz, 1H), 7.23 - 7.22 (m, 2H), 4.91 - 4.89 (m, 1H), 2.64 - 2.54 (m, 2H), 2.33 - 2.27 (m, 1H), 1.99 - 1.93 (m, 1H), 1.85 - 1.71 (m, 1H). **^{13}C NMR** (126 MHz, $CDCl_3$): δ 165.60, 165.54, 139.64, 128.63, 127.80, 126.07, 63.00, 32.75, 30.79, 17.85. **IR** (cm^{-1}): 3029, 2970, 1739, 1633, 1365. **MS:** HR-ESI calculated for [$C_{11}H_{13}NO_2$+H^+]: 192.1025, found, 192.1022. **m.p.** 139 - 143 ℃. *(R)*-**10a** was isolated in 48% yield and 98% ee (Table 4-7, entry 1). $[\alpha]_D^{22}$= +95 °(c=1.00, acetone).

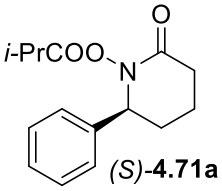

(S)-**4.71a**

Isolated in 51% yield and 89% ee (Table 4-7, entry 1): **^{1}H NMR** (500 MHz, $CDCl_3$) δ 7.35 - 7.27 (m, 4H), 4.83 - 4.80 (m, 1H), 2.67 - 2.64 (m, 2H), 2.50 - 2.48 (m, 1H), 2.30 - 2.27 (m, 1H), 2.05 - 1.97 (m, 1H), 1.93 - 1.84 (m, 2H), 0.98 - 0.96 (d, *J* = 10 Hz, 6H). **^{13}C NMR** (126 MHz, $CDCl_3$): δ 173.61, 167.37, 139.25, 128.47, 127.98, 126.59, 66.70, 33.98, 33.17, 31.79, 29.61, 18.50, 18.45. **IR** (cm^{-1}): 2978, 1809, 1744, 1005. **MS**: HR-ESI calculated for [$C_{15}H_{19}NO_3$+Na^+]: 284.1263, found 284.1247. **HPLC** (10% isopropanol/hexanes, OD-H): *(S)* enantiomer: 9.0 min; *(R)* enantiomer: 10.5 min; $[\alpha]_D^{22}$= −84 ° (c=1.00, acetone).

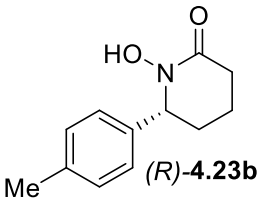

(R)-**4.23b**

Racemate was prepared in 34% yield. **^{1}H NMR** (600 MHz, $CDCl_3$) δ 8.45 (br, 1H), 7.20 - 7.18 (d, *J* = 5 Hz, 2H), 7.12 - 7.10 (d, *J* = 5 Hz, 2H), 4.88 - 4.86 (m, 1H), 2.61 - 2.59 (m, 2H), 2.35 (s, 3H), 2.29 - 2.27 (m, 1H), 1.97 - 1.93 (m, 1H), 1.85 - 1.82 (m, 1H), 1.76 - 1.72 (m, 1H). **^{13}C NMR** (126 MHz, $CDCl_3$): δ 165.38, 137.64, 136.58, 129.35, 126.02, 62.72, 32.83, 30.73, 21.08, 17.97. **IR** (cm^{-1}): 2937, 1636, 1282, 1075. **MS:** HR-ESI calculated for [$C_{12}H_{15}NO_2$+H^+]: 206.1181, found, 206.1169.; **m.p.** 151

- 153 ℃. *(R)*-**10b** was isolated in 44% yield and 96% ee (Table 4-7, entry 2). $[\alpha]_D^{22}$= +31 °(c=1.00, acetone).

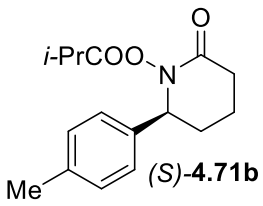

(S)-**4.71b**

Isolated in 54% yield and 88% ee (Table 4-7, entry 2): **^{1}H NMR** (500 MHz, $CDCl_3$) δ 7.19 - 7.17 (d, *J* = 5 Hz, 2H), 7.16 - 7.14 (d, *J* = 5 Hz, 2H), 4.81 - 4.78 (m, 1H), 2.70 - 2.64 (m, 2H), 2.54 - 2.48 (m, 1H), 2.34 (s, 3H), 2.29 - 2.25, 2.04 - 1.97 (m, 1H), 1.94 - 1.82 (m, 2H), 1.00 - 0.99 (d, *J* = 5 Hz, 6H).**^{13}C NMR** (126 MHz, $CDCl_3$): δ 173.74, 167.36, 137.76, 136.35, 129.18, 126.57, 66.47, 34.06, 33.24, 31.86, 21.09, 18.61, 18.56. **IR** (cm^{-1}): 2935, 1654, 1332, 1070. **MS:** HR-ESI calculated for [$C_{16}H_{21}NO_3$+H^+]: 276.1600, found, 276.1589. **HPLC** (5% isopropanol/hexanes, OD-H): *(S)* enantiomer: 13.7 min; *(R)* enantiomer: 15.6 min; $[\alpha]_D^{22}$= −71 °(c=1.00, acetone).

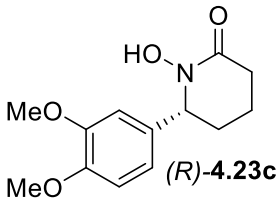

(R)-**4.23c**

Racemate was prepared in 34% yield. **^{1}H NMR** (500 MHz, $CDCl_3$) δ 8.49 (br, 1H), 6.89 - 6.87 (d, *J* = 5 Hz, 1H), 6.80 - 6.78 (d, *J* = 5 Hz, 1H), 6.74 (s, 1H), 4.86 (m, 1H), 3.89 (s, 6H), 2.65 - 2.58 (m, 2H), 2.32 - 2.27 (m, 1H), 2.00 - 1.93 (m, 1H), 1.90 - 1.84 (m, 1H), 1.80 - 1.74 (m, 1H). **^{13}C NMR** (126 MHz, $CDCl_3$): δ 165.69, 149.24, 148.68, 132.09, 118.38, 111.17, 109.24, 63.01, 55.96, 55.94, 32.95, 30.84, 18.11. **IR** (cm^{-1}): 2970, 1739, 1366, 1229, 1217. **MS:** HR-ESI calculated for [$C_{13}H_{17}NO_4$+H^+]: 274.1055, found, 274.1047.; **m.p.** 164 - 168 ℃. *(R)*-**10c** was isolated in 42% yield and 95% ee (Table 4-7, entry 3). $[\alpha]_D^{22}$= +64 °(c=1.00, acetone).

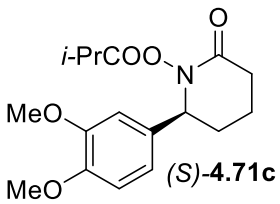

(S)-**4.71c**

Isolated in 53% yield and 91% ee (Table 4-7, entry 3): **^{1}H NMR** (500 MHz, $CDCl_3$) δ 6.85 - 6.81 (m, 3H), 4.78 - 4.76 (m, 1H), 3.88 (s, 3H), 3.87 (s, 3H), 2.73 - 2.63 (m, 1H), 2.54 - 2.50 (m, 1H), 2.28 - 2.24 (m, 1H), 2.05 - 1.98 (m, 1H), 1.93 - 1.85 (m, 1H), 1.02 - 1.00 (d, *J* = 5 Hz, 6H). **^{13}C NMR** (126 MHz, $CDCl_3$): δ 149.08, 148.77, 131.87, 119.08, 110.82, 109.44, 55.96, 55.92, 34.34, 33.28, 31.88, 18.65,

18.55. **IR** (cm^{-1}): 3156, 3061, 1772, 1366, 1260, 1230. **MS:** HR-ESI calculated for [$C_{17}H_{23}NO_5$+H^+]: 344.1474, found, 344.1460. **HPLC** (5% isopropanol/hexanes, OD-H): *(S)* enantiomer: 36.0 min; *(R)* enantiomer: 41.6 min; $[\alpha]_D^{22}$= −84 °(c=1.00, acetone).

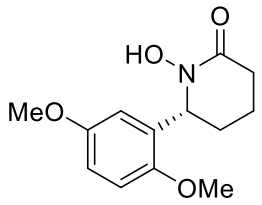

(R)-**4.23d**

Racemate was prepared in 31% yield. **^{1}H NMR** (500 MHz, $CDCl_3$) δ 6.85 - 6.83 (d, *J* = 5 Hz, 1H), 6.77 - 6.75 (d, *J* = 5 Hz, 1H), 6.72 (s, 1H), 4.83 - 4.81 (m, 1H), 3.87 (s, 3H), 3.85 (s, 3H), 2.60 - 2.55 (m, 2H), 2.27 - 2.22 (m, 1H), 1.95 - 1.90 (m, 1H), 1.83 - 1.79 (m, 1H), 1.75 - 1.70 (m, 1H). **^{13}C NMR** (126 MHz, $CDCl_3$): δ 166.00, 149.15, 148.56, 132.13, 118.35, 111.10, 109.20, 63.28, 55.88, 32.86, 31.02, 17.90. **IR** (cm^{-1}): 2970, 1739, 1684, 1366, 1217. **MS:** HR-ESI calculated for [$C_{13}H_{17}NO_4$+H^+]: 252.1236, found, 252.1224.; **m.p.** 179 - 181 ℃. *(R)*-**10d** was isolated in 45% yield and 84% ee (Table 4-7, entry 4). $[\alpha]_D^{22}$= +34 °(c=1.00, acetone).

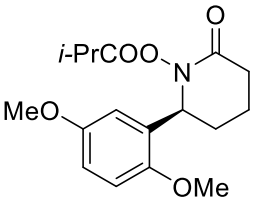

(S)-**4.71d**

Isolated in 51% yield and 83% ee (Table 4-7, entry 4): **^{1}H NMR** (500 MHz, $CDCl_3$) δ 6.90 (s, 1H), 6.80 - 6.76 (dd, *J* = 5 Hz, 2H), 5.23 - 5.20 (m, 1H), 3.76 (s, 3H), 3.75 (s, 3H), 2.64 - 2.60 (m, 2H), 2.57 - 2.51 (m, 1H), 2.31 - 2.25 (m, 1H), 2.00 - 1.93 (m, 1H), 1.86 - 1.78 (m, 2H), 1.04 - 1.02 (d, 6H). **^{13}C NMR** (126 MHz, $CDCl_3$): δ 173.68, 167.58, 153.55, 150.51, 128.38, 113.47, 113.04, 111.66, 60.45, 55.86, 55.74, 33.23, 31.82, 31.35, 18.97, 18.59, 18.55. **IR** (cm^{-1}): 2972, 1778, 1685, 1075. **MS:** HR-ESI calculated for [$C_{17}H_{23}NO_5$+H^+]: 322.1654, found, 322.1643. **HPLC** (5% isopropanol/hexanes, OD-H): *(S)* enantiomer: 16.1 min; *(R)* enantiomer: 21.7 min; $[\alpha]_D^{22}$= −34 ° (c=1.00, acetone).

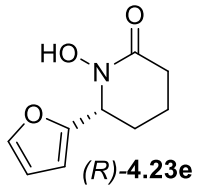

(R)-**4.23e**

Racemate was prepared in 37% yield. **^{1}H NMR** (500 MHz, $CDCl_3$) δ 8.72 (br, 1H), 7.38 (s, 1H), 6.36 (m, 1H), 6.30 (m, 1H), 4.94 (m, 1H), 2.55 - 2.52 (m, 2H), 1.96 - 1.94 (m, 2H), 1.80 - 1.77 (m, 1H). **^{13}C NMR** (126 MHz, $CDCl_3$): δ 165.98, 151.70, 142.28, 110.38, 107.94, 57.23, 28.88, 18.17. **IR** (cm^{-1}): 2927, 1684, 1559. **MS**: HR-ESI calculated for [$C_9H_{11}NO_3$+H^+]: 182.0817, found, 182.0808.; **m.p.** 149 ℃ (dec). *(R)*-**10e** was isolated in 43% yield and 97% ee (Table 4-7, entry 4). $[\alpha]_D^{22}$= +83 °(c=1.00, acetone).

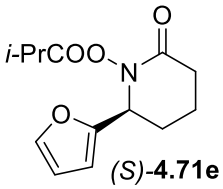

(S)-**4.71e**

Isolated in 53% yield and 92% ee (Table 4-7, entry 4): **^{1}H NMR** (600 MHz, $CDCl_3$) δ 7.35 - 7.34 (d, *J* = 6 Hz, 1H), 6.30 - 6.29 (d, *J* = 6 Hz, 1H), 6.25 (s, 1H), 4.86 - 4.84 (t, *J* = 6 Hz, 1H), 2.62 - 2.54 (m, 3H), 2.25 - 2.21 (m, 2H), 1.99 - 1.92 (m, 1H), 1.86 - 1.77 (m, 1H), 1.11 - 1.09 (t, *J* = 6 Hz, 6H). **^{13}C NMR** (126 MHz, $CDCl_3$): δ 173.57, 166.33, 151.24, 142.34, 110.12, 108.09, 59.31, 32.86, 31.78, 29.59, 19.12, 18.62, 18.55. **IR** (cm^{-1}): 2978, 1809, 1744, 1469, 1005. **MS**: HR-ESI calculated for [$C_{13}H_{17}NO_4$+Na^+]: 274.1055, found, 274.1050. **HPLC** (5% isopropanol/hexanes, OD-H): *(S)* enantiomer: 15.6 min; *(R)* enantiomer: 18.2 min; $[\alpha]_D^{22}$= −84 °(c=1.00, acetone).

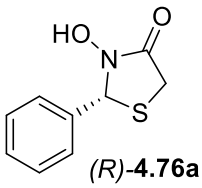

(R)-**4.76a**

Racemate is a known compound.[25] Prepared in 33% yield. **^{1}H NMR** (600 MHz, $CDCl_3$) δ 8.59 (br, 1H), 7.42 - 7.37 (m, 5H), 5.77 - 5.76 (m, 1H), 3.75 - 3.72 (dd, J_1 = 12 Hz, J_2 = 6 Hz, 2H). **^{13}C NMR** (151 MHz, $CDCl_3$): δ 167.04, 137.16, 129.48, 128.95, 127.17, 63.20, 28.90. **IR** (cm^{-1}): 3015, 2970, 1739, 1633, 1365, 1229. **MS:** HR-ESI calculated for [$C_9H_9NO_2S$+H^+]: 196.0432, found, 196.0423. *(R)*-**15a** was isolated in 42% yield and 95% ee (Table 4-8, entry 1). $[\alpha]_D^{22}$= +86 °(c=1.00, acetone).

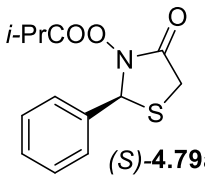

(S)-**4.79a**

Isolated in 53% yield and 86% ee (Table 4-8, entry 1): **^{1}H NMR** (600 MHz, $CDCl_3$) δ 7.46 - 7.37 (m, 5H), 5.82 (m, 1H), 3.75 - 3.67 (dd, J_1 = 18 Hz, J_2 = 6 Hz, 2H), 2.62 - 2.56 (m, 1H), 1.09 - 1.06 (d, J = 6 Hz, 3H). **^{13}C NMR** (151 MHz, $CDCl_3$): δ 173.35, 166.68, 135.77, 129.71, 128.80, 127.81, 62.14, 31.80, 28.24, 18.62. **IR** (cm^{-1}): 3125, 1734, 1073. **MS:** HR-ESI calculated for [$C_{13}H_{15}NO_3S$+Na^+]: 288.0670, found, 288.0660. **HPLC** (5% isopropanol/hexanes, AS-H): *(S)* enantiomer: 11.6 min; *(R)* enantiomer: 15.9 min; $[\alpha]_D^{22}$= −61 °(c=1.00, acetone).

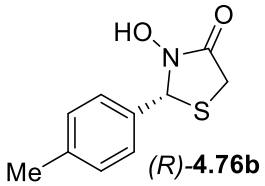

(R)-**4.76b**

Racemate was prepared in 31% yield. **^{1}H NMR** (500 MHz, $CDCl_3$) δ 7.31 - 7.30 (d, J = 5 Hz), 7.20 - 7.19 (d, J = 5 Hz), 6.46 (m, 1H), 3.69 (m, 2H), 2.37 (s, 3H). **^{13}C NMR** (126 MHz, $CDCl_3$): δ 174.54, 139.24, 136.91, 129.68, 126.34, 58.70, 33.01, 21.19. **IR** (cm^{-1}): 3016, 2970, 1739, 1366, 1229. **MS:** HR-ESI calculated for [$C_{10}H_{11}NO_2S$+Na^+]: 232.0408, found, 232.0413.; **m.p.** 144-149 ℃. *(R)*-**15b** was isolated in 43% yield and 94% ee (Table 4-8, entry 2). $[\alpha]_D^{22}$= +81 °(c=1.00, acetone).

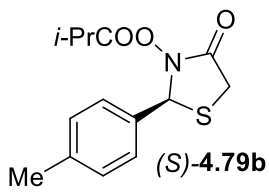

(S)-**4.79b**

Isolated in 42% yield and 88% ee (Table 4-8, entry 2): **^{1}H NMR** (500 MHz, $CDCl_3$) δ 7.16 - 7.15 (d, J = 6 Hz, 2H), 6.33 - 6.32 (d, J = 6 Hz, 2H), 3.98 - 3.95 (d, J = 15 Hz, 1H), 3.72 - 3.69 (d, J = 15 Hz), 2.34 (s, 3H), 1.37 - 1.32 (m, 1H), 1.17 - 1.13 (t, J = 10 Hz, 3H). **^{13}C NMR** (126 MHz, $CDCl_3$): δ 177.52, 171.68, 138.22, 137.96, 129.58, 124.91, 61.67, 35.07, 34.42, 34.08, 21.11. **IR** (cm^{-1}): 2974, 2929, 1709, 1189. **MS**: HR-ESI calculated for [$C_{14}H_{17}NO_3S$+H^+]: 302.0827, found, 302.0829. **HPLC** (5% isopropanol/hexanes, AS-H): *(S)* enantiomer: 5.5 min; *(R)* enantiomer: 6.9 min; $[\alpha]_D^{22}$= −43 ° (c=1.00, acetone).

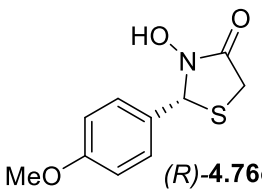

(R)-**4.76c**

Racemate was prepared in 38% yield. **^{1}H NMR** (600 MHz, $CDCl_3$) δ 9.35 (br, 1H), 7.35 - 7.34 (d, *J* = 6 Hz, 2H), 6.92 - 6.91 (d, *J* = 6 Hz, 2H), 5.74 (m, 1H), 3.81 (s, 3H), 3.70 - 3.61 (dd, J_1 = 18 Hz, J_2 = 6 Hz, 2H). **^{13}C NMR** (151 MHz, $CDCl_3$): δ 167.15, 160.39, 128.79, 114.23, 77.21, 77.00, 76.79, 63.25, 55.33, 28.95. **IR** (cm^{-1}): 2974, 1789, 1721, 1514. **MS**: HR-ESI calculated for [$C_{10}H_{11}NO_3S+H^+$]: 226.0538, found, 226.0528.; **m.p.** 147-149 ℃. *(R)*-**15c** was isolated in 43% yield and 85% ee (Table 4-8, entry 2). $[\alpha]_D^{22}$= +62 °(c=1.00, acetone).

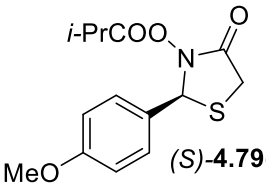

(S)-**4.79c**

Isolated in 47% yield and 89% ee (Table 4-8, entry 3): **^{1}H NMR** (600 MHz, $CDCl_3$) δ 7.38 - 7.37 (d, *J* = 6 Hz, 2H), 6.90 - 6.88 (d, *J* = 6 Hz, 2H), 5.79 - 5.78 (m, 1H), 3.81 (s, 3H), 3.73 - 3.64 (dd, J_1 = 18 Hz, J_2 = 6 Hz, 2H), 2.63 - 2.55 (m, 1H), 1.09 - 1.07 (d, *J* = 6Hz). **^{13}C NMR** (151 MHz, $CDCl_3$): δ 173.35, 166.52, 160.63, 129.35, 127.33, 114.10, 61.89, 55.32, 31.77, 28.26, 18.63. **IR** (cm^{-1}): 2957, 2865, 1684, 1612, 1306. **MS**: HR-ESI calculated for [$C_{14}H_{17}NO_4S+H^+$]: 296.0957, found, 296.0953. **HPLC** (5% isopropanol/hexanes, AS-H): *(S)* enantiomer: 21.7 min; *(R)* enantiomer: 36.6 min; $[\alpha]_D^{22}$= −76 °(c=1.00, acetone).

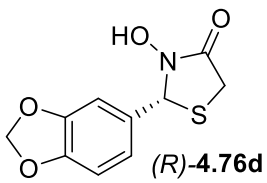

(R)-**4.76d**

Racemate was prepared in 31% yield. **^{1}H NMR** (500 MHz, $CDCl_3$) δ 8.28 (br, 1H), 6.92 (s, *J* = 5 Hz, 1H), 6.88 - 6.87 (d, *J* = 5 Hz, 1H), 6.80 - 6.79 (d, *J* = 5 Hz, 1H), 5.99 (s, 2H), 5.68 - 5.68 (m, 1H), 3.73 - 3.70 (d, *J* = 15 Hz, 1H), 3.66 - 3.63 (d, *J* = 15 Hz, 1H). **^{13}C NMR** (126 MHz, $CDCl_3$): δ 166.79, 148.74, 148.38, 130.67, 121.62, 108.25, 107.18, 101.51, 63.20, 28.84. **IR** (cm^{-1}): 2971, 1792, 1446. **MS**: HR-ESI calculated for [$C_{10}H_9NO_4S+H^+$]: 240.0331, found, 240.0325.; **m.p.** 168-170 ℃. *(R)*-**15d** was isolated in 42% yield and 85% ee (Table 4-8, entry 4). $[\alpha]_D^{22}$= +71 °(c=1.00, acetone).

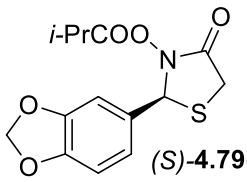

(S)-**4.79d**

Isolated in 53% yield and 95% ee (Table 4-8, entry 4): **^{1}H NMR** (500 MHz, $CDCl_3$) δ 7.01 (s, 1H), 6.85- 6.84 (d, *J* = 5 Hz, 1H), 6.76 - 6.75 (d, *J* = 5 Hz, 1H), 6.00 - 5.99 (d, *J* = 5Hz, 2H), 5.75 - 5.74 (d, *J* = 5 Hz, 1H), 3.72 - 3.69 (d, *J* = 15 Hz, 1H), 3.67 - 3.64 (d, *J* = 15 Hz, 1H), 2.65 - 2.59 (m, 1H), 1.14 - 1.10 (m, 6H). **^{13}C NMR** (126 MHz, $CDCl_3$): δ 173.39, 166.47, 148.88, 148.27, 129.39, 122.05, 107.97, 107.78, 101.50, 62.15, 31.82, 28.20, 18.69. **IR** (cm^{-1}): 2971, 1787, 1726, 1491. **MS**: HR-ESI calculated for [$C_{14}H_{15}NO_2S+H^+$]: 310.0749, found, 310.0746. **HPLC** (5% isopropanol/hexanes, AS-H): *(S)* enantiomer: 38.0 min; *(R)* enantiomer: 57.0 min; $[\alpha]_D^{22}$= −97 °(c=1.00, acetone).

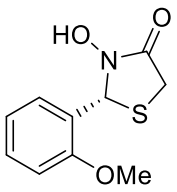

(R)-**4.76e**

Racemate was prepared in 28% yield. **^{1}H NMR** (500 MHz, $CDCl_3$) δ 9.45 (br, 1H), 7.36 - 7.29 (m, 2H), 7.02 - 7.00 (d, *J* = 6 Hz, 1H), 6.94 - 6.93 (t, 1H), 6.17 (m, 1H), 3.88 (s, 3H) 3.73 - 3.62 (dd, J_1 = 18 Hz, J_2 = 6 Hz, 2H). **^{13}C NMR** (126 MHz, $CDCl_3$): δ 152.24, 125.30, 122.05, 121.48, 116.12, 106.21, 53.95, 50.92. **IR** (cm^{-1}): 2970, 2927, 2849, 1739, 1366, 1229, 1217. **MS**: HR-ESI calculated for [$C_{10}H_{11}NO_3S+H^+$]: 226.0538, found, 226.0530.; **m.p.** 156-158 ℃. *(R)*-**15e** was isolated in 43% yield and 75% ee (Table 4-8, entry 5). $[\alpha]_D^{22}$= +92 °(c=1.00, acetone).

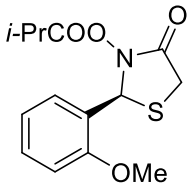

(S)-**4.79e**

Isolated in 55% yield and 89% ee (Table 4-8, entry 5): **^{1}H NMR** (600 MHz, $CDCl_3$) δ 7.42 - 7.31 (m, 2H), 7.00 - 6.97 (m, 1H), 6.91 - 6.89 (d, *J* = 6 Hz, 1H), 6.18 (m, 1H) 3.85, 3.69 - 3.62 (dd, J_1 = 18 Hz, J_2 = 6 Hz, 2H), 2.65 - 2.59 (m, 1H), 1.16 - 1.15 (d, *J* = 6 Hz), 1.08 - 1.06 (d, *J* = 6 Hz). **^{13}C NMR** (151 MHz, $CDCl_3$): δ 173.35, 167.28, 157.31, 130.32, 127.74, 124.83, 120.82, 110.77, 56.56, 55.57, 31.81, 27.78, 18.65, 18.61. **IR** (cm^{-1}): 2975, 2938, 1788, 1722, 1248. **MS**: HR-ESI calculated for [$C_{14}H_{17}NO_4S+H^+$]: 296.0957, found, 296.0947. **HPLC** (5% isopropanol/hexanes, AS-H): *(S)* enantiomer: 16.5 min; *(R)* enantiomer: 30.6 min; $[\alpha]_D^{22}$= −76 °(c=1.00, acetone).

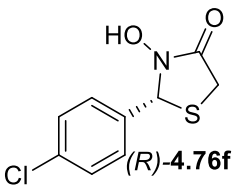

(R)-**4.76f**

Racemate was prepared in 29% yield. Isolated as a white solid (28 mg, 45% yield) after chromatography (5→40% EtOAc/hexanes. **^{1}H NMR** (500 MHz, $CDCl_3$) δ 7.55 - 7.53 (d, *J* = 10 Hz, 2H), 7.30 - 7.28 (d, *J* = 10 Hz, 2H), 5.72 (m, 1H), 3.75 - 3.71 (d, *J* = 20 Hz, 1H), 3.69 - 3.65 (d, *J* = 20 Hz, 1H). **^{13}C NMR** (126 MHz, $CDCl_3$): δ 206.96, 134.29, 133.83, 132.96, 129.27, 128.09, 127.82, 127.20, 126.91, 126.70, 123.71, 63.28, 30.92. **IR** (cm^{-1}): 2970, 1739, 1366, 1229, 1217. **MS**: HR-ESI calculated for [$C_9H_8ClNO_2S+H^+$]: 230.0043, found, 230.0039.; **m.p.** 174 ℃ (dec). *(R)*-**15f** was isolated in 45% yield and 85% ee (Table 4-8, entry 6). $[\alpha]_D^{22}$= +39 °(c=1.00, acetone).

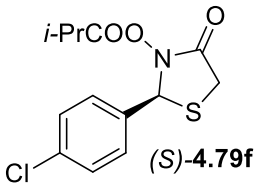

(S)-**4.79f**

Isolated in 53% yield and 56% ee (Table 4-8, entry 6): **^{1}H NMR** (500 MHz, $CDCl_3$) δ 7.41 - 7.39 (d, *J* = 5 Hz, 2H), 7.38 - 7.36 (d, *J* = 5 Hz, 2H), 5.79 (m, 1H), 3.76 - 3.72 (d, *J* = 20 Hz, 1H), 3.70 - 3.66 (d, *J* = 20 Hz, 1H), 2.64 - 2.58 (m, 1H), 1.12 - 1.09 (t, *J* = 4.5 Hz, 6H). **^{13}C NMR** (126 MHz, $CDCl_3$): δ 173.33, 166.60, 135.64, 134.39, 129.20, 129.08, 67.97, 61.49, 31.82, 28.19, 18.65. **IR** (cm^{-1}): 2971, 1786, 1734, 1413, 1217. **MS**: HR-ESI calculated for [$C_{13}H_{14}ClNO_3S+H^+$]: 300.0461, found, 300.0458. **HPLC** (5% isopropanol/hexanes, AS-H): *(S)* enantiomer: 16.2 min; *(R)* enantiomer: 20.2 min; $[\alpha]_D^{22}$= −14 °(c=1.00, acetone).

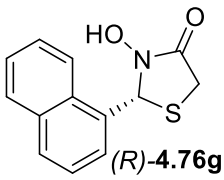

(R)-**4.76g**

Racemate was prepared in 31% yield. **^{1}H NMR** (500 MHz, $CDCl_3$) δ 7.92 - 7.90 (d, *J* = 10 Hz, 1H), 7.86 - 7.84 (m, 2H), 7.53 - 7.51 (m, 2H), 5.93 (m, 1H), 3.82 - 3.79 (d, *J* = 10 Hz, 1H), 3.72 - 3.70 (d, *J* = 10 Hz, 1H). **^{13}C NMR** (126 MHz, $CDCl_3$): δ 206.96, 134.29, 133.83, 132.96, 129.27, 128.09, 127.82, 127.20, 126.91, 126.70, 123.71, 63.28, 30.92. **IR** (cm^{-1}): 2970, 2857, 1772, 1734. **MS**: HR-ESI calculated for [$C_{13}H_{11}NO_2S+H^+$]: 246.0589, found, 246.0578.; **m.p.** 163 -**4.79**7 ℃. *(R)*-**15g** was isolated in 43% yield and 89% ee (Table 4-8, entry 7). $[\alpha]_D^{22}$= +76 °(c=1.00, acetone).

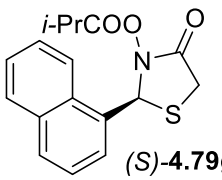

(S)-**4.79g**

Isolated in 51% yield and 83% ee (Table 4-8, entry 7): **^{1}H NMR** (500 MHz, $CDCl_3$) δ 7.99 - 7.97 (d, *J* = 10 Hz, 1H), 7.91 - 7.90 (d, *J* = 5 Hz, 1H), 7.87 - 7.86 (d, *J* = 5 Hz, 1H), 7.75 - 7.74 (d, *J* = 5 Hz, 1H), 7.59 - 7.51 (m, 3H), 6.65 (m, 1H), 3.82 - 3.79 (d, *J* = 15 Hz, 1H), 3.74 - 3.71 (d, *J* = 15 Hz, 1H), 2.64 - 2.56 (m, 1H), 1.21 - 1.19 (d, *J* = 10 Hz, 3H), 1.14 - 1.13 (d, *J* = 10 Hz, 3H). **^{13}C NMR** (126 MHz, $CDCl_3$): δ 173.63, 167.46, 133.79, 130.37, 129.63, 129.10, 126.83, 126.11, 125.48, 58.84, 31.82, 28.02, 18.73, 18.67. **IR** (cm^{-1}): 2970, 2850, 1734, 1733.7. **MS**: HR-ESI calculated for [$C_{17}H_{17}NO_3S+Na^+$]: 338.0827, found, 338.0819. **HPLC** (5% isopropanol/hexanes, AS-H): *(S)* enantiomer: 16.1 min; *(R)* enantiomer: 19.5 min; $[\alpha]_D^{22}$= −64 °(c=1.00, acetone).

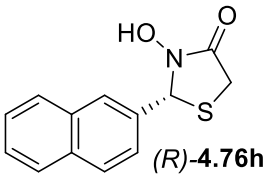

(R)-**4.76h**

Racemate was prepared in 29% yield. **^{1}H NMR** (500 MHz, $CDCl_3$) δ 8.85 (br, 1H), 7.93 - 7.85 (m, 3H), 7.60 - 7.51 (m, 4H), 6.58 (m, 1H), 3.81, 3.81 - 3.78 (d, *J* = 15 Hz, 1H), 3.75 - 3.72 (d, *J* = 15 Hz, 1H). **^{13}C NMR** (126 MHz, $CDCl_3$): δ 168.17, 133.96, 132.77, 130.19, 129.46, 129.21, 126.86, 126.11, 125.54, 123.12, 121.99, 60.23, 28.92. **IR** (cm^{-1}): 2985, 2841, 1792, 1436, 1229. **MS**: HR-ESI calculated for [$C_{13}H_{11}NO_2S+H^+$]: 246.0589, found, 246.0585.; **m.p.** 144-190 ℃ (dec). ***(R)*-15h** was isolated in 45% yield and 70% ee (Table 4-8, entry 8). $[\alpha]_D^{22}$= +76 °(c=1.00, acetone).

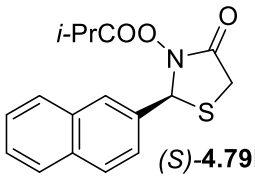

(S)-**4.79h**

Isolated in 53% yield and 89% ee (Table 4-8, entry 8): **^{1}H NMR** (500 MHz, $CDCl_3$) δ 7.92 - 7.90 (d, *J* = 10 Hz, 1H), 7.88 - 7.82 (m, 3H), 7.65 - 7.63 (d, *J* = 10 Hz, 1H), 7.56 - 7.53 (m, 2H), 6.01 (m, 1H), 3.81 - 3.78 (d, *J* = 15 Hz, 1H), 3.76 - 3.73 (d, *J* = 15 Hz, 1H), 2.60 -2.55 (m, 1H), 1.09 - 1.07 (d, *J* = 10 Hz, 3H), 1.06 - 1.04 (d, *J* = 10 Hz, 3H). **^{13}C NMR** (126 MHz, $CDCl_3$): δ 173.42, 166.64, 133.88, 133.18, 132.78, 129.10, 128.00, 127.83, 127.58, 126.96, 126.65, 124.32, 62.34, 31.77, 28.26, 18.62, 18.60. **IR** (cm^{-1}): 2970, 2930, 2853, 1727, 1367, 1217. **MS**: HR-ESI calculated [$C_{17}H_{17}NO_3S+Na^+$]:

338.0827, found, 338.0828. **HPLC** (5% isopropanol/hexanes, AS-H): *(S)* enantiomer: 18.8 min; *(R)* enantiomer: 24.1 min; $[\alpha]_D^{22} = -61$ °(c=1.00, acetone).

1. NMR DATA

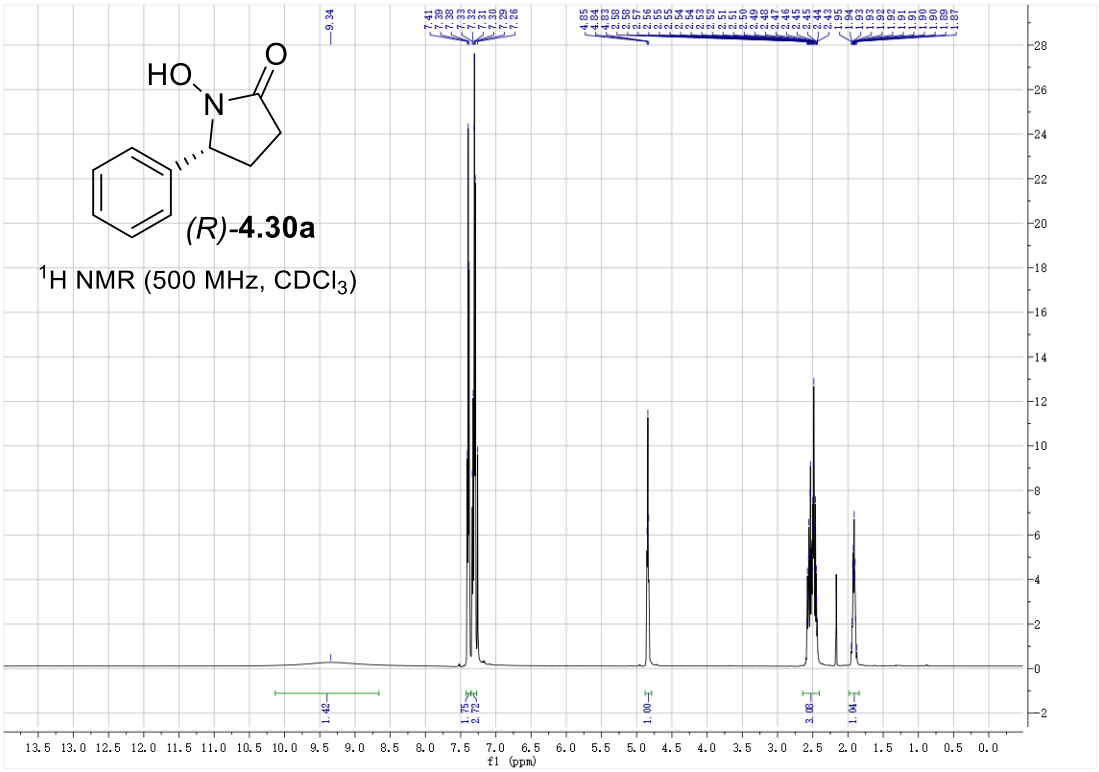
HO
N
O
(R)-4.30a
1H NMR (500 MHz, CDCl3)
f1 (ppm)

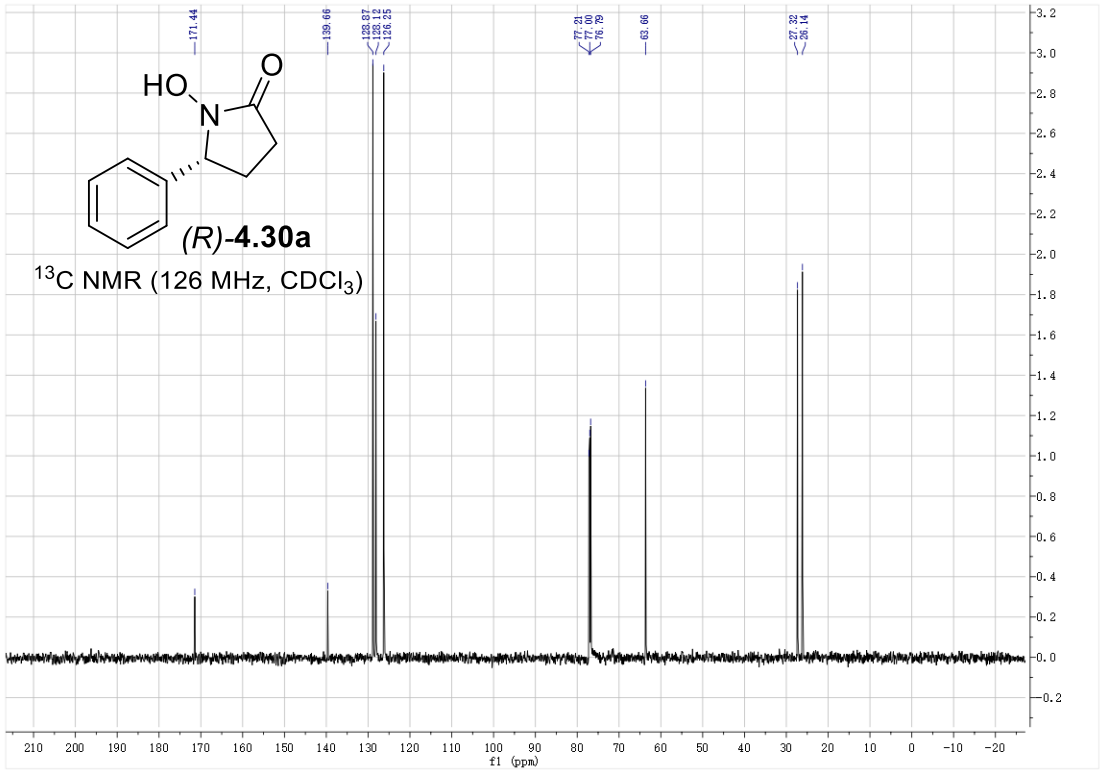
HO
N
O
(R)-4.30a
13C NMR (126 MHz, CDCl3)
f1 (ppm)

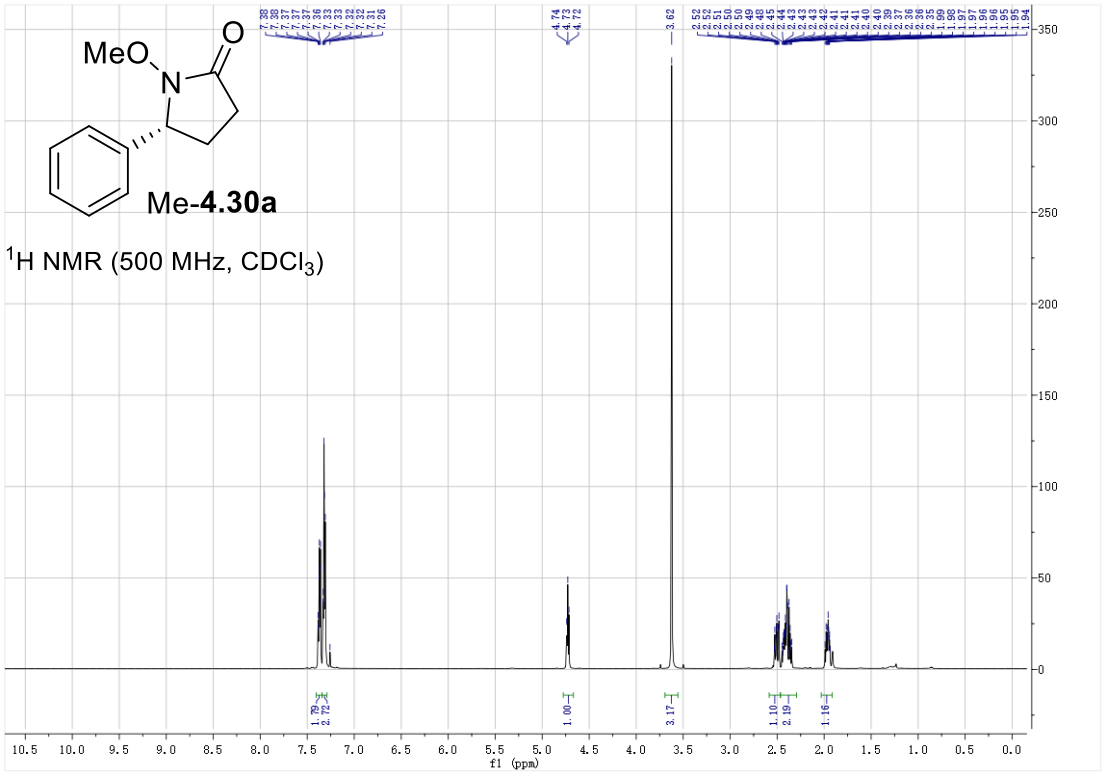
MeO
N
O
Me-4.30a
1H NMR (500 MHz, CDCl3)
f1 (ppm)

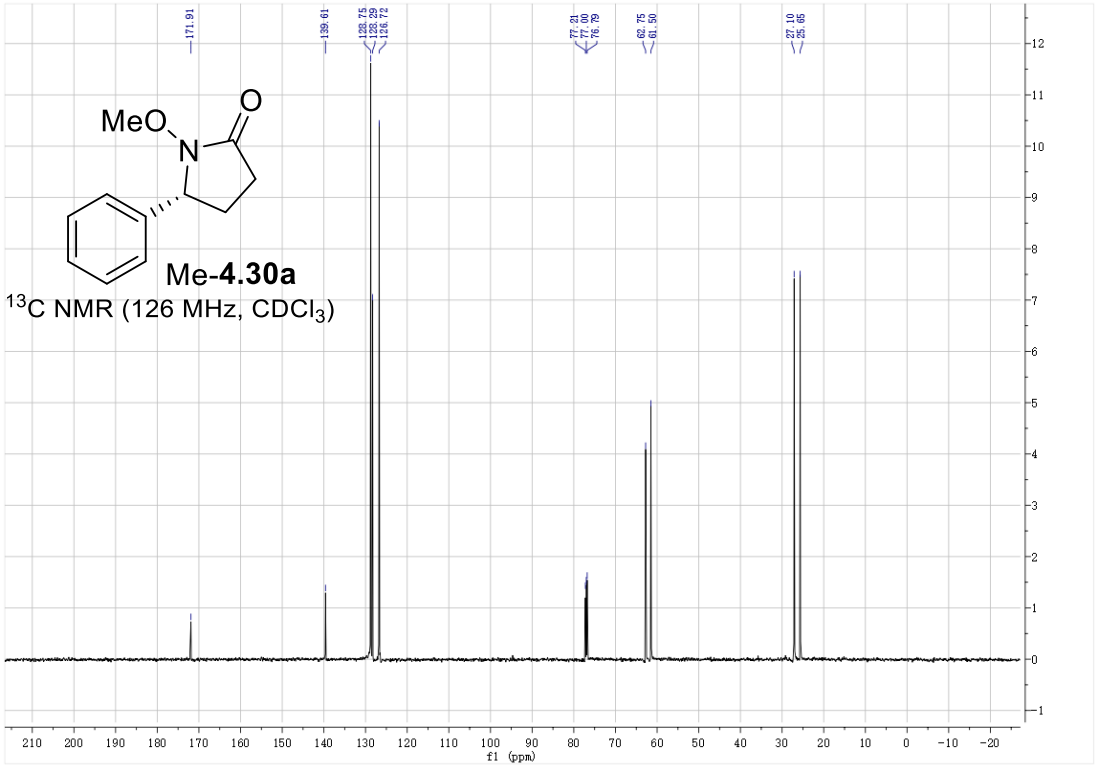
MeO
N
O
Me-4.30a
13C NMR (126 MHz, CDCl3)
f1 (ppm)

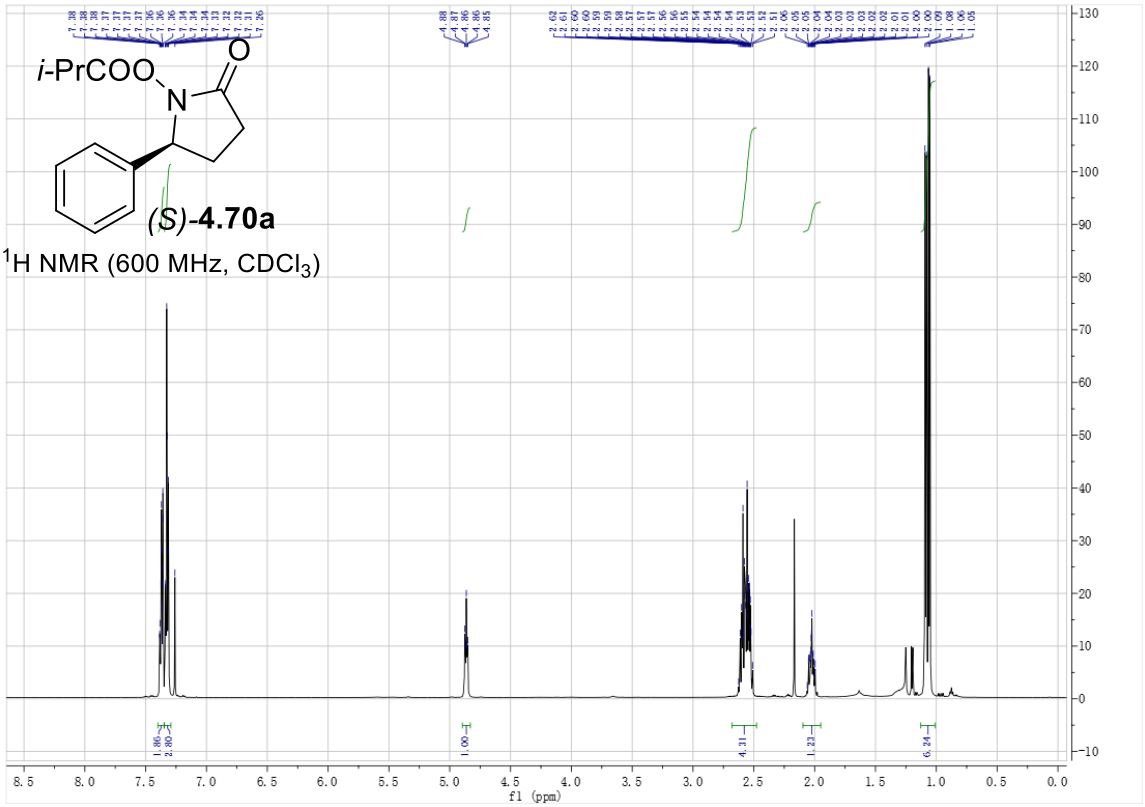
i-PrCOO
N
O
(S)-4.70a
1H NMR (600 MHz, CDCl3)
f1 (ppm)

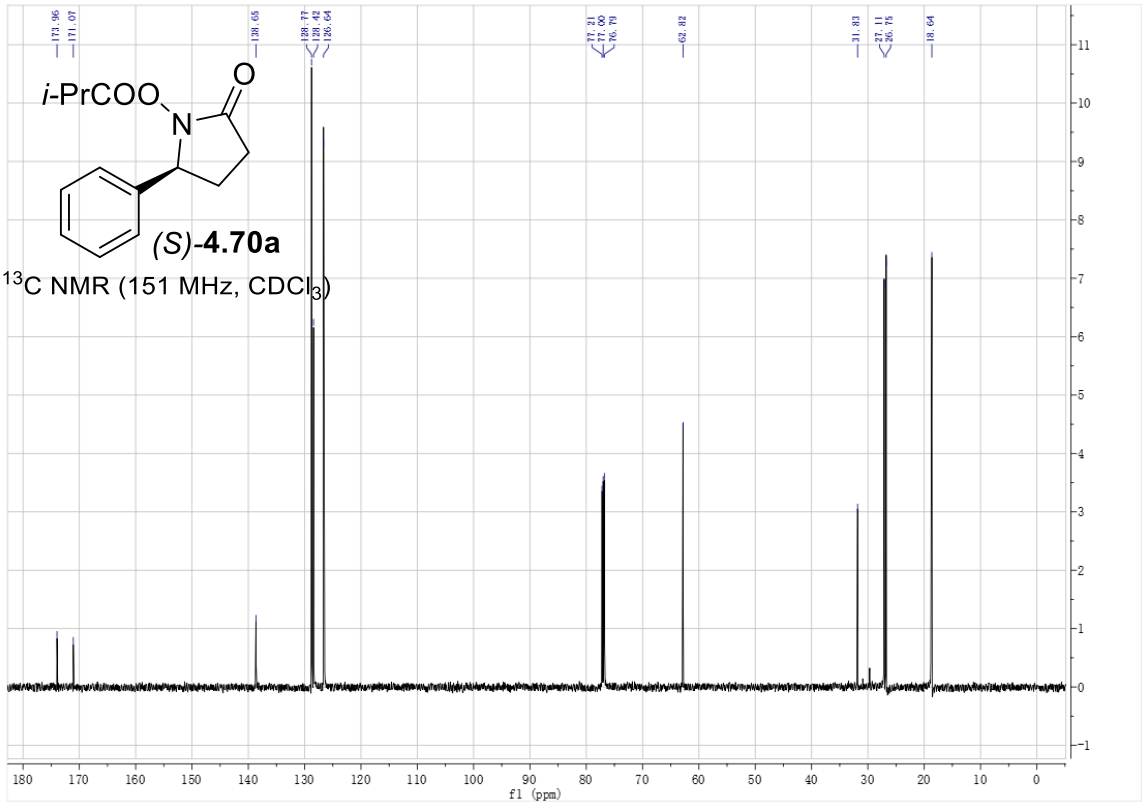
i-PrCOO
N
O
(S)-4.70a
13C NMR (151 MHz, CDCl3)
f1 (ppm)

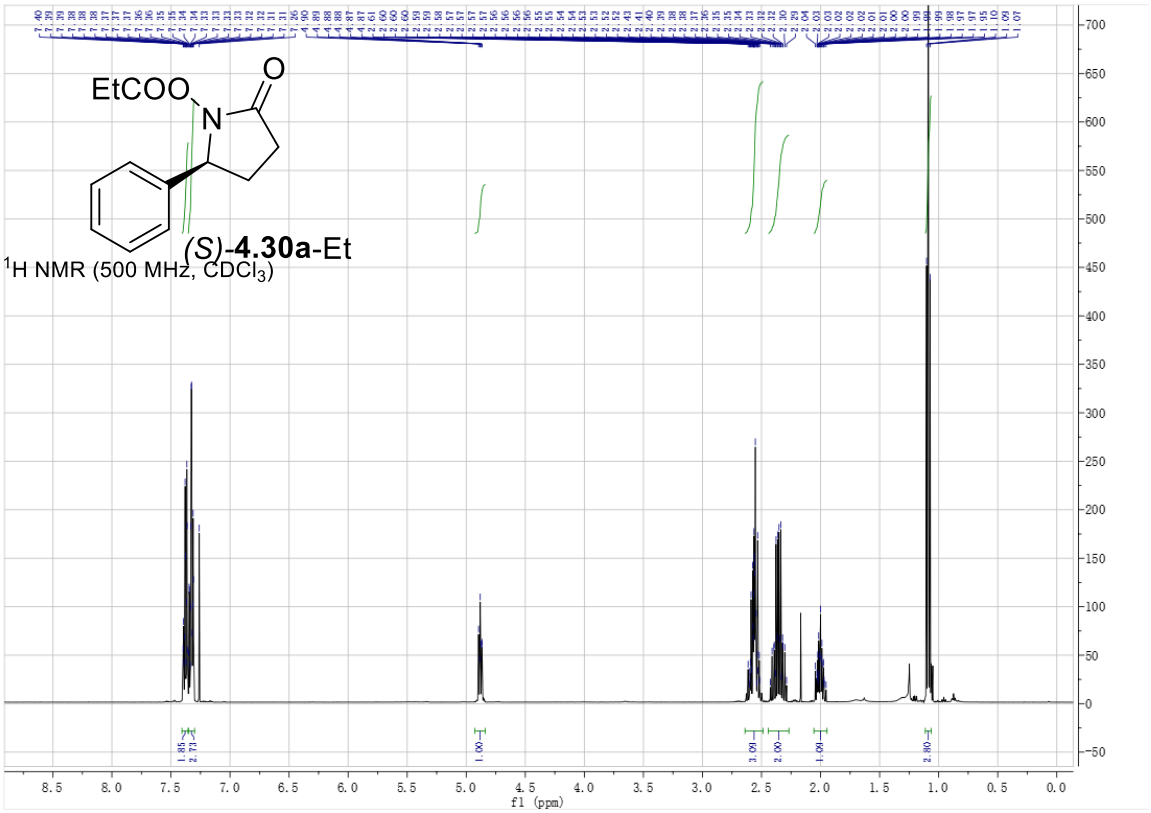
EtCOO
N
O
(S)-4.30a-Et
1H NMR (500 MHz, CDCl3)
f1 (ppm)

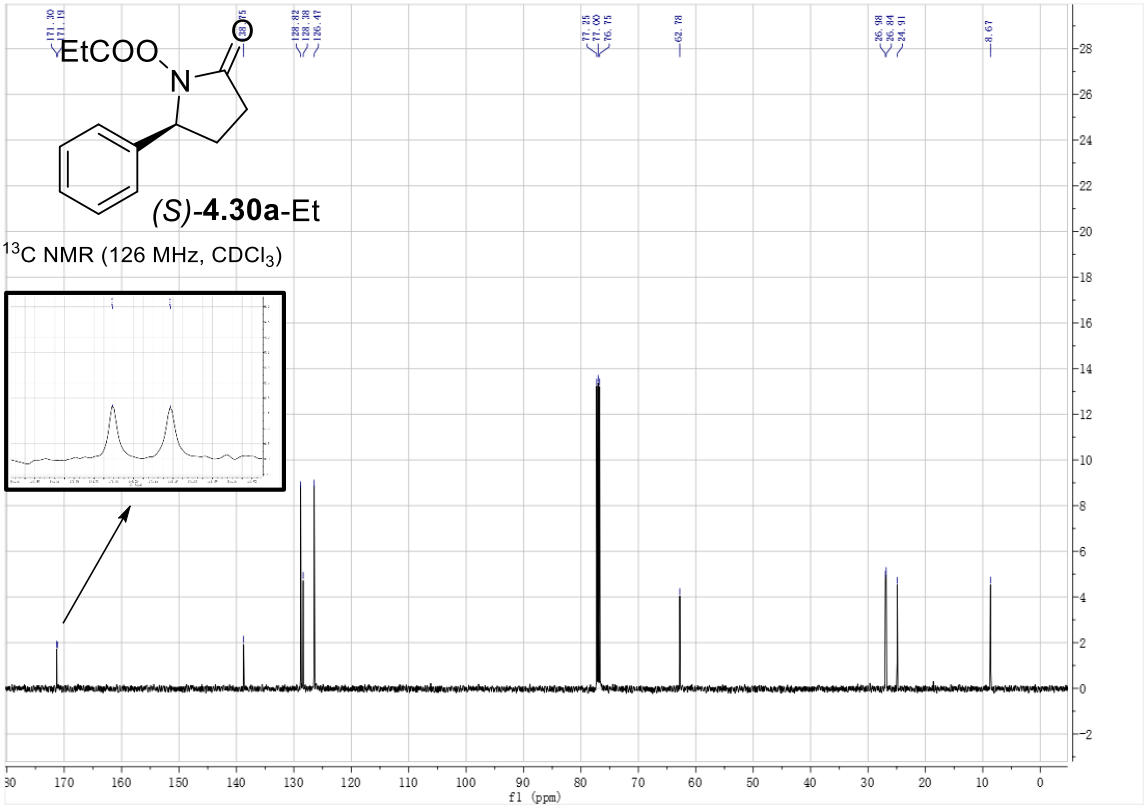
EtCOO
N
O
(S)-4.30a-Et
13C NMR (126 MHz, CDCl3)
f1 (ppm)

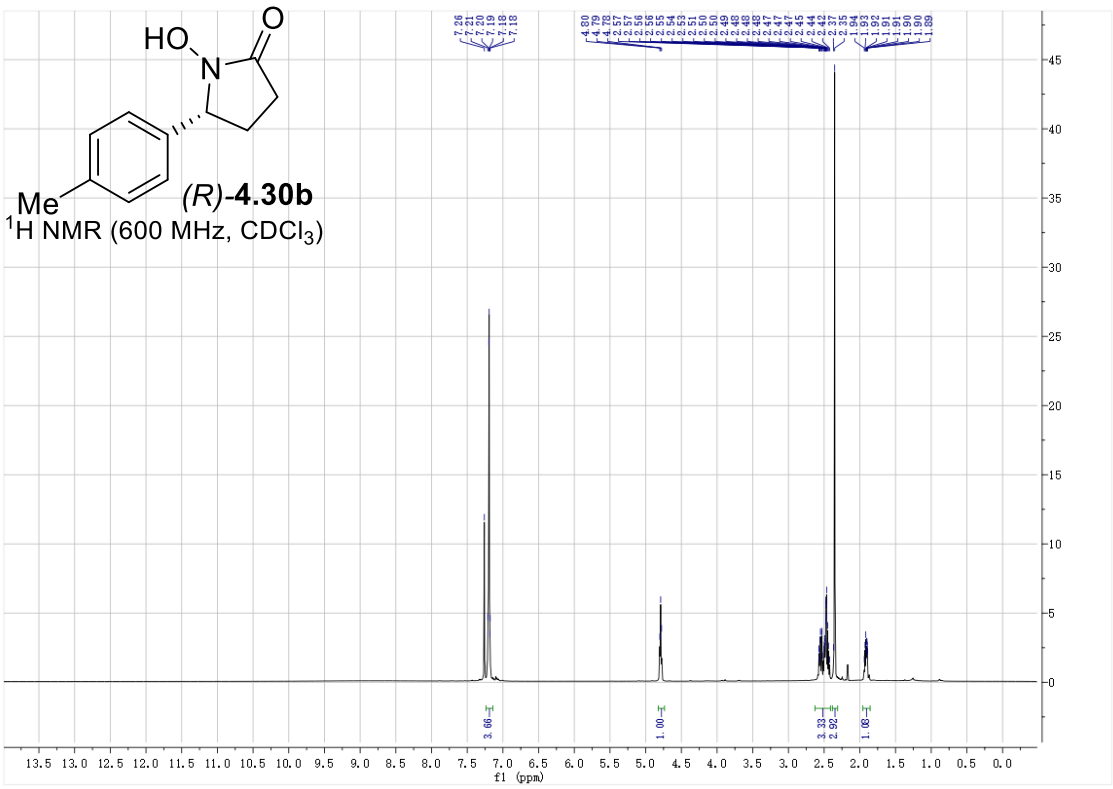
HO
N
O
Me
(R)-4.30b
1H NMR (600 MHz, CDCl3)
f1 (ppm)

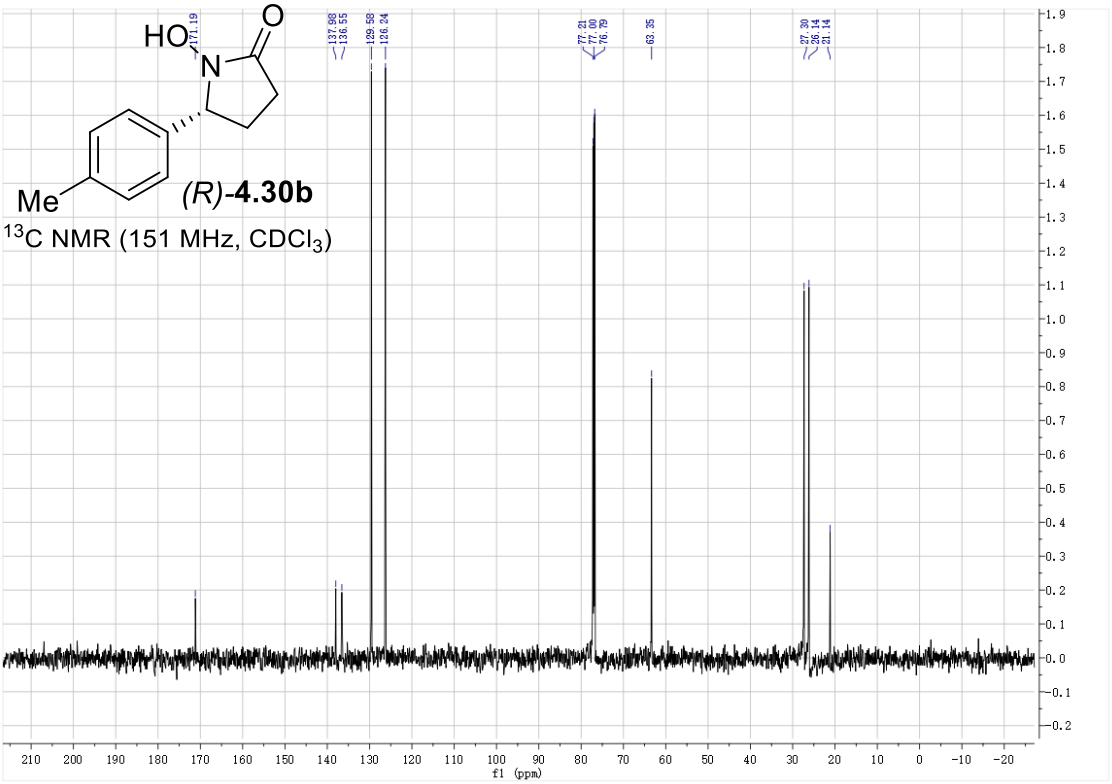
HO
N
O
Me
(R)-4.30b
13C NMR (151 MHz, CDCl3)
f1 (ppm)

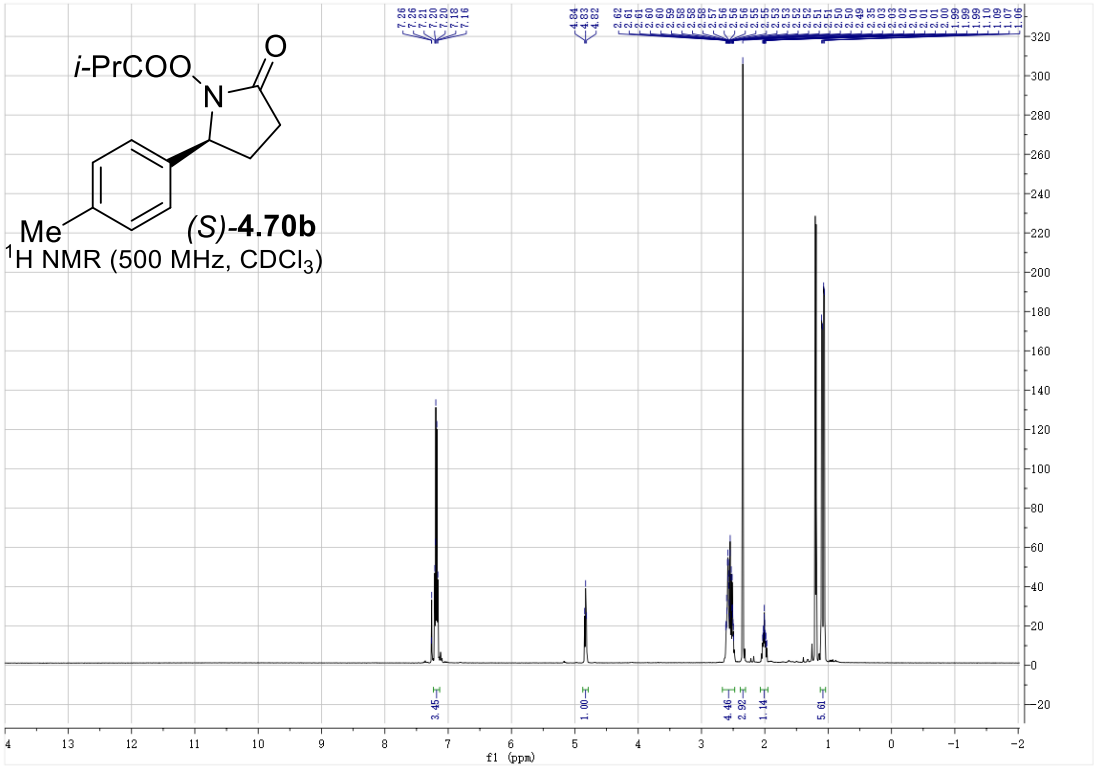
i-PrCOO
N
O
Me
(S)-4.70b
1H NMR (500 MHz, CDCl3)
f1 (ppm)

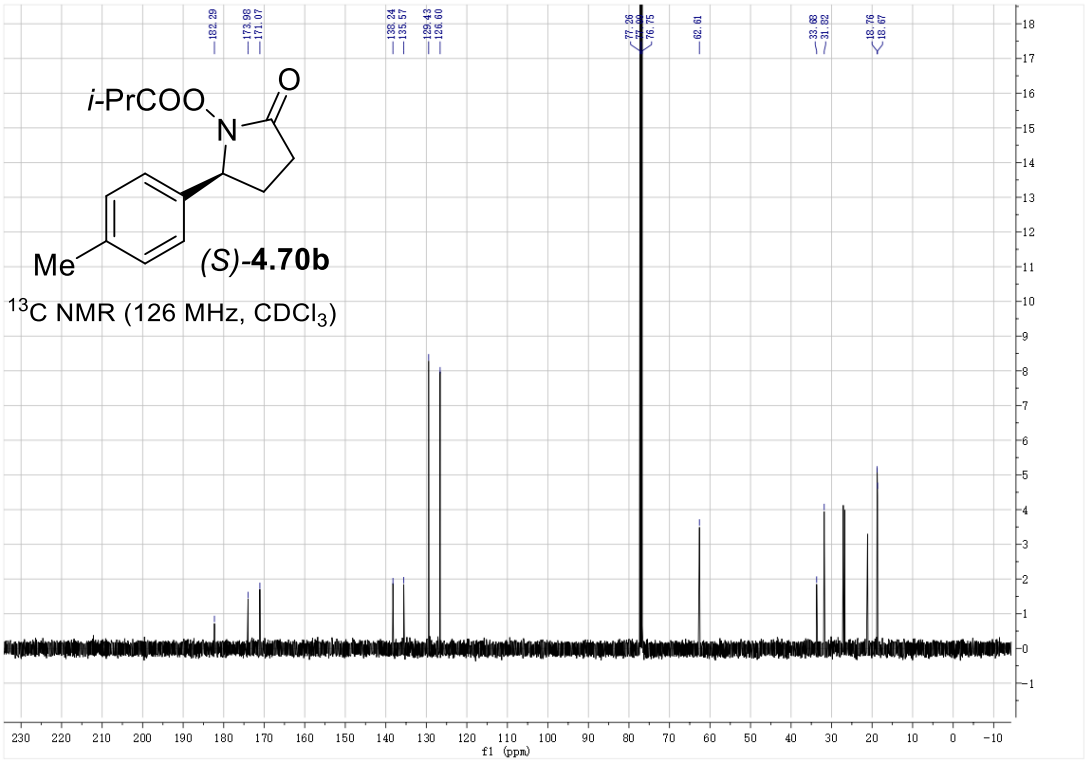
i-PrCOO
N
O
Me
(S)-4.70b
13C NMR (126 MHz, CDCl3)
f1 (ppm)

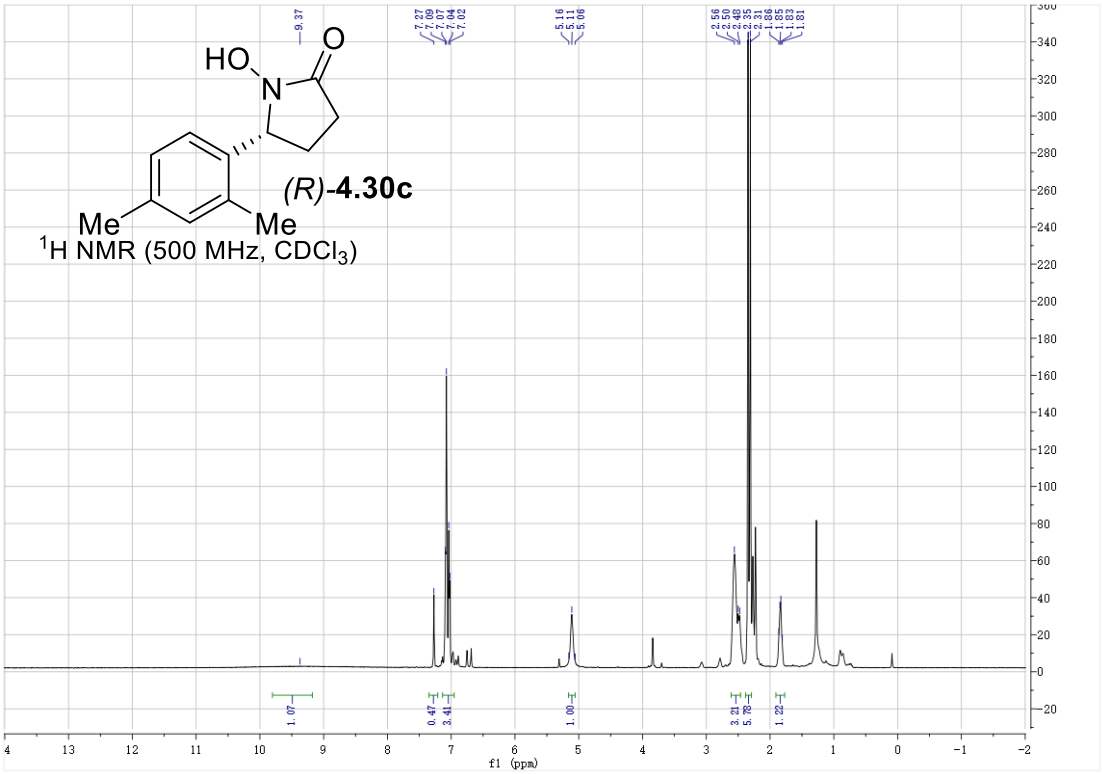
HO
N
O
Me
Me
(R)-4.30c
1H NMR (500 MHz, CDCl3)
f1 (ppm)

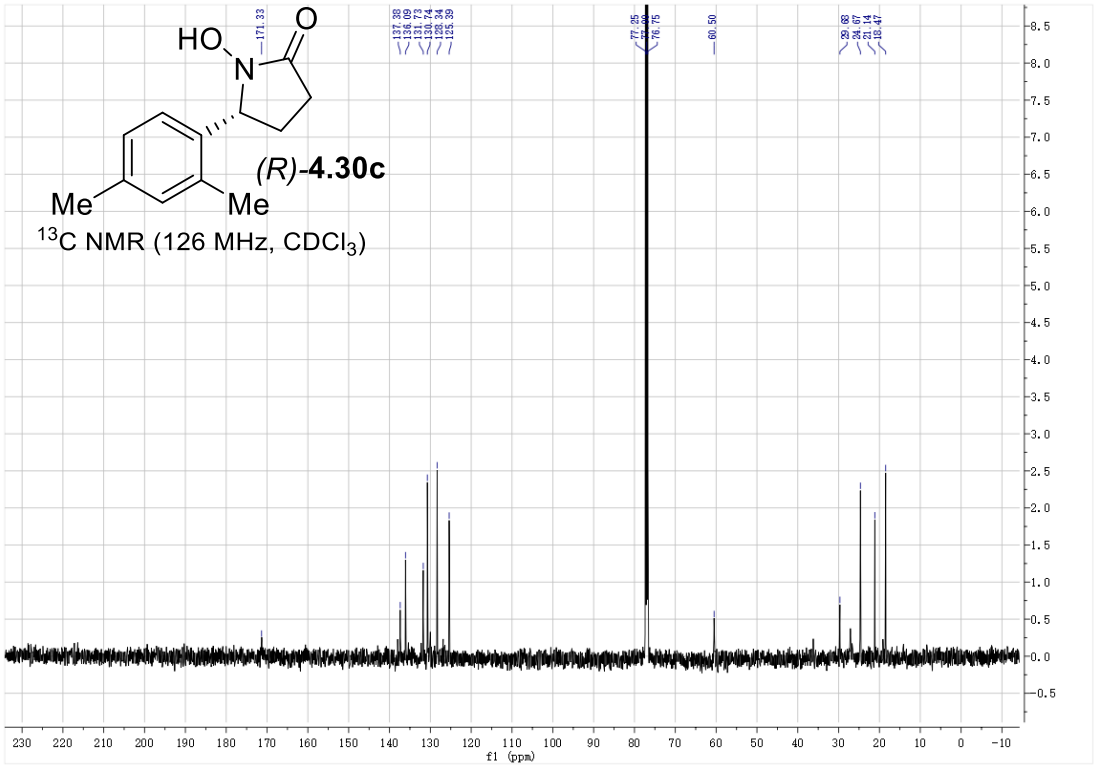
HO
N
O
Me
Me
(R)-4.30c
13C NMR (126 MHz, CDCl3)
f1 (ppm)

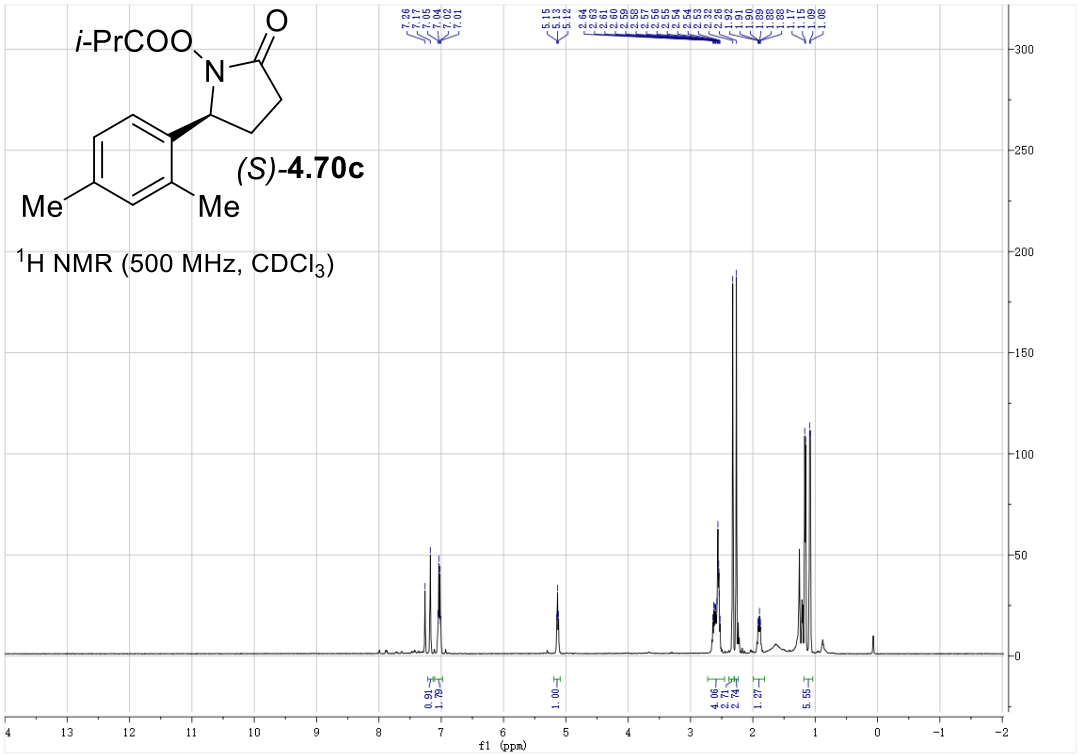
i-PrCOO
N
O
(S)-4.70c
Me
Me
1H NMR (500 MHz, CDCl3)
f1 (ppm)

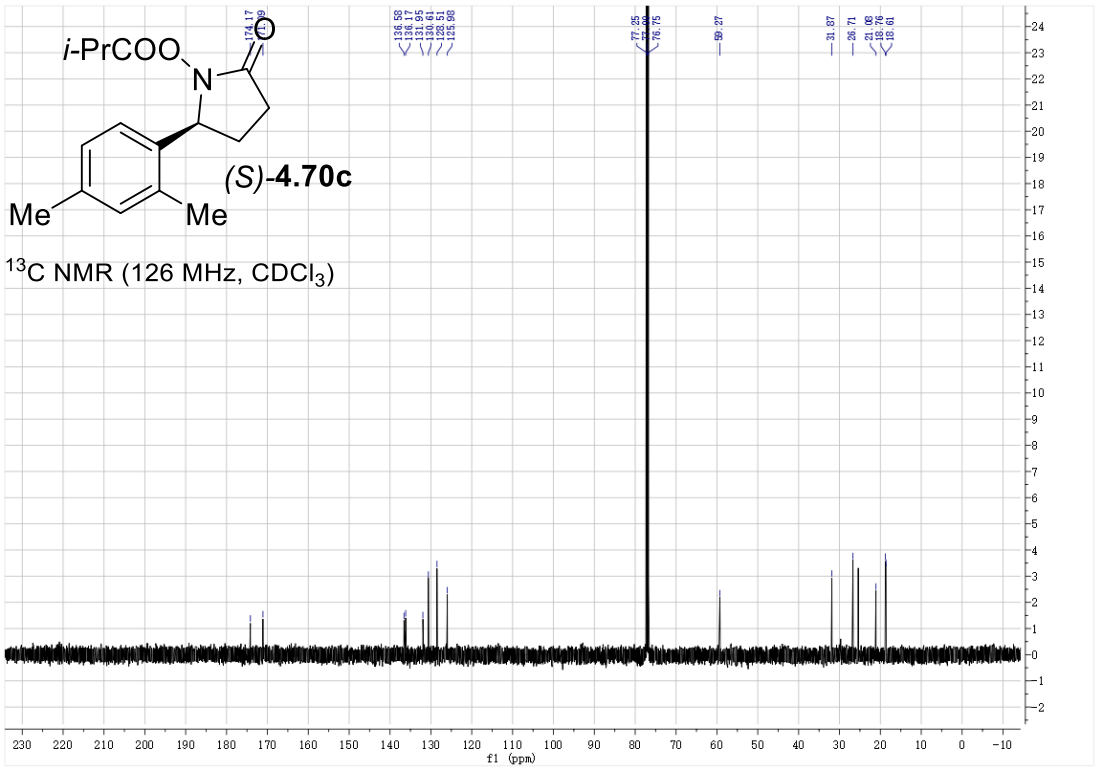
i-PrCOO
N
O
(S)-4.70c
Me
Me
13C NMR (126 MHz, CDCl3)
f1 (ppm)

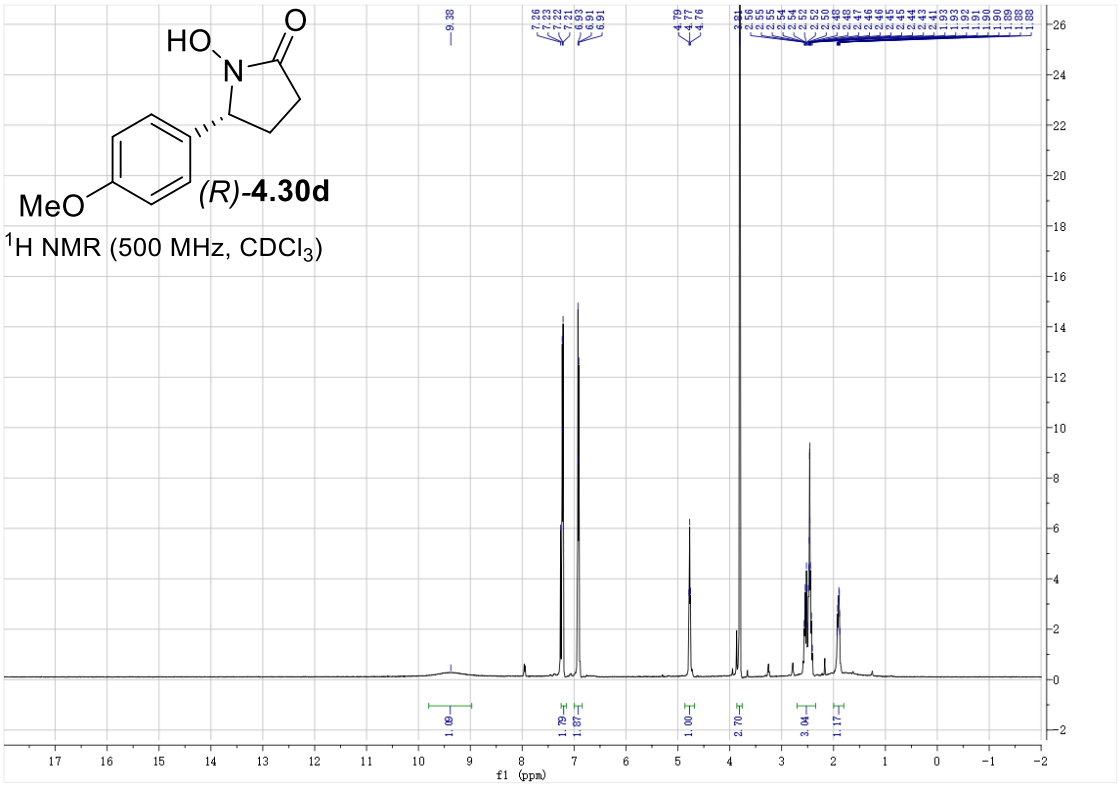
HO
N
O
MeO
(R)-4.30d
1H NMR (500 MHz, CDCl3)
f1 (ppm)

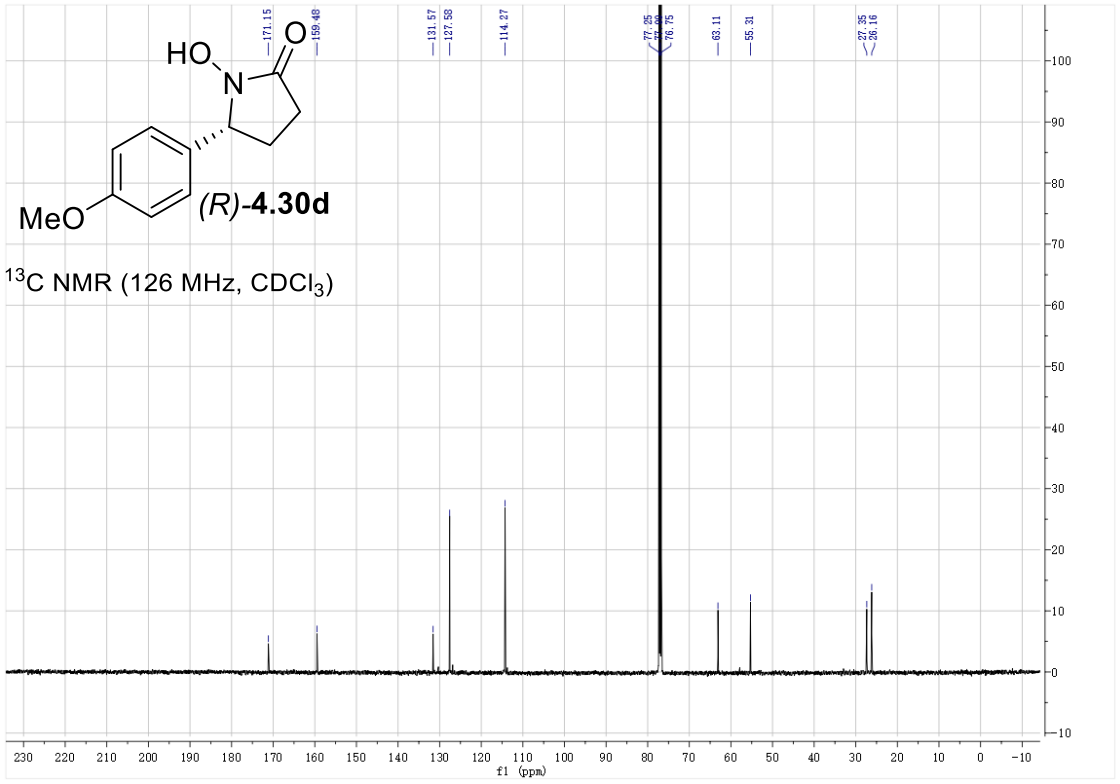
HO
N
O
MeO
(R)-4.30d
13C NMR (126 MHz, CDCl3)
f1 (ppm)

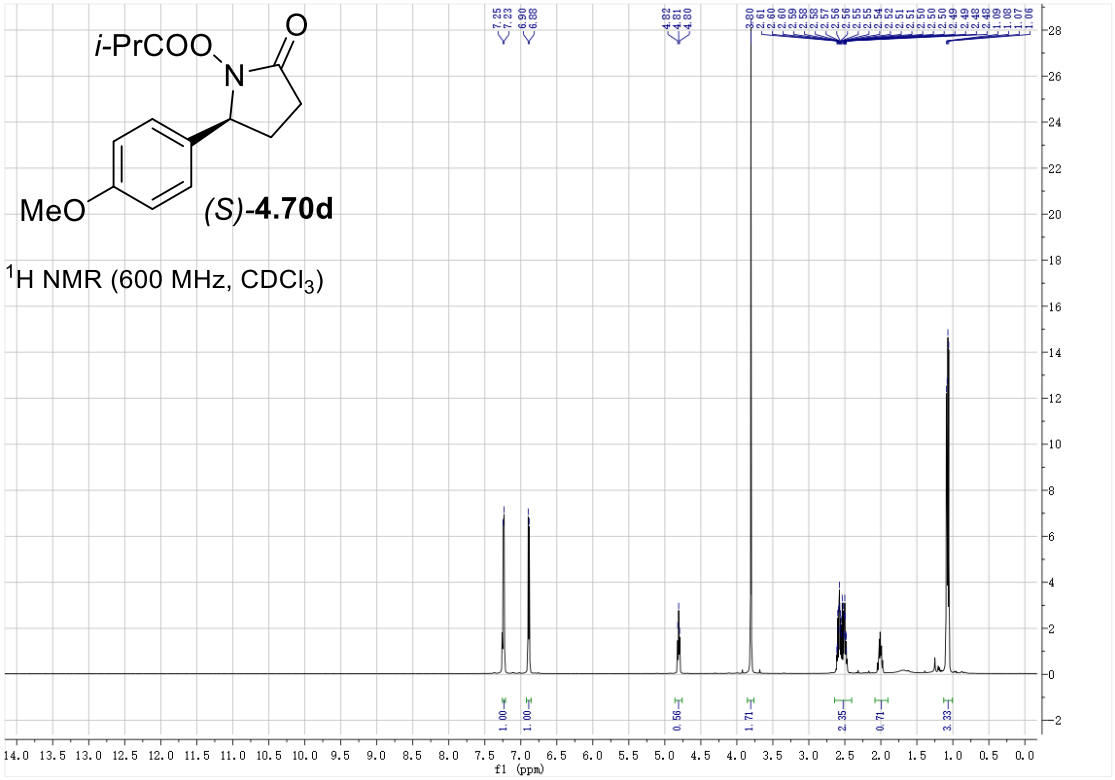
i-PrCOO
N
O
MeO
(S)-4.70d
1H NMR (600 MHz, CDCl3)
f1 (ppm)

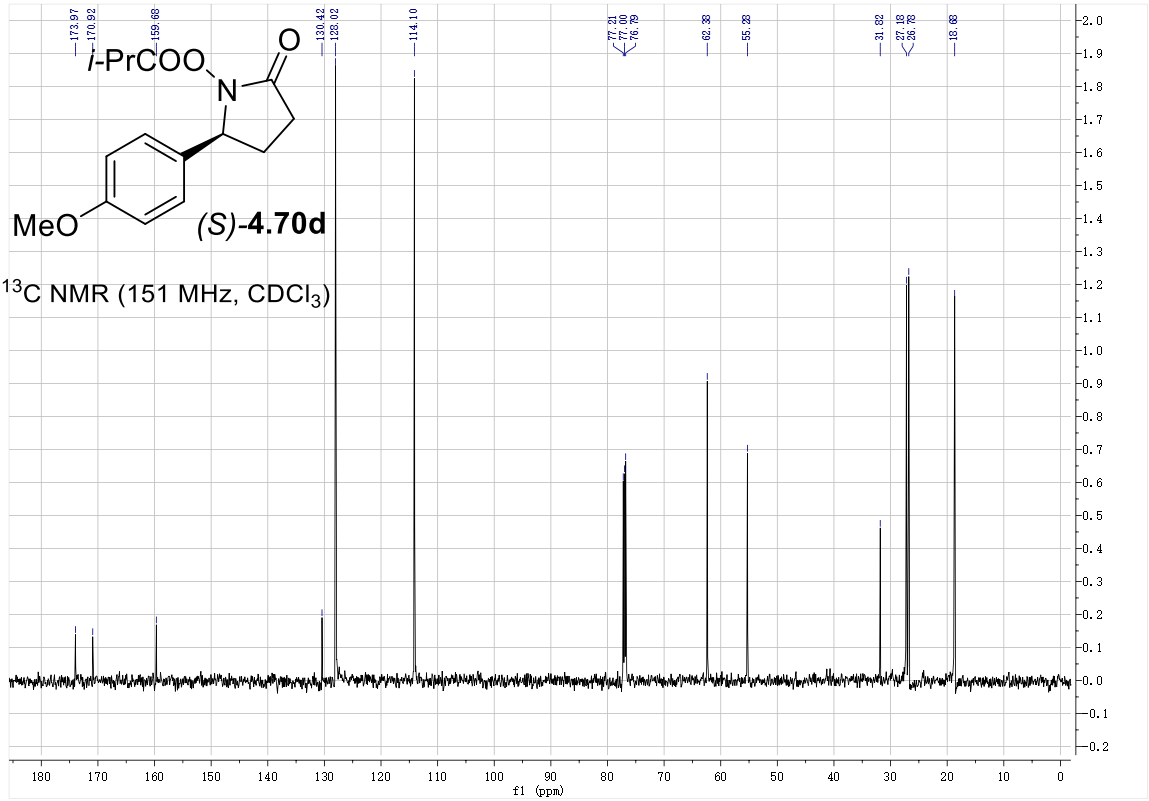
i-PrCOO
N
O
MeO
(S)-4.70d
13C NMR (151 MHz, CDCl3)
f1 (ppm)

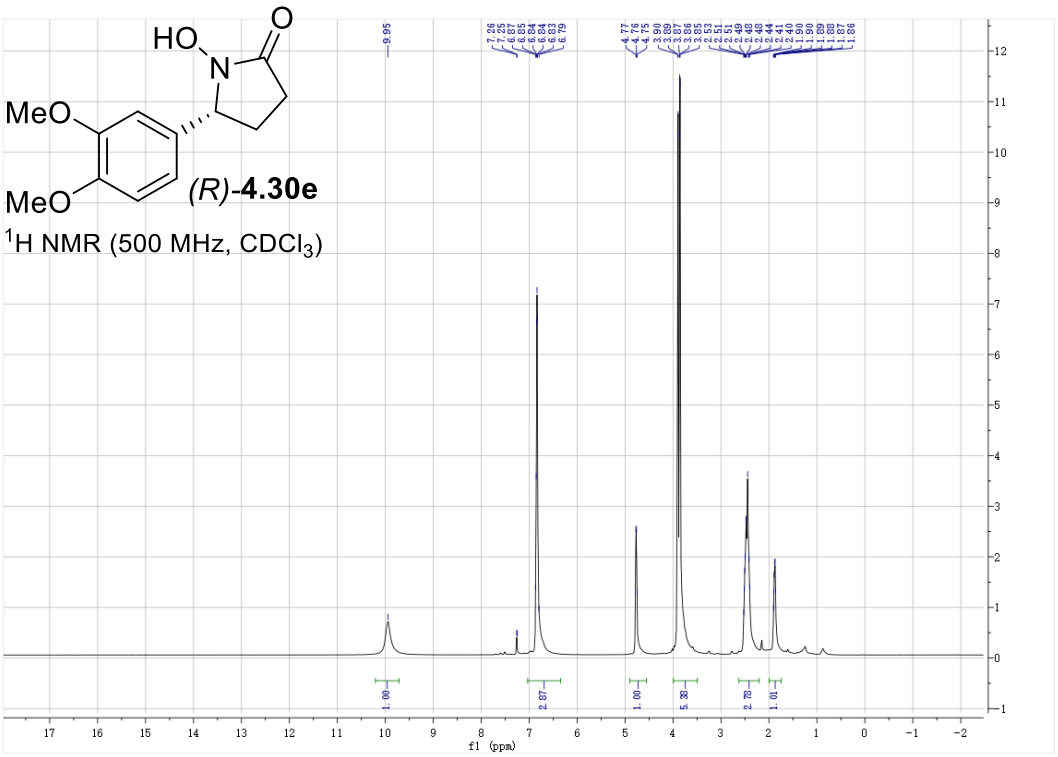
HO
N
O
MeO
MeO
(R)-4.30e
1H NMR (500 MHz, CDCl3)
f1 (ppm)

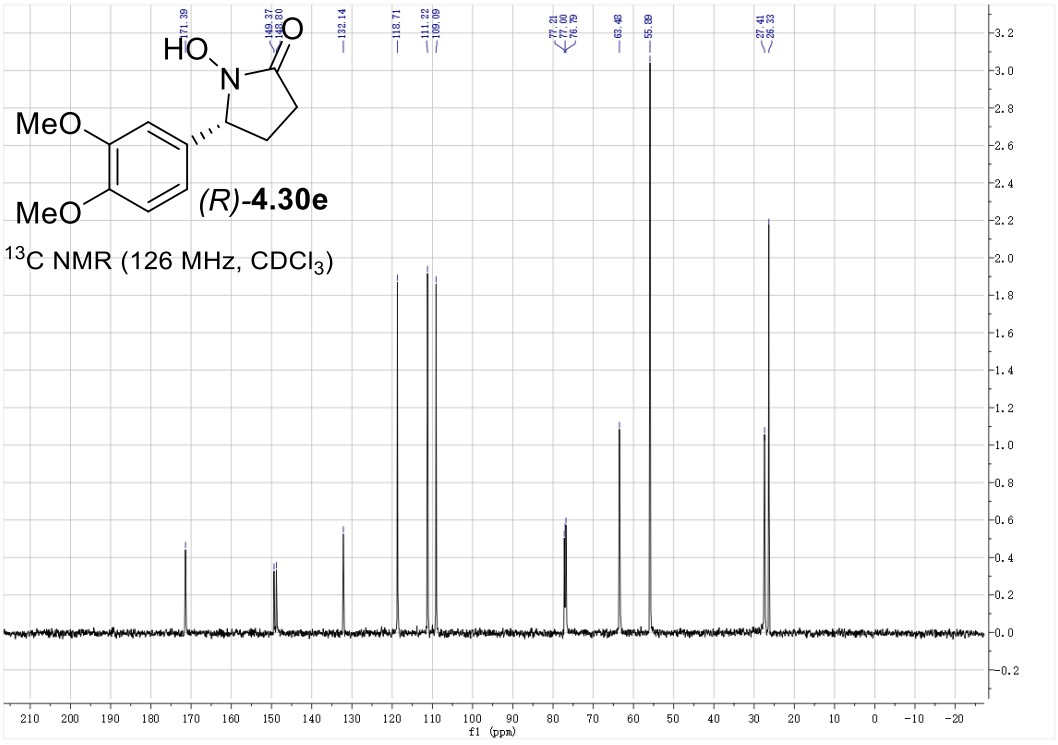
HO
N
O
MeO
MeO
(R)-4.30e
13C NMR (126 MHz, CDCl3)
f1 (ppm)

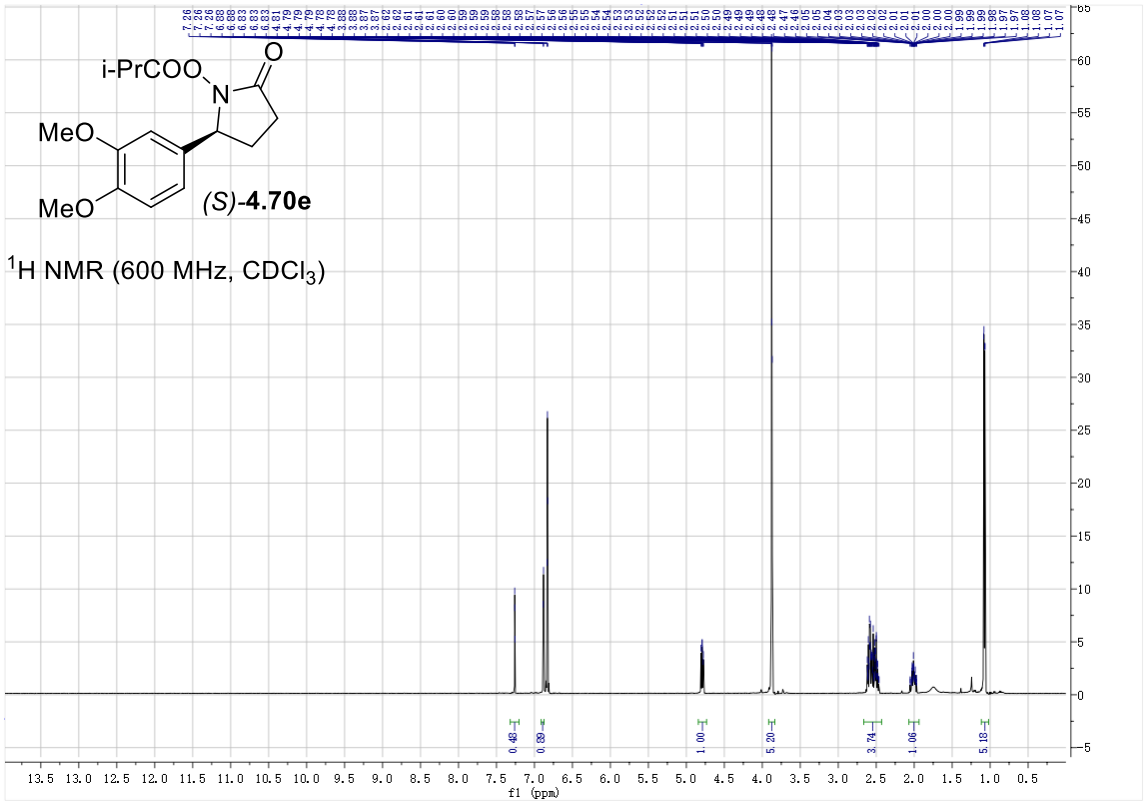
i-PrCOO
N
O
MeO
MeO
(S)-4.70e
1H NMR (600 MHz, CDCl3)
f1 (ppm)

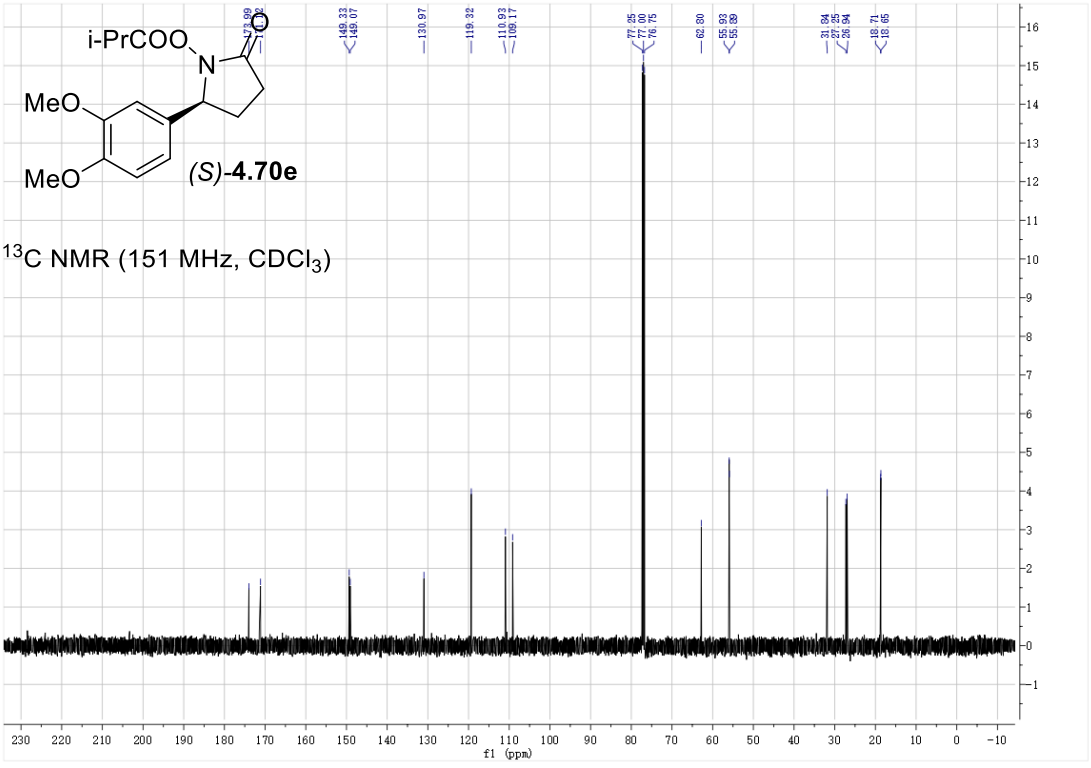
i-PrCOO
N
O
MeO
MeO
(S)-4.70e
13C NMR (151 MHz, CDCl3)
f1 (ppm)

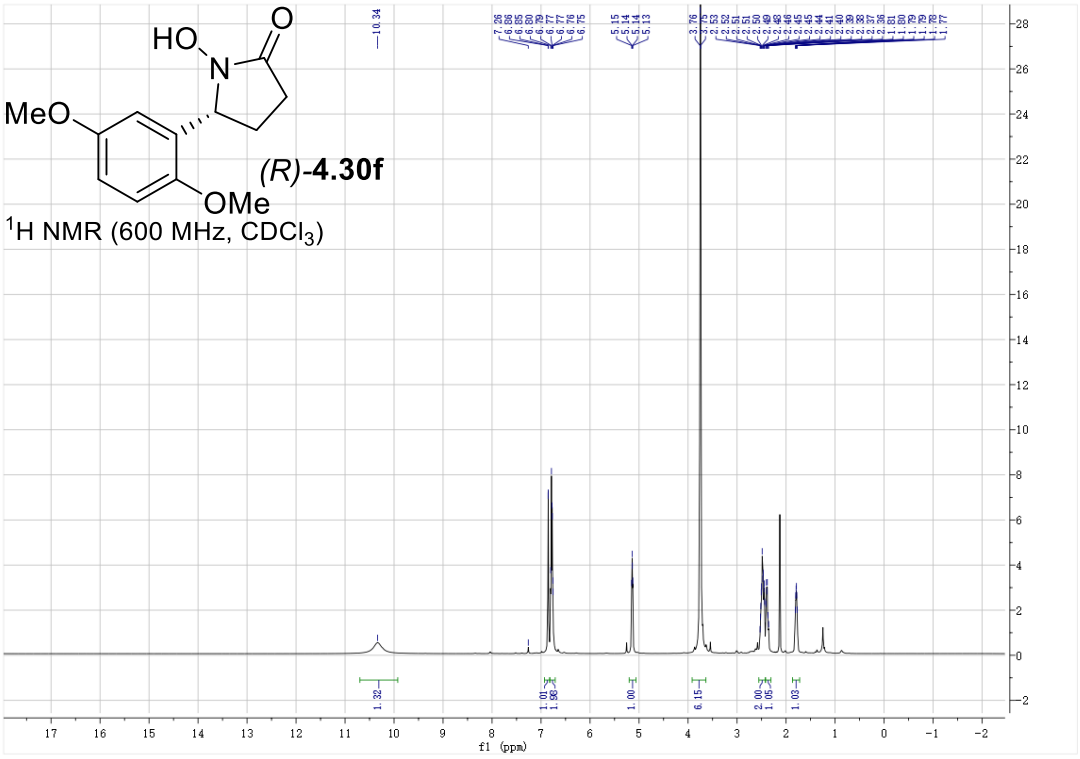
HO
N
O
MeO
OMe
(R)-4.30f
1H NMR (600 MHz, CDCl3)
f1 (ppm)

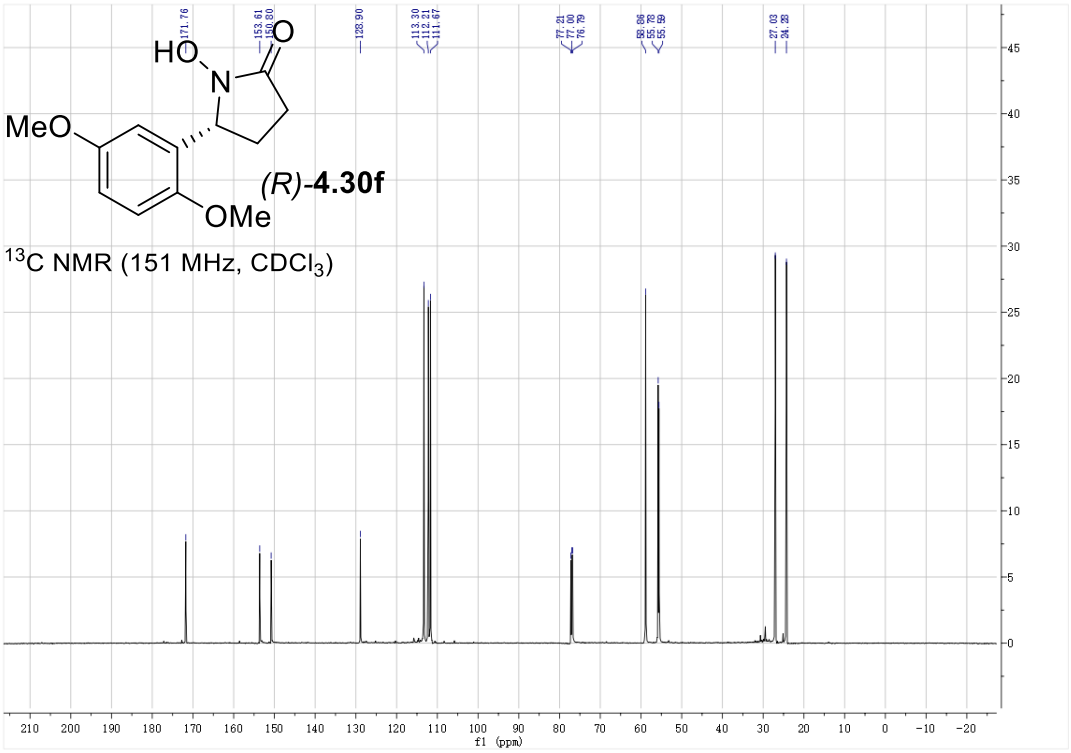
HO
N
O
MeO
OMe
(R)-4.30f
13C NMR (151 MHz, CDCl3)
f1 (ppm)

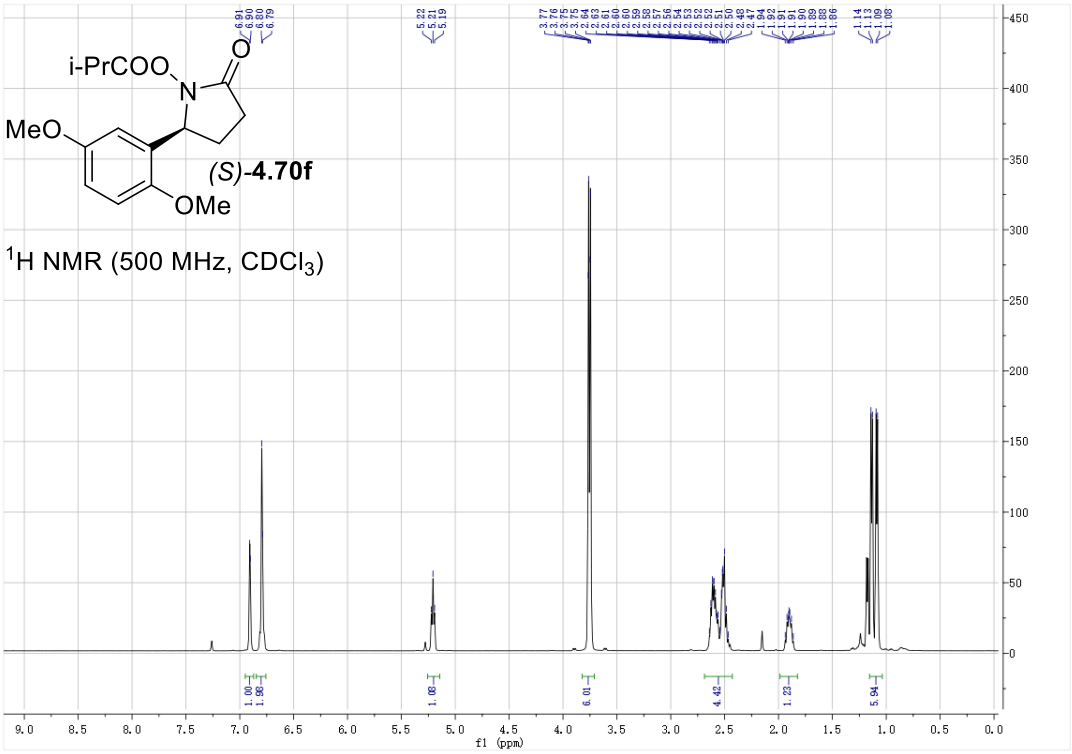
i-PrCOO
N
O
MeO
OMe
(S)-4.70f
1H NMR (500 MHz, CDCl3)
f1 (ppm)

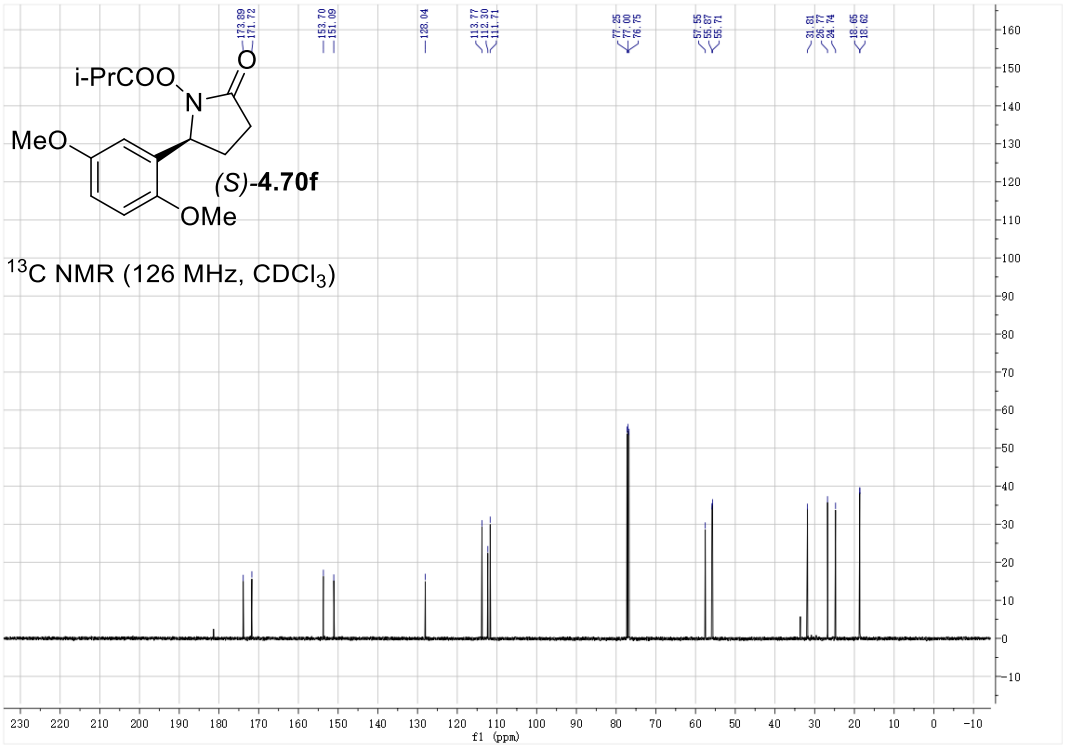
i-PrCOO
N
O
MeO
OMe
(S)-4.70f
13C NMR (126 MHz, CDCl3)
f1 (ppm)

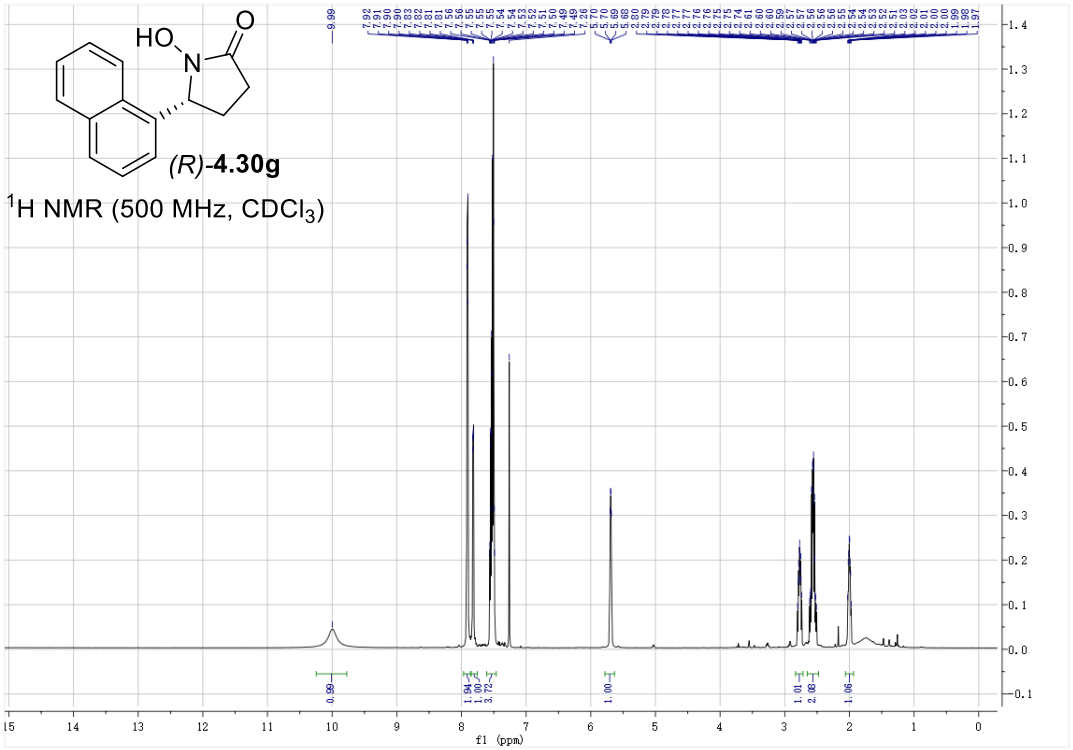
HO
N
O
(R)-4.30g
1H NMR (500 MHz, CDCl3)
f1 (ppm)

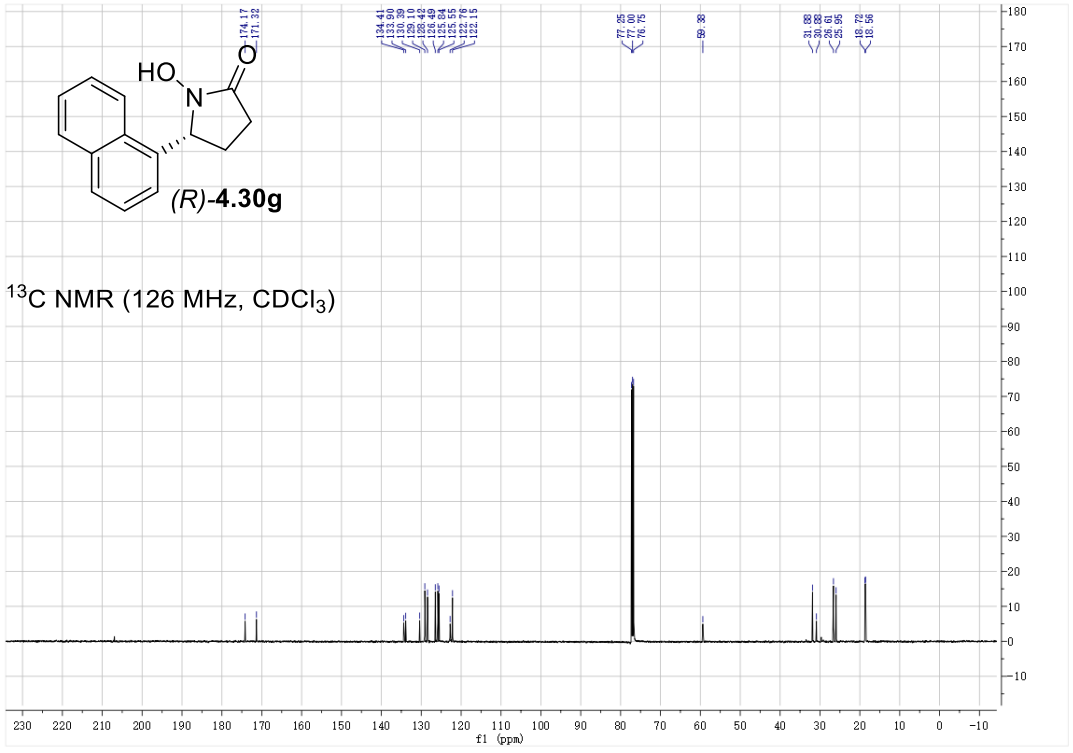
HO
N
O
(R)-4.30g
13C NMR (126 MHz, CDCl3)
f1 (ppm)

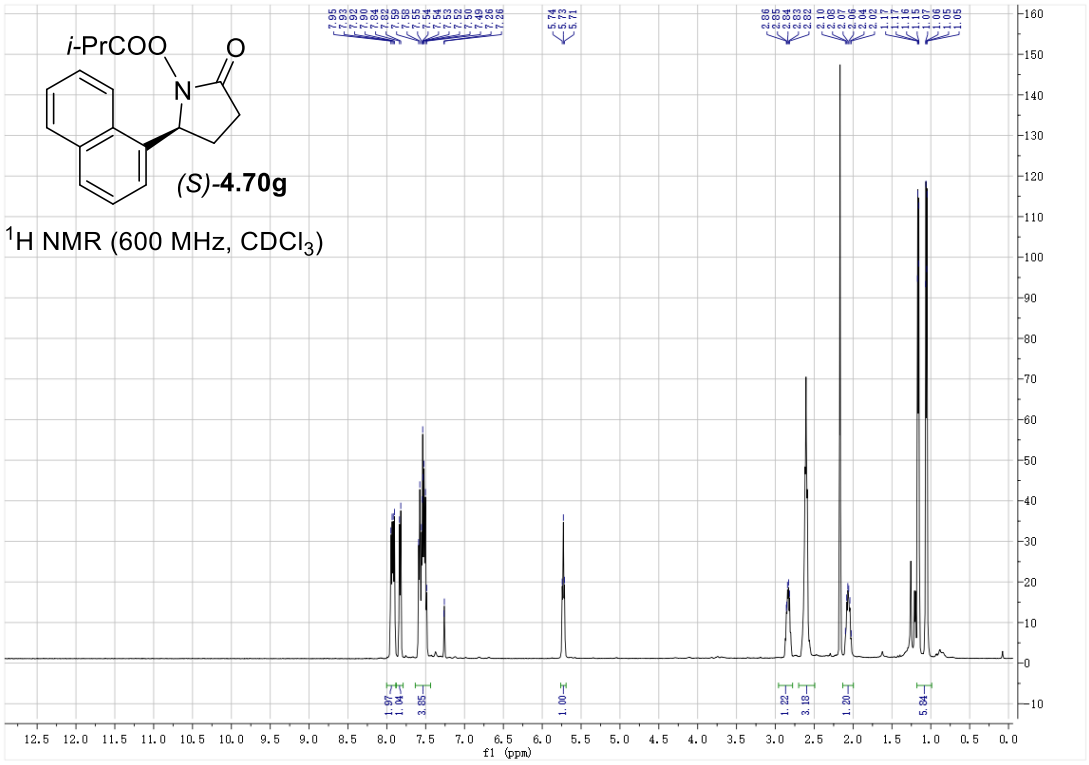
i-PrCOO
O
N
(S)-4.70g
1H NMR (600 MHz, CDCl3)
f1 (ppm)

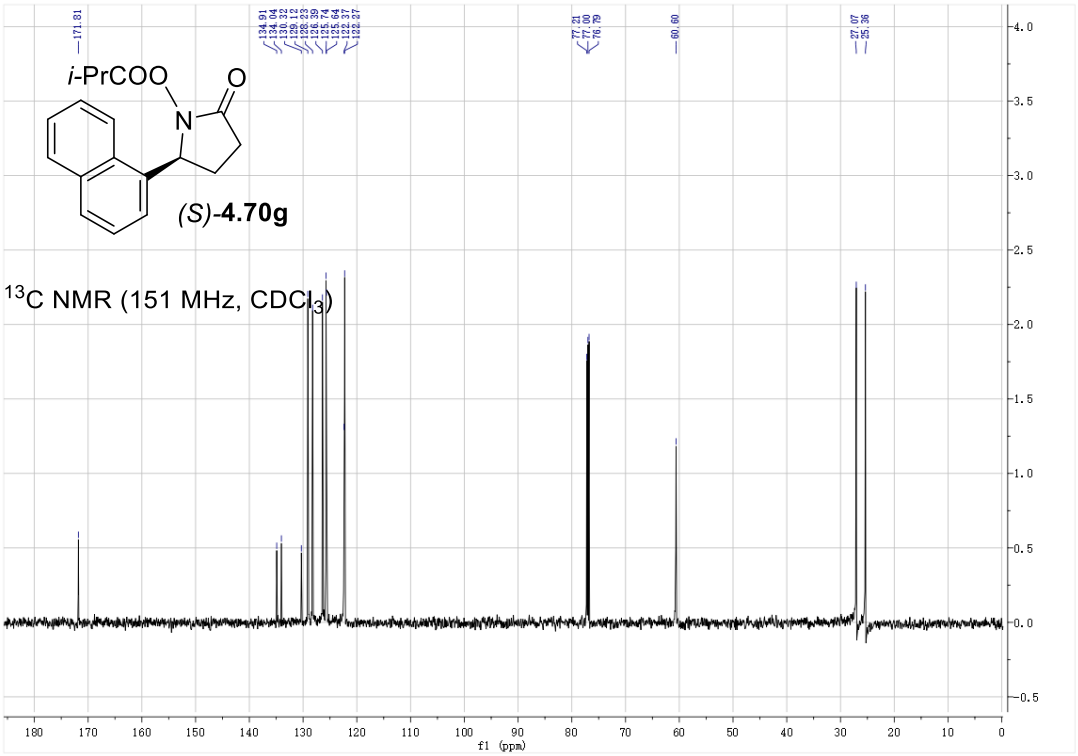
i-PrCOO
O
N
(S)-4.70g
13C NMR (151 MHz, CDCl3)
f1 (ppm)

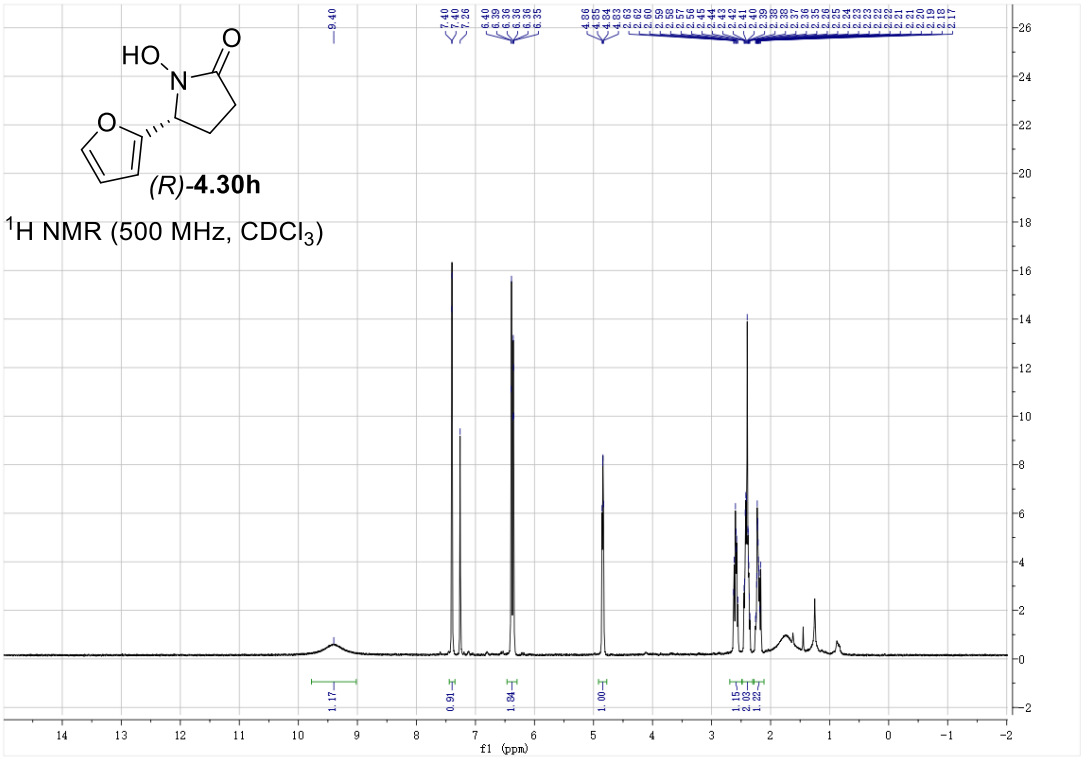
HO
N
O
O
(R)-4.30h
1H NMR (500 MHz, CDCl3)
f1 (ppm)

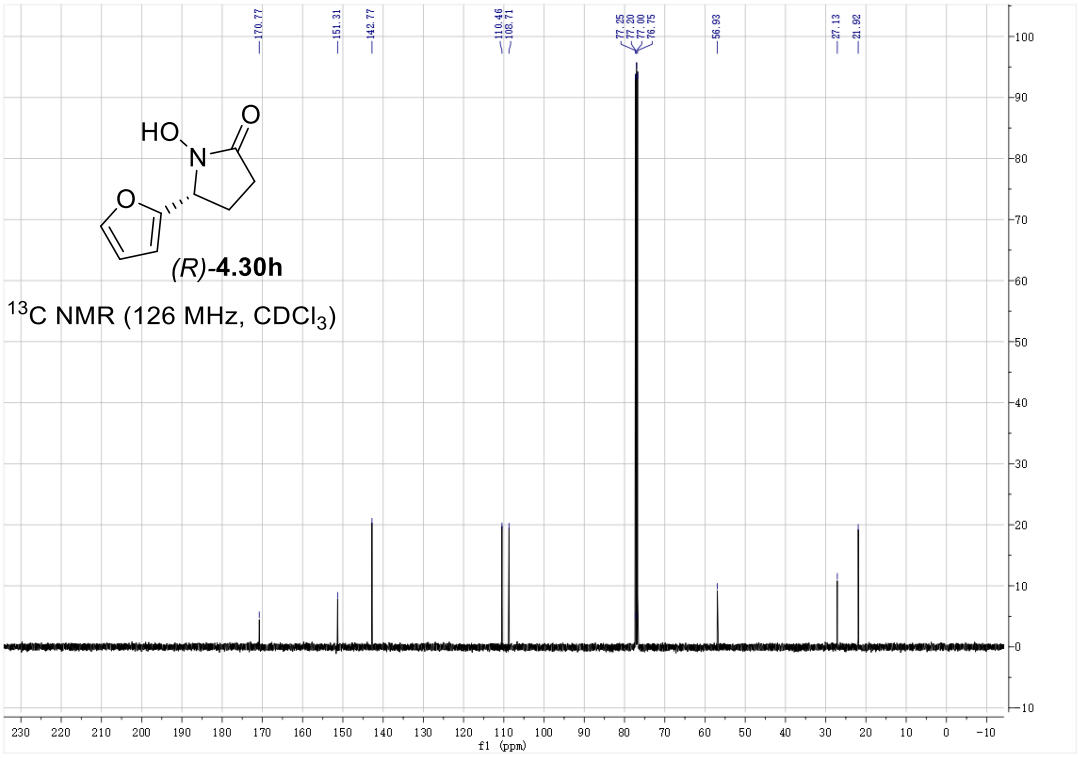
HO
N
O
O
(R)-4.30h
13C NMR (126 MHz, CDCl3)
f1 (ppm)

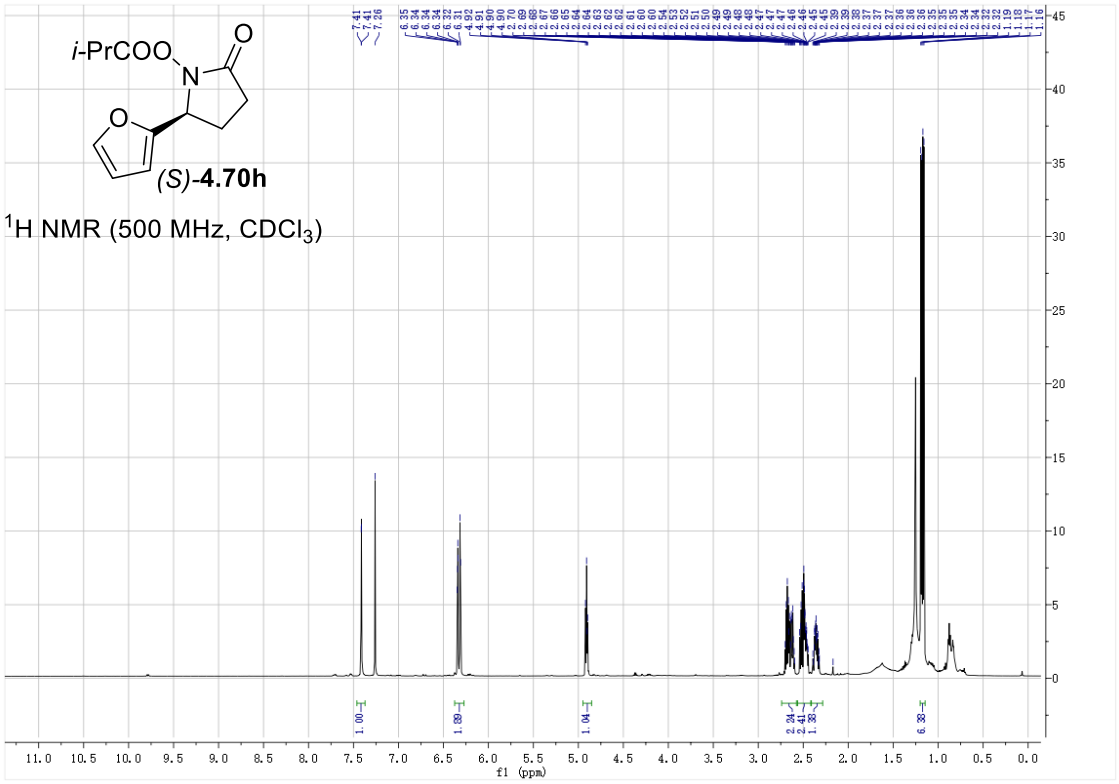
i-PrCOO
N
O
O
(S)-4.70h
1H NMR (500 MHz, CDCl3)
f1 (ppm)

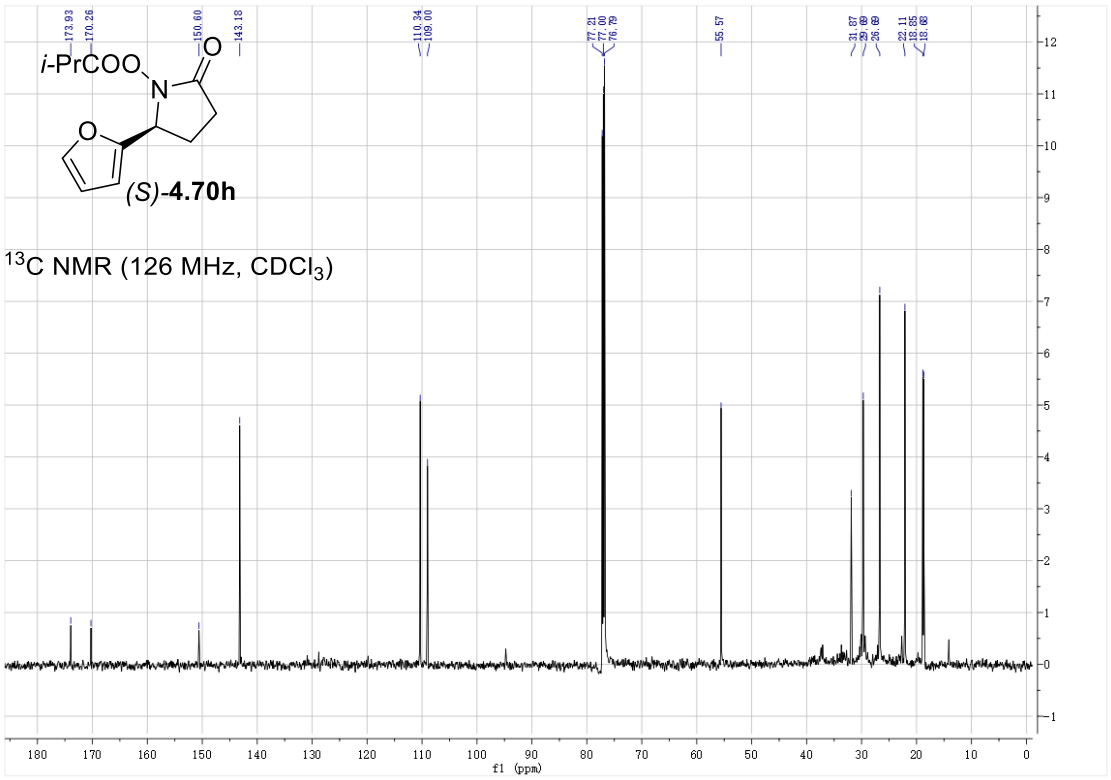
i-PrCOO
N
O
O
(S)-4.70h
13C NMR (126 MHz, CDCl3)
f1 (ppm)

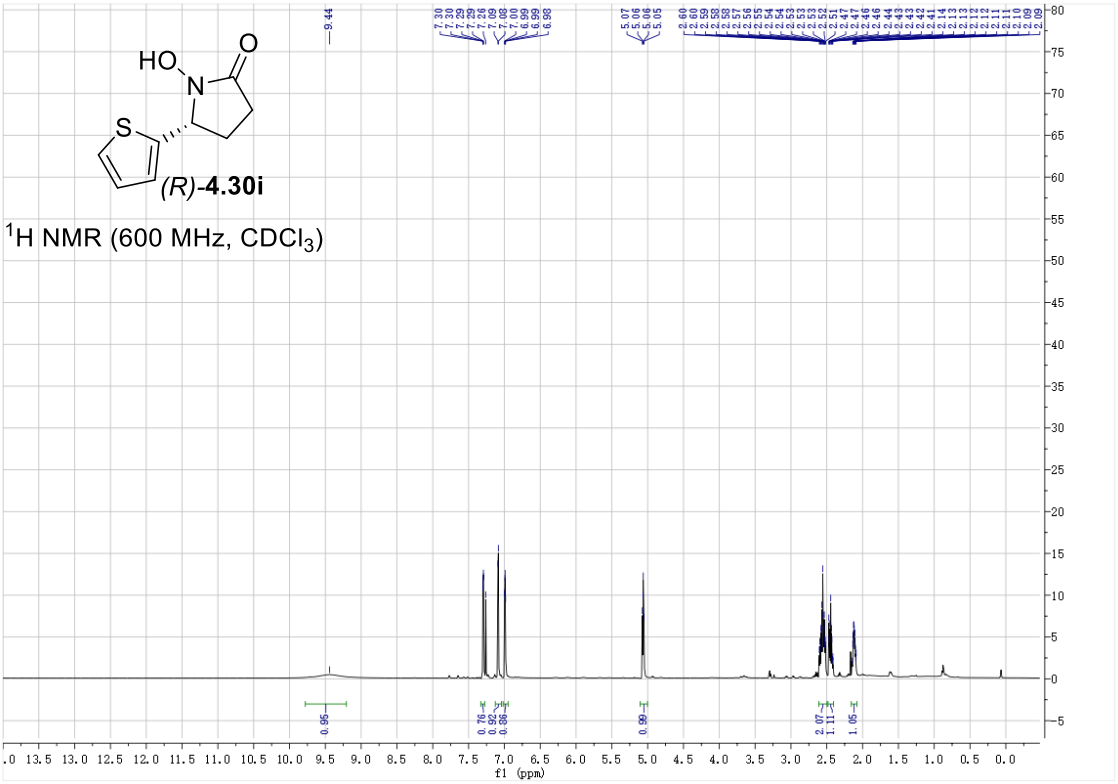
HO
N
O
S
(R)-4.30i
1H NMR (600 MHz, CDCl3)
f1 (ppm)

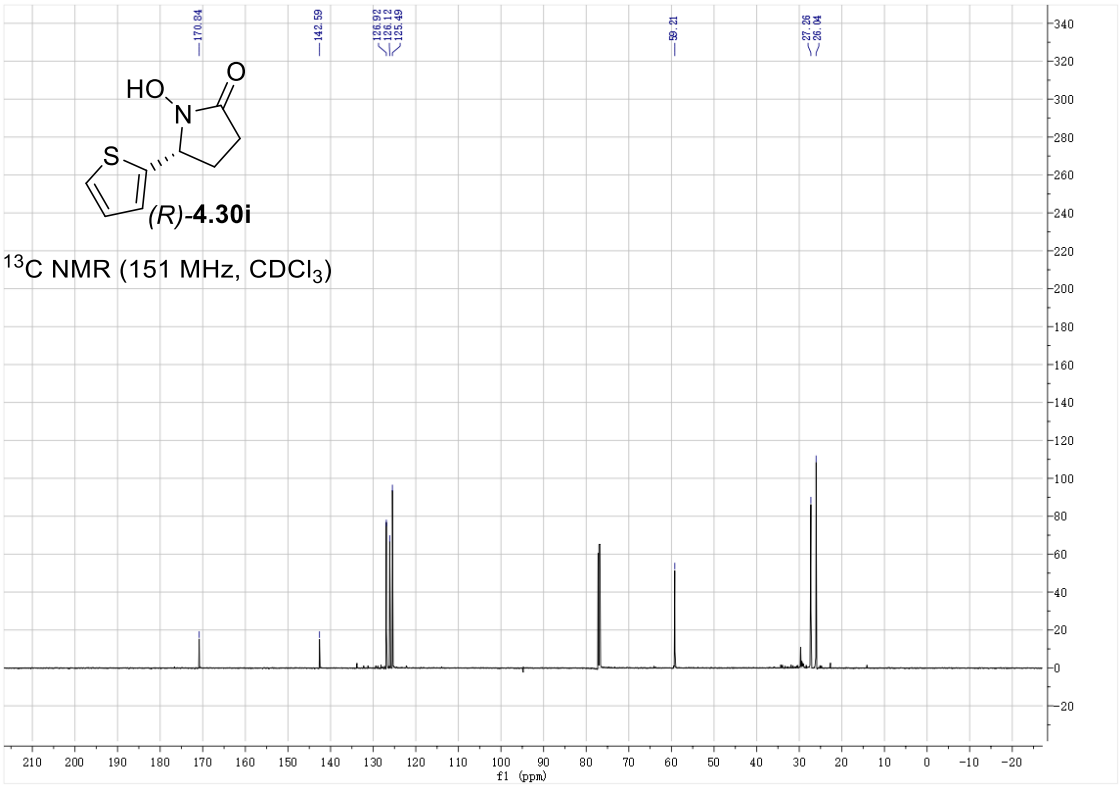
HO
N
O
S
(R)-4.30i
13C NMR (151 MHz, CDCl3)
f1 (ppm)

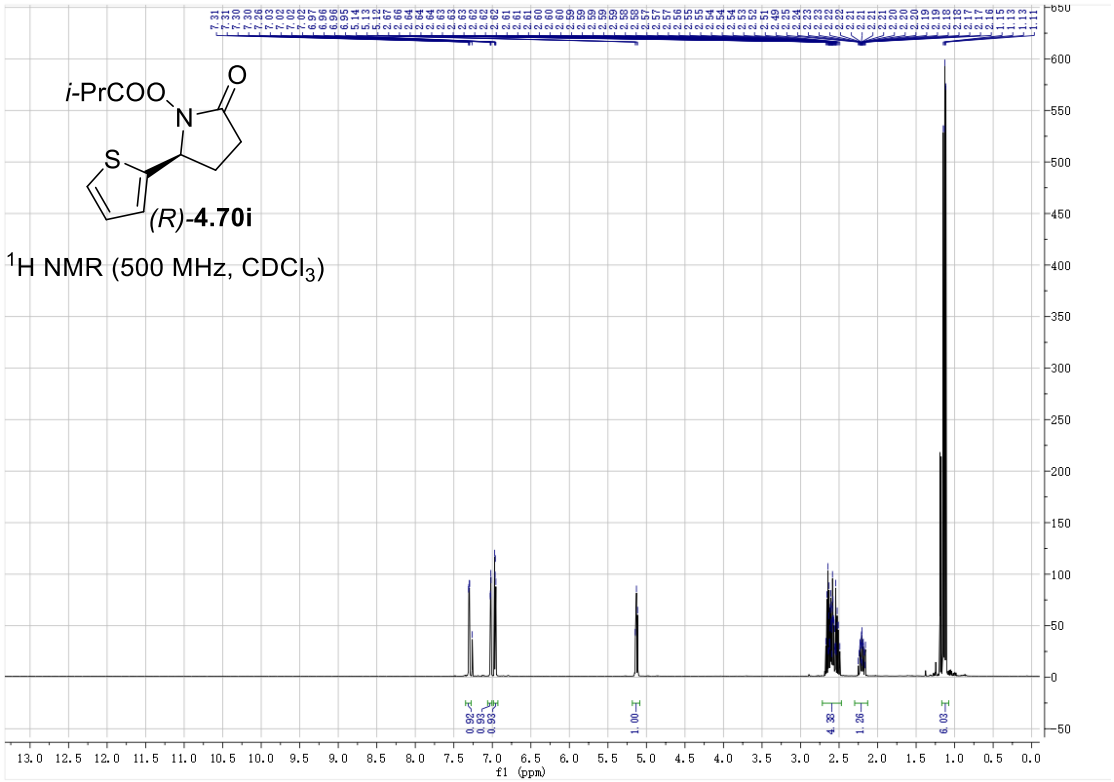
i-PrCOO
N
O
S
(R)-4.70i
1H NMR (500 MHz, CDCl3)
f1 (ppm)

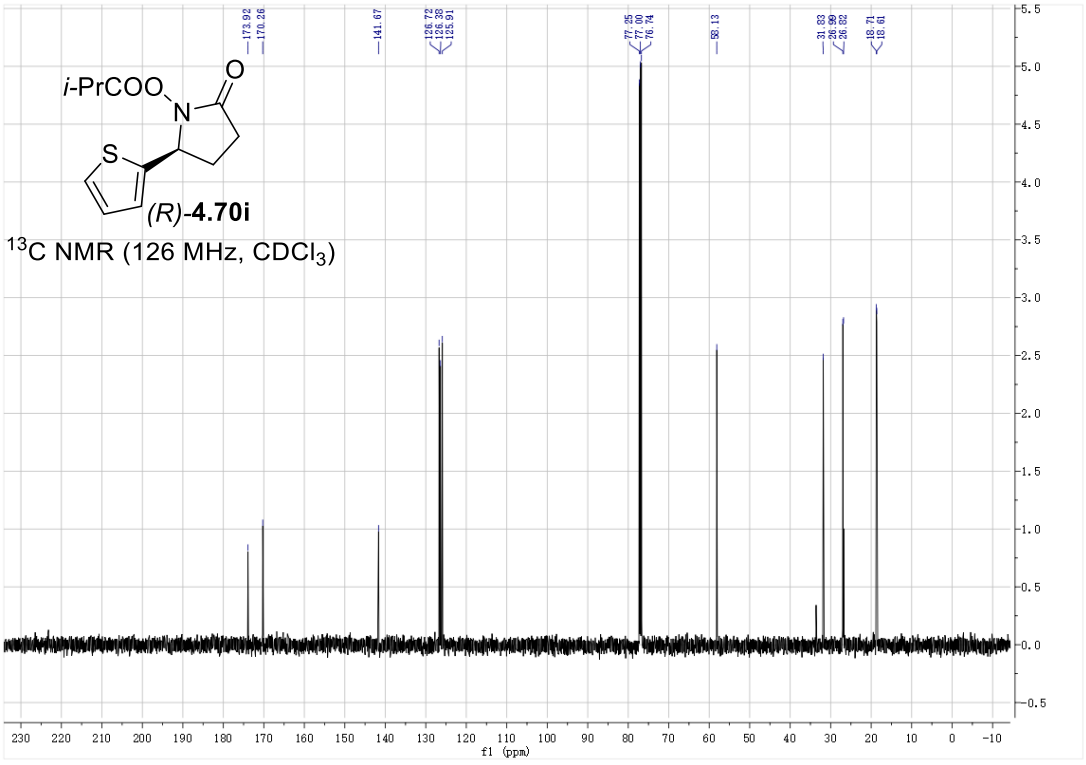
i-PrCOO
N
O
S
(R)-4.70i
13C NMR (126 MHz, CDCl3)
f1 (ppm)

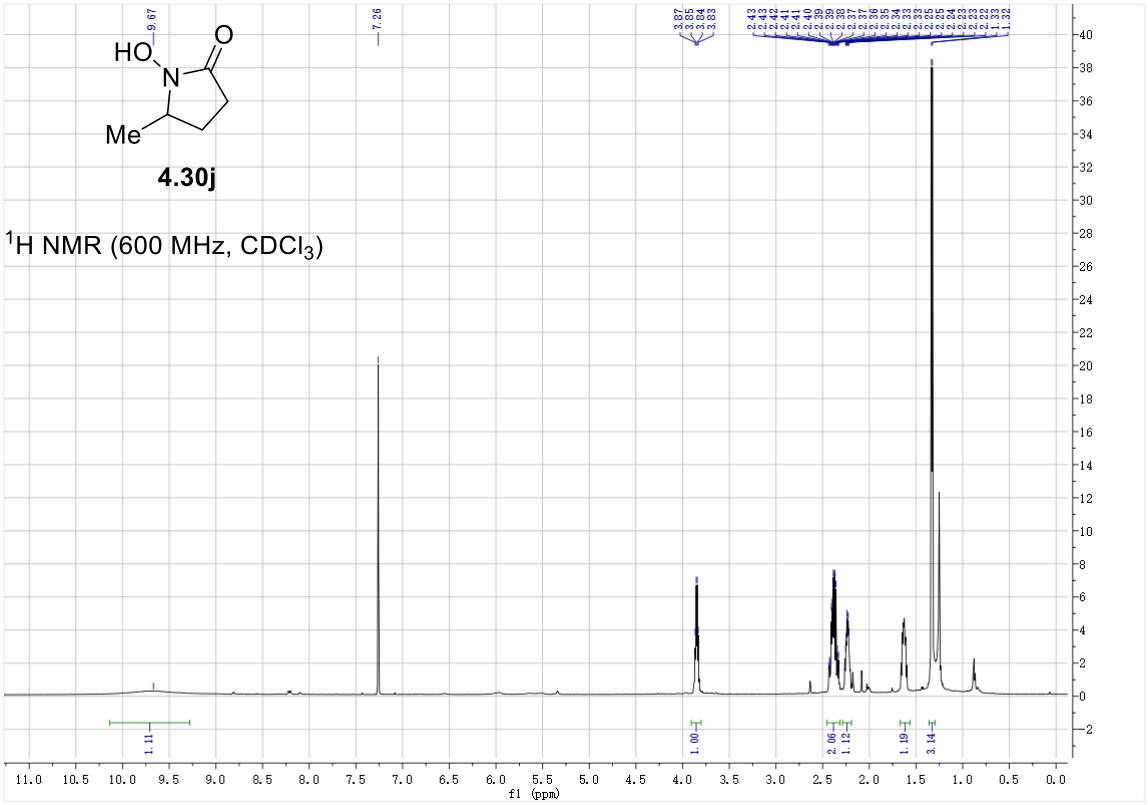
HO
N
O
Me
4.30j
1H NMR (600 MHz, CDCl3)
f1 (ppm)

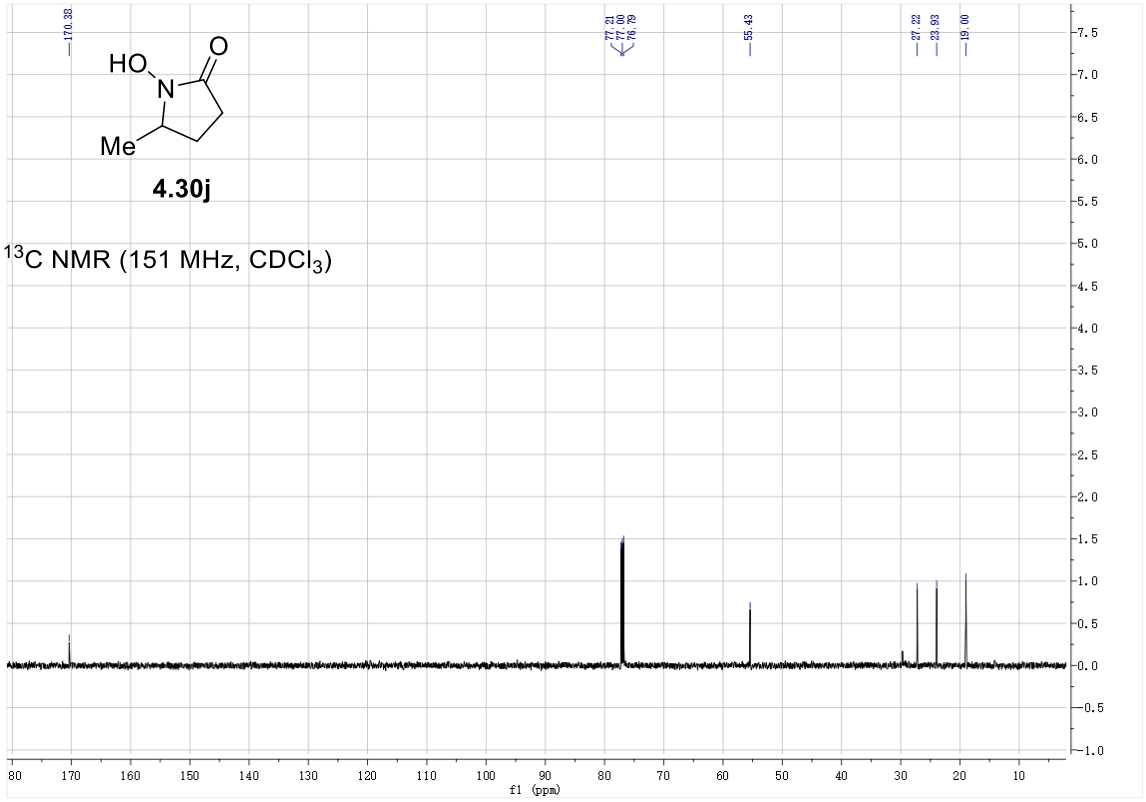
HO
N
O
Me
4.30j
13C NMR (151 MHz, CDCl3)
f1 (ppm)

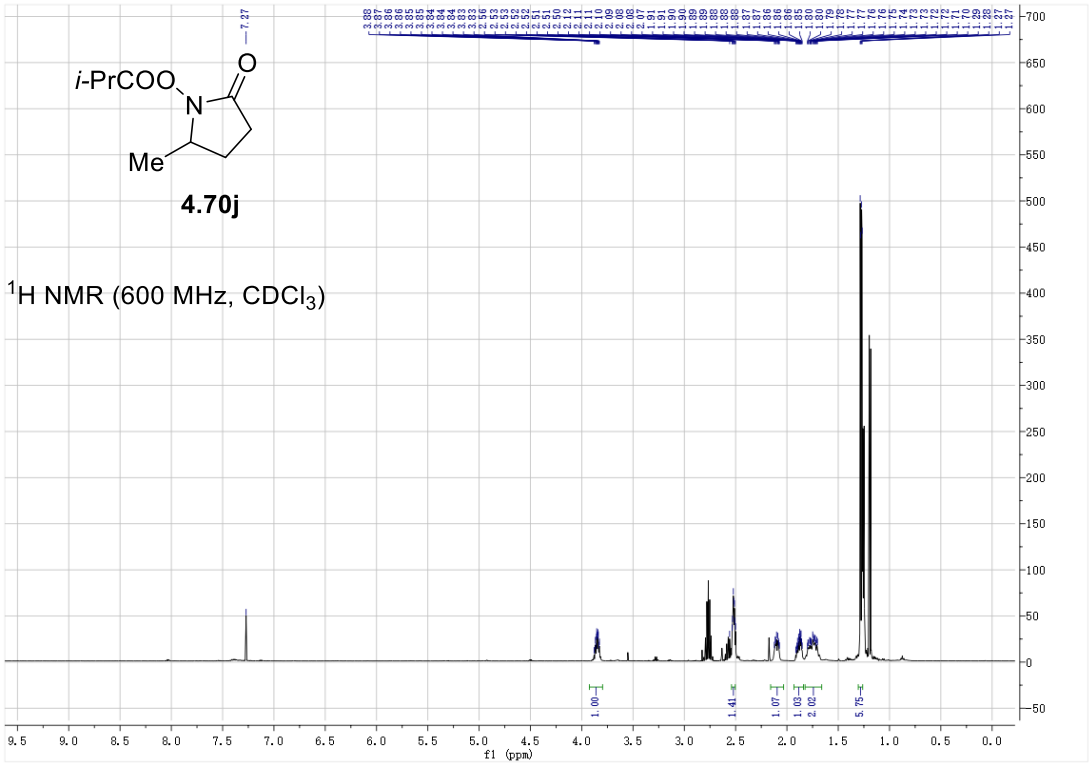
i-PrCOO
N
O
Me
4.70j
1H NMR (600 MHz, CDCl3)
f1 (ppm)

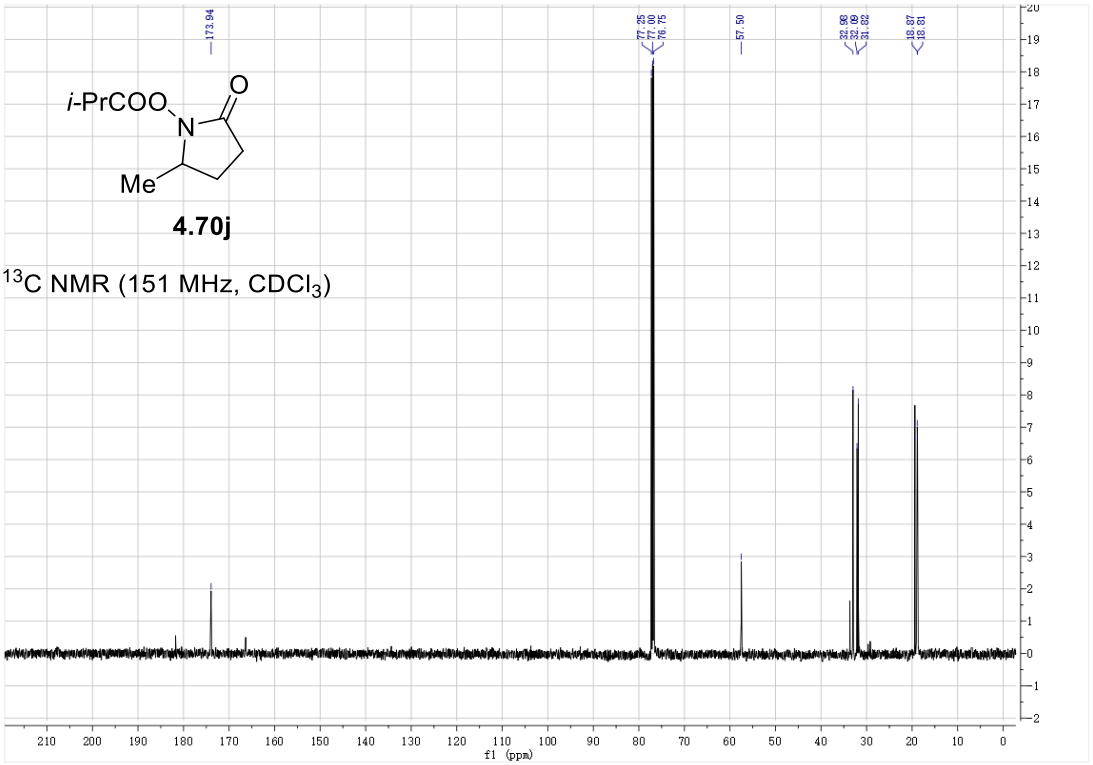
i-PrCOO
N
O
Me
4.70j
13C NMR (151 MHz, CDCl3)
f1 (ppm)

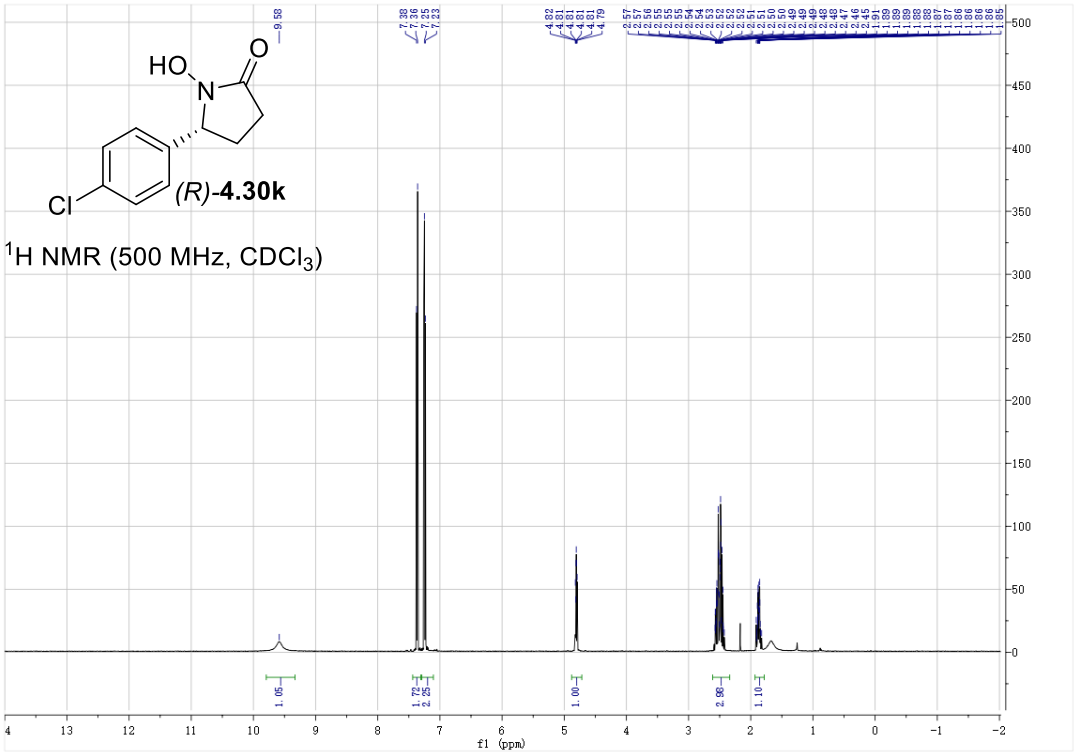
HO
N
O
Cl
(R)-4.30k
^{1}H NMR (500 MHz, CDCl$_3$)
f1 (ppm)

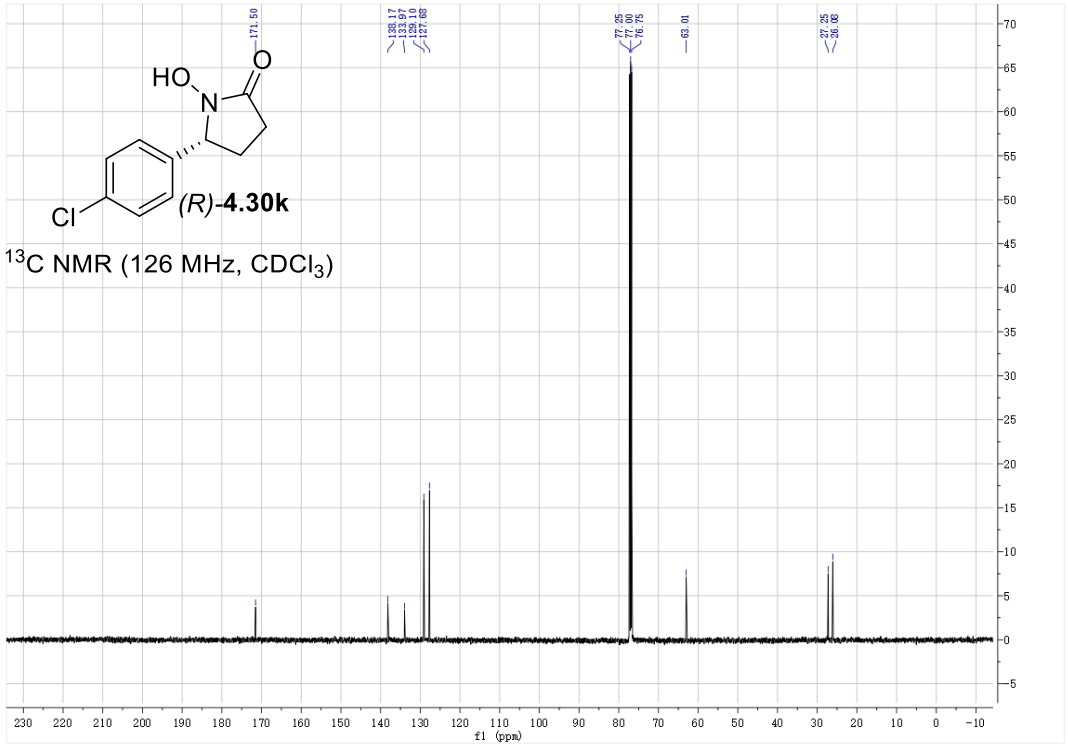
HO
N
O
Cl
(R)-4.30k
^{13}C NMR (126 MHz, CDCl$_3$)
f1 (ppm)

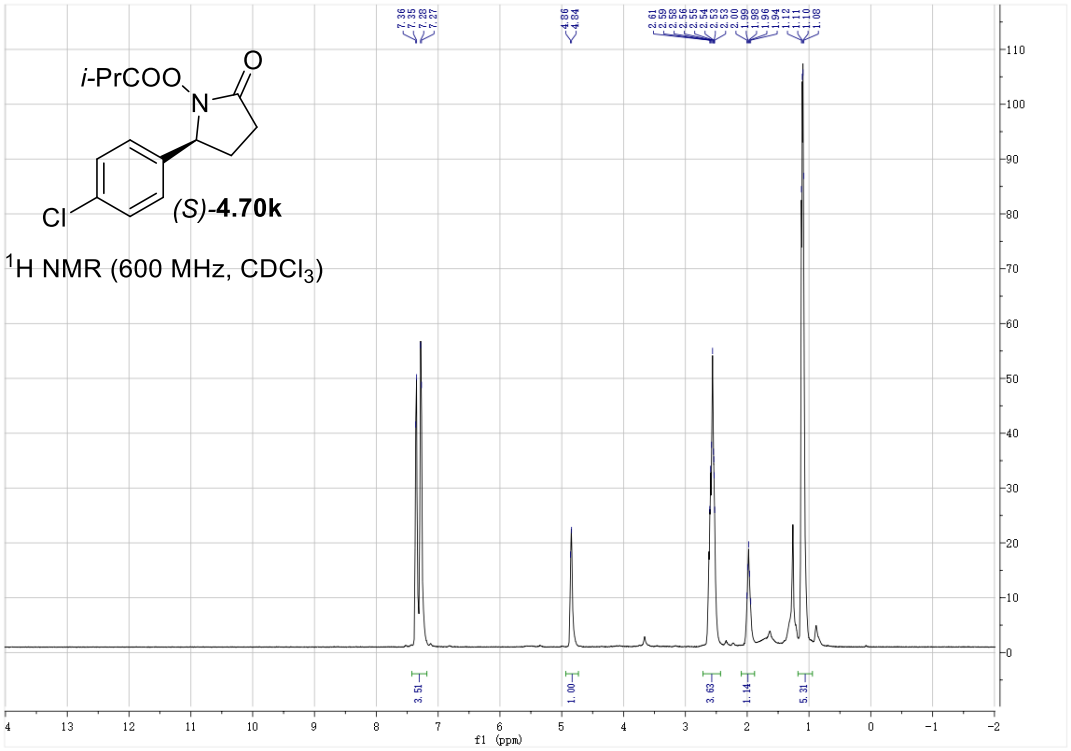
i-PrCOO
N
O
Cl
(S)-4.70k
1H NMR (600 MHz, CDCl3)
f1 (ppm)

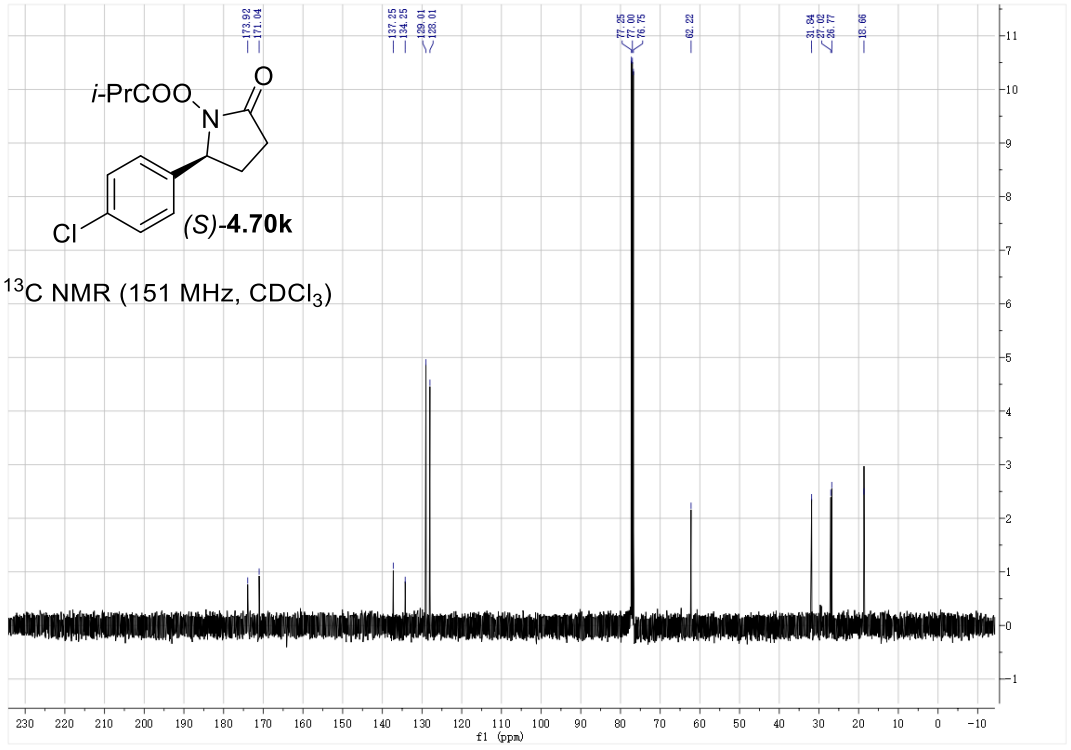
i-PrCOO
N
O
Cl
(S)-4.70k
13C NMR (151 MHz, CDCl3)
f1 (ppm)

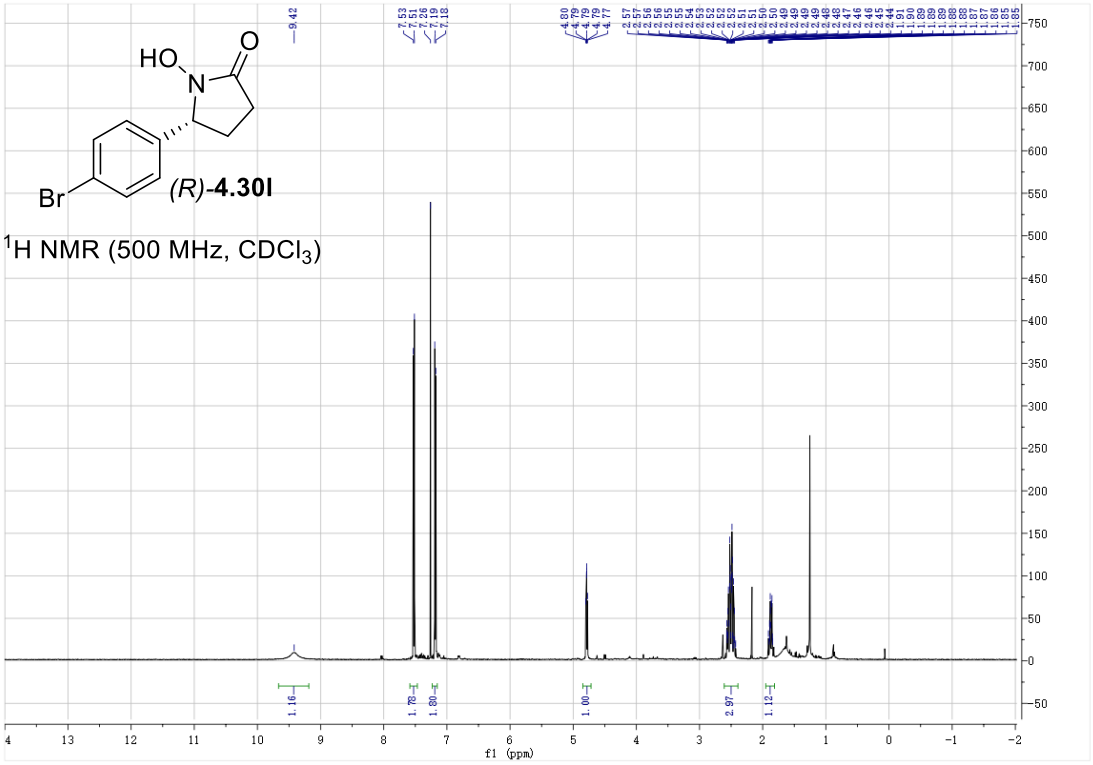
HO
N
O
Br
(R)-4.30l
1H NMR (500 MHz, CDCl3)
f1 (ppm)

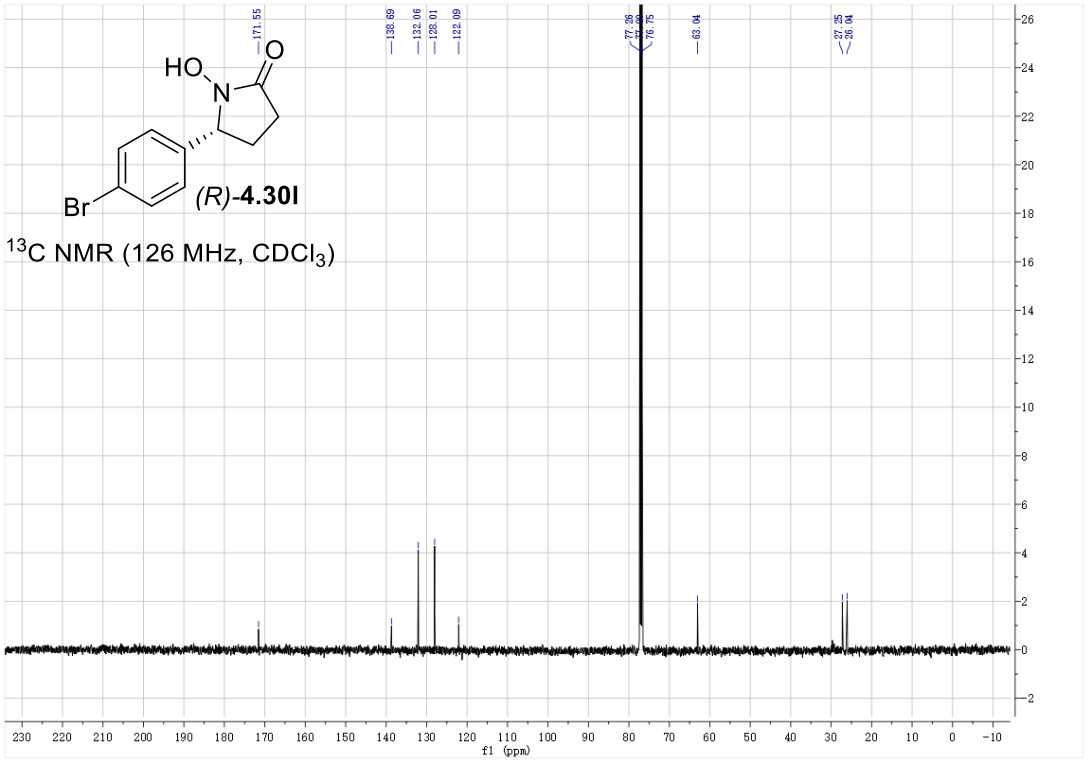
HO
N
O
Br
(R)-4.30l
13C NMR (126 MHz, CDCl3)
f1 (ppm)

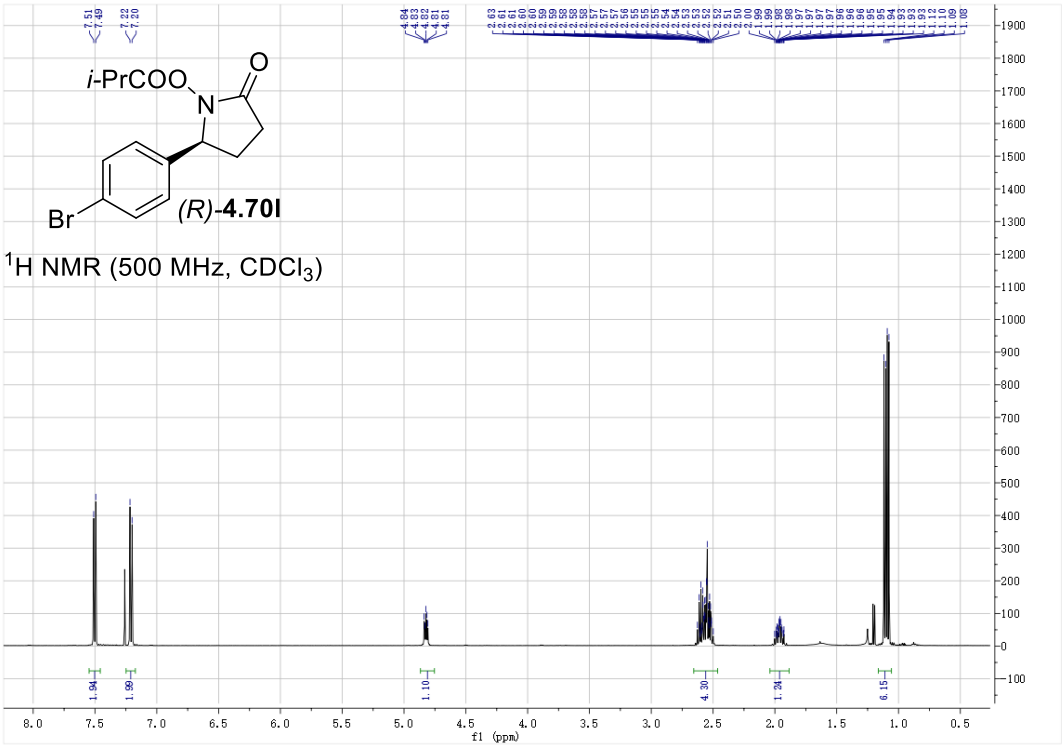
i-PrCOO
N
O
Br
(R)-4.70l
1H NMR (500 MHz, CDCl3)
f1 (ppm)

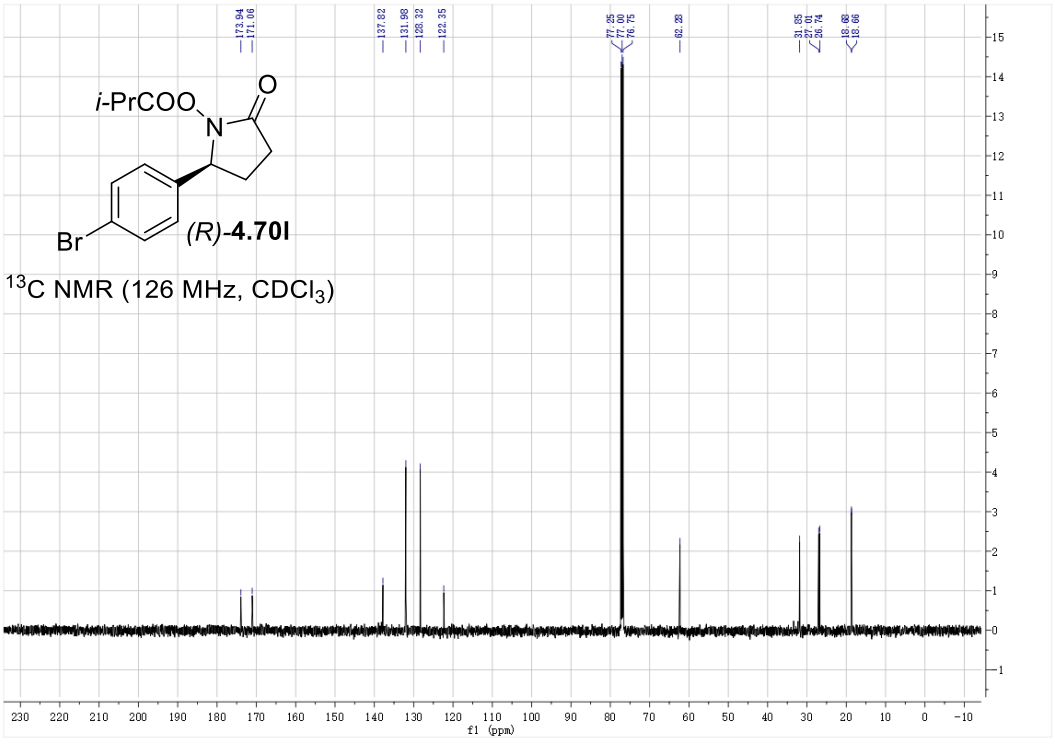
i-PrCOO
N
O
Br
(R)-4.70l
13C NMR (126 MHz, CDCl3)
f1 (ppm)

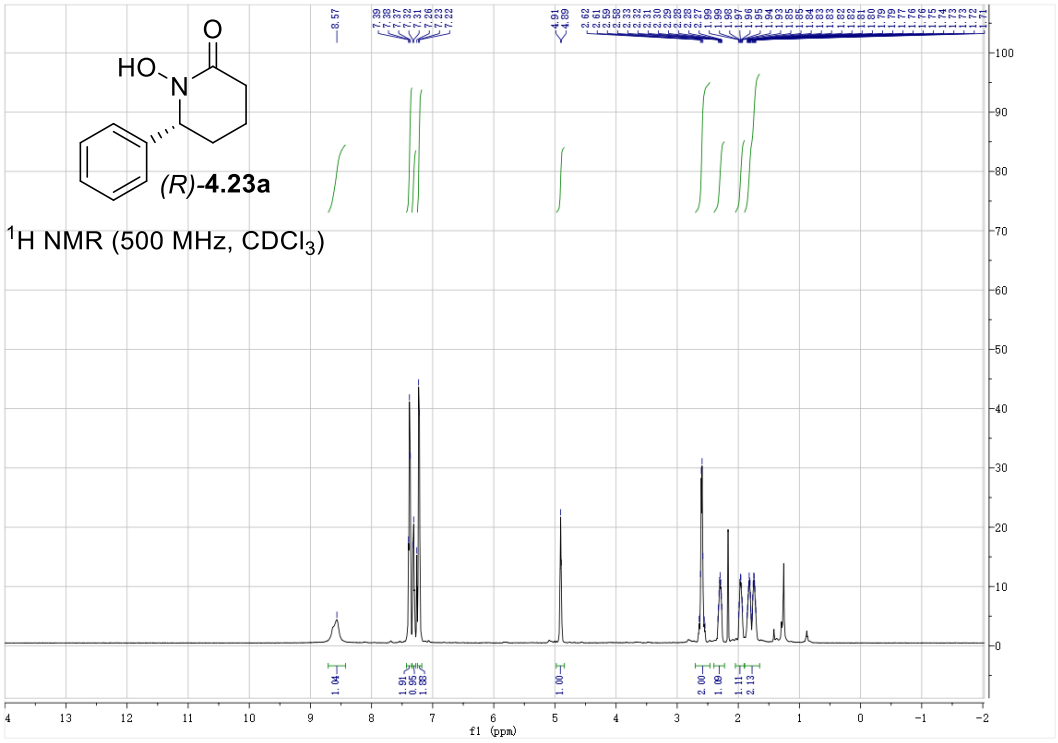
HO
N
O
(R)-4.23a
1H NMR (500 MHz, CDCl3)
f1 (ppm)

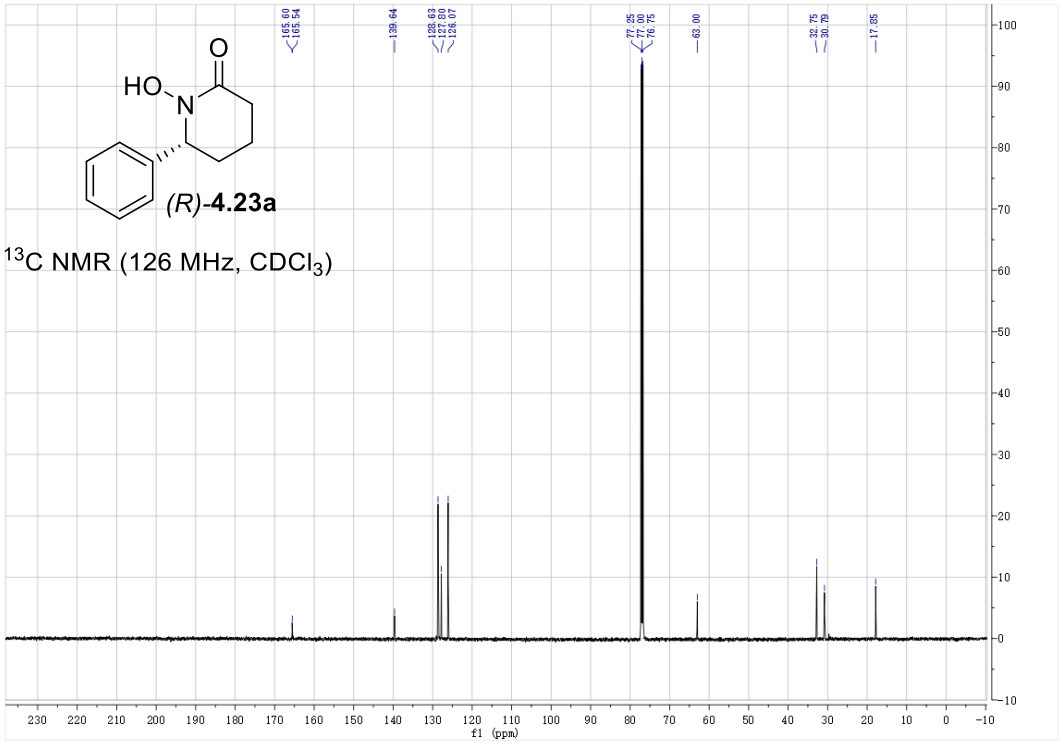
HO
N
O
(R)-4.23a
13C NMR (126 MHz, CDCl3)
f1 (ppm)

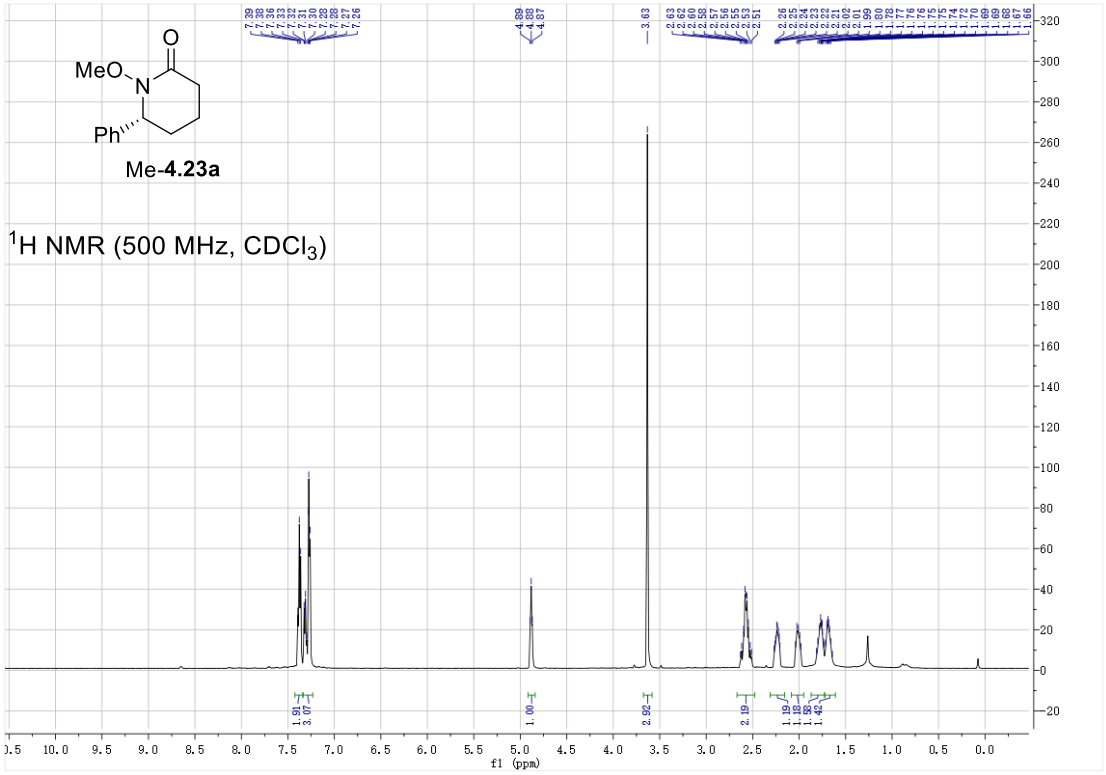
MeO
N
O
Ph
Me-4.23a
1H NMR (500 MHz, CDCl3)
f1 (ppm)

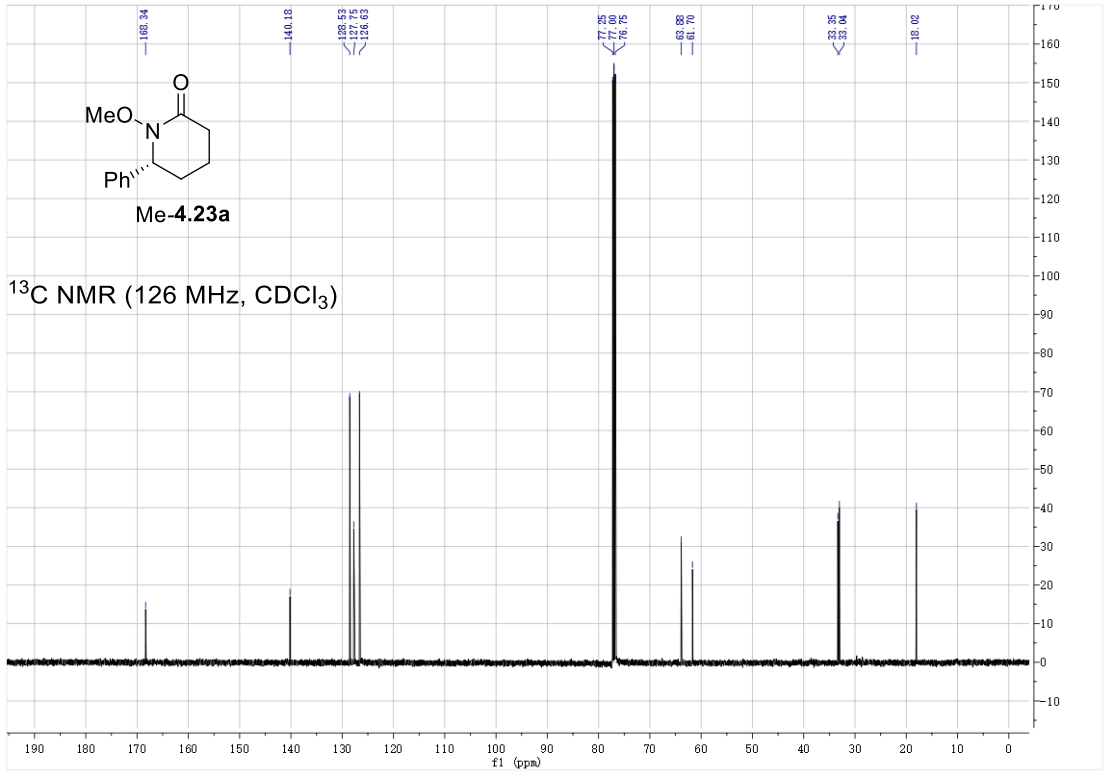
MeO
N
O
Ph
Me-4.23a
13C NMR (126 MHz, CDCl3)
f1 (ppm)

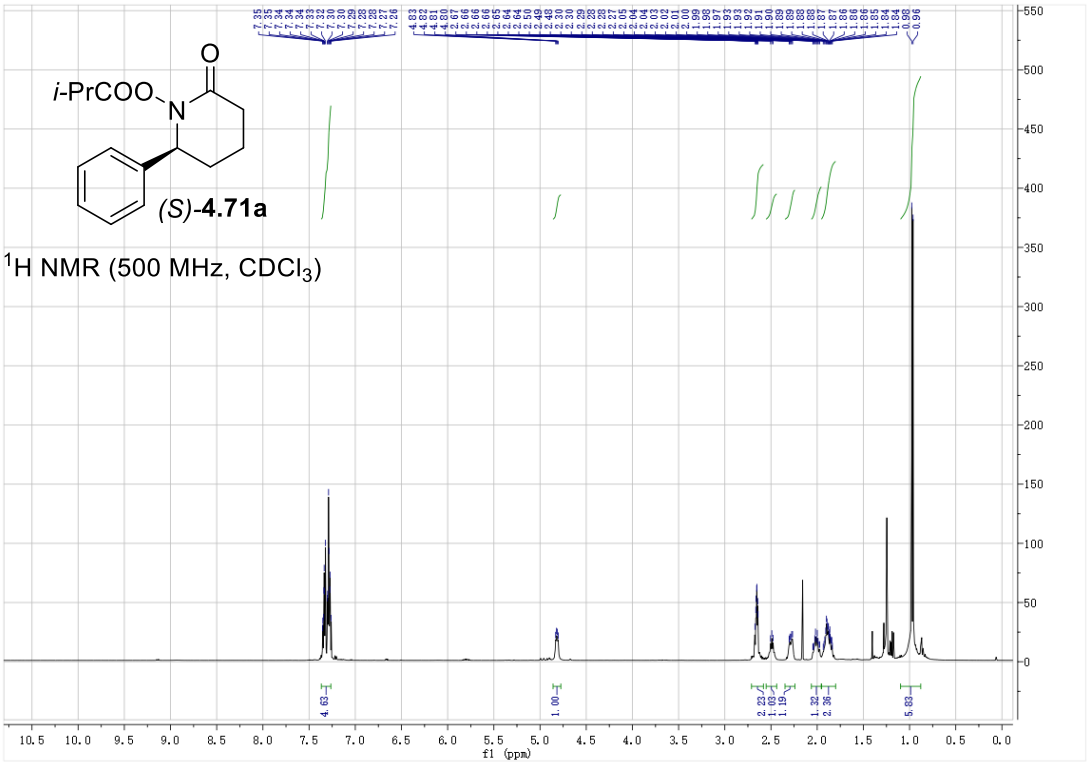
i-PrCOO
N
O
(S)-4.71a
1H NMR (500 MHz, CDCl3)
f1 (ppm)

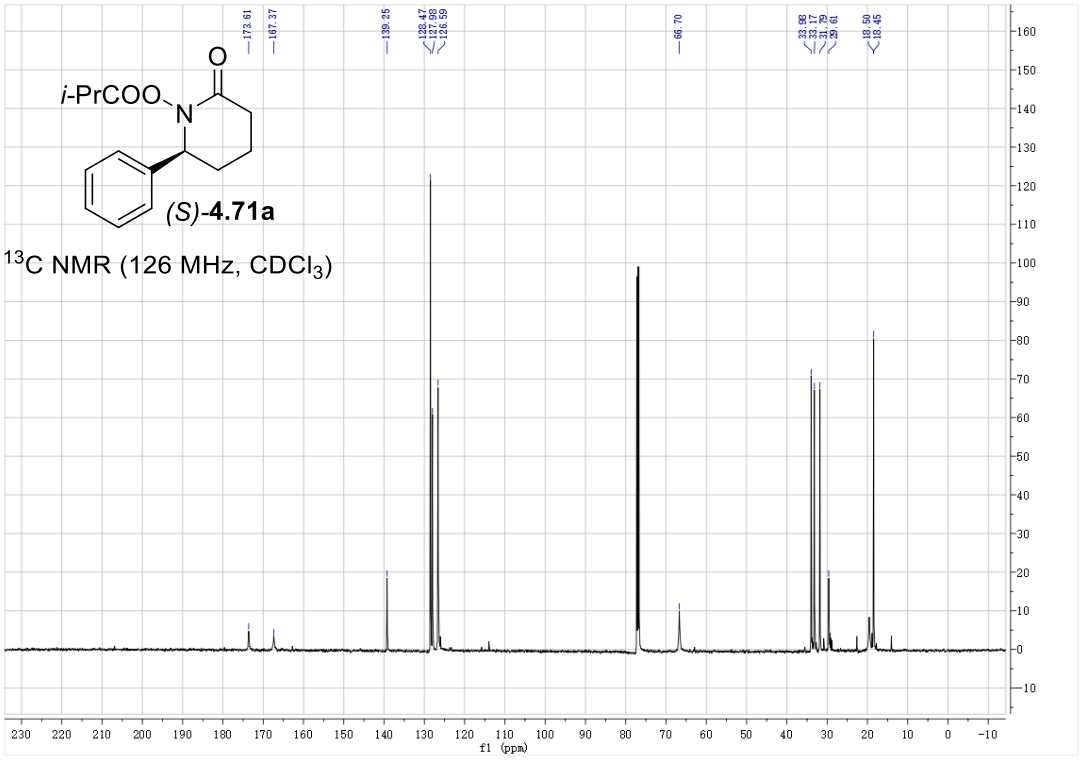
i-PrCOO
N
O
(S)-4.71a
13C NMR (126 MHz, CDCl3)
f1 (ppm)

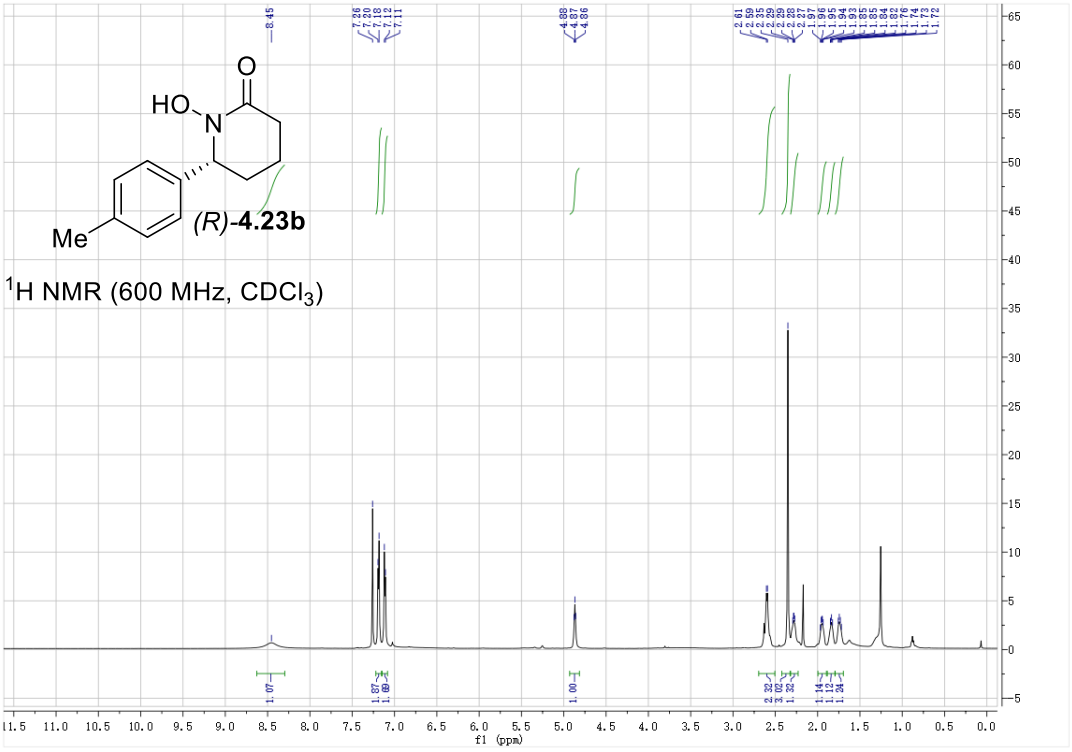
HO
N
O
Me
(R)-4.23b
1H NMR (600 MHz, CDCl3)
f1 (ppm)

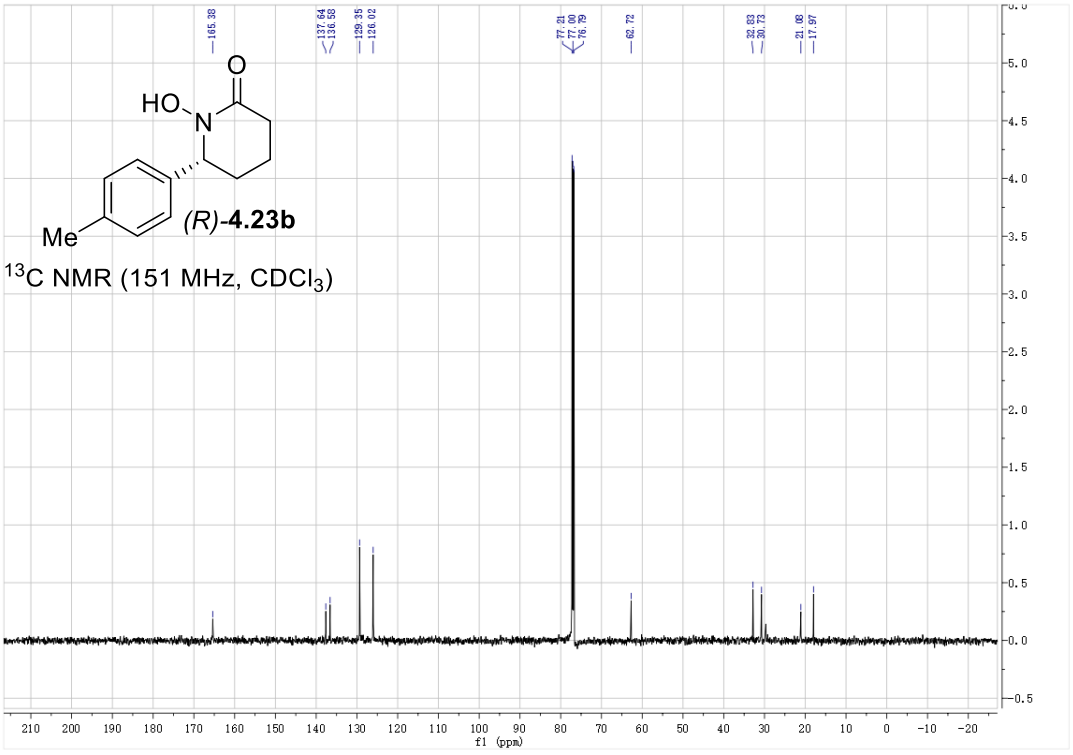
HO
N
O
Me
(R)-4.23b
13C NMR (151 MHz, CDCl3)
f1 (ppm)

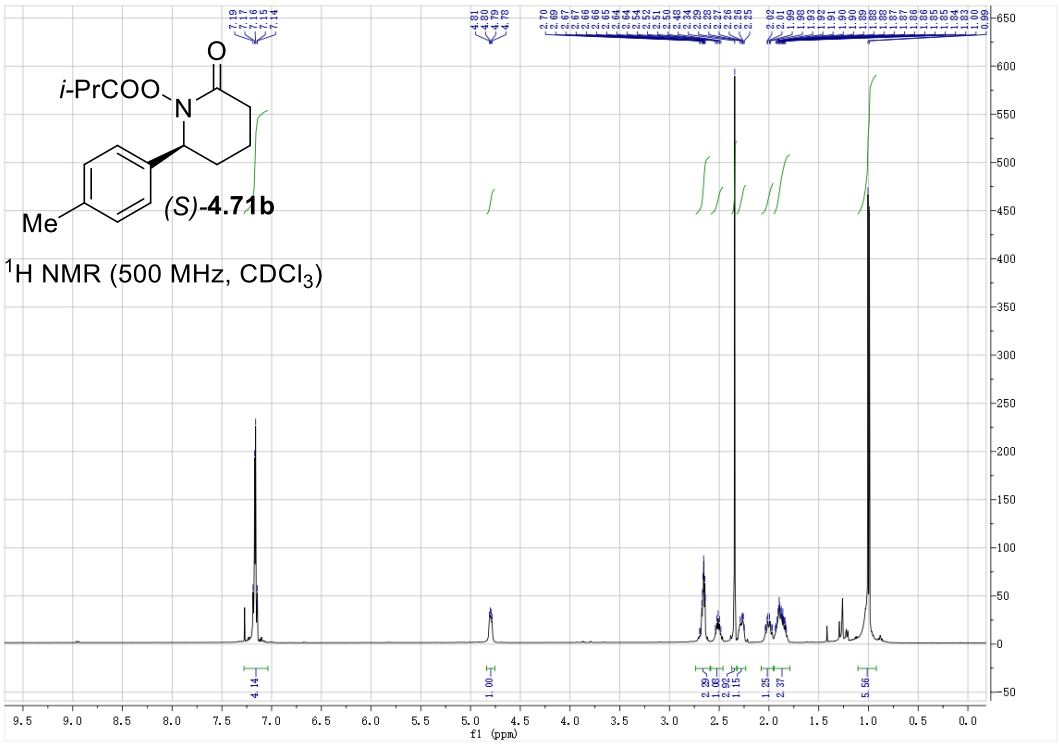
i-PrCOO
N
O
Me
(S)-4.71b
1H NMR (500 MHz, CDCl3)
f1 (ppm)

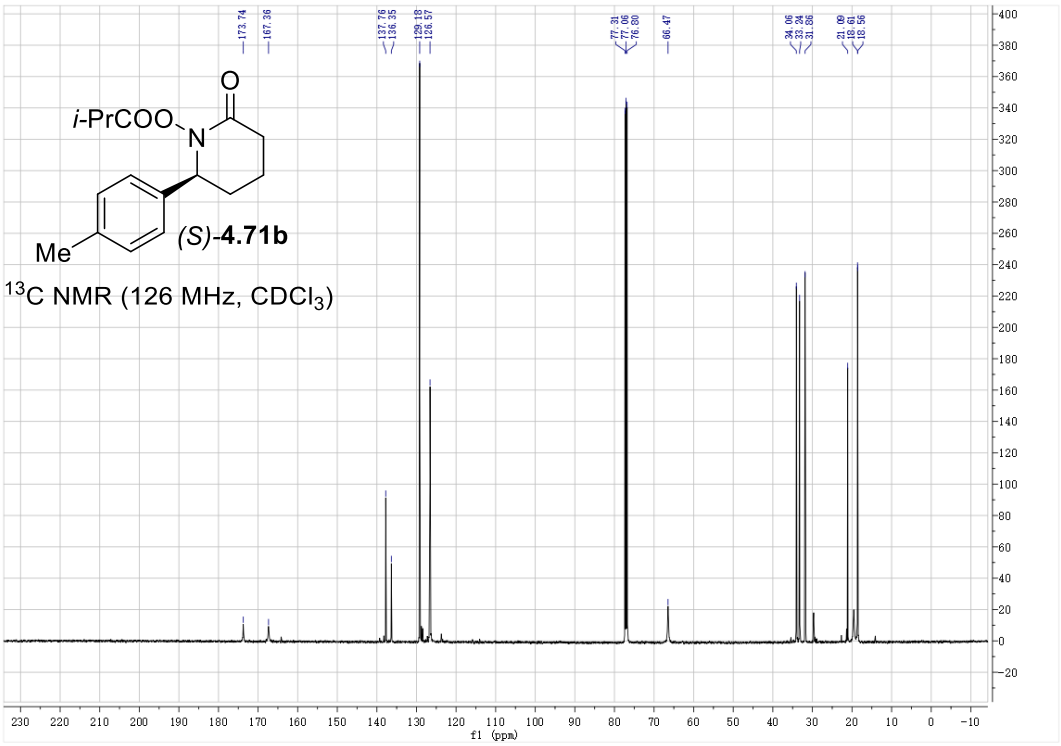
i-PrCOO
N
O
Me
(S)-4.71b
13C NMR (126 MHz, CDCl3)
f1 (ppm)

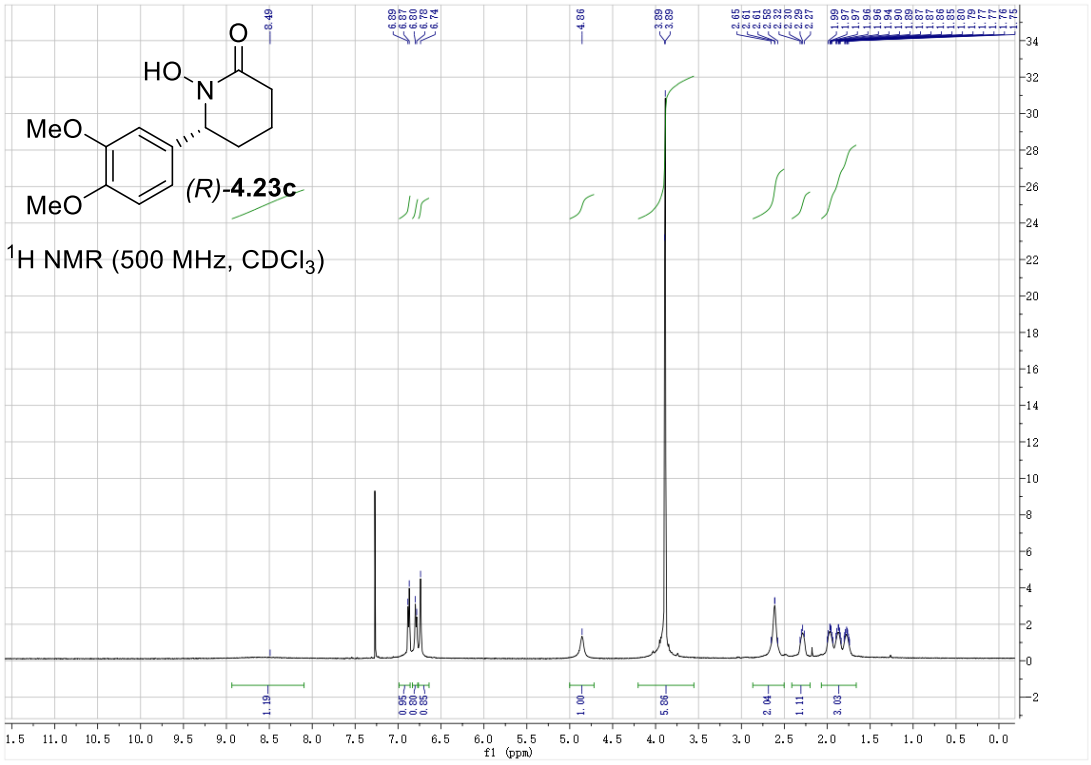
HO
N
O
MeO
MeO
(R)-4.23c
1H NMR (500 MHz, CDCl3)
f1 (ppm)

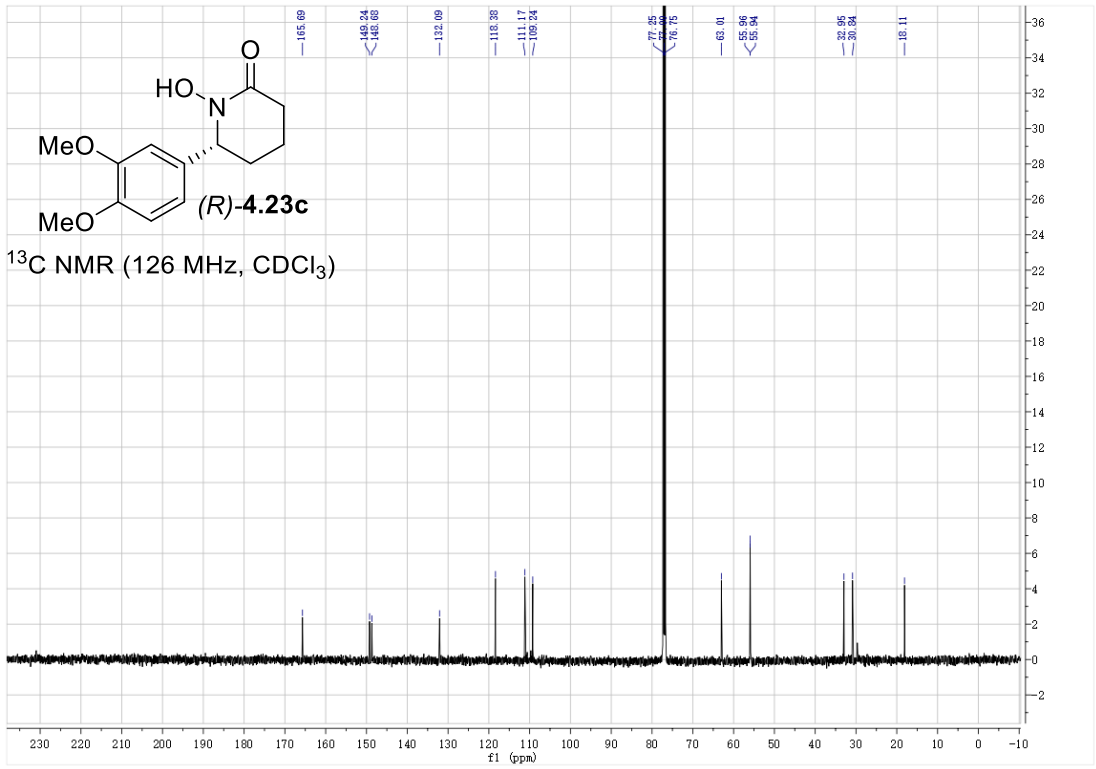
HO
N
O
MeO
MeO
(R)-4.23c
13C NMR (126 MHz, CDCl3)
f1 (ppm)

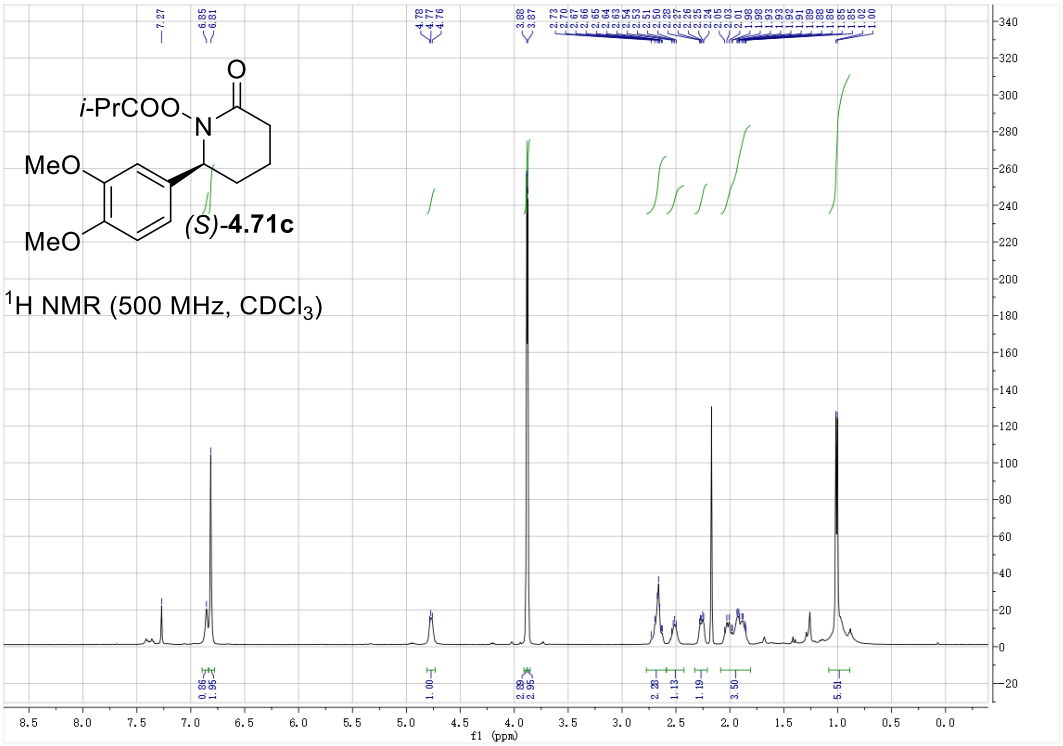
i-PrCOO
N
O
MeO
MeO
(S)-4.71c
1H NMR (500 MHz, CDCl3)
f1 (ppm)

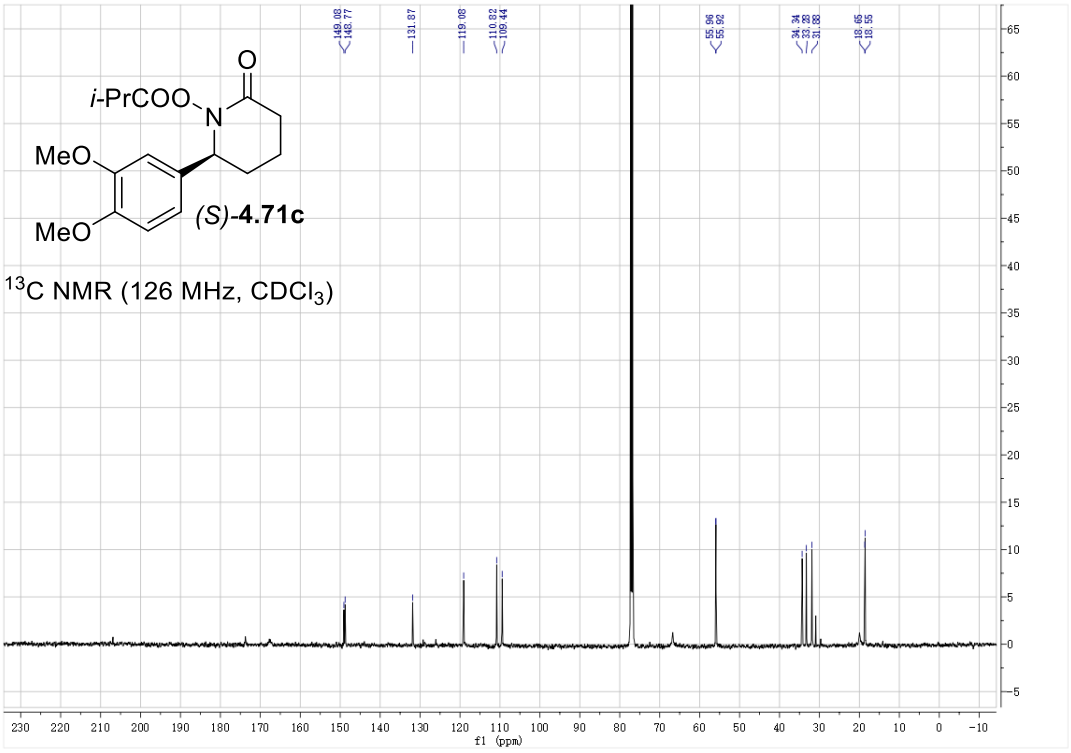
i-PrCOO
N
O
MeO
MeO
(S)-4.71c
13C NMR (126 MHz, CDCl3)
f1 (ppm)

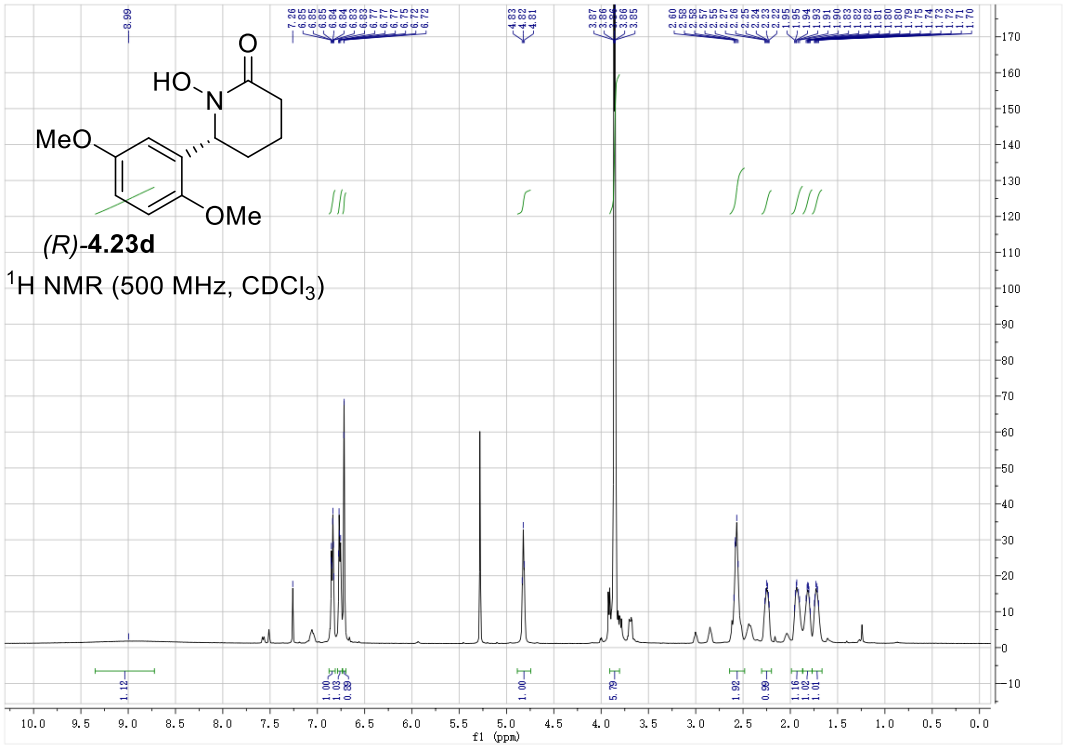
HO
N
O
MeO
OMe
(R)-4.23d
1H NMR (500 MHz, CDCl3)
f1 (ppm)

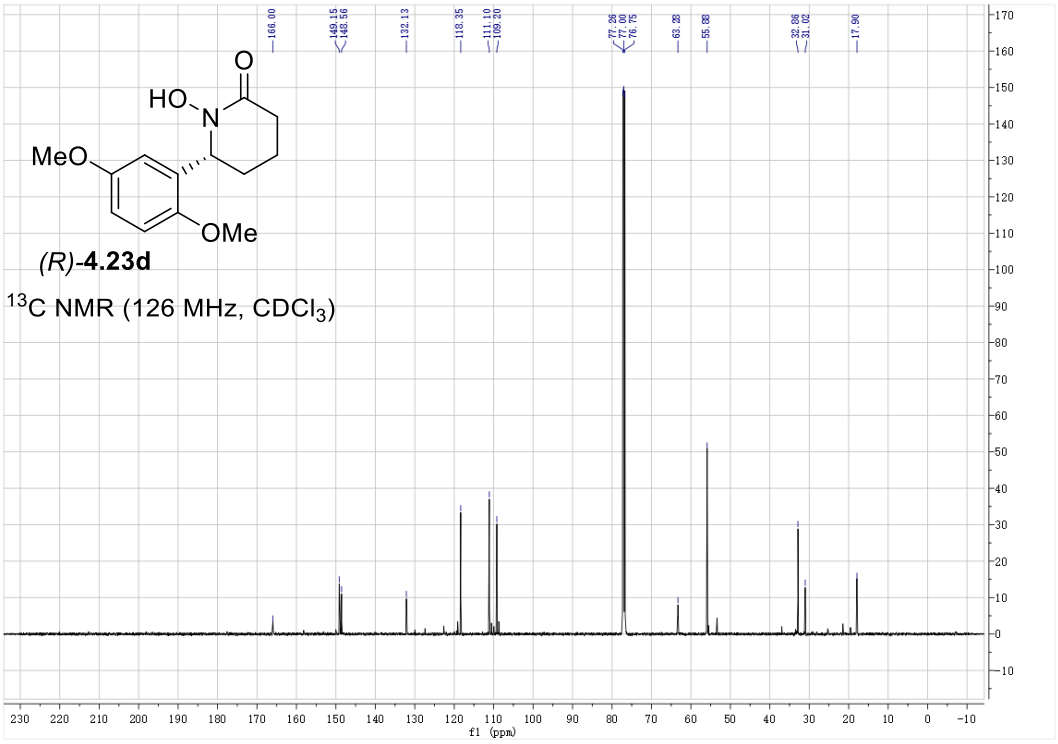
HO
N
O
MeO
OMe
(R)-4.23d
13C NMR (126 MHz, CDCl3)
f1 (ppm)

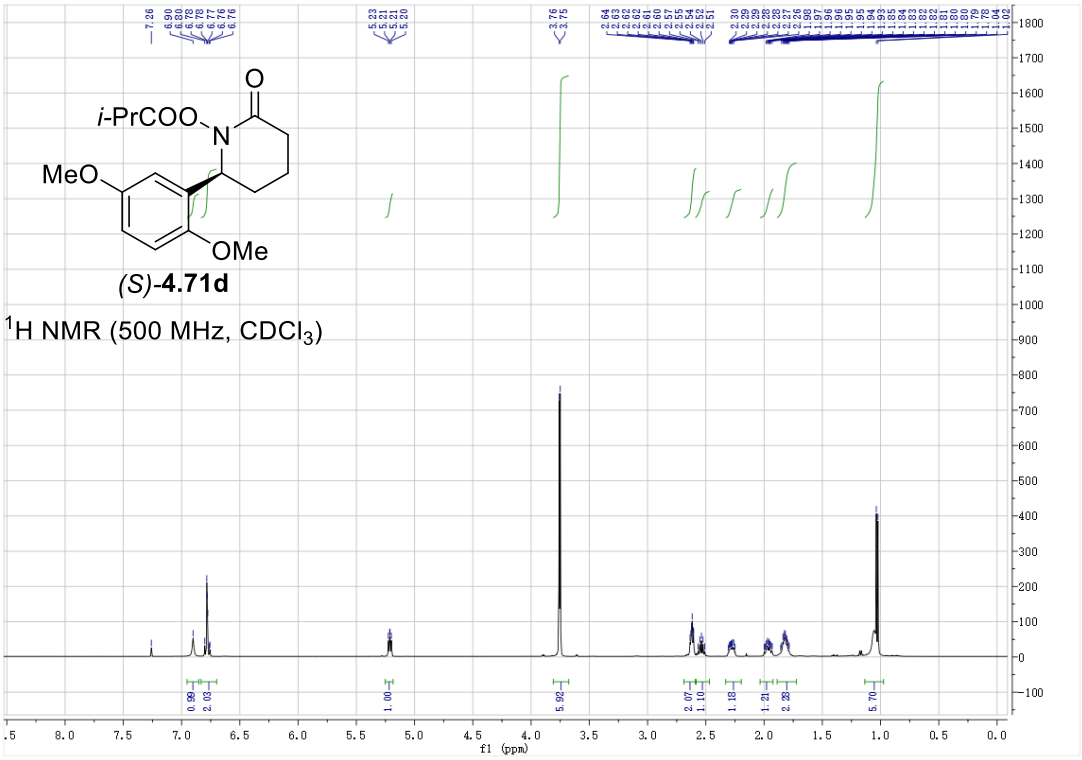
i-PrCOO
N
O
MeO
OMe
(S)-4.71d
1H NMR (500 MHz, CDCl3)
f1 (ppm)

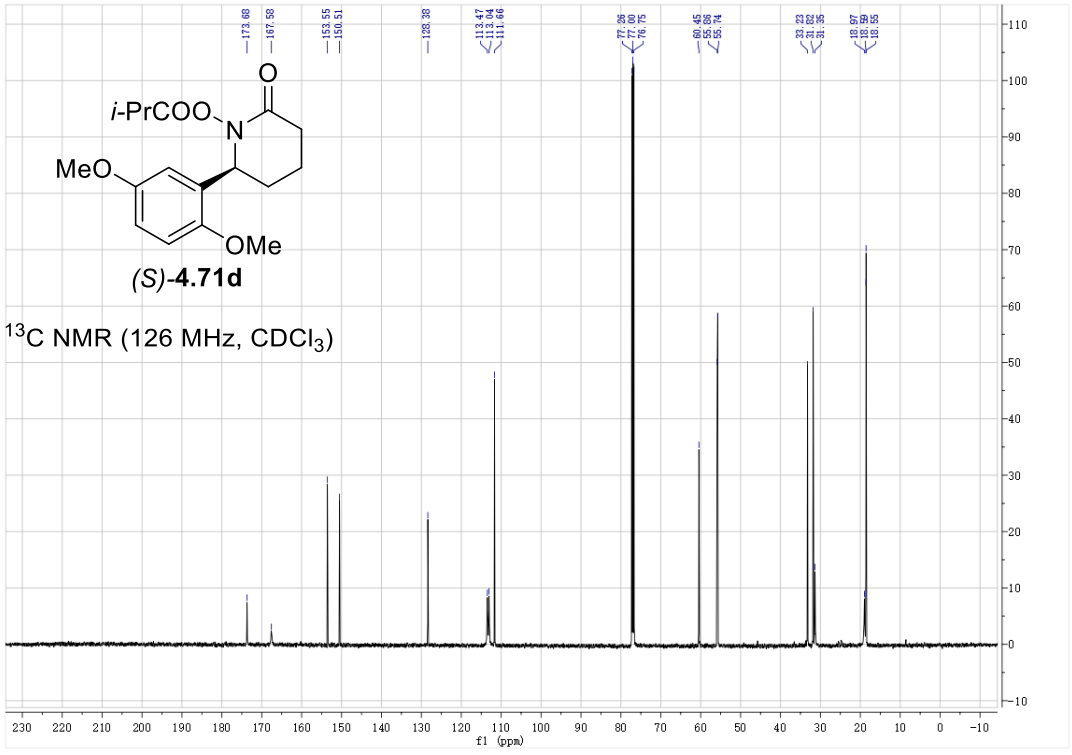
i-PrCOO
N
O
MeO
OMe
(S)-4.71d
13C NMR (126 MHz, CDCl3)
f1 (ppm)

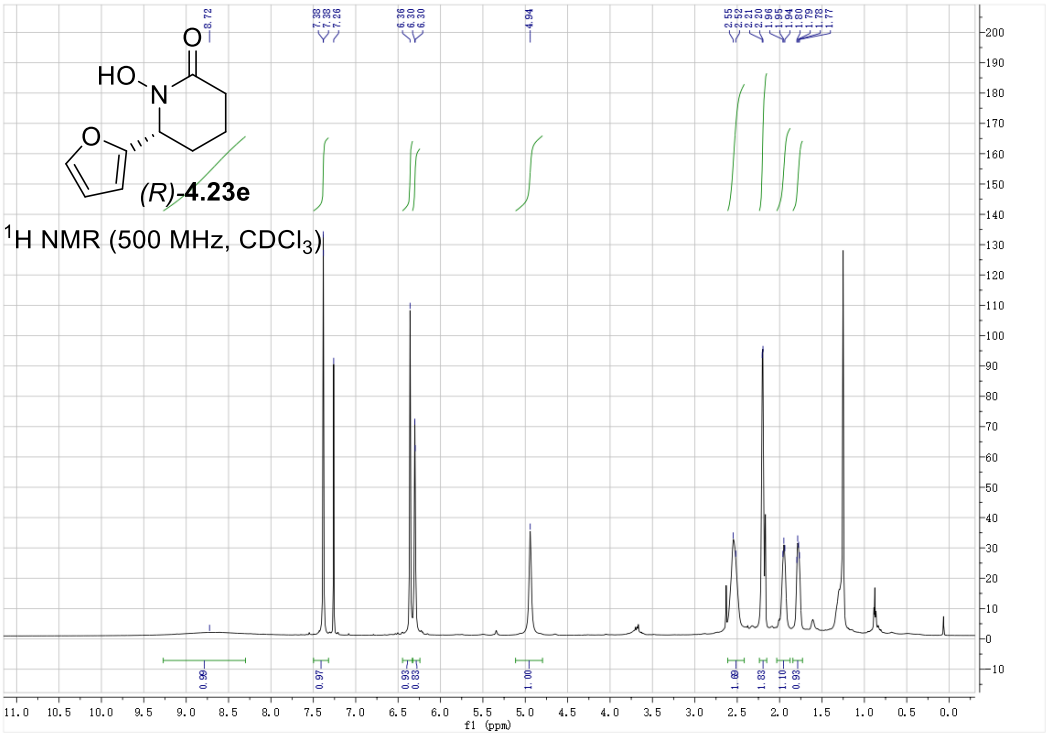
(R)-4.23e
1H NMR (500 MHz, CDCl3)
f1 (ppm)

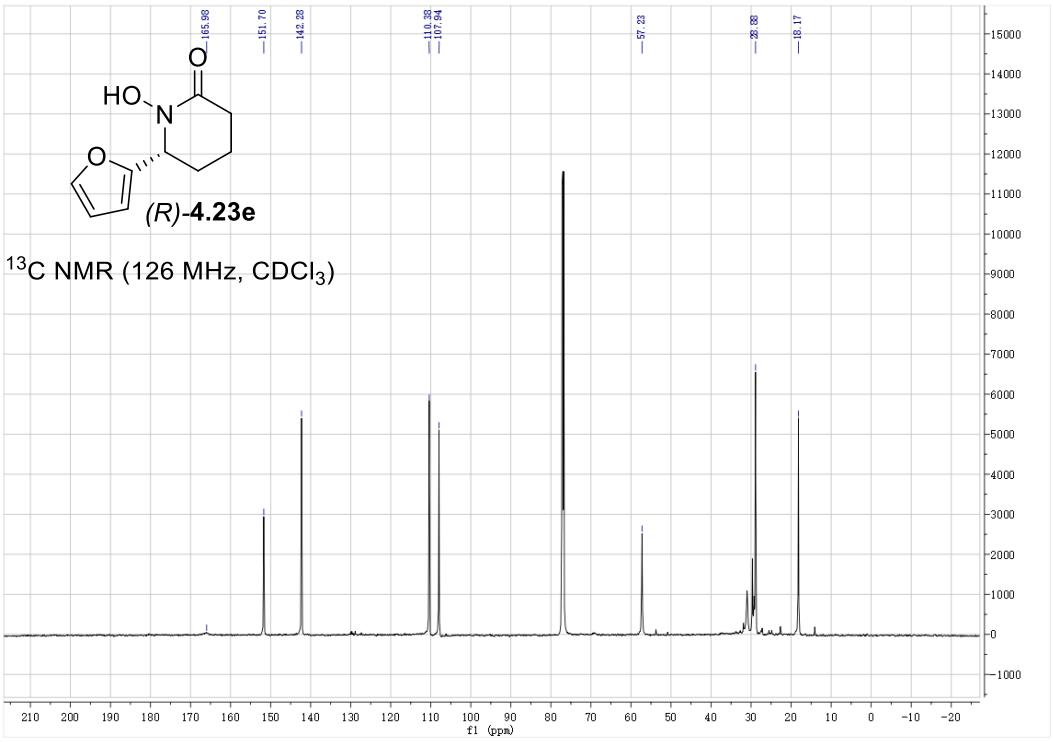
(R)-4.23e
13C NMR (126 MHz, CDCl3)
f1 (ppm)

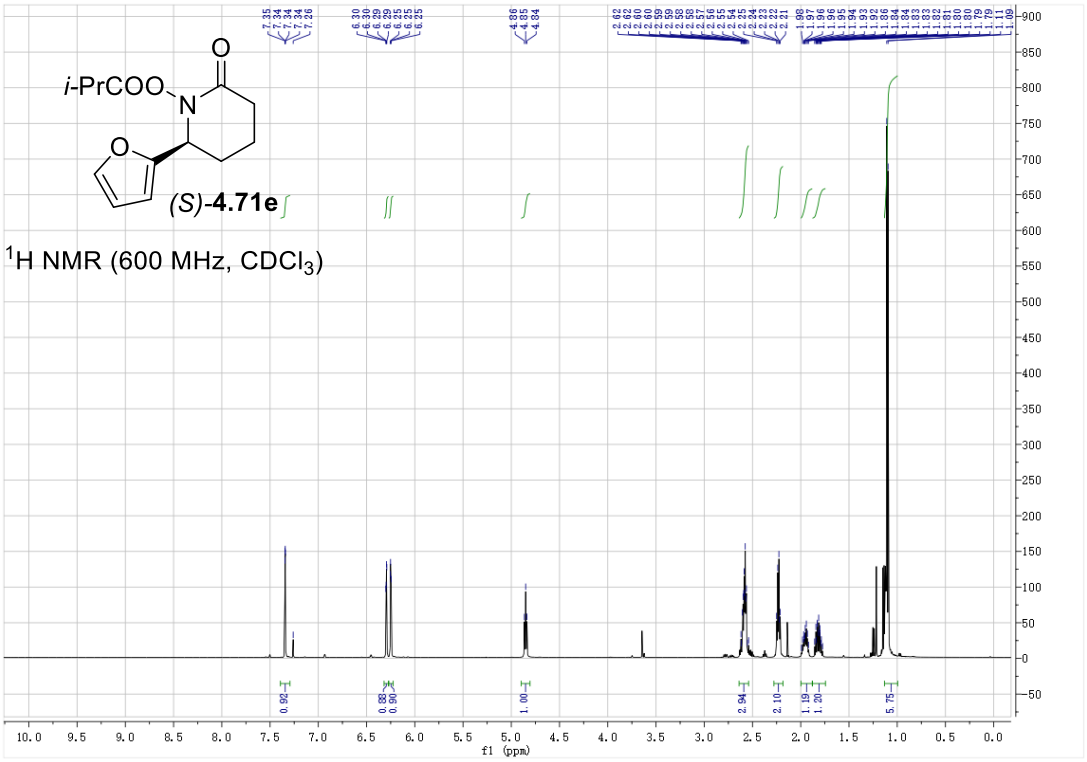
i-PrCOO
N
O
O
(S)-4.71e
1H NMR (600 MHz, CDCl3)
f1 (ppm)

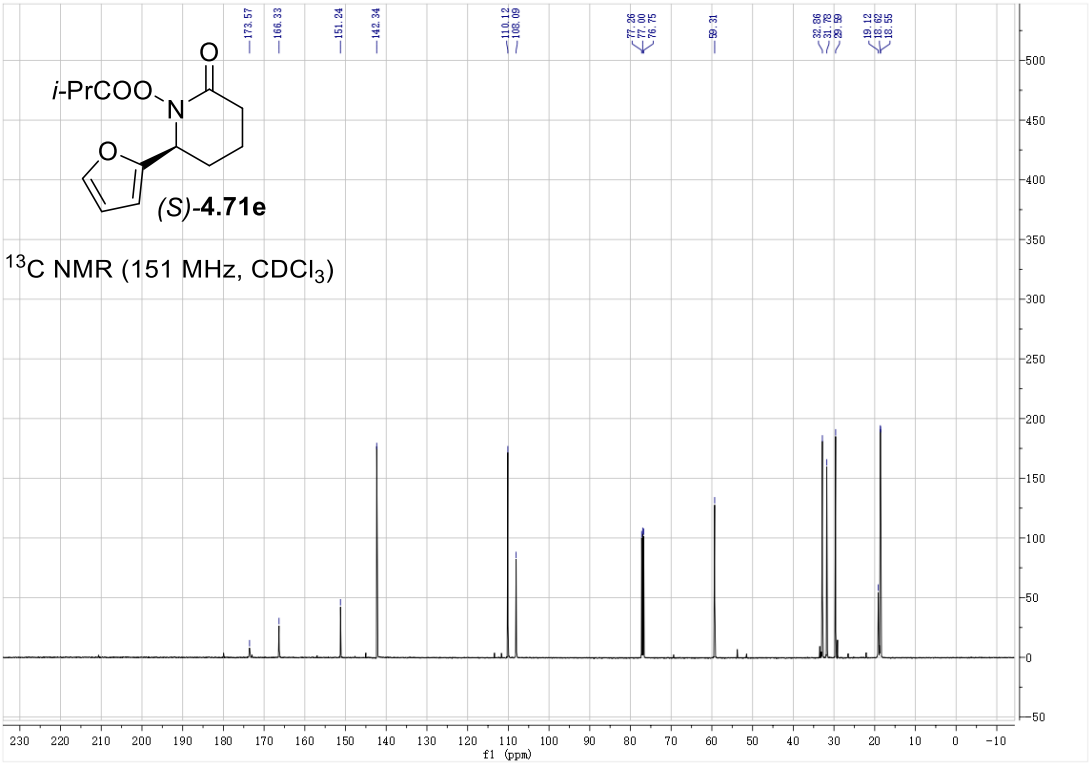
i-PrCOO
N
O
O
(S)-4.71e
13C NMR (151 MHz, CDCl3)
f1 (ppm)

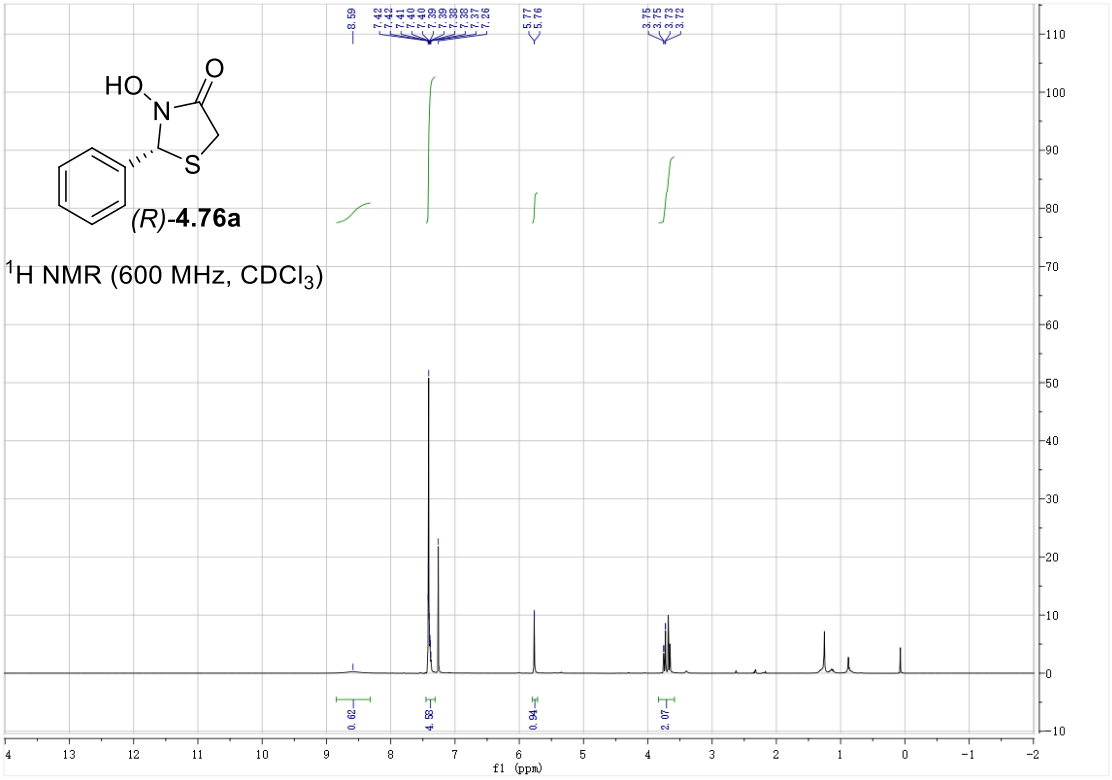
HO
N
O
S
(R)-4.76a
1H NMR (600 MHz, CDCl3)
f1 (ppm)

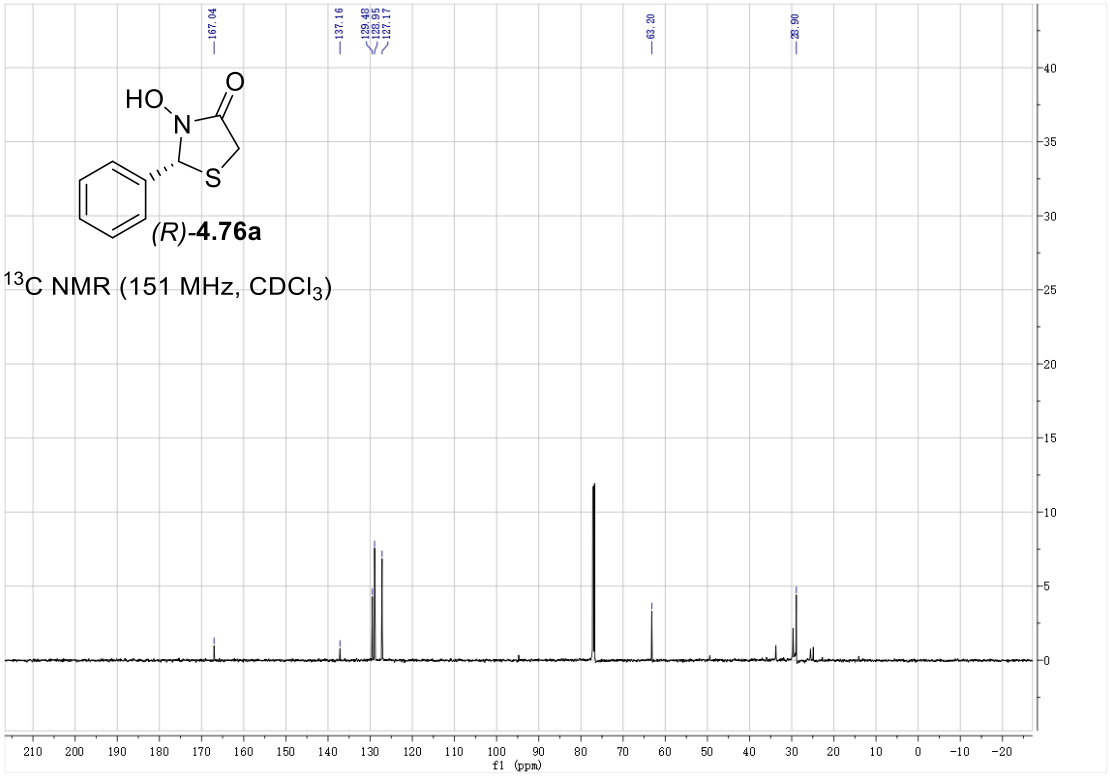
HO
N
O
S
(R)-4.76a
13C NMR (151 MHz, CDCl3)
f1 (ppm)

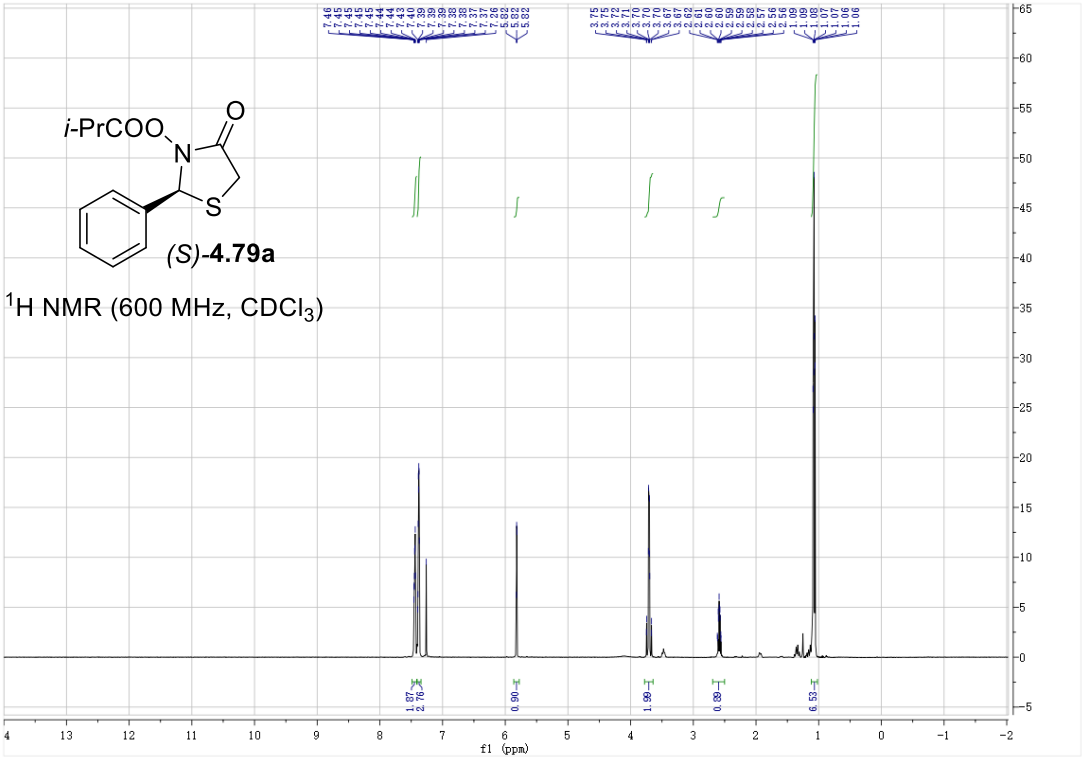
i-PrCOO
N
O
S
(S)-4.79a
1H NMR (600 MHz, CDCl3)
f1 (ppm)

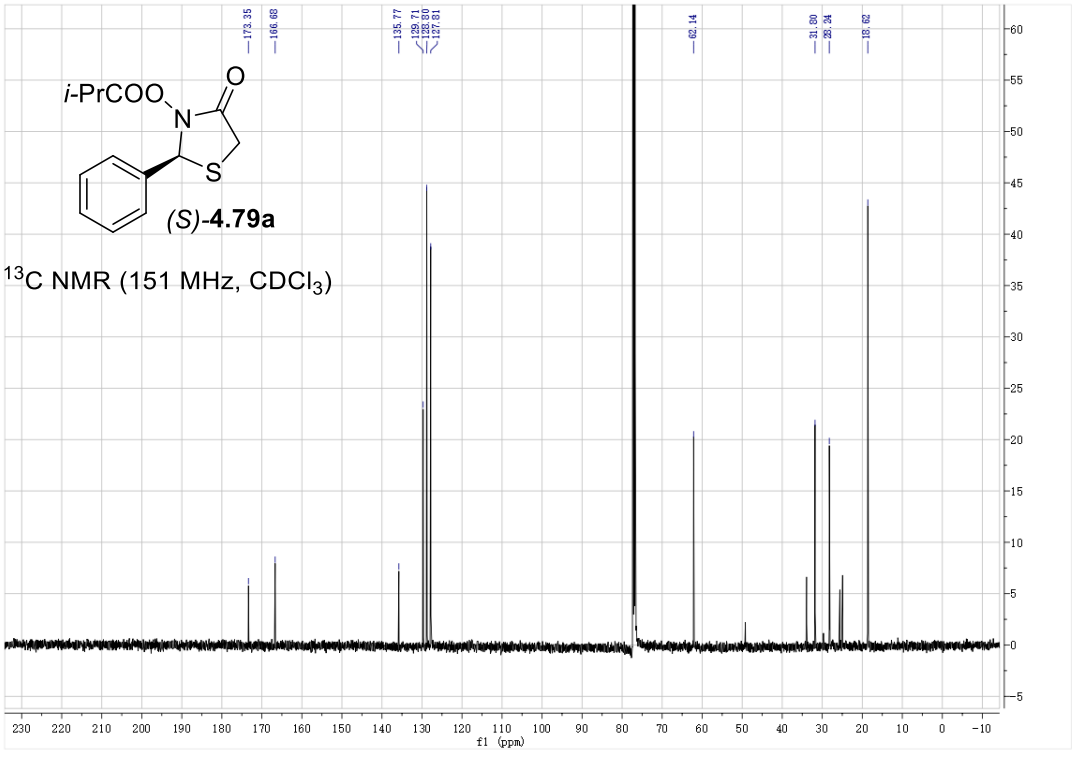
i-PrCOO
N
O
S
(S)-4.79a
13C NMR (151 MHz, CDCl3)
f1 (ppm)

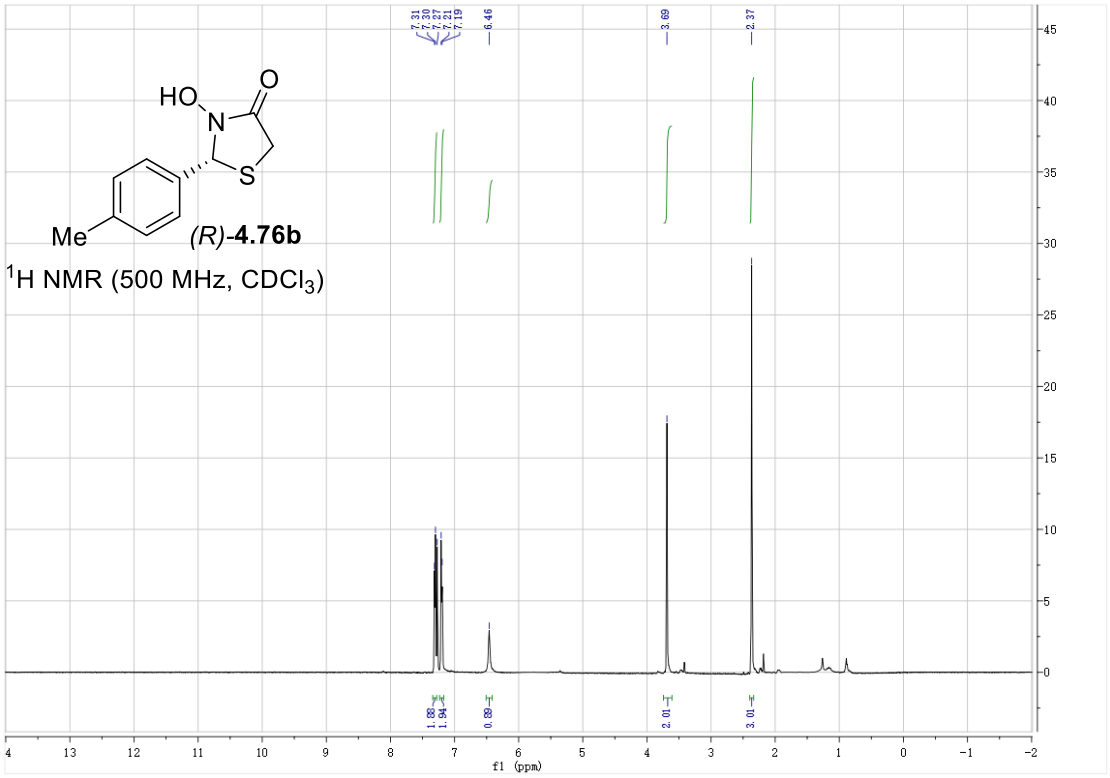
HO
N
O
S
Me
(R)-4.76b
1H NMR (500 MHz, CDCl3)
7.31
7.30
7.27
7.21
7.19
6.46
3.69
2.37
1.88
1.94
0.89
2.01
3.01
f1 (ppm)

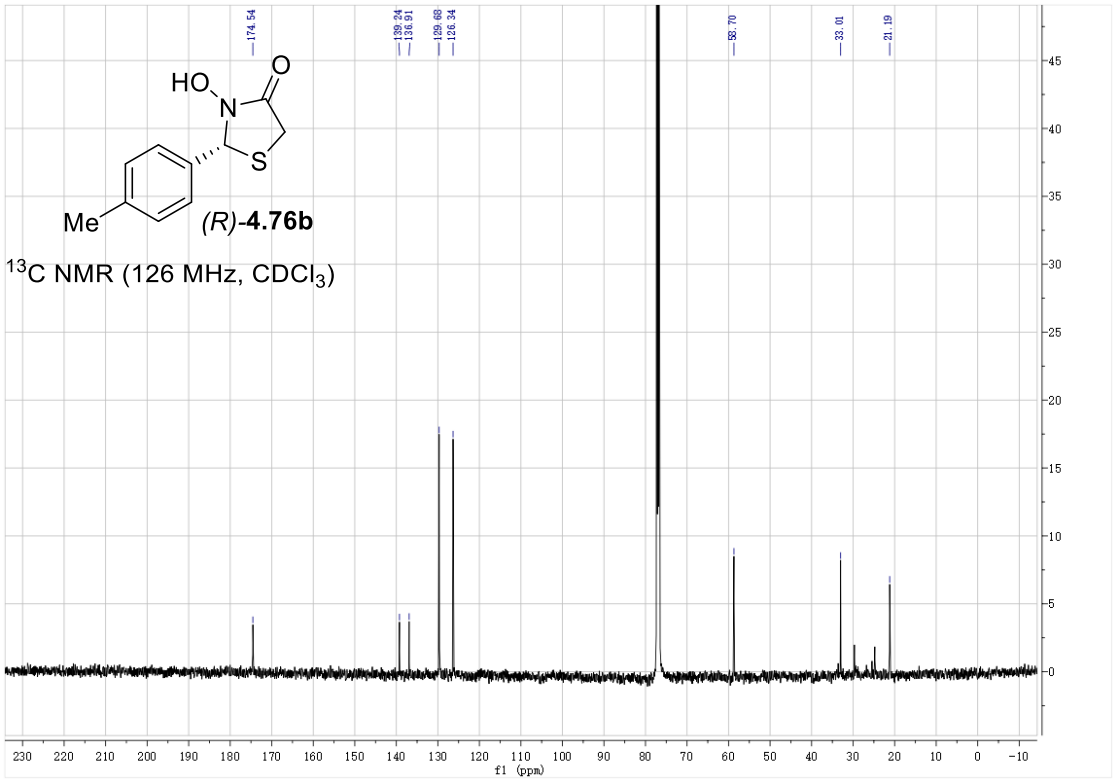
HO
N
O
S
Me
(R)-4.76b
13C NMR (126 MHz, CDCl3)
174.54
139.84
136.91
129.69
126.34
58.70
33.01
21.19
f1 (ppm)

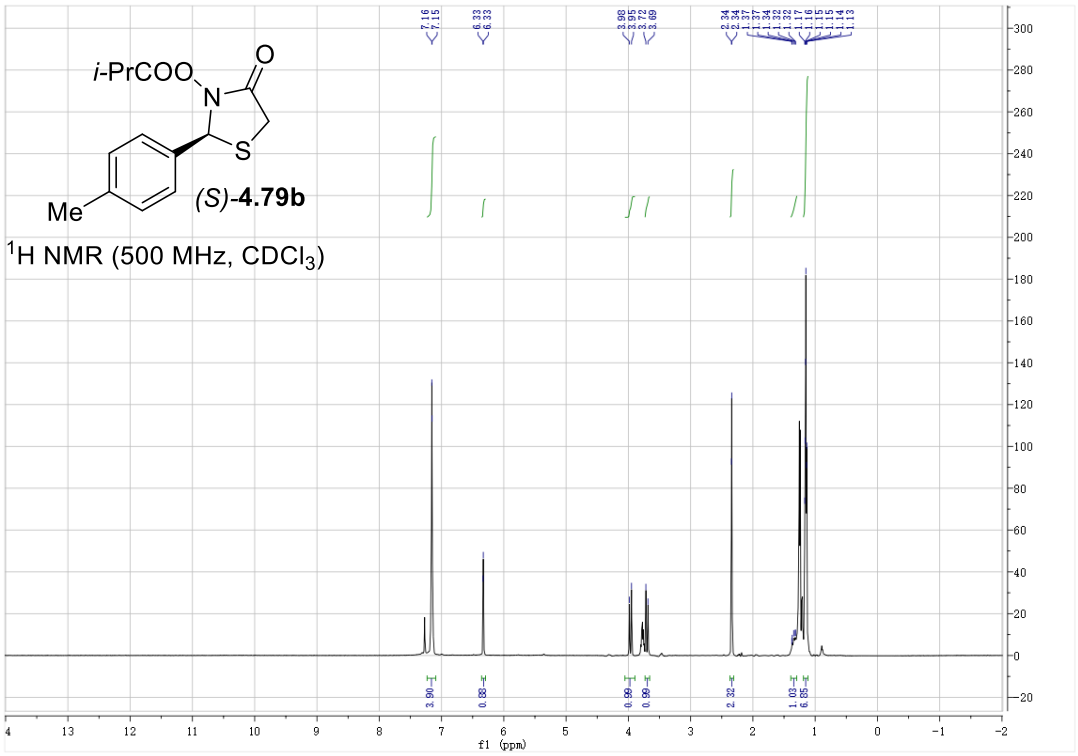
i-PrCOO
N
O
S
Me
(S)-4.79b
1H NMR (500 MHz, CDCl3)
f1 (ppm)

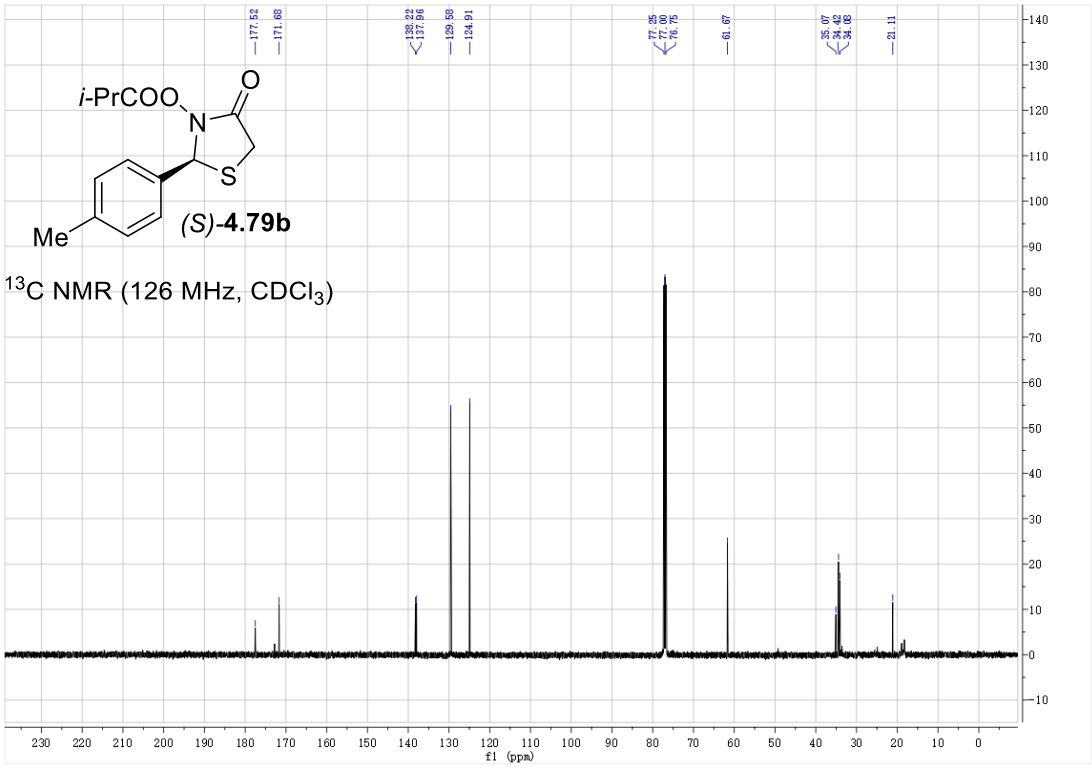
i-PrCOO
N
O
S
Me
(S)-4.79b
13C NMR (126 MHz, CDCl3)
f1 (ppm)

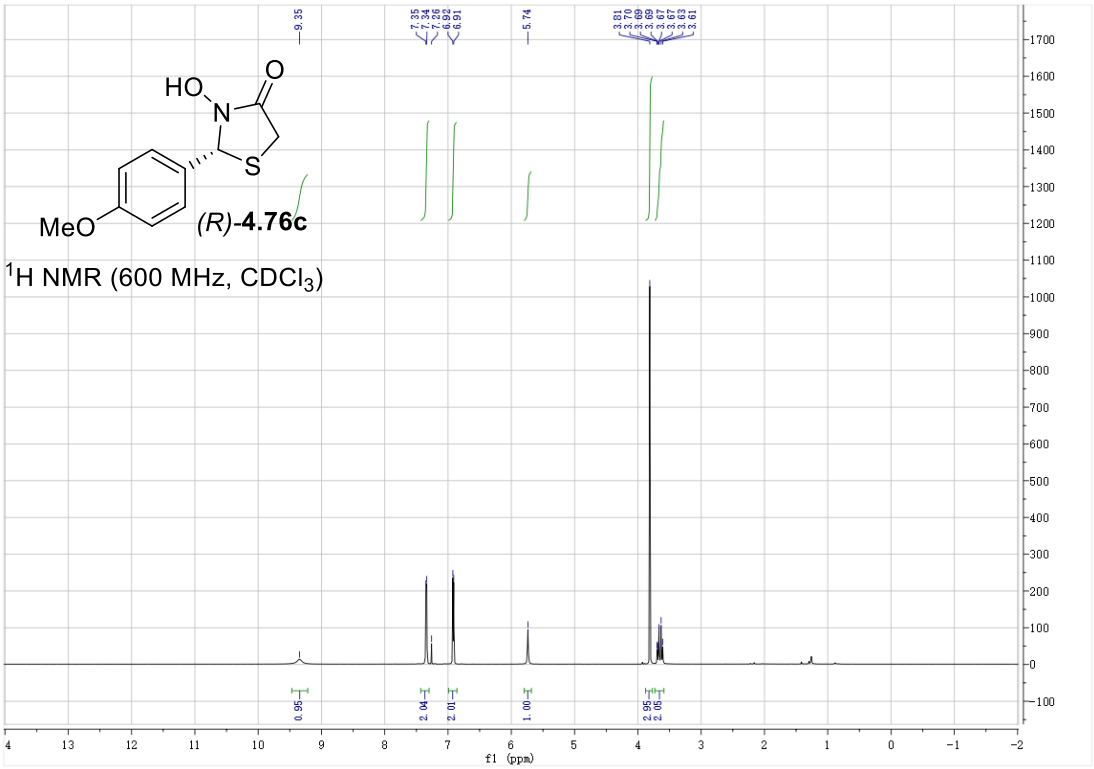
HO
N
O
S
MeO
(R)-4.76c
1H NMR (600 MHz, CDCl3)
9.35
7.35
7.34
7.35
6.92
6.91
5.74
3.81
3.70
3.69
3.69
3.67
3.67
3.63
3.61
0.95
2.04
2.01
1.00
2.95
2.00
f1 (ppm)

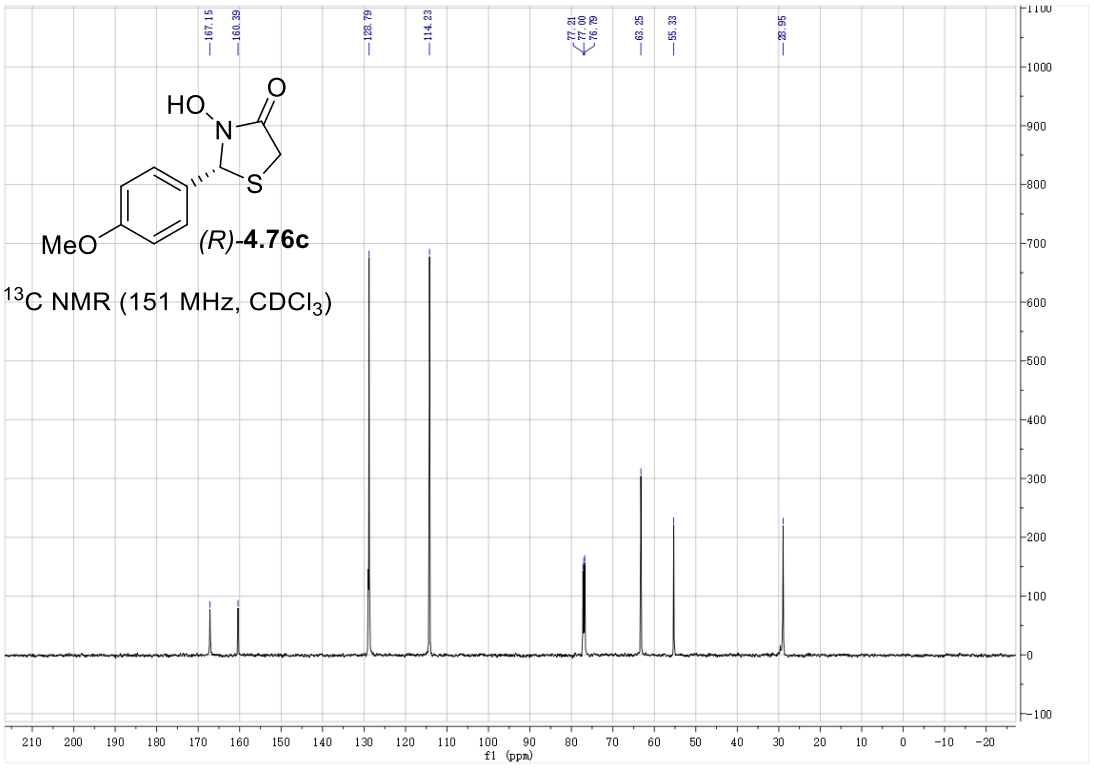
HO
N
O
S
MeO
(R)-4.76c
13C NMR (151 MHz, CDCl3)
167.15
160.39
128.79
114.23
77.21
77.00
76.79
63.25
55.33
28.95
f1 (ppm)

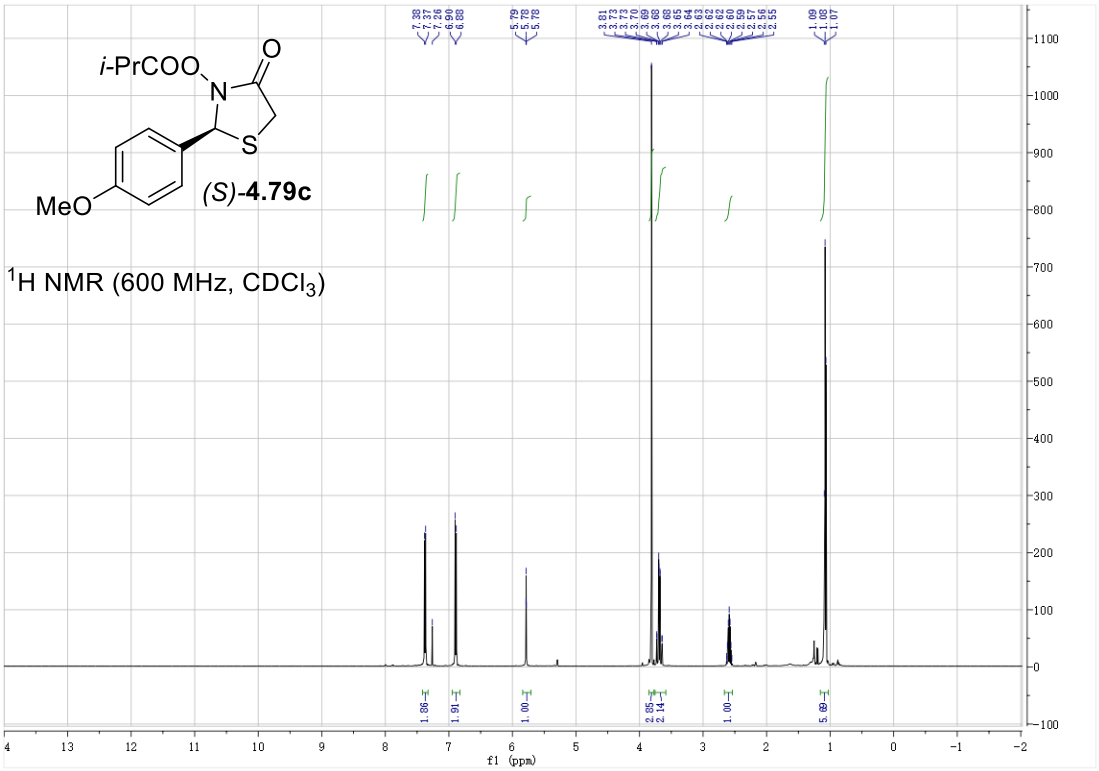
i-PrCOO
N
O
S
MeO
(S)-4.79c
1H NMR (600 MHz, CDCl3)
f1 (ppm)

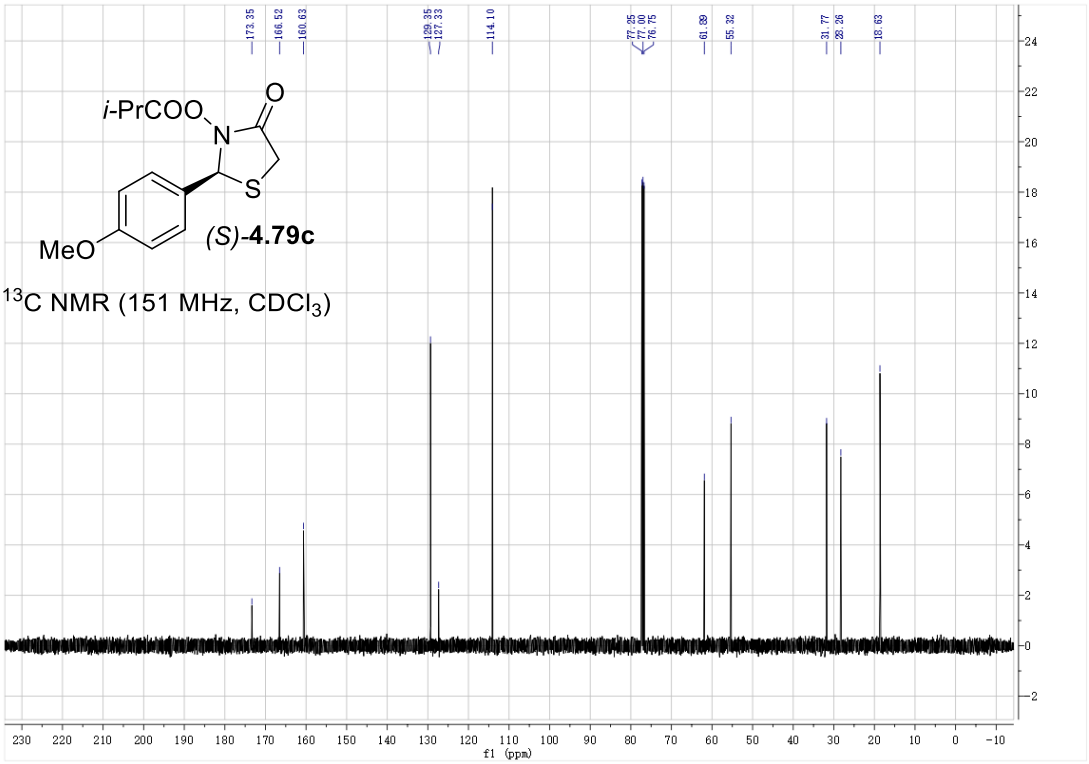
i-PrCOO
N
O
S
MeO
(S)-4.79c
13C NMR (151 MHz, CDCl3)
f1 (ppm)

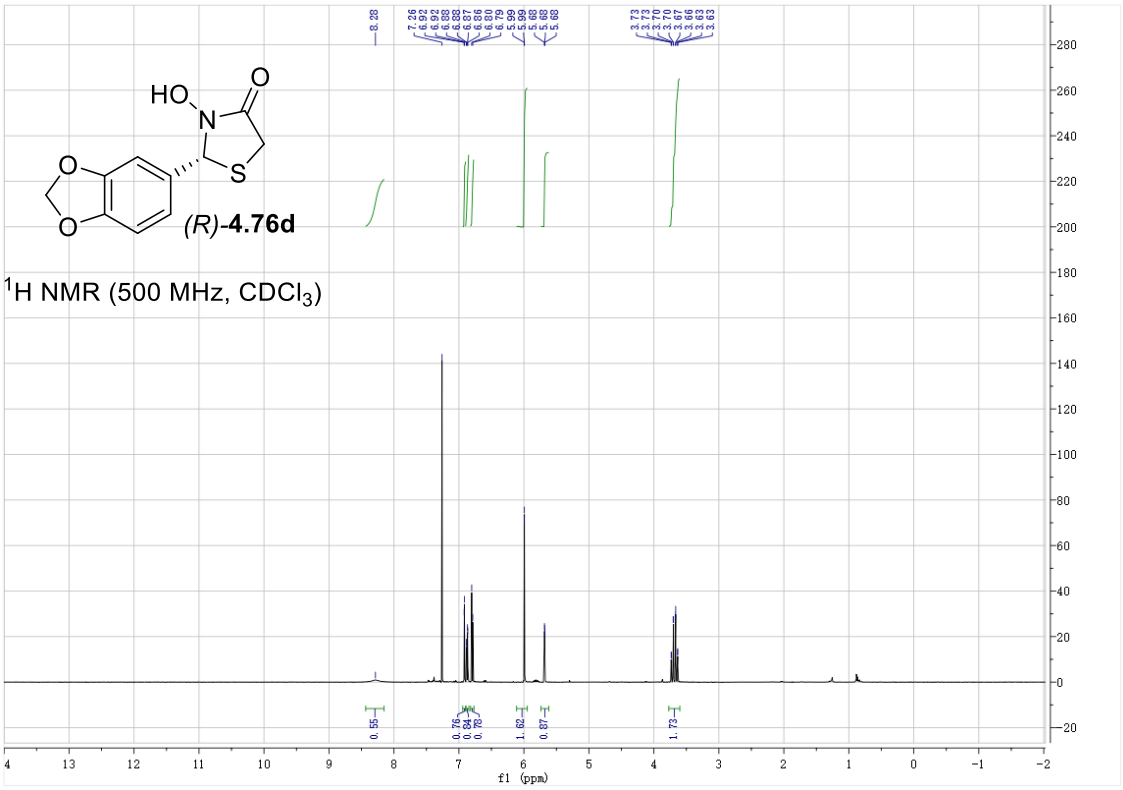
HO
N
O
S
O
O
(R)-4.76d
1H NMR (500 MHz, CDCl3)
f1 (ppm)

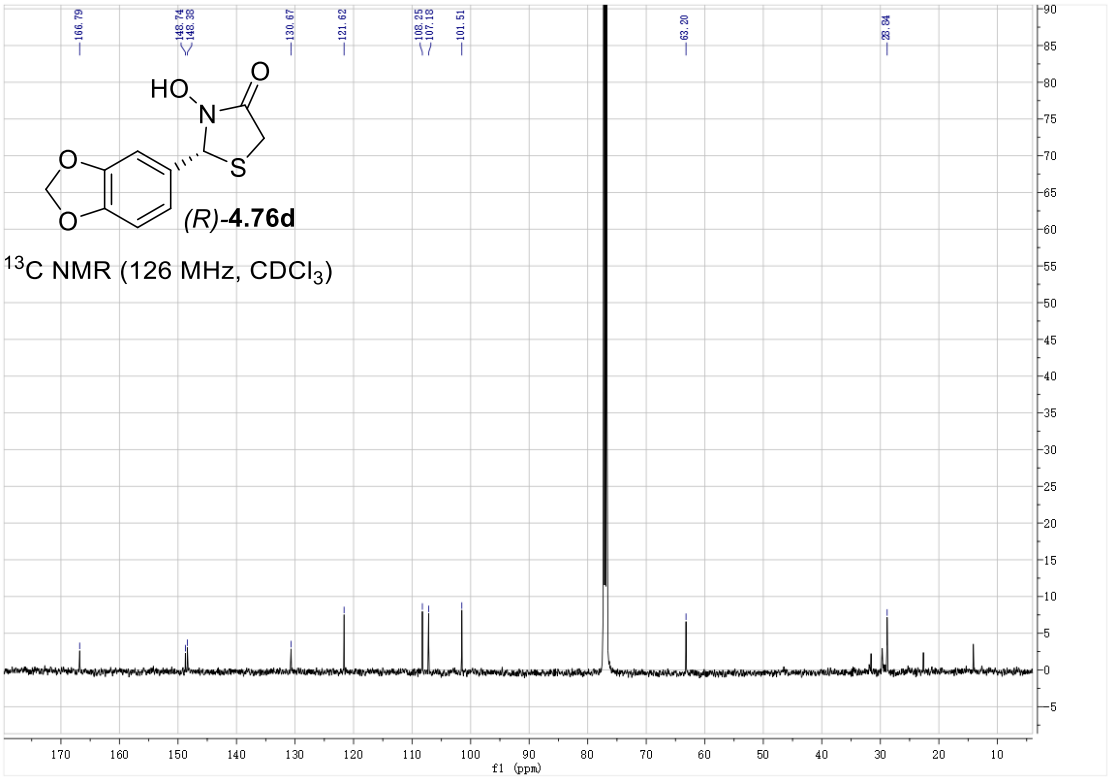
HO
N
O
S
O
O
(R)-4.76d
13C NMR (126 MHz, CDCl3)
f1 (ppm)

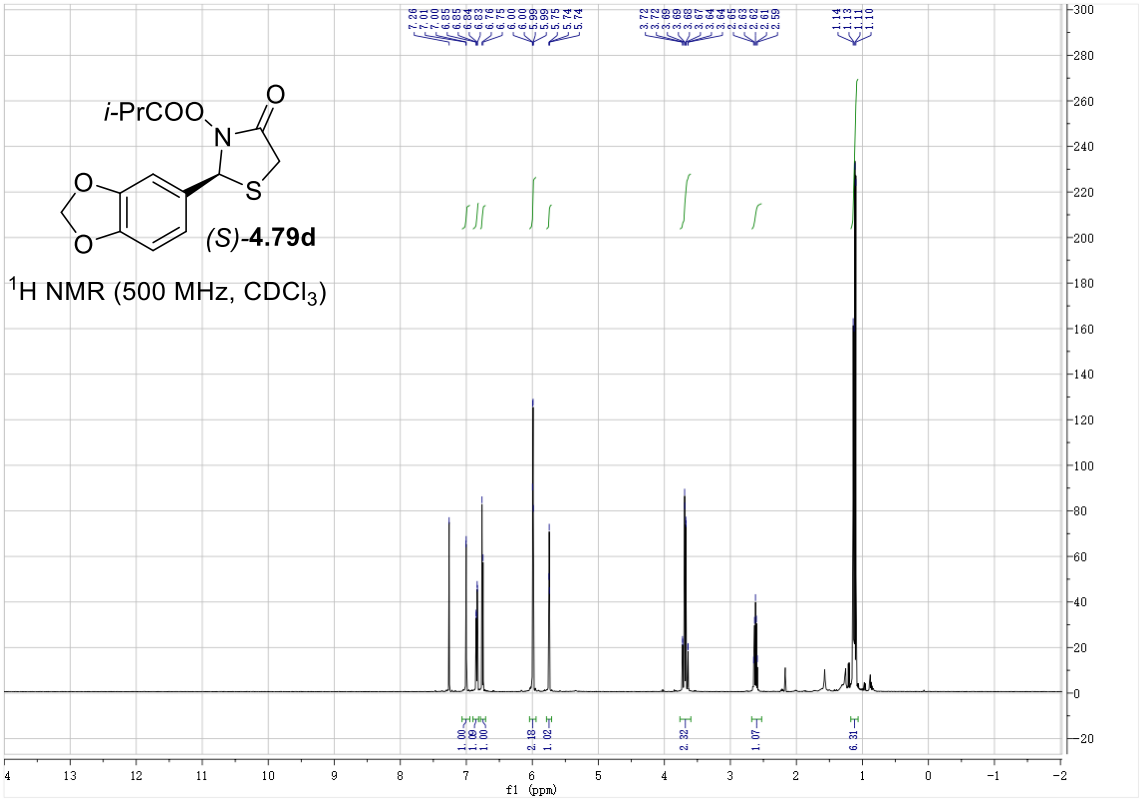
i-PrCOO
N
O
S
O
O
(S)-4.79d
1H NMR (500 MHz, CDCl3)
f1 (ppm)

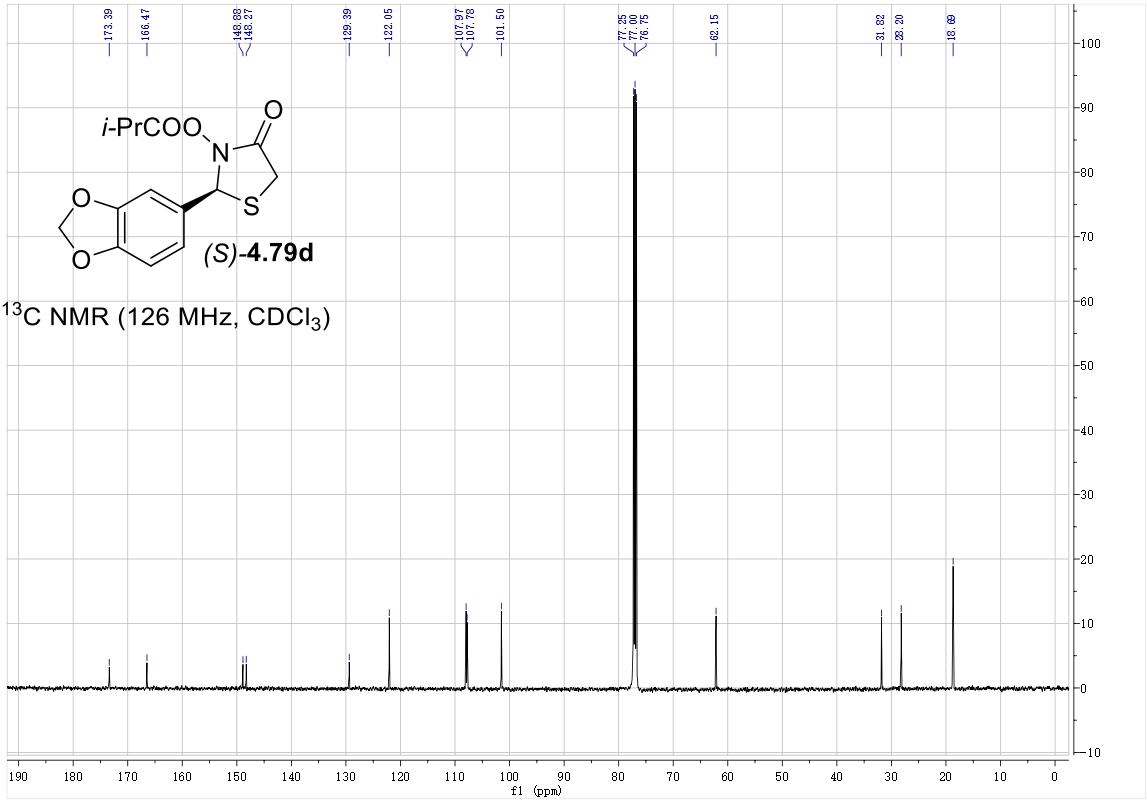
i-PrCOO
N
O
S
O
O
(S)-4.79d
13C NMR (126 MHz, CDCl3)
f1 (ppm)

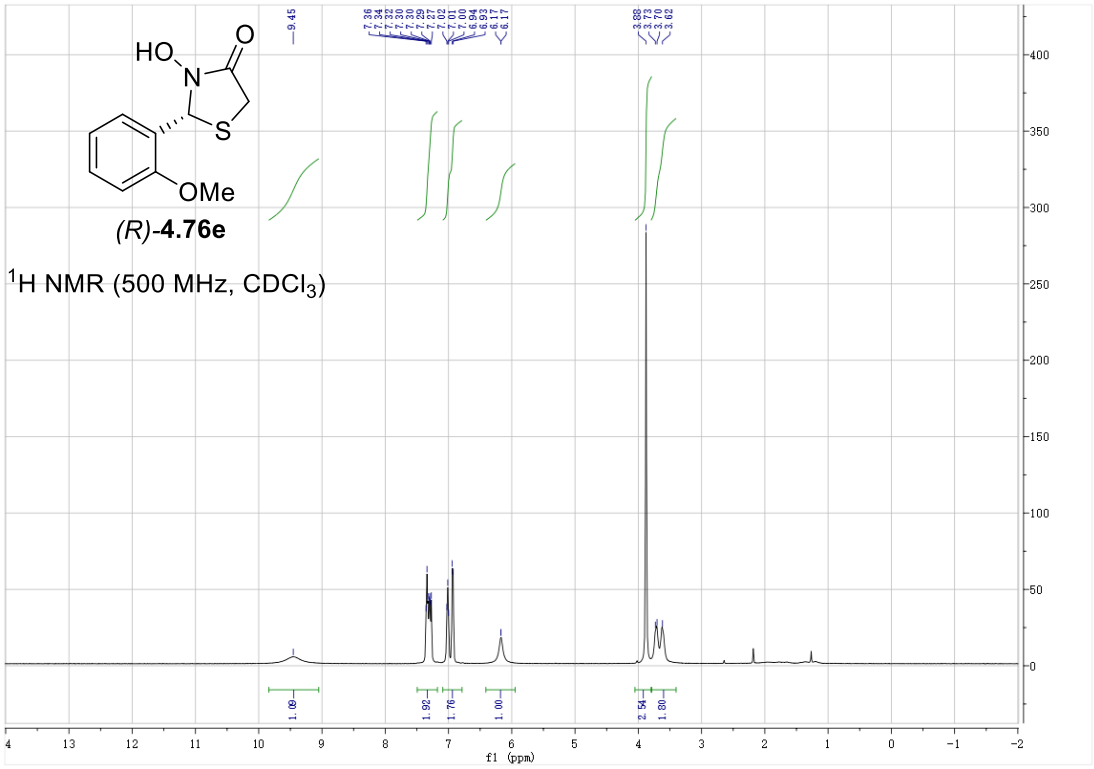
HO
N
O
S
OMe
(R)-4.76e
1H NMR (500 MHz, CDCl3)
f1 (ppm)

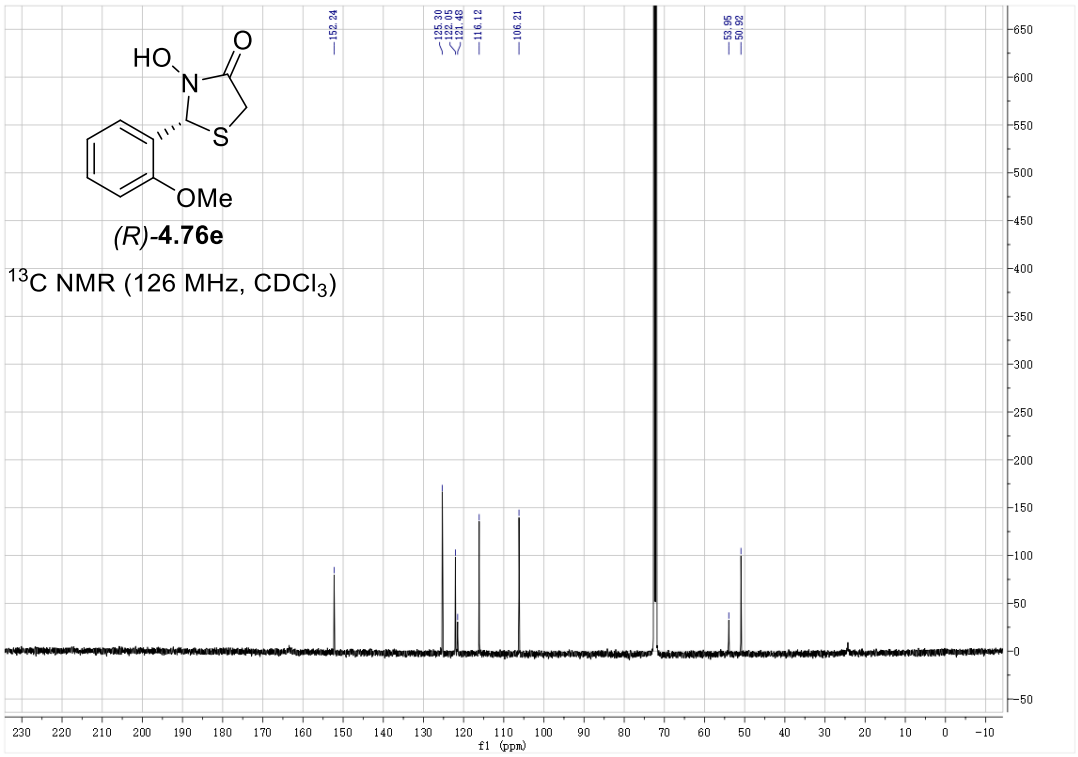
HO
N
O
S
OMe
(R)-4.76e
13C NMR (126 MHz, CDCl3)
f1 (ppm)

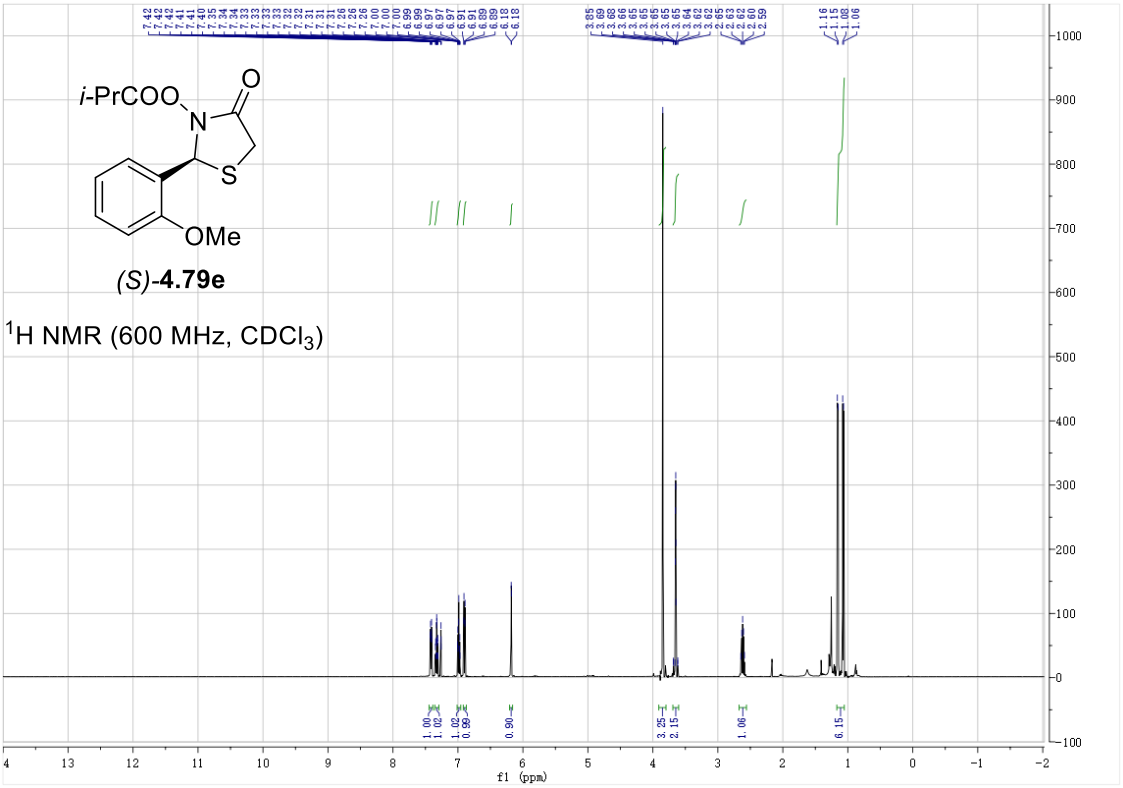
i-PrCOO
N
O
S
OMe
(S)-4.79e
1H NMR (600 MHz, CDCl3)
f1 (ppm)

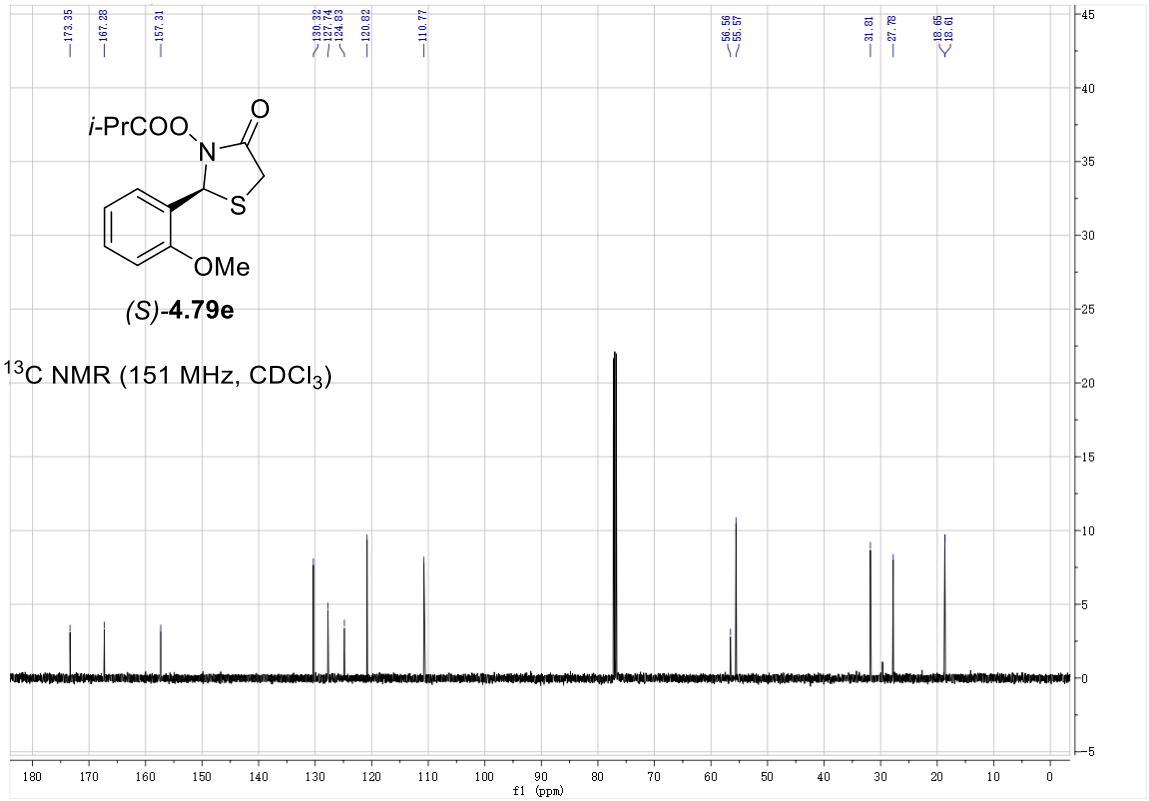
i-PrCOO
N
O
S
OMe
(S)-4.79e
13C NMR (151 MHz, CDCl3)
f1 (ppm)

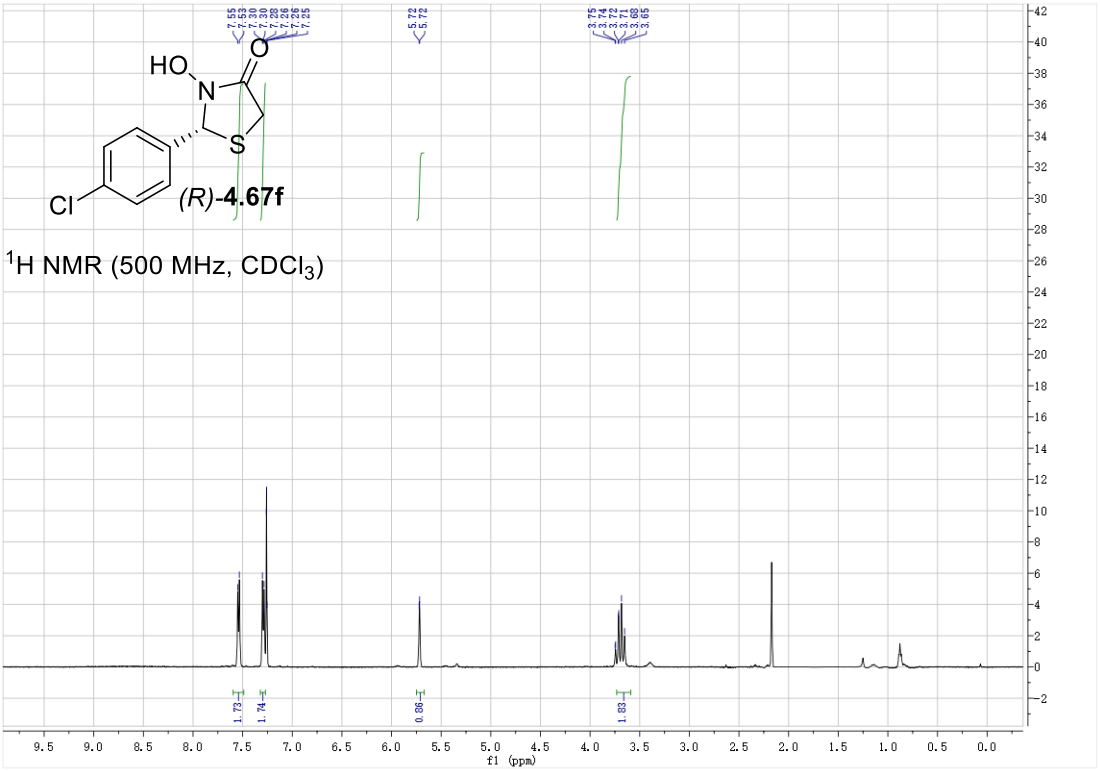
HO
N
O
S
Cl
(R)-4.67f
1H NMR (500 MHz, CDCl3)
f1 (ppm)

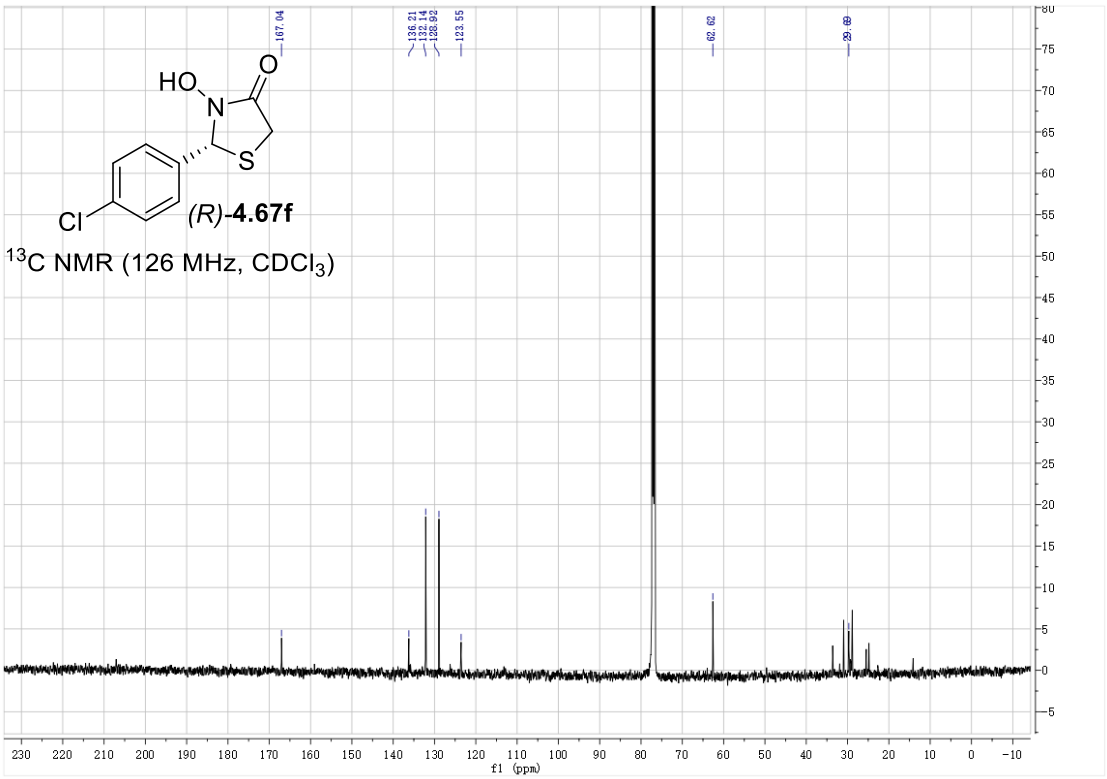
HO
N
O
S
Cl
(R)-4.67f
13C NMR (126 MHz, CDCl3)
f1 (ppm)

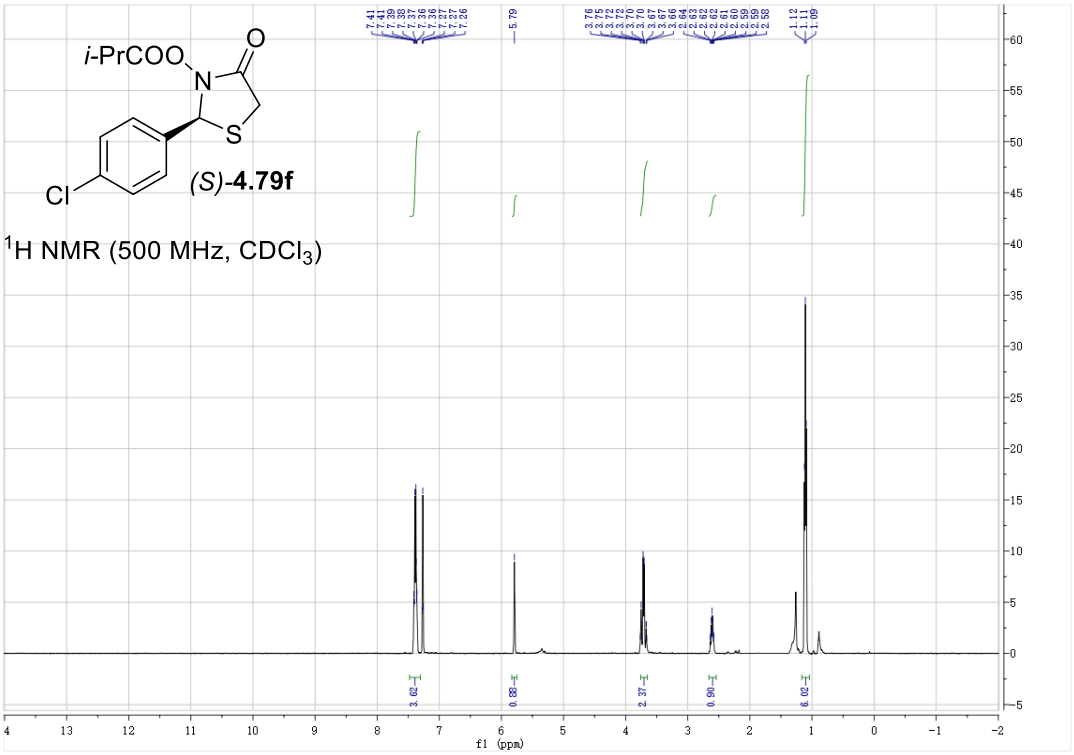
i-PrCOO
O
N
S
Cl
(S)-4.79f
1H NMR (500 MHz, CDCl3)
f1 (ppm)

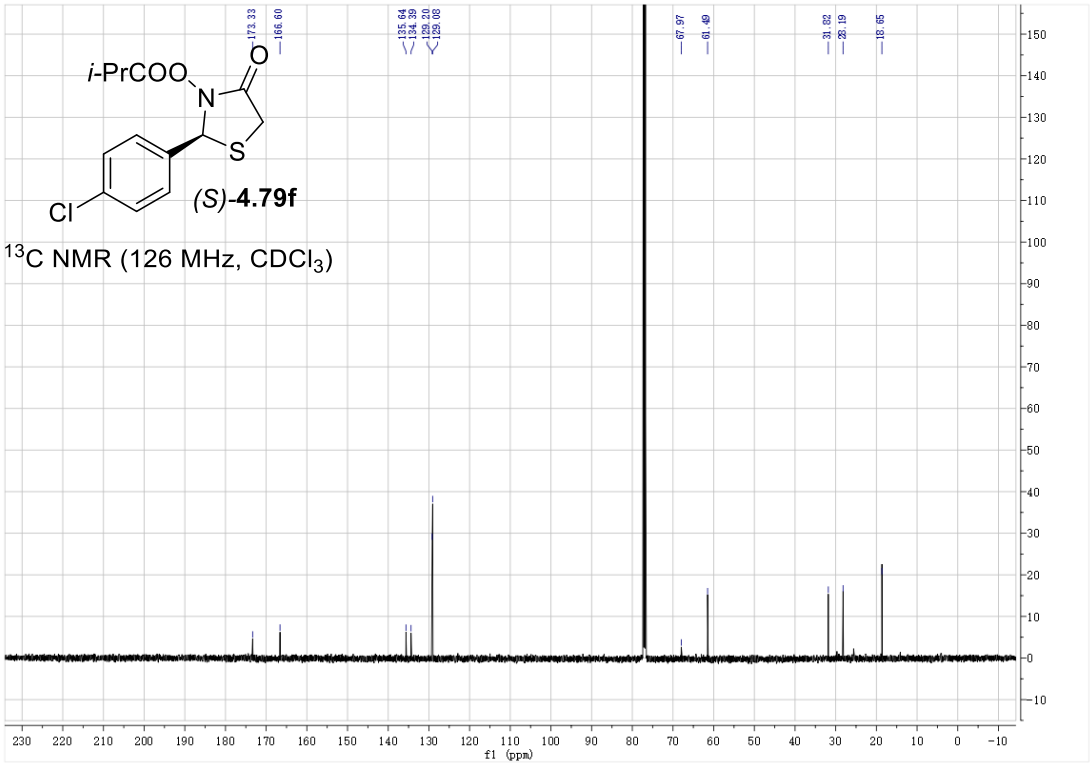
i-PrCOO
O
N
S
Cl
(S)-4.79f
13C NMR (126 MHz, CDCl3)
f1 (ppm)

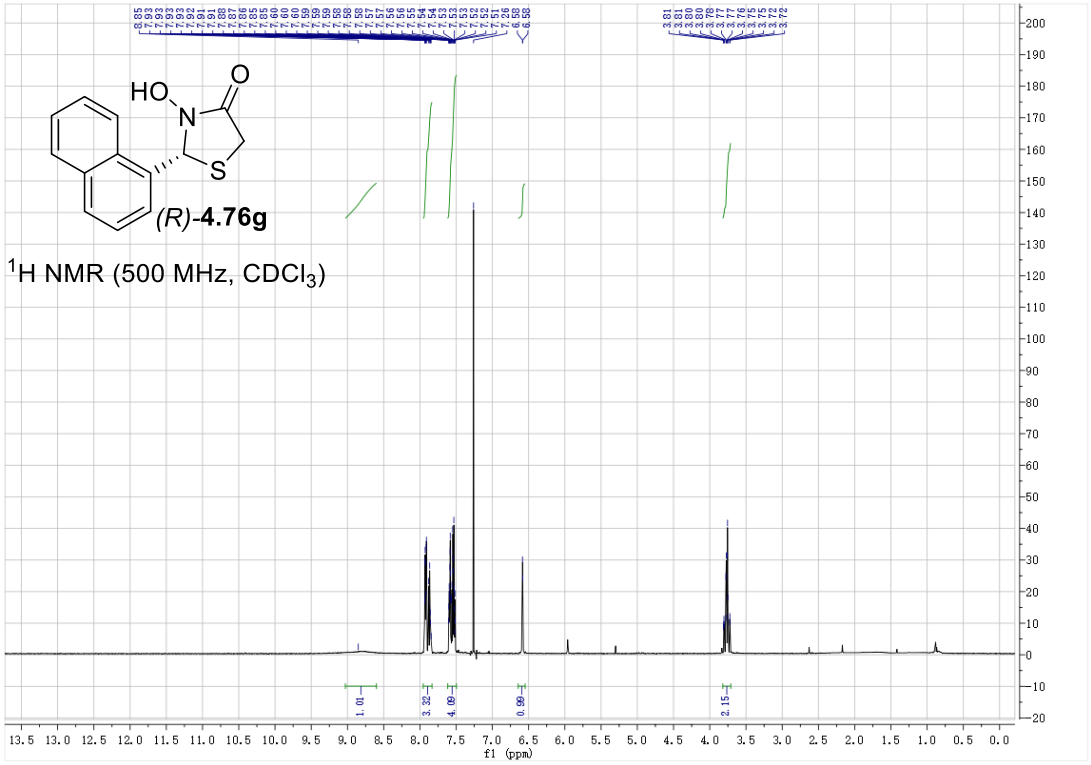
HO
N
O
S
(R)-4.76g
1H NMR (500 MHz, CDCl3)
f1 (ppm)

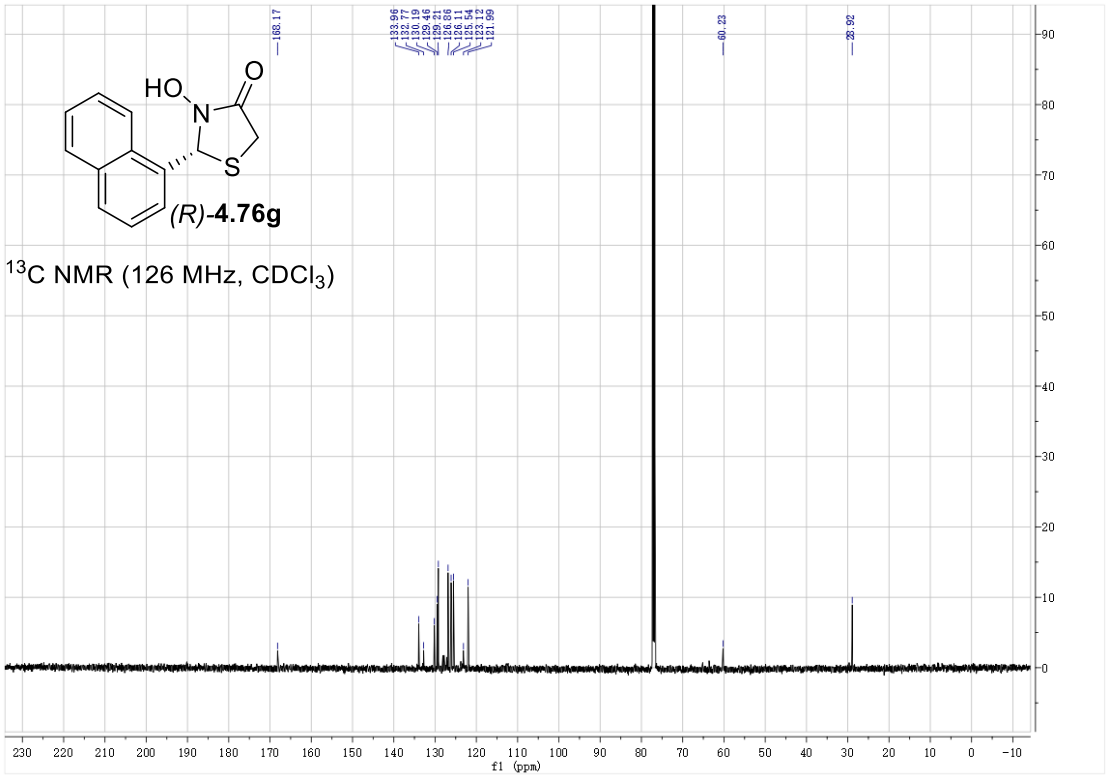
HO
N
O
S
(R)-4.76g
13C NMR (126 MHz, CDCl3)
f1 (ppm)

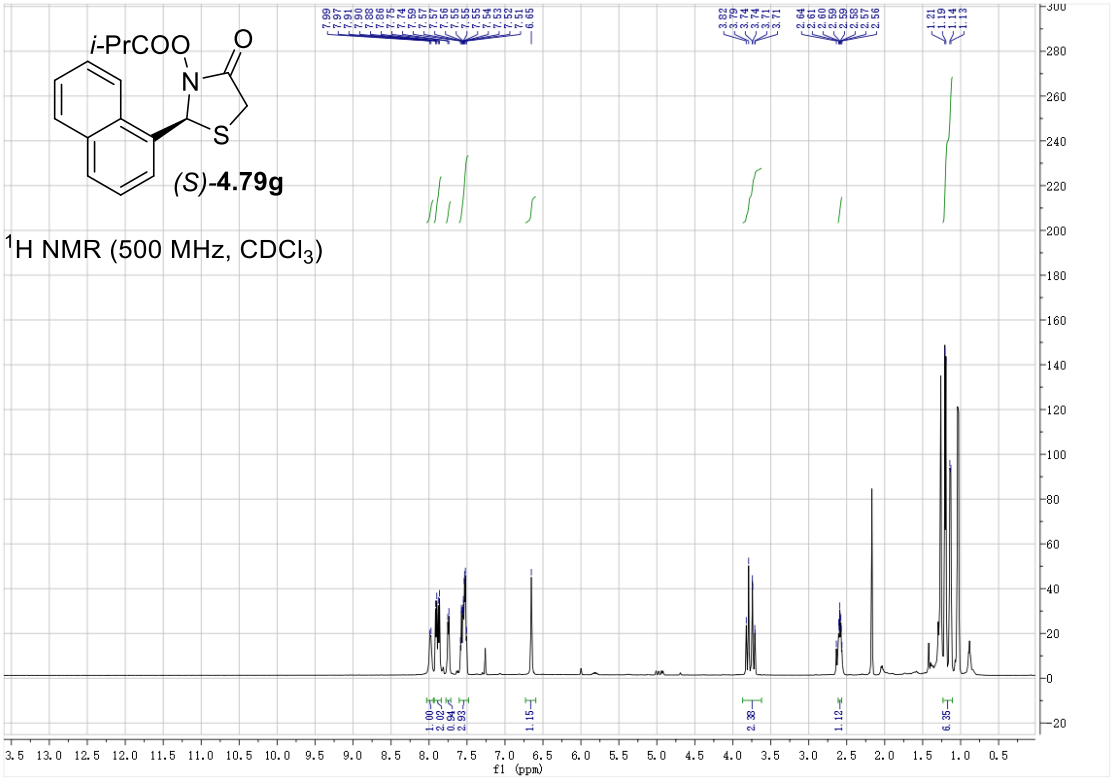
i-PrCOO
O
N
S
(S)-4.79g
1H NMR (500 MHz, CDCl3)
f1 (ppm)

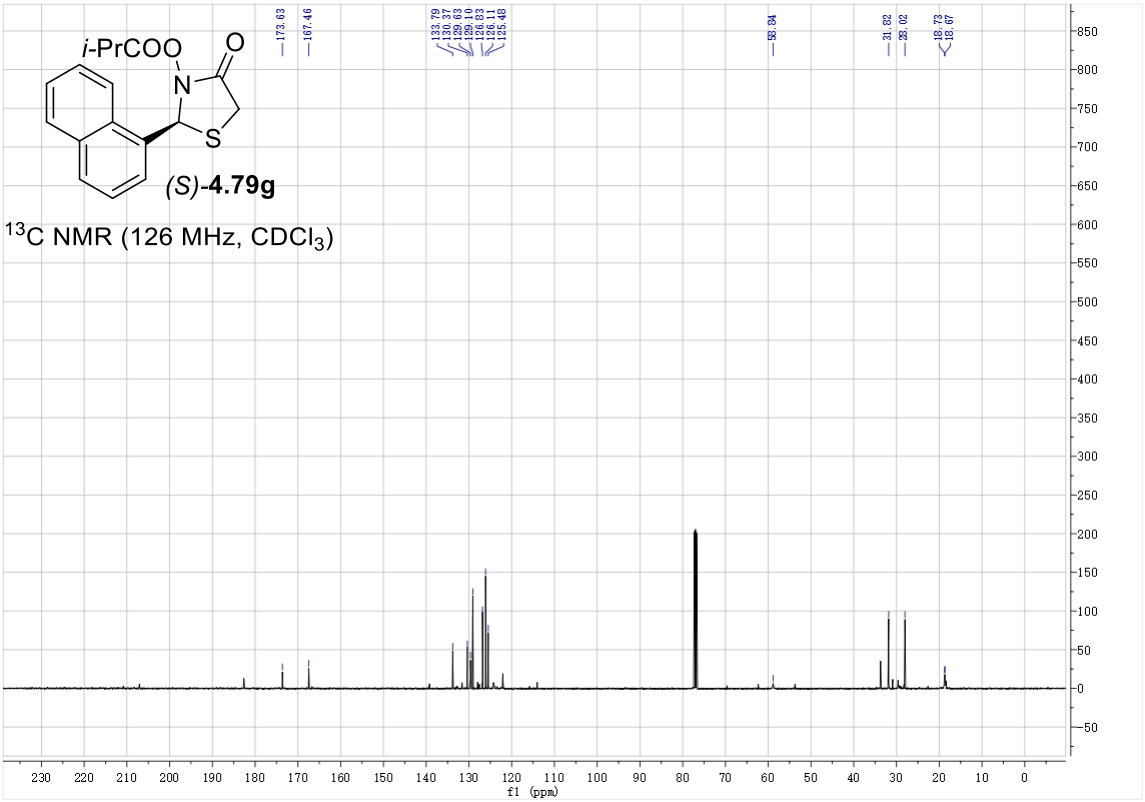
i-PrCOO
O
N
S
(S)-4.79g
13C NMR (126 MHz, CDCl3)
f1 (ppm)

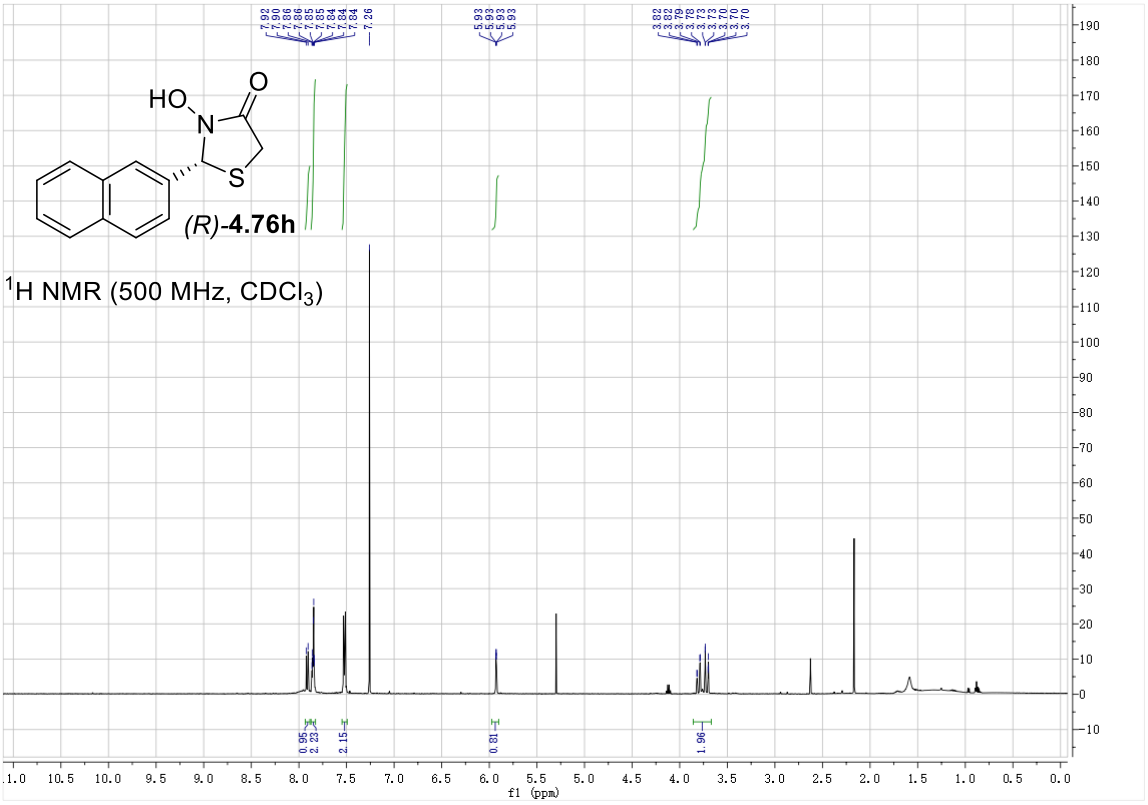
HO
N
O
S
(R)-4.76h
1H NMR (500 MHz, CDCl3)
f1 (ppm)

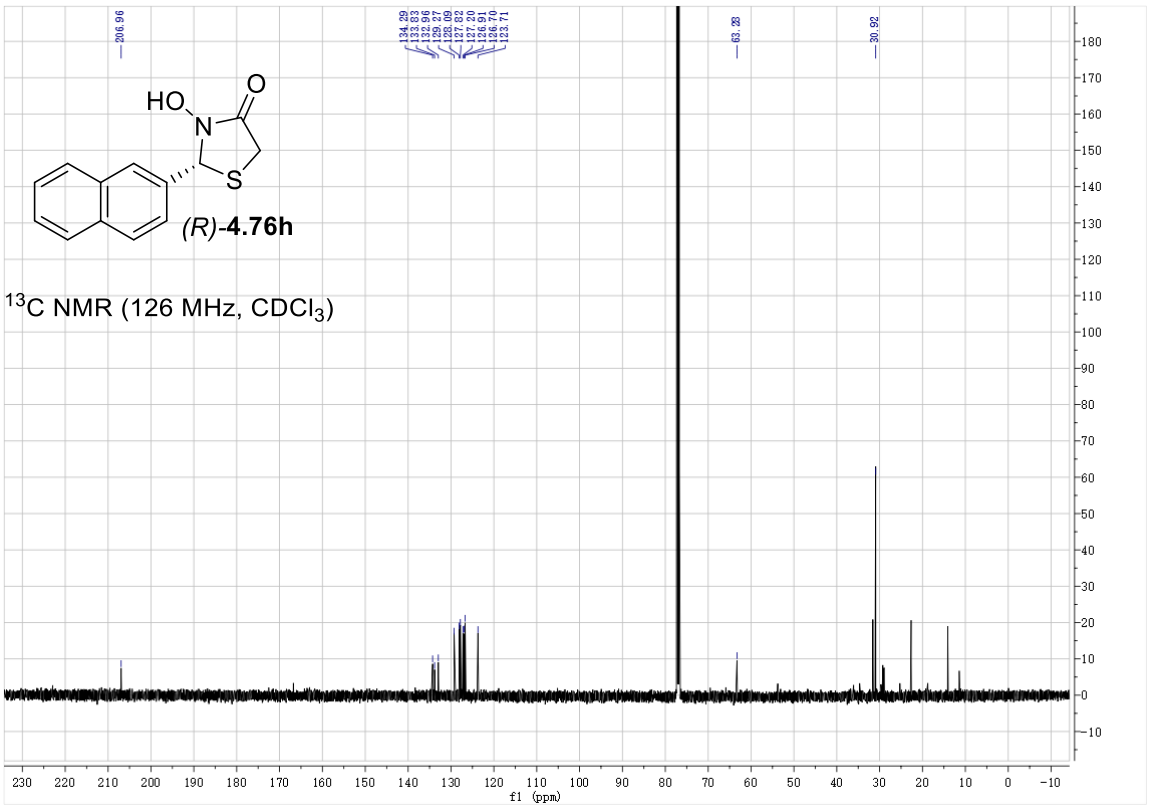
HO
N
O
S
(R)-4.76h
13C NMR (126 MHz, CDCl3)
f1 (ppm)

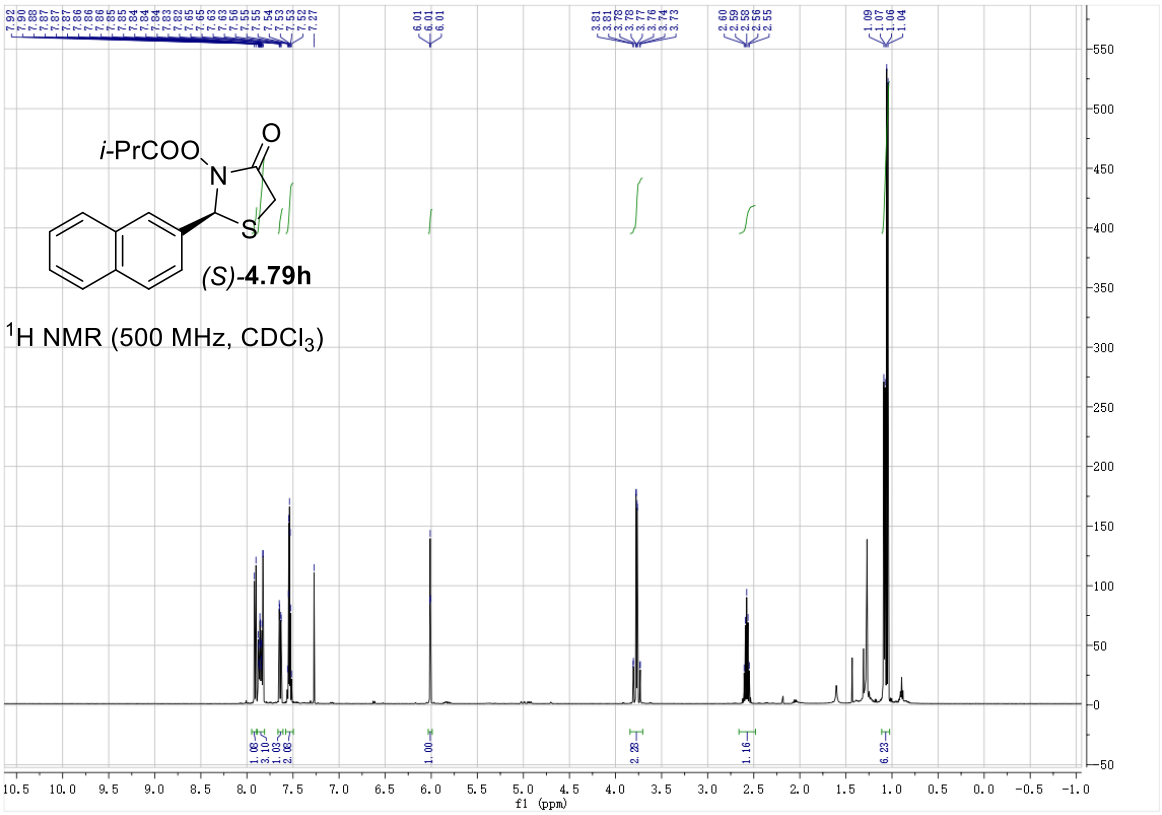
i-PrCOO
N
O
S
(S)-4.79h
1H NMR (500 MHz, CDCl3)
f1 (ppm)

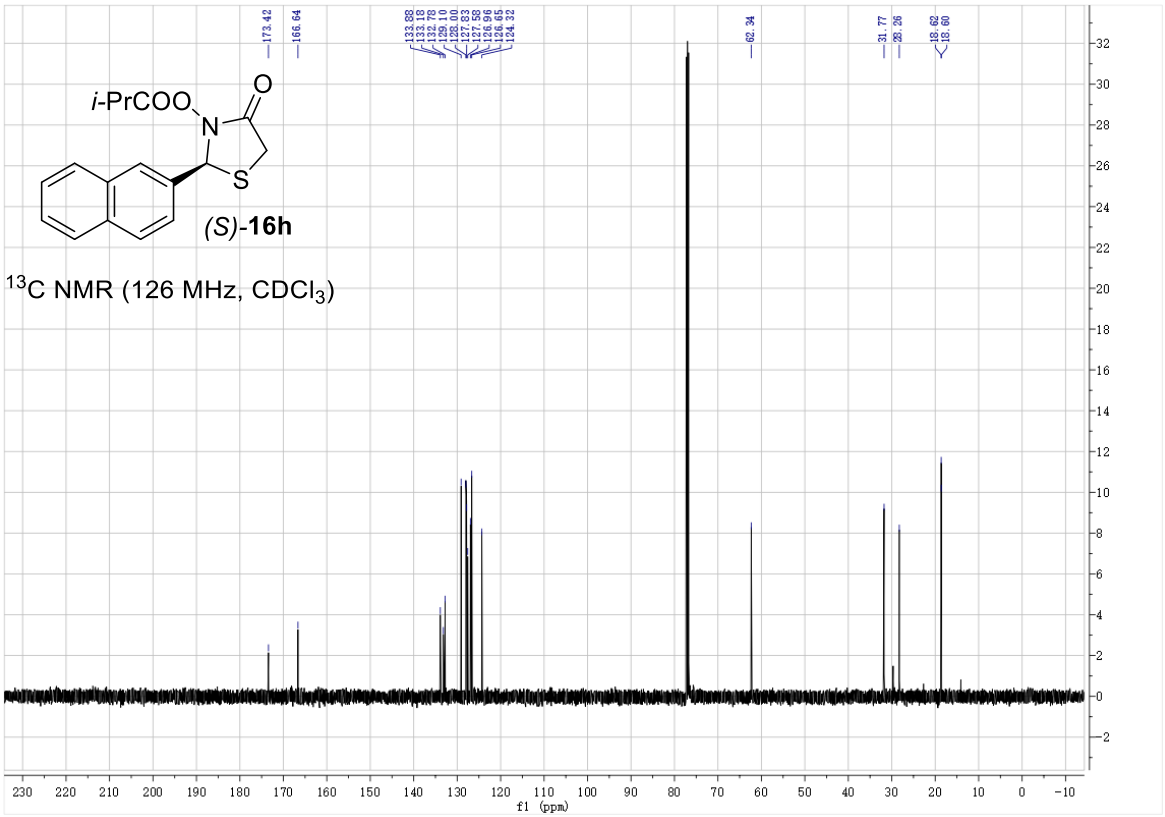
i-PrCOO
N
O
S
(S)-16h
13C NMR (126 MHz, CDCl3)
f1 (ppm)

2. HPLC DATA

(±)-**4.70a**

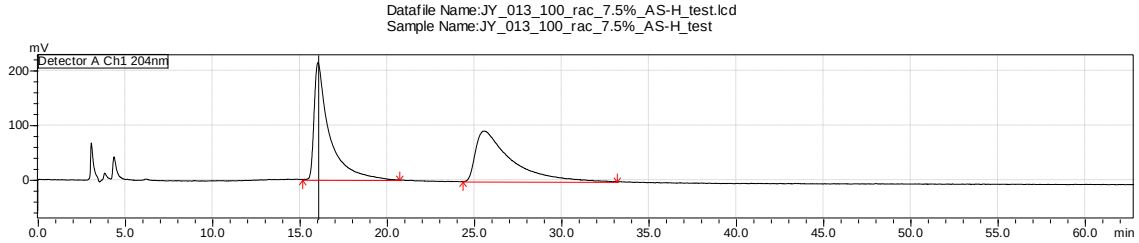

Peak#	Ret. Time	Area	Height	Conc.	Area%
1	16.066	12979526	214187	50.079	50.079
2	25.594	12938551	92020	49.921	49.921
Total		25918078	306207	100.000	100.000

(S)-**4.70a** (Table 4-5, entry 2a)

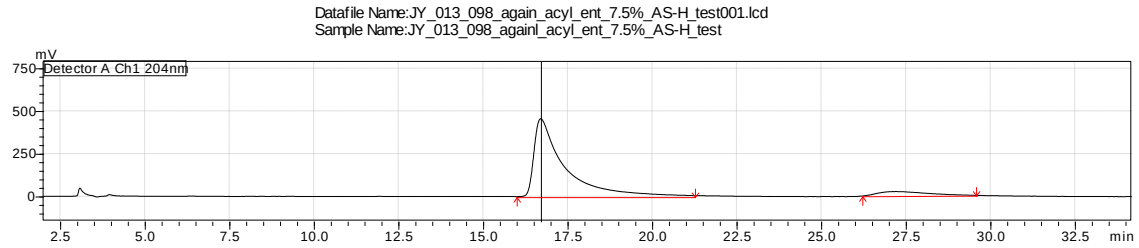

Peak#	Ret. Time	Area	Height	Conc.	Area%
1	16.715	29301962	458223	91.808	91.808
2	27.212	2614632	25619	8.192	8.192
Total		31916593	48384	100.000	100.000

(R)-**4.70a** (Table 4-5, entry 2a)

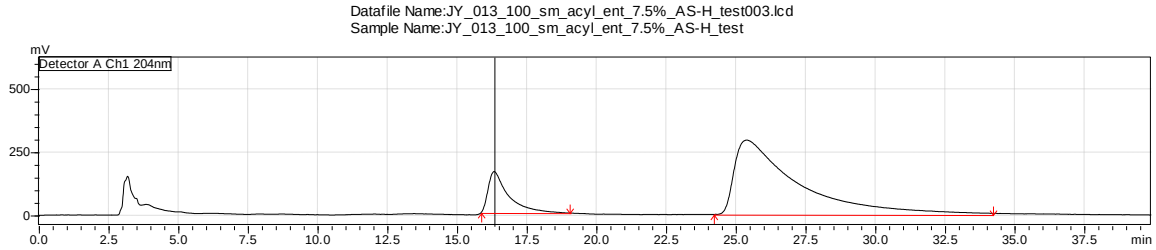

Peak#	Ret. Time	Area	Height	Conc.	Area%
1	16.337	8142979	162595	14.949	14.949
2	25.390	46327032	293717	85.051	85.051
Total		54470011	456312	100.000	100.000

(±)-**4.70a-Et**

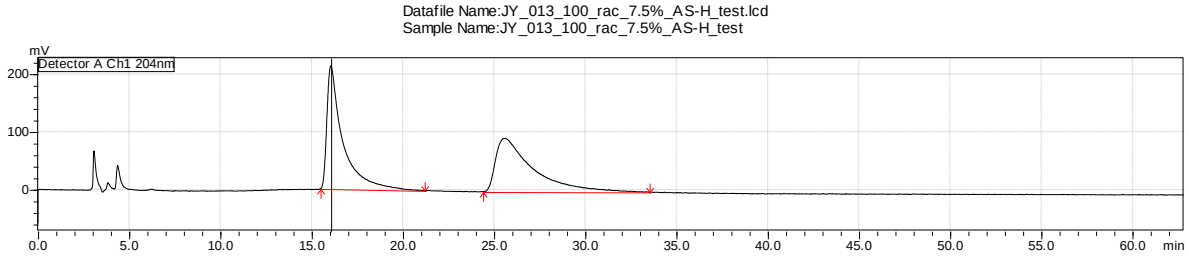

Peak#	Ret. Time	Area	Height	Conc.	Area%
1	16.066	12879859	212947	49.595	49.595
2	25.594	13090200	92337	50.405	50.405
Total		25970059	305284	100.000	100.000

(S)-**4.70a-Et** (Table 4-5, 3a)

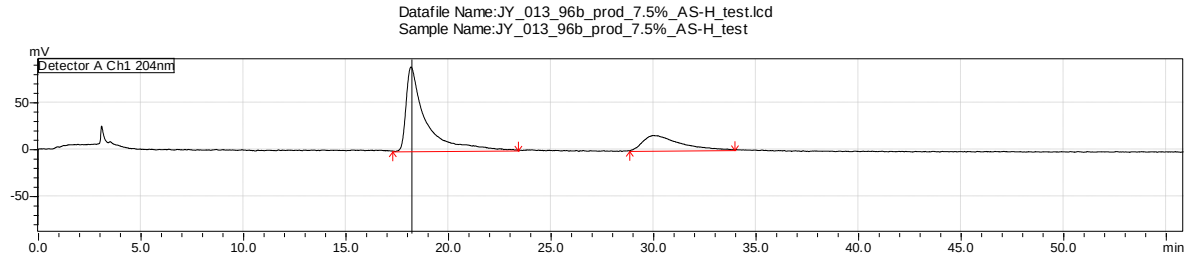

Peak#	Ret. Time	Area	Height	Conc.	Area%
1	18.206	5876798	89611	74.798	74.798
2	30.013	1980044	16093	25.202	25.202
Total		7856842	105704	100.000	100.000

(±)-**4.70b**

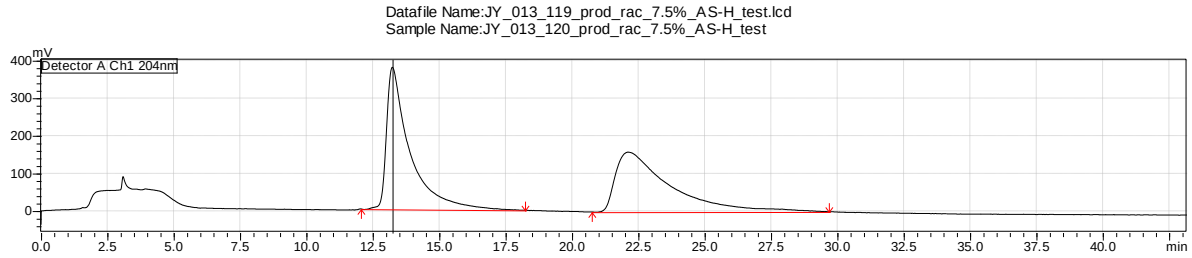

Peak#	Ret. Time	Area	Height	Conc.	Area%
1	13.244	22957946	377094	50.459	50.459
2	22.127	22540178	159104	49.541	49.541
Total		45498125	536197	100.000	100.000

(S)-**4.70b** (Table 4-6, 1a)

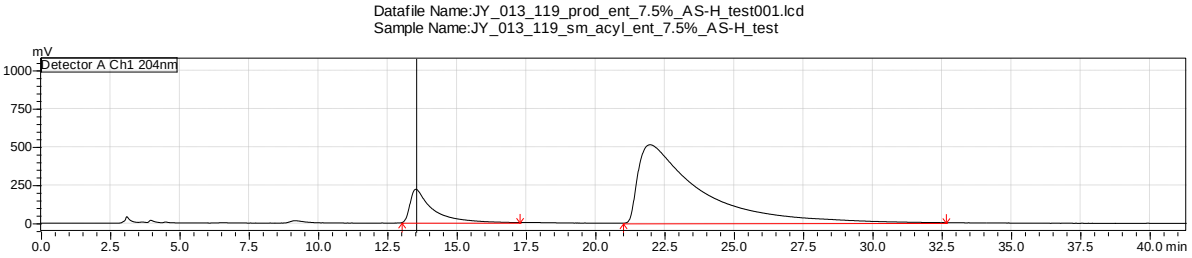

Peak#	Ret. Time	Area	Height	Conc.	Area%
1	13.534	12090287	217604	13.268	13.268
2	21.988	79034786	513255	86.732	86.732
Total		91125072	730859	100.000	100.000

(R)-**4.70b** (Table 4-6, 1a)

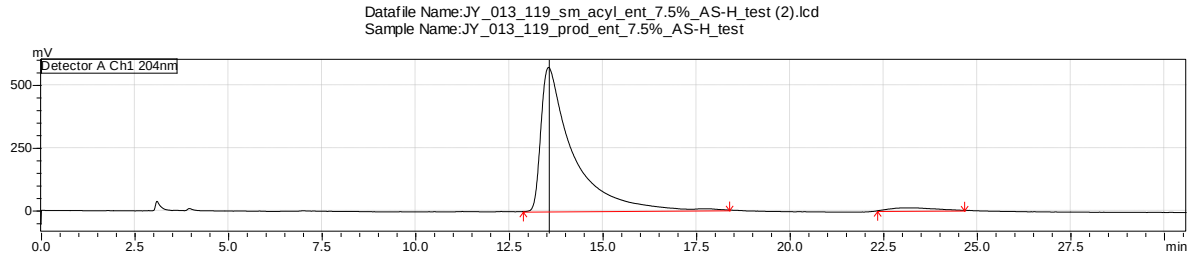

Peak#	Ret. Time	Area	Height	Conc.	Area%
1	13.564	33879619	572525	97.337	97.337
2	23.147	926884	11316	2.663	2.663
Total		34806503	583841	100.000	100.000

(±)-**4.70c**

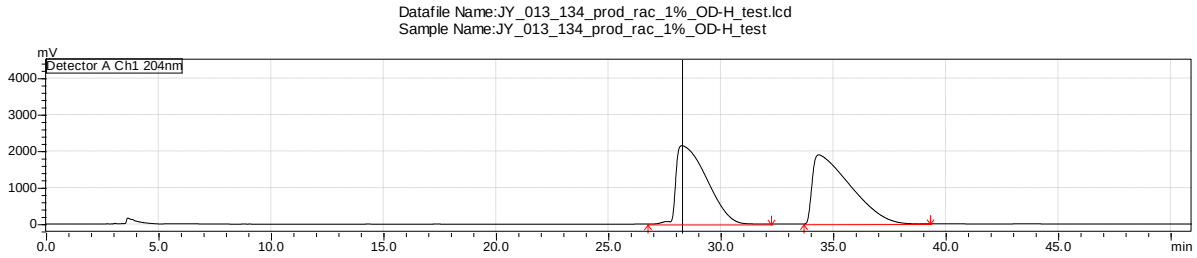

Peak#	Ret. Time	Area	Height	Conc.	Area%
1	28.281	204431245	2153102	48.017	48.017
2	34.367	221314755	1892503	51.983	51.983
Total		425746000	4045606	100.000	100.000

(S)-**4.70c** (Table 4-6, 2a)

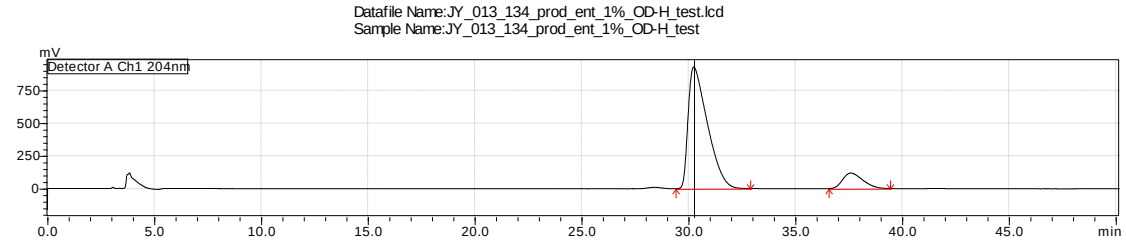

Peak#	Ret. Time	Area	Height	Conc.	Area%
1	30.260	58200475	928790	88.138	88.138
2	37.611	7833211	118936	11.862	11.862
Total		66033686	1047726	100.000	100.000

(R)-**4.70c** (Table 4-6, 2a)

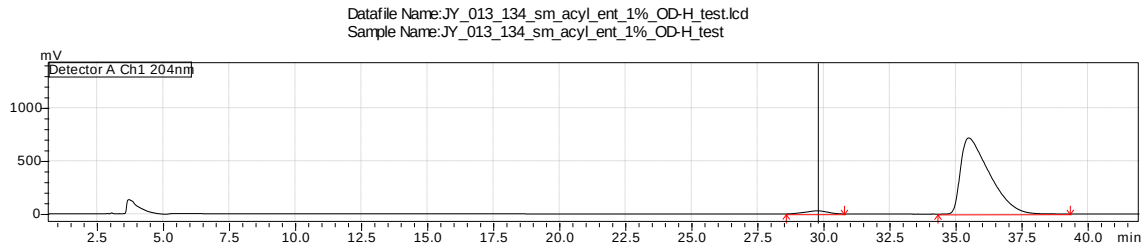

Peak#	Ret. Time	Area	Height	Conc.	Area%
1	29.785	1736639	29412	3.079	3.079
2	35.506	54668079	717872	96.921	96.921
Total		56404717	747284	100.000	100.000

(±)-**4.70d**

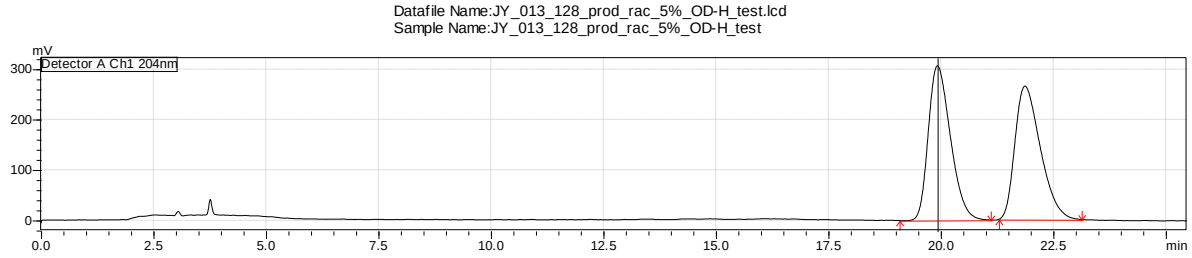

Peak#	Ret. Time	Area	Height	Conc.	Area%
1	19.930	10491961	306678	50.162	50.162
2	21.875	10424137	264725	49.838	49.838
Total		20916098	571403	100.000	100.000

(S)-**4.70d** (Table 4-6, 3a)

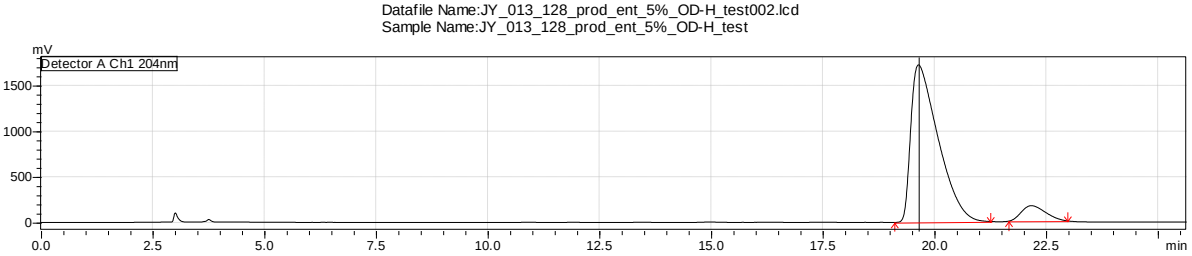

Peak#	Ret. Time	Area	Height	Conc.	Area%
1	19.649	73083229	1720805	92.042	92.042
2	22.178	6318740	168368	7.958	7.958
Total		79401969	1889174	100.000	100.000

(R)-**4.70d** (Table 4-6, 3a)

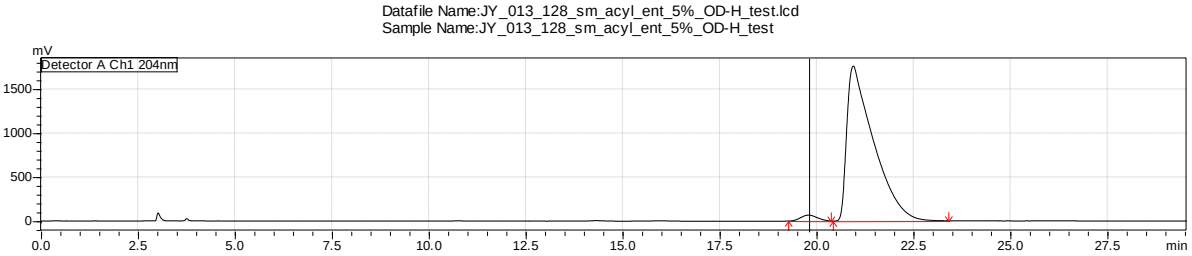

Peak#	Ret. Time	Area	Height	Conc.	Area%
1	19.805	1898399	65448	2.201	2.201
2	20.953	84359148	1761077	97.799	97.799
Total		86257547	1826525	100.000	100.000

(±)-**4.70e**

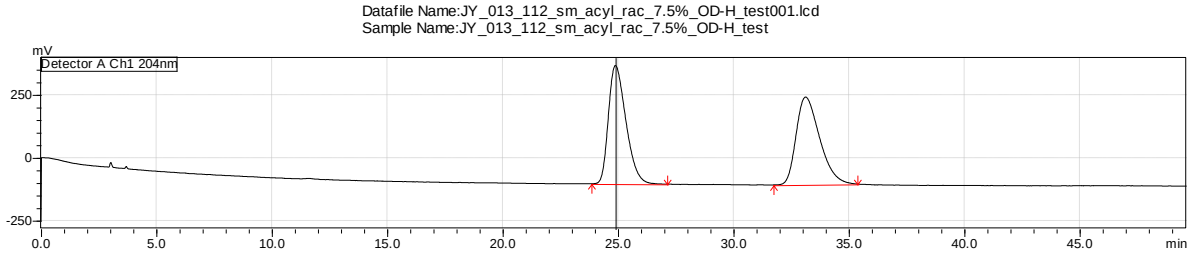

Peak#	Ret. Time	Area	Height	Conc.	Area%
1	24.895	24804175	470577	50.157	50.157
2	33.132	24648809	348029	49.843	49.843
Total		49452984	818605	100.000	100.000

(S)-**4.70e** (Table 4-6, 4a)

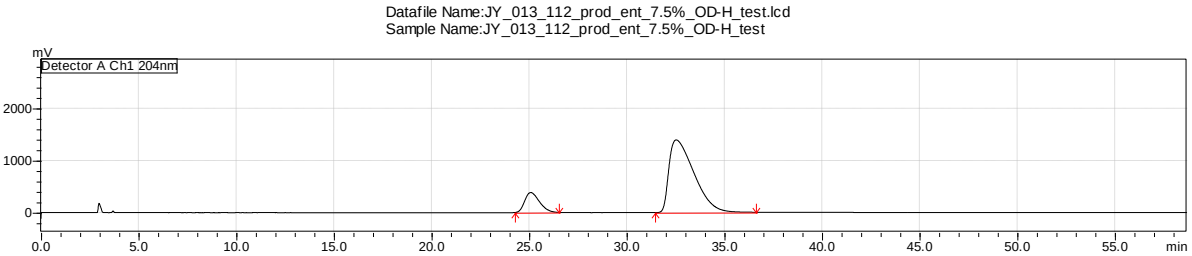

Peak#	Ret. Time	Area	Height	Conc.	Area%
1	25.093	20034374	382889	13.921	13.921
2	32.542	123880829	1392648	86.079	86.079
Total		143915203	1775537	100.000	100.000

(R)-**4.70e** (Table 4-6, 4a)

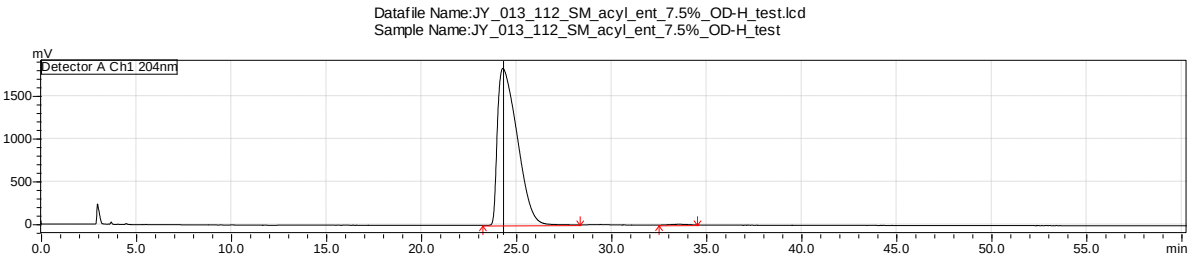

Peak#	Ret. Time	Area	Height	Conc.	Area%
1	24.312	132323315	1831725	99.629	99.629
2	33.555	493103	8486	0.371	0.371
Total		132816417	1840211	100.000	100.000

(±)-**4.70f**

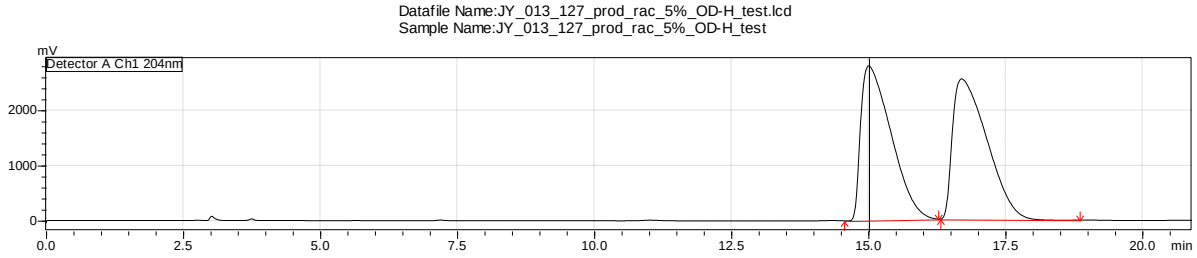

Peak#	Ret. Time	Area	Height	Conc.	Area%
1	15.011	108008723	2804740	49.348	49.348
2	16.709	110862970	2547612	50.652	50.652
Total		218871693	5352352	100.000	100.000

(S)-**4.70f** (Table 4-6, 5a)

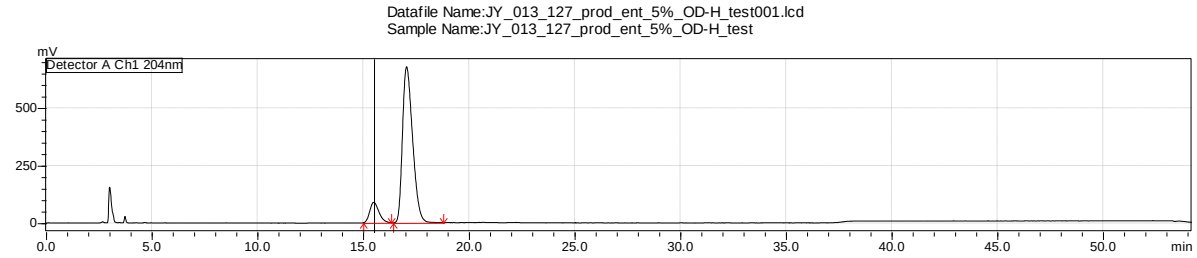

Peak#	Ret. Time	Area	Height	Conc.	Area%
1	15.518	2663674	88925	10.556	10.556
2	17.067	22570569	677629	89.444	89.444
Total		25234244	766555	100.000	100.000

(R)-**4.70f** (Table 4-6, 5a)

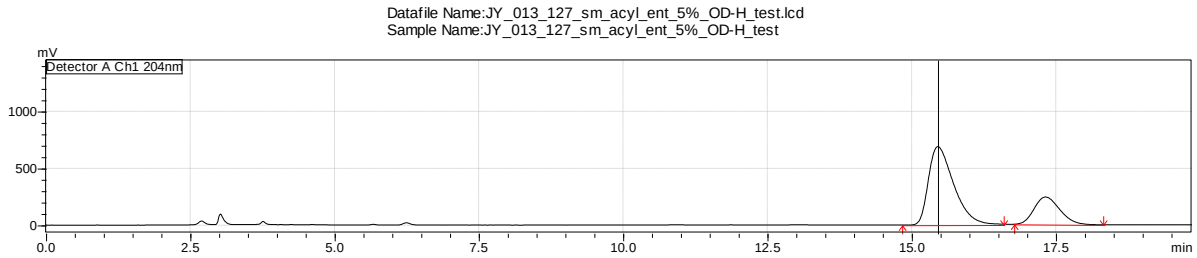

Peak#	Ret. Time	Area	Height	Conc.	Area%
1	15.456	21033422	689487	73.859	73.859
2	17.322	7444402	241055	26.141	26.141
Total		28477824	930541	100.000	100.000

(±)-**4.70g**

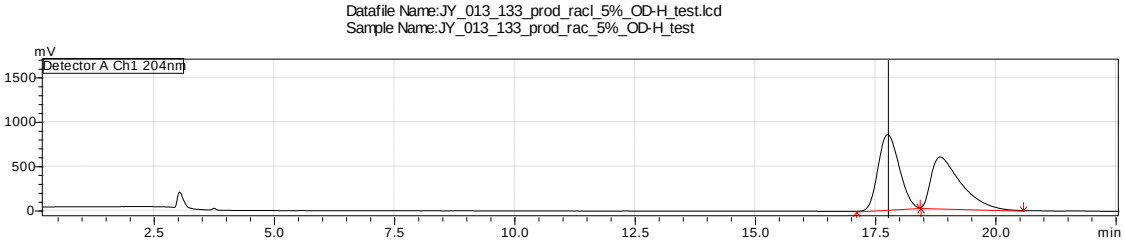

Peak#	Ret. Time	Area	Height	Conc.	Area%
1	17.763	25600898	845442	50.841	50.841
2	18.855	24753925	578238	49.159	49.159
Total		50354822	1423680	100.000	100.000

(S)-**4.70g** (Table 4-6, 6a)

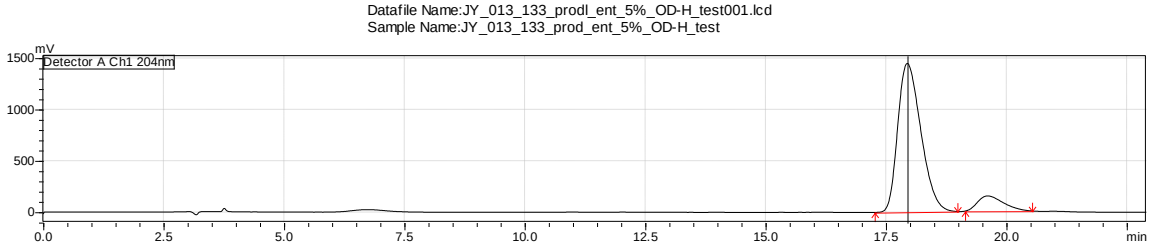

Peak#	Ret. Time	Area	Height	Conc.	Area%
1	17.947	48343806	1447381	89.759	89.759
2	19.618	5515499	147615	10.241	10.241
Total		53859305	1594996	100.000	100.000

(R)-**4.70g** (Table 4-6, 6a)

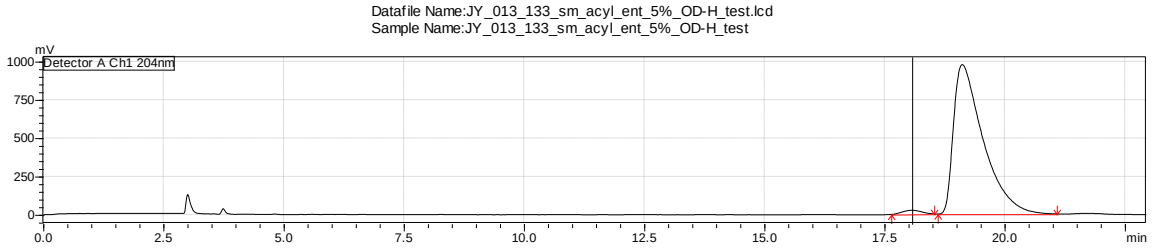

Peak#	Ret. Time	Area	Height	Conc.	Area%
1	18.078	704299	25768	1.658	1.658
2	19.123	41770700	974804	98.342	98.342
Total		42474999	1000572	100.000	100.000

(±)-**4.70h**

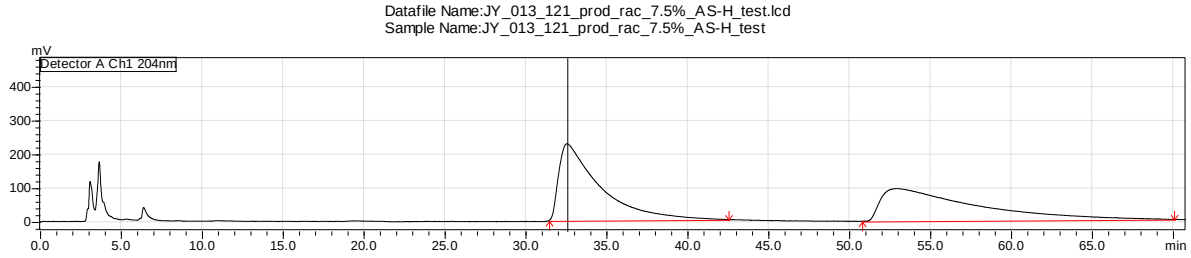

Peak#	Ret. Time	Area	Height	Conc.	Area%
1	32.572	39849110	227204	50.960	50.960
2	52.919	38347618	96179	49.040	49.040
Total		78196728	323382	100.000	100.000

(S)-**4.70h** (Table 4-6, 7a)

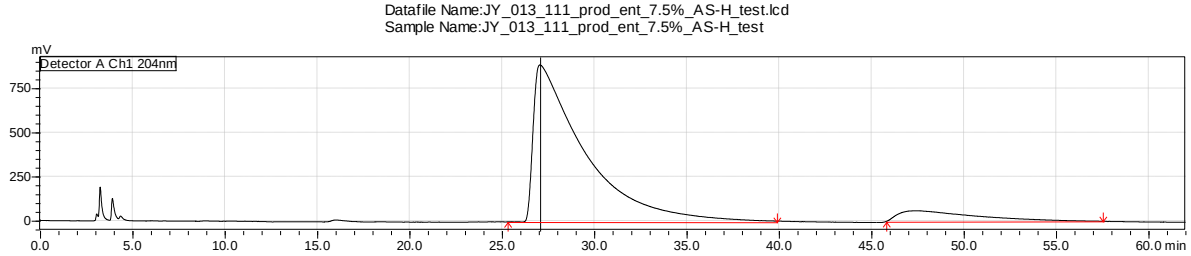

Peak#	Ret. Time	Area	Height	Conc.	Area%
1	27.067	171636003	889228	90.739	90.739
2	47.407	17517185	60667	9.261	9.261
Total		189153188	949895	100.000	100.000

(R)-**4.70h** (Table 4-6, 7a)

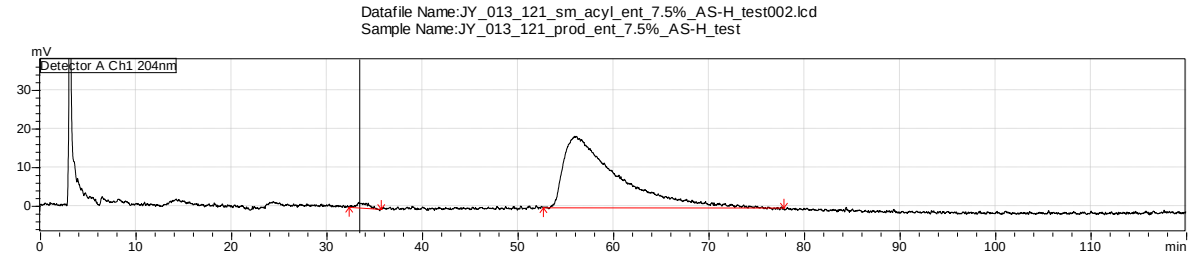

Peak#	Ret. Time	Area	Height	Conc.	Area%
1	33.413	87326	1305	1.236	1.236
2	56.152	6975743	18325	98.764	98.764
Total		7063069	19629	100.000	100.000

(±)-**4.70i**

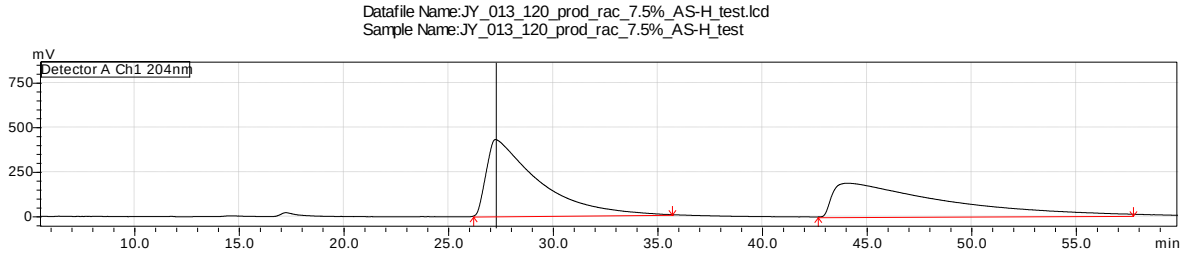

Peak#	Ret. Time	Area	Height	Conc.	Area%
1	27.271	73078450	429366	51.656	51.656
2	44.183	68392063	188390	48.344	48.344
Total		141470513	617756	100.000	100.000

(S)-**4.70i** (Table 4-6, 8a)

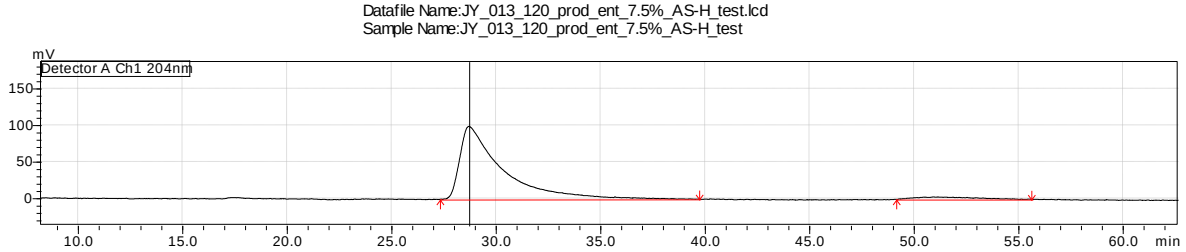

Peak#	Ret. Time	Area	Height	Conc.	Area%
1	28.727	13974923	99638	95.667	95.667
2	50.965	632947	3325	4.333	4.333
Total		14607870	102963	100.000	100.000

(R)-**4.70h** (Table 4-6, 8a)

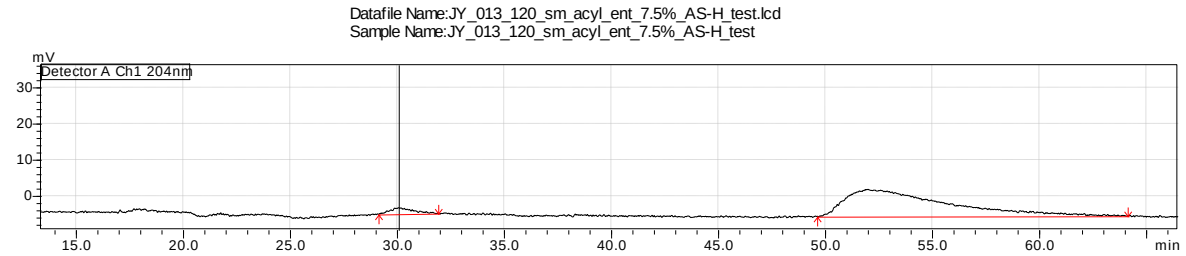

Peak#	Ret. Time	Area	Height	Conc.	Area%
1	30.084	124714	1722	4.874	4.874
2	52.017	2433947	7477	95.126	95.126
Total		2558661	9199	100.000	100.000

(±)-**4.70j**

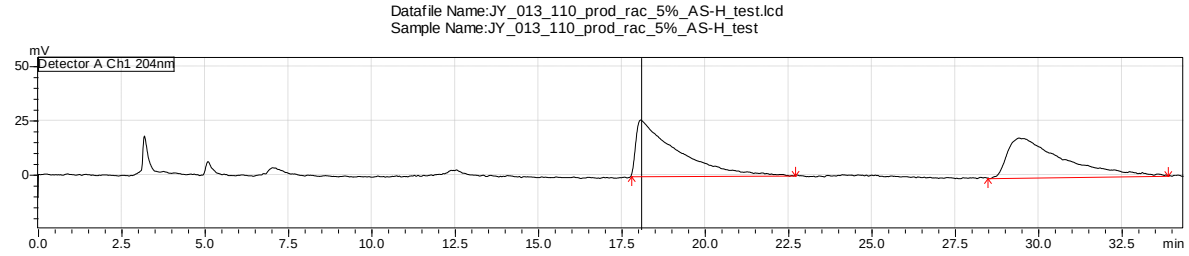

Peak#	Ret. Time	Area	Height	Conc.	Area%
1	18.091	2156720	25789	50.780	50.780
2	29.431	2090502	18210	49.220	49.220
Total		4247222	43999	100.000	100.000

(S)-**4.70j** (Table 4-6, 9a)

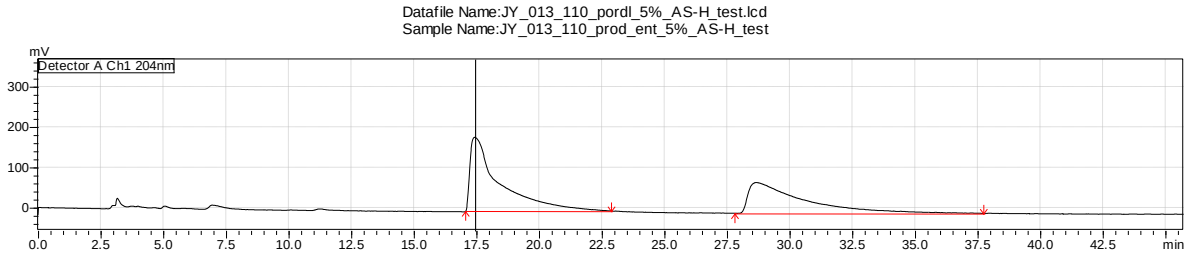

Peak#	Ret. Time	Area	Height	Conc.	Area%
1	17.441	14750238	182192	56.200	56.200
2	28.686	11495777	75886	43.800	43.800
Total		26246015	258078	100.000	100.000

(R)-**4.70j** (Table 4-6, 9a)

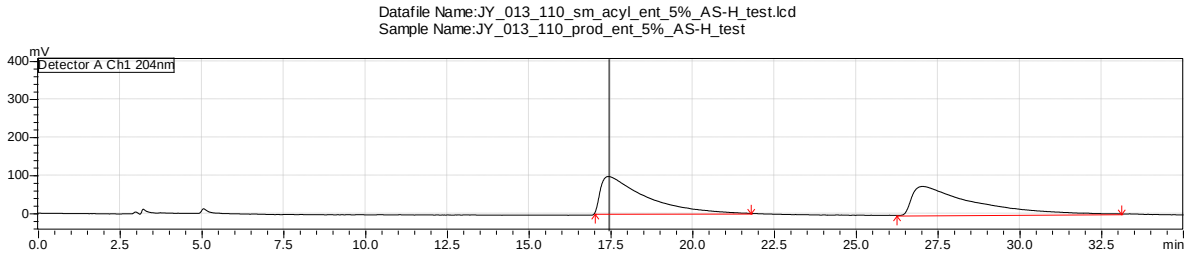

Peak#	Ret. Time	Area	Height	Conc.	Area%
1	17.444	9109398	97237	48.724	48.724
2	27.042	9586468	75600	51.276	51.276
Total		18695866	172837	100.000	100.000

(±)-**4.70k**

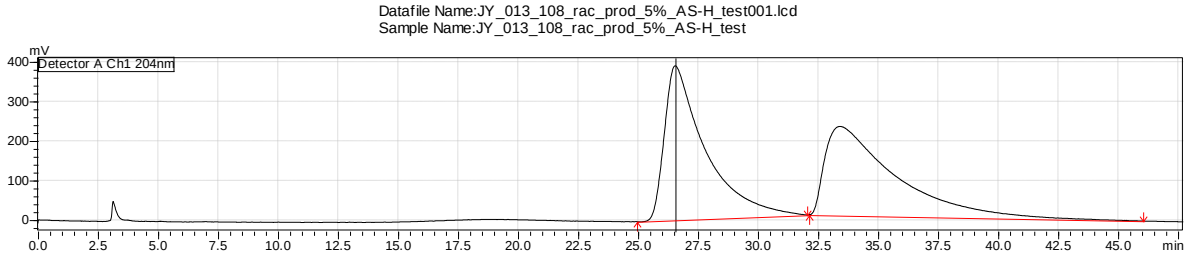

Peak#	Ret. Time	Area	Height	Conc.	Area%
1	26.558	46070327	390283	50.264	50.264
2	33.422	45585641	224771	49.736	49.736
Total		91655968	615054	100.000	100.000

(S)-**4.70k** (Table 4-6, 10a)

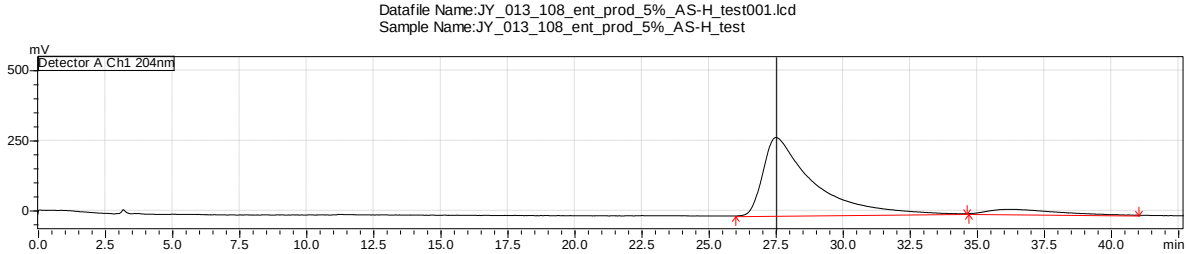

Peak#	Ret. Time	Area	Height	Conc.	Area%
1	27.518	35706242	279087	92.425	92.425
2	36.395	2926292	17337	7.575	7.575
Total		38632534	296424	100.000	100.000

(R)-**4.70k** (Table 4-6, 10a)

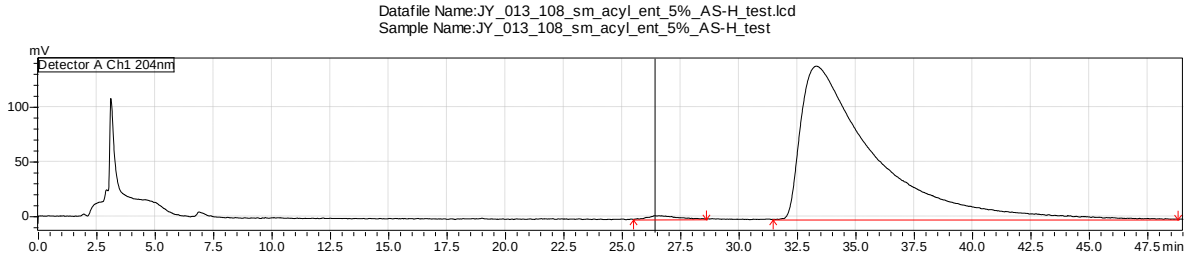

Peak#	Ret. Time	Area	Height	Conc.	Area%
1	26.397	267160	3211	0.881	0.881
2	33.334	30072655	139943	99.119	99.119
Total		30339815	143154	100.000	100.000

(±)-**4.70l**

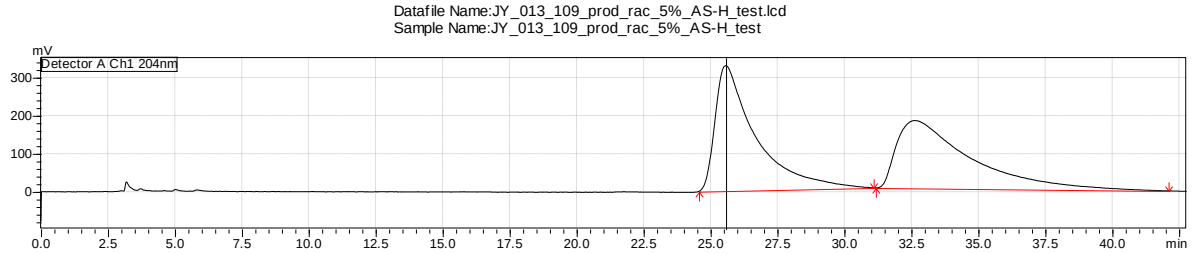

Peak#	Ret. Time	Area	Height	Conc.	Area%
1	25.578	34545270	329008	50.471	50.471
2	32.634	33899833	177831	49.529	49.529
Total		68445102	506839	100.000	100.000

(S)-**4.70l** (Table 4-6, 12a)

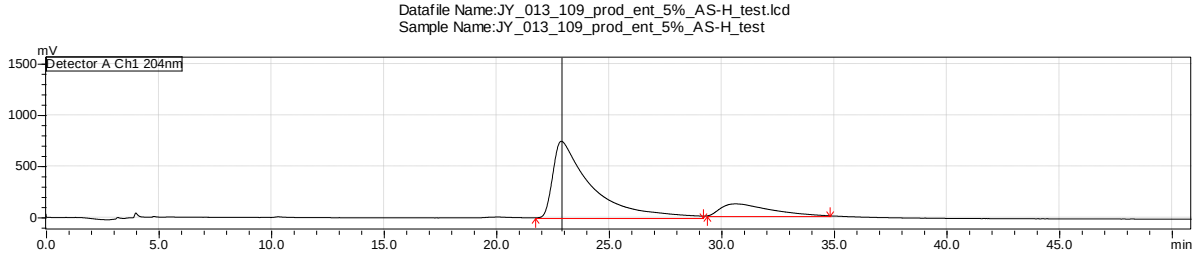

Peak#	Ret. Time	Area	Height	Conc.	Area%
1	22.898	88117976	747575	83.347	83.347
2	30.642	17606743	117684	16.653	16.653
Total		105724718	865259	100.000	100.000

(R)-**4.70l** (Table 4-6, 12a)

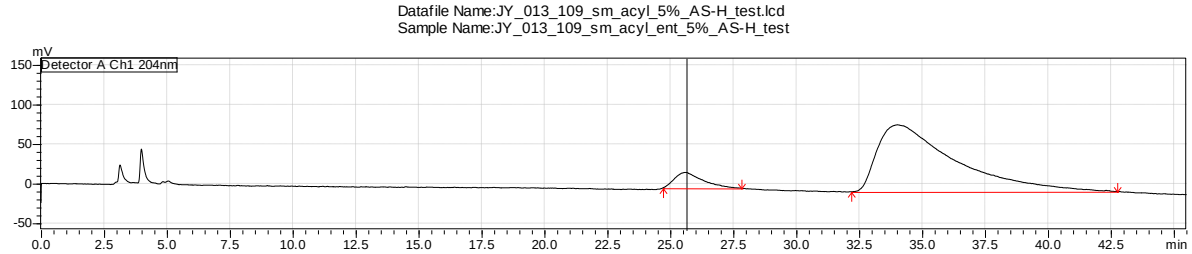

Peak#	Ret. Time	Area	Height	Conc.	Area%
1	25.638	1532030	19708	7.791	7.791
2	34.030	18132987	84514	92.209	92.209
Total		19665017	104223	100.000	100.000

(±)-**4.71a**

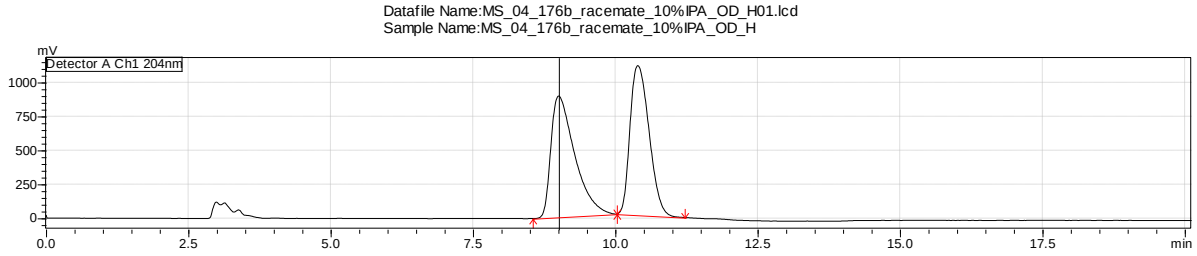

Peak#	Ret. Time	Area	Height	Conc.	Area%
1	9.008	25872114	891261	50.257	50.257
2	10.398	25607532	1100190	49.743	49.743
Total		51479646	1991451	100.000	100.000

(S)-**4.71a** (Table 4-7, 1a)

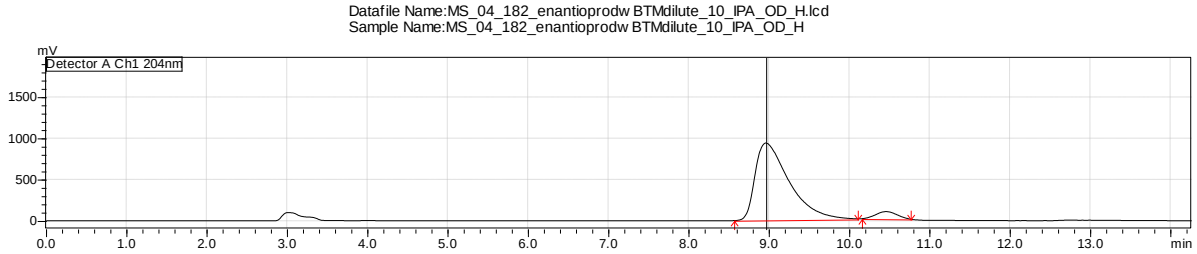

Peak#	Ret. Time	Area	Height	Conc.	Area%
1	8.966	27595334	935786	94.486	94.486
2	10.462	1610284	88392	5.514	5.514
Total		29205618	1024177	100.000	100.000

(R)-**4.71a** (Table 4-7, 1a)

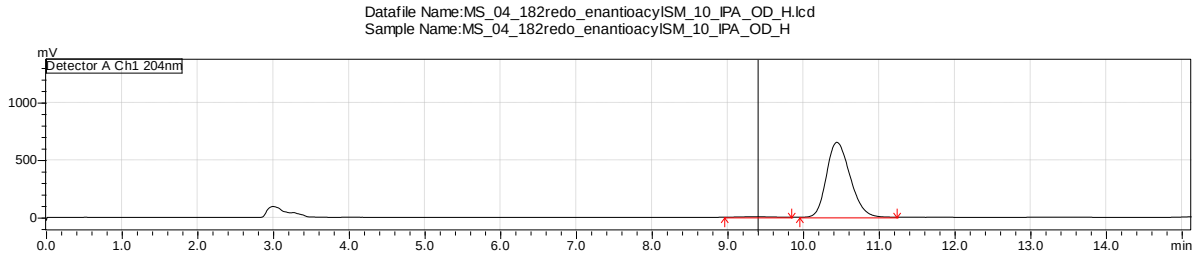

Peak#	Ret. Time	Area	Height	Conc.	Area%
1	9.398	120285	4607	0.844	0.844
2	10.447	14131175	651220	99.156	99.156
Total		14251460	655828	100.000	100.000

(±)-**4.71b**

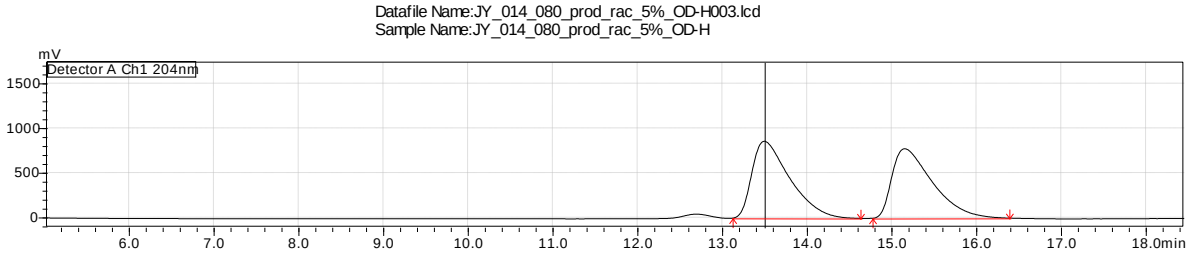

Peak#	Ret. Time	Area	Height	Conc.	Area%
1	13.503	26807802	860696	50.863	50.863
2	15.158	25898507	778033	49.137	49.137
Total		52706309	1638729	100.000	100.000

(S)-**4.71b** (Table 4-7, 2a)

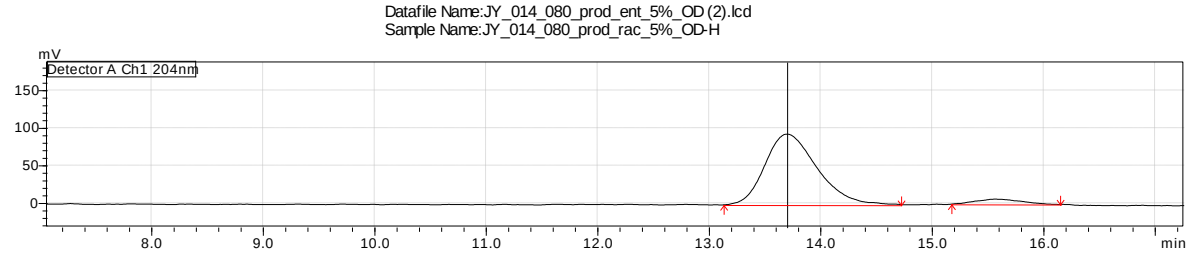

Peak#	Ret. Time	Area	Height	Conc.	Area%
1	13.702	3056168	94083	94.141	94.141
2	15.569	190201	6799	5.859	5.859
Total		3246369	100881	100.000	100.000

(R)-**4.71b** (Table 4-7, 2a)

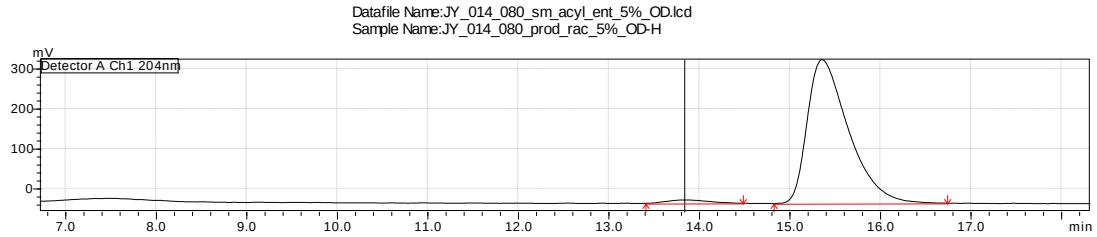

Peak#	Ret. Time	Area	Height	Conc.	Area%
1	13.837	263606	8420	2.261	2.261
2	15.362	11396111	359602	97.739	97.739
Total		11659717	36802	100.000	100.000

(±)-**4.71c**

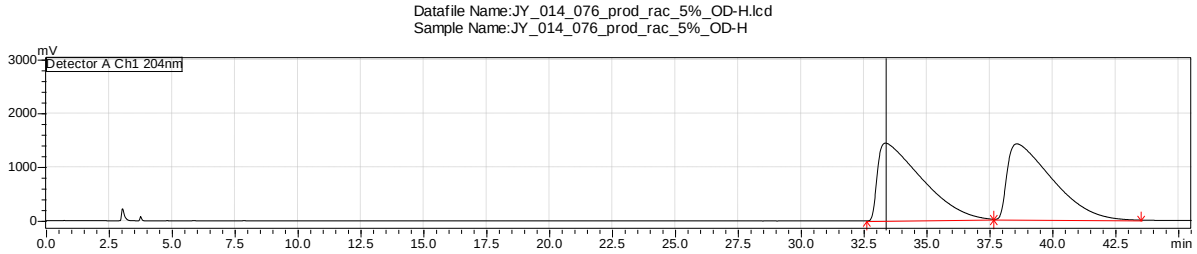

Peak#	Ret. Time	Area	Height	Conc.	Area%
1	33.376	174932817	1443860	50.092	50.092
2	38.597	174293431	1406930	49.908	49.908
Total		349226248	2850790	100.000	100.000

(S)-**4.71c** (Table 4-7, 3a)

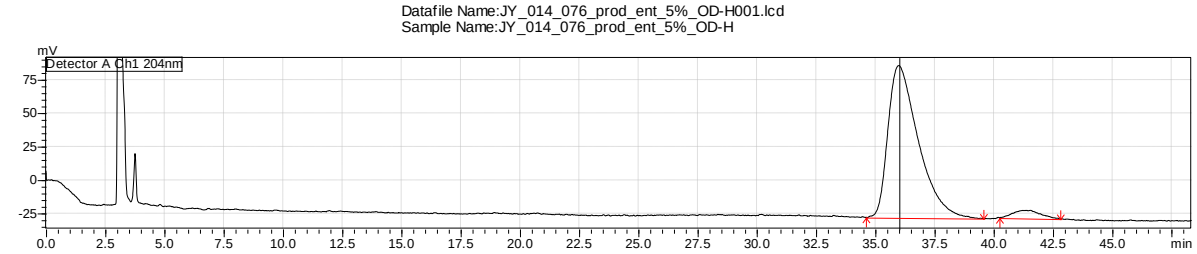

Peak#	Ret. Time	Area	Height	Conc.	Area%
1	36.015	10107164	113821	95.472	95.472
2	41.555	479377	6031	4.528	4.528
Total		10586542	119853	100.000	100.000

(R)-**4.71c** (Table 4-7, 3a)

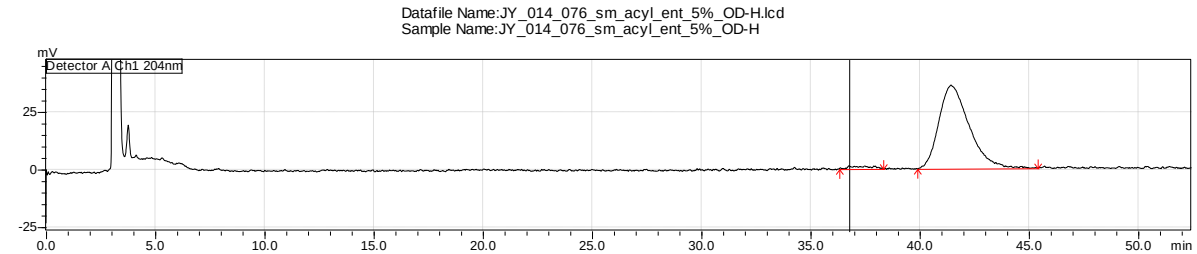

Peak#	Ret. Time	Area	Height	Conc.	Area%
1	36.776	83496	1388	2.350	2.350
2	41.442	3470135	36243	97.650	97.650
Total		3553630	37630	100.000	100.000

(±)-**4.71d**

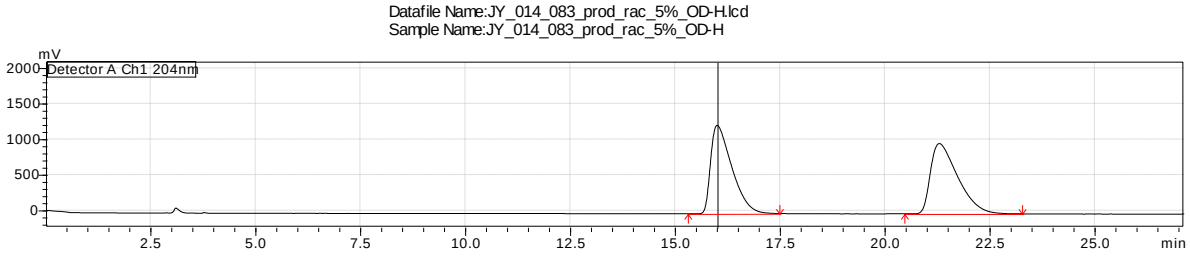

Peak#	Ret. Time	Area	Height	Conc.	Area%
1	16.013	43516339	1241269	49.403	49.403
2	21.306	44568894	987036	50.597	50.597
Total		88085233	2228305	100.00	100.000

(S)-**4.71d** (Table 4-7, 4a)

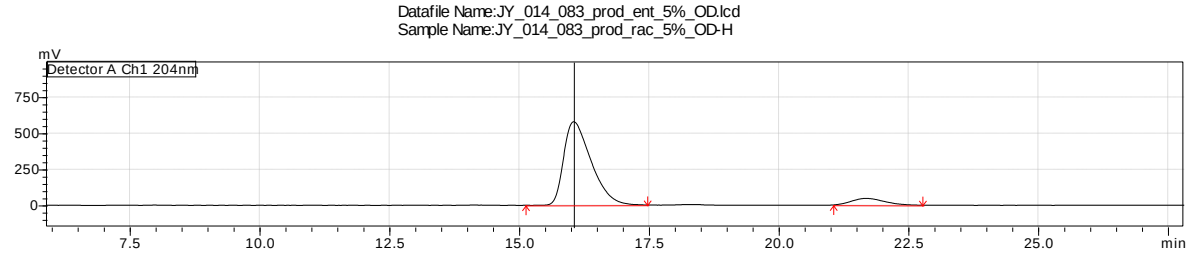

Peak#	Ret. Time	Area	Height	Conc.	Area%
1	16.057	21228236	577982	91.458	91.458
2	21.698	1982790	45976	8.542	8.542
Total		23211025	623958	100.000	100.00

(R)-**4.71d** (Table 4-7, 4a)

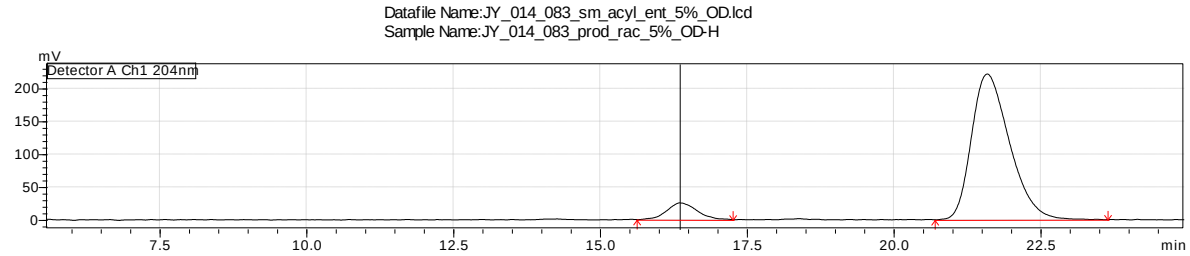

Peak#	Ret. Time	Area	Height	Conc.	Area%
1	16.358	901435	25412	8.274	8.274
2	21.597	9993027	221759	91.726	91.726
Total		10894462	247171	100.000	100.000

(±)-**4.71e**

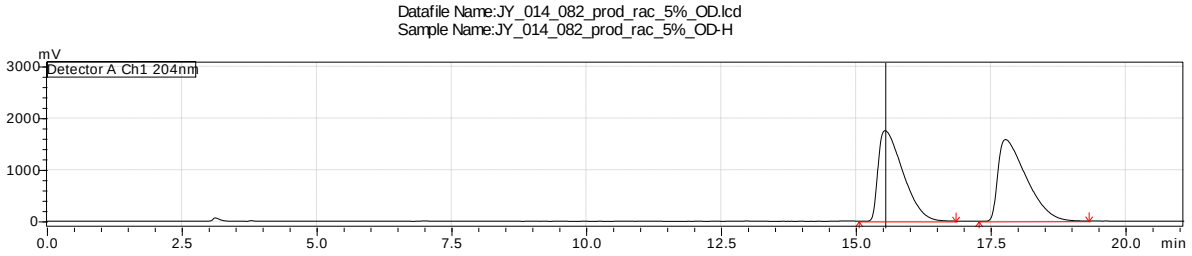

Peak#	Ret. Time	Area	Height	Conc.	Area%
1	15.545	55862166	1752775	49.219	49.219
2	17.779	57634983	1580070	50.781	50.781
Total		113497148	3332846	100.000	100.000

(S)-**4.71e** (Table 4-7, 5a)

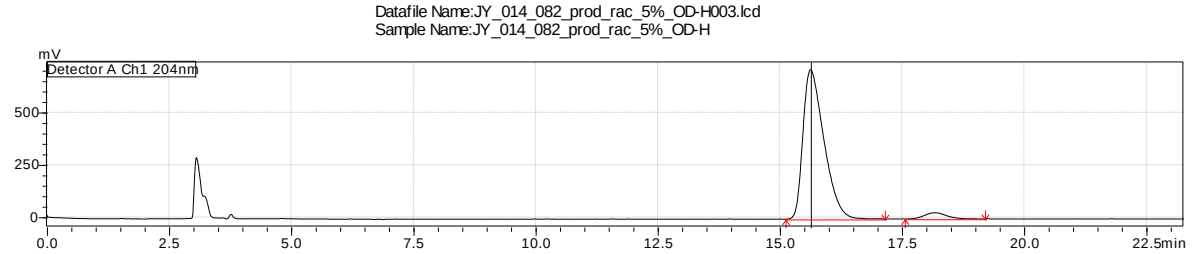

Peak#	Ret. Time	Area	Height	Conc.	Area%
1	15.633	21334445	714495	95.815	95.815
2	18.178	931931	29614	4.185	4.185
Total		22266375	744109	100.000	100.000

(R)-**4.71e** (Table 4-7, 5a)

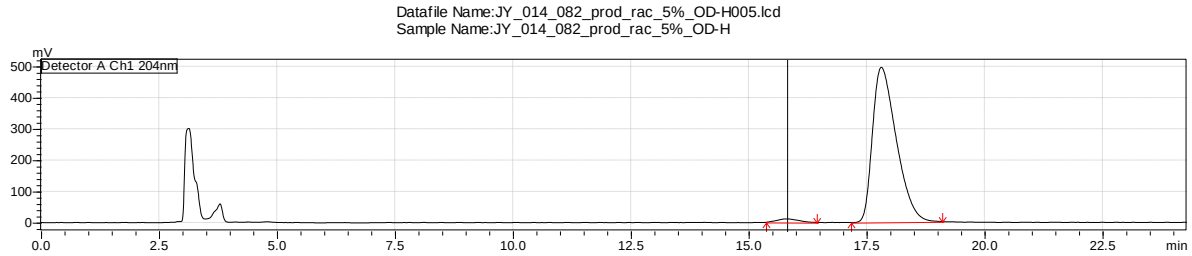

Peak#	Ret. Time	Area	Height	Conc.	Area%
1	15.812	341280	11165	1.926	1.926
2	17.815	17377599	495959	98.074	98.074
Total		17718879	507124	100.000	100.000

(±)-**4.79a**

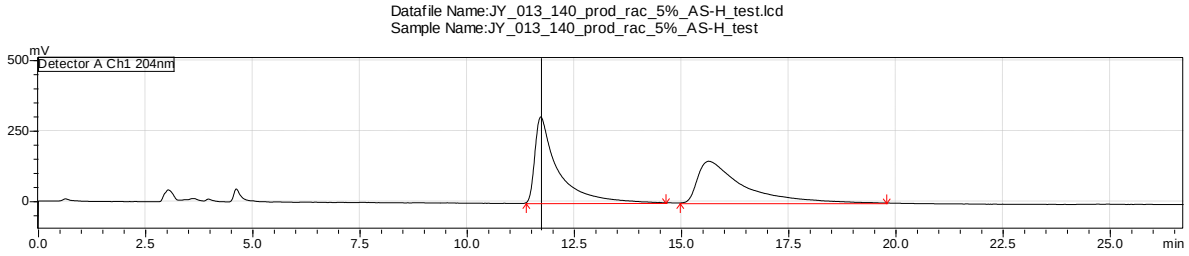

Peak#	Ret. Time	Area	Height	Conc.	Area%
1	11.731	11316892	305059	50.983	50.983
2	15.648	10880595	147997	49.017	49.017
Total		22197486	453056	100.000	100.000

(S)-**4.79a** (Table 4-8, 1a)

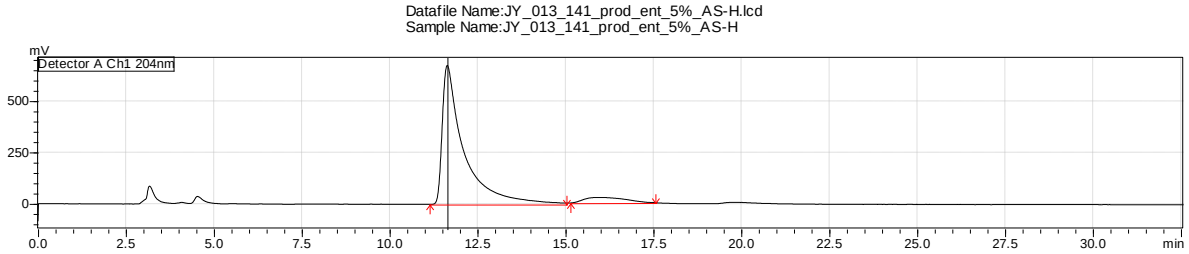

Peak#	Ret. Time	Area	Height	Conc.	Area%
1	11.644	28773513	676490	93.027	93.027
2	15.904	2156791	26523	6.973	6.973
Total		30930304	703013	100.000	100.000

(R)-**4.79a** (Table 4-8, 1a)

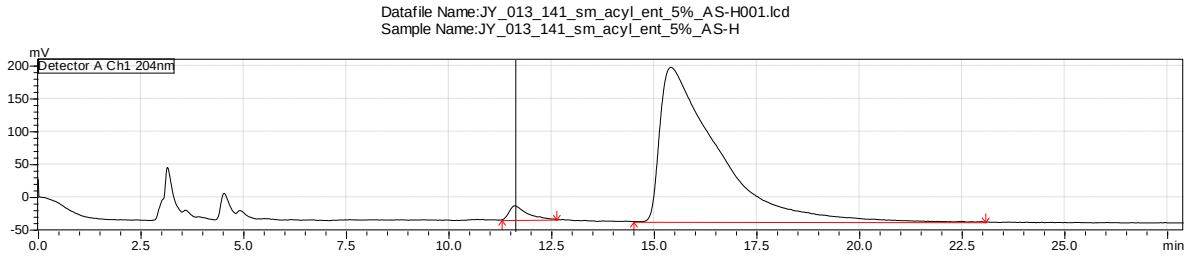

Peak#	Ret. Time	Area	Height	Conc.	Area%
1	11.623	634423	21356	2.712	2.712
2	15.423	22757702	235105	97.288	97.288
Total		23392125	256460	100.000	100.000

(±)-**4.79b**

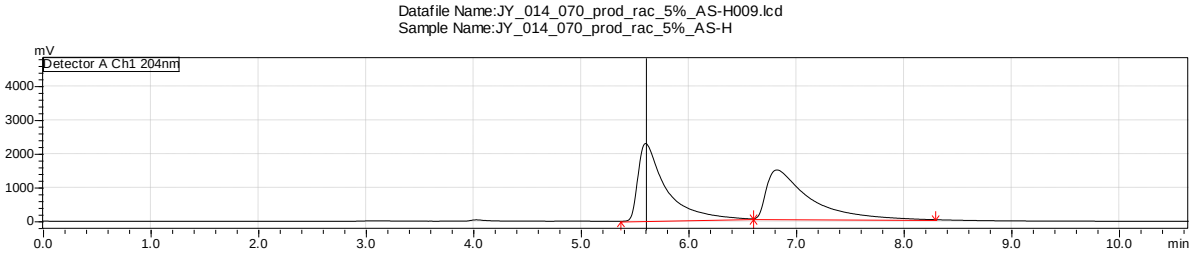

Peak#	Ret. Time	Area	Height	Conc.	Area%
1	5.603	40982972	2288822	50.845	50.845
2	6.823	39621025	1451917	49.155	49.155
Total		80603998	3740739	100.000	100.000

(S)-**4.79b** (Table 4-8, 2a)

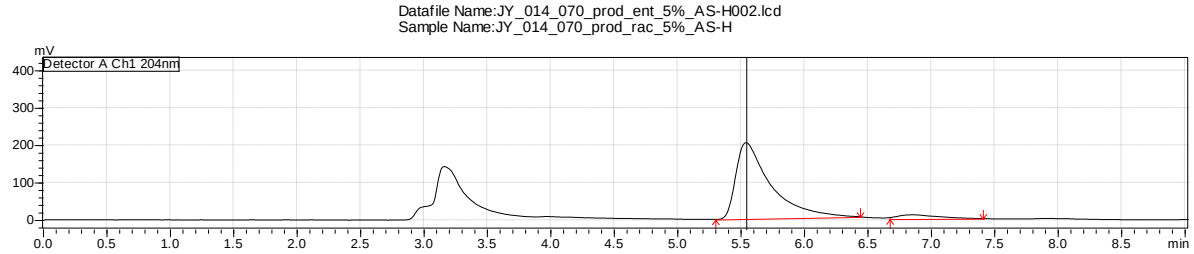

Peak#	Ret. Time	Area	Height	Conc.	Area%
1	5.544	3882254	203965	94.413	94.413
2	6.859	229721	10548	5.587	5.587
Total		4111975	214514	100.000	100.000

(R)-**4.79b** (Table 4-8, 2a)

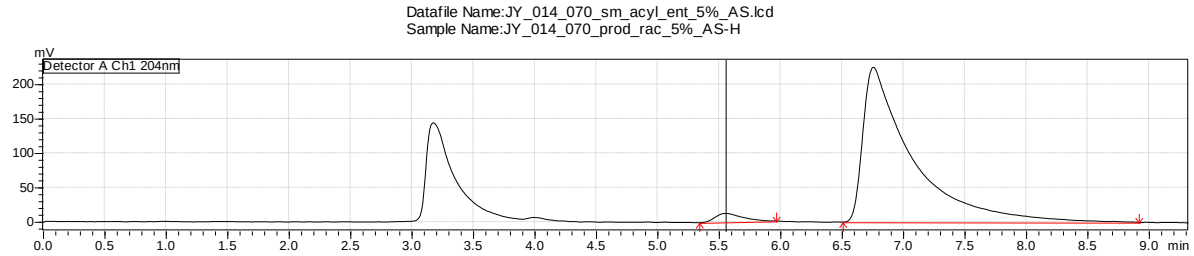

Peak#	Ret. Time	Area	Height	Conc.	Area%
1	5.556	194443	12735	3.010	3.010
2	6.760	6264620	225332	96.990	96.990
Total		6459062	238067	100.000	100.000

(±)-**4.79c**

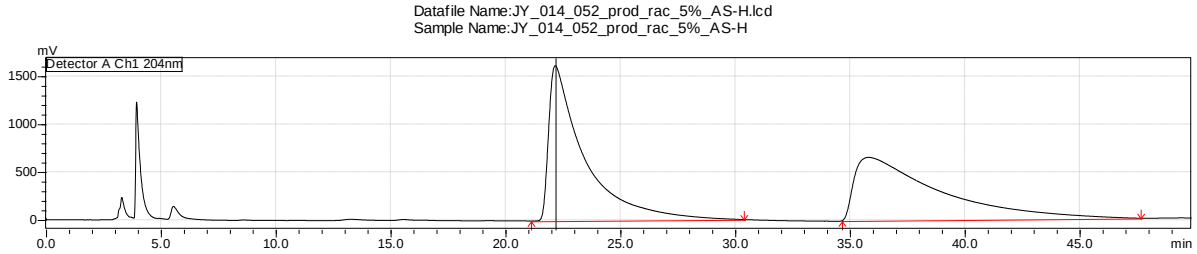

Peak#	Ret. Time	Area	Height	Conc.	Area%
1	22.179	174316130	161958	50.901	50.901
2	35.843	168141619	660038	49.099	49.099
Total		342457750	2279619	100.000	100.000

(S)-**4.79c** (Table 4-8, 3a)

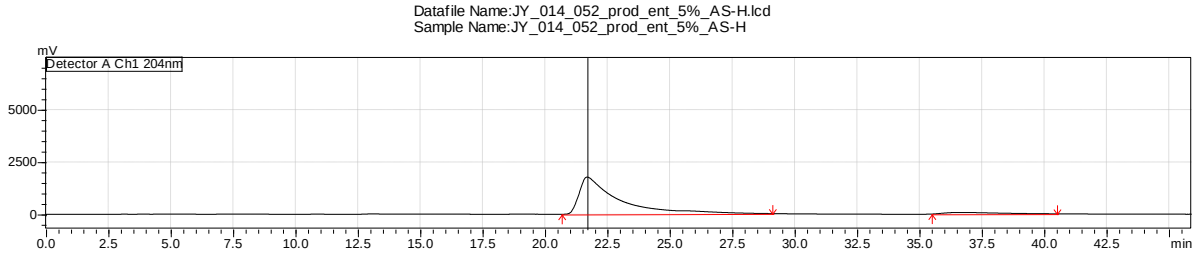

Peak#	Ret. Time	Area	Height	Conc.	Area%
1	21.696	191895407	1772977	94.658	94.658
2	36.634	10830339	72969	5.342	5.342
Total		202725746	1845946	100.000	100.000

(R)-**4.79c** (Table 4-8, 3a)

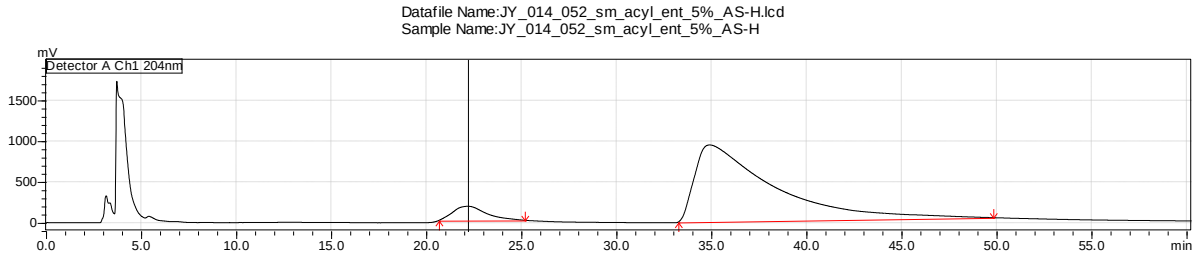

Peak#	Ret. Time	Area	Height	Conc.	Area%
1	22.194	21147838	174213	7.283	7.283
2	34.920	269231674	941746	92.717	92.717
Total		290379511	1115960	100.000	100.000

(±)-**4.79d**

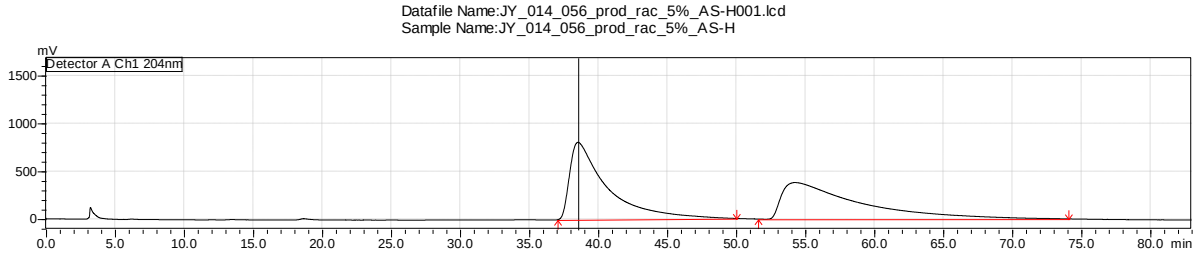

Peak#	Ret. Time	Area	Height	Conc.	Area%
1	38.556	152114767	808065	50.844	50.844
2	54.275	147063615	381454	49.156	49.156
Total		299178382	1189519	100.000	100.000

(S)-**4.79d** (Table 4-8, 4a)

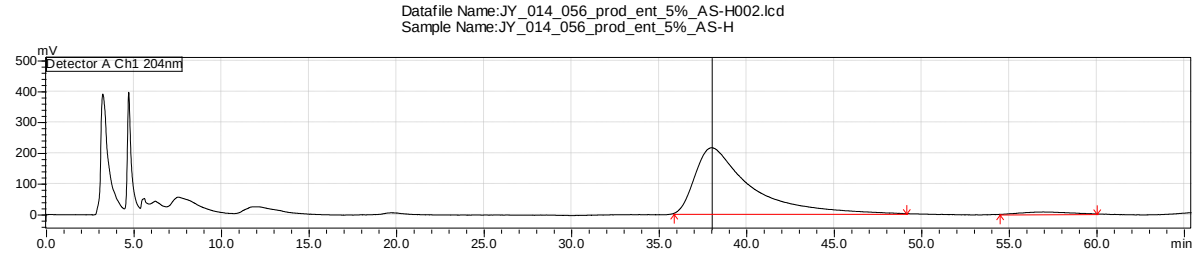

Peak#	Ret. Time	Area	Height	Conc.	Area%
1	38.031	46016106	213867	97.343	97.343
2	56.980	1256008	7215	2.657	2.657
Total		47272115	221082	100.000	100.000

(R)-**4.79d** (Table 4-8, 4a)

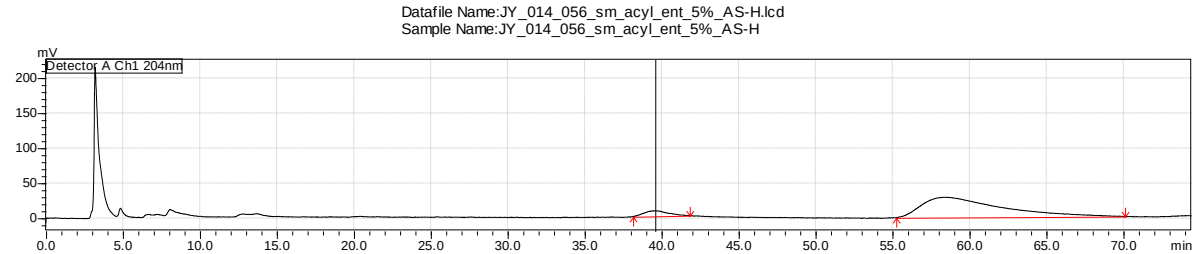

Peak#	Ret. Time	Area	Height	Conc.	Area%
1	39.578	817125	7631	7.433	7.433
2	58.365	10176341	28825	92.567	92.567
Total		10993466	36456	100.000	100.000

(±)-**4.79e**

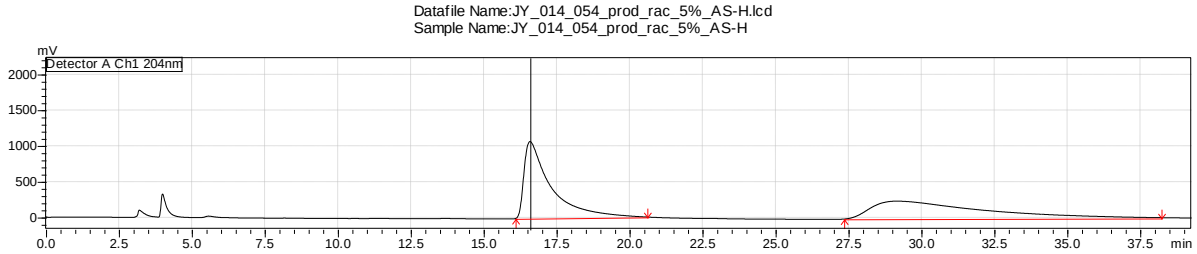

Peak#	Ret. Time	Area	Height	Conc.	Area%
1	16.595	68917181	1075120	51.302	51.302
2	29.238	65417962	248508	48.698	48.698
Total		134335143	1323628	100.000	100.000

(S)-**4.79e** (Table 4-8, 5a)

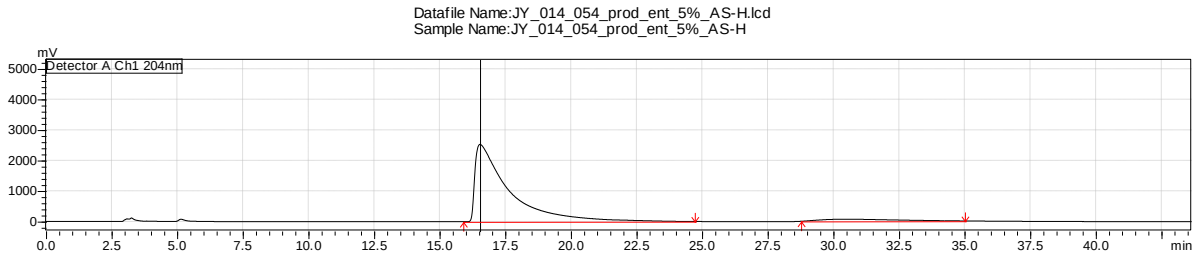

Peak#	Ret. Time	Area	Height	Conc.	Area%
1	16.540	227198518	2530616	94.598	94.598
2	30.553	12973886	65513	5.402	5.402
Total		240172403	2596130	100.000	100.000

(R)-**4.79e** (Table 4-8, 5a)

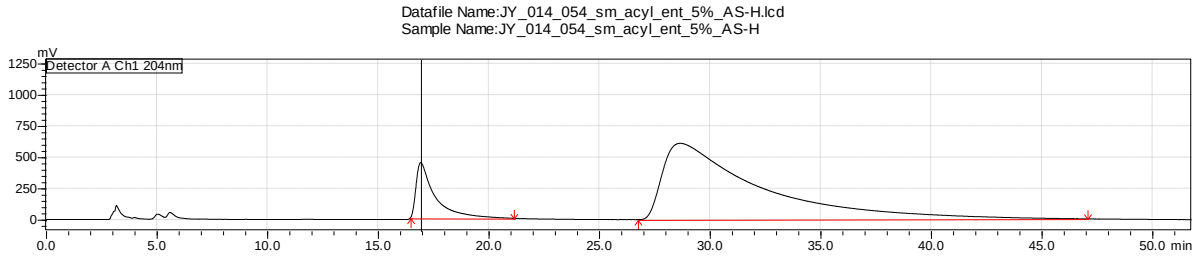

Peak#	Ret. Time	Area	Height	Conc.	Area%
1	16.950	26228789	444632	12.503	12.503
2	28.679	183553226	610404	87.497	87.497
Total		209782016	1055036	100.000	100.000

(±)-**4.79f**

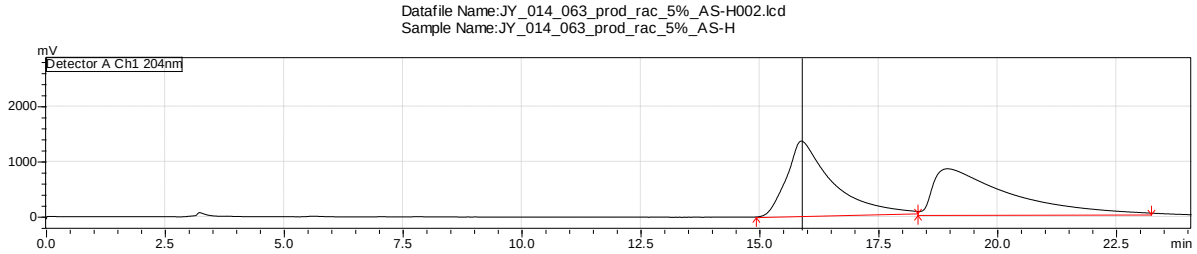

Peak#	Ret. Time	Area	Height	Conc.	Area%
1	15.888	89699233	1354091	49.599	49.599
2	18.959	91148801	829593	50.401	50.401
Total		180848034	2183684	100.000	100.000

(S)-**4.79f** (Table 4-8, 6a)

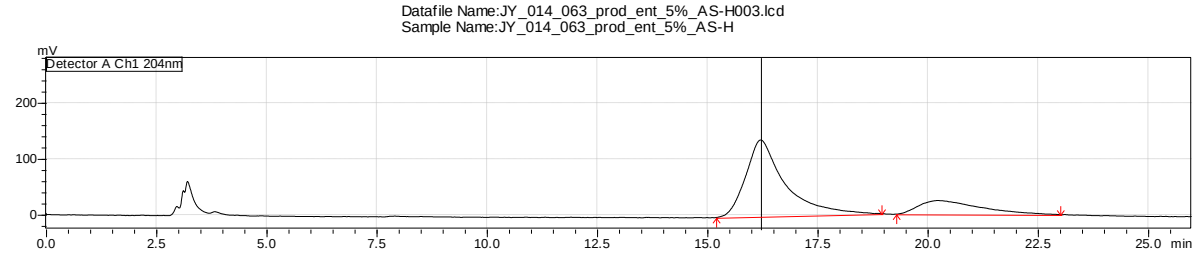

Peak#	Ret. Time	Area	Height	Conc.	Area%
1	16.218	8457892	136632	78.123	78.123
2	20.230	2368500	24620	21.877	21.877
Total		10826392	161252	100.000	100.000

(R)-**4.79f** (Table 4-8, 6a)

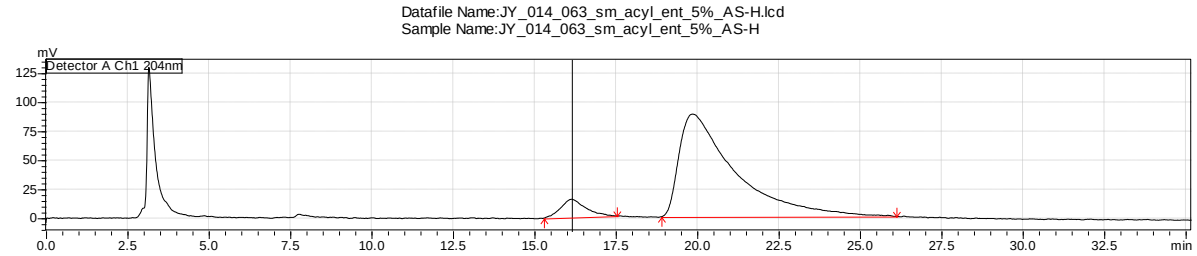

Peak#	Ret. Time	Area	Height	Conc.	Area%
1	16.149	837091	15632	7.385	7.385
2	19.872	10497377	88353	92.615	92.615
Total		11334467	103985	100.000	100.000

(±)-**4.79g**

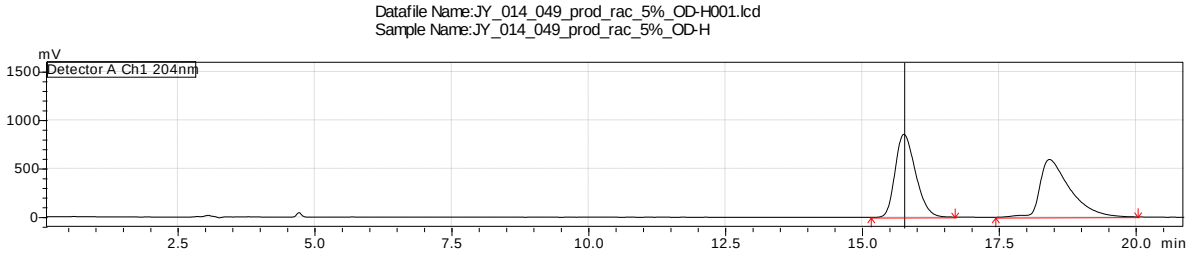

Peak#	Ret. Time	Area	Height	Conc.	Area%
1	15.768	22170577	856021	49.571	49.571
2	18.428	22554637	594265	50.429	50.429
Total		44725214	1450286	100.000	100.000

(S)-**4.79g** (Table 4-8, 7a)

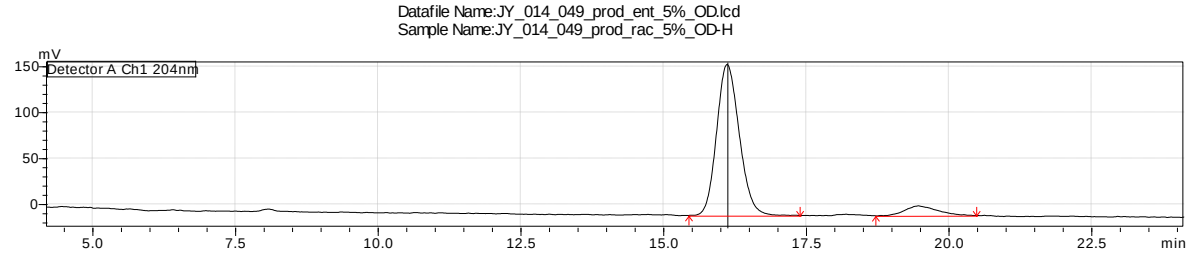

Peak#	Ret. Time	Area	Height	Conc.	Area%
1	16.124	4534995	164402	91.508	91.508
2	19.477	420826	10677	8.492	8.492
Total		4955821	175080	100.000	100.000

(R)-**4.79g** (Table 4-8, 7a)

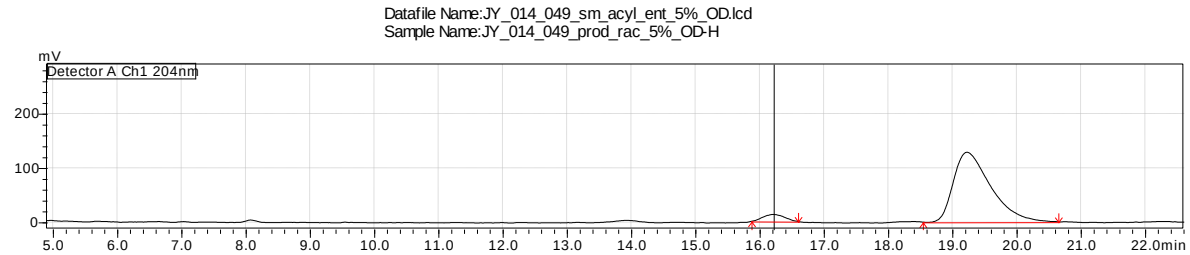

Peak#	Ret. Time	Area	Height	Conc.	Area%
1	16.222	296496	12716	5.427	5.427
2	19.231	5166576	128553	94.573	94.573
Total		5463072	141268	100.000	100.000

(±)-**4.79h**

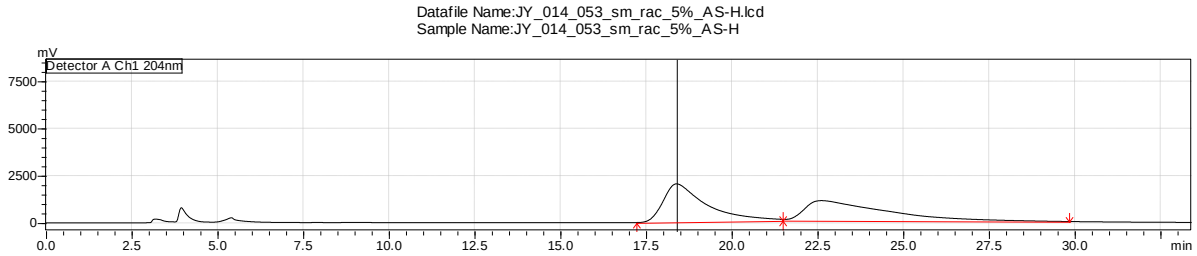

Peak#	Ret. Time	Area	Height	Conc.	Area%
1	18.394	175516715	2018980	50.541	50.541
2	22.629	171758640	1058342	49.459	49.459
Total		347275355	3077322	100.000	100.000

(S)-**4.79h** (Table 4-8, 8a)

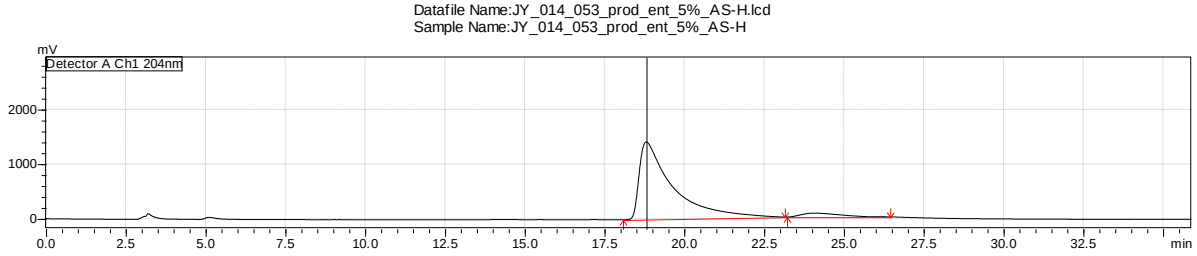

Peak#	Ret. Time	Area	Height	Conc.	Area%
1	18.813	102405856	1414247	94.701	94.701
2	24.102	5729721	69795	5.299	5.299
Total		108135577	1484042	100.000	100.000

(R)-**4.79h** (Table 4-8, 8a)

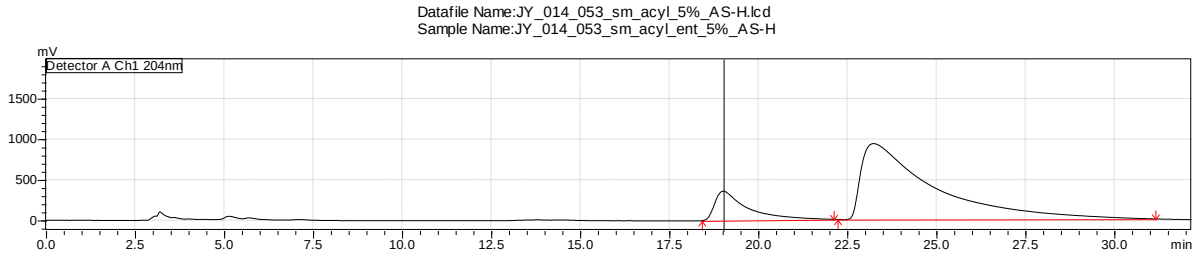

Peak#	Ret. Time	Area	Height	Conc.	Area%
1	19.025	22889982	360940	14.947	14.947
2	23.244	130248675	932530	85.053	85.053
Total		153138657	1293470	100.000	100.000

4.6 References.

1. Grobben, Y.; de Man, J.; Van Doornmalen, A. M.; Muller, M.; Willemsen-Seegers, N.; Vu-Pham, D.; Mulder, W. R.; Prinsen, M. B. W.; de Wit, J.; Sterren-burg, J. G.; Van Cauter, F.; Ouden, J. E. D.; Van Al-tena, A. M.; Massuger, L. F.; Uitdehaag, J. C. M.; Buijsman, R. C.; Zaman, G. J. R., Targeting indoleam-ine 2,3-dioxygenase in cancer models using the novel small molecule inhibitor NTRC 3883-0. *Front. Immunol.* **2020**.

2. Peilleron, L., Retailleau, P., Cariou, K., Synthesis of Cyclic N -Hydroxylated Ureas and Oxazolidinone Oximes Enabled by Chemoselective Iodine(III)-Mediated Radical or Cationic Cyclizations of Unsaturated N –Alkoxyureas. *Adv. Synth. Catal.* **2019**, *361*, 5160-5169

3. Yang, X.; Song, L.; Hao, X.; Wang, Y.; Fu, H. 1-Hydroxy-2-pyrrolidone compounds as calcium an-tagonists and their preparation, pharmaceutical compositions and use in the treatment of nervous system diseases. CN102491929A, 2012.

4. Binanzer, M.; Hsieh, S.-Y.; Bode, J. W., Catalytic Kinetic Resolution of Cyclic Secondary Amines. *J. Am. Chem. Soc.* **2011,** *133* (49), 19698-19701.

5. Wanner, B.; Kreituss, I.; Gutierrez, O.; Kozlowski, M. C.; Bode, J. W., Catalytic Kinetic Resolution of Disubstituted Piperidines by Enantioselective Acylation: Synthetic Utility and Mechanistic Insights. *J. Am. Chem. Soc.* **2015,** *137* (35), 11491-11497.

6. Dooley, C. J.; Burtea, A.; Mitilian, C.; Dao, W. T.; Qu, B.; Salzameda, N. T.; Rychnovsky, S. D., Using the Competing Enantioselective Conversion Method to Assign the Absolute Configuration of Cyclic Amines with Bode's Acylation Reagents. *J. Org. Chem.* **2020**, *85* (16), 10750-10759.

7. Frazier, Charles P.; Engelking, Jarred R.; Javier, Read de Alaniz. Copper-Catalyzed Aerobic Oxidation of Hydroxamic Acids Leads to a Mild and Versatile Acylnitroso Ene Reaction. *J. Am. Chem. Soc.* **2011**, *133*, 27, 10430-10433.

8. (a) Arjun, A.; Karissa, M.; Jeffery C. S. Access to 4-Oxazolidinones: A (3 + 2) Cycloaddition Approach. *Org. Lett.* **2016**, *18*, 23, 6082-6085. (b) Acharya, A.; Anumandla, D.; Jeffrey, C. S. Dearomative Indole Cycloaddition Reactions of Aza-Oxyallyl Cationic Intermediates: Modular Access to Pyrroloindolines. *J. Am. Chem. Soc.* **2015,** *137*, 14858.

9. Hadimani, M. B.; Mukherjee, R.; Banerjee, R.; Shoman, M. E.; Aly, O. M.; King, S. B., Ring expansions of acyloxy nitroso compounds. *Tetrahedron Lett.* **2015**, *56*, 5870-5873.

10. Yamada, K.; Kishikawa, K.; Yamamoto, M. Stereospecificity of the photorearrangement of nitronate anions and its utilization for stereospecific cleavage of cyclic compounds. *J. Org. Chem.* **1987**, *52*, 2327-30.

11. Bannykh, A. V.; Bakulina, O. Y.; Dar'in, D. V.; Krasavin, M., Hydroxylamine as an ammonia equivalent: access to NH-tetrahydroisoquinolonic derivatives from aldoximes by the Castagnoli-Cushman reaction followed by reduction. *Mendeleev Commun.* **2019**, *29*, 337-338.

12. (a) Hiraoka, S.; Matsumoto, T.; Matsuzaka, K.; Sato, T.; Chida, N., Approach to Fully Substituted Cyclic Nitrones from N-Hydroxylactam Derivatives: Development and Application to the Total Synthesis of Cylindricine C. *Angew. Chem., Int. Ed.* **2019**, *58*, 4381-4385. (b) Katahara, S.; Kobayashi, S.; Fujita, K.; Matsumoto, T.; Sato, T.; Chida, N., An Iridium-Catalyzed Reductive Approach to Nitrones from N-Hydroxyamides. *J. Am. Chem. Soc.* **2016**, *138*, 5246-5249.

13. Yokosaka, T.; Hamajima, A.; Nemoto, T.; Hamada, Y., Asymmetric synthesis of highly functionalized γ-lactams through an organocatalytic aza-Michael-Michael reaction cascade using fumaric acid amide esters as multi-reactive substrates. *Tetrahedron Lett.* **2012**, *53*, 1245-1248.

14. Jaekel, M.; Qu, J.; Schnitzer, T.; Helmchen, G., Addition of Organometallic Reagents to Chiral N-Methoxylactams; Enantioselective Syntheses of Pyrrolidines and Piperi-dines. *Chem. - Eur. J.* **2013,** *19*, 16746-16755.

15. Lee, C. Y.; Kwon, Y. I.; Jang, H. S.; Lee, S.; Chun, Y. L.; Jung, J.; Kim, S.-G., Organocatalytic Enantioselective [4+3]-Cycloadditions of Azaoxyallyl Cations with 2-Aminophenyl Enones. *Adv. Synth. Catal.* **2021,** *363*, 4197-4203.

16. Hoshino, Y.; Oyaizu, M.; Koyanagi, Y.; Honda, K., Enantiomerically enriched bicyclic hydroxamic acids in one-step from α-aminohydroxamic acids and keto acids via cyclocondensation. *Synth. Commun.* **2013**, *43* (18), 2484-2492.

17. (a) Binanzer, M.; Hsieh, S.-Y.; Bode, J. W., Catalytic Kinetic Resolution of Cyclic Secondary Amines. *J. Am. Chem. Soc.* **2011,** *133* (49), 19698-19701. (b) Wanner, B.; Kreituss, I.; Gutierrez, O.; Kozlowski, M. C.; Bode, J. W., Catalytic Kinetic Resolution of Disubstituted Piperidines by Enantioselective Acylation: Synthetic Utility and Mechanistic Insights. *J. Am. Chem. Soc.* **2015,** *137* (35), 11491-11497.

18. Li, X.; Jiang, H.; Uffman, E. W. Guo, L.; Zhang, Y.; Yang, X.; Birman, V. B., Kinetic Resolution of Secondary Alcohols Using Amidine-Based Catalysts. *J. Org. Chem.* **2012,** *77*, 1722-1737.

19. Nakata, K.; Gotoh, K.; Ono, K.; Futami, K.; Shiina, I., Kinetic Resolution of Racemic 2-Hydroxy-γ-butyrolactones by Asymmetric Esterification Using Diphenylacetic Acid with Pivalic Anhydride and a Chiral Acyl-Transfer Catalyst. *Org. Lett.* **2013,** *15*, 1170-1173.

20. Birman, V. B.; Jiang, H.; Li, X.; Guo, L.; Uffman, E. W. "Kinetic Resolution of 2-Oxazolidinones via Catalytic, Enantioselective N-Acylation" *J. Am. Chem. Soc.* **2006,** *128*, 6536-6537.

21 . (a) Yang, X.; Bumbu, V. D.; Birman, V. B. Kinetic Resolution of β-Lactams via Enantioselective N-Acylation. *Org. Lett.* **2011**, *13*, 4755-4757. (b) Yang, X.; Bumbu, V. D.; Liu, P.; Li, X.; Jiang, H.; Uffman, E. W. Guo, L.; Zhang, W.; Jiang, X.; Houk, K. N.; Birman, V. B. Catalytic, Enantioselective N-Acylation of Lactams and Thiolactams Using Amidine-Based Catalysts. *J. Am. Chem. Soc.*, **2012**, *134*, 17605-17612.

22. (a) Ahlemeyer, N. A.; Birman, V. B., Asymmetric Catalytic Synthesis of Thiochromenes via an Acyl Transfer-Initiated Cascade. *Org. Lett.* **2016**, *18*, 3454-3457. (b) Ahlemeyer, N. A.; Streff, E. V.; Muthupandi, P.; Birman, V. B., Dramatic Acceleration of an Acyl Transfer-Initiated Cascade by Using Electron-Rich Amidine-Based Catalysts. *Org. Lett.* **2017**, *19*, 6486-6489. (c) Birman, V. B. *Aldrichimica Acta.* **2016**, *49*, 23.

23. Jackson, Chris M.; Blass, Benjamin; Coburn, Keith; Djandjighian, Laurent; Fadayel, Gina; Fluxe, Andrew J.; Hodson, Steven J.; Janusz, John M.; Murawsky, Michael; Ridgeway, James M.; White, Ronald E.; Wu, Shengde. Evolution of thiazolidine-based blockers of human Kv1.5 for the treatment of atrial arrhythmias. Bioorganic & Medicinal Chemistry Letters (2007), 17, (1), 282-284.

24. Srivastava, T.; Haq, W.; Katti, S. B., Carbodiimide mediated synthesis of 4-thiazolidinones by one-pot three-component condensation. Tetrahedron 2002, 58, 7619-7624.

25. Reported without characterization: (b) Jackson, C. M.; Blass, B.; Coburn, K.; Djandjighian, L.; Fadayel, G.; Fluxe, A. J.; Hodson, S. J.; Janusz, J. M.; Murawsky, M.; Ridgeway, J. M.; White, R. E.; Wu, S., Evolution of thiazolidine-based blockers of human Kv1.5 for the treatment of atrial arrhythmias. *Bioorg. Med. Chem. Lett.* **2007,** *17*, 282-284.

26. Birman, V. B.; Li, X., Benzotetramisole: A Remarkably Enantioselective Acyl Transfer Catalyst. *Org. Lett.* **2006,** *8*, 1351-1354.

27. Birman, V. B.; Jiang, H., Kinetic Resolution of Alcohols Using a 1,2-Dihydroimidazo[1,2-a]quinoline Enantioselective Acylation Catalyst. *Org. Lett.* **2005,** *7*, 3445-3447.

28. Belmessieri, D.; Joannesse, C.; Woods, P. A.; MacGregor, C.; Jones, C.; Campbell, C. D.; Johnston, C. P.; Duguet, N.; Concellon, C.; Bragg, R. A.; Smith, A. D., Structure-enantioselectivity effects in 3,4-dihydropyrimido[2,1-b]benzothiazole-based isothioureas as enantioselective acylation catalysts. *Org. Biomol. Chem.* **2011,** *9*, 559-570.

29. Hiraoka, S.; Matsumoto, T.; Matsuzaka, K.; Sato, T.; Chida, N., Approach to Fully Substituted Cyclic Nitrones from N-Hydroxylactam Derivatives: Development and Application to the Total Synthesis of Cylindricine C. *Angew. Chem., Int. Ed.* **2019,** *58*, 4381-4385.

30. Katahara, S.; Kobayashi, S.; Fujita, K.; Matsumoto, T.; Sato, T.; Chida, N., An Iridium-Catalyzed Reductive Approach to Nitrones from N-Hydroxyamides. *J. Am. Chem. Soc.* **2016,** *138*, 5246-5249.

31. Sakai, N.; Kobayashi, T.; Ogiwara, Y. One-pot Synthesis of Tetralin Derivatives from 3-Benzoylpropionic Acids: Indium-catalyzed Hydrosilylation of Ketones and Carboxylic Acids and Intramolecular Cyclization. *Chemistry Letters*. **2015**, *44*, (11), 1503-1505.

32. Kagan, H. B.; Fiaud, J. C., Kinetic resolution. *Top. Stereochem.* **1988,** *18*, 249-330.